

Dissertation zu Erlangung des Doktorgrades
der Fakultät für Chemie und Pharmazie
der Ludwig-Maximilians-Universität München

N-Substituted Glycosylamines and their Coordination Chemistry with Palladium(II)

Oliver Konrad Richter

aus

München, Deutschland

2020

Erklärung

Die Dissertation wurde im Sinne von § 7 der Promotionsordnung vom 28. November 2011 von Herrn Prof. Dr. Klüfers betreut.

Eidesstattliche Versicherung

Diese Dissertation wurde eigenständig und ohne unerlaubte Hilfe erarbeitet.

München, den 02. November 2020

Oliver Richter

Dissertation eingereicht am: 05.11.2020

Erstgutachter: Prof. Dr. Peter Klüfers

Zweitgutachter: Prof. Dr. Hans-Christian Böttcher

Mündliche Prüfung am: 15.12.2020

Diese Arbeit wurde in der Zeit von Januar 2014 bis November 2020 am Department für Chemie der Ludwig-Maximilians-Universität am Lehrstuhl für Bioanorganische Chemie und Koordinationschemie unter Anleitung von Herrn Prof. Dr. Klüfers durchgeführt.

Contents

List of Figures	III
Abbreviations	VII
Overview of Crystal Structures	IX
1. Introduction	1
1.1. The Biological Importance of Carbohydrates and Amino Sugars	1
1.2. The Chemistry of Glycosylamines	3
1.3. Palladium(II) and Platinum(II) Complexes	6
1.4. Characterization of Glycosylamines and their Pd ^{II} Complexes	7
1.5. Aim of this Work	9
2. Results	10
2.1. <i>N</i> -Substituted Glycosylamines	10
2.1.1. <i>N</i> -Alkylpentosylamines	10
2.1.1.1. <i>N</i> -Alkyl-D-arabinosylamines	11
2.1.1.2. <i>N</i> -Alkyl-D-lyxosylamines	14
2.1.1.3. <i>N</i> -Alkyl-D-ribosylamines	16
2.1.1.4. <i>N</i> -Alkyl-D-xylosylamines	19
2.1.2. <i>N</i> -Alkylhexosylamines	21
2.1.2.1. <i>N</i> -Alkyl-D-galactosylamines	21
2.1.2.2. <i>N</i> -Alkyl-D-glucosylamines	23
2.1.2.3. <i>N</i> -Alkyl-L-gulosylamines	25
2.1.2.4. <i>N</i> -Alkyl-D-mannosylamines	27
2.1.2.5. <i>N</i> -Alkyl-L-rhamnosylamines	28
2.1.3. <i>N</i> -Alkyl-2-deoxyglycosylamines	31
2.1.3.1. <i>N</i> -Alkyl-2-deoxy-D- <i>erythro</i> -pentosylamines	31
2.1.3.2. <i>N</i> -Alkyl-2-deoxy-D- <i>arabino</i> -hexosylamines	34
2.1.3.3. <i>N</i> -Alkyl-2-deoxy- <i>lyxo</i> -D-hexosylamines	35
2.1.4. <i>N</i> -Phenylglycosylamines	37
2.1.4.1. <i>N</i> -Phenylpentosylamines	37
2.1.4.2. <i>N</i> -Phenylhexosylamines	42
2.1.4.3. <i>N</i> -Phenyl-2-deoxyglycosylamines	44
2.2. Coordination Chemistry of <i>N</i> -Substituted Glycosylamines with Palladium(II) . .	47
2.2.1. <i>N</i> -Alkylpentosylamines	48
2.2.1.1. <i>N</i> -Alkyl-D-arabinosylamines	48
2.2.1.2. <i>N</i> -Alkyl-D-lyxosylamines	51

2.2.1.3.	<i>N</i> -Alkyl-D-ribosylamines	54
2.2.1.4.	<i>N</i> -Alkyl-D-xylosylamines	59
2.2.2.	<i>N</i> -Alkylhexosylamines	65
2.2.2.1.	<i>N</i> -Alkyl-D-galactosylamines	65
2.2.2.2.	<i>N</i> -Alkyl-D-glucosylamines	68
2.2.2.3.	<i>N</i> -Alkyl-L-gulosylamines	72
2.2.2.4.	<i>N</i> -Alkyl-D-mannosylamines	76
2.2.2.5.	<i>N</i> -Alkyl-L-rhamnosylamines	79
2.2.3.	<i>N</i> -Alkyl-2-deoxy-D-glycosylamines	81
2.2.3.1.	<i>N</i> -Alkyl-2-deoxy-D- <i>erythro</i> -pentosylamines	81
2.2.3.2.	<i>N</i> -Alkyl-2-deoxy-D- <i>arabino</i> -hexosylamines	83
2.2.3.3.	<i>N</i> -Alkyl-2-deoxy-D- <i>lyxo</i> -hexosylamines	85
2.2.4.	<i>N</i> -Phenylglycosylamines	88
2.2.4.1.	<i>N</i> -Phenylpentosylamines	88
2.2.4.2.	<i>N</i> -Phenylhexosylamines	91
3.	Discussion	93
3.1.	Comparison of <i>N</i> -Substituted Glycosylamines to their corresponding Glycoses . .	93
3.2.	Effects of the Aglycon on the Configuration of <i>N</i> -Substituted Glycosylamines . .	95
3.3.	The Chelation Preferences of <i>N</i> -Substituted Glycosylamines	96
3.4.	Influencing Factors for the Chelation of the Imine Form	98
3.5.	The exceptional Coordination Behavior of <i>N</i> -Alkyl-2-deoxyglycosylamines	99
4.	Summary	101
5.	Experimental Section	103
5.1.	Methods and Materials	103
5.2.	NMR Spectroscopy	103
5.3.	Reagents and Solvents	104
5.4.	Preparation of Palladium Precursor Compounds	105
5.5.	Preparation of <i>N</i> -Substituted Alkylglycosylamines	106
5.5.1.	Preparation of <i>N</i> -Alkylpentosylamines	106
5.5.1.1.	Preparation of <i>N</i> -Alkylarabinosylamines	106
5.5.1.2.	Preparation of <i>N</i> -Alkylxylosylamines	112
5.5.1.3.	Preparation of <i>N</i> -Alkylribosylamines	116
5.5.1.4.	Preparation of <i>N</i> -Alkylxylosylamines	122
5.5.2.	Preparation of <i>N</i> -Alkylhexosylamines	126
5.5.2.1.	Preparation of <i>N</i> -Alkylgalactosylamines	126
5.5.2.2.	Preparation of <i>N</i> -Alkylglucosylamines	132
5.5.2.3.	Preparation of <i>N</i> -Alkylgulosylamines	136
5.5.2.4.	Preparation of <i>N</i> -Alkylmannosylamines	140
5.5.2.5.	Preparation of <i>N</i> -Alkylrhamnosylamines	144
5.5.3.	Preparation of <i>N</i> -Alkyl-2-deoxy-D-glycoamines	147
5.5.3.1.	Preparation of <i>N</i> -Alkyl-2-deoxy-D- <i>erythro</i> -pentosylamines	147

5.5.3.2.	Preparation of <i>N</i> -Alkyl-2-deoxy-D- <i>arabino</i> -hexosylamines	153
5.5.3.3.	Preparation of <i>N</i> -Alkyl-2-deoxy-D- <i>lyxo</i> -hexosylamines	157
5.5.4.	Preparation of <i>N</i> -Phenylglycosylamines	162
5.6.	Preparation of Complexes with Palladium(II)	170
5.6.1.	Complexes featuring <i>N</i> -Alkyl-D-arabinosylamines	170
5.6.2.	Complexes featuring <i>N</i> -Alkyl-D-lyxosylamines	173
5.6.3.	Complexes featuring <i>N</i> -Alkyl-D-ribosylamines	177
5.6.4.	Complexes featuring <i>N</i> -Alkyl-D-xylosylamines	181
5.6.5.	Complexes featuring <i>N</i> -Alkyl-D-galactosylamines	186
5.6.6.	Complexes featuring <i>N</i> -Alkyl-D-glucosylamines	189
5.6.7.	Complexes featuring <i>N</i> -Alkyl-L-gulosylamines	192
5.6.8.	Complexes featuring <i>N</i> -Alkyl-D-mannosylamines	196
5.6.9.	Complexes featuring <i>N</i> -Alkyl-L-rhamnosylamines	199
5.6.10.	Complexes featuring <i>N</i> -Alkyl-2-deoxy-D- <i>erythro</i> -pentosylamines	201
5.6.11.	Complexes featuring <i>N</i> -Alkyl-2-deoxy-D- <i>arabino</i> -hexosylamines	202
5.6.12.	Complexes featuring <i>N</i> -Alkyl-2-deoxy-D- <i>lyxo</i> -hexosylamines	204
5.6.13.	Complexes featuring <i>N</i> -phenyl-D-glycosylamines	205
A.	¹³C{¹H} NMR Spectra of coordinated Glycosylamines	209
B.	Packing Diagrams of the Crystal Structures	255
C.	Crystallographic Tables	263

List of Figures

1.1.	The repeating unit of the polysaccharide cellulose	1
1.2.	The repeating unit of the polymeric amino sugar chitin	2
1.3.	Structure of the aminoglycosides gentamycin and streptomycin	2
1.4.	Mechanism of acrylamide formation from D-glucose and L-asparagin in heated foods	3
1.5.	Isomerization between the different species of glycosylamines in aqueous solution	4
1.6.	Ring inversion shown for the α - and β -anomer of D-arabinopyranosylamine . . .	5
1.7.	Conformations of the anomers of D-xylofuranosylamine and D-xylofuranose . . .	5
1.8.	Platinum-based antineoplastic drugs	6
1.9.	Overview of the by BERGER <i>et al.</i> synthesized platinum(II) amino sugar complexes	7
1.10.	Glucosamine derative metal complexes synthesized by Tanaka <i>et al.</i>	7
1.11.	Schematic visualization of the KARPLUS relation	8
2.1.	Detected isomers and conformations of the synthesized <i>N</i> -alkyl-D-arabinosylamines	12
2.2.	Detected isomers and conformations of the synthesized <i>N</i> -alkyl-D-lyxosylamines .	14
2.3.	Detected isomers of the synthesized <i>N</i> -alkyl-D-ribosylamines	16
2.4.	Detected isomers of the synthesized <i>N</i> -alkyl-D-xyloamines	19
2.5.	Detected isomers of the synthesized <i>N</i> -alkyl-D-galactosylamines	21
2.6.	Detected isomers of the synthesized <i>N</i> -alkyl-D-glucosylamines	23
2.7.	The molecular structure of the 4C_1 - β -D-Glc1NMe molecule in 1	25
2.8.	Detected isomers of the synthesized <i>N</i> -alkyl-L-gulosylamines	26
2.9.	Detected isomers of the synthesized <i>N</i> -alkyl-D-mannosylamines	27
2.10.	Detected isomers of the synthesized <i>N</i> -alkyl-L-rhamnopyranosylamines	28
2.11.	The molecular structure of the 1C_4 - β -L-Rha1NEt molecule in 2	30
2.12.	Detected isomers of the synthesized <i>N</i> -alkyl-2-deoxy-D- <i>erythro</i> -pentosylamines . .	31
2.13.	Detected isomers of the synthesized <i>N</i> -alkyl-2-deoxy-D- <i>arabino</i> -hexosylamines . .	34
2.14.	Detected isomers of the synthesized <i>N</i> -alkyl-2-deoxy-D- <i>lyxo</i> -hexosylamines	35
2.15.	Detected configurations of the synthesized <i>N</i> -phenyl-D-pentosylamines	38
2.16.	The molecular structure of the β -D-Lyx1NPh- 4C_1 molecule in 3	39
2.17.	The molecular structure of the 1C_4 - α -D-Rib1NPh molecule in 4	40
2.18.	The molecular structure of the β -D-Xyl1NPh- 4C_1 molecule in 5	41
2.19.	Detected configurations of the synthesized <i>N</i> -phenyl-D-hexosylamines	43
2.20.	The molecular structure of the 4C_1 - β -D- <i>ara</i> -dHex1NPh molecule in 6	45
2.21.	The molecular structure of the 4C_1 - β -D- <i>lyx</i> -dHex1NPh molecule in 7	46
2.22.	Palladium(II) reagents containing the auxiliary ligands en, tmeda and chxn . . .	47
2.23.	Complex species resulting from the reaction of Ara1NR with Pd-en and HIO ₃ . .	48
2.24.	Complex species resulting from the reaction of Lyx1NR with Pd-en and HIO ₃ . .	51
2.25.	Complex species resulting from the reaction of Rib1NR with Pd-en and HIO ₃ . .	55

2.26. Complex species resulting from the reaction of Xyl1NR with Pd-en and HIO ₃ . . .	60
2.27. The structure of the [Pd(en)(⁴ C ₁ -β-D-Xylp1NMe2H ₋₁ -κ ² N ¹ ,O ²)] ⁺ ion in 8 . . .	62
2.28. Complex species resulting from the reaction of Gal1NR with Pd-en and HIO ₃ . . .	65
2.29. Complex species resulting from the reaction of Glc1NR with Pd-en and HIO ₃ . . .	68
2.30. Complex species resulting from the reaction of Gul1NR with Pd-en and HIO ₃ . . .	72
2.31. ¹³ C NMR spectra for the treatment of L-Gul1NMe with Pd-en and iodic acid . . .	76
2.32. Complex species resulting from the reaction of Man1NR with Pd-en and HIO ₃ . . .	76
2.33. Complex species resulting from the reaction of Rha1NR with Pd-en and HIO ₃ . . .	79
2.34. Complex species resulting from the reaction of <i>ery</i> -dPent1NR with Pd-en and HIO ₃ . . .	81
2.35. Complex species resulting from the reaction of <i>ara</i> -dHex1NR with Pd-en and HIO ₃ . . .	83
2.36. Complex species resulting from the reaction of <i>lyx</i> -dHex1NR with Pd-en and HIO ₃ . . .	85
2.37. Complex species resulting from the reaction of Pent1NPh with Pd-en and HIO ₃ . . .	88
2.38. Imine species resulting from the reaction of Pent1NPh with Pd-en and HIO ₃ . . .	90
2.39. Complex species resulting from the reaction of Hex1NPh with Pd-en and HIO ₃ . . .	91
A.1. Resulting ¹³ C NMR spectra for the treatment of D-Ara1NMe with Pd-en	210
A.2. Resulting ¹³ C NMR spectra for the treatment of D-Ara1NEt with Pd-en	211
A.3. Resulting ¹³ C NMR spectra for the treatment of D-Ara1NPr with Pd-en	212
A.4. Resulting ¹³ C NMR spectra for the treatment of D-Ara1N <i>i</i> Pr with Pd-en	213
A.5. Resulting ¹³ C NMR spectra for the treatment of D-Lyx1NMe with Pd-en	214
A.6. Resulting ¹³ C NMR spectra for the treatment of D-Lyx1NEt with Pd-en	215
A.7. Resulting ¹³ C NMR spectra for the treatment of D-Lyx1NPr with Pd-en	216
A.8. Resulting ¹³ C NMR spectra for the treatment of D-Lyx1N <i>i</i> Pr with Pd-en	217
A.9. Resulting ¹³ C NMR spectra for the treatment of D-Lyx1N <i>t</i> Bu with Pd-en	218
A.10. Resulting ¹³ C NMR spectra for the treatment of D-Rib1NMe with Pd-en	219
A.11. Resulting ¹³ C NMR spectra for the treatment of D-Rib1NEt with Pd-en	220
A.12. Resulting ¹³ C NMR spectra for the treatment of D-Rib1NPr with Pd-en	221
A.13. Resulting ¹³ C NMR spectra for the treatment of D-Rib1N <i>i</i> Pr with Pd-en	222
A.14. Resulting ¹³ C NMR spectra for the treatment of D-Rib1N <i>t</i> Bu with Pd-en	223
A.15. Resulting ¹³ C NMR spectra for the treatment of D-Xyl1NMe with Pd-en	224
A.16. Resulting ¹³ C NMR spectra for the treatment of D-Xyl1NEt with Pd-en	225
A.17. Resulting ¹³ C NMR spectra for the treatment of D-Xyl1NPr with Pd-en	226
A.18. Resulting ¹³ C NMR spectra for the treatment of D-Xyl1N <i>i</i> Pr with Pd-en	227
A.19. Resulting ¹³ C NMR spectra for the treatment of D-Xyl1N <i>t</i> Bu with Pd-en	228
A.20. Resulting ¹³ C NMR spectra for the treatment of D-Gal1NMe with Pd-en	229
A.21. Resulting ¹³ C NMR spectra for the treatment of D-Gal1NEt with Pd-en	230
A.22. Resulting ¹³ C NMR spectra for the treatment of D-Gal1NPr with Pd-en	231
A.23. Resulting ¹³ C NMR spectra for the treatment of D-Gal1N <i>i</i> Pr with Pd-en	232
A.24. Resulting ¹³ C NMR spectra for the treatment of D-Gal1N <i>t</i> Bu with Pd-en	233
A.25. Resulting ¹³ C NMR spectra for the treatment of D-Glc1NMe with Pd-en	234
A.26. Resulting ¹³ C NMR spectra for the treatment of D-Glc1NEt with Pd-en	235
A.27. Resulting ¹³ C NMR spectra for the treatment of D-Glc1NPr with Pd-en	236
A.28. Resulting ¹³ C NMR spectra for the treatment of D-Glc1N <i>i</i> Pr with Pd-en	237
A.29. Resulting ¹³ C NMR spectra for the treatment of D-Glc1N <i>t</i> Bu with Pd-en	238

A.30. Resulting ^{13}C NMR spectra for the treatment of D-Gul1NMe with Pd-en	239
A.31. Resulting ^{13}C NMR spectra for the treatment of D-Gul1NEt with Pd-en	240
A.32. Resulting ^{13}C NMR spectra for the treatment of D-Gul1NPr with Pd-en	241
A.33. Resulting ^{13}C NMR spectra for the treatment of D-Gul1N <i>i</i> Pr with Pd-en	242
A.34. Resulting ^{13}C NMR spectra for the treatment of D-Gul1N <i>t</i> Bu with Pd-en	243
A.35. Resulting ^{13}C NMR spectra for the treatment of D-Man1NEt with Pd-en	244
A.36. Resulting ^{13}C NMR spectra for the treatment of D-Man1NPr with Pd-en	245
A.37. Resulting ^{13}C NMR spectra for the reactions of D-Man1NR with Pd-en	246
A.38. Resulting ^{13}C NMR spectra for the reactions of L-Rha1NR with Pd-en	247
A.39. Resulting ^{13}C NMR spectra for the treatment of D- <i>ery</i> -dPent1NMe with Pd-en	248
A.40. Resulting ^{13}C NMR spectra for the treatment of D- <i>ery</i> -dPent1NEt with Pd-en	249
A.41. Resulting ^{13}C NMR spectra for the treatment of D- <i>ara</i> -dHex1NMe with Pd-en	250
A.42. Resulting ^{13}C NMR spectra for the treatment of D- <i>ara</i> -dHex1NEt with Pd-en	251
A.43. Resulting ^{13}C NMR spectra for the treatment of D- <i>ara</i> -dHex1N <i>i</i> Pr with Pd-en	252
A.44. Resulting ^{13}C NMR spectra for the treatment of D- <i>lyx</i> -dHex1NMe with Pd-en	253
A.45. Resulting ^{13}C NMR spectra for the treatment of D- <i>lyx</i> -dHex1NEt with Pd-en	254
B.1. Packing diagram of 1 in the monoclinic space group $C2$	255
B.2. Packing diagram of 2 in the monoclinic space group $P2_1$	256
B.3. Packing diagram of 3 in the orthorhombic space group $P2_12_12_1$	257
B.4. Packing diagram of 4 in the orthorhombic space group $P2_12_12_1$	258
B.5. Packing diagram of 5 in the triclinic space group $P1$	259
B.6. Packing diagram of 6 in the orthorhombic space group $P2_12_12_1$	260
B.7. Packing diagram of 7 in the orthorhombic space group $P2_12_12_1$	261
B.8. Packing diagram of 8 in the orthorhombic space group $P2_12_12_1$	262

Abbreviations

<i>a</i>	acyclic
Ac	acetyl
Ara	arabinose
Bn	benzyl
<i>C</i>	chair (conformation)
calcd	calculated
chxn	(1 <i>R</i> ,2 <i>R</i>)-1,2-diaminocyclohexane
CIS	coordination-induced shift
conc.	concentrated
COSY	correlated spectroscopy
δ	chemical shift
d	doublet
dd	doublet of doublets
DEPT	Distortionless Enhancement by Polarization Transfer
DFT	Density Functional Theory
DMSO	dimethyl sulfoxide
DNA	deoxyribonucleic acid
<i>E</i>	envelope (conformation)
EA	elemental analysis
en	ethan-1,2-diamine
eq	equivalent
<i>ery</i>	<i>erythro</i>
Et	ethyl
<i>f</i>	furanose
FAB	Fast Atom Bombardment
Gal	galactose
Glc	glucose
Gul	gulose
h	hour
HMBC	heteronuclear multiple bond correlation
HMQC	heteronuclear multiple quantum coherence
<i>i</i> Pr	<i>iso</i> -propyl
IUPAC	International Union of Pure and Applied Chemistry
<i>J</i>	coupling constant
<i>lyx</i>	<i>lyxo</i>

Lyx	lyxose
m	multiplet
<i>m</i>	<i>meta</i>
Man	Mannose
Me	methyl
MS	mass spectrometry
n. i.	not identified
NMR	Nuclear Magnetic Resonance
<i>o</i>	<i>ortho</i>
Pd-en	aqueous solution of dihydroxido-(ethane-1,2-diamine)-palladium(II)
Pr	propyl
<i>p</i>	pyranose
<i>p</i>	<i>para</i>
Ph	phenyl
ppm	parts per million
q	quartet
R	rest
Rib	ribose
Rha	rhamnose
RT	room temperature
s	singlet
sp	superposed
t	triplet
<i>t</i> Bu	<i>tert</i> -butyl
tmeda	<i>N,N,N',N'</i> -tetramethylethane-1,2-diamine
Xyl	xylose

Overview of Crystal Structures

- 1 ${}^4C_1\text{-}\beta\text{-D-Glcp1NMe}\cdot\text{MeNH}_2$
- 2 ${}^1C_4\text{-}\beta\text{-L-Rhap1NEt}$
- 3 ${}^4C_1\text{-}\beta\text{-D-Lyxp1NPh}$
- 4 ${}^4C_1\text{-}\alpha\text{-D-Ribp1NPh}\cdot 0.5\text{H}_2\text{O}$
- 5 ${}^4C_1\text{-}\beta\text{-D-Xylp1NPh}$
- 6 ${}^4C_1\text{-}\beta\text{-D-ara-dHexp1NPh}$
- 7 ${}^4C_1\text{-}\beta\text{-D-lyx-dHexp1NPh}\cdot 0.33\text{H}_2\text{O}$
- 8 $[\text{Pd}(\text{en})({}^4C_1\text{-}\beta\text{-D-Xylp1NMe2H}_{-1}\text{-}\kappa N^1, \kappa O^2)]\text{IO}_3\cdot 4\text{H}_2\text{O}$

1. Introduction

1.1. The Biological Importance of Carbohydrates and Amino Sugars

Carbohydrates form the most abundant class of biomolecules and are constituents of all plants, animals and microorganisms. Simple polysaccharides, such as amylose in starch and cellulose (figure 1.1), serve as food reserves as well as structural components in cell walls. These polymeric structures are composed of monomeric building blocks, called monosaccharides. In the case of amylose and cellulose, D-glucose, the most prominent carbohydrate, functions as the monosaccharide. The chemistry of monosaccharides—also often referred to as glycoses—is mostly characterized by their great versatility due to the multitude of functional groups in a rather small molecule.^[1]

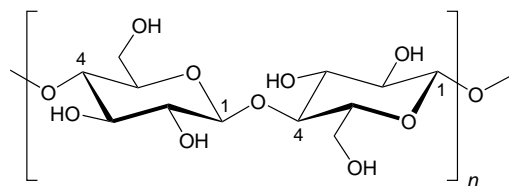


Figure 1.1. The repeating unit of the polysaccharide cellulose.

During the last decades the development of more effective methods for the characterization and investigation of carbohydrate structures led to the perception that the biological relevance of carbohydrates well exceeds their primary role as energy storage and structural component. Glycosylated carbohydrates play a key role in many biological processes such as fertilization, embryogenesis, immune defense, viral replication, tissue repair and cell growth. This newfound importance of carbohydrates for living systems led to the establishment of a new research field called glycobiology.^[2]

Many of the aforementioned biological processes involve glycans containing amino sugars as building blocks. Examples include polymeric glycosaminoglycans as the mammalian blood anticoagulant heparin and the joint lubricant hyaluronic acid or peptidoglycans as components of the bacterial cell walls. Amino sugars are defined as monosaccharides in which at least one hydroxyl group is replaced by an amino group.^[3] The most common long-chain polymer featuring an amino sugar as monomeric unit found in nature is chitin (figure 1.2). Chitin is the prevailing constituent of the exoskeleton of insects and crustaceans and has a structure similar to cellulose with only the hydroxyl group at the C2 position of the backbone polymer chain being replaced by an acetamido group.^[4] In 1875, LEDDERHOSE was the first to isolate a monomeric amino sugar, when he obtained colorless crystals of D-glucosamine hydrochloride by boiling a lobster shell in hydrochloric acid.^[5]

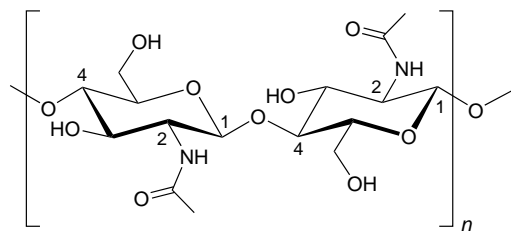


Figure 1.2. The repeating unit of the polymeric amino sugar chitin.

Amino sugars are further the main constituents of oligomeric aminoglycoside antibiotics as gentamycin and streptomycin (figure 1.3), which are of great medical importance. Their mechanism of action is based on the interference of the aminoglycosides with the protein biosynthesis by acting on the bacterial ribosome, leading to rapid cell death.^[6]

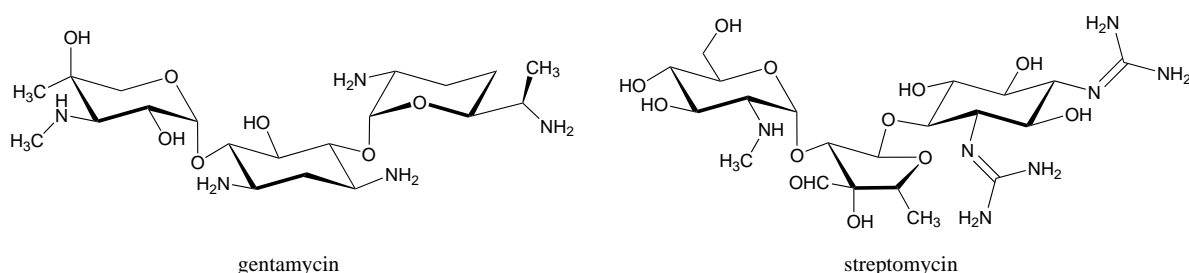


Figure 1.3. Structure of the aminoglycosides gentamycin and streptomycin.

If the amino group of an amino sugar is located at the anomeric carbon atom those compounds are generally referred to as glycosylamines or *N*-glycosides. Glycosylamines represent a particular class of its own since their chemical behavior and biological relevance is predominately distinct from all other amino sugars. The immense importance of glycosylamines first became obvious with the determination of the composition and structure of ribonucleic and deoxyribonucleic acid in the 20th century. The included nucleobases, coding the genetic information in all life forms, are linked via a *N*-glycosidic bond to the anomeric carbon atom of a pentose (ribose or 2-deoxyribose), forming nucleosides. Hence, nucleosides are regarded as the most prominent representatives of the class of glycosylamines.^[3]

Glycosylamines are also found as reactive intermediates in the MAILLARD reaction, a reaction between amino acids and reducing sugars that gives food its brown color and distinctive flavor upon cooking.^[7] Almost fifty years after the elucidation of the reaction mechanism, the MAILLARD reaction became again a center of interest, when the potential human carcinogen acrylamide was detected in various heated foods.^[8-10] The currently proposed mechanism for the formation of acrylamide in heating processes is depicted in figure 1.4 and involves the formation of glycosylamine and SCHIFF base species as intermediates and subsequent elimination of either ammonia or a substituted imine.^[11]

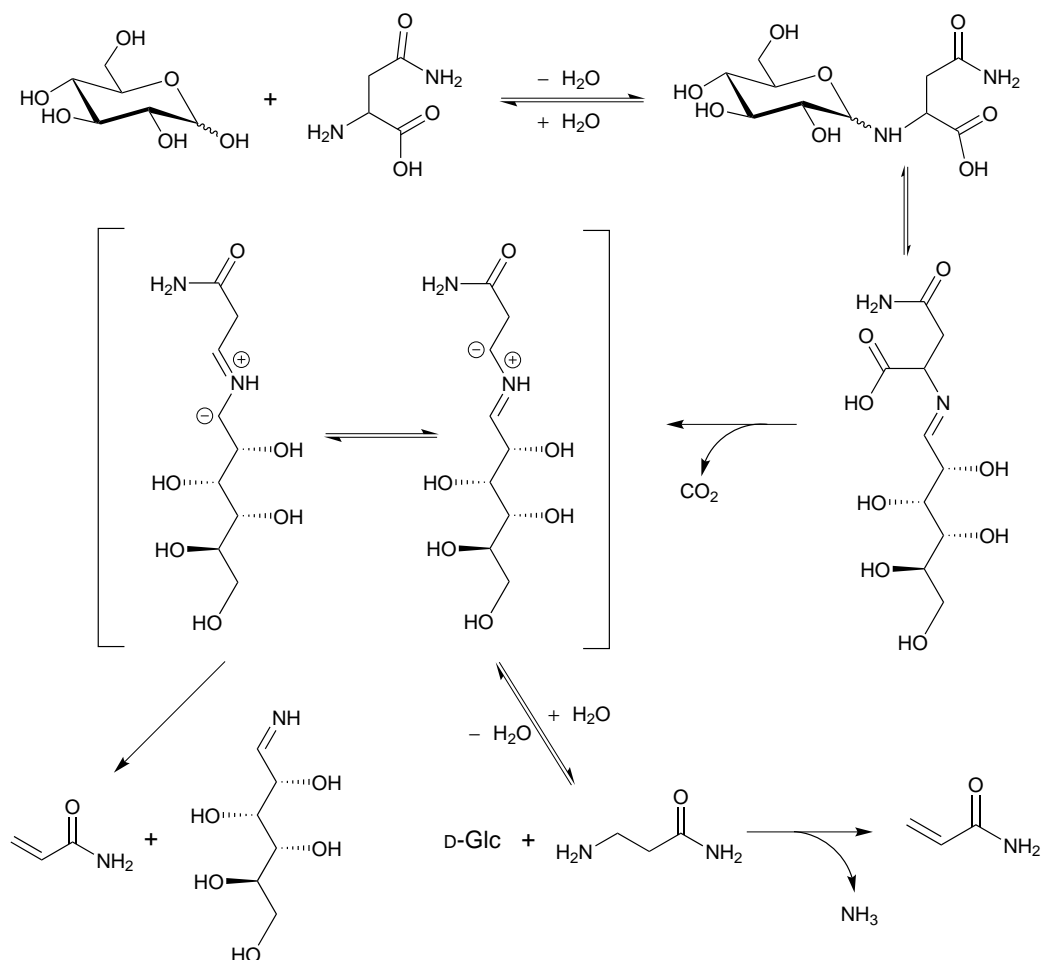


Figure 1.4. Mechanism of acrylamide formation from D-glucose and L-asparagine in heated foods as postulated by ZYZAK *et al.*^[11]

Furthermore, *N*-alkylated derivatives of glycosylamines have been investigated as β -glucocerebrosidase inhibitors for a potential treatment of the GAUCHER's disease,^[12] as glycolipid analogs in alternative antigen delivery systems^[13] and as compounds exhibiting antifungal activities; thus, being promising candidates as biocidal additives for food packaging.^[14]

1.2. The Chemistry of Glycosylamines

For reducing sugars the equilibrium between the carbonyl open chain form, its hydrate and the prevailing cyclic hemiacetal or hemiketal forms upon dissolution in water is long known and well researched.^[15,16] The observed cyclic species differ in their ring size (pyranoses and furanoses) and their configuration at the anomeric carbon atom.^[17] The formation of different anomers is accompanied by a change in optical rotation known as mutarotation. For glycosylamines a similar behavior was first described by ISBELL and FRUSH in course of kinetic measurements on the mutarotation and hydrolysis reaction of D-pentosylamines.^[18,19] In contrast to glycoses, the mutarotation of glycosylamines is not sufficiently catalyzed under basic conditions, suggesting that mutarotation and hydrolysis take place through an intermediate immonium ion.^[18] This

assumption was further verified by NMR-spectroscopic studies on D-pentosylamines by ZHU *et al.*, showing the presence of two diastereomeric acyclic hemiaminals in solution.^[20] These hemiaminal species function as intermediates in the course of the hydrolysis of glycosylamines since the subsequent elimination of ammonia yields the corresponding glycoses. Over the recent years further NMR-spectroscopic studies on the equilibrium state of unsubstituted and *N*-alkylated glycosylamines in aqueous solution were conducted by SCHWARZ and LINDNER.^[21-23] An exemplary scheme of all relevant species of D-glucosylamine in aqueous solution is illustrated in figure 1.5.

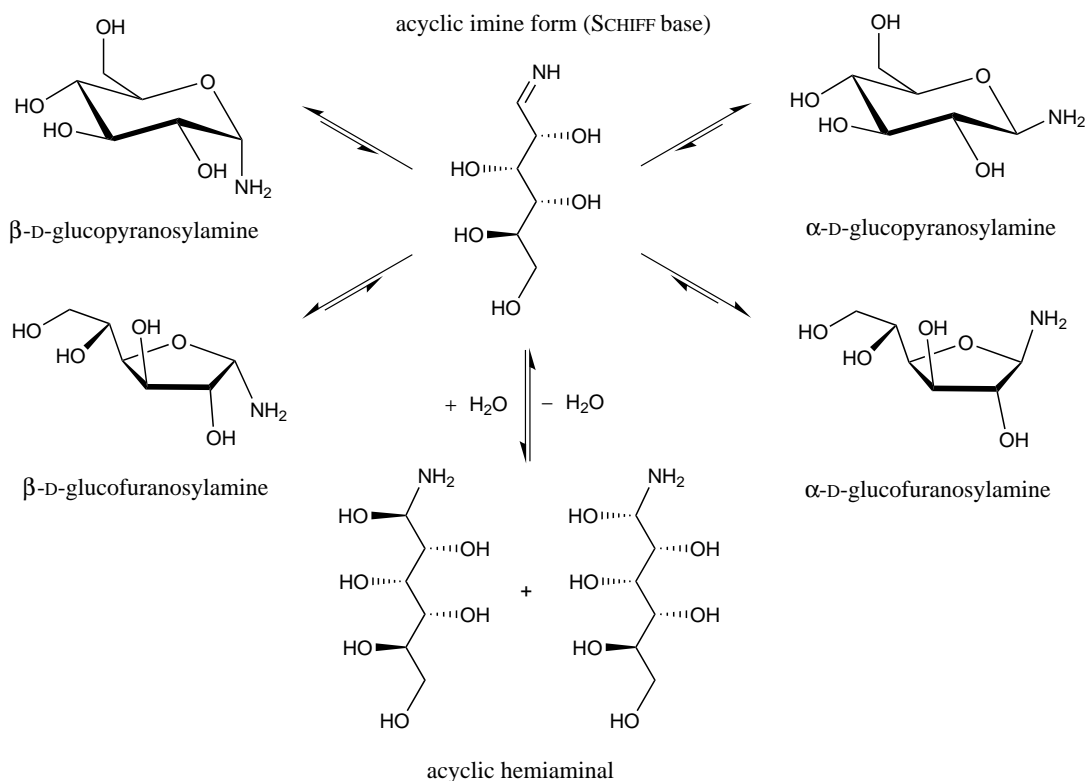


Figure 1.5. Isomerization between the different species of glycosylamines in aqueous solution and the reaction with water to the corresponding diastereomeric hemiaminals shown for D-glucosylamine.

The research of SCHWARZ and LINDNER revealed a striking dominance of the β -anomer for D-xylosylamine and D-glucosylamine in comparison to D-xylose and D-glucose in aqueous solution. This observation arises from the absence of an anomeric effect for carbohydrates bearing an amino function at the anomeric carbon atom;^[24] thus, leading to a significant preference of an equatorial orientation of the C1–N bond in D-glycosylamines.^[20]

Just like pyranoses and furanoses, pyranosylamines and furansosylamines potentially exhibit a broad variety of different conformations. Generally, in six-membered rings these possible conformations include chair, boat and twist-boat forms. But in the case of pyranosylamines only two discrete chair conformations have yet been described: the 4C_1 and 1C_4 conformation. These conformations can be converted into each other by ring inversion, with the boat and twist-boat form being intermediates on the conversion path. In the case of D-arabinopyranosylamine,

NMR-spectroscopic studies reveal a preference of the 1C_4 conformation for the α -anomer, while the β -anomer favors the 4C_1 conformation, as depicted in figure 1.6.^[22] This observation is in accordance with the general rule, that equatorial substituents confer stability to a chair form, while axial substituents are destabilizing.^[25]

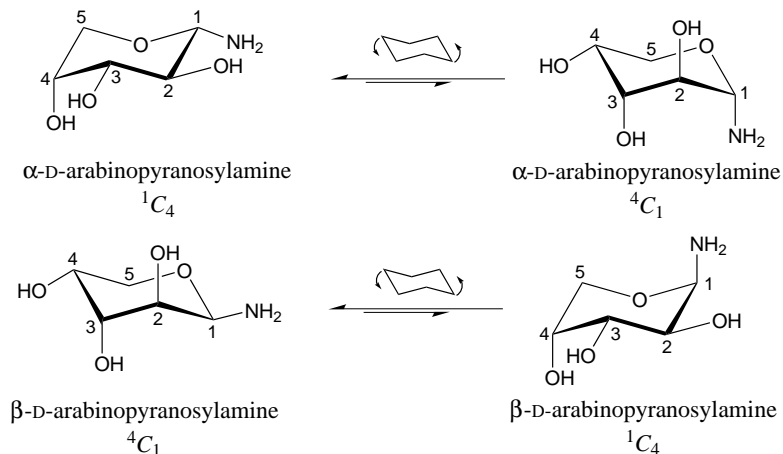


Figure 1.6. Ring inversion shown for the α - and β -anomer of D-arabinopyranosylamine, indicating the prevailing conformation in aqueous solution.

For furanose forms the determination of the present ring form is more complicated, since five-membered rings have the ability to adopt twenty idealized forms (ten envelope and ten twist forms). These nonplanar forms interconvert readily *via* pseudorotation or inversion, the latter involving the planar form as intermediate.^[26] As in most cases the formation of furanosylamines is less favored than the formation of pyranosylamines in solution, only few studies on their conformation were performed. NMR-spectroscopic experiments conducted by ZHU *et al.* indicate the preference of the E_2 and 2E for the α -anomer and β -anomer of D-xylofuranosylamine in solution, respectively, while for D-xylofuranose the conformation for the α -anomer is near E_1 and near 1E for the β -anomer (figure 1.7). This observation is accounted to the anomeric effect in xylofuranoses, leading to an increased stability of the quasi-axial orientation for the C1–O1 bond. Due to the absence of an anomeric effect in glycosylamines the C1–N1 bond strictly favors the quasi-equatorial position in furanosylamines.^[20]

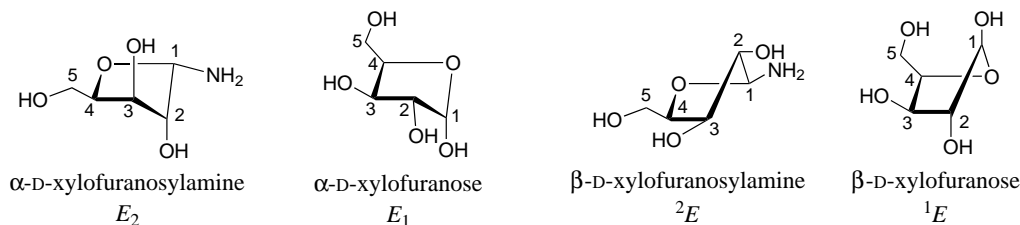


Figure 1.7. Preferred conformations for the anomers of D-xylofuranosylamine and D-xylofuranose according to ZHU *et al.*^[20]

1.3. Palladium(II) and Platinum(II) Complexes

Palladium(II) and platinum(II) ions show similar characteristics regarding their coordination chemistry. Both are divalent noble metal cations and strictly form low-spin complexes exhibiting a square-planar geometry with diamagnetic properties due to their d^8 electron configuration. A wide pool of palladium(II) compounds are of major importance as catalysts in various industrial processes (e.g. the WACKER process) as well as in organic synthesis (e.g. the HECK reaction).^[27] The research on platinum(II) complexes on the other hand mainly focuses on their activity as chemotherapeutic agents. ROSENBERG *et al.* first serendipitously discovered and reported the antitumor activity of platinum compounds.^[28] In advanced studies *cis*-diamminedichlorido-platinum(II) (cisplatin, figure 1.8) proved to be the most promising platinum-based antitumor drug candidate and was approved for clinical use by the U.S. Food and Drug Administration in 1978.^[29] The mechanism leading to this anti-cancer activity is mainly designated to the covalent binding of the PtN_2 -fragment to the N7 position of guanine in the DNA. The resulting intrastrand crosslinks inhibit DNA repair and DNA synthesis in the fast multiplying cancer cells.^[30] Today's other notable platinum-based antineoplastic drugs include oxaliplatin and carboplatin (figure 1.8), which distinguish themselves from cisplatin by changes in the neutral spectator ligand and anionic leaving ligand. Such changes lead to a reduction of undesirable side effects (most notably nephrotoxicity, neurotoxicity and nausea), but can also decrease the potency of the drug.^[31]

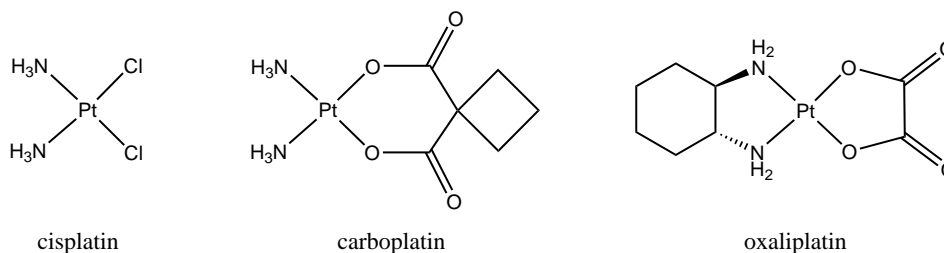


Figure 1.8. Platinum-based antineoplastic drugs.

Since the exchange of the ligand has such a large impact on the reactivity of a platinum-based drug, the search for alternative ligand candidates plays a key role in this still thriving research field. Some of the numerous drug candidates proposed in the literature incorporate amino sugars as spectator ligands. For example, HLAVKA *et al.* first described the anti-cancer activity of not further specified compounds resulting from the treatment of various glycosylamines and D-glucosamine with platinum(II) chloride in water.^[32] In a more recent publication BERGER *et al.* substituted the cyclohexane-1,2-diamine auxiliary ligand in oxaliplatin by a 2,3-diamino-2,3-dideoxy-D-glucose ligand and characterized the four complexes depicted in figure 1.9. The synthesized compounds vary in their anionic ligand utilized as leaving group and thus exhibit different cytotoxic activities.^[33]

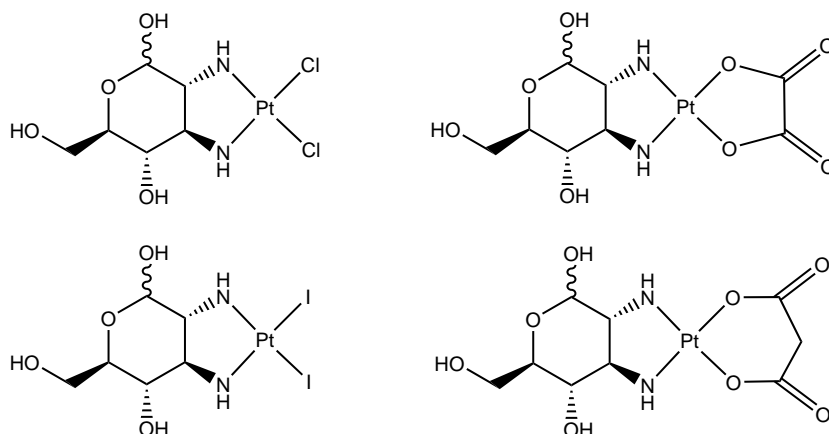


Figure 1.9. Overview of the by Berger *et al.* synthesized platinum(II) amino sugar complexes.^[33]

Beyond this broad range of investigated ligands, there is also great interest in the use of other metal ions for inorganic anti-cancer drugs. Palladium-based alternatives proved to have anti-neoplastic properties similar to platinum complexes but with different stability and kinetics (palladium complexes are up to 10^5 times more reactive)^[34] at a lower cost.^[31] In an exemplary work TANAKA *et al.* investigated and compared the anti-cancer effects of glycoconjugated palladium(II) and platinum(II) complexes with a glucosamine derivative as the featured ligand illustrated in figure 1.10.^[35]

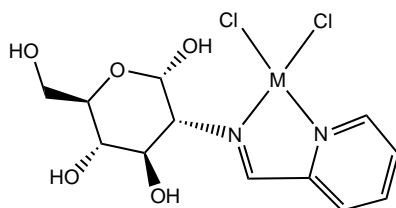


Figure 1.10. Structure of the glucosamine derivative metal complexes with $M = \text{Pd}, \text{Pt}$ synthesized by TANAKA *et al.*^[35]

1.4. Characterization of Glycosylamines and their Pd^{II} Complexes

The most common analytical method to determine the configuration and conformation of glycosylamines in solution is NMR spectroscopy. In comparison to the corresponding glycoses the $^{13}\text{C}\{^1\text{H}\}$ NMR signal for the C1 atom of the glycosylamines is shifted in the upper field due to the substitution of the attached hydroxyl group by an amino function. All other carbon atoms of the carbohydrate scaffold show comparable chemical shifts. Furanoid isomers can be identified by a chemical shift larger than 80 ppm for the C4 atom.^[36]

The KARPLUS equation allows a further determination of the present configuration and conformation as it describes the correlation between the coupling constant and the dihedral torsion angle of two vicinal hydrogen atoms.^[37] Although the KARPLUS equation gives distinct values for every angle, it is only used empirically throughout this work. As can be seen in figure 1.11, in pyranoid systems a coupling constant of 1 Hz to 4 Hz indicates an axial-equatorial or an

equatorial-equatorial arrangement of two vicinal hydrogen atoms, while coupling constants from 8 Hz to 12 Hz match an axial-axial orientation. In some cases dynamic fluctuation between two species in solution, as for example between the 4C_1 and the 1C_4 conformation, allow no unambiguous determination by the aforementioned measures.^[38]

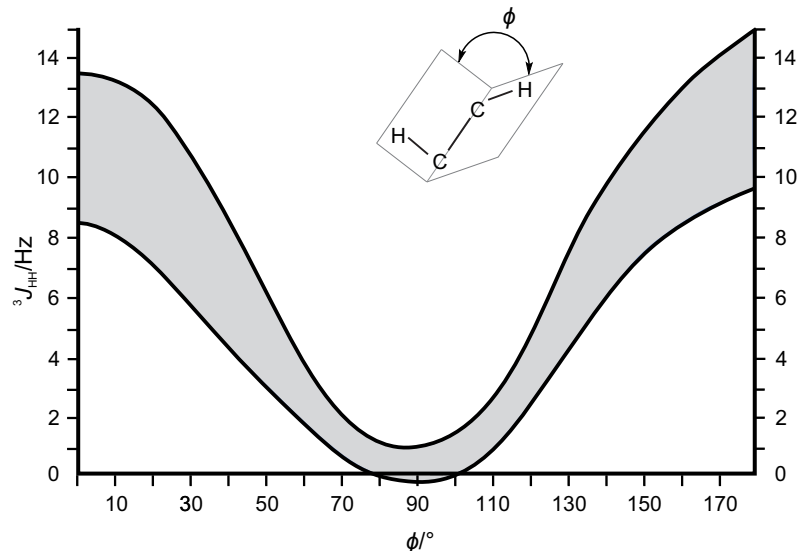


Figure 1.11. Schematic visualization of the KARPLUS relation, showing the correlation between the coupling constant ${}^3J_{\text{HH}}$ and the H–C–C–H dihedral torsion angle ϕ in nuclear magnetic resonance spectroscopy.

The configuration and conformation of glycosylamines as ligands in palladium(II) complexes can be determined in the same manner as for the free glycosylamines due to the diamagnetism of the obtained complexes. The coordination sites of the metal fragments on glycosylamines can be identified by the observation of the coordination-induced shift (CIS). The CIS is a result of the changes in the electron density within ligands upon coordination and its value is obtained by subtracting chemical shifts of each nucleus in the complexed and the free ligand.

$$\Delta\delta(\text{CIS}) = \delta_{\text{complexed}} - \delta_{\text{free}} \quad (1.1)$$

In most cases the resulting binding mode in solution is determined in regard to the CIS for ${}^{13}\text{C}\{{}^1\text{H}\}$ NMR signals of carbon atoms attached to the coordinating functional group. Characteristic values in the case of unsubstituted glycosylamines are 1 ppm to 3 ppm for the C1 atom coordinating *via* a neutral amino function, while CIS values from 6 ppm to 12 ppm are observed for carbon atoms with coordinating alkoxide moieties.^[22]

1.5. Aim of this Work

In first studies on the chelation properties of *N*-alkyl-D-glycosylamines towards palladium(II) probes performed by LINDNER, unexpected metalation of the acyclic imine form was NMR-spectroscopically detected besides the anticipated formation of pyranosylamine-palladium complexes. This remarkable behavior was observed for *N*-ethyl-D-arabinosylamine and for *N*-methyl- and *N*-ethyl-D-lyxosylamine as well as for non-substituted D-lyxosylamine. The methyl and ethyl derivatives of *N*-alkyl-D-glucosylamine on the other hand showed no indications for a similar metalation of the respective imine form.^[22]

On the basis of these initial findings, the aim of this work is to identify and elucidate the influencing factors for this intermittent metalation of the open-chain isomer and to provide further analytical evidence for the formation of these remarkable complex species. Therefore, in a first step, the pool of *N*-substituted glycosylamines available as ligands is extended. These synthesized *N*-substituted glycosylamines are subsequently treated with various palladium(II) probes. The resulting structures and percentage distributions for the glycosylamine-metal complexes formed in the reaction solutions are determined by NMR-spectroscopic methods. In the best case also single crystals suitable for X-ray diffraction studies are obtained from the corresponding reaction solutions to gain additional structural information and analytical evidence for the investigated glycosylamine-palladium complexes. The results gathered from these experiments should help to formulate tendencies for the influence of the used ligand as well as of the included metal probe on the potential metalation of the acyclic imine form of a glycosylamine.

2. Results

2.1. *N*-Substituted Glycosylamines

The *N*-substituted glycosylamines described in this work were primarily synthesized for their use as ligands in reactions with palladium(II) and platinum(II) probes. These reactions intend to lead to a better understanding of the coordination behavior of glycosylamines in general. Since the synthesis and characteristics of the majority of the investigated *N*-substituted glycosylamines has not yet been reported in the literature, the first part of this work exclusively focuses on their synthesis and chemical characteristics.

The purity of the synthesized *N*-substituted glycosylamine was analyzed by elemental analysis, fast atom bombardment mass spectrometry and ^1H and $^{13}\text{C}\{^1\text{H}\}$ NMR spectroscopy in D_2O and $\text{DMSO-}d_6$. For further characterization, $^1\text{H}, ^1\text{H}$ -COSY, $^1\text{H}, ^{13}\text{C}$ -HMQC, $^1\text{H}, ^{13}\text{C}$ -HMBC and DEPT135 NMR experiments were performed in order to allow an exact assignment of the NMR signals in the carbohydrate scaffold and the determination of the present isomers.

Besides the basic analytic characterization, the equilibrium of the formed isomers in various solvents as well as the extent of their hydrolysis was investigated more closely. The percentage distributions of the isomers detected in solution were determined with the help of NMR-spectroscopic methods. The comparison of the respective isomers' integrals in the measured ^1H NMR spectra represents the method of choice for this kind of quantification. Superposition of signals is a common problem in ^1H NMR spectra and often hinders an exact determination of the percentage distribution. In this case, the integrals measured in the associated $^{13}\text{C}\{^1\text{H}\}$ NMR spectra were taken into account. This method is slightly less accurate, but still reveals the composition of the solution with a deviation of up to $\pm 5\%$.^[36]

Furthermore, the molecular structure was determined through single-crystal X-ray diffraction for all crystalline *N*-substituted glycosylamines. Using the thereby obtained atom coordinates, the associated puckering parameters Q , θ and ϕ according to CREMER and POPLÉ were calculated with PLATON for the pyranosylamine rings.

2.1.1. *N*-Alkylpentosylamines

N-Alkylpentosylamines are readily synthesized through the condensation reaction of an aldose with a primary aliphatic amine in either methanolic or ethanolic solution. The formation of the desired *N*-alkylpentosylamine proceeds *via* the nucleophilic attack of the alkylamine on the carbonyl carbon atom of the monosaccharide in its open-chain form, leading to the substitution of the hydroxy group at the anomeric carbon atom by an alkylamine moiety.

Procedures for the synthesis of various pentosylamines as described by LINDNER were applied and slightly modified in this work.^[22] Essentially, those reactions proceeded at good rates under ice cooling or at room temperature. The subsequent isolation of the desired *N*-alkylpentosylamines

from the reaction mixture was achieved by either precipitation, and thereby taking advantage of the lower solubility of the product in alcoholic solution, or *via* evaporation of all solvents and reactants, since short-chained aliphatic amines are highly volatile. It has to be noted, that the purification step including the precipitation yielded the desired products in a better purity, but was not always applicable.

All four D-aldopentoses (D-arabinose, D-lyxose, D-ribose and D-xylose) were used as reactants, while the reacting alkylamines were methylamine, ethylamine, propylamine, *iso*-propylamine and *tert*-butylamine.

Many of the synthesized *N*-alkylpentosylamines showed significant rates of hydrolysis, resulting in the back reaction to the originally applied aldose and alkylamine. The stability of the *N*-alkylpentosylamines differ for every pentose and the extent of the hydrolytic cleavage can readily be monitored by NMR spectroscopy in D₂O. The rate of hydrolysis increases with rising temperature, pH-value and steric demand of the alkylamino substituent. These tendencies were already described by STEPANENKO and coworkers, who furthermore found evidence for a correlation between the decreasing stability and an increasing conformational instability of the sugar component.^[39] In order to avoid this formation of the initial reactants, accompanied by the emergence of extra NMR signals, the majority of NMR spectra in D₂O were measured at 4 °C to reduce the hydrolytic side reaction. Furthermore, NMR spectra of the *N*-alkylpentosylamines in dry DMSO-*d*₆ were collected to minimize hydrolysis and therefore guaranteeing the detection of any contamination of the product with residues of the reactants.

Similar to their corresponding pentose analogues, the synthesized *N*-alkylpentosylamines exhibit various configurations and conformations in solution. The occurring anomerization results in an equilibrium between the α - and β - forms of pyranosylamines and furanosylamines. Additionally, some *N*-alkylpentopyranosylamine isomers tend to show a dynamic fluctuation between the ⁴C₁ conformation and ¹C₄ conformation through ring inversion.

2.1.1.1. *N*-Alkyl-D-arabinosylamines

The reaction of D-arabinose with various alkylamines yielded the *N*-alkyl-D-arabinosylamines displayed in figure 2.1. D-Ara1NMe and D-Ara1NEt could be stored at 4 °C under inert gas atmosphere for several weeks before slowly decomposing to a brown residue. D-Ara1NPr, D-Ara1N*i*Pr and D-Ara1N*t*Bu on the other hand showed immediate signs of hydrolysis when exposed to air and had to be stored under inert gas atmosphere at -20 °C to avoid decomposition.

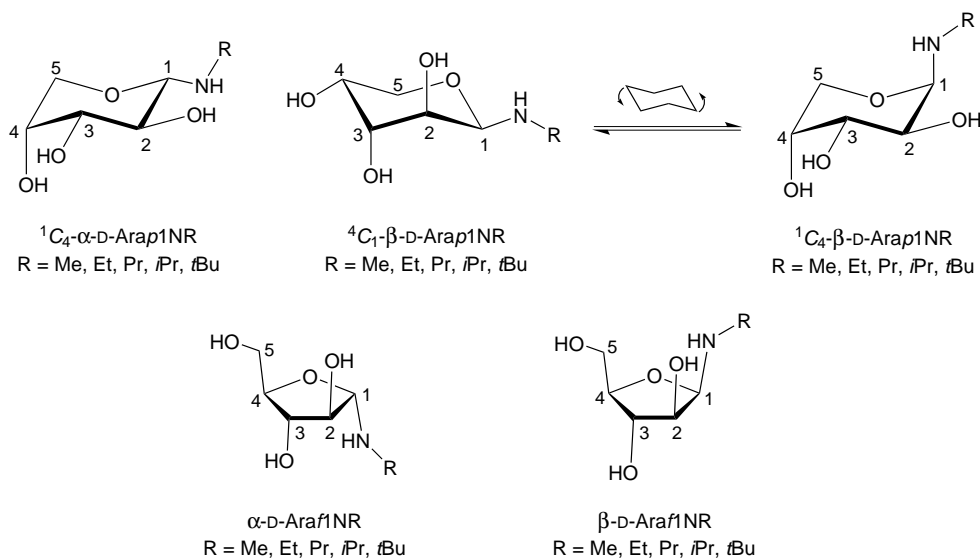


Figure 2.1. In D_2O and $DMSO-d_6$ detected isomers and conformations of the synthesized *N*-alkyl-D-arabinosylamines.

As can be seen in table 2.1, the α -anomer represents the predominant isomer for the *N*-alkyl-D-arabinosylamines in D_2O and in $DMSO-d_6$. The ${}^3J_{H,H}$ values found for the α -anomers (listed in table 2.2) verify the clear preference of the 1C_4 conformation featuring three equatorial oriented substituents. These spectroscopic findings are in accordance with the crystal structures of 1C_4 - α -D-Ara1NMe and 1C_4 - α -D-Ara1NEt previously reported by LINDNER.^[22]

Table 2.1. Percentage distribution of the different isomers for the synthesized *N*-alkyl-D-arabinosylamines from 1H or ${}^{13}C\{^1H\}$ NMR spectra measured in D_2O and in $DMSO-d_6$ at room temperature.

	D_2O				$DMSO-d_6$			
	αp	βp	αf	βf	αp	βp	αf	βf
D-Ara1NMe	64	18	10	8	36	32	20	12
D-Ara1NEt	66	15	12	7	60	19	13	8
D-Ara1NPr	70	18	8	4	55	23	13	9
D-Ara1N <i>i</i> Pr	78	14	6	2	56	22	15	7
D-Ara1N <i>t</i> Bu	100	0	0	0	30	27	22	21

The less abundant β -anomers feature two substituents in equatorial position and two substituents in axial position in the 1C_4 conformation and in the 4C_1 conformation. Thus, a dynamic fluctuation between both conformations was assumed. The experimental ${}^3J_{H,H}$ values for the *N*-alkyl- β -D-arabinosylamines, listed in table 2.2, noticeably decreased with an increasing steric demand of the alkylamino substituent located at anomeric carbon atom. This observation indicates a reasonable preference of the 4C_1 conformation to keep the more bulky substituents in the energetically favored equatorial position. In the case of D-Ara1N*t*Bu no evidence for the presence of the corresponding β -pyranosylamine form in aqueous solution was found. The ${}^{13}C\{^1H\}$ NMR shifts assigned to the carbohydrate scaffold and the C α atom of the alkylamino group of all detected *N*-alkyl-D-arabinopyranosylamines are listed in table 2.3.

Table 2.2. Experimental and calculated ${}^3J_{\text{H,H}}$ values in Hz for both anomers of the detected *N*-alkyl-D-arabinopyranosylamines from ${}^1\text{H}$ NMR spectra measured in D_2O . Dashes indicate that due to superposition of signals no coupling constant could be determined.

	${}^3J_{1,2}$	${}^3J_{2,3}$	${}^3J_{3,4}$	${}^3J_{4,5eq}$	${}^3J_{4,5ax}$
1C_4 - α -D-Ara1NR (calcd.)	8.6	9.6	3.2	2.5	0.6
α -D-Arap1NMe	8.6	9.5	3.7	2.3	1.2
α -D-Arap1NEt	8.6	9.5	3.5	2.3	1.2
α -D-Arap1NPr	8.6	9.4	3.6	2.3	1.2
α -D-Arap1NiPr	8.5	9.4	3.6	2.3	1.2
α -D-Arap1NtBu	8.7	–	–	1.9	–
4C_1 - α -D-Ara1NR (calcd.)	2.4	4.3	3.5	4.3	10.1
1C_4 - β -D-Ara1NR (calcd.)	3.1	9.6	3.2	2.5	0.6
β -D-Arap1NMe	2.6	–	–	–	–
β -D-Arap1NEt	2.2	–	–	–	–
β -D-Arap1NPr	2.1	–	–	–	–
β -D-Arap1NiPr	1.8	–	–	–	–
4C_1 - β -D-Ara1NR (calcd.)	0.9	4.3	3.5	4.3	10.1

Table 2.3. Selected ${}^{13}\text{C}\{{}^1\text{H}\}$ NMR chemical shifts (δ/ppm) of the *N*-alkyl-D-arabinopyranosylamines detected in D_2O or $\text{DMSO-}d_6$ (*).

	C1	C2	C3	C4	C5	C α
α -D-Arap1NMe	92.2	70.9	73.8	69.4	67.7	31.5
α -D-Arap1NEt	90.8	71.2	73.8	69.4	67.7	39.9
α -D-Arap1NPr	91.1	71.1	73.8	69.4	67.8	47.6
α -D-Arap1NiPr	89.0	71.5	73.9	69.4	67.7	45.4
α -D-Arap1NtBu	87.6	71.3	73.9	69.6	67.3	51.2
β -D-Arap1NMe	87.1	69.3	70.3	66.1	63.6	31.7
β -D-Arap1NEt	85.1	70.5	70.7	65.7	63.8	39.8
β -D-Arap1NPr	85.3	70.8	70.8	65.6	63.9	47.5
β -D-Arap1NiPr	82.3	71.3	69.5	65.2	64.1	44.1
β -D-Arap1NtBu*	81.2	70.8	71.4	64.7	63.1	49.5

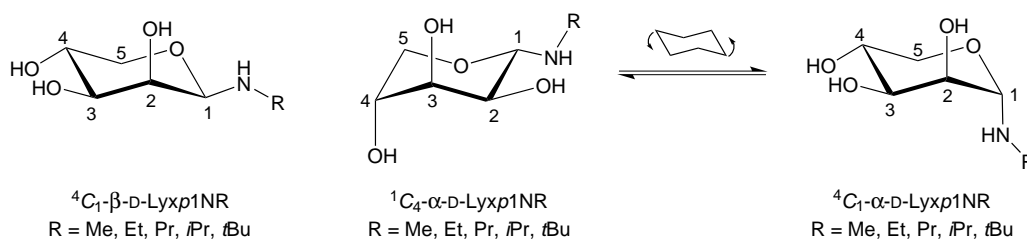
Additionally, both furanoid anomers were detected in aqueous solutions of all synthesized *N*-alkyl-D-arabinosylamines, except for D-Ara1NtBu. This exception, which also applied to the previously mentioned pyranoid β -anomer, presumably derives from the significant steric demand of the *tert*-butylamino moiety. The amount of the furanoid form is slightly increased in DMSO compared to aqueous solutions (table 2.1). The measured ${}^3J_{1,2}$ values range between 4.9 Hz to 5.1 Hz for the *N*-alkyl- α -D-arabinosylamines and 3.6 Hz to 3.7 Hz for the corresponding β -anomers, respectively. The ${}^{13}\text{C}\{{}^1\text{H}\}$ NMR shifts assigned to the carbohydrate scaffold and the C α atom of the alkylamino group of all detected *N*-alkyl-D-arabinofuranosylamines are listed below in table 2.4.

Table 2.4. Selected $^{13}\text{C}\{^1\text{H}\}$ NMR chemical shifts (δ/ppm) of the *N*-alkyl-D-arabinosylamines detected in D_2O or $\text{DMSO-}d_6$ (*).

	C1	C2	C3	C4	C5	C α
α -D-Araf1NMe	95.1	79.9	76.0	81.9	61.8	31.1
α -D-Araf1NEt	93.8	80.4	76.1	81.9	61.8	39.7
α -D-Araf1NPr	94.4	80.2	75.9	81.9	61.7	47.3
α -D-Araf1NiPr	91.4	80.8	76.1	81.9	61.8	44.7
α -D-Araf1N <i>t</i> Bu*	91.4	81.6	76.3	82.3	62.1	49.5
β -D-Araf1NMe	92.8	77.2	76.3	83.1	62.5	32.3
β -D-Araf1NEt	91.2	77.3	76.4	83.3	62.5	40.7
β -D-Araf1NPr	91.7	77.5	76.4	83.6	62.5	48.3
β -D-Araf1NiPr	88.9	77.6	76.6	83.8	62.5	45.3
β -D-Araf1N <i>t</i> Bu*	86.3	77.0	76.4	83.4	62.1	49.4

2.1.1.2. *N*-Alkyl-D-lyxosylamines

The reaction of D-lyxose with various alkylamines yielded the corresponding *N*-alkyl-D-lyxosylamines displayed in figure 2.2. All products were obtained as white or slightly beige powders with only D-Lyx1NiPr and D-Lyx1N*t*Bu showing significant signs of decomposition when exposed to air and when stored at 4 °C under inert gas atmosphere for months.

Figure 2.2. In D_2O and $\text{DMSO-}d_6$ detected isomers and conformations of the synthesized *N*-alkyl-D-lyxosylamines.

As shown in table 2.5, the prevailing isomer in aqueous solution for all *N*-alkyl-D-lyxosylamines is the β -pyranosylamine anomer. The only other species detected in aqueous solution, excluding hydrolysis products, is the corresponding pyranoid α -anomer. The measured amount of the α -anomer is higher in DMSO than in water. In the case of D-Lyx1N*t*Bu the concentration of the α -anomer even exceeds the β -anomer in DMSO. There were no traces of furanoid isomers detected in the NMR spectra of any of the investigated *N*-alkyl-D-lyxosylamines, neither in D_2O or in $\text{DMSO-}d_6$. The $^{13}\text{C}\{^1\text{H}\}$ NMR shifts assigned to the carbohydrate scaffold and the C α atom of the alkylamino group are listed in table 2.5.

Table 2.5. Percentage distribution of the different isomers for the synthesized *N*-alkyl-D-lyxosylamines from ^1H or $^{13}\text{C}\{^1\text{H}\}$ NMR spectra measured in D_2O at room temperature or at 4°C^* and in $\text{DMSO-}d_6$ at room temperature.

	D_2O		$\text{DMSO-}d_6$	
	βp	αp	βp	αp
D-Lyx1NMe	69	31	56	44
D-Lyx1NEt	73	27	57	43
D-Lyx1NPr	74	26	59	41
D-Lyx1N <i>i</i> Pr	77	23	62	38
D-Lyx1N <i>t</i> Bu*	64	36	46	54

The experimental $^3J_{1,2}$ values for the *N*-alkyl- β -D-lyxosylamines, listed in table 2.6, match the calculated values for the expected sole presence of the 4C_1 conformation with only one axial substituent. For the corresponding α -anomers on the other hand, the measured $^3J_{1,2}$ values lie in between the idealized $^3J_{1,2}$ coupling constants for the 4C_1 and 1C_4 conformation of α -D-lyxopyranoses. Thus, a dynamic fluctuation between the 1C_4 conformation and the 4C_1 conformation is assumed for the synthesized *N*-alkyl- α -D-lyxosylamines. And yet the 1C_4 conformation appears to be favored since the found $^3J_{1,2}$ values are located closer to the idealized $^3J_{1,2}$ value for the 1C_4 conformation. This preference increases with growing steric demand of the alkylamino substituent in order to avoid an adverse axial orientation of a bulky substituent, as can be clearly seen in the case of α -D-Lyx1N*t*Bu.

Table 2.6. Experimental and calculated $^3J_{\text{H,H}}$ values in Hz for the detected isomers of the synthesized *N*-alkyl-D-lyxopyranosylamines from ^1H NMR spectra measured in D_2O . Dashes indicate that due to superposition of signals no coupling constant could be determined.

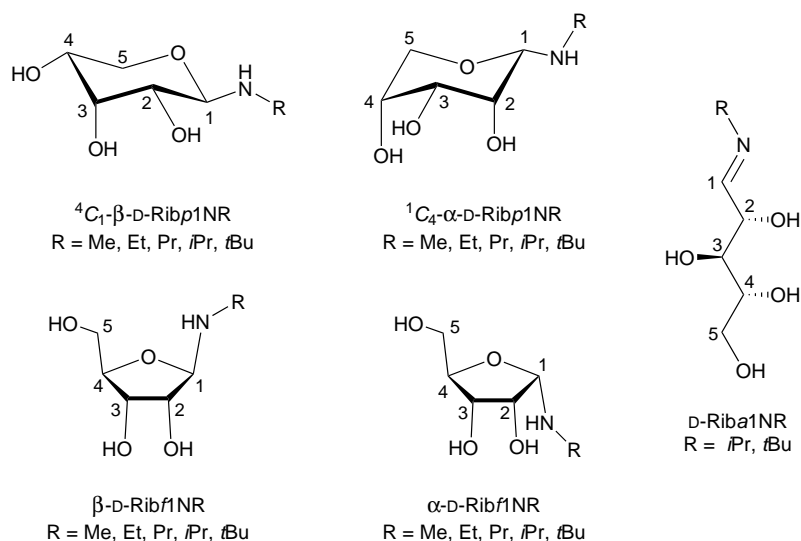
	$^3J_{1,2}$	$^3J_{2,3}$	$^3J_{3,4}$	$^3J_{4,5eq}$	$^3J_{4,5ax}$
4C_1 - β -D-Lyx1NR (calcd.)	1.1	3.5	9.6	4.3	10.1
β -D-Lyx <i>p</i> 1NMe	1.2	3.3	9.6	5.5	10.4
β -D-Lyx <i>p</i> 1NEt	1.1	3.4	9.6	5.5	10.4
β -D-Lyx <i>p</i> 1NPr	1.1	3.4	9.6	5.6	10.4
β -D-Lyx <i>p</i> 1N <i>i</i> Pr	1.1	3.4	9.6	5.6	11.3
β -D-Lyx <i>p</i> 1N <i>t</i> Bu	1.1	–	–	–	–
1C_4 - β -D-Lyx1NR (calcd.)	3.1	3.5	4.3	2.5	0.6
4C_1 - α -D-Lyx1NR (calcd.)	2.6	3.5	9.6	4.3	10.1
α -D-Lyx <i>p</i> 1NMe	6.6	3.3	–	–	4.7
α -D-Lyx <i>p</i> 1NEt	6.8	3.3	–	–	–
α -D-Lyx <i>p</i> 1NPr	6.9	3.1	–	–	–
α -D-Lyx <i>p</i> 1N <i>i</i> Pr	6.9	3.1	–	–	–
α -D-Lyx <i>p</i> 1N <i>t</i> Bu	7.6	–	–	–	–
1C_4 - α -D-Lyx1NR (calcd.)	8.7	3.5	4.3	2.5	0.6

Table 2.7. Selected $^{13}\text{C}\{^1\text{H}\}$ NMR chemical shifts (δ/ppm) of the *N*-alkyl-D-lyxopyranosylamines detected in D_2O or $\text{DMSO-}d_6$ (*).

	C1	C2	C3	C4	C5	C α
β -D-Lyxp1NMe	89.7	71.4	74.4	67.2	67.0	31.6
β -D-Lyxp1NEt	87.8	71.6	74.4	67.2	67.0	39.5
β -D-Lyxp1NPr	88.2	71.6	74.5	67.2	67.0	47.1
β -D-Lyxp1N <i>i</i> Pr	85.4	71.8	74.5	67.2	67.1	43.8
β -D-Lyxp1N <i>t</i> Bu	85.3	71.1	74.7	67.2	66.6	51.1
α -D-Lyxp1NMe	89.1	69.3	71.1	69.2	64.7	31.2
α -D-Lyxp1NEt	87.6	69.4	71.1	69.2	64.6	39.6
α -D-Lyxp1NPr	87.9	69.4	71.2	69.2	64.7	47.3
α -D-Lyxp1N <i>i</i> Pr	85.5	69.2	70.9	69.2	64.4	45.0
α -D-Lyxp1N <i>t</i> Bu	84.3	69.8	71.1	69.4	64.7	51.2

2.1.1.3. *N*-Alkyl-D-ribosylamines

The reaction of D-ribose with various alkylamines yielded the in figure 2.3 displayed *N*-alkyl-D-ribosylamines. While D-Rib1NMe, D-Rib1NEt, D-Rib1NPr were obtained as yellow to brown syrup-like liquids at room temperature, D-Rib1N*i*Pr and D-Rib1N*t*Bu could be isolated as off-white solids. All compounds showed an immense susceptibility towards hydrolysis and had to be stored at -25°C under inert gas atmosphere.

Figure 2.3. In D_2O and $\text{DMSO-}d_6$ detected isomers of the synthesized *N*-alkyl-D-ribosylamines.

As shown in table 2.8, the pyranoid β -anomer represents the most abundant isomer in aqueous solution for all synthesized *N*-alkyl-D-ribosylamines. Next to the prevailing species, significant amounts of the corresponding α -anomer in its pyranosylamine form and smaller amounts of both anomers of the respective furanosylamines were detected. The abundance of these minor species appeared to be slightly increased in solutions of DMSO. Another noteworthy finding was the detection of traces of the open-chain imine form in the case of D-Rib1N*i*Pr and D-Rib1N*t*Bu

in DMSO. Both acyclic isomers were identified by the prominent $^{13}\text{C}\{^1\text{H}\}$ NMR signal of the imine moiety (C1) at 162.8 ppm and 159.7 ppm as well as the corresponding ^1H NMR signals at 7.70 ppm and 7.69 ppm, respectively.

Table 2.8. Percentage distribution of the different isomers for the synthesized *N*-alkyl-D-ribosylamines from ^1H or $^{13}\text{C}\{^1\text{H}\}$ NMR spectra measured in D_2O at 4 °C and in $\text{DMSO-}d_6$ at room temperature.

	D_2O				$\text{DMSO-}d_6$				
	βp	αp	βf	αf	βp	αp	βf	αf	<i>a</i>
D-Rib1NMe	42	41	10	7	44	32	17	7	0
D-Rib1NEt	55	34	8	3	40	37	16	7	0
D-Rib1NPr	44	44	8	4	40	35	15	10	0
D-Rib1N <i>i</i> Pr	50	38	8	4	40	36	13	9	2
D-Rib1N <i>t</i> Bu	52	39	9	0	42	23	19	14	2

The measured $^3J_{\text{H,H}}$ values for the β -anomers of the *N*-alkyl-D-ribosylamines, listed in table 2.9, prove that the favored conformation is the expected 4C_1 conformation with three equatorial substituents. Derived from their small $^3J_{1,2}$ values, the α -anomers on the other hand seem to strictly reside in the 1C_4 conformation. By adopting this conformation it is guaranteed that the alkylamino substituent is always located at the energetically favored equatorial position. The $^{13}\text{C}\{^1\text{H}\}$ NMR shifts assigned to the carbohydrate scaffold and the $\text{C}\alpha$ atom of the alkylamino group for the ribopyranosylamines are listed in table 2.10.

Table 2.9. Experimental and calculated $^3J_{\text{H,H}}$ values in Hz for the detected isomers of the synthesized *N*-alkyl-D-ribosylamines from ^1H NMR spectra measured in D_2O . Dashes indicate that due to superposition of signals no coupling constant could be determined.

	$^3J_{1,2}$	$^3J_{2,3}$	$^3J_{3,4}$	$^3J_{4,5eq}$	$^3J_{4,5ax}$
4C_1 - β -D-Rib1NR (calcd.)	8.7	3.5	3.5	4.3	10.1
β -D-Rib <i>p</i> 1NMe	8.4	2.7	2.7	4.9	11.0
β -D-Rib <i>p</i> 1NEt	8.4	3.0	3.0	4.9	11.1
β -D-Rib <i>p</i> 1NPr	8.5	3.0	3.0	4.8	11.0
β -D-Rib <i>p</i> 1N <i>i</i> Pr	8.4	2.7	2.7	4.9	11.0
β -D-Rib <i>p</i> 1N <i>t</i> Bu	8.6	2.7	2.4	–	–
1C_4 - β -D-Rib1NR (calcd.)	2.4	3.5	3.2	2.5	0.6
1C_4 - α -D-Rib1NR (calcd.)	0.9	3.5	3.2	2.5	0.6
α -D-Rib <i>p</i> 1NMe	1.1	–	–	–	–
α -D-Rib <i>p</i> 1NEt	1.0	–	–	–	–
α -D-Rib <i>p</i> 1NPr	0.9	–	–	–	–
α -D-Rib <i>p</i> 1N <i>i</i> Pr	1.2	–	–	–	–
α -D-Rib <i>p</i> 1N <i>t</i> Bu	0.9	–	–	–	–
4C_1 - α -D-Rib1NR (calcd.)	3.1	3.5	3.5	4.3	10.1

Table 2.10. Selected $^{13}\text{C}\{^1\text{H}\}$ NMR chemical shifts (δ/ppm) of the *N*-alkyl-D-ribofuranosylamines detected in D_2O or $\text{DMSO-}d_6$ ($*$).

	C1	C2	C3	C4	C5	Cα
β -D-Rib p 1NMe	88.4	72.2	70.6	67.6	63.9	31.4
β -D-Rib p 1NEt	86.9	72.5	70.8	67.6	63.8	40.0
β -D-Rib p 1NPr	87.2	72.4	70.7	67.6	63.8	47.6
β -D-Rib p 1NiPr	85.1	72.7	71.0	67.6	63.7	45.2
β -D-Rib p 1NtBu	83.5	73.7	71.1	67.6	63.5	51.1
α -D-Rib p 1NMe	89.4	71.2	69.3	69.2	63.5	31.6
α -D-Rib p 1NEt	87.6	70.9	69.4	69.2	63.5	39.5
α -D-Rib p 1NPr	87.9	71.0	69.4	69.2	63.5	47.1
α -D-Rib p 1NiPr	85.0	71.0	69.4	69.2	63.5	44.5
α -D-Rib p 1NtBu	85.1	72.4	69.4	69.3	63.3	50.9

The determined $^3J_{1,2}$ values for the furanoid isomers in D_2O lie within the range from 4.4 Hz to 4.7 Hz for the β -anomers and from 3.2 Hz to 3.8 Hz for the respective α -anomers. The $^{13}\text{C}\{^1\text{H}\}$ NMR shifts assigned to the carbohydrate scaffold and the C α atom of the alkylamino group for the ribofuranosylamines are listed in table 2.11.

Table 2.11. Selected $^{13}\text{C}\{^1\text{H}\}$ NMR chemical shifts (δ/ppm) of the *N*-alkyl-D-ribofuranosylamines detected in D_2O or $\text{DMSO-}d_6$ ($*$).

	C1	C2	C3	C4	C5	Cα
β -D-Rib f 1NMe	95.5	71.2	74.5	82.9	62.4	31.7
β -D-Rib f 1NEt	94.1	71.2	74.9	82.9	62.4	40.3
β -D-Rib f 1NPr	94.5	71.2	74.8	82.8	62.3	47.8
β -D-Rib f 1NiPr	91.7	71.2	75.3	82.9	62.3	43.6
β -D-Rib f 1NtBu	90.6	71.2	76.1	82.9	62.4	51.1
α -D-Rib f 1NMe	92.5	72.1	71.8	81.0	61.8	31.8
α -D-Rib f 1NEt	90.8	72.1	72.0	80.9	61.8	40.1
α -D-Rib f 1NPr	91.1	72.1	72.1	80.9	61.8	47.6
α -D-Rib f 1NiPr	88.1	72.2	72.1	80.9	61.8	45.3
α -D-Rib f 1NtBu*	86.2	71.3	71.0	81.4	62.0	49.3

2.1.1.4. *N*-Alkyl-D-xylosylamines

The reaction of D-xylose with various alkylamines yielded the *N*-alkyl-D-xylosylamines displayed in figure 2.4. D-Xyl1NMe, D-Xyl1NEt and D-Xyl1NPr were obtained as neat powders, storeable for days at room temperature before showing signs of hydrolysis. On the other hand the synthesis of D-Xyl1N*i*Pr and D-Xyl1N*t*Bu yielded the products as syrup-like liquids with a significant sensitivity towards hydrolysis. All compounds were stored at 4 °C and under inert gas atmosphere for a few months before slowly decomposing to a brown caramel-like residue.

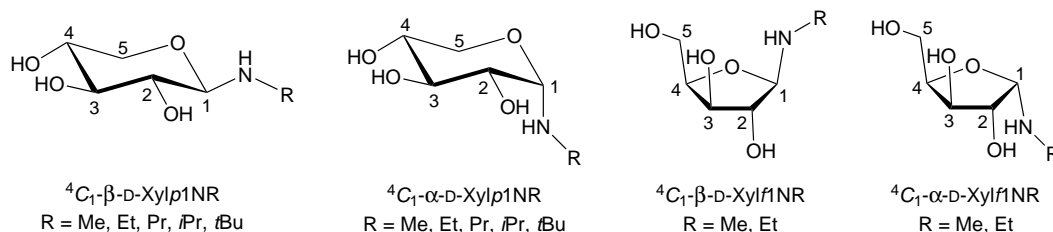


Figure 2.4. In D₂O and DMSO-*d*₆ detected isomers of the synthesized *N*-alkyl-D-xylosylamines.

The β-pyranosylamine isomers represent the prevailing species in aqueous solution for all synthesized *N*-alkyl-D-xylosylamines, as shown in table 2.12 below. This dominance of one isomer appears even more pronounced at lower temperatures. Other species, observed in the NMR spectra, besides the hydrolysis products D-xylose and the corresponding alkylamine, were identified as the α-pyranosylamine isomers by their small ³J_{H,H} values listed in table 2.13. While the α-anomer is present in all aqueous solutions of the synthesized *N*-alkyl-D-xylopyranosylamines, its anomeric ratio never exceeded 10 % at 4 °C. Both pyranoid anomers strictly adopt the ⁴C₁ conformation in order to minimize the presence of equatorial hydroxy groups.

Table 2.12. Percentage distribution of the different isomers for the synthesized *N*-alkyl-D-xylosylamines detected in ¹H or ¹³C{¹H} NMR spectra measured in D₂O at 4 °C and room temperature and in DMSO-*d*₆ at room temperature.

	D ₂ O (RT)				D ₂ O (4 °C)				DMSO- <i>d</i> ₆			
	β <i>p</i>	α <i>p</i>	β <i>f</i>	α <i>f</i>	β <i>p</i>	α <i>p</i>	β <i>f</i>	α <i>f</i>	β <i>p</i>	α <i>p</i>	β <i>f</i>	α <i>f</i>
D-Xyl1NMe	87	11	2	0	94	6	0	0	72	23	3	2
D-Xyl1NEt	87	11	2	0	97	3	0	0	84	12	2	2
D-Xyl1NPr	90	10	0	0	98	2	0	0	85	15	0	0
D-Xyl1N <i>i</i> Pr	94	6	0	0	94	6	0	0	88	12	0	0
D-Xyl1N <i>t</i> Bu	98	2	0	0	98	2	0	0	67	33	0	0

In addition, traces of the β-furanosylamine anomer of D-Xyl1NMe and D-Xyl1NEt were detected in their respective NMR spectra at room temperature. The ³J_{1,2} values associated to these isomers in water are 3.0 Hz and 2.9 Hz, respectively.

A higher abundance of the *N*-alkyl-α-D-xylopyranosylamines was observed in DMSO. In those solutions the α/β ratio reached up to 1:2 and in the case of D-Xyl1NMe and D-Xyl1NEt also small amounts of the corresponding furanosylamine isomers were detected. The ¹³C{¹H} NMR shifts assigned to the carbohydrate scaffold and the Cα atom of the alkylamino group for the detected D-xylosylamines are listed in table 2.14.

2. Results

Table 2.13. Experimental and calculated ${}^3J_{\text{H,H}}$ values in Hz for the detected isomers of the synthesized *N*-alkyl-D-xylosylamines from ${}^1\text{H}$ NMR spectra measured in D_2O . Dashes indicate that due to superposition of signals no coupling constant could be determined.

	${}^3J_{1,2}$	${}^3J_{2,3}$	${}^3J_{3,4}$	${}^3J_{4,5a}$	${}^3J_{4,5b}$
4C_1 - β -D-Xyl1NR (calcd.)	8.7	9.8	9.6	4.3	10.1
β -D-Xylp1NMe	9.0	9.0	9.1	5.5	11.0
β -D-Xylp1NEt	8.8	8.9	9.1	5.4	11.0
β -D-Xylp1NPr	8.8	8.9	9.1	5.5	11.4
β -D-Xylp1NiPr	8.7	–	9.1	5.3	11.0
β -D-Xylp1NtBu	8.7	8.9	9.1	5.4	11.0
4C_1 - β -D-Xyl1NR (calcd.)	2.4	4.3	4.3	2.5	0.6
4C_1 - α -D-Xyl1NR (calcd.)	3.1	9.8	9.6	4.3	10.1
α -D-Xylp1NMe	3.7	–	–	–	–
α -D-Xylp1NEt	3.5	–	–	–	–
α -D-Xylp1NPr	3.4	–	–	–	–
α -D-Xylp1NiPr	2.8	–	–	–	–
α -D-Xylp1NtBu	3.7	–	–	–	–
4C_1 - α -D-Xyl1NR (calcd.)	0.9	4.3	4.3	2.5	0.6

Table 2.14. Selected ${}^{13}\text{C}\{{}^1\text{H}\}$ NMR chemical shifts (δ/ppm) of the *N*-alkyl-D-xylosylamines detected in D_2O or $\text{DMSO}-d_6$ (*). Dashes indicate that due to superposition of signals no chemical shift could be determined.

	C1	C2	C3	C4	C5	C α
β -D-Xylp1NMe	92.2	73.4	77.4	70.2	66.9	31.6
β -D-Xylp1NEt	90.8	73.6	77.5	70.2	66.7	40.0
β -D-Xylp1NPr	91.1	73.5	77.4	70.1	66.8	47.5
β -D-Xylp1NiPr	89.0	73.9	77.6	70.1	66.8	45.5
β -D-Xylp1NtBu	87.5	73.8	77.5	70.3	66.2	51.1
α -D-Xylp1NMe	87.8	71.2	72.1	69.7	63.0	31.4
α -D-Xylp1NEt	86.0	71.2	71.7	69.5	63.7	39.8
α -D-Xylp1NPr	86.2	71.2	71.7	69.5	63.6	47.4
α -D-Xylp1NiPr	83.4	71.0	71.2	69.2	64.7	44.5
α -D-Xylp1NtBu*	82.0	71.6	72.1	69.7	62.1	49.4
β -D-Xylf1NMe	96.7	80.2	76.1	80.5	61.2	31.7
β -D-Xylf1NEt	95.7	80.6	76.1	80.7	61.1	40.1
α -D-Xylf1NMe*	92.2	75.8	75.8	79.0	66.9	32.8
α -D-Xylf1NEt*	90.3	75.4	75.4	78.9	60.3	–

2.1.2. *N*-Alkylhexosylamines

N-Alkylhexosylamines were synthesized in a similar fashion as the in chapter 2.1.1 described *N*-alkylpentosylamines. The aldohexoses used as reactants for the synthesis of *N*-alkylhexosylamines in this work include D-galactose, D-glucose, L-gulose, D-mannose and the 6-deoxy-aldohexose L-rhamnose. The reaction of these aldohexoses with various alkylamines (methylamine, ethylamine, propylamine, *iso*-propylamine and *tert*-butylamine) gave numerous *N*-alkylhexosylamines with deviating results in terms of their yield, purity, stability and hygroscopy. Contrary to *N*-alkylpentosylamines, the fluctuation between the 4C_1 and 1C_4 conformation of *N*-alkylhexosylamines is frozen to the conformer featuring the terminal hydroxymethyl function in equatorial position (4C_1 for D- and 1C_4 for L-enantiomers). Exhibiting a similar behavior as their reducing sugar analogues, *N*-alkylhexosylamines furthermore mostly form pyranoid isomers in aqueous solution. This reduced configurational variety and increased conformational stability leads to the formation of less sensitive products, when compared to many of the previously described *N*-alkylpentosylamines.

2.1.2.1. *N*-Alkyl-D-galactosylamines

The synthesis of various *N*-alkyl-D-galactosylamines gave D-Gal1NMe, D-Gal1NEt, D-Gal1NPr, D-Gal1N*i*Pr and D-Gal1N*t*Bu (depicted in 2.5) as white and off-white powders in good yields and purity. Compared to similar reactions with other D-aldoses, noticeably larger amounts of solvent and longer reaction times were necessary for the complete synthesis of *N*-alkyl-D-galactosylamines. All obtained compounds could be stored at 4 °C under inert gas atmosphere for months without showing signs of decomposition.

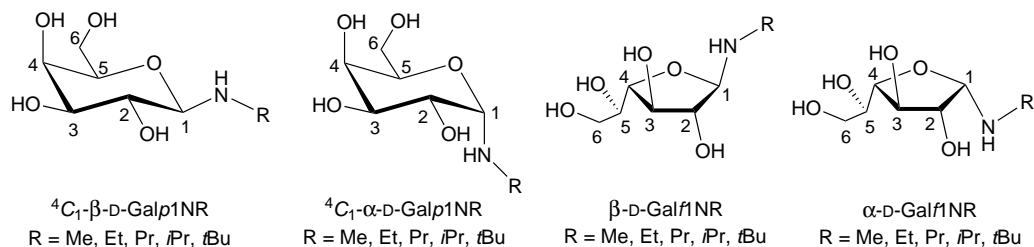


Figure 2.5. In D₂O and DMSO-*d*₆ detected isomers of the synthesized *N*-alkyl-D-galactosylamines.

As can be seen in table 2.15, the β -pyranosylamine isomer represents the prevailing species for all synthesized *N*-alkyl-D-galactosylamines in D₂O and in DMSO-*d*₆. The pyranoid α -anomer was not detected for D-Gal1N*i*Pr and D-Gal1N*t*Bu in aqueous solution and only in small concentrations for the remaining compounds. Both anomers were identified using the KARPLUS relation by their ${}^3J_{1,2}$ values of 8.5 Hz to 8.8 Hz and 5.0 Hz to 5.3 Hz, respectively. These experimental values are in accordance with the calculated ${}^3J_{1,2}$ coupling constant of 8.7 Hz for 4C_1 - α -D-Gal1NR species, but slightly differ from the calculated ${}^3J_{1,2}$ value of 3.1 Hz for the corresponding β -anomer in the 4C_1 conformation. The ${}^{13}C\{^1H\}$ NMR shifts assigned to the carbohydrate scaffold and the C α of the pyranoid anomers are listed in table 2.16.

Table 2.15. Percentage distribution of the different isomers for the synthesized *N*-alkyl-D-galactosylamines detected in ^1H or $^{13}\text{C}\{^1\text{H}\}$ NMR spectra in D_2O and in $\text{DMSO-}d_6$ at room temperature.

	D_2O				$\text{DMSO-}d_6$			
	βp	αp	βf	αf	βp	αp	βf	αf
D-Gal1NMe	90	6	4	0	52	11	21	16
D-Gal1NEt	92	4	4	0	44	14	21	21
D-Gal1NPr	90	5	5	0	49	11	21	19
D-Gal1NiPr	>98	0	<2	0	45	11	21	23
D-Gal1NtBu	100	0	0	0	40	12	15	33

Table 2.16. Selected $^{13}\text{C}\{^1\text{H}\}$ NMR chemical shifts (δ/ppm) of the *N*-alkyl-D-galactopyranosylamines detected in D_2O or in $\text{DMSO-}d_6$ (*).

	C1	C2	C3	C4	C5	C6	C α
β -D-Galp1NMe	91.8	71.0	74.3	69.7	76.5	61.8	31.5
β -D-Galp1NEt	90.4	71.2	74.3	69.6	76.5	61.8	39.9
β -D-Galp1NPr	90.7	71.2	74.3	69.6	76.5	61.7	47.5
β -D-Galp1NiPr	88.6	71.6	74.5	69.6	76.4	61.8	45.5
β -D-Galp1NtBu	87.1	71.4	74.4	69.8	76.1	61.9	51.1
α -D-Galp1NMe	88.4	68.3	69.4	69.7	69.9	61.6	31.0
α -D-Galp1NEt	86.9	68.3	69.4	69.8	70.4	61.6	39.6
α -D-Galp1NPr	87.1	68.3	69.4	69.8	70.3	61.6	47.1
α -D-Galp1NiPr*	85.5	68.0	68.7	69.4	70.0	60.4	46.5
α -D-Galp1NtBu*	82.5	68.1	68.6	69.8	70.0	60.3	49.4

N-Alkyl-D-galactosylamines are the only group within all *N*-alkyl-D-hexosylamines investigated in this work to form detectable amounts of furanoid isomers in solution, particularly in DMSO. In aqueous solution only the β -furanosylamine form can be found, while in DMSO both furanoid anomers are present and their concentration well exceeds the α -pyranosylamine isomer. Furthermore, the amount of detected furansylamines appears to be almost in no relation to the steric demand of the featured alkylamino substituent in DMSO. The corresponding $^3J_{1,2}$ values for the β -furanosylamine isomers in water range between 5.3 Hz and 5.7 Hz. The $^{13}\text{C}\{^1\text{H}\}$ NMR shifts assigned to the carbohydrate scaffold and the C α atom of the furanoid anomers are listed in table 2.17.

Table 2.17. Selected $^{13}\text{C}\{^1\text{H}\}$ NMR chemical shifts (δ/ppm) of the *N*-alkyl-D-galactofuranosylamines detected in D_2O or in $\text{DMSO}-d_6$ (*).

	C1	C2	C3	C4	C5	C6	C α
β -D-Galp1NMe	94.9	79.5	76.3	80.9	71.6	63.4	31.5
β -D-Galp1NEt	93.6	80.1	76.4	80.9	71.6	63.4	40.1
β -D-Galp1NPr	94.0	79.9	76.4	80.9	71.6	63.4	47.8
β -D-Galp1N <i>i</i> Pr	91.6	80.7	76.5	80.9	70.3	63.4	46.0
β -D-Galp1N <i>t</i> Bu *	90.9	80.3	76.0	81.1	71.0	63.1	49.6
α -D-Galp1NMe *	91.9	76.7	76.3	82.4	70.8	62.7	32.7
α -D-Galp1NEt *	90.0	76.7	76.3	82.4	70.8	62.7	40.1
α -D-Galp1NPr *	90.5	76.7	76.3	82.4	70.9	62.7	48.1
α -D-Galp1N <i>i</i> Pr *	88.3	76.7	76.3	82.3	70.8	62.7	45.6
α -D-Galp1N <i>t</i> Bu *	85.2	76.5	76.2	82.1	70.4	62.9	49.6

2.1.2.2. *N*-Alkyl-D-glucosylamines

The reaction of D-glucose with various alkylamines yielded both anomers of *N*-alkyl-D-glucopyranosylamines, as depicted in figure 2.6. The products were obtained as colorless to slightly yellow powders. All compounds showed notable sensitivity towards moisture and air, however, the tendency of the compounds to hydrolyze increased significantly with the size of the alkylamino moiety. D-Glc1NMe, D-Glc1NEt and D-Glc1NPr were stored under inert gas atmosphere at 4 °C for months without showing signs of decomposition, while under the same conditions D-Glc1N*i*Pr and D-Glc1N*t*Bu decomposed to brown viscous liquids within weeks.

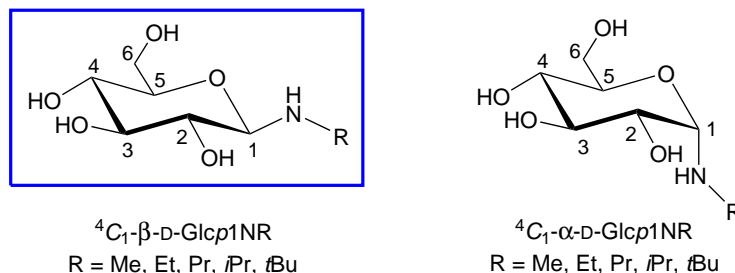


Figure 2.6. In D_2O and $\text{DMSO}-d_6$ detected isomers of the synthesized *N*-alkyl-D-glucosylamines. The structure of the blue-framed isomer is confirmed for R = Me by X-ray structure analysis (1).

As can be seen in table 2.18, the β -anomer represents the clearly dominating isomer for all *N*-alkyl-D-glucopyranosylamines in water or DMSO, with the amounts of the α -anomer being slightly higher in DMSO.

Table 2.18. Percentage distribution of the different isomers for the synthesized *N*-alkyl-D-glucosylamines detected in ^1H or $^{13}\text{C}\{^1\text{H}\}$ NMR spectra measured in D_2O and in $\text{DMSO-}d_6$ at room temperature.

	D_2O		$\text{DMSO-}d_6$	
	βp	αp	βp	αp
D-Glc1NMe	91	9	85	15
D-Glc1NEt	94	6	93	7
D-Glc1NPr	95	5	95	5
D-Glc1NiPr	92	8	85	15
D-Glc1NtBu	100	0	78	22

In accordance with the KARPLUS relation the *N*-alkyl- α -D-glucopyranosylamines possess smaller $^3J_{1,2}$ values with 4.5 Hz to 5.0 Hz than the corresponding β -anomers with 8.8 Hz to 8.9 Hz. The $^3J_{\text{H,H}}$ values found for the β -anomers coincide with the calculated coupling constants for the 4C_1 conformation. But as already mentioned for *N*-alkyl-D-galactosylamines in chapter 2.1.2.1, the experimental $^3J_{1,2}$ values found for the α -anomers are higher than the idealized value of 3.1 Hz. Despite this observation, two-dimensional NMR methods clearly confirm the correct assignment of the H1 atom for the α -anomers.

There was no evidence found for the presence of any furanoid isomers in the NMR spectra, neither in water nor in DMSO. The $^{13}\text{C}\{^1\text{H}\}$ NMR chemical shifts of the carbohydrate scaffold and of the C α atom of the alkylamino group of all detected *N*-alkyl-D-glucopyranosylamines are listed in table 2.19.

Table 2.19. Selected $^{13}\text{C}\{^1\text{H}\}$ NMR chemical shifts (δ/ppm) of the *N*-alkyl-D-glucopyranosylamines detected in D_2O or in $\text{DMSO-}d_6$ (*).

	C1	C2	C3	C4	C5	C6	C α
β -D-Glcp1NMe	91.3	73.4	77.4	70.6	77.4	61.5	31.5
β -D-Glcp1NEt	89.7	73.6	77.4	70.5	77.5	61.5	39.9
β -D-Glcp1NPr	90.2	73.6	77.4	70.5	77.5	61.5	47.6
β -D-Glcp1NiPr	88.2	74.0	77.3	70.6	77.6	61.6	45.5
β -D-Glcp1NtBu	86.7	73.8	76.9	70.7	77.6	61.7	50.9
α -D-Glcp1NMe	88.2	71.4	73.6	70.6	71.2	61.4	31.4
α -D-Glcp1NEt	86.8	71.6	73.6	70.8	71.0	61.4	39.7
α -D-Glcp1NPr	87.0	71.4	73.5	70.6	71.2	61.5	47.7
α -D-Glcp1NiPr	85.3	71.2	73.6	70.3	70.7	61.4	46.0
α -D-Glcp1NtBu*	82.2	71.2	73.8	70.1	70.8	61.2	49.6

Colorless, needle-like crystals suitable for X-ray diffraction of D-Glc1NMe were obtained from the ethanolic reaction solution at 4 °C. The crystal structure was solved in the monoclinic space group *C*2. The asymmetric unit of the determined molecular structure, displayed in figure 2.7, contains one molecule of *N*-methyl- 4C_1 - β -D-glucopyranosylamine along with one methylamine molecule (**1**). The determined molecular structure is in accordance with the previously outlined NMR-spectroscopic results, suggesting a clear preference of the β -D-Glcp1NMe anomer residing in the 4C_1 conformation in solution. The identified hydrogen bonds in the structure are listed in table 2.20.

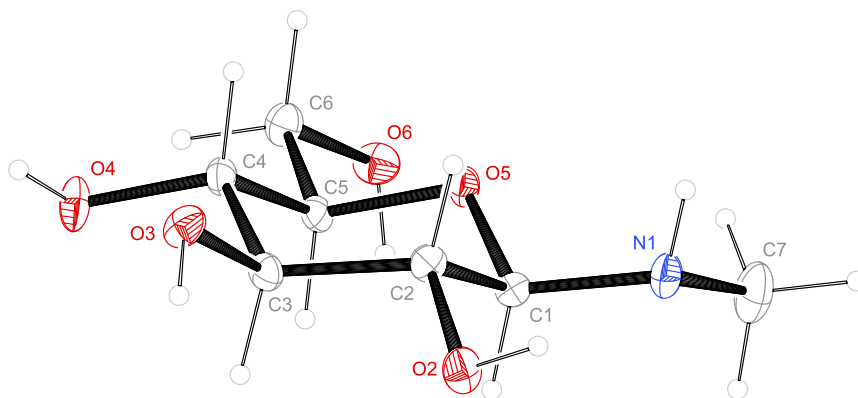


Figure 2.7. The molecular structure of the 4C_1 - β -D-Glc1NMe molecule in **1**. ORTEP plot is drawn with 50 % probability ellipsoids. Selected interatomic distances (\AA) and angles ($^\circ$), standard deviations of the last digit in parentheses: O5–C1 1.434(4), C1–C2 1.534(4), C1–N1 1.435(2), N1–C7 1.467(3), C2–O2 1.427(4), C1–N1–C7 114.0(2), O5–C1–N1 110.5(3), O2–C2–C1 111.4(2), O2–C2–C3 107.4(3), N1–C1–C2 110.9(2), O5–C1–C2 108.4(2); puckering parameters^[40] of the pyranose ring O5–C1–C2–C3–C4–C5: $Q = 0.602(3) \text{ \AA}$, $\theta = 8.1(3)^\circ$, $\phi = 343(2)^\circ$.

Table 2.20. Distances in \AA and angles in $^\circ$ of the hydrogen bonds in **1**. Standard deviations of the last digit are given in parentheses; values without standard deviation are related to hydrogen atoms at calculated positions. Symmetry codes are given as footnotes at the bottom of the table. D: donor, A: acceptor.

D	H	A	D–H	H \cdots A	D \cdots A	D–H \cdots A
O2	H82	N1 ⁱ	0.84	2.04	2.877(4)	172
O3	H83	N2 ⁱⁱ	0.84	1.90	2.707(5)	160
O4	H82	O3 ⁱⁱⁱ	0.84	1.95	2.743(4)	157
O6	H86	O6 ^{iv}	0.84	2.03	2.847(3)	163
N2	H721	O3 ⁱ	0.91(8)	2.57(8)	3.013(5)	110(5)

ⁱ $-x + 1, y, -z + 1$; ⁱⁱ $-x + 1, y - 1, -z + 1$;

ⁱⁱⁱ $-x + 1, y, -z + 2$; ^{iv} $-x + 1/2, y - 1/2, -z + 1$

2.1.2.3. *N*-Alkyl-L-gulosylamines

The reaction of L-gulose with the used alkylamines yielded the corresponding *N*-alkyl-L-gulosylamines as hygroscopic powders. The obtained compounds had to be stored under inert gas atmosphere at -20°C to prevent them from decomposing to a viscous, brown residue. The in solution detected isomers for all synthesized *N*-alkyl-L-gulosylamines are depicted in figure 2.8.

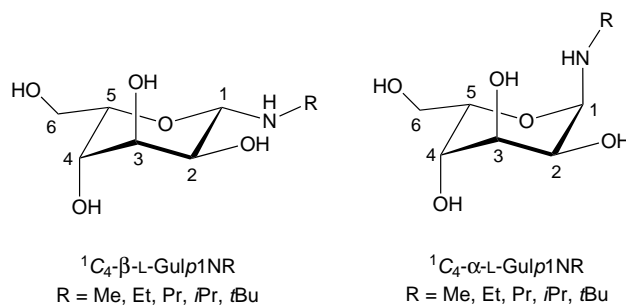


Figure 2.8. In D_2O and $DMSO-d_6$ detected isomers of the synthesized *N*-alkyl-L-gulosylamines.

As can be seen in table 2.21, only the β -pyranosylamine isomer is detected in aqueous solution. The β -anomers are readily identified by their ${}^3J_{1,2}$ values of 9.2 Hz to 9.4 Hz due to the anti-arranged hydrogen atoms in this configuration. The calculated ${}^3J_{1,2}$ value for the β -anomer in the expected 1C_4 conformation lies with 8.7 Hz slightly beneath the experimental values. The corresponding α -anomers are only found in small amounts in DMSO. All NMR spectra measured in D_2O , even at 4 °C, show notable amounts of L-gulose due to the high susceptibility towards hydrolysis of the investigated *N*-alkyl-L-gulosylamines. The ${}^{13}C\{^1H\}$ NMR chemical shifts of the carbohydrate scaffold and of the $C\alpha$ atom of the alkylamino group of all *N*-alkyl-D-gulopyranosylamines are listed in table 2.22.

Table 2.21. Percentage distribution of the different isomers for the synthesized *N*-alkyl-L-gulosylamines detected in 1H or ${}^{13}C\{^1H\}$ NMR spectra measured in D_2O at 4 °C and in $DMSO-d_6$ at room temperature.

	D_2O		$DMSO-d_6$	
	βp	αp	βp	αp
D-Gul1NMe	100	0	86	14
D-Gul1NEt	100	0	82	18
D-Gul1NPr	100	0	80	20
D-Gul1N <i>i</i> Pr	100	0	78	22
D-Gul1N <i>t</i> Bu	100	0	82	18

Table 2.22. Selected ${}^{13}C\{^1H\}$ NMR chemical shifts (δ /ppm) of the *N*-alkyl-L-gulopyranosylamines detected in D_2O or in $DMSO-d_6$ (*).

	C1	C2	C3	C4	C5	C6	C α
β -L-Gulp1NMe	88.4	68.2	71.7	70.3	74.5	61.8	31.3
β -L-Gulp1NEt	87.0	68.4	71.7	70.3	74.5	61.8	39.7
β -L-Gulp1NPr	87.3	68.4	71.8	70.3	74.6	61.8	47.4
β -L-Gulp1N <i>i</i> Pr	85.2	68.8	71.8	70.4	74.5	61.8	45.2
β -L-Gulp1N <i>t</i> Bu	83.7	68.5	71.7	70.6	74.2	61.8	51.1
α -L-Gulp1NMe*	87.7	64.8	72.0	69.5	65.2	60.6	31.4
α -L-Gulp1NEt*	86.2	64.7	72.0	69.4	65.2	60.5	38.9
α -L-Gulp1NPr*	86.5	64.7	72.0	69.4	65.2	60.5	46.7
α -L-Gulp1N <i>i</i> Pr*	84.1	64.6	71.9	69.3	65.3	60.4	43.5
α -L-Gulp1N <i>t</i> Bu*	82.6	64.5	71.9	69.1	64.2	60.3	49.1

2.1.2.4. *N*-Alkyl-D-mannosylamines

The treatment of D-mannose with alkylamines led to the formation of the *N*-alkyl-D-mannosylamines illustrated in figure 2.9. All compounds were obtained as white powders in good yields and only D-Man1*Ni*Pr and D-Man1*Nt*Bu showed moderate signs of susceptibility towards hydrolysis and decomposition when exposed to air. All compounds were stored under inert gas atmosphere at 4 °C.

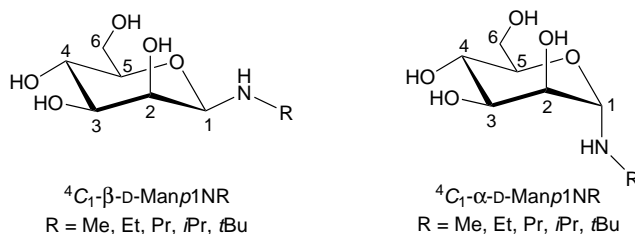


Figure 2.9. In D₂O and DMSO-*d*₆ detected isomers of the synthesized *N*-alkyl-D-mannosylamines.

As shown in table 2.23, the β -pyranosylamine form represents the predominant isomer for all investigated *N*-alkyl-D-mannosylamines in aqueous solution as well as in DMSO. The β -anomers exhibit ${}^3J_{1,2}$ values of 1.0 Hz to 1.1 Hz, which coincide with the calculated ${}^3J_{1,2}$ value of 1.1 Hz for the respective 4C_1 conformation. The calculated ${}^3J_{1,2}$ value for the corresponding α -anomers is with 2.6 Hz only slightly larger. The experimental ${}^3J_{1,2}$ values determined for the less abundant *N*-alkyl- α -D-mannosylamine isomers range between 1.5 Hz and 1.8 Hz. Furanoid isomers of the synthesized *N*-alkyl-D-mannosylamines were not detected, neither in water nor in DMSO. The ${}^{13}\text{C}\{^1\text{H}\}$ NMR chemical shifts of the carbohydrate scaffold and of the C α atom of the alkylamino group of all *N*-alkyl-D-mannopyranosylamines are listed in table 2.24.

Table 2.23. Percentage distribution of the different isomers for the synthesized *N*-alkyl-D-mannosylamines detected in ${}^1\text{H}$ or ${}^{13}\text{C}\{^1\text{H}\}$ NMR spectra measured in D₂O and in DMSO-*d*₆ at room temperature.

	D ₂ O		DMSO- <i>d</i> ₆	
	βp	αp	βp	αp
D-Man1NMe	84	16	86	14
D-Man1NEt	87	13	81	19
D-Man1NPr	85	15	90	10
D-Man1 <i>Ni</i> Pr	90	10	88	12
D-Man1 <i>Nt</i> Bu	100	0	76	24

Table 2.24. Selected $^{13}\text{C}\{^1\text{H}\}$ NMR chemical shifts (δ/ppm) of the *N*-alkyl-D-mannopyranosylamines detected in D_2O or in $\text{DMSO-}d_6$ (*).

	C1	C2	C3	C4	C5	C6	C α
β -D-Manp1NMe	88.7	71.5	74.5	67.9	77.9	61.9	31.6
β -D-Manp1NEt	86.9	71.8	74.5	67.9	77.9	61.9	39.5
β -D-Manp1NPr	87.2	71.8	74.5	67.9	77.9	61.9	47.1
β -D-Manp1N <i>i</i> Pr	84.5	72.0	74.7	67.9	77.9	61.9	43.8
β -D-Manp1N <i>t</i> Bu	86.7	73.8	76.9	70.7	77.6	61.7	50.9
α -D-Manp1NMe	89.8	71.5	71.2	67.6	72.4	61.7	31.0
α -D-Manp1NEt	88.3	71.6	71.2	67.6	72.4	61.7	39.4
α -D-Manp1NPr	88.6	71.6	71.2	67.6	72.4	61.7	47.1
α -D-Manp1N <i>i</i> Pr	86.1	71.9	71.2	67.7	72.4	61.7	44.3
α -D-Manp1N <i>t</i> Bu *	82.2	71.2	73.8	70.1	70.8	61.2	49.6

2.1.2.5. *N*-Alkyl-L-rhamnosylamines

The treatment of L-rhamnose with methylamin, ethylamine and *iso*-propylamine led to the successful synthesis of L-Rha1NMe, L-Rha1NEt and L-Rha1N*i*Pr (depicted in figure 2.10). All products were obtained as pure, white powders *via* precipitation from the reaction solution. The compounds showed only a minimal susceptibility towards hydrolysis and were stored under inert gas atmosphere at 4 °C for months without showing any signs of decomposition.

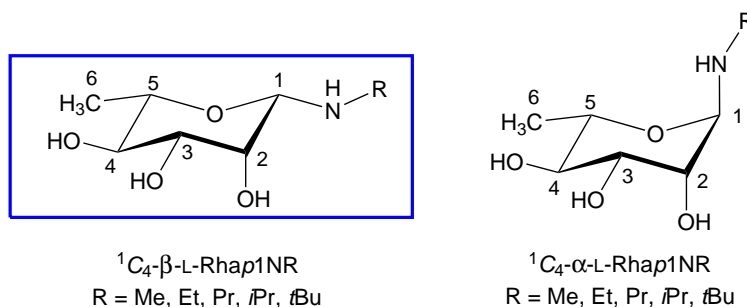


Figure 2.10. In D_2O and $\text{DMSO-}d_6$ detected isomers of the synthesized *N*-alkyl-L-rhamnopyranosylamines. The structure of the blue-framed isomer is confirmed for R = Et by X-ray analysis (**2**).

The chemical characteristics of the synthesized *N*-alkyl-L-rhamnosylamines in solution are largely similar to those of the in chapter 2.1.2.4 described *N*-alkyl-D-mannosylamines. These commonalities come as no surprise as rhamnose is the 6-deoxy analogue of mannose and the use of the other enantiomer has no impact on the physical properties. As can be seen in table 2.25, the β -anomers are the in water and DMSO prevailing species and have an experimental $^3J_{1,2}$ values of about 1.1 Hz. The less abundant α -pyranosylamine isomers have a $^3J_{1,2}$ values of about 1.6 Hz. The $^{13}\text{C}\{^1\text{H}\}$ NMR chemical shifts of the carbohydrate scaffold and of the C α atom of the alkylamino group of all *N*-alkyl-L-rhamnopyranosylamines are listed in table 2.26.

Table 2.25. Percentage distribution of the different isomers for the synthesized *N*-alkyl-L-rhamnopyranosylamines detected in ^1H or $^{13}\text{C}\{^1\text{H}\}$ NMR spectra measured in D_2O and in $\text{DMSO}-d_6$ at room temperature.

	D_2O		$\text{DMSO}-d_6$	
	βp	αp	βp	αp
L-Rha1NMe	86	14	80	20
L-Rha1NEt	87	13	80	20
L-Rha1N <i>i</i> Pr	90	10	88	12

Table 2.26. Selected $^{13}\text{C}\{^1\text{H}\}$ NMR chemical shifts (δ/ppm) of the *N*-alkyl-L-rhamnopyranosylamines in D_2O or in $\text{DMSO}-d_6$ (*).

	C1	C2	C3	C4	C5	C6	Cα
β -L-Rhap1NMe	88.7	71.8	74.2	73.0	73.8	17.4	31.6
β -L-Rhap1NEt	86.8	71.9	74.2	73.1	73.8	17.4	39.5
β -L-Rhap1N <i>i</i> Pr	84.3	72.1	74.3	73.1	73.8	17.4	43.7
α -L-Rhap1NMe	89.9	71.6	70.9	72.8	68.1	17.3	31.0
α -L-Rhap1NEt	88.3	71.8	70.9	72.8	68.1	17.3	39.5
α -L-Rhap1N <i>i</i> Pr	86.2	72.0	70.8	72.9	68.1	17.3	44.4

Colorless, rod-shaped crystals suitable for X-ray diffraction of L-Rha1NMe were obtained from the methanolic reaction solution at 4°C . The crystal structure was solved in the monoclinic space group $P2_1$. The asymmetric unit of the determined molecular structure, displayed in figure 2.11, contains one molecule of *N*-methyl- $^1\text{C}_4$ - β -L-rhamnopyranosylamine without any further solvent molecules (**2**). The found molecular structure is in accordance with the aforementioned NMR-spectroscopic results, indicating the preference of the β -L-Rhap1NMe anomer residing in the $^1\text{C}_4$ conformation in solution. The hydrogen bonds present in the structure are listed in table 2.27.

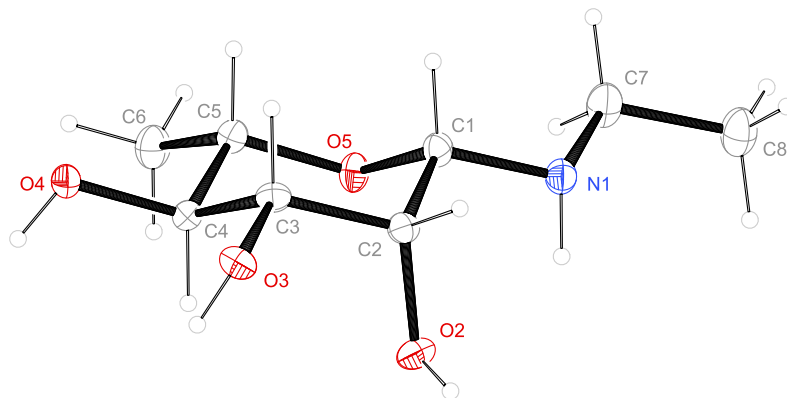


Figure 2.11. The molecular structure of the β -L-Rha1NEt- 1C_4 molecule in **2**. ORTEP plot is drawn with 50 % probability ellipsoids. Interatomic distances (\AA) and angles ($^\circ$) (standard deviations of the last digit in parentheses): O5–C1 1.442(2), C1–C2 1.532(2), C1–N1 1.440(2), N1–C7 1.471(3), O2–C2 1.428(2), C1–N1–C7 114.84(16), N1–C1–O5 110.20(15), O2–C2–C1 108.99(15), O2–C2–C3 111.50(16), N1–C1–C2 110.08(15), O5–C1–C2 109.81(15); puckering parameters^[40] of the pyranose ring O5–C1–C2–C3–C4–C5: $Q = 0.605(2)$ \AA , $\theta = 180.0(19)^\circ$, $\phi = 160(6)^\circ$.

Table 2.27. Distances in \AA and angles in $^\circ$ of the hydrogen bonds in **2**. Standard deviations of the last digit are given in parentheses; values without standard deviation are related to hydrogen atoms at calculated positions. Symmetry codes are given as footnotes at the bottom of the table. D: donor, A: acceptor.

D	H	A	D–H	H...A	D...A	D–H...A
O2	H82	N1 ⁱ	0.84	2.09	2.907(2)	163
O3	H83	O4 ⁱⁱ	0.84	1.91	2.741(2)	169
O4	H84	O3 ⁱⁱ	0.84	1.87	2.701(2)	168
N1	H71	O2	0.90(3)	2.43(3)	2.816(2)	107(2)

ⁱ $-x, y - 1/2, -z + 1$; ⁱⁱ $-x + 1, y - 1/2, -z + 1$

2.1.3. *N*-Alkyl-2-deoxyglycosylamines

The synthesis and characteristics of *N*-alkylated 2-deoxy-D-glycosylamines have not yet been reported in the literature, which comes as a surprise due to the fundamental role of 2-deoxy-D-aldoses and their derivatives in life sciences. Especially 2-deoxy-D-ribose in its role as structural component of DNA is of major biological importance. Solely theoretical studies on the molecular structure of an analogous 2-deoxy- β -D-ribofuranosylamine have yet been published.^[41] 2-Deoxy-D-glucose on the other hand functions as a competitive inhibitor in the glycolysis and is therefore used and proposed for various medical purposes. The synthesis and crystal structure of 2-deoxy-D-glycosylamine and 2-deoxy-D-galactosylamine was first reported by SCHWARZ,^[21] but *N*-substituted derivatives of these compounds have not yet been described in the literature. The term 2-deoxy-D-ribose is misleading as 2-deoxy-D-arabinose could be used just as well for the same compound. Thus, the nomenclature recommended by the IUPAC for 2-deoxy-aldoses is used throughout the following chapters: *erythro*-D-pentosylamine (D-*ery*-dPent1N) refers to 2-deoxy-D-ribosylamine, *arabino*-D-hexosylamine (D-*ara*-dHex1N) to 2-deoxy-D-glucosylamine and *lyxo*-D-pentosylamine (D-*lyx*-dHex1N) to 2-deoxy-D-galactosylamine.

2.1.3.1. *N*-Alkyl-2-deoxy-D-*erythro*-pentosylamines

The *N*-alkyl-2-deoxy-D-*erythro*-pentosylamines depicted in figure 2.12 were synthesized through the reaction of 2-deoxy-D-*erythro*-pentose with the corresponding alkylamine in methanolic or ethanolic solution. D-*ery*-dPent1NMe and D-*ery*-dPent1NEt were obtained as gelatinous substances, while D-*ery*-dPent1NPr, D-*ery*-dPent1N*i*Pr and D-*ery*-dPent1N*t*Bu could be isolated as solids. Although the compounds showed no apparent signs of susceptibility towards hydrolysis, they were preventively stored under inert gas atmosphere at $-20\text{ }^{\circ}\text{C}$.

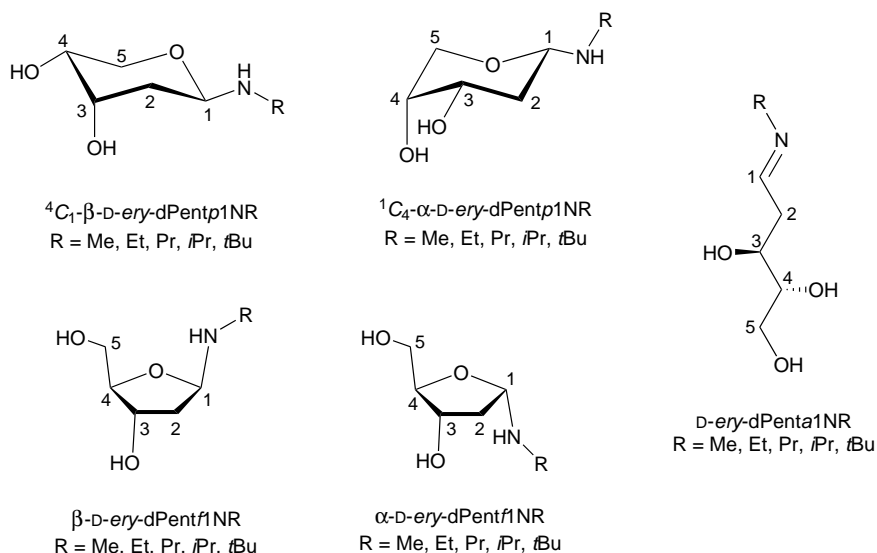


Figure 2.12. In D_2O and $\text{DMSO-}d_6$ detected isomers of the synthesized *N*-alkyl-2-deoxy-D-*erythro*-pentosylamines.

As can be seen in table 2.28, the synthesized *N*-alkyl-2-deoxy-D-*erythro*-pentosylamines exhibit a

broad variety of isomers in aqueous solution as well as in DMSO. The pyranoid β -anomer prevails in water for all compounds, in the case of *D-ery*-dPent1N*t*Bu it is the sole detected isomer. In contrast, the ratio between both pyranoid anomers appears more balanced in DMSO for most *N*-alkyl-2-deoxy-*D-erythro*-pentosylamines. Due to the superposition of the numerous signals of the different isomers in the ^1H NMR spectra no definite assignment regarding the coupling constants was feasible. Nevertheless, a preference of the 4C_1 conformation for the β -pyranosylamine and of the 1C_4 conformation for the α -pyranosylamine was assumed since both conformations feature two substituents, including the alkylamino moiety, in equatorial position. The $^{13}\text{C}\{^1\text{H}\}$ NMR chemical shifts of the carbohydrate scaffold and of the $\text{C}\alpha$ atom of the alkylamino group of all *N*-alkyl-2-deoxy-*D-erythro*-pentopyranosylamines are listed in table 2.29.

Table 2.28. Percentage distribution of the different isomers of the synthesized *N*-alkyl-2-deoxy-*D-erythro*-pentosylamines from ^1H or $^{13}\text{C}\{^1\text{H}\}$ NMR spectra measured in D_2O and in $\text{DMSO-}d_6$ at room temperature.

	D_2O				$\text{DMSO-}d_6$				
	βp	αp	βf	αf	βp	αp	βf	αf	a
<i>D-ery</i> -dPent1NMe	53	24	14	9	30	35	16	13	6
<i>D-ery</i> -dPent1NEt	64	24	8	4	30	33	17	14	6
<i>D-ery</i> -dPent1NPr	65	22	11	2	76	6	8	6	4
<i>D-ery</i> -dPent1N <i>i</i> Pr	62	24	12	2	31	39	13	11	6
<i>D-ery</i> -dPent1N <i>t</i> Bu	100	0	0	0	50	11	17	11	11

Table 2.29. Selected $^{13}\text{C}\{^1\text{H}\}$ NMR chemical shifts (δ/ppm) of the *N*-alkyl-2-deoxy-*D-erythro*-pentopyranosylamines in D_2O or in $\text{DMSO-}d_6$ (*).

	C1	C2	C3	C4	C5	$\text{C}\alpha$
β - <i>D-ery</i> -dPent <i>p</i> 1NMe	88.0	34.1	67.6	68.5	67.9	31.1
β - <i>D-ery</i> -dPent <i>p</i> 1NEt	86.5	34.3	67.5	68.5	67.9	39.4
β - <i>D-ery</i> -dPent <i>p</i> 1NPr	86.9	34.2	67.5	68.5	67.5	47.0
β - <i>D-ery</i> -dPent <i>p</i> 1N <i>i</i> Pr	84.0	34.7	67.6	68.6	67.9	44.0
β - <i>D-ery</i> -dPent <i>p</i> 1N <i>t</i> Bu	82.4	36.8	66.9	68.3	65.4	49.6
α - <i>D-ery</i> -dPent <i>p</i> 1NMe	85.1	35.6	66.5	67.6	63.6	31.2
α - <i>D-ery</i> -dPent <i>p</i> 1NEt	83.4	35.9	66.7	67.5	63.7	39.5
α - <i>D-ery</i> -dPent <i>p</i> 1NPr	83.8	36.0	66.7	67.5	63.7	47.1
α - <i>D-ery</i> -dPent <i>p</i> 1N <i>i</i> Pr	80.9	36.7	66.9	67.5	63.9	44.1
α - <i>D-ery</i> -dPent <i>p</i> 1N <i>t</i> Bu*	79.4	39.1	66.7	67.3	63.6	49.6

Next to the pyranoid isomers, noticeable amounts of both furanoid anomers were detected in water and in DMSO. The β -furanosylamine anomer prevails in water for all investigated compounds, except for *D-ery*-dPent1N*t*Bu for which no furanoid forms were detected. The detected amount of α -furanosylamine decreases in water with increasing steric demand of the alkylamino moiety. This observation does not apply in DMSO, where the ratio between both furanoid anomers is more balanced. The $^{13}\text{C}\{^1\text{H}\}$ NMR chemical shifts of the carbohydrate scaffold and of the $\text{C}\alpha$ atom of the alkylamino group for all *N*-alkyl-2-deoxy-*erythro*-*D*-pentopyranosylamines are listed

in table 2.30.

Table 2.30. Selected $^{13}\text{C}\{^1\text{H}\}$ NMR chemical shifts (δ/ppm) of the *N*-alkyl-2-deoxy-*erythro*-D-pentofuranosylamines in D_2O or in $\text{DMSO-}d_6$ (*).

	C1	C2	C3	C4	C5	Cα
β -D- <i>ery</i> -dPentf1NMe	92.5	39.3	72.2	85.9	62.9	31.5
β -D- <i>ery</i> -dPentf1NEt	91.0	40.6*	72.2	86.0	62.9	39.2
β -D- <i>ery</i> -dPentf1NPr	91.4	40.5*	72.2	85.9	62.9	47.7
β -D- <i>ery</i> -dPentf1NiPr	88.6	41.2	72.2	86.1	62.9	45.3
β -D- <i>ery</i> -dPentf1NtBu*	86.5	42.1	71.1	85.9	62.9	49.5
α -D- <i>ery</i> -dPentf1NMe	91.9	39.3	71.5	84.5	62.1	31.5
α -D- <i>ery</i> -dPentf1NEt	90.3	40.2*	71.4	84.4	62.1	39.7
α -D- <i>ery</i> -dPentf1NPr	90.6	40.2*	71.5	84.4	62.1	47.2
α -D- <i>ery</i> -dPentf1NiPr	87.7	40.5	71.5	84.4	62.2	44.5
α -D- <i>ery</i> -dPentf1NtBu*	86.3	41.5	70.8	84.1	62.1	49.7

It is noteworthy that a fifth species in addition to the furanoid and pyranoid anomers is present in the NMR spectra of all synthesized *N*-alkyl-2-deoxy-*erythro*-D-pentosylamines in DMSO. These species are identified as the corresponding open-chain forms by their prominent signals in the downfield region of the ^1H NMR and $^{13}\text{C}\{^1\text{H}\}$ NMR assigned to the imine function. The $^{13}\text{C}\{^1\text{H}\}$ NMR chemical shifts of the carbohydrate scaffold and of the C α atom of the alkylamino group for the detected acyclic *N*-alkyl-2-deoxy-*erythro*-D-pentosylamines are listed in table 2.31.

Table 2.31. Selected $^{13}\text{C}\{^1\text{H}\}$ NMR chemical shifts (δ/ppm) of the detected open-chain form for *N*-alkyl-2-deoxy-*erythro*-D-pentosylamines in $\text{DMSO-}d_6$.

	C1	C2	C3	C4	C5	Cα
D- <i>ery</i> -dPenta1NMe	165.3	39.0	69.5	74.6	63.2	47.4
D- <i>ery</i> -dPenta1NEt	163.2	38.9	69.6	74.6	63.2	54.7
D- <i>ery</i> -dPenta1NPr	163.7	38.8	69.6	74.6	63.2	62.3
D- <i>ery</i> -dPenta1NiPr	161.1	42.2	69.6	74.6	63.2	63.9
D- <i>ery</i> -dPenta1NtBu	158.0	39.2	69.7	74.6	63.1	56.4

2.1.3.2. *N*-Alkyl-2-deoxy-D-*arabino*-hexosylamines

The reaction of 2-deoxy-D-*arabino*-hexose with alkylamines yielded the in figure 2.13 depicted *N*-alkyl-2-deoxy-D-*arabino*-hexosylamines. All products were isolated as white solids, which showed no apparent signs of hydrolysis and decomposition when stored at 4 °C under inert gas atmosphere or upon short exposure to air.

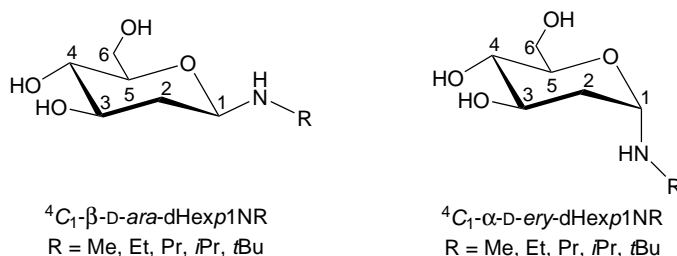


Figure 2.13. In D₂O and DMSO-*d*₆ detected isomers of the synthesized *N*-alkyl-2-deoxy-D-*arabino*-hexosylamines.

As can be seen in table 2.32, all investigated *N*-alkyl-2-deoxy-D-*arabino*-hexosylamines exhibited a clear prevalence of the β -pyranosylamine anomer in aqueous solution and in DMSO. The NMR spectra in D₂O also reveal notable amounts of hydrolysis products for all investigated *N*-alkyl-2-deoxy-D-*arabino*-hexosylamines due to the poor solubility of the compounds in water. This behavior culminates in the sole presence of 2-deoxy-D-*arabino*-hexosylamine and *tert*-butylamine in the NMR spectra of D-*ara*-dHex1N*t*Bu in D₂O. The ¹³C{¹H} NMR chemical shifts of the carbohydrate scaffold and of the C α atom of the alkylamino group for all *N*-alkyl-2-deoxy-D-*arabino*-hexopyranosylamines are listed in table 2.33.

Table 2.32. Percentage distribution of the different configurations of the synthesized *N*-alkyl-2-deoxy-D-*arabino*-D-hexosylamines measured in ¹H or ¹³C{¹H} NMR spectra in D₂O and in DMSO-*d*₆ at room temperature.

	D ₂ O		DMSO- <i>d</i> ₆	
	βp	αp	βp	αp
D- <i>ara</i> -dHex1NMe	85	15	81	19
D- <i>ara</i> -dHex1NEt	87	13	83	17
D- <i>ara</i> -dHex1NPr	88	12	83	17
D- <i>ara</i> -dHex1N <i>i</i> Pr	89	11	85	15
D- <i>ara</i> -dHex1N <i>t</i> Bu	hydrolysis		88	12

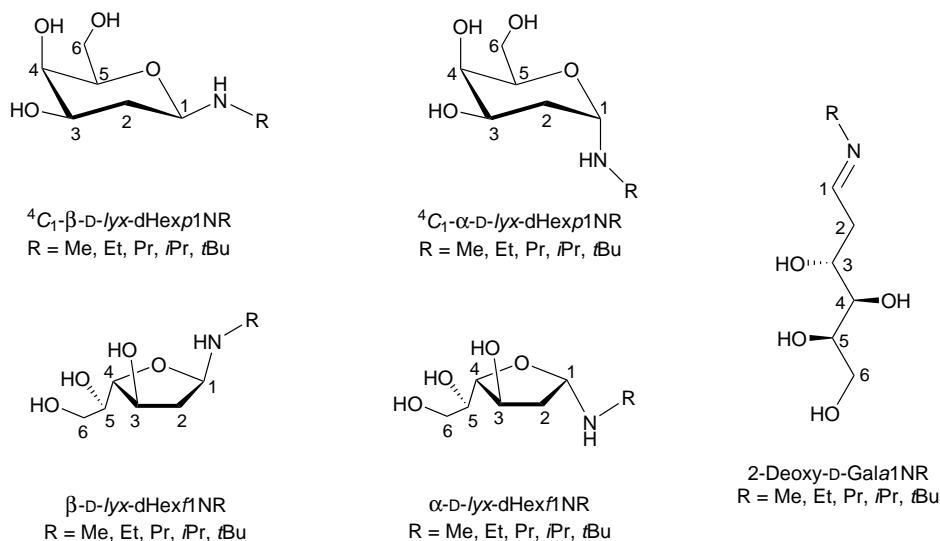
The ¹³C{¹H} NMR chemical shifts of the carbohydrate scaffold and of the C α atom of the alkylamino group for all *N*-alkyl-2-deoxy-D-*arabino*-hexopyranosylamines are listed in table 2.33.

Table 2.33. Selected $^{13}\text{C}\{^1\text{H}\}$ NMR chemical shifts (δ/ppm) of the *N*-alkyl-2-deoxy-*arabino*-D-hexosylamines in D_2O or in $\text{DMSO}-d_6$ (*).

	C1	C2	C3	C4	C5	C6	C α
β -D- <i>ara</i> -dHexp1NMe	87.5	38.6	71.9	71.9	77.6	61.7	31.1
β -D- <i>ara</i> -dHexp1NEt	86.0	38.8	72.0	71.9	77.7	61.8	39.5
β -D- <i>ara</i> -dHexp1NPr	86.4	38.9	72.0	71.9	77.7	61.8	47.2
β -D- <i>ara</i> -dHexp1 <i>i</i> Pr	83.8	39.4	72.1	72.0	77.7	61.7	43.1
β -D- <i>ara</i> -dHexp1 <i>t</i> Bu*	82.6	41.4	72.3	72.0	77.4	61.8	49.6
α -D- <i>ara</i> -dHexp1NMe	85.2	36.4	68.8	71.8	72.0	61.5	30.8
α -D- <i>ara</i> -dHexp1NEt	83.6	37.6	68.8	71.8	72.1	61.5	39.2
α -D- <i>ara</i> -dHexp1NPr	83.8	37.7	68.9	71.9	72.1	61.5	46.9
α -D- <i>ara</i> -dHexp1 <i>i</i> Pr	81.1	37.8	68.8	71.9	72.1	61.6	43.8
α -D- <i>ara</i> -dHexp1 <i>t</i> Bu*	79.2	39.1	68.2	70.4	72.8	61.4	49.6

2.1.3.3. *N*-Alkyl-2-deoxy-*lyxo*-D-hexosylamines

The treatment of 2-deoxy-*lyxo*-D-hexose with various alkylamines yielded the *N*-alkyl-2-deoxy-D-*lyxo*-hexosylamines depicted in figure 2.14. All compounds were obtained as syrup-like residues, which could be solidified for a short time when they were frozen in liquid nitrogen. In this state the compounds showed severe signs of hygroscopicity. Due to their sensitivity, all *N*-alkyl-2-deoxy-D-*lyxo*-hexosylamines were stored under inert gas atmosphere at -20°C .

Figure 2.14. In D_2O and $\text{DMSO}-d_6$ detected isomers of the synthesized *N*-alkyl-2-deoxy-D-*lyxo*-hexosylamines.

In comparison to their C4 epimers, *N*-alkyl-2-deoxy-D-*lyxo*-hexosylamines exhibit a greater variety of isomers in aqueous solution. As can be seen in table 2.34, for D-*lyx*-dHex1NMe and D-*lyx*-dHex1NEt all furanoid and pyranoid anomers are detected collectively in solution. However, with increasing steric demand of the alkylamino function the amount of furanoid forms and the α -pyranosylamine anomer detected in noticeably decreases. This trend was not observed

in the respective NMR spectra in DMSO- d_6 , in which even small concentrations of the acyclic imine form are visible.

Table 2.34. Percentage distribution of the different configurations of the synthesized *N*-alkyl-2-deoxy-D-*lyxo*-hexosylamines measured in ^1H or $^{13}\text{C}\{^1\text{H}\}$ NMR spectra in D_2O and in DMSO- d_6 at room temperature.

	D_2O				DMSO- d_6				
	βp	αp	βf	αf	βp	αp	βf	αf	a
D- <i>lyx</i> -dHex1NMe	62	16	14	8	52	12	20	12	4
D- <i>lyx</i> -dHex1NEt	75	13	9	3	54	12	20	10	4
D- <i>lyx</i> -dHex1NPr	85	11	4	0	48	18	21	13	0
D- <i>lyx</i> -dHex1N <i>i</i> Pr	96	2	2	0	48	12	22	14	4
D- <i>lyx</i> -dHex1N <i>t</i> Bu		hydrolysis			36	15	25	15	9

The $^{13}\text{C}\{^1\text{H}\}$ NMR chemical shifts measured for the carbohydrate scaffold and for the C α atom of the alkylamino group of all *N*-alkyl-2-deoxy-D-*lyxo*-hexosylamines are listed in table 2.35 for the pyranoid isomers, in table 2.36 for the furanoid isomers and in table 2.37 for the respective imine forms.

Table 2.35. Selected $^{13}\text{C}\{^1\text{H}\}$ NMR chemical shifts (δ/ppm) of the *N*-alkyl-2-deoxy-D-*lyxo*-hexopyranosylamines in D_2O or in DMSO- d_6 (*).

	C1	C2	C3	C4	C5	C6	C α
β -D- <i>lyx</i> -dHexp1NMe	87.9	34.2	67.7	69.2	76.8	62.2	31.1
β -D- <i>lyx</i> -dHexp1NEt	86.3	34.4	67.7	69.2	76.8	62.2	39.4
β -D- <i>lyx</i> -dHexp1NPr	86.8	34.4	67.7	69.3	76.9	62.3	47.1
β -D- <i>lyx</i> -dHexp1N <i>i</i> Pr	83.8	34.9	67.8	69.3	76.9	62.3	43.7
β -D- <i>lyx</i> -dHexp1N <i>t</i> Bu*	83.4	37.2	67.0	69.6	76.3	61.3	50.1
α -D- <i>lyx</i> -dHexp1NMe	85.3	31.7	65.5	68.2	69.1	62.3	31.0
α -D- <i>lyx</i> -dHexp1NEt	83.7	31.7	65.4	68.2	69.2	62.3	39.3
α -D- <i>lyx</i> -dHexp1NPr	84.0	31.7	65.5	68.2	69.3	62.3	47.1
α -D- <i>lyx</i> -dHexp1N <i>i</i> Pr	81.0	32.8	65.3	68.2	69.3	62.4	43.6
α -D- <i>lyx</i> -dHexp1N <i>t</i> Bu*	80.0	34.6	65.4	68.0	69.1	61.1	50.0

Table 2.36. Selected $^{13}\text{C}\{^1\text{H}\}$ NMR chemical shifts (δ/ppm) of the *N*-alkyl-2-deoxy-D-*lyxo*-hexopyranosylamines in D_2O or in $\text{DMSO-}d_6$ (*).

	C1	C2	C3	C4	C5	C6	C α
β -D- <i>lyx</i> -dHexf1NMe	92.7	40.3	72.1	85.9	70.5	63.5	31.8
β -D- <i>lyx</i> -dHexf1NEt	91.2	40.6	72.2	85.9	70.5	63.6	40.4
β -D- <i>lyx</i> -dHexf1NPr	91.8	40.6	72.3	86.1	70.6	63.6	48.2
β -D- <i>lyx</i> -dHexf1NiPr	88.3	41.1	72.3	86.1	70.6	63.6	45.3
β -D- <i>lyx</i> -dHexf1NtBu*	86.7	43.3	72.3	85.7	71.8	63.8	50.2
α -D- <i>lyx</i> -dHexf1NMe	92.2	39.8	73.1	84.0	72.0	61.6	31.1
α -D- <i>lyx</i> -dHexf1NEt	90.6	40.0	73.1	83.8	72.0	63.6	40.4
α -D- <i>lyx</i> -dHexf1NPr*	90.4	40.8	71.6	83.5	71.2	63.1	47.1
α -D- <i>lyx</i> -dHexf1NiPr*	87.9	41.2	71.6	83.4	71.3	63.1	43.8
α -D- <i>lyx</i> -dHexf1NtBu*	87.0	42.8	71.9	83.4	71.2	63.8	50.2

Table 2.37. Selected $^{13}\text{C}\{^1\text{H}\}$ NMR chemical shifts (δ/ppm) of the detected open-chain form for *N*-alkyl-2-deoxy-D-*lyxo*-hexosylamines in $\text{DMSO-}d_6$.

	C1	C2	C3	C4	C5	C6	C α
D- <i>lyx</i> -dHexa1NMe	165.5	39.9	69.9	68.6	72.9	63.0	47.4
D- <i>lyx</i> -dHexa1NEt	163.2	36.2	69.1	68.7	72.9	63.0	54.8
D- <i>lyx</i> -dHexa1NiPr	161.2	40.0	69.9	68.7	72.9	63.0	60.5
D- <i>lyx</i> -dHexa1NtBu	158.6	40.5	70.3	69.3	73.4	63.5	56.8

2.1.4. *N*-Phenylglycosylamines

N-Phenylglycosylamines differ considerably from the previously described *N*-alkylglycosylamines regarding their chemical properties. In the first place, *N*-phenylglycosylamines are much more stable since they show no signs of hydrolysis. They can be readily synthesized by heating the corresponding glucose with aniline in methanol. Although aniline has a nucleophilicity comparable to aliphatic amines,^[42] further activation through the addition of catalytic amounts of acid is required for most reactions. Upon cooling the reaction solution the desired products precipitated or crystallized in good yields. Reactions for the synthesis of *N*-aryl glycosylamines are known for a long time and commonly described in the literature.^[43,44] Surprisingly, the only crystal structures of *N*-phenylglycosylamines yet reported are *N*-phenyl- β -D-mannopyranosylamine and *N*-phenyl- β -D-galactopyranosylamine.^[45,46]

The glycoses used as reactants in this chapter include aldopentoses (D-arabinose, D-lyxose, D-ribose, D-xylose), aldohexoses (D-glucose, L-gulose, D-mannose) and 2-deoxy-D-glycoses (2-deoxy-D-*erythro*-pentose, 2-deoxy-D-*arabino*-hexose, 2-deoxy-D-*lyxo*-hexose).

2.1.4.1. *N*-Phenylpentosylamines

The treatment of D-aldopentoses with aniline led to the formation of D-Ara1NPh, D-Lyx1NPh, D-Rib1NPh and D-Xyl1NPh (depicted in figure 2.15) in good yields and purity. In the case of D-Lyx1NPh, D-Rib1NPh and D-Xyl1NPh crystals suitable for X-ray diffraction were obtained from the respective reaction solutions. All aforementioned compounds proved to be relatively

stable, even when exposed to air. Hence, the compounds could be stored at 4 °C for months without showing any signs of decomposition.

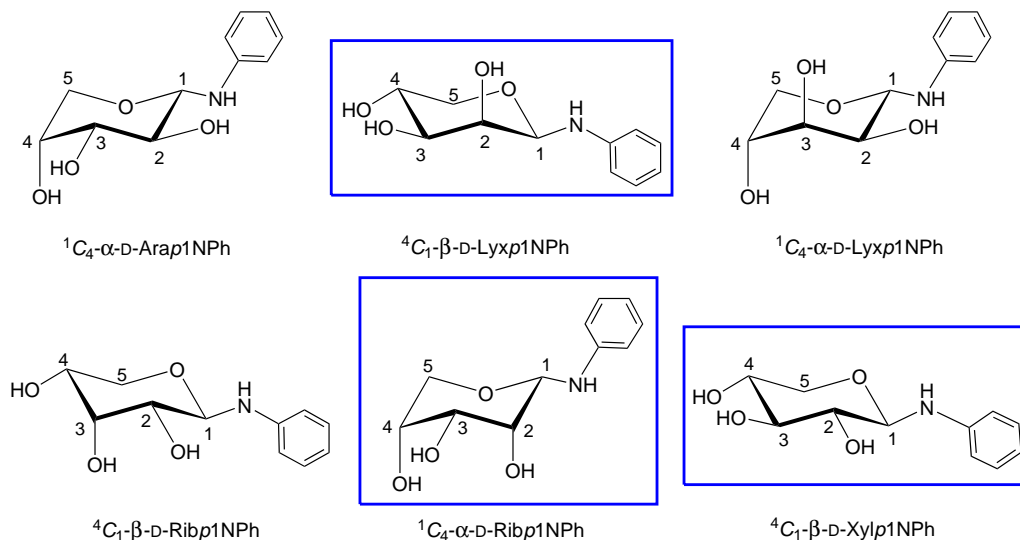


Figure 2.15. In D₂O or solid state detected isomers of the synthesized *N*-phenyl-D-pentosylamines. The structures of the blue-framed isomers are confirmed by X-ray analysis (**3**, **4**, **5**).

As listed in table 2.38, only pyranoid isomers are detected in aqueous solution for the synthesized *N*-phenyl-D-xylosylamines. D-Lyx1NPh is the only compound to show an balanced equilibrium between both anomers, while for the other compounds one anomer is clearly prevailing in water. But as can be seen on the example of D-Rib1NPh, this does not necessarily mean that the other anomer is nonexistent: While there is no evidence found for the presence of α -D-Rib1NPh in the respective NMR spectrum in D₂O, it is the predominant anomer in DMSO-*d*₆ and the featured configuration in crystal structure **4**. This observation can be attributed to the fact that one anomer exhibits a better water solubility than the other. And since all *N*-phenyl-D-pentosylamines are poorly soluble in water at room temperature, this characteristic can lead to a clear preference of one anomer in water as well as to disproportionate amounts of the highly soluble hydrolysis product in the NMR spectra. In DMSO on the other hand distributions comparable to those of the *N*-alkyl-D-pentosylamines previously reported in chapter 2.1.1 were found. Notable amounts of furanoid isomers were only detected for D-Lyx1NPh and D-Rib1NPh in DMSO.

Table 2.38. Percentage distribution of the different isomers of the synthesized *N*-phenyl-D-pentosylamines detected in ¹H or ¹³C{¹H} NMR spectra in D₂O and in DMSO-*d*₆ at room temperature.

	D ₂ O		DMSO- <i>d</i> ₆			
	αp	βp	αp	βp	αf	βf
D-Ara1NPh	100	0	37	31	21	11
D-Lyx1NPh	42	58	45	55	0	0
D-Rib1NPh	0	100	31	37	11	21
D-Xyl1NPh	8	92	0	100	0	0

The measured ³J_{1,2} value of 8.6 Hz matches the favored ¹C₄ conformation for α -D-Ara1NPh,

while the values of 8.9 Hz and 8.7 Hz verify the presence the β -anomers for β -D-Rib1NPh and β -D-Xyl1NPh in their 4C_1 conformation. The detected small amounts of 4C_1 - α -D-Xyl1NPh correlate with the measured ${}^3J_{1,2}$ coupling constant of 4.2 Hz. In the case of α -D-Ara1NPh the high experimental ${}^3J_{1,2}$ value of 8.0 Hz indicates that there is almost no dynamic fluctuation between the 1C_4 and 4C_1 conformation as exhibited by the corresponding *N*-alkyl- α -D-lyxosylamines, described in chapter 2.1.1.2. 4C_1 - β -D-Lyx1NPh was identified by its characteristically small ${}^3J_{1,2}$ value of 1.3 Hz. The ${}^{13}C\{^1H\}$ NMR shifts assigned to the carbohydrate scaffold and the *ipso* carbon atom of the *N*-phenyl-D-pentosylamines are listed in table 2.39.

Table 2.39. Selected ${}^{13}C\{^1H\}$ and ${}^{15}N$ NMR chemical shifts (δ /ppm) of the detected *N*-phenyl-D-pentopyranosylamines in D_2O at 4 °C or in $DMSO-d_6$ at room temperature(*).

	C1	C2	C3	C4	C5	C _i	N
α -D-Arap1NPh	86.1	70.9	73.9	69.5	67.6	146.3	-302.5
β -D-Arap1NPh*	79.6	70.4	70.6	64.8	63.3	146.6	-304.8
β -D-Lyxp1NPh	82.7	71.1	74.3	67.1	66.3	145.3	-304.7
α -D-Lyxp1NPh	82.8	68.7	71.1	69.7	65.1	146.2	-303.5
β -D-Ribp1NPh	81.5	70.5	69.8	66.7	62.0	145.0	-303.8
α -D-Ribp1NPh*	81.7	70.1	69.8	67.8	62.9	173.3	-296.9
β -D-Xylp1NPh	86.2	73.2	77.5	70.0	66.4	146.1	-302.5
α -D-Xylp1NPh	82.1	70.8	72.6	69.7	62.3	146.0	-310.5

The presence of 4C_1 - β -D-Lyx1NPh in solution was verified by X-ray diffraction studies on the colorless platelet-like crystals obtained from the methanolic reaction solution. The structure presented in figure 2.16 was solved in the orthorhombic space group $P2_12_12_1$ and displays the asymmetric unit containing one *N*-phenyl- β -D-lyxosylamine molecule in its 4C_1 conformation (**3**). No further molecules are included the asymmetric unit and the phenylamino substituent appears slightly disordered. The hydrogen bonds present in the structure are listed in table 2.40.

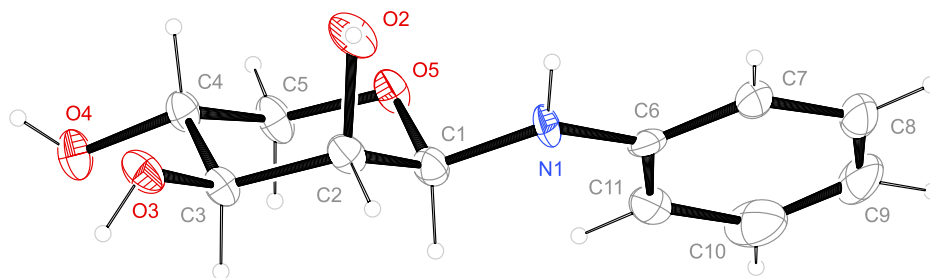


Figure 2.16. The molecular structure of the 4C_1 - β -D-Lyx1NPh molecule in **3**. ORTEP plot is drawn with 50 % probability ellipsoids. Interatomic distances (\AA) and angles ($^\circ$) (standard deviations of the last digit in parentheses, values for disordered atoms are averaged and without deviations): C1-N1 1.402, N1-C6 1.401, O5-C1 1.4529(19), C1-C2 1.519(2), C1-O2 1.421(2), C1-N1-C6 125.5, O5-C1-N1 108.9, C2-C1-N1 111.7, C2-C1-O5 109.81(13), O2-C2-C1 108.31(13), O2-C2-C3 111.40(13); puckering parameters^[40] of the pyranose ring O5-C1-C2-C3-C4-C5: $Q = 0.5658(17)$ \AA , $\theta = 3.24(18)^\circ$, $\phi = 278(3)^\circ$.

Table 2.40. Distances in Å and angles in ° of the hydrogen bonds in **3**. Standard deviations of the last digit are given in parentheses; values without standard deviation are related to hydrogen atoms at calculated positions. Symmetry codes are given as footnotes at the bottom of the table. D: donor, A: acceptor.

D	H	A	D–H	H...A	D...A	D–H...A
O3	H83	O5 ⁱ	0.84	1.87	2.7019(16)	168
O4	H84	O3 ⁱⁱ	0.84	1.88	2.6757(16)	159
O2	H82	O4 ⁱⁱⁱ	0.84	1.96	2.7760(16)	162
N1	H71	O2	0.84	2.39	2.688(14)	102

ⁱ $x + 1, y, z$; ⁱⁱ $-x + 3, y + 1/2, -z + 1/2$; ⁱⁱⁱ $x, y - 1, z$

Only the β -anomer of D-Rib1NPh was NMR-spectroscopically detected in aqueous solution, but the corresponding α -anomer was obtained as colorless platelet-like crystals from the methanolic reaction solution. These findings indicate that the α -D-Rib1NPh has significantly lower solubility than the respective β -anomer in methanol and water. The crystal structure was solved in the orthorhombic space group $P2_12_12_1$ and its asymmetric unit contains two *N*-phenyl- β -D-ribosylamines molecule in 1C_4 conformation and an additional water molecule (**4**). The structure of one comprised 1C_4 - α -D-Rib1NPh molecule is depicted in figure 2.17. Since the X-ray crystal diffraction measurement on **4** was conducted at room temperature, the probability ellipsoids appear larger than in previously displayed ORTEP plots. The hydrogen bonds present in the structure are listed in table 2.41.

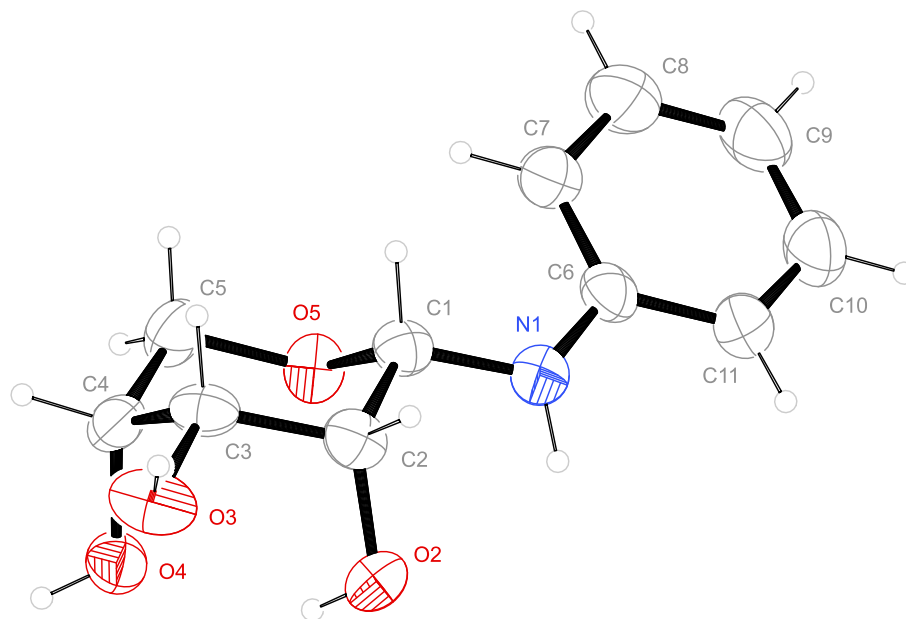


Figure 2.17. The molecular structure of the 1C_4 - α -D-Rib1NPh molecule in **4**. ORTEP plot is drawn with 50 % probability ellipsoids. Averaged interatomic distances (Å) and angles (°): C1–N1 1.409, N1–C7 1.394, O5–C1 1.448, C1–C2 1.523, C2–O2 1.423, C1–N1–C7 122.2, O5–C1–N1 108.8, C2–C1–N1 112.1, C2–C1–O5 109.4, O2–C2–C1 110.8, O2–C2–C3 109.4 ; averaged puckering parameters^[40] of the pyranose rings O5–C1–C2–C3–C4–C5: $Q = 0.581$ Å, $\theta = 357^\circ$, $\phi = 226^\circ$.

Table 2.41. Distances in Å and angles in ° of the hydrogen bonds in **4**. Standard deviations of the last digit are given in parentheses; values without standard deviation are related to hydrogen atoms at calculated positions. Symmetry codes are given as footnotes at the bottom of the table. D: donor, A: acceptor.

D	H	A	D–H	H···A	D···A	D–H···A
O21	H821	O41	0.82	2.06	2.756(3)	143
O22	H822	O21	0.82	2.26	3.040(3)	158
O31	H831	O51 ⁱ	0.82	1.86	2.683(3)	162
O32	H832	O21 ⁱ	0.82	2.05	2.838(3)	161
O41	H841	O91 ⁱⁱ	0.82	1.94	2.737(3)	165
O42	H842	O31 ⁱⁱⁱ	0.82	1.92	2.735(3)	171
N11	H711	O21	0.86(3)	2.48(3)	2.835(4)	106(2)
N12	H712	O32 ^{iv}	0.81(3)	2.21(4)	3.021(3)	177(3)
O91	H911	O52 ⁱⁱ	0.87(5)	1.95(5)	2.819(3)	175(5)
O91	H912	O42 ⁱⁱⁱ	0.90(5)	1.84(5)	2.729(3)	169(4)

ⁱ $x+1, y, z$; ⁱⁱ $-x+1, y-1/2, -z+1/2$; ⁱⁱⁱ $-x+2, y+1/2, -z+1/2$;
^{iv} $-x+2, y+1/2, -z+1/2$; ^v $-x+2, y-1/2, -z+1/2$

Furthermore, crystals of D-Xyl1NPh suitable for X-ray diffraction studies were obtained from the respective reaction solution. The structure was solved in the triclinic space group $P1$. The determined asymmetric unit consists of four molecules of *N*-phenyl- β -D-xylopyranosylamine in the 4C_1 conformation without including any other molecules (**5**). One exemplary 4C_1 - β -D-Xyl1NPh molecule from the crystal structure is displayed in figure 2.18. This crystallographic finding is in accordance with the previously mentioned NMR-spectroscopic results showing a clear preference of the β -anomer for D-Xyl1NPh in all solvents. The hydrogen bonds present in the structure are listed in table 2.42.

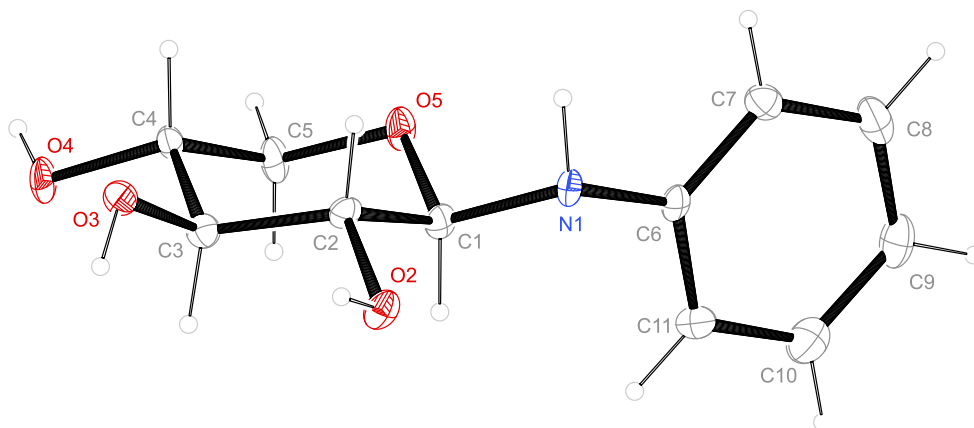


Figure 2.18. The molecular structure of a β -D-Xyl1NPh- 4C_1 molecule in **5**. ORTEP plot is drawn with 50% probability ellipsoids. Averaged interatomic distances (Å) and angles (°): O5–C1 1.447, C1–C2 1.525, C1–N1 1.418, N1–C7 1.409, C2–O2 1.427, C1–N1–C7 121.2, O5–C1–N1 109.9, O2–C2–C1 108.4, O2–C2–C3 109.4, C2–C1–N1 109.9, O5–C1–C2 108.6; averaged puckering parameters^[40] of the pyranose rings O5–C1–C2–C3–C4–C5: $Q = 0.585$ Å, $\theta = 9.6^\circ$, $\phi = 293^\circ$.

Table 2.42. Distances in Å and angles in ° of the hydrogen bonds in **5**. Standard deviations of the last digit are given in parentheses; values without standard deviation are related to hydrogen atoms at calculated positions. Symmetry codes are given as footnotes at the bottom of the table. D: donor, A: acceptor.

D	H	A	D–H	H···A	D···A	D–H···A
O21	H821	O31	0.84	2.59	2.896(4)	103
O21	H821	O44 ⁱ	0.84	1.95	2.780(4)	168
O22	H822	N12	0.84	2.55	2.883(4)	105
O23	H823	O42 ⁱⁱ	0.84	2.01	2.835(4)	165
O24	H824	O32 ⁱⁱ	0.84	1.83	2.668(4)	171
O31	H831	O24 ⁱⁱⁱ	0.84	1.94	2.711(4)	151
O32	H832	O43	0.84	1.93	2.734(4)	160
O33	H833	O22	0.84	1.93	2.733(4)	159
O34	H834	O22	0.84	2.09	2.712(4)	131
O41	H841	O34 ⁱⁱⁱ	0.84	2.12	2.737(4)	130
O42	H842	O51	0.84	2.12	2.955(4)	172
O43	H843	O23 ^{iv}	0.84	2.57	2.924(4)	106
O43	H843	N13 ^{iv}	0.84	2.14	2.969(4)	170
O44	H844	O24 ^{iv}	0.84	2.37	3.186(3)	163
N11	H711	O33	0.85(6)	3.053(5)	3.021(3)	153(5)
N12	H712	O21 ^v	0.93(6)	2.28(6)	3.124(5)	151(5)
N13	H713	O31 ⁱⁱⁱ	1.00(6)	2.18(6)	3.105(5)	154(5)
N14	H714	O23	0.92(6)	3.274(5)	3.021(3)	154(5)

ⁱ $x, y - 1, z$; ⁱⁱ $x + 1, y, z$; ⁱⁱⁱ $x - 1, y - 1, z$; ^{iv} $x - 1, y, z$;
^v $x, y + 1, z$

2.1.4.2. N-Phenylhexosylamines

The reaction of various aldohexoses with aniline led to the successful isolation of D-Glc1NPh, L-Gul1NPh and D-Man1NPh. The products were obtained in good yields and as pure, white powders. D-Man1NPh even crystallized in the respective reaction solution upon storage at 4 °C. The obtained crystals were suitable for X-ray diffraction studies and the determined structure (β -configuration and 4C_1 conformation) matched the crystal structure already published by OJALA *et al.*^[45] All synthesized compounds are stable with respect to the exposure to air and humidity and hence could be stored without additional precautions.

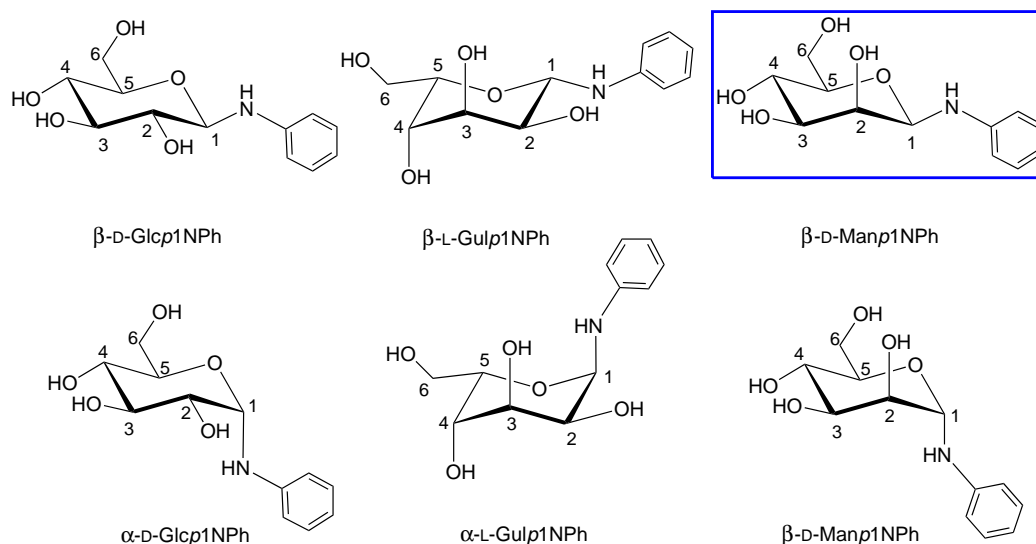


Figure 2.19. In D_2O or $DMSO-d_6$ detected isomers of the synthesized *N*-phenyl-D-hexosylamines. The structure of the blue-framed isomer is confirmed by X-ray analysis.

As can be seen in table 2.43, the β -pyranosylamine isomer clearly prevails in aqueous solution for all investigated *N*-phenylhexosylamines. The respective α -pyranosylamine isomer is only observed in small amounts for D-Glc1NPh. On the other hand the α -anomer is present in the case of all three investigated *N*-phenylhexosylamines in $DMSO$, but in a lower concentration than the corresponding β -anomer. This finding is not as unexpected as for the *N*-phenylpentosylamines, previously described in chapter 2.1.4.2, since the extra additional hydroxymethyl moiety improves the solubility in water and the corresponding *N*-alkylhexosylamines also only showed minimal or no formation of the respective α -anomers. The $^{13}C\{^1H\}$ NMR shifts assigned to the carbohydrate scaffold and the *ipso* carbon atom of the *N*-phenylhexosylamines are listed in table 2.44.

Table 2.43. Percentage distribution of the different isomers of the synthesized *N*-phenyl-D-hexosylamines detected in 1H or $^{13}C\{^1H\}$ NMR spectra in D_2O and in $DMSO-d_6$ at room temperature.

	D_2O		$DMSO-d_6$	
	βp	αp	βp	αp
D-Glc1NPh	86	14	72	28
L-Gul1NPh	100	0	84	16
D-Man1NPh	100	0	74	16

Table 2.44. Selected $^{13}\text{C}\{^1\text{H}\}$ and ^{15}N NMR chemical shifts (δ/ppm) of the detected *N*-phenyl-D-hexopyranosylamines in D_2O at 4°C or in $\text{DMSO-}d_6$ at room temperature(*).

	C1	C2	C3	C4	C5	C6	C_i	N
β -D-Glcp1NPh	85.5	73.3	77.1	70.4	77.5	61.4	146.3	-302.7
α -D-Glcp1NPh	82.7	71.1	73.5	70.6	71.0	61.2	146.6	-312.6
β -L-Gulp1NPh	82.6	68.2	71.5	70.0	74.2	61.5	145.3	-302.2
α -L-Gulp1NPh*	81.6	64.1	71.8	69.0	65.9	60.1	146.8	-306.1
β -D-Manp1NPh	83.0	71.6	74.5	67.6	77.6	61.7	145.5	-304.2
α -D-Manp1NPh*	82.7	71.3	73.5	70.7	71.2	61.1	147.7	-305.9

2.1.4.3. *N*-Phenyl-2-deoxyglycosylamines

The reaction of various 2-deoxyglycosylamines with aniline led to the successful isolation of D-*ery*-dPent1NPh, D-*ara*-dHex1NPh and D-*lyx*-dHex1NPh. While both synthesized *N*-phenyl-2-deoxyhexosylamines could be isolated as crystals, *N*-phenyl-2-deoxy-D-*erythro*-glycosylamines was obtained as a white solid. All compounds showed no signs of hydrolysis or decomposition when exposed to air, even for longer periods.

In aqueous solution all investigated *N*-phenyl-2-deoxyglycosylamines were only detected in their respective β -pyranosylamine form. All compounds exhibit a poor solubility in water and thus minimal amounts of further species could be distinguished from the signal noise in the NMR spectrum, especially if these isomers are even less soluble (as observed for the α -anomers of the *N*-phenylhexosylamines described in chapter 2.1.4.2). Due to this solubility behavior all measured NMR spectra also feature large amounts of the more soluble respective reactants, formed through the hydrolysis of the product. But also in $\text{DMSO-}d_6$ no obvious evidence for the presence of the respective α -anomers, furanoid isomers or even the imine form was found. The $^{13}\text{C}\{^1\text{H}\}$ NMR shifts assigned to the carbohydrate scaffold and the *ipso* carbon atom of the *N*-phenyl-2-deoxyglycosylamines are listed in table 2.45.

Table 2.45. Selected $^{13}\text{C}\{^1\text{H}\}$ and ^{15}N NMR chemical shifts (δ/ppm) of the detected *N*-phenyl-2-deoxyglycosylamines in D_2O or in $\text{DMSO-}d_6$ (*) at room temperature. Dashes indicate that the corresponding atom is not featured in the compound or that no matching signal was detected in the NMR spectra.

	C1	C2	C3	C4	C5	C6	C_i	N
β -D- <i>ery</i> -dPent1NPh	82.3	35.6	67.4	68.6	63.4	-	-	-294.7*
β -D- <i>ara</i> -dHex1NPh	82.0	38.7	71.8	72.0	77.3	61.7	146.3	-298.5
β -D- <i>lyx</i> -dHex1NPh	82.2	33.7	67.5	69.8	76.2	61.9	146.0	-297.6

Upon storage at 4°C brownish plate-like crystals of D-*ara*-dHex1NPh suitable for X-ray diffraction studies were obtained from the methanolic reaction solution. The structure was solved in the orthorhombic space group $P2_12_12_1$. The determined asymmetric unit consists of a single molecule of *N*-phenyl- β -D-*arabino*-hexopyranosylamine in the 4C_1 conformation without any further solvent molecules (**6**). The β -D-*ara*-dHex1NPh molecule from the crystal structure is

displayed in figure 2.20. This crystallographic finding is in accordance with the previously mentioned NMR-spectroscopic results showing a clear preference of the β -anomer. The hydrogen bonds present in the structure are listed in table 2.46.

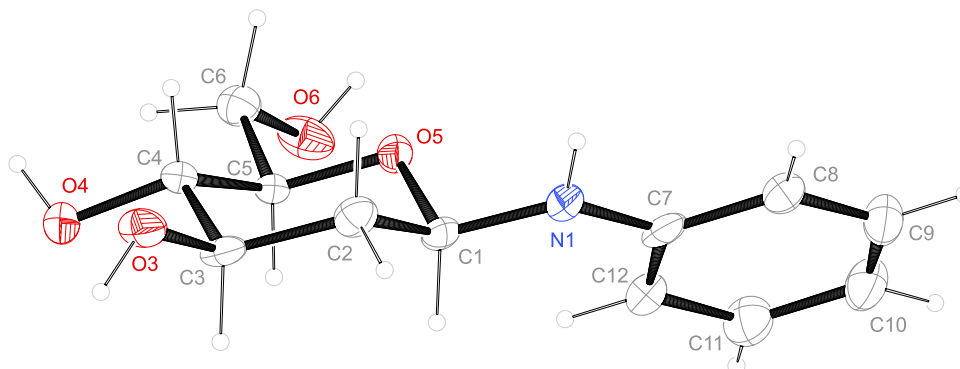


Figure 2.20. The molecular structure of the 4C_1 - β -D-*ara*-dHex1NPh molecule in **6**. ORTEP plot is drawn with 50 % probability ellipsoids. Interatomic distances (\AA) and angles ($^\circ$) (standard deviations of the last digit in parentheses): O5–C1 1.475(4), C1–C2 1.516(5), C1–N1 1.405(4), N1–C7 1.410(4), C1–N1–C7 123.3(3), N1–C1–O5 108.9(3), N1–C1–C2 113.0(3), O5–C1–C2 108.3(3); puckering parameters^[40] of the pyranose ring O5–C1–C2–C3–C4–C5: $Q = 0.581(3)$ \AA , $\theta = 5.4(3)^\circ$, $\phi = 226(4)^\circ$.

Table 2.46. Distances in \AA and angles in $^\circ$ of the hydrogen bonds in **6**. Standard deviations of the last digit are given in parentheses; values without standard deviation are related to hydrogen atoms at calculated positions. Symmetry codes are given as footnotes at the bottom of the table. D: donor, A: acceptor.

D	H	A	D–H	H \cdots A	D \cdots A	D–H \cdots A
O3	H83	O5 ⁱ	0.84	1.94	2.781(3)	178
O4	H84	O3 ⁱⁱ	0.84	1.85	2.684(3)	173
O6	H86	O4 ⁱⁱⁱ	0.84	1.89	2.723(3)	171
N1	H71	O6 ^{iv}	0.82	2.14	2.957(3)	169

ⁱ $x + 1, y, z;$ ⁱⁱ $x, y - 1, z;$ ⁱⁱⁱ $x - 1, y, z;$

^{iv} $-x + 1, y + 1/2, -z + 1/2$

Furthermore, colorless block-like crystals of D-*lyx*-dHex1NPh suitable for X-ray diffraction studies were obtained from the methanolic reaction solution at 4 $^\circ\text{C}$. The structure was solved in the orthorhombic space group $P2_12_12_1$. The determined asymmetric unit features three molecules of *N*-phenyl- β -D-*lyxo*-hexopyranosylamine in the 4C_1 conformation and an additional methanol molecule (**7**). An exemplary β -D-*lyx*-dHex1NPh molecule from the asymmetric unit is depicted in figure 2.21. This crystallographic finding is also in accordance with the previously mentioned NMR-spectroscopic results showing a clear preference of the β -anomer. The hydrogen bonds present in the structure are listed in table 2.47.

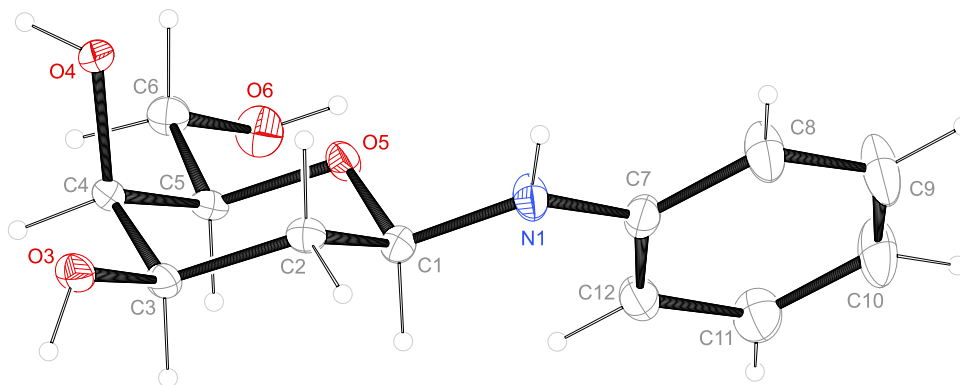


Figure 2.21. The molecular structure of the 4C_1 - β -D-*lyx*-dHex1NPh molecule in **7**. ORTEP plot is drawn with 50% probability ellipsoids. Averaged interatomic distances (\AA) and angles ($^\circ$): O5–C1 1.457, C1–C2 1.518, C1–N1 1.120, N1–C7 1.394, C1–N1–C7 123.0, N1–C1–O5 109.4, N1–C1–C2 112.9, O5–C1–C2 108.3; averaged puckering parameters^[40] of the pyranose rings O5–C1–C2–C3–C4–C5: $Q = 0.587 \text{ \AA}$, $\theta = 6.7^\circ$, $\phi = 155^\circ$.

Table 2.47. Distances in \AA and angles in $^\circ$ of the hydrogen bonds in **7**. Standard deviations of the last digit are given in parentheses; values without standard deviation are related to hydrogen atoms at calculated positions. Symmetry codes are given as footnotes at the bottom of the table. D: donor, A: acceptor.

D	H	A	D–H	H...A	D...A	D–H...A
O31	H831	O43	0.84	1.94	2.742(2)	159
O32	H832	O51 ⁱ	0.84	2.03	2.820(2)	156
O33	H833	O52 ⁱⁱ	0.84	1.99	2.825(2)	176
O41	H841	O33 ⁱⁱⁱ	0.84	1.93	2.734(3)	170
O42	H842	O32 ⁱ	0.84	1.86	2.702(2)	174
O43	H843	O31 ⁱⁱⁱ	0.84	1.88	2.692(3)	161
O61	H861	O42	0.84	1.90	3.028(3)	175
O62	H862	O41 ^{iv}	0.84	1.91	2.743(3)	175
O63	H863	O53	0.84	2.50	2.802(2)	102
O63	H863	O7	0.84	1.97	2.805(3)	172
O7	H87	–	0.84	–	–	–
N1	H71	O61 ^v	0.94(3)	2.18(3)	2.688(14)	161(3)
N2	H72	O62 ^v	0.90(3)	2.06(3)	2.943(3)	165(2)
N3	H73	O63 ^v	0.87(3)	2.04(3)	2.912(3)	179(3)

ⁱ $x + 1/2, -y + 1/2, -z + 1$; ⁱⁱ $x - 1/2, -y + 3/2, -z + 1$;

ⁱⁱⁱ $x + 1/2, -y + 3/2, -z + 1$; ^{iv} $x + 1, y, z$; ^v $x - 1, y, z$

2.2. Coordination Chemistry of *N*-Substituted Glycosylamines with Palladium(II)

In order to investigate the coordination behavior of *N*-substituted glycosylamines towards palladium(II), the previously synthesized compounds were dissolved in a solution containing a palladium(II) probe. In literature mostly dihydroxido palladium(II) complexes including a diamine auxiliary ligand are used as probes.^[38,47,48] The reagents serving as PdN₂-fragment source in this work are depicted in figure 2.22. The *C*₂ symmetry present in the auxiliary ligands prevents the formation of stereoisomers and thus facilitates the NMR-spectroscopic characterization of the obtained glycosylamin complexes.

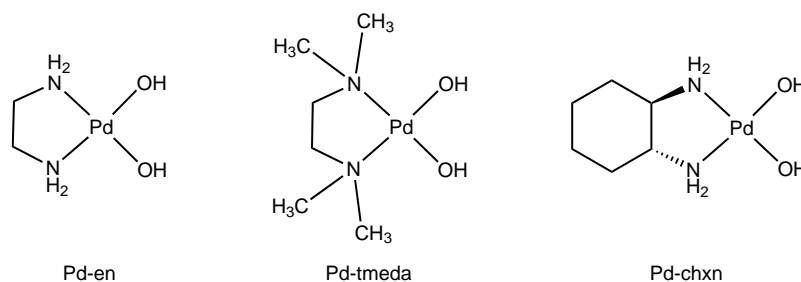


Figure 2.22. Palladium(II) reagents containing the auxiliary ligands en, tmEDA and chxn.

This work primarily features the use of Pd-en as palladium probe since in the case of Pd-en the superposition of NMR shifts of the auxiliary ligand and the coordinating glycosylamine is minimized. The NMR signals of the ethylene moiety of the auxiliary ligand ethane-1,2-diamine are usually located around 2.5 ppm in ¹H NMR spectra and around 46 ppm in ¹³C{¹H} NMR spectra. In all following illustrations of the identified glycosylamine palladium complex species, the PdN₂-fragment including the corresponding auxiliary ligand is labeled with the red symbol [Pd].

Since the hydrolysis of the glycosylamines is accelerated under alkaline conditions, stoichiometric amounts of iodic acid were added to the reaction mixtures in order to control the pH value of the resulting solutions. Despite this addition, in many cases the hydrolytic cleavage of the used glycosylamines could not be completely prevented and was analytically detected by the emergence of NMR signals assigned to the corresponding alkylamines and aldoses. A more apparent visual observation indicating a potential hydrolysis is the formation of a black precipitate or even a mirror on the glass of the reaction vessel, identified as elemental palladium. This reaction derives from the reducing character of the formed aldose and can be compared with the reaction of aldehyds with TOLLENS' reagent.

Furthermore, undesired palladium complexes featuring an aldose or an alkylamine as ligand were identified in some measured NMR spectra or even isolated as crystalline solids. All reactions and NMR-spectroscopic measurements were executed at 4 °C to reduce the hydrolysis of the ligands to a minimum level. The influence of the used glycosylamine, the manner of the *N*-substitution and the concentration of the palladium(II) reagent on the extent of the occurring hydrolysis represents another aspect of the following investigations.

The stoichiometry of the used reactants was adjusted correspondingly to allow different depro-

tonation states of the hydroxy functions of the glycosylamine. Thus, while the oxygen atoms coordinate the metal as alkoxides, the amino function serves as a neutral donor ligand in the resulting complex compounds. The exact binding mode, configuration and conformation of the glycosylamine ligands was determined by using NMR-spectroscopic methods with particular focus on the observed coordination-induced shifts (CIS) of the $^{13}\text{C}\{^1\text{H}\}$ NMR signals in the carbohydrate scaffold and alkyl or aryl substituent. The NMR spectra including the assignment of the signals to the formed complex species in all experiments described in this chapter can be found in the appendix of this work (chapter A).

2.2.1. *N*-Alkylpentosylamines

The coordination chemistry of *N*-alkylpentosylamines is largely characterized by the equilibrium of the α - and β -pyranosylamine form and the acyclic imine form in between the anomers. Contrary to palladium(II)-aldopentose complexes,^[49] no detectable coordination of furanoid forms was observed in the conducted experiments. An additional factor in the coordination chemistry of *N*-alkylpentosylamines represents the possible dynamic fluctuation between different conformations, particularly the ${}^4\text{C}_1 \rightleftharpoons {}^1\text{C}_4$ chair inversion.

2.2.1.1. *N*-Alkyl-D-arabinosylamines

In the performed reactions of the investigated *N*-alkyl-D-arabinosylamines with Pd-en in the molar ratios 1:1:1 and 1:2:1, the three complex species depicted in figure 2.23 were identified in the resulting reaction solutions.

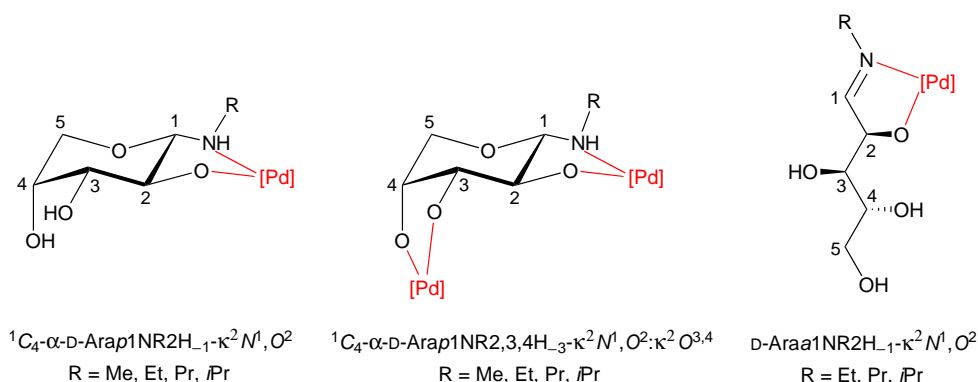


Figure 2.23. Complex species detected in reaction solutions resulting from the treatment of *N*-alkyl-D-arabinosylamines with Pd-en and iodic acid.

As can be seen in table 2.48, upon addition of one equivalent Pd-en to *N*-alkyl-D-arabinosylamines a clear preference of the ${}^1\text{C}_4\text{-}\alpha\text{-D-Arap1NR2H}_{-1}\text{-}\kappa^2\text{N}^1, \text{O}^2$ species became evident for all ligands with the exception of D-Ara1N*t*Bu. In the case of D-Ara1N*t*Bu all reaction attempts resulted in the instant hydrolysis of the ligand and subsequent complexation of D-arabinose. The $\kappa^2\text{N}^1, \text{O}^2$ chelation of the ligand's open-chain form was detected to a small extent in reaction solutions containing the ethyl-, propyl- and *iso*-propyl derivatives. The amount of additional species, mostly metalated and non-metalated hydrolysis products, detected in the reaction solutions increased with the steric demand of the featured alkylamino function.

Table 2.48. Percentage distribution of the metalated species resulting from the treatment of *N*-alkyl-D-arabinosylamines with Pd-en and iodic acid in the molar ratio 1:1:1 at 4 °C.

	Me	Et	Pr	<i>i</i> Pr
1C_4 - α -D-Arap1NR2H ₋₁ - κ^2N^1,O^2	100	82	75	76
D-Araa1NR2H ₋₁ - κ^2N^1,O^2	0	10	10	10
other species	0	8	15	14

The preferred *trans*-vicinal κ^2N^1,O^2 binding of Pd-en to α -*N*-alkyl-D-arabinosylamines was identified by the characteristic CIS values displayed in table 2.49. The present α -configuration and non-fluctuating 1C_4 conformation in the ligands in the monometalated complex species was further verified by the measured ${}^3J_{1,2}$ values, which range between 8.7 Hz to 8.9 Hz as a result of the *anti*-orientation of the hydrogen atoms. All other coupling constants determined for the complexes generally match the values previously listed in chapter 2.1.1.1 for the in water prevailing α -anomer of the free ligand. In contrast to uncomplexed *N*-alkyl-D-arabinosylamines, no evidence for a metalation of the corresponding β -anomers was found in the reaction solutions.

Table 2.49. Selected ${}^{13}C\{^1H\}$ NMR chemical shifts (δ /ppm) and shift differences ($\Delta\delta$) to the free ligand of the detected monometalated *N*-alkyl-D-arabinopyranosylamines with Pd-en in D₂O at 4 °C. The $\Delta\delta$ values indicating a CIS are printed bold.

		C1	C2	C3	C4	C5	C α
α -D-Ara1NMe	δ	92.2	70.9	73.8	69.4	67.7	31.5
1C_4 - α -D-Arap1NMe2H ₋₁	δ	94.8	77.2	75.3	69.0	70.5	36.7
κ^2N^1,O^2	$\Delta\delta$	2.6	6.3	1.5	-0.4	2.8	5.2
α -D-Ara1NEt	δ	90.8	71.2	73.8	69.4	67.7	39.9
1C_4 - α -D-Arap1NEt2H ₋₁	δ	89.9	77.0	75.4	69.0	70.5	42.2
κ^2N^1,O^2	$\Delta\delta$	-0.9	5.8	1.6	-0.4	2.8	2.3
α -D-Ara1NPr	δ	91.1	71.1	73.8	69.4	67.8	47.6
1C_4 - α -D-Arap1NPr2H ₋₁	δ	91.1	77.1	75.4	69.0	70.5	49.9
κ^2N^1,O^2	$\Delta\delta$	0.0	6.0	1.6	-0.4	2.7	2.3
α -D-Ara1NiPr	δ	89.0	71.5	73.9	69.4	67.7	45.4
1C_4 - α -D-Arap1NiPr2H ₋₁	δ	90.8	77.4	75.5	68.9	70.5	50.9
κ^2N^1,O^2	$\Delta\delta$	1.8	5.9	1.9	-0.4	2.8	5.5

The κ^2N^1,O^2 chelation of the open-chain form of *N*-alkyl-D-arabinosylamines, observed for the ethyl-, propyl- and *iso*-propyl derivatives, was readily identified by the distinctive 1H NMR signals assigned to the protons of the imine function. These signals are located at 7.92 ppm, 7.91 ppm and 7.91 ppm, respectively. In ${}^{13}C\{^1H\}$ NMR spectra the presence of the acyclic species became obvious by the extremely downfield shifted C1 atoms and noticeably deviating NMR signal patterns in comparison to the previously described pyranoid species. The ${}^{13}C\{^1H\}$ NMR shifts of the detected chelated open-chain species are listed in table 2.50.

Table 2.50. Selected $^{13}\text{C}\{^1\text{H}\}$ NMR chemical shifts (δ/ppm) of the detected monometalated open-chain species of *N*-alkyl-D-arabinoamines with Pd-en in D_2O at 4°C .

		C1	C2	C3	C4	C5	Cα
D-Ara α 1NEt2H $_{-1}$ - κ^2N^1,O^2	δ	186.1	85.8	71.7	71.5	63.5	55.6
D-Ara α 1NPr2H $_{-1}$ - κ^2N^1,O^2	δ	187.2	85.7	71.7	71.4	63.4	62.7
D-Ara α 1NiPr2H $_{-1}$ - κ^2N^1,O^2	δ	183.3	86.1	71.8	71.6	63.5	60.0

The addition of two equivalents Pd-en to *N*-alkyl-D-arabinosylamines clearly led to a preferred $\kappa^2N^1,O^2:\kappa^2O^{3,4}$ chelation of the α -anomer. Aside from the doubly metalated species, smaller amounts of the previously described cyclic and acyclic monometalated species were detected in all reaction solutions. The NMR-spectroscopically determined percentage distributions of the different species are displayed in table 2.51. Remarkably, no evidence for a $\kappa^2N^1,O^2:\kappa^2O^{3,4}$ chelation of the imine form was found for any of the investigated *N*-alkyl-D-arabinosylamines. A monometalation of the imine form occurred for the same ligand derivatives as in the equimolar experiments. Regarding the further species detected in the NMR spectra, an additional presence of the solely $\kappa^2O^{3,4}$ monometalated α -anomer and dimetalated β -anomer was assumed, but a definite characterization of the complexes was not possible due to their low concentration and the superposition of signals.

Table 2.51. Percentage distribution of the metalated species resulting from the treatment of *N*-alkyl-D-arabinosylamines with Pd-en and iodic acid in the molar ratio 1:2:1 at 4°C .

	Me	Et	Pr	<i>i</i>Pr
1C_4 - α -D-Ara ρ 1NR2,3,4H $_{-3}$ - $\kappa^2N^1,O^2:\kappa^2O^{3,4}$	73	66	64	52
1C_4 - α -D-Ara ρ 1NR2H $_{-1}$ - κ^2N^1,O^2	19	21	12	9
D-Ara α 1NR2H $_{-1}$ - κ^2N^1,O^2	0	4	6	15
other species	8	9	18	24

Considering the favorable orientation of the functional groups, it is assumed that the α -anomer in the 1C_4 conformation is coordinated by the two PdN $_2$ -fragments. A complete evaluation of this hypothesis by the analysis of the coupling constants was not feasible due to the overlapping of different species in the respective ^1H NMR spectra. The $^{13}\text{C}\{^1\text{H}\}$ NMR chemical shifts and determined CIS values, which nevertheless clearly indicate the double metalation of the *N*-alkyl-D-arabinosylamines, are listed in table 2.52.

Table 2.52. Selected $^{13}\text{C}\{^1\text{H}\}$ NMR chemical shifts (δ/ppm) and shift differences ($\Delta\delta$) to the free ligand of the detected doubly metalated *N*-alkyl-D-arabinopyranosylamines with Pd-en in D_2O at 4°C . The $\Delta\delta$ values indicating a CIS are printed bold.

		C1	C2	C3	C4	C5	C α
α -D-Ara1NMe	δ	92.2	70.9	73.8	69.4	67.7	31.5
$^1\text{C}_4$ - α -D-Arap1NMe2,3,4H $_{-3}$	δ	94.7	80.9	85.1	79.2	69.6	37.0
$\kappa^2\text{N}^1, \text{O}^2; \kappa^2\text{O}^{3,4}$	$\Delta\delta$	2.5	10.0	11.3	9.8	1.9	5.5
α -D-Ara1NEt	δ	90.8	71.2	73.8	69.4	67.7	39.9
$^1\text{C}_4$ - α -D-Arap1NEt2,3,4H $_{-3}$	δ	89.6	80.7	85.1	79.2	69.6	42.2
$\kappa^2\text{N}^1, \text{O}^2; \kappa^2\text{O}^{3,4}$	$\Delta\delta$	-1.2	9.5	11.3	9.8	1.9	2.3
α -D-Ara1NPr	δ	91.1	71.1	73.8	69.4	67.8	47.6
$^1\text{C}_4$ - α -D-Arap1NPr2,3,4H $_{-3}$	δ	90.8	80.9	85.2	79.2	69.6	50.0
$\kappa^2\text{N}^1, \text{O}^2; \kappa^2\text{O}^{3,4}$	$\Delta\delta$	-0.3	9.8	11.4	9.8	1.8	2.4
α -D-Ara1NiPr	δ	89.0	71.5	73.9	69.4	67.7	45.4
$^1\text{C}_4$ - α -D-Arap1NiPr2,3,4H $_{-3}$	δ	90.9	81.0	85.4	79.2	69.7	50.6
$\kappa^2\text{N}^1, \text{O}^2; \kappa^2\text{O}^{3,4}$	$\Delta\delta$	1.9	9.5	11.5	9.8	2.0	5.2

2.2.1.2. *N*-Alkyl-D-lyxosylamines

The four complex species depicted in figure 2.24 were identified in reaction solutions containing *N*-alkyl-D-lyxosylamines, Pd-en and iodic acid in various molar ratios.

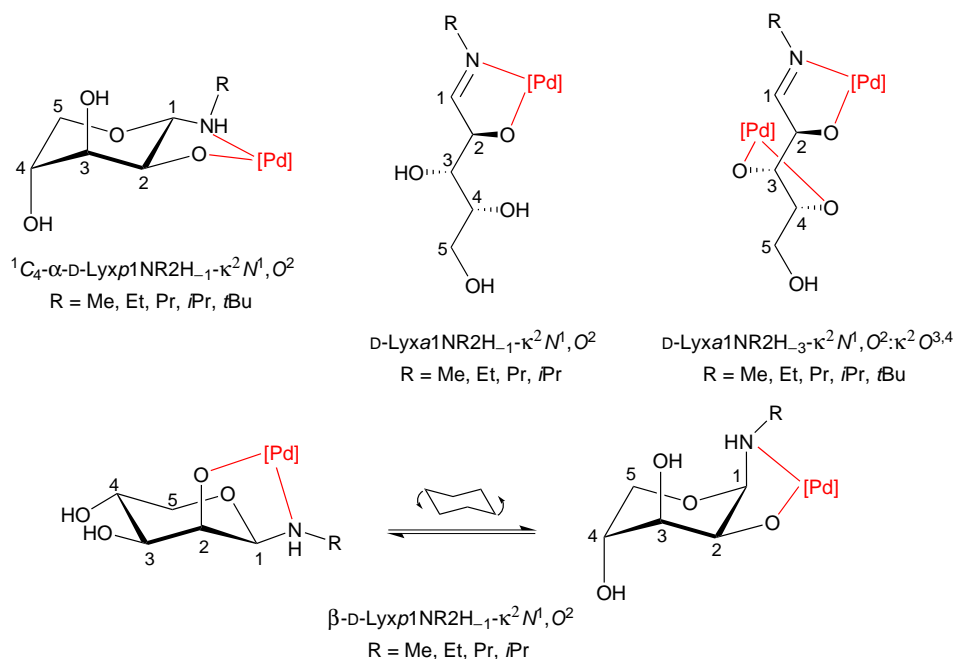


Figure 2.24. Complex species detected in reaction solutions resulting from the treatment of *N*-alkyl-D-lyxosylamines with Pd-en and iodic acid.

As the percentage distribution in table 2.53 shows, the preference of a certain species in equimolar reaction solutions largely depends on the *N*-alkyl-D-lyxosylamine included in the reaction. As

for the methyl and ethyl derivatives the κ^2N^1,O^2 chelation of the ligand in its pyranoid form dominates, *N*-propyl- and *N*-(*iso*-propyl)-*D*-lyxosylamine on the other hand favor the metalation of the acyclic imine form. Additionally, the metalation of the corresponding β -pyranosylamine form was detected for all derivatives with unbranched alkylamino moieties, but to a lesser extent. Surprisingly, for α -*D*-Lyx1*Nt*Bu only the coordination of the ligand in its cyclic form is observed. But due to the rapid hydrolysis of the *tert*-butyl derivative, the main species detected in the NMR spectrum were metalated and non-metalated hydrolysis products.

Table 2.53. Percentage distribution of the metalated species resulting from the treatment of *N*-alkyl-*D*-lyxosylamines with Pd-en and iodic acid in the molar ratio 1:1:1 at 4 °C.

	Me	Et	Pr	<i>i</i> Pr	<i>t</i> Bu
1C_4 - α - <i>D</i> -Lyxp1NR2H ₋₁ - κ^2N^1,O^2	36	28	10	36	36
<i>D</i> -Lyxa1NR2H ₋₁ - κ^2N^1,O^2	28	16	78	64	0
β - <i>D</i> -Lyxp1NR2H ₋₁ - κ^2N^1,O^2	17	15	8	0	0
other species	19	41	4	0	74

The cyclic complex species feature a κ^2N^1,O^2 metalation of the α -anomer and were observed for all investigated *N*-alkyl-*D*-lyxosylamines. This binding mode was identified by the CIS values shown in table 2.54. The presence of the α -configuration and 1C_4 conformation was further verified by the measured ${}^3J_{1,2}$ values of 9.3 Hz to 9.6 Hz for the respective complex species. Hence, in comparison to the free α -anomer, the ${}^3J_{1,2}$ values are remarkably higher as any possibility of a dynamic fluctuation by chair inversion is prevented by the occurring *trans*-vicinal chelation.

Table 2.54. Selected ${}^{13}C\{^1H\}$ NMR chemical shifts (δ /ppm) and shift differences ($\Delta\delta$) to the free ligand of the detected monometalated *N*-alkyl- α -*D*-lyxopyranosylamines with Pd-en in D₂O at 4 °C. The $\Delta\delta$ values indicating a CIS are printed bold.

		C1	C2	C3	C4	C5	C α
α - <i>D</i> -Lyx1NMe	δ	89.1	69.3	71.1	69.2	64.7	31.2
1C_4 - α - <i>D</i> -Lyxp1NMe2H ₋₁	δ	91.0	75.3	72.3	69.6	67.9	36.8
κ^2N^1,O^2	$\Delta\delta$	1.9	6.0	1.2	0.4	3.2	5.6
α - <i>D</i> -Lyx1NEt	δ	87.6	69.4	71.1	69.2	64.6	39.6
1C_4 - α - <i>D</i> -Lyxp1NEt2H ₋₁	δ	86.2	75.2	72.4	69.3	67.9	42.4
κ^2N^1,O^2	$\Delta\delta$	-1.4	5.8	1.3	0.1	3.3	2.8
α - <i>D</i> -Lyx1NPr	δ	87.9	69.4	71.2	69.2	64.7	47.3
1C_4 - α - <i>D</i> -Lyxp1NPr2H ₋₁	δ	87.4	75.3	72.4	69.6	67.9	50.1
κ^2N^1,O^2	$\Delta\delta$	-0.5	5.9	1.2	0.4	3.2	2.8
α - <i>D</i> -Lyx1NiPr	δ	85.7	69.7	71.1	69.3	64.7	45.0
1C_4 - α - <i>D</i> -Lyxp1NiPr2H ₋₁	δ	86.8	75.5	72.5	69.6	67.9	50.8
κ^2N^1,O^2	$\Delta\delta$	1.1	5.8	1.4	0.3	3.2	5.8

For all *N*-alkyl-*D*-lyxosylamines with unbranched methylamino moieties, a second complex species featuring the ligand as cyclic pyranosylamine isomer was detected. The exceptional ${}^{13}C\{^1H\}$ NMR chemical shifts and CIS values listed in table 2.55 indicate a possible *cis*-vicinal metalation of the β -anomer. For this chelation mode a dynamic fluctuation between the 1C_4 and 4C_1 conforma-

tion is conceivable, although the 4C_1 conformation should be sterically favored. The fluctuation hinders a direct comparison to the free β -anomer, which, as shown in chapter 2.1.1.2, strictly resides in the 4C_1 conformation. Since this coordination mode was only detected as a minor species, the most coupling constants could not be determined due to superposed 1H NMR signals. But as expected the determined ${}^3J_{1,2}$ values of 4.3 Hz to 5.1 Hz neither match the sole presence of the 4C_1 or 1C_4 conformation in the metalated β -lyxopyranosylamine species.

Table 2.55. Selected ${}^{13}C\{{}^1H\}$ NMR chemical shifts (δ /ppm) and shift differences ($\Delta\delta$) to the free ligand of the detected monometalated *N*-alkyl- β -D-lyxopyranosylamines with Pd-en in D_2O at 4 °C. The $\Delta\delta$ values indicating a CIS are printed bold.

		C1	C2	C3	C4	C5	C α
β -D-Lyx1NMe	δ	89.7	71.4	74.4	67.2	67.0	31.6
β -D-Lyx <i>p</i> 1NMe2H $_{-1}$	δ	93.0	78.8	72.6	68.8	61.0	37.0
κ^2N^1,O^2	$\Delta\delta$	3.3	7.4	-1.8	1.6	-6.2	5.4
β -D-Lyx1NMe	δ	87.8	71.6	74.4	67.2	67.0	39.5
β -D-Lyx <i>p</i> 1NEt2H $_{-1}$	δ	89.2	79.1	71.5	68.4	62.0	42.8
κ^2N^1,O^2	$\Delta\delta$	1.6	7.5	-2.9	1.2	-5.0	3.3
β -D-Lyx1NPr	δ	88.2	71.6	74.5	67.2	67.0	47.1
β -D-Lyx <i>p</i> 1NPr2H $_{-1}$	δ	91.0	79.1	72.6	68.3	67.5	50.2
κ^2N^1,O^2	$\Delta\delta$	2.8	7.5	-2.0	1.1	0.5	3.1

The κ^2N^1,O^2 metalation of the open-chain form led to the emergence of distinctive 1H and ${}^{13}C\{{}^1H\}$ NMR signals in the downfield region of the recorded spectra which were assigned to the respective imine functions. An overview of the ${}^{13}C\{{}^1H\}$ NMR signals for the mononuclear imine species is given in table 2.56. The 1H NMR chemical shifts of the imine hydrogen atom range between 8.01 ppm to 8.09 ppm, depending on the nature of the alkylamino moiety.

A more detailed analysis of the 1H NMR was feasible for reaction solutions, in which the imine complex species was clearly predominant, as in the case of D-Lyx*a*1NPr2H $_{-1}$ - κ^2N^1,O^2 . The determined coupling constants of ${}^3J_{1,2}=1.2$ Hz, ${}^3J_{2,3}=6.3$ Hz and ${}^3J_{3,4}=2.1$ Hz match the expected gauche-, anti- and gauche-orientation of the respective hydrogen atoms in the postulated zigzag conformation of the open-chain form.

Table 2.56. Selected ${}^{13}C\{{}^1H\}$ NMR chemical shifts (δ /ppm) of the detected monometalated open-chain species of *N*-alkyl-D-lyxoamines with Pd-en in D_2O at 4 °C.

		C1	C2	C3	C4	C5	C α
D-Lyx <i>a</i> 1NMe2H $_{-1}$ - κ^2N^1,O^2	δ	187.8	86.5	74.6	71.2	63.3	48.8
D-Lyx <i>a</i> 1NEt2H $_{-1}$ - κ^2N^1,O^2	δ	186.3	86.5	74.6	71.2	63.3	55.7
D-Lyx <i>a</i> 1NPr2H $_{-1}$ - κ^2N^1,O^2	δ	187.3	86.3	74.7	71.2	63.3	62.7
D-Lyx <i>a</i> 1N <i>i</i> Pr2H $_{-1}$ - κ^2N^1,O^2	δ	183.5	86.7	74.7	71.2	63.3	60.1
D-Lyx <i>a</i> 1N <i>t</i> Bu2H $_{-1}$ - κ^2N^1,O^2	δ	181.8	85.9	75.2	71.1	63.3	63.1

As can be seen in table 2.57, reactions of *N*-alkyl-D-lyxosylamines with two equivalents of Pd-en led to only one binuclear coordination mode. These species feature a $\kappa^2N^1,O^2:\kappa^2O^{3,4}$ metalation of the open-chain form and prevail in the respective reaction solutions of all derivatives. The pres-

ence of this doubly metalated species was accompanied by the formation of the aforementioned monometalated complex species and other not identified reaction products. All reaction solutions showed more evident signs of decomposition than the corresponding equimolar reactions, easily recognizable through the rapid formation of elemental palladium.

Table 2.57. Percentage distribution of the metalated species resulting from the treatment of *N*-alkyl-D-lyxosylamines with Pd-en and iodic acid in the molar ratio 1:2:1 at 4 °C.

	Me	Et	Pr	<i>i</i> Pr	<i>t</i> Bu
D-Lyx <i>a</i> 1NR2,3,4H ₋₃ -κ ² N ¹ ,O ² :κ ² O ^{3,4}	33	58	50	100	73
¹ C ₄ -α-D-Lyx <i>p</i> 1NR2H ₋₁ -κ ² N ¹ ,O ²	26	18	0	0	0
D-Lyx <i>a</i> 1NR2H ₋₁ -κ ² N ¹ ,O ²	0	24	0	0	27
other species	41	0	50	0	0

The ¹³C{¹H} NMR chemical shifts of the detected doubly metalated open-chain species are listed in table 2.58. The binding of a second PdN₂-fragment was characterized by the observed chemical shift differences in comparison to the monometalated imine species of about 13 ppm and about 12 ppm found for the C3 and C4 atom, respectively. The ¹H NMR signals ($\delta = 8.07$ ppm to 8.18 ppm) of the imine hydrogen atom appear slightly downfield shifted compared to their monometalated analogues. The reduced quality of the recorded ¹H NMR spectra, due to the rapid formation of elemental palladium, hindered a more detailed determination of the exact conformation of the doubly metalated imine ligand.

Table 2.58. Selected ¹³C{¹H} NMR chemical shifts (δ /ppm) of the detected doubly metalated open-chain species of *N*-alkyl-D-lyxosylamines with Pd-en in D₂O at 4 °C.

		C1	C2	C3	C4	C5	C α
D-Lyx <i>a</i> 1NMe2,3,4H ₋₃ -κ ² N ¹ ,O ² :κ ² O ^{3,4}	δ	189.6	88.9	87.5	83.4	64.6	48.7
D-Lyx <i>a</i> 1NEt2,3,4H ₋₃ -κ ² N ¹ ,O ² :κ ² O ^{3,4}	δ	187.9	88.9	87.6	83.5	64.6	55.8
D-Lyx <i>a</i> 1NPr2,3,4H ₋₃ -κ ² N ¹ ,O ² :κ ² O ^{3,4}	δ	188.9	89.0	87.4	83.3	64.6	62.8
D-Lyx <i>a</i> 1N <i>i</i> Pr2,3,4H ₋₃ -κ ² N ¹ ,O ² :κ ² O ^{3,4}	δ	184.9	88.5	88.2	83.6	64.7	60.4
D-Lyx <i>a</i> 1N <i>t</i> Bu2,3,4H ₋₃ -κ ² N ¹ ,O ² :κ ² O ^{3,4}	δ	183.0	89.0	87.4	84.0	64.5	63.2

2.2.1.3. *N*-Alkyl-D-ribosylamines

Comparing all four pentosylamines, the treatment of *N*-alkyl-D-ribosylamines with Pd-en yielded the largest variety of complex species in aqueous solution. All identified metalated species from the reactions in the molar ratios 1:1:1 and 1:2:1 are depicted in figure 2.25.

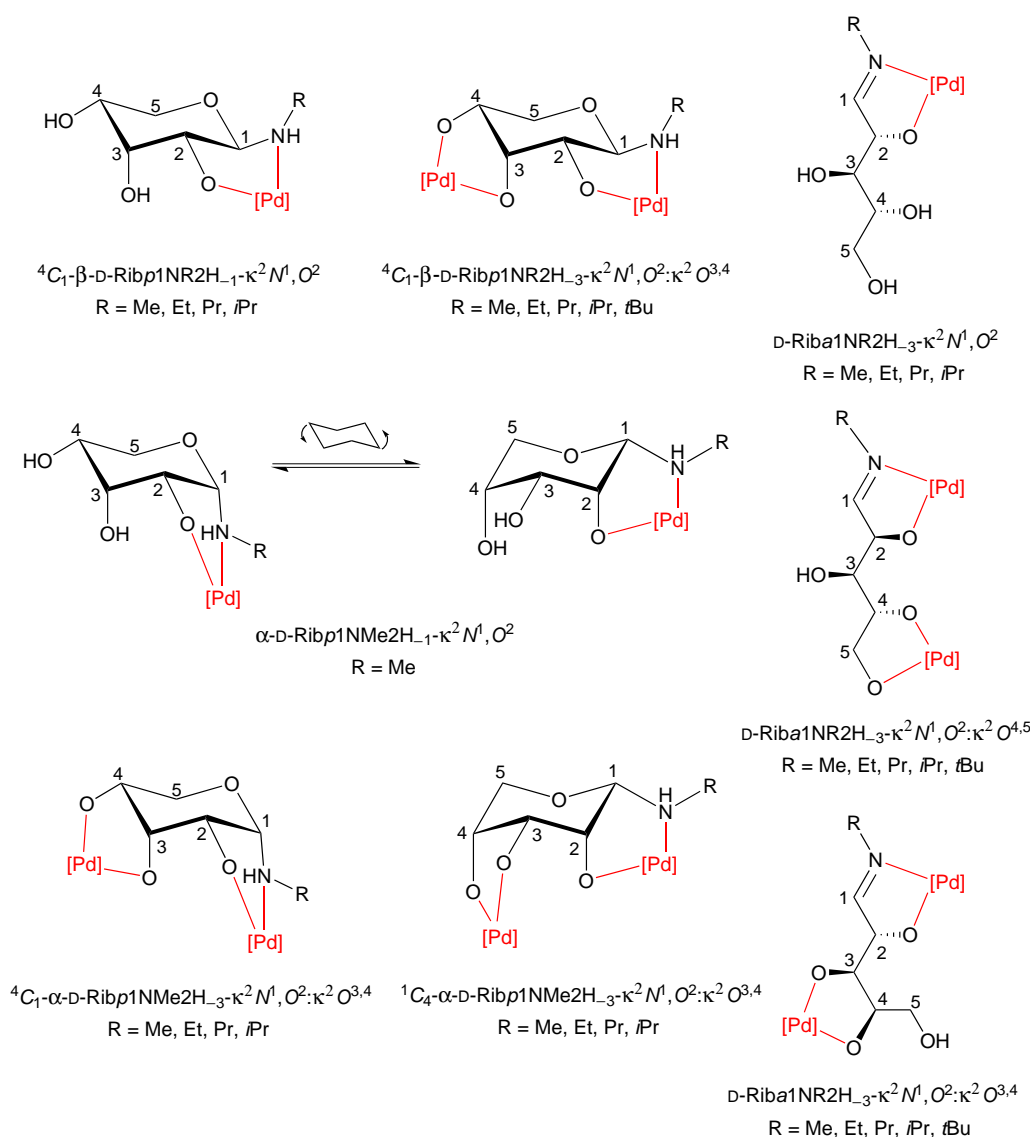


Figure 2.25. Complex species detected in reaction solutions resulting from the treatment of *N*-alkyl-D-ribosylamines with Pd-en and iodic acid.

As shown in table 2.59, the $\kappa^2 N^1, O^2$ -metalated β -anomer was detected as the main species in equimolar reactions for all investigated *N*-alkyl-D-ribosylamines, except for the *tert*-butyl derivative. The determined amount of chelated open-chain isomer increases with growing complexity of the alkylamino moiety, culminating in 60 % of complexed acyclic species for *N*-(*tert*-butyl)-D-ribosylamine. An additional chelation of the α -anomer was only observed in reactions with *N*-methyl-D-ribosylamine.

Table 2.59. Percentage distribution of the metalated species resulting from the treatment of *N*-alkyl-*D*-ribosylamines with Pd-en and iodic acid in the molar ratio 1:1:1 at 4 °C.

	Me	Et	Pr	<i>i</i> Pr	<i>t</i> Bu
4C_1 - β -D-Rib p 1NR2H $_{-1}$ - κ^2N^1,O^2	58	88	58	71	14
α -D-Rib p 1NR2H $_{-1}$ - κ^2N^1,O^2	25	0	0	0	0
D-Rib a 1NR2H $_{-1}$ - κ^2N^1,O^2	13	12	26	29	60
other species	4	0	16	0	26

The aforementioned κ^2N^1,O^2 metalation of the β -anomer was identified by the measured ${}^{13}C\{^1H\}$ NMR chemical shifts and associated CIS values shown in table 2.60. The calculated CIS values for the C1, C2 and C α atoms all lie within the common range for the respective alkylamino moiety featured in the ligand. The determined ${}^3J_{1,2}$ values range between 9.1 Hz and 9.4 Hz, thus, according to the KARPLUS relation, strongly suggesting the sole presence of the 4C_1 conformation in these species. These findings, indicating a *trans*-vicinal chelation, are largely congruent with the in chapter 2.1.1.3 described conformational behavior of free *N*-alkyl- β -*D*-ribosylamines.

Table 2.60. Selected ${}^{13}C\{^1H\}$ NMR chemical shifts (δ /ppm) and shift differences ($\Delta\delta$) to the free ligand of the detected monometalated *N*-alkyl- β -*D*-ribopyranosylamines with Pd-en in D $_2$ O at 4 °C. The $\Delta\delta$ values indicating a CIS are printed bold.

		C1	C2	C3	C4	C5	C α
β -D-Rib1NMe	δ	88.4	72.2	70.6	67.6	63.9	31.4
4C_1 - β -D-Rib p 1NMe2H $_{-1}$	δ	90.8	78.1	72.1	66.9	64.8	36.9
κ^2N^1,O^2	$\Delta\delta$	2.4	5.9	1.5	-0.7	0.9	5.5
β -D-Rib1NEt	δ	86.9	72.5	70.8	67.6	63.8	40.0
4C_1 - β -D-Rib p 1NEt2H $_{-1}$	δ	86.1	78.0	72.2	66.8	64.8	42.4
κ^2N^1,O^2	$\Delta\delta$	-0.8	5.5	1.4	-0.8	1.0	2.4
β -D-Rib1NPr	δ	87.2	72.4	70.7	67.6	63.8	47.6
4C_1 - β -D-Rib p 1NPr2H $_{-1}$	δ	87.3	78.1	72.2	66.9	64.8	50.2
κ^2N^1,O^2	$\Delta\delta$	0.1	5.7	1.5	-0.7	1.0	2.6
β -D-Rib1N <i>i</i> Pr	δ	85.1	72.7	71.0	67.6	63.7	45.2
4C_1 - β -D-Rib p 1N <i>i</i> Pr2H $_{-1}$	δ	86.8	78.3	72.5	66.8	64.8	50.8
κ^2N^1,O^2	$\Delta\delta$	1.1	5.6	1.5	-0.8	1.1	5.6

As previously outlined in chapter 2.1.1.3, uncomplexed α -D-Rib1NMe strictly resides in the 1C_4 conformation. But upon addition of Pd-en, the measured ${}^3J_{1,2}$ value for the α -anomer increases to 2.5 Hz (free ligand: ${}^3J_{1,2}$ =1.1 Hz) as a result of the occurring *cis*-vicinal κ^2N^1,O^2 chelation and hence indicating a dynamic fluctuation between the 1C_4 and 4C_1 conformation in the yielded complex species. Although the observed ${}^{13}C\{^1H\}$ NMR chemical shifts also indicate the formation of this additional pyranoid species, the absence of comparative ${}^{13}C\{^1H\}$ NMR chemical shifts for the fluctuating free ligand impeded the determination of meaningful CIS values for this coordination mode.

A metalation of the respective imine isomer was detected for all *N*-alkyl-*D*-ribosylamines and unambiguously identified by the observed distinctive ${}^{13}C\{^1H\}$ NMR chemical shifts listed in table 2.61. In the cases of Rib1N*i*Pr and Rib1N*t*Bu the corresponding open-chain species was

also detected to a minimal extent for the free ligand in DMSO- d_6 . Although it must be noted that the measurements were conducted in different solvents, this allows a comparison of the observed $^{13}\text{C}\{^1\text{H}\}$ NMR chemical shifts between the free and the complexed ligand. The resulting shift differences are about 19 ppm and 15 ppm for the C1 and C2 atom, respectively. The C α atom of the alkylamino moiety, however, showed only a slight downfield shift upon coordination. While the ^1H NMR signals assigned to the imine hydrogen atom in the free open-chain isomer are found at 7.70 ppm for Rib1N*i*Pr and 7.69 ppm for Rib1N*t*Bu, the corresponding ^1H NMR signals for the metalated *N*-alkyl-D-ribosylamines open-chain species are located at 7.90 ppm and 7.99 ppm, respectively.

Table 2.61. Selected $^{13}\text{C}\{^1\text{H}\}$ NMR chemical shifts (δ /ppm) of the detected monometalated open-chain species of *N*-alkyl-D-riboamines with Pd-en in D₂O at 4 °C.

		C1	C2	C3	C4	C5	C α
D-Rib1NMe2H ₋₁ - κ^2N^1,O^2	δ	186.4	86.7	74.6	72.7	63.4	48.7
D-Rib1NEt2H ₋₁ - κ^2N^1,O^2	δ	184.9	86.8	74.2	72.5	63.4	55.6
D-Rib1NPr2H ₋₁ - κ^2N^1,O^2	δ	185.8	86.6	74.4	72.8	63.4	62.7
D-Rib1N <i>i</i> Pr2H ₋₁ - κ^2N^1,O^2	δ	182.0	87.2	74.1	72.2	63.4	60.0
D-Rib1N <i>t</i> Bu2H ₋₁ - κ^2N^1,O^2	δ	180.3	86.7	74.1	72.3	63.5	57.0

In the reaction solutions with *N*-alkyl-D-ribosylamines and two equivalents of Pd-en, it could be observed that a total of four binuclear coordination modes coexist simultaneously. These species feature the $\kappa^2N^1,O^2:\kappa^2O^{3,4}$ and the $\kappa^2N^1,O^2:\kappa^2O^{4,5}$ chelation of the acyclic imine form as well as the $\kappa^2N^1,O^2:\kappa^2O^{3,4}$ metalation of the pyranoid α - and β -anomer. In the reaction including β -D-Rib1N*t*Bu only the imine complex species could be identified with definite certainty. As can be seen in table 2.62, the amount of metalated β -anomer clearly prevails in comparison to the coordination of the corresponding α -anomer, especially for ligands with sterically more demanding alkylamino moieties. On the contrary, the detected amounts of the two doubly metalated imine species are almost equal in all investigated reaction solutions. The concentration of the imine complexes species in the reaction solutions increases with the size of alkylamino function of the featured *N*-alkyl-D-ribosylamines.

Table 2.62. Percentage distribution of the metalated species resulting from the treatment of *N*-alkyl-D-ribosylamines with Pd-en and iodic acid in the molar ratio 1:2:1 at 4 °C.

	Me	Et	Pr	<i>i</i> Pr	<i>t</i> Bu
4C_1 - β -D-Ribp1NR2H ₋₃ - $\kappa^2N^1,O^2:\kappa^2O^{3,4}$	50	50	25	37	0
α -D-Ribp1NR2H ₋₃ - $\kappa^2N^1,O^2:\kappa^2O^{3,4}$	31	16	10	5	0
D-Rib1NR2,3,4H ₋₃ - $\kappa^2N^1,O^2:\kappa^2O^{3,4}$	8	17	23	27	22
D-Rib1NR2,4,5H ₋₃ - $\kappa^2N^1,O^2:\kappa^2O^{4,5}$	6	17	22	27	24
other species	5	0	20	4	54

In the case of doubly metalated *N*-alkyl- β -D-ribosylamines the first Pd-en fragment binds in *trans*-vicinal fashion to the alkylamino group at the C1 atom and the alkoxido group at the C2 atom. The second fragment is chelated in *cis*-vicinal fashion by the two deprotonated alkoxido functions at the C3 and C4 atom. This coordination mode was confirmed by the measured

$^{13}\text{C}\{^1\text{H}\}$ NMR chemical shifts and derived CIS values listed in table 2.63. Although superposition of signals and poor signal to noise ratio in the recorded ^1H NMR spectra allowed no definite determination of the $^3J_{1,2}$ or other coupling constants, a preference of the 4C_1 conformation in this species is assumed. This assumption is based on the previously verified presence of the 4C_1 conformation in the corresponding monometalated species as well as on the energetically favored equatorial orientation of the majority of functional groups in this conformation.

Table 2.63. Selected $^{13}\text{C}\{^1\text{H}\}$ NMR chemical shifts (δ/ppm) and shift differences ($\Delta\delta$) to the free ligand of the detected doubly metalated *N*-alkyl- β -D-ribosepyranosylamines with Pd-en in D_2O at 4°C . The $\Delta\delta$ values indicating a CIS are printed bold.

		C1	C2	C3	C4	C5	C α
β -D-Rib1NMe	δ	88.4	72.2	70.6	67.6	63.9	31.4
4C_1 - β -D-Ribp1NMe2,3,4H $_{-3}$	δ	91.2	77.9	83.2	76.9	67.6	36.8
$\kappa^2N^1,O^2;\kappa^2O^{3,4}$	$\Delta\delta$	2.8	7.3	12.6	9.3	3.7	5.4
β -D-Rib1NEt	δ	86.9	72.5	70.8	67.6	63.8	40.0
4C_1 - β -D-Ribp1NEt2,3,4H $_{-3}$	δ	86.2	77.7	83.2	77.0	67.7	42.4
$\kappa^2N^1,O^2;\kappa^2O^{3,4}$	$\Delta\delta$	-0.7	5.5	12.5	10.1	3.9	2.4
β -D-Rib1NPr	δ	87.2	72.4	70.7	67.6	63.8	47.6
4C_1 - β -D-Ribp1NPr2,3,4H $_{-3}$	δ	87.5	77.8	83.2	76.9	67.6	50.2
$\kappa^2N^1,O^2;\kappa^2O^{3,4}$	$\Delta\delta$	0.3	5.4	12.5	9.3	3.8	2.6
β -D-Rib1NiPr	δ	85.1	72.7	71.0	67.6	63.7	45.2
4C_1 - β -D-Ribp1NiPr2,3,4H $_{-3}$	δ	86.9	78.0	83.4	76.9	67.7	50.9
$\kappa^2N^1,O^2;\kappa^2O^{3,4}$	$\Delta\delta$	1.8	5.3	12.4	9.3	4.0	5.7

The chelation of two PdN $_2$ -fragments by the α -anomer was observed for more ligand derivatives as the corresponding monometalation, which was only detected in the case of D-Rib1NMe. The $^{13}\text{C}\{^1\text{H}\}$ NMR chemical shifts found for these binuclear species are listed in table 2.64. In the case of the methyl derivative, the described *cis*-vicinal coordination of a second palladium(II) ion resulted in NMR shift differences of 4.9 ppm and 4.4 ppm for the C3 and C4 atom, respectively, when compared to the analogue monometalated species. In contrast to the mononuclear species, the assumption of a dynamic fluctuation between the 1C_4 and 4C_1 conformation is not reasonable for the doubly metalated α -anomers.

Table 2.64. Selected $^{13}\text{C}\{^1\text{H}\}$ NMR chemical shifts (δ/ppm) and shift differences ($\Delta\delta$) to the free ligand of the detected doubly metalated *N*-alkyl- α -D-ribosepyranosylamines with Pd-en in D_2O at 4°C .

		C1	C2	C3	C4	C5	C α
α -D-Ribp1NMe2,3,4H $_{-3}$ - $\kappa^2N^1,O^2;\kappa^2O^{3,4}$	δ	91.2	81.8	75.8	71.0	60.4	35.8
α -D-Ribp1NEt2,3,4H $_{-3}$ - $\kappa^2N^1,O^2;\kappa^2O^{3,4}$	δ	86.0	81.6	75.9	70.9	60.6	40.7
α -D-Ribp1NPr2,3,4H $_{-3}$ - $\kappa^2N^1,O^2;\kappa^2O^{3,4}$	δ	87.3	81.6	75.8	70.8	60.7	48.4
α -D-Ribp1NiPr2,3,4H $_{-3}$ - $\kappa^2N^1,O^2;\kappa^2O^{3,4}$	δ	86.7	81.6	75.9	71.7	60.4	48.9

In all reaction solutions of *N*-alkyl-D-riboseylamines containing two equivalents of palladium probe(II), two distinctive ^1H and $^{13}\text{C}\{^1\text{H}\}$ NMR signals with almost similar integrals were de-

tected in the downfield regions of the respective spectra. This observation derives from the presence of two different doubly metalated open-chain species in the reaction solutions. Both species differ in the coordination mode of the second PdN₂ fragment. While one species features the anticipated $\kappa^2O^{3,4}$ chelation of the additional metal ion, $\kappa^2O^{4,5}$ chelation is realized in the other species. The unusual binding of the terminal C5 hydroxy group was identified by the observed downfield shift for the C5 atom, which is readily assigned through DEPT 135 NMR experiments. The observed chemical shift differences upon coordination in comparison to the corresponding monometalated species average about 13 ppm for the C3 atom and about 10 ppm for the C4 atom as well as for the C5 atom. In the case of a $\kappa^2O^{3,4}$ binding the calculated shift difference for the C5 atom averages about -1 ppm, which is in accordance with the non-coordination of the associated hydroxy function. Conversely, for the $\kappa^2O^{4,5}$ coordination mode the signal assigned to the C3 atom experiences only a minor downfield shift of about 2.5 ppm. An overview of all relevant $^{13}\text{C}\{^1\text{H}\}$ NMR chemical shifts for both species is given in table 2.65.

Table 2.65. Selected $^{13}\text{C}\{^1\text{H}\}$ NMR chemical shifts (δ/ppm) of the detected doubly metalated open-chain species of *N*-alkyl-D-ribosylamines with Pd-en in D₂O at 4 °C.

		C1	C2	C3	C4	C5	C α
D-Rib a1NMe2,3,4H ₋₃ - κ^2N^1, O^2 : $\kappa^2O^{3,4}$	δ	189.5	87.7	87.6	82.6	62.6	48.8
D-Rib a1NEt2,3,4H ₋₃ - κ^2N^1, O^2 : $\kappa^2O^{3,4}$	δ	187.8	87.6	85.7	82.7	62.6	55.9
D-Rib a1NPr2,3,4H ₋₃ - κ^2N^1, O^2 : $\kappa^2O^{3,4}$	δ	188.7	87.6	85.7	82.7	62.5	62.8
D-Rib a1NiPr2,3,4H ₋₃ - κ^2N^1, O^2 : $\kappa^2O^{3,4}$	δ	184.4	87.3	86.1	82.7	62.6	60.4
D-Rib a1NtBu2,3,4H ₋₃ - κ^2N^1, O^2 : $\kappa^2O^{3,4}$	δ	182.7	87.6	85.5	82.7	62.6	63.0
D-Rib a1NMe2,4,5H ₋₃ - κ^2N^1, O^2 : $\kappa^2O^{4,5}$	δ	185.8	86.1	77.1	82.1	73.5	48.8
D-Rib a1NEt2,4,5H ₋₃ - κ^2N^1, O^2 : $\kappa^2O^{4,5}$	δ	184.3	86.1	77.0	82.2	73.5	55.9
D-Rib a1NPr2,4,5H ₋₃ - κ^2N^1, O^2 : $\kappa^2O^{4,5}$	δ	185.2	86.0	77.0	82.3	73.5	62.9
D-Rib a1NiPr2,4,5H ₋₃ - κ^2N^1, O^2 : $\kappa^2O^{4,5}$	δ	181.3	86.2	77.0	82.4	73.5	62.9
D-Rib a1NtBu2,4,5H ₋₃ - κ^2N^1, O^2 : $\kappa^2O^{4,5}$	δ	179.5	86.7	76.9	82.5	73.5	63.4

2.2.1.4. *N*-Alkyl-D-xylosylamines

As described in chapter 2.1.1.4, α - and β -pyranosylamine isomers are found in neutral and alkaline aqueous solutions for all investigated uncomplexed *N*-alkyl-D-xylosylamines, with the β -anomer representing the strictly favored isomer. Upon addition of Pd-en and iodic acid, a variety of palladium complexes featuring multiple forms of the *N*-alkyl-D-xylosylamines as bidentate ligands were detected. The five different complex species identified by NMR spectroscopy in the reaction solutions containing different amounts of the palladium(II) metal probe are depicted in figure 2.26.

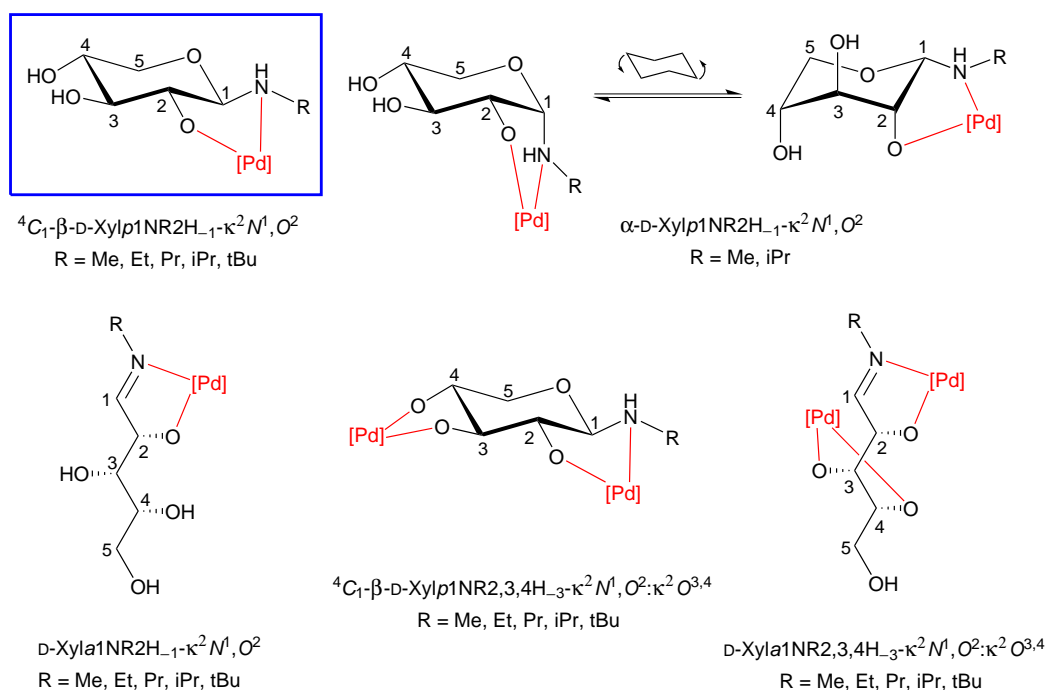


Figure 2.26. Complex species detected in reaction solutions resulting from the treatment of *N*-alkyl-D-xylosylamines with Pd-en and iodic acid.

As can be seen in table 2.66, upon addition of equimolar amounts of Pd-en and iodic acid, all investigated *N*-alkyl-D-xylosylamines except for the *tert*-butyl derivative showed a clear preference of the κ^2N^1,O^2 metalation of the β -pyranosylamine form. The chelation of the acyclic imine was observed for all derivatives, but in the case of D-Xylp1NMe and D-Xylp1NEt only in minimal amounts. For β -D-Xylp1N*t*Bu on the other hand, the metalation of the open-chain form appears to be clearly favored. Furthermore, in reaction solutions with D-Xylp1NMe and D-Xylp1N*i*Pr indications for a similar chelation of the respective α -anomer were found.

Table 2.66. Percentage distribution of the metalated species resulting from the treatment of *N*-alkyl-D-xylosylamines with Pd-en and iodic acid in the molar ratio 1:1:1 at 4 °C.

	Me	Et	Pr	<i>i</i> Pr	<i>t</i> Bu
${}^4C_1\text{-}\beta\text{-D-Xylp1NR2H}_{-1}\text{-}\kappa^2N^1,O^2$	85	98	76	78	12
$\alpha\text{-D-Xylp1NR2H}_{-1}\text{-}\kappa^2N^1,O^2$	3	0	0	8	0
$\text{D-Xyla1NR2H}_{-1}\text{-}\kappa^2N^1,O^2$	4	2	24	14	50
other species	8	0	0	0	38

The *trans*-vicinal chelation of the β -anomer was identified by the ${}^{13}\text{C}\{^1\text{H}\}$ NMR chemical shifts and derived CIS values, listed in table 2.67. The measured ${}^3J_{1,2}$ values of 7.8 Hz to 8.9 Hz verify the *anti*-configuration of the respective hydrogen atom and thus the presence of the 4C_1 conformation for the complex species. All other determined coupling constants are also in accordance with the values found for the free *N*-alkyl- β -D-xylosylamines, previously described in chapter 2.1.1.4.

Table 2.67. Selected $^{13}\text{C}\{^1\text{H}\}$ NMR chemical shifts (δ/ppm) and shift differences ($\Delta\delta$) to the free ligand of the detected monometalated *N*-alkyl- β -D-xylopyranosylamines with Pd-en in D_2O at 4°C . The $\Delta\delta$ values indicating a CIS are printed bold.

		C1	C2	C3	C4	C5	Cα
β -D-Xylp1NMe	δ	92.2	73.4	77.4	70.2	66.9	31.6
$^4\text{C}_1$ - β -D-Xylp1NMe2H $_{-1}$	δ	94.9	80.2	78.0	69.8	68.6	36.8
$\kappa^2\text{N}^1, \text{O}^2$	$\Delta\delta$	2.7	6.8	0.6	-0.4	1.5	5.2
β -D-Xylp1NEt	δ	90.8	73.6	77.5	70.2	66.9	40.0
$^4\text{C}_1$ - β -D-Xylp1NEt2H $_{-1}$	δ	90.2	80.0	78.0	69.7	68.6	42.3
$\kappa^2\text{N}^1, \text{O}^2$	$\Delta\delta$	-0.6	6.4	0.5	-0.5	1.9	2.3
β -D-Xylp1NPr	δ	91.1	73.5	77.4	70.1	66.8	47.5
$^4\text{C}_1$ - β -D-Xylp1NPr2H $_{-1}$	δ	91.4	80.1	78.0	69.7	68.6	50.0
$\kappa^2\text{N}^1, \text{O}^2$	$\Delta\delta$	0.3	6.6	0.6	-0.4	1.8	2.5
β -D-Xylp1NiPr	δ	89.0	73.9	77.6	70.1	66.8	45.5
$^4\text{C}_1$ - β -D-Xylp1NiPr2H $_{-1}$	δ	90.9	80.3	78.1	69.7	68.5	50.9
$\kappa^2\text{N}^1, \text{O}^2$	$\Delta\delta$	1.9	6.4	0.5	-0.4	1.7	5.4
β -D-Xylp1NtBu	δ	87.5	73.8	77.5	70.3	66.2	51.1
$^4\text{C}_1$ - β -D-Xylp1NtBu2H $_{-1}$	δ	91.6	78.2	81.0	69.8	68.6	58.8
$\kappa^2\text{N}^1, \text{O}^2$	$\Delta\delta$	4.1	4.4	4.5	-0.5	2.4	7.7

From the equimolar reaction solution containing D-Xylp1NMe, colorless, block-like crystals of $[\text{Pd}(\text{en})(^4\text{C}_1\text{-}\beta\text{-D-Xylp1NMe2H}_{-1}\text{-}\kappa^2\text{N}^1, \text{O}^2)]\text{IO}_3$ tetrahydrate (**8**) were obtained after overlaying the solution with acetone and subsequent storage at 4°C for one week. The crystals were suitable for X-ray diffraction studies and the crystal structure was solved in the space group $P2_12_12_1$. The Flack parameter for the structure of **8** was refined to be $-0.004(8)$.

The determined molecular structure (depicted in figure 2.27) confirmed the results of the collected NMR data: one single Pd(en)-fragment coordinates the equatorial methylamino function located at the C1 atom and the equatorial alkoxido function at the C2 atom of the *N*-methyl- β -D-xylosylamine in its $^4\text{C}_1$ conformation. The identified hydrogen bonds in the structure are listed in table 2.68.

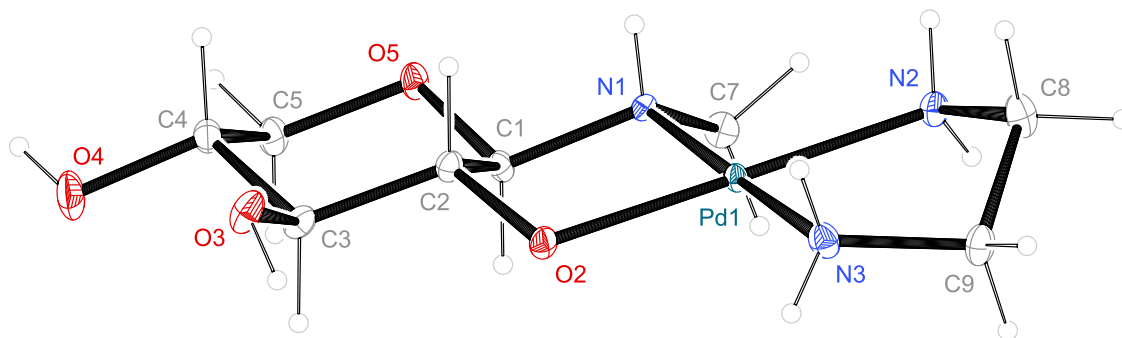


Figure 2.27. The molecular structure of the $[\text{Pd}(\text{en})(^4C_1\text{-}\beta\text{-D-Xylp1NMe}_2\text{H}_{-1}\text{-}\kappa^2\text{N}^1, \text{O}^2)]^+$ ion in **8**. ORTEP plot is drawn with 50 % probability ellipsoids. Interatomic distances (\AA) and angles ($^\circ$) (standard deviations of the last digit in parentheses): Pd1–N1 2.058(3), Pd1–O2 2.003(3), Pd1–N2 2.040(3), Pd1–N3 2.033(4), N1–C1 1.468(4), N1–C6 1.483(4), O5–C1 1.418(4), C2–C1 1.525(4), O2–C2 1.404(4), N1–Pd1–O2 85.61, N2–Pd1–N3 84.16; chelate torsion angles ($^\circ$): N1–C1–C2–O2 56.9, N2–C1–C2–N3 53.0; puckering parameters^[40] of the pyranose ring O5–C1–C2–C3–C4–C5: $Q = 0.589(3)$ \AA , $\theta = 0.0(3)^\circ$, $\phi = 26(14)^\circ$.

Table 2.68. Distances in \AA and angles in $^\circ$ of the hydrogen bonds in **8**. Standard deviations of the last digit are given in parentheses; values without standard deviation are related to hydrogen atoms at calculated positions. Symmetry codes are given as footnotes at the bottom of the table. D: donor, A: acceptor.

D	H	A	D–H	H...A	D...A	D–H...A
N2	H721	O6 ⁱ	0.85(4)	2.28(4)	3.082(4)	157(3)
N2	H722	O7 ⁱⁱ	0.91(4)	1.99(4)	2.893(4)	176(3)
O91	H911	O7	0.83(1)	2.064(18)	2.870(3)	163(4)
O91	H912	O8 ⁱⁱⁱ	0.83(1)	1.876(17)	2.690(3)	165(4)
O92	H921	O93 ^{iv}	0.83(1)	1.938(14)	2.758(4)	172(4)
O92	H922	O91	0.83(1)	2.147(16)	2.953(4)	164(4)
O93	H931	O92 ^v	0.83(1)	2.039(18)	2.855(4)	169(5)
O93	H932	O8	0.83(1)	2.01(2)	2.798(3)	159(5)
O4	H84	O91 ⁱⁱⁱ	0.84	2.07	2.871(3)	159.7
O3	H83	O7 ^{vi}	0.84	1.87	2.690(3)	163.8
N3	H731	O92 ^{vii}	0.89(4)	2.30(4)	3.140(4)	156(3)
N3	H732	O6 ^{vi}	0.80(4)	2.22(4)	2.987(4)	161(4)
N1	H711	O6 ⁱⁱ	0.80(4)	2.04(4)	2.824(4)	169(4)

ⁱ $-x + 3/2, -y + 1, z - 1/2$; ⁱⁱ $-x + 1/2, -y + 1, z - 1/2$; ⁱⁱⁱ $x - 1, y, z$;
^{iv} $x - 1/2, -y + 1/2, -z + 1$; ^v $x + 1, y, z$; ^{vi} $x - 1/2, -y + 3/2, -z + 1$;
^{vii} $-x, y + 1/2, -z + 1/2$

The additionally observed metalation of the α -anomer of D-Xylp1NMe and D-Xyl1NPr was identified by the determined, in comparison to the complexed β -anomers smaller, $^3J_{1,2}$ values of 4.4 Hz and 5.5 Hz. Although the possibility of a dynamic fluctuation could not be excluded with absolute certainty, the obtained $^3J_{1,2}$ values indicate a reasonable preference of the 4C_1 conformation in the respective species, especially for the *iso*-propyl derivative. The corresponding, partially unusual, CIS values listed in table 2.69, can be attributed to the for glycosylamine complexes uncommon *cis*-vicinal coordination pattern in combination with the possibility of a

dynamic fluctuation.

Table 2.69. Selected $^{13}\text{C}\{^1\text{H}\}$ NMR chemical shifts (δ/ppm) and shift differences ($\Delta\delta$) to the free ligand of the detected monometalated *N*-alkyl- α -D-xylopyranosylamines with Pd-en in D_2O at 4°C . The $\Delta\delta$ values indicating a CIS are printed bold.

		C1	C2	C3	C4	C5	Cα
α -D-Xylp1NMe	δ	87.8	71.2	72.1	69.7	63.0	31.4
α -D-Xylp1NMe2H $_{-1}$	δ	93.4	76.7	73.4	69.1	63.5	37.0
$\kappa^2\text{N}^1,\text{O}^2$	$\Delta\delta$	5.6	5.5	1.3	-0.6	0.5	5.6
α -D-Xylp1NiPr	δ	83.4	71.0	71.2	69.2	64.7	44.5
α -D-Xylp1NiPr2H $_{-1}$	δ	88.9	78.2	75.3	69.1	64.0	52.3
$\kappa^2\text{N}^1,\text{O}^2$	$\Delta\delta$	5.5	7.2	4.1	-0.1	-0.7	7.8

An overview of the $^{13}\text{C}\{^1\text{H}\}$ NMR chemical shifts assigned to the detected $\kappa^2\text{N}^1,\text{O}^2$ -chelated acyclic imine species is given in table 2.70. These species were identified, even in small concentrations, by their distinctive ^1H and $^{13}\text{C}\{^1\text{H}\}$ NMR signals of the imine function between 7.90 ppm to 7.99 ppm and 181.3 ppm to 187.4 ppm, respectively.

Table 2.70. Selected $^{13}\text{C}\{^1\text{H}\}$ NMR chemical shifts (δ/ppm) of the detected monometalated open-chain species of *N*-alkyl-D-xyloamines with Pd-en in D_2O at 4°C .

		C1	C2	C3	C4	C5	Cα
D-Xyla1NMe2H $_{-1}$ - $\kappa^2\text{N}^1,\text{O}^2$	δ	187.4	87.3	72.7	71.1	63.3	48.6
D-Xyla1NEt2H $_{-1}$ - $\kappa^2\text{N}^1,\text{O}^2$	δ	185.9	87.4	72.8	71.0	63.3	55.5
D-Xyla1NPr2H $_{-1}$ - $\kappa^2\text{N}^1,\text{O}^2$	δ	186.7	87.3	72.5	71.4	63.2	62.6
D-Xyla1NiPr2H $_{-1}$ - $\kappa^2\text{N}^1,\text{O}^2$	δ	183.2	87.7	72.9	70.9	63.3	59.7
D-Xyla1NtBu2H $_{-1}$ - $\kappa^2\text{N}^1,\text{O}^2$	δ	181.3	87.2	72.8	71.1	63.2	62.9

The treatment of *N*-alkyl-D-xylosylamines with up to two equivalents palladium(II) probe led to the additional formation of two doubly metalated species in the respective reaction solutions. This observation is accompanied by a decline of the concentration of the aforementioned mononuclear species, although varying amounts of these species are present in all investigated solutions. Double metalation was observed for the pyranoid β -anomer and the acyclic imine form. As can be seen in table 2.71 the amount of detected species featuring the open-chain form as ligand is remarkably higher in comparison to the equimolar reactions. This tendency becomes especially evident for the derivatives featuring a sterically more demanding alkylamino function.

Table 2.71. Percentage distribution of the metalated species resulting from the treatment of *N*-alkyl-D-xylosylamines with Pd-en and iodic acid in the molar ratio 1:2:1 at 4°C .

	Me	Et	Pr	<i>i</i>Pr	<i>t</i>Bu
$^4\text{C}_1$ - β -D-Xylp1NR2H $_{-3}$ - $\kappa^2\text{N}^1,\text{O}^2$: $\kappa^2\text{O}^{3,4}$	68	31	35	60	0
D-Xyla1NR2,3,4H $_{-3}$ - $\kappa^2\text{N}^1,\text{O}^2$: $\kappa^2\text{O}^{3,4}$	24	12	50	29	75
other species	8	57	15	11	25

The double metalation of the *N*-alkyl- β -D-xylopyranosylamines is realized in *trans*-vicinal fashion for both Pd-en fragments and characterized by the $^{13}\text{C}\{^1\text{H}\}$ NMR chemical shifts and derived CIS values listed in table 2.72. There were no indications found for the presence of a dynamic fluctuation in this species or for a possible double metalation of the corresponding α -anomer.

Table 2.72. Selected $^{13}\text{C}\{^1\text{H}\}$ NMR chemical shifts (δ /ppm) and shift differences ($\Delta\delta$) to the free ligand of the detected doubly metalated *N*-alkyl-D-xylopyranosylamines with Pd-en in D_2O at 4 °C. The $\Delta\delta$ values indicating a CIS are printed bold.

		C1	C2	C3	C4	C5	C α
β -D-Xylp1NMe	δ	92.2	73.4	77.4	70.2	66.9	31.6
$^4\text{C}_1$ - β -D-Xylp1NMe2,3,4H $_{-3}$	δ	95.4	82.1	88.3	79.7	68.2	37.2
$\kappa^2\text{N}^1, \text{O}^2: \kappa^2\text{O}^{3,4}$	$\Delta\delta$	3.2	8.7	10.9	9.5	1.3	6.0
β -D-Xylp1NEt	δ	90.8	73.6	77.5	70.2	66.9	40.0
$^4\text{C}_1$ - β -D-Xylp1NEt2,3,4H $_{-3}$	δ	90.6	81.9	88.4	79.7	68.2	42.5
$\kappa^2\text{N}^1, \text{O}^2: \kappa^2\text{O}^{3,4}$	$\Delta\delta$	-0.2	8.3	10.9	9.5	1.3	2.5
β -D-Xylp1NPr	δ	91.1	73.5	77.4	70.1	66.8	47.5
$^4\text{C}_1$ - β -D-Xylp1NPr2,3,4H $_{-3}$	δ	91.8	82.0	88.4	79.7	68.2	50.2
$\kappa^2\text{N}^1, \text{O}^2: \kappa^2\text{O}^{3,4}$	$\Delta\delta$	0.7	8.5	11.0	9.3	1.4	2.7
β -D-Xylp1NiPr	δ	89.0	73.9	77.6	70.1	66.8	45.5
$^4\text{C}_1$ - β -D-Xylp1NiPr2,3,4H $_{-3}$	δ	91.6	82.3	88.4	79.7	68.2	50.9
$\kappa^2\text{N}^1, \text{O}^2: \kappa^2\text{O}^{3,4}$	$\Delta\delta$	2.6	8.4	10.8	9.6	1.4	5.4
β -D-Xylp1N <i>t</i> Bu	δ	87.5	73.8	77.5	70.3	66.2	51.1
$^4\text{C}_1$ - β -D-Xylp1N <i>t</i> Bu2,3,4H $_{-3}$	δ	97.3	82.8	89.4	78.5	68.4	57.0
$\kappa^2\text{N}^1, \text{O}^2: \kappa^2\text{O}^{3,4}$	$\Delta\delta$	9.8	9.0	11.9	8.2	2.2	5.9

Regarding the double metalation of the open-chain form, no indications for other coordination modes than the observed $\kappa^2\text{N}^1, \text{O}^2: \kappa^2\text{O}^{3,4}$ binding were found. The $^{13}\text{C}\{^1\text{H}\}$ NMR chemical shifts assigned to these species are listed in table 2.73 and the respective signals of the imine hydrogen atom appear with values from 8.72 ppm to 8.94 ppm clearly shifted downfield in comparison to the signals found for their monometalated analogues. The $^{13}\text{C}\{^1\text{H}\}$ NMR chemical shifts of the C3 and C4 atoms of the dimetalated species exhibit a downfield shift about 13 ppm and 9 ppm, respectively, as result of the additional coordination.

Table 2.73. Selected $^{13}\text{C}\{^1\text{H}\}$ NMR chemical shifts (δ /ppm) of the detected doubly metalated open-chain species of *N*-alkyl-D-xyloamines with Pd-en in D_2O at 4 °C.

		C1	C2	C3	C4	C5	C α
D-Xyla1NMe2,3,4H $_{-3}$ - $\kappa^2\text{N}^1, \text{O}^2: \kappa^2\text{O}^{3,4}$	δ	187.9	88.2	85.2	79.9	65.6	48.7
D-Xyla1NEt2,3,4H $_{-3}$ - $\kappa^2\text{N}^1, \text{O}^2: \kappa^2\text{O}^{3,4}$	δ	186.1	88.3	85.2	79.9	65.6	55.5
D-Xyla1NPr2,3,4H $_{-3}$ - $\kappa^2\text{N}^1, \text{O}^2: \kappa^2\text{O}^{3,4}$	δ	187.1	88.2	85.4	80.1	66.5	62.8
D-Xyla1NiPr2,3,4H $_{-3}$ - $\kappa^2\text{N}^1, \text{O}^2: \kappa^2\text{O}^{3,4}$	δ	183.3	88.5	85.4	80.0	65.6	59.5
D-Xyla1N <i>t</i> Bu2,3,4H $_{-3}$ - $\kappa^2\text{N}^1, \text{O}^2: \kappa^2\text{O}^{3,4}$	δ	181.9	88.0	85.5	80.3	65.4	61.1

2.2.2. *N*-Alkylhexosylamines

Due to the additional hydroxy function, *N*-alkylhexosylamines provide more possible coordination modes for palladium(II) probes than the previously discussed *N*-alkylpentosylamines. As shown in chapter 2.1.2 all investigated free *N*-alkylhexosylamines are essentially found in hexopyranosylamine forms in aqueous solution. The conformational fluctuation of these hexopyranosylamines through ring inversion between 4C_1 and 1C_4 is frozen to the conformer that carries the terminal hydroxymethyl moiety in equatorial position. These factors limit the number of possible coordination patterns for *N*-alkylhexosylamines in comparison to the previously discussed *N*-alkylpentosylamines.

2.2.2.1. *N*-Alkyl-D-galactosylamines

The NMR spectra obtained from the reactions of *N*-alkyl-D-galactosylamines with Pd-en and iodic acid are characterized by a remarkably distinct species distribution. All investigated reaction solutions essentially show the three species depicted in figure 2.28.

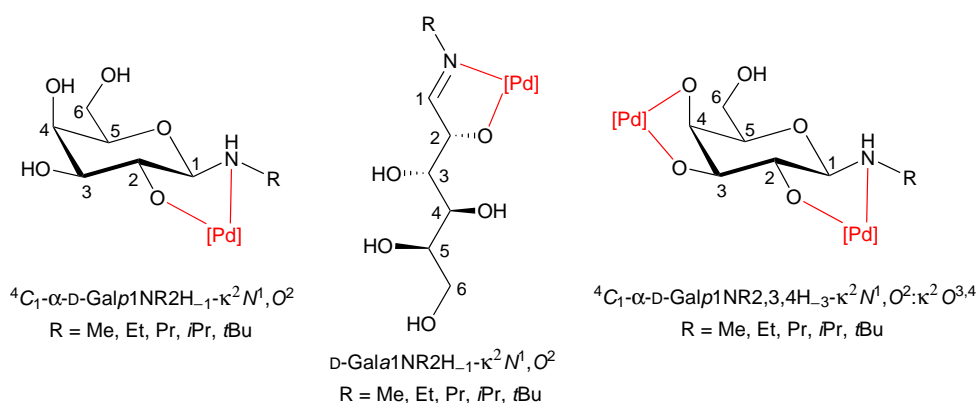


Figure 2.28. Complex species detected in reaction solutions resulting from the treatment of *N*-alkyl-D-galactosylamines with Pd-en and iodic acid.

As can be seen in table 2.74, all equimolar reactions yield κ^2 N 1 ,O 2 -monometalated *N*-alkyl- β -D-galactosylamines species as the prevailing product in aqueous solution. The respective κ^2 N 1 ,O 2 metalation of the open-chain becomes more apparent in the measured NMR spectra of reactions featuring an increased steric demand at the ligand's alkylamino substituent. But even in the reaction featuring *N*-(*tert*-butyl)-D-galactosylamine as ligand, the amount of acyclic species did not exceed one quarter in the total species distribution. The presence of further species in the reactions with β -D-Galp1NPr, β -D-Galp1NiPr and β -D-Galp1N*t*Bu is caused by the ligands higher sensitivity towards hydrolysis, leading to the formation and subsequent complexation of D-galactose.

Table 2.74. Percentage distribution of the metalated species resulting from the treatment of *N*-alkyl-D-galactosylamines with Pd-en and iodic acid in the molar ratio 1:1:1 at 4 °C.

	Me	Et	Pr	<i>i</i> Pr	<i>t</i> Bu
β -D-Galp1NR2H ₋₁ - κ^2N^1,O^2	98	95	76	81	58
D-Gal α 1NR2H ₋₁ - κ^2N^1,O^2	2	5	8	7	24
other species	0	0	16	12	18

Due to the superposition of signals in the obtained ¹H NMR spectra, most coupling constants, including ³J_{1,2}, could not be determined with definite certainty. But the found characteristic CIS values, listed in table 2.75, along with the preference of the β -anomer for all investigated *N*-alkyl-D-galactosylamines in water, clearly indicate a *trans*-vicinal κ^2N^1,O^2 metalation of the β -anomer.

Table 2.75. Selected ¹³C{¹H} NMR chemical shifts (δ /ppm) and shift differences ($\Delta\delta$) to the free ligand of the detected monometalated *N*-alkyl-D-galactopyranosylamines with Pd-en in D₂O at 4 °C. The $\Delta\delta$ values indicating a CIS are printed bold.

		C1	C2	C3	C4	C5	C6	C α
β -D-Galp1NMe	δ	91.8	71.0	74.3	69.7	76.5	61.8	31.5
β -D-Galp1NMe2H ₋₁	δ	94.5	77.3	75.3	69.3	79.3	61.6	36.9
κ^2N^1,O^2	$\Delta\delta$	2.7	6.3	1.0	-0.4	2.8	-0.2	5.4
β -D-Galp1NEt	δ	90.4	71.2	74.3	69.6	76.5	61.8	39.9
β -D-Galp1NEt2H ₋₁	δ	89.6	77.2	75.4	69.3	79.3	61.5	42.2
κ^2N^1,O^2	$\Delta\delta$	-0.8	6.0	1.1	-0.3	2.8	-0.3	2.3
β -D-Galp1NPr	δ	90.7	71.2	74.3	69.6	76.5	61.7	47.5
β -D-Galp1NPr2H ₋₁	δ	90.8	77.3	75.4	69.2	79.2	61.4	49.9
κ^2N^1,O^2	$\Delta\delta$	0.1	6.1	1.2	-0.4	2.7	-0.3	2.4
β -D-Galp1NiPr	δ	88.6	71.6	74.5	69.6	76.4	61.8	45.5
β -D-Galp1NiPr2H ₋₁	δ	90.4	77.5	75.5	69.1	79.3	61.4	50.8
κ^2N^1,O^2	$\Delta\delta$	1.8	5.9	1.0	-0.5	2.9	-0.4	5.3
β -D-Galp1N <i>t</i> Bu	δ	87.1	71.4	74.4	69.8	76.1	61.9	51.1
β -D-Galp1N <i>t</i> Bu2H ₋₁	δ	91.2	78.3	75.5	69.1	79.3	61.4	58.8
κ^2N^1,O^2	$\Delta\delta$	4.1	6.9	1.1	-0.7	3.2	-0.5	7.7

The κ^2N^1,O^2 -chelation of the acyclic imine form of *N*-alkyl-D-galactopyranosylamines was identified by the determined characteristic ¹³C{¹H} NMR chemical shifts listed in table 2.76. Additionally, the respective metalated open-chain forms exhibit prominent downfield ¹H NMR signals, assigned to the hydrogen atom of the imine group, in the range from 7.89 ppm to 7.99 ppm.

On the basis of the determined percentage distribution shown in table 2.77 it becomes evident that in all performed reactions containing two equivalents of Pd-en the $\kappa^2N^1,O^2;\kappa^2O^{3,4}$ chelation of the β -anomer prevails. The corresponding ¹³C{¹H} NMR chemical shifts and CIS values for the respective species are listed in table 2.78. Residues of monometalated species were only found in reaction solutions containing the *iso*-propyl or *tert*-butyl derivative. Due to their low concentration the other detected minor species were not unambiguously identified, but appeared to be of cyclic nature. Furthermore, it is noteworthy that no indications for a possible

2. Results

$\kappa^2N^1,O^2:\kappa^2O^{3,4}$ - or $\kappa^2N^1,O^2:\kappa^2O^{4,5}$ metalation were found in the respective NMR spectra.

Table 2.76. Selected $^{13}C\{^1H\}$ NMR chemical shifts (δ /ppm) of the detected monometalated open-chain species of *N*-alkyl-D-galactosylamines with Pd-en in D₂O at 4 °C.

		C1	C2	C3	C4	C5	C6	C α
D-Gal α 1NMe2H ₋₁ - κ^2N^1,O^2	δ	187.9	85.6	70.8	70.2	70.7	63.7	48.6
D-Gal α 1NEt2H ₋₁ - κ^2N^1,O^2	δ	186.3	85.7	70.8	70.2	70.7	63.7	55.6
D-Gal α 1NPr2H ₋₁ - κ^2N^1,O^2	δ	187.4	85.8	70.7	70.2	70.6	63.7	62.6
D-Gal α 1NiPr2H ₋₁ - κ^2N^1,O^2	δ	183.5	86.0	70.9	70.2	70.8	63.7	60.0
D-Gal α 1NtBu2H ₋₁ - κ^2N^1,O^2	δ	181.5	85.6	71.2	70.2	70.8	63.7	62.9

Table 2.77. Percentage distribution of the metalated species resulting from the treatment of *N*-alkyl-D-galactosylamines with Pd-en and iodic acid in the molar ratio 1:2:1 at 4 °C.

	Me	Et	Pr	<i>i</i> Pr	<i>t</i> Bu
4C_1 - β -D-Galp1NR2,3,4H ₋₃ - $\kappa^2N^1,O^2:\kappa^2O^{3,4}$	92	92	94	64	70
D-Gal α 1NR2H ₋₁ - κ^2N^1,O^2	0	0	0	11	20
4C_1 - α -D-Galp1NR2H ₋₁ - κ^2N^1,O^2	0	0	0	17	10
other species	8	8	6	8	0

Table 2.78. Selected $^{13}C\{^1H\}$ NMR chemical shifts (δ /ppm) and shift differences ($\Delta\delta$) to the free ligand of the detected doubly metalated *N*-alkyl-D-galactopyranosylamines with Pd-en in D₂O at 4 °C. The $\Delta\delta$ values indicating a CIS are printed bold.

		C1	C2	C3	C4	C5	C6	C α
β -D-Galp1NMe	δ	91.8	71.0	74.3	69.7	76.5	61.8	31.5
β -D-Galp1NMe2,3,4H ₋₃	δ	94.6	79.8	85.3	81.1	78.5	62.5	37.2
$\kappa^2N^1,O^2:\kappa^2O^{3,4}$	$\Delta\delta$	2.8	8.8	11.0	11.4	2.0	0.7	5.7
β -D-Galp1NEt	δ	90.4	71.2	74.3	69.6	76.5	61.8	39.9
β -D-Galp1NEt2,3,4H ₋₃	δ	89.5	80.9	85.9	79.8	78.5	62.5	42.2
$\kappa^2N^1,O^2:\kappa^2O^{3,4}$	$\Delta\delta$	-0.9	9.7	11.6	10.2	2.0	0.7	2.3
β -D-Galp1NPr	δ	90.7	71.2	74.3	69.6	76.5	61.7	47.5
β -D-Galp1NPr2,3,4H ₋₃	δ	90.7	81.1	85.9	79.7	78.5	62.4	49.9
$\kappa^2N^1,O^2:\kappa^2O^{3,4}$	$\Delta\delta$	0.0	9.9	11.6	10.1	2.0	0.7	2.4
β -D-Galp1NiPr	δ	88.6	71.6	74.5	69.6	76.4	61.8	45.5
β -D-Galp1NiPr2,3,4H ₋₃	δ	90.6	81.2	86.0	79.7	78.6	62.4	50.6
$\kappa^2N^1,O^2:\kappa^2O^{3,4}$	$\Delta\delta$	2.0	9.6	11.5	10.1	2.2	0.6	5.1
β -D-Galp1NtBu	δ	87.1	71.4	74.4	69.8	76.1	61.9	51.1
β -D-Galp1NtBu2H ₋₁	δ	91.1	82.0	86.2	79.6	78.6	62.3	58.7
κ^2N^1,O^2	$\Delta\delta$	4.0	10.6	11.8	9.8	2.5	-0.4	7.6

2.2.2.2. *N*-Alkyl-D-glucosylamines

As shown in chapter 2.1.2.2 the β -pyranosylamine form represents the preferred isomer in neutral and alkaline aqueous solution for uncomplexed *N*-alkyl-D-glucosylamines. Upon addition of Pd-en as coordinating agent and iodic acid, a variety of heteroleptic palladium complexes, depicted in figure 2.29, with *N*-alkyl-D-glucosylamines as bidentate ligands were identified *via* NMR spectroscopy in aqueous solution.

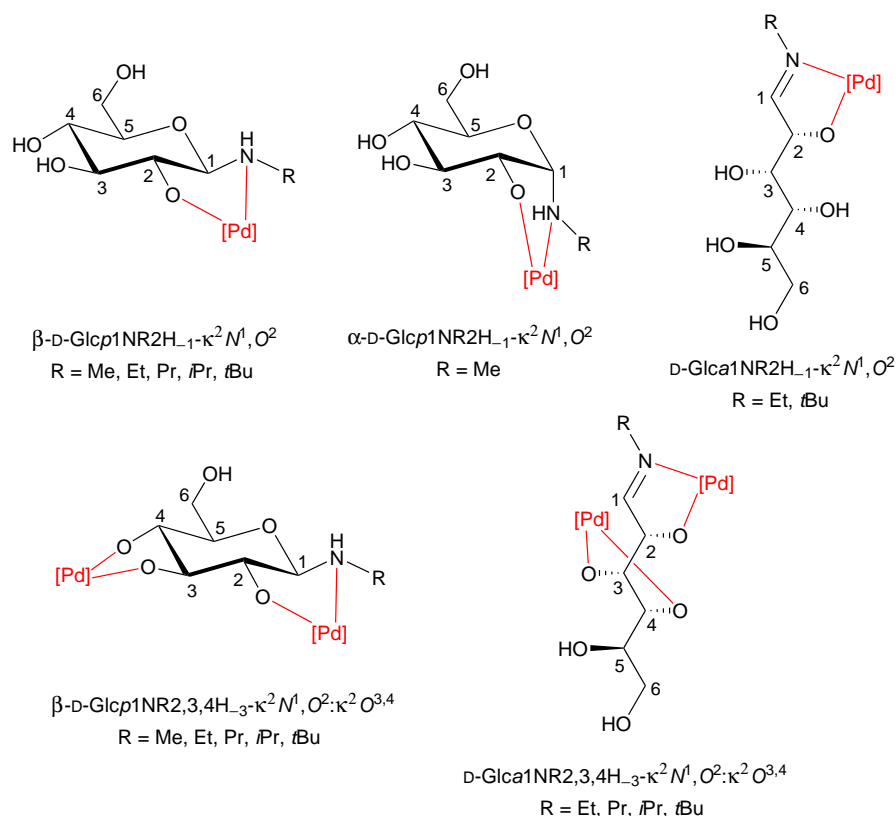


Figure 2.29. Complex species detected in reaction solutions resulting from the treatment of *N*-alkyl-D-glucosylamines with Pd-en and iodic acid.

As shown in the table 2.79, the κ^2 N¹,O² chelation of the β -anomer represents the prevailing coordination mode for equimolar reactions with *N*-alkyl-D-glucosylamines and Pd-en. A metalation of the respective α -anomer was only observed for the methyl derivative. Traces of the complex species featuring the ligand in its open-chain form were only detected in reaction solutions containing D-Glc1NEt and D-Glc1N*i*Pr. The equimolar experiments with D-Glc1N*i*Pr and D-Glc1N*t*Bu showed higher hydrolysis rates for the ligand and thus noticeable amounts of free and complexed D-Glucose were detected in the reaction solutions. Associated to this sensitivity, a rapid formation of palladium black was observed during these reactions.

Table 2.79. Percentage distribution of the metalated species resulting from the treatment of *N*-alkyl-D-glucosylamines with Pd-en and iodic acid in the molar ratio 1:1:1 at 4 °C.

	Me	Et	Pr	<i>i</i> Pr	<i>t</i> Bu
β -D-Glcp1NR2H ₋₁ - κ^2N^1,O^2	84	76	94	78	52
α -D-Glcp1NR2H ₋₁ - κ^2N^1,O^2	12	0	0	0	0
D-Glca1NR2H ₋₁ - κ^2N^1,O^2	0	4	0	0	7
other species	4	20	6	22	41

The presence of the sterically favored β -anomer in the prevailing complex species is indicated by the measured ${}^3J_{1,2}$ values of 7.9 Hz to 9.4 Hz. Additionally, all further determined coupling constants in the complexes match the values found for the free *N*-alkyl- β -D-glucopyranosylamine isomers in aqueous solution. The ${}^{13}\text{C}\{^1\text{H}\}$ NMR chemical shifts and derived CIS values for the β -pyranosylamine complex species are listed in table 2.80 and are in accordance with the expected values for a κ^2N^1,O^2 coordination mode.

Table 2.80. Selected ${}^{13}\text{C}\{^1\text{H}\}$ NMR chemical shifts (δ /ppm) and shift differences ($\Delta\delta$) to the free ligand of the detected monometalated *N*-alkyl-D-glucopyranosylamines with Pd-en in D₂O at 4 °C. The $\Delta\delta$ values indicating a CIS are printed bold.

		C1	C2	C3	C4	C5	C6	C α
β -D-Glcp1NMe	δ	91.3	73.4	77.4	70.6	77.4	61.5	31.5
β -D-Glcp1NMe2H ₋₁	δ	94.1	80.2	79.0	69.8	77.9	61.1	36.8
κ^2N^1,O^2	$\Delta\delta$	2.8	6.8	1.6	-0.8	0.5	-0.4	5.3
β -D-Glcp1NEt	δ	89.7	73.6	77.4	70.5	77.5	61.5	39.9
β -D-Glcp1NEt2H ₋₁	δ	89.5	80.2	79.0	69.9	77.9	61.1	42.4
κ^2N^1,O^2	$\Delta\delta$	-0.2	6.6	1.6	-0.6	0.4	-0.4	2.5
β -D-Glcp1NPr	δ	90.2	73.6	77.4	70.5	77.5	61.5	47.6
β -D-Glcp1NPr2H ₋₁	δ	90.7	80.1	79.0	69.7	77.9	61.0	50.1
κ^2N^1,O^2	$\Delta\delta$	0.5	6.5	1.6	-0.8	0.4	-0.5	2.5
β -D-Glcp1N <i>i</i> Pr	δ	88.2	74.0	77.3	70.6	77.6	61.6	45.5
β -D-Glcp1N <i>i</i> Pr2H ₋₁	δ	90.0	80.4	79.1	69.7	78.1	61.1	50.9
κ^2N^1,O^2	$\Delta\delta$	1.8	6.4	1.8	-0.9	0.5	-0.5	5.4
β -D-Glcp1N <i>t</i> Bu	δ	86.6	73.8	76.9	70.7	77.6	61.7	50.9
β -D-Glcp1N <i>t</i> Bu2H ₋₁	δ	90.7	81.0	79.1	69.9	78.2	61.3	58.8
κ^2N^1,O^2	$\Delta\delta$	4.1	7.2	2.2	-0.8	0.5	-0.5	7.9
α -D-Glcp1NMe	δ	88.2	71.4	73.6	70.6	71.2	61.4	31.4
α -D-Glcp1NMe2H ₋₁	δ	93.1	76.6	74.0	69.3	69.6	61.4	36.6
κ^2N^1,O^2	$\Delta\delta$	4.9	5.2	0.4	-1.3	-1.6	0.0	5.2

A metalation of the energetically less favorable α -anomer was only observed in the case of D-Glc1NMe and is indicated by the smaller ${}^3J_{1,2}$ coupling constant of 6.0 Hz (free α -D-Glc1NMe: 5.0 Hz). This complex species exhibits with 4.9 ppm for the C1 atom and 5.2 ppm for the C2 atom rather unusual CIS values. Only the CIS value for the C α atom lies with 5.2 ppm within the expected range. Unlike in the case of the chelation of the α -anomer for some *N*-alkyl-D-xylosylamines described in chapter 2.2.1.4, the possibility of a dynamic fluctuation between

the two chair conformations can be excluded for all D-glycosylamines derivatives as in the 1C_4 conformation the hydroxymethyl group at the C5 atom would adopt the sterically unfavorable axial position.

The minimal amounts of open-chain complex species for D-Glc1NEt and D-Glc1N*i*Pr were detected by their prominent ${}^{13}C\{^1H\}$ NMR chemical shifts, listed in table 2.80, and the corresponding 1H NMR signals assigned to the imine hydrogen atom at 7.98 ppm and 7.90 ppm, respectively.

Table 2.81. Selected ${}^{13}C\{^1H\}$ NMR chemical shifts (δ /ppm) of the detected monometalated open-chain species of *N*-alkyl-D-glucosylamines with Pd-en in D₂O at 4 °C.

		C1	C2	C3	C4	C5	C6	Cα
D-Glc1NEt2H ₋₁ - κ^2N^1,O^2	δ	186.0	88.0	71.9	69.3	71.4	63.5	55.3
D-Glc1N <i>t</i> Bu2H ₋₁ - κ^2N^1,O^2	δ	181.5	87.9	72.0	69.1	71.4	63.6	62.8

The species distribution given in table 2.82 reveals a clear preference of the coordination of the β -pyranosylamine form for all *N*-alkyl-D-glucosylamines in experiments including two equivalents of Pd-en. Despite the excess of palladium(II) probe, all derivatives formed considerable amounts of the previously described monometalated species, indicating a high stability of the mononuclear complexes. Nevertheless, the doubly metalated complex species prevail in all reaction solutions, except in the reaction with D-Glc1N*t*Bu. The amount of complexes including the ligand in its open-chain form is noticeably higher in experiments with an excess of palladium probe than in the corresponding equimolar reactions.

Table 2.82. Percentage distribution of the metalated species resulting from the treatment of *N*-alkyl-D-glucosylamines with Pd-en and iodic acid in the molar ratio 1:2:1 at 4 °C.

	Me	Et	Pr	<i>i</i>Pr	<i>t</i>Bu
β -D-Glc <i>p</i> 1NR2,3,4H ₋₃ - $\kappa^2N^1,O^2;\kappa^2O^{3,4}$	72	54	68	48	20
D-Glc <i>a</i> 1NR2,3,4H ₋₃ - $\kappa^2N^1,O^2;\kappa^2O^{3,4}$	0	6	14	12	14
β -D-Glc <i>p</i> 1NR2H ₋₁ - κ^2N^1,O^2	12	32	10	40	40
other species	16	8	10	0	26

The experimental ${}^{13}C\{^1H\}$ NMR chemical shifts and CIS values listed in table 2.83 verify the $\kappa^2O^{3,4}$ binding of a second Pd-en fragment in a *trans*-vicinal manner for all investigated *N*-alkyl-D-glucosylamines.

Table 2.83. Selected $^{13}\text{C}\{^1\text{H}\}$ NMR chemical shifts (δ/ppm) and shift differences ($\Delta\delta$) to the free ligand of the detected doubly metalated *N*-alkyl-D-glucopyranosylamines with Pd-en in D_2O at 4°C . The $\Delta\delta$ values indicating a CIS are printed bold.

		C1	C2	C3	C4	C5	C6	Cα
β -D-Glcp1NMe	δ	91.3	73.4	77.4	70.6	77.4	61.5	31.5
β -D-Glcp1NMe2,3,4H $_{-3}$	δ	95.0	82.2	88.3	80.1	79.2	61.6	37.2
$\kappa^2\text{N}^1, \text{O}^2: \kappa^2\text{O}^{3,4}$	$\Delta\delta$	3.7	8.8	10.9	9.5	1.8	0.1	5.7
β -D-Glcp1NEt	δ	89.7	73.6	77.4	70.5	77.5	61.5	39.9
β -D-Glcp1NEt2,3,4H $_{-3}$	δ	90.2	82.0	88.4	80.0	79.3	61.5	42.5
$\kappa^2\text{N}^1, \text{O}^2: \kappa^2\text{O}^{3,4}$	$\Delta\delta$	0.5	8.4	11.0	9.5	1.8	0.0	2.6
β -D-Glcp1NPr	δ	90.2	73.6	77.4	70.5	77.5	61.5	47.6
β -D-Glcp1NPr2,3,4H $_{-3}$	δ	91.3	82.1	88.3	79.9	79.2	61.5	50.3
$\kappa^2\text{N}^1, \text{O}^2: \kappa^2\text{O}^{3,4}$	$\Delta\delta$	1.1	8.5	10.9	9.4	1.7	0.0	2.7
β -D-Glcp1NiPr	δ	88.2	74.0	77.3	70.6	77.6	61.6	45.5
β -D-Glcp1NiPr2,3,4H $_{-3}$	δ	91.0	82.4	88.4	79.9	79.3	61.5	50.8
$\kappa^2\text{N}^1, \text{O}^2: \kappa^2\text{O}^{3,4}$	$\Delta\delta$	2.8	8.4	11.1	9.3	1.7	-0.1	5.3
β -D-Glcp1NtBu	δ	86.6	73.8	76.9	70.7	77.6	61.7	50.9
β -D-Glcp1NtBu2,3,4H $_{-3}$	δ	91.7	83.4	88.3	80.2	79.0	61.7	58.8
$\kappa^2\text{N}^1, \text{O}^2: \kappa^2\text{O}^{3,4}$	$\Delta\delta$	5.1	9.6	11.4	9.5	1.4	0.0	7.9

The doubly metalated open-chain species differ from the corresponding monometalated derivatives in the $^{13}\text{C}\{^1\text{H}\}$ NMR chemical shifts measured for the C3 and C4 atoms. The calculated shift differences average 13.4 ppm for the C3 atom and 11.6 ppm for the C4 atom, unambiguously indicating a $\kappa^2\text{N}^1, \text{O}^2: \kappa^2\text{O}^{3,4}$ metalation of the acyclic isomers. No traces of species featuring further possible coordination modes, as e.g. a $\kappa^2\text{N}^1, \text{O}^2: \kappa^2\text{O}^{4,5}$ binding, were detected in the reaction solutions.

Table 2.84. Selected $^{13}\text{C}\{^1\text{H}\}$ NMR chemical shifts (δ/ppm) of the detected doubly metalated open-chain species of *N*-alkyl-D-glucosylamines with Pd-en in D_2O at 4°C .

		C1	C2	C3	C4	C5	C6	Cα
D-Glca1NEt2,3,4H $_{-3}$ - $\kappa^2\text{N}^1, \text{O}^2: \kappa^2\text{O}^{3,4}$	δ	186.4	88.7	85.4	80.7	73.5	65.2	55.3
D-Glca1NPr2,3,4H $_{-3}$ - $\kappa^2\text{N}^1, \text{O}^2: \kappa^2\text{O}^{3,4}$	δ	187.4	88.2	85.5	80.8	73.4	65.2	62.7
D-Glca1NiPr2,3,4H $_{-3}$ - $\kappa^2\text{N}^1, \text{O}^2: \kappa^2\text{O}^{3,4}$	δ	183.5	88.5	85.3	80.7	73.6	65.3	59.2
D-Glca1NtBu2,3,4H $_{-3}$ - $\kappa^2\text{N}^1, \text{O}^2: \kappa^2\text{O}^{3,4}$	δ	182.2	88.1	85.5	80.7	73.9	65.1	62.7

All reactions involving an excess of palladium(II) probe, showed notable signs for the formation of elemental palladium during the reaction process. The rate of this formation appears to accelerate with the steric demand of the alkylamino moiety of the included ligand and hence correlates with the hydrolysis sensitivity of the ligand. Thus, as observed in the case of the *tert*-butyl derivative, the through hydrolytic cleavage released *tert*-butylamine readily substitutes the hydroxide ligand and forms competing complex species. Furthermore, the excess of palladium(II) probe led to an additional coordination of deprotonated D-glucose, indicated by the emergence of $^{13}\text{C}\{^1\text{H}\}$ NMR signals in the range from 102 ppm to 107 ppm.

2.2.2.3. *N*-Alkyl-L-gulosylamines

In reaction solutions containing varying amounts of Pd-en, iodic acid and *N*-alkyl-L-gulosylamines the single, doubly and triple metalated species depicted in figure 2.30 were identified. While the characterized monometalated species feature the ligands in their cyclic and acyclic form, double and triple metalation occurs on the open-chain imine form.

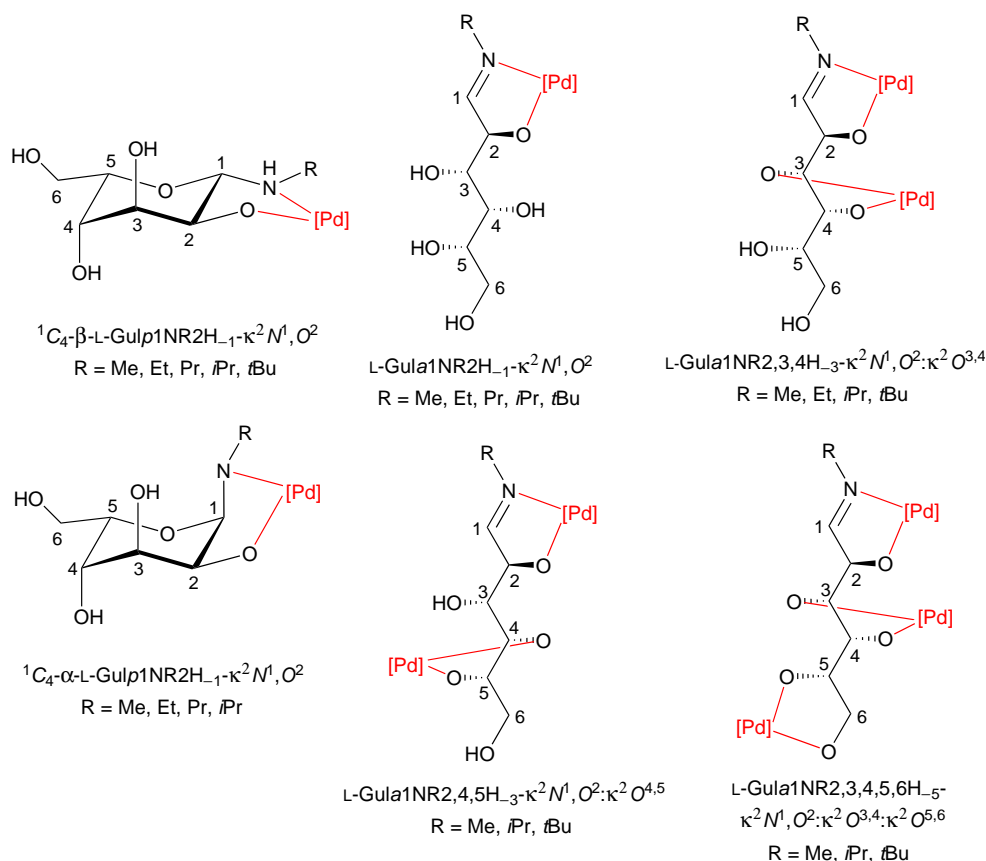


Figure 2.30. Complex species detected in reaction solutions resulting from the treatment of *N*-alkyl-L-gulosylamines with Pd-en and iodic acid.

As shown in the table 2.85, the conducted equimolar experiments strictly led to a κ^2N^1,O^2 chelation of the investigated *N*-alkyl-L-gulosylamines. The identified complex species only distinguish from each other in the included isomer. For methyl and ethyl derivatives the complexation of the β -anomer prevailed, while also smaller amounts of metalated α -anomer were found. The chelation of the open-chain form became more apparent in experiments with *iso*-propyl and *tert*-butyl derivatives. Other species identified in the reaction solutions were mostly free *N*-alkyl-L-gulosylamines and the associated hydrolytic cleavage product L-gulose.

Table 2.85. Percentage distribution of the metalated species resulting from the treatment of *N*-alkyl-*L*-gulosylamines with Pd-en and iodic acid in the molar ratio 1:1:1 at 4 °C.

	Me	Et	Pr	<i>i</i> Pr	<i>t</i> Bu
1C_4 - β - <i>L</i> -Gulp1NR2H ₋₁ - κ^2N^1,O^2	72	76	52	54	27
1C_4 - α - <i>L</i> -Gulp1NR2H ₋₁ - κ^2N^1,O^2	16	14	5	6	0
<i>L</i> -Gul α 1NR2H ₋₁ - κ^2N^1,O^2	8	6	12	23	54
other species	4	4	31	17	19

In most cases the chelation of the *N*-alkyl- β -*L*-gulosylamines was favored in the reaction solution. The corresponding complexes were readily identified by the characteristic CIS values found for the C1, C2 and C α atoms (listed in table 2.86) and the measured ${}^3J_{1,2}$ values, which range between 9.2 Hz and 9.5 Hz. Furthermore also all other determined coupling constants indicate the expected strict presence of the 1C_4 conformation for the ligands.

Table 2.86. Selected ${}^{13}C\{^1H\}$ NMR chemical shifts (δ /ppm) and shift differences ($\Delta\delta$) to the free ligand of the detected monometalated *N*-alkyl-*L*-gulopyranosylamines with Pd-en in D₂O at 4 °C. The $\Delta\delta$ values indicating a CIS are printed bold.

		C1	C2	C3	C4	C5	C6	C α
β - <i>L</i> -Gul1NMe	δ	88.4	68.2	71.7	70.3	74.5	61.8	31.3
1C_4 - β - <i>L</i> -Gulp1NMe2H ₋₁	δ	91.2	75.5	72.5	69.9	76.5	61.6	36.8
κ^2N^1,O^2	$\Delta\delta$	2.8	7.3	-0.8	0.4	2.0	-0.2	5.5
β - <i>L</i> -Gul1NEt	δ	87.0	68.4	71.7	70.3	74.5	61.8	39.7
1C_4 - β - <i>L</i> -Gulp1NEt2H ₋₁	δ	86.3	75.2	72.5	69.8	76.5	61.5	42.3
κ^2N^1,O^2	$\Delta\delta$	-0.7	6.8	0.8	-0.5	2.0	-0.3	2.6
β - <i>L</i> -Gul1N1NPr	δ	87.3	68.4	71.8	70.3	74.6	61.8	47.4
1C_4 - β - <i>L</i> -Gulp1NPr2H ₋₁	δ	87.5	75.4	72.5	69.8	76.5	61.4	50.0
κ^2N^1,O^2	$\Delta\delta$	0.2	7.0	0.7	-0.5	1.9	-0.4	2.6
β - <i>L</i> -Gul1NiPr	δ	85.2	68.8	71.8	70.4	74.5	61.8	45.2
1C_4 - β - <i>L</i> -Gulp1NiPr2H ₋₁	δ	86.8	75.6	72.7	69.7	76.7	61.4	50.8
κ^2N^1,O^2	$\Delta\delta$	1.6	6.8	0.9	-0.7	2.2	-0.4	5.6
β - <i>L</i> -Gul1N <i>t</i> Bu	δ	83.7	68.5	71.7	70.6	74.2	61.8	51.1
1C_4 - β - <i>L</i> -Gulp1N <i>t</i> Bu2H ₋₁	δ	87.3	76.3	73.3	69.7	77.1	61.4	58.8
κ^2N^1,O^2	$\Delta\delta$	3.6	7.8	1.6	-0.9	2.9	-0.4	7.7

The minor pyranoid species detected in all reaction solutions, except for those containing the *tert*-butyl derivative, was identified as the κ^2N^1,O^2 -chelated α -anomer. A direct comparison of the ${}^{13}C\{^1H\}$ NMR chemical shifts between those complexes and the corresponding free ligands was not feasible since the free α -anomer was not NMR-spectroscopically detected in D₂O.

The complex species including the *N*-alkyl-*L*-gulosylamines in their acyclic imine form were characterized by their downfield NMR signals assigned to the imine carbon and hydrogen atom. The 1H NMR signals of the H1 atom are located between 8.04 ppm and 8.08 ppm and the corresponding ${}^{13}C\{^1H\}$ NMR signals between 187.7 ppm and 181.6 ppm. Although no reference values for the open-chain isomers of the free *N*-alkyl-*L*-gulosylamines are available, the downfield-shifted ${}^{13}C\{^1H\}$ NMR signals of the C2 atoms listed in table 2.87 indicate a κ^2N^1,O^2 chelation.

Table 2.87. Selected $^{13}\text{C}\{^1\text{H}\}$ NMR chemical shifts (δ/ppm) of the detected monometalated open-chain species of *N*-alkyl-L-gulosylamines with Pd-en in D_2O at 4 °C.

		C1	C2	C3	C4	C5	C6	C α
L-Gul a 1NMe2H $_{-1}$ - κ^2N^1,O^2	δ	187.7	86.5	75.2	70.8	73.2	63.0	48.8
L-Gul a 1NEt2H $_{-1}$ - κ^2N^1,O^2	δ	186.2	86.5	75.3	70.8	73.3	63.0	55.8
L-Gul a 1NPr2H $_{-1}$ - κ^2N^1,O^2	δ	187.3	86.3	75.3	70.8	73.3	63.0	62.8
L-Gul a 1NiPr2H $_{-1}$ - κ^2N^1,O^2	δ	183.3	86.7	75.3	70.7	73.3	63.0	60.2
L-Gul a 1NtBu2H $_{-1}$ - κ^2N^1,O^2	δ	181.6	86.1	75.7	70.6	73.3	62.9	63.1

If the amount of palladium(II) probe is increased to two equivalents, doubly and also triple metalated species were detected in the resulting reaction solutions. Remarkably, all identified multinuclear complexes feature the *N*-alkyl-L-gulosylamines in the respective open-chain imine form as ligand. Furthermore, as shown in table 2.88, significant amounts of the monometalated pyranoid species was found for the methyl, ethyl and propyl derivative. This indicates a high stability of the mononuclear species, even when exposed to an excess of palladium(II) probe. In the case of the *iso*-propyl and *tert*-butyl derivatives, almost exclusively acyclic imine forms were featured. This preference of acyclic species for all *N*-alkyl-L-gulosylamines can be attributed to the fact that the *anti*-orientation of the C3 and C4 hydroxy groups in the 1C_4 conformation is not suitable for a complexation of a second PdN $_2$ -fragment. Further species detected in the experiments were mostly complexed and non-complexed D-glucose. In the case of L-Gul1NMe also an additional pyranoid species was visible in the NMR spectra, but could not be unambiguously characterized. For L-Gul1NPr rapid hydrolysis of the ligand and the vigorous formation of elementary palladium yielded a NMR spectrum insufficient for detailed analysis.

Table 2.88. Percentage distribution of the metalated species resulting from the treatment of *N*-alkyl-L-gulosylamines with Pd-en and iodic acid in the molar ratio 1:2:1 at 4 °C.

	Me	Et	Pr	<i>i</i> Pr	<i>t</i> Bu
L-Gul a 1NR2,3,4H $_{-3}$ - $\kappa^2N^1,O^2;\kappa^2O^{3,4}$	27	46	0	46	23
L-Gul a 1NR2,4,5H $_{-3}$ - $\kappa^2N^1,O^2;\kappa^2O^{4,5}$	0	0	0	35	61
L-Gul a 1NR2,3,4,5,6H $_{-5}$ - $\kappa^2N^1,O^2;\kappa^2O^{3,4};\kappa^2O^{5,6}$	8	0	0	15	16
1C_4 - β -D-Gul p 1NR2H $_{-1}$ - κ^2N^1,O^2	46	48	38	4	0
other species	19	6	62	0	0

Two different dimetalated acyclic species, identified as the $\kappa^2N^1,O^2;\kappa^2O^{3,4}$ and $\kappa^2N^1,O^2;\kappa^2O^{4,5}$ chelate, were detected. While the $\kappa^2N^1,O^2;\kappa^2O^{3,4}$ chelate was present in the reaction solution of every *N*-alkyl-L-gulosylamines with two equivalents of palladium probe, the $\kappa^2N^1,O^2;\kappa^2O^{4,5}$ chelate was only found in experiments with L-Gul1NiPr and L-Gul1NtBu. An overview of the $^{13}\text{C}\{^1\text{H}\}$ NMR chemical shifts assigned to both species is given in table 2.89. The $\kappa^2N^1,O^2;\kappa^2O^{3,4}$ complex was characterized by shift differences of about 10 ppm for the C3 atom and 11 ppm for the C4 atom in comparison to the respective monometalated open-chain species. The $\kappa^2N^1,O^2;\kappa^2O^{4,5}$ complex on the other hand was identified by the shift difference of about 18 ppm for the C5 atom and the aforementioned 11 ppm for the C4 atom. The hydroxy group at the C3 atom remained uncomplexed in this species and thus experienced no significant downfield shift.

Table 2.89. Selected $^{13}\text{C}\{^1\text{H}\}$ NMR chemical shifts (δ/ppm) of the detected doubly metalated open-chain species of *N*-alkyl-L-gulosylamines with Pd-en in D_2O at 4°C .

		C1	C2	C3	C4	C5	C6	Cα
L-Gula1NMe2,3,4H ₋₃ - κ^2N^1, O^2 : $\kappa^2O^{3,4}$	δ	190.3	88.0	85.8	81.5	73.9	62.3	48.8
L-Gula1NEt2,3,4H ₋₃ - κ^2N^1, O^2 : $\kappa^2O^{3,4}$	δ	188.6	88.3	85.7	81.5	74.0	62.4	55.8
L-Gula1NiPr2,3,4H ₋₃ - κ^2N^1, O^2 : $\kappa^2O^{3,4}$	δ	185.3	88.3	85.7	81.5	74.0	62.4	60.1
L-Gula1NtBu2,3,4H ₋₃ - κ^2N^1, O^2 : $\kappa^2O^{3,4}$	δ	183.9	88.2	86.2	81.4	74.0	62.3	62.9
L-Gula1NMe2,4,5H ₋₃ - κ^2N^1, O^2 : $\kappa^2O^{4,5}$	δ	190.9	88.8	79.5	81.3	92.0	63.3	48.7
L-Gula1NiPr2,4,5H ₋₃ - κ^2N^1, O^2 : $\kappa^2O^{4,5}$	δ	185.5	88.8	79.6	81.4	92.2	63.3	60.3
L-Gula1NtBu2,4,5H ₋₃ - κ^2N^1, O^2 : $\kappa^2O^{4,5}$	δ	182.9	87.7	79.7	82.0	92.6	63.3	63.0

In reactions featuring L-Gul1NiPr and L-Gul1NtBu and two equivalents of Pd-en a third acyclic species was present in all recorded NMR spectra. The $^{13}\text{C}\{^1\text{H}\}$ NMR chemical shifts listed in table 2.90 were assigned to this species and indicate the formation of a trinuclear complex. All carbon atoms experience a significant downfield shift as result of the complexation, most noticeably the C6 atom, which is easily identified in the performed DEPT135 NMR experiments.

Table 2.90. Selected $^{13}\text{C}\{^1\text{H}\}$ NMR chemical shifts (δ/ppm) of the detected triple metalated open-chain species of *N*-alkyl-L-gulosylamines with Pd-en in D_2O at 4°C .

		C1	C2	C3	C4	C5	C6	Cα
L-Gula1NMe2,3,4,5,6H ₋₅ - κ^2N^1, O^2 : $\kappa^2O^{3,4}$: $\kappa^2O^{5,6}$	δ	190.9	86.8	85.3	83.1	88.8	72.4	48.7
L-Gula1NiPr2,3,4,5,6H ₋₅ - κ^2N^1, O^2 : $\kappa^2O^{3,4}$: $\kappa^2O^{5,6}$	δ	185.9	86.9	85.6	83.4	89.0	72.4	60.2
L-Gula1NtBu2,3,4,5,6H ₋₅ - κ^2N^1, O^2 : $\kappa^2O^{3,4}$: $\kappa^2O^{5,6}$	δ	184.0	87.4	86.7	83.5	88.8	72.5	63.1

The increase of the palladium concentration in a reaction with *N*-methyl-L-gulosylamines up to three equivalents resulted in the NMR spectrum displayed in figure 2.31. The spectrum shows all of the three above mentioned acyclic species L-Gula1NMe2,3,4H₋₃- κ^2N^1, O^2 : $\kappa^2O^{3,4}$ (37%), L-Gula1NMe2H₋₃- κ^2N^1, O^2 : $\kappa^2O^{4,5}$ (21%) and L-Gula1NMe2,3,4,5,6H₋₅- κ^2N^1, O^2 : $\kappa^2O^{3,4}$: $\kappa^2O^{5,6}$ (17%) next to the monometalated pyranoid 1C_4 - β -D-Gulp1NR2H₋₁- κ^2N^1, O^2 (19%) species and small amounts of an unidentified cyclic species (6%).

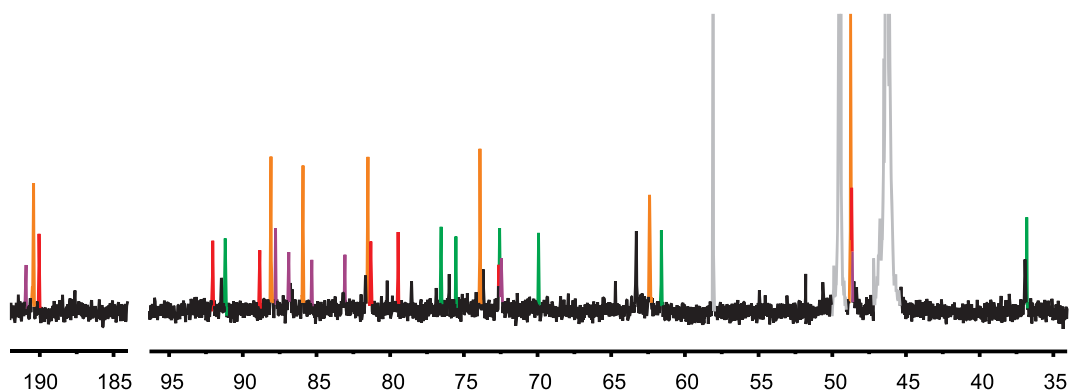


Figure 2.31. Resulting $^{13}\text{C}\{^1\text{H}\}$ NMR spectra for the treatment of L-Gula1NMe with Pd-en and iodic acid in the molar ratio 1:3:1 after 3 h at 4°C in D_2O . Orange: L-Gula1NMe $_{2,3,4}\text{H}_{-3-\kappa^2\text{N}^1, \text{O}^2:\kappa^2\text{O}^{3,4}}$, red: L-Gula1NMe $_{2,3,4}\text{H}_{-3-\kappa^2\text{N}^1, \text{O}^2:\kappa^2\text{O}^{4,5}}$, green: $^1\text{C}_4\text{-}\beta\text{-D-Gulp1NR2H}_{-1-\kappa^2\text{N}^1, \text{O}^2}$, purple: L-Gula1NMe $_{2,3,4,5,6}\text{H}_{-5-\kappa^2\text{N}^1, \text{O}^2:\kappa^2\text{O}^{3,4}:\kappa^2\text{O}^{5,6}}$, grey: Pd-en, EtOH and MeOH.

2.2.2.4. N-Alkyl-D-mannosylamines

In the investigated reaction solutions containing equimolar amounts of *N*-alkyl-D-mannosylamines, Pd-en and iodic acid two complex species were unambiguously identified. For the third major species detected in solution, the configuration and conformation of the binding ligand could only be assumed. These three species and the binuclear complex species resulting from experiments with two equivalents of Pd-en are depicted in figure 2.32.

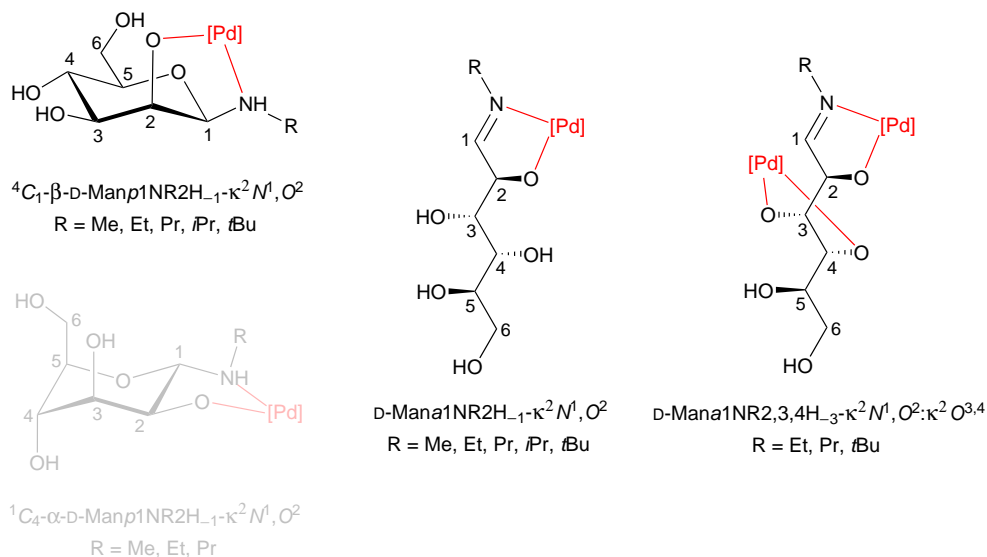


Figure 2.32. Complex species detected in reaction solutions resulting from the treatment of *N*-alkyl-D-mannosylamines with Pd-en and iodic acid. Assumed complex species without clear evidence for their presence are displayed grayed out.

The percentage distributions determined from the conducted equimolar experiments are listed in table 2.91 and indicate a remarkable variability of the coordination behavior of *N*-alkyl-D-

mannosylamines towards palladium(II) probes. While for D-Man1NMe and D-Man1NEt cyclic isomers prevailed upon coordination, the sterically more demanding *iso*-propyl and *tert*-butyl derivatives exhibited a tendency to favor the metalation of the open-chain form. In the case of D-Man1NMe, D-Man1NEt and D-Man1NPr two differing cyclic species were detected in the respective reaction solutions. Other detected species include the free reactant D-Man1NMe in the corresponding experiment and not identifiable species in the reactions with D-Man1N*i*Pr and D-Man1N*t*Bu. Indications for a hydrolysis of the ligand were only found in reaction solutions containing *N-tert*-butyl-D-mannosylamine.

Table 2.91. Percentage distribution of the metalated species resulting from the treatment of *N*-alkyl-D-mannosylamines with Pd-en and iodic acid in the molar ratio 1:1:1 at 4 °C.

	Me	Et	Pr	<i>i</i> Pr	<i>t</i> Bu
4C_1 - β -D-Man <i>p</i> 1NR2H ₋₁ - κ^2N^1,O^2	40	38	38	24	28
1C_4 - α -D-Man <i>p</i> 1NR2H ₋₁ - κ^2N^1,O^2	22	36	22	0	0
D-Man <i>a</i> 1NR2H ₋₁ - κ^2N^1,O^2	20	22	40	62	46
other species	18	4	0	14	26

The predominant complex species including a cyclic ligand features the β -mannopyranosylamine form and hence a *cis*-vicinal κ^2N^1,O^2 chelation of the palladium ion. Although the found CIS values for these complexes, listed in table 2.92, are noticeably higher than in the previously discussed cases, a κ^2N^1,O^2 binding is highly likely. This is mainly explained by the absence of any other apparent configurations, which allow a reasonable coordination of the palladium ion. Due to the problem of overlapping signals in the 1H NMR spectra of the respective experiments, a definite assignment and determination of the coupling constants was not feasible.

Table 2.92. Selected ${}^{13}C\{{}^1H\}$ NMR chemical shifts (δ /ppm) and shift differences ($\Delta\delta$) to the free ligand of the detected monometalated *N*-alkyl-D-mannopyranosylamines with Pd-en in D₂O at 4 °C. The $\Delta\delta$ values indicating a CIS are printed bold.

		C1	C2	C3	C4	C5	C6	C α
β -D-Man <i>p</i> 1NMe	δ	88.7	71.5	74.5	67.9	77.9	61.9	31.6
β -D-Man <i>p</i> 1NMe2H ₋₁	δ	94.2	78.6	72.6	67.5	78.7	61.8	36.5
κ^2N^1,O^2	$\Delta\delta$	5.5	7.2	-1.9	-0.4	0.7	-0.1	4.9
β -D-Man <i>p</i> 1NEt	δ	86.9	71.8	74.5	67.9	77.9	61.9	39.5
β -D-Man <i>p</i> 1NEt2H ₋₁	δ	89.9	79.2	72.7	67.6	78.8	61.7	43.7
κ^2N^1,O^2	$\Delta\delta$	3.0	7.4	-1.8	-0.3	0.9	-0.3	4.2
β -D-Man <i>p</i> 1NPr	δ	87.2	71.8	74.5	67.9	77.9	61.9	47.1
β -D-Man <i>p</i> 1NPr2H ₋₁	δ	90.2	79.2	72.8	67.5	78.8	61.7	50.8
κ^2N^1,O^2	$\Delta\delta$	3.0	7.4	-1.7	-0.4	0.8	-0.3	3.7
β -D-Man <i>p</i> 1N <i>i</i> Pr	δ	84.5	72.0	74.7	67.9	77.9	61.9	43.8
β -D-Man <i>p</i> 1N <i>i</i> Pr2H ₋₁	δ	92.8	79.2	73.0	67.0	79.0	61.6	52.1
κ^2N^1,O^2	$\Delta\delta$	8.3	7.2	-1.7	-0.9	1.1	-0.3	8.3
β -D-Man <i>p</i> 1N <i>t</i> Bu	δ	84.4	73.1	74.8	67.8	77.6	61.9	51.0
β -D-Man <i>p</i> 1N <i>t</i> Bu2H ₋₁	δ	93.5	80.0	73.1	66.8	78.8	61.5	57.7
κ^2N^1,O^2	$\Delta\delta$	9.1	6.9	-1.7	-1.0	1.2	-0.4	6.7

The formation of a second complex species featuring a cyclic ligand was observed in some experiments, but the associated coordination mode could not be initially elucidated. Conceivable scenarios include the ligand coordinating as furanoid isomer, a coordination of the PdN₂-fragment without involvement of the methylamino function or the fluctuation of the *N*-alkyl-D-mannosylamines from the ⁴C₁ conformation to the unlikely ¹C₄ conformation. The reason why the presence of the latter is assumed will be outlined in the discussion of this work.

The *N*-alkyl-D-mannosylamine complexes featuring the acyclic isomer as ligand are characterized by the prominent ¹H and ¹³C{¹H} NMR signals in the downfield region of the obtained NMR spectra, assigned to the coordinating imine function. The corresponding ¹H NMR signals are unambiguously identified by their chemical shifts ranging from 8.02 ppm to 8.09 ppm. The ¹³C{¹H} NMR signals assigned to the carbohydrate scaffold and C α atom are listed in table 2.93.

Table 2.93. Selected ¹³C{¹H} NMR chemical shifts (δ /ppm) of the detected monometalated open-chain species of *N*-alkyl-D-mannosylamines with Pd-en in D₂O at 4 °C.

		C1	C2	C3	C4	C5	C6	C α
D-Mana1NMe2H ₋₁ - κ^2N^1,O^2	δ	188.2	86.6	73.8	70.2	71.2	63.7	48.8
D-Mana1NEt2H ₋₁ - κ^2N^1,O^2	δ	186.6	86.5	73.9	70.2	71.2	63.7	55.7
D-Mana1NPr2H ₋₁ - κ^2N^1,O^2	δ	187.4	85.8	74.0	70.2	71.1	63.7	62.8
D-Mana1NiPr2H ₋₁ - κ^2N^1,O^2	δ	183.7	86.6	74.0	70.2	71.1	63.7	60.1
D-Mana1NtBu2H ₋₁ - κ^2N^1,O^2	δ	182.1	85.8	74.7	70.1	70.1	63.7	63.1

In reaction solutions of *N*-alkyl-D-mannosylamines containing an excess of Pd-en only one doubly metalated species, featuring the open-chain isomer as ligand, was detected. The chelation of a second PdN₂-fragment by the acyclic imine strictly occurs on the alkoxide functions at the C3 and C4 atom and was verified by the chemical shift differences of between 13 ppm and 14 ppm for both carbon atoms in comparison to the corresponding monometalated acyclic complex species. An overview of the ¹³C{¹H} NMR chemical shifts assigned to the acyclic doubly metalated species is given in table 2.94.

Surprisingly, no indications for a $\kappa^2N^1,O^2:\kappa^2O^{3,4}$ chelation of a pyranoid or furanoid isomer were observed in the respective reactions. Only small amounts of the previously mentioned monometalated species were detected next to the doubly metalated open-chain species.

Table 2.94. Selected ¹³C{¹H} NMR chemical shifts (δ /ppm) of the detected doubly metalated open-chain species of *N*-alkyl-D-mannosylamines with Pd-en in D₂O at 4 °C.

		C1	C2	C3	C4	C5	C6	C α
D-Mana1NEt2,3,4H ₋₃ - $\kappa^2N^1,O^2:\kappa^2O^{3,4}$	δ	188.1	88.6	87.8	83.9	73.3	64.2	55.8
D-Mana1NPr2,3,4H ₋₃ - $\kappa^2N^1,O^2:\kappa^2O^{3,4}$	δ	189.2	88.7	87.6	83.9	73.3	64.2	62.9
D-Mana1NtBu2,3,4H ₋₃ - $\kappa^2N^1,O^2:\kappa^2O^{3,4}$	δ	183.1	88.4	87.9	84.2	73.3	64.4	63.1

It is noteworthy, that all reactions of *N*-alkyl-D-mannosylamines with two equivalents of palladium(II) probe led to an immediate formation of a black precipitate, most likely palladium black. Despite the reaction temperature of 4 °C, most reaction vessels and NMR tubes showed a mirror of elementary palladium after the full reaction and analysis time. These side reactions and accompanied reduction of palladium often resulted in not analyzable NMR spectra.

2.2.2.5. *N*-Alkyl-L-rhamnosylamines

As anticipated because of the structural similarity, the observed coordination behavior of *N*-alkyl-L-rhamnosylamines towards palladium(II) probes is quite similar to the previously in chapter 2.2.2.4 described findings for *N*-alkyl-D-mannosylamines. Hence, the treatment of the investigated rhamnosylamine derivatives with Pd-en and iodic acid also led to the characterization of the three mononuclear species depicted in figure 2.33.

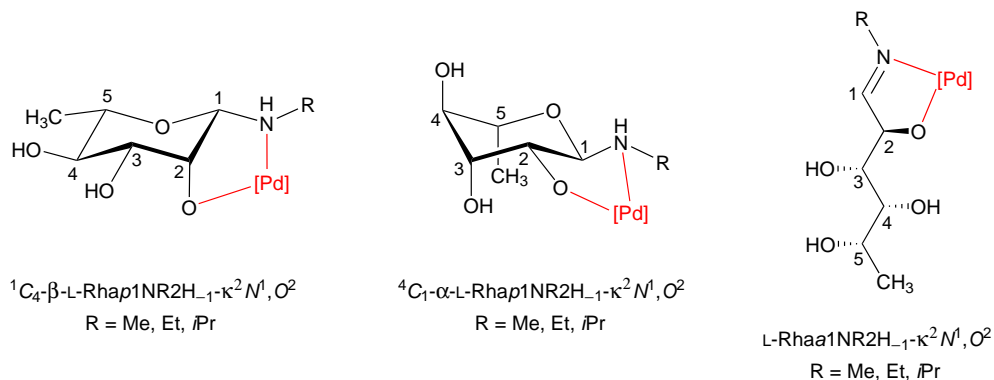


Figure 2.33. Complex species and conformational fluctuation detected in reaction solutions resulting from the treatment of *N*-alkyl-L-rhamnosylamines with Pd-en and iodic acid.

As shown in table 2.95, for *N*-alkyl-L-rhamnosylamines the amount of metalation of the acyclic isomer in equimolar reactions increases with the size of the alkylamino moiety in the ligand. As a consequence, the concentration of complex species featuring the ligand in its pyranoid form diminishes, especially the coordination of the α -anomer. While the NMR spectra obtained from the equimolar reaction solutions were of good quality and showed almost no side products, reactions of *N*-alkyl-L-rhamnosylamines with an excess of palladium(II) probe showed a rapid decomposition accompanied by the visible formation of elementary palladium and leading to the reception of not analyzable NMR spectra.

Table 2.95. Percentage distribution of the metalated species resulting from the treatment of *N*-alkyl-L-rhamnosylamines with Pd-en and iodic acid in the molar ratio 1:1:1 at 4 °C.

	Me	Et	<i>i</i> Pr
${}^1C_4\text{-}\beta\text{-L-Rhap1NR2H}_{-1}\text{-}\kappa^2N^1,O^2$	58	42	42
${}^4C_1\text{-}\alpha\text{-L-Rhap1NR2H}_{-1}\text{-}\kappa^2N^1,O^2$	28	26	12
L-Rhaa1NR2H ₋₁ -κ ² N ¹ ,O ²	14	20	46
other species	0	12	0

The in table 2.96 listed CIS values for the chelation of the β -L-rhamnopyranosylamine form are similar to the values described in chapter 2.2.2.4 for *N*-alkyl- β -D-mannopyranosylamines. Hence, a similar structure and *cis*-vicinal coordination mode is assumed. But unlike in the case of their 6-hydroxy analogues, the majority of the coupling constants for the coordinating *N*-alkyl- β -L-rhamnosylamines could be obtained from the respective ¹H NMR spectra. The determined ³J_{1,2} values of 1.0 Hz to 1.2 Hz and also other coupling constants verify the coordination of the

β -anomer and the presence of the 1C_4 conformation in this species.

Table 2.96. Selected ${}^{13}C\{^1H\}$ NMR chemical shifts (δ /ppm) and shift differences ($\Delta\delta$) to the free ligand of the detected monometalated *N*-alkyl-L-rhamnopyranosylamines with Pd-en in D_2O at 4 °C. The $\Delta\delta$ values indicating a CIS are printed bold.

		C1	C2	C3	C4	C5	C6	Cα
β -L-Rha1NMe	δ	88.7	71.8	74.2	73.0	73.8	17.4	31.6
1C_4 - β -L-Rhap1NMe2H $_{-1}$	δ	94.8	78.9	74.8	72.4	72.8	17.6	36.4
κ^2N^1,O^2	$\Delta\delta$	6.1	7.1	0.6	-0.6	-1.0	0.2	4.8
β -L-Rha1NEt	δ	86.8	71.9	74.2	73.1	73.8	17.4	39.5
1C_4 - β -L-Rhap1NEt2H $_{-1}$	δ	90.0	79.3	74.8	72.5	72.8	17.6	43.7
κ^2N^1,O^2	$\Delta\delta$	3.2	7.4	0.6	-0.6	-1.0	0.2	4.2
β -L-Rha1NiPr	δ	84.3	72.1	74.3	73.1	73.8	17.4	43.7
1C_4 - β -L-Rhap1NiPr2H $_{-1}$	δ	92.9	79.4	75.0	72.4	72.7	17.8	52.2
κ^2N^1,O^2	$\Delta\delta$	8.6	7.3	0.7	-0.7	-1.1	0.4	8.5

For the other complex species featuring the ligands in their pyranoid form the metalation of the respective α -anomers is assumed. This κ^2N^1,O^2 chelation would not be feasible if the ligand strictly resides in the energetically favored 1C_4 conformation as the considered functional groups would be *anti*-oriented. Conversely, in the 4C_1 conformation a *trans*-vicinal binding of the PdN $_2$ -fragment is realizable. Due to the lower steric demand of the functional group in axial position at the C5 atom (methyl *vs.* hydroxymethyl group), this coordination mode is not as improbable as for the respective mannosylamine analogues. This assumption is further supported by the determined ${}^3J_{1,2}$ values which range from 5.9 Hz to 6.2 Hz and hence indicate the preference of the 4C_1 conformation.

The monometalation of the acyclic imine form is characterized by the immense downfield shift of the NMR signals assigned to the C1 atom. The 1H NMR signals for the imine hydrogen atom are located at 8.07 ppm to 8.08 ppm in the respective 1H NMR spectra. The distinctive ${}^{13}C\{^1H\}$ NMR chemical shifts for the chelated open-chain form are given in table 2.97.

Table 2.97. Selected ${}^{13}C\{^1H\}$ NMR chemical shifts (δ /ppm) of the detected monometalated open-chain species of *N*-alkyl-L-rhamnosylamines with Pd-en in D_2O at 4 °C.

		C1	C2	C3	C4	C5	C6	Cα
L-Rhaa1NMe2H $_{-1}$ - κ^2N^1,O^2	δ	187.9	86.8	74.6	73.8	67.4	19.7	48.8
L-Rhaa1NEt2H $_{-1}$ - κ^2N^1,O^2	δ	186.4	86.8	74.6	73.9	67.4	19.7	55.7
L-Rhaa1NiPr2H $_{-1}$ - κ^2N^1,O^2	δ	183.4	87.0	74.6	74.0	67.4	19.7	60.1

encountering energetic limitations. Furanose rings usually exhibit a dynamic puckering leading to a variety of possible conformations,^[50] but for the observed complex species it is assumed that due to the κ^2N^1,O^3 chelation the C^2E conformation is strictly realized. As a consequence of the large amount of hydrolysis products in the investigated reaction solutions and the associated overlapping of 1H NMR signals, no further verification of the coordination mode and structure through the determination of coupling constants was possible. The lack of additional functional groups inhibits the possibility of a second metalation of the α -furanosylamine isomer in reactions including an excess of palladium(II) probe.

Table 2.99. Selected $^{13}C\{^1H\}$ NMR chemical shifts (δ /ppm) and shift differences ($\Delta\delta$) to the free ligand of the detected monometalated *N*-alkyl-2-deoxy-*D*-*erythro*-pentofuranosylamines with Pd-en in D_2O at 4 °C. The $\Delta\delta$ values indicating a CIS are printed bold.

		C1	C2	C3	C4	C5	Cα
α - <i>D</i> - <i>ery</i> -dPentf1NMe	δ	91.9	39.3	71.5	84.5	62.1	31.5
α - <i>D</i> - <i>ery</i> -dPentf1NMe3H ₋₁	δ	92.4	38.1	72.8	90.7	62.7	36.8
κ^2N^1,O^3	$\Delta\delta$	0.5	-1.2	1.3	6.2	1.6	5.3
α - <i>D</i> - <i>ery</i> -dPentf1NEt	δ	90.3	40.2	71.4	84.4	62.1	39.7
α - <i>D</i> - <i>ery</i> -dPentf1NEt3H ₋₁	δ	92.3	39.6	73.0	88.4	62.8	40.3
κ^2N^1,O^3	$\Delta\delta$	2.0	-0.6	1.6	4.0	0.7	0.6

The formation of six-membered chelate rings was also observed in the detected complex species exhibiting a single and double metalation of the open-chain form of *N*-methyl- and *N*-ethyl-2-deoxy-*D*-*erythro*-pentosylamines. The presence of these chelated imine isomers in solution becomes strikingly evident by the prominent 1H NMR signals, assigned to the imine hydrogen atom, at 7.75 ppm and 7.81 ppm for the mononuclear complex as well as 7.68 ppm and 7.75 ppm for the binuclear species. All corresponding $^{13}C\{^1H\}$ NMR chemical shifts and resulting CIS values are listed in table 2.100. It has to be noted that the mentioned CIS values are calculated from values obtained in different solvents since the imine form of the free ligand was only detected in $DMSO-d_6$. The binding of the first palladium fragment to the imine occurs at the N1 and O3 atoms and appears to be slightly favored over the aforementioned chelation of the furanoid isomer in equimolar experiments. The doubly metalated species feature an additional PdN₂-fragment bound to the alkoxide groups at the C4 and C5 atom, exhibiting the common five-membered coordination pattern. This coordination mode involving the terminal functional group is readily identified by the induced downfield shift observed for the C5 atom in the DEPT 135 NMR experiment and is only detected in reaction solutions containing two equivalents of palladium probe. In the respective experiments the doubly metalated open-chain isomers clearly represents the prevailing species.

Table 2.100. Selected $^{13}\text{C}\{^1\text{H}\}$ NMR chemical shifts (δ /ppm) and shift differences ($\Delta\delta$) to the free ligand in $\text{DMSO-}d_6$ of the detected open-chain species of *N*-alkyl-2-deoxy-D-*erythro*-pentosylamines with Pd-en in D_2O at 4°C .

		C1	C2	C3	C4	C5	Cα
D- <i>ery</i> -dPenta1NMe	δ	165.3	39.0	69.5	74.6	63.2	47.4
D- <i>ery</i> -dPenta1NMe3H $_{-1}$	δ	179.8	37.2	75.1	68.4	63.0	48.8
$\kappa^2\text{N}^1, \text{O}^3$	$\Delta\delta$	14.5	-1.8	5.6	-6.2	-0.2	1.4
D- <i>ery</i> -dPenta1NMe3,4,5H $_{-3}$	δ	174.0	39.3	69.3	84.8	75.7	51.7
$\kappa^2\text{N}^1, \text{O}^3; \kappa^2\text{O}^{4,5}$	$\Delta\delta$	8.7	-0.2	1.0	10.2	12.5	4.3
D- <i>ery</i> -dPenta1NEt	δ	163.2	38.9	69.6	74.6	63.2	54.7
D- <i>ery</i> -dPenta1NEt3H $_{-1}$	δ	173.3	39.5	75.1	68.1	64.5	57.9
$\kappa^2\text{N}^1, \text{O}^3$	$\Delta\delta$	10.1	0.6	5.5	-6.5	1.3	3.2
D- <i>ery</i> -dPenta1NEt3,4,5H $_{-3}$	δ	173.3	40.0	69.2	84.8	75.6	58.1
$\kappa^2\text{N}^1, \text{O}^3; \kappa^2\text{O}^{4,5}$	$\Delta\delta$	10.1	1.1	-0.4	10.2	12.4	3.4

2.2.3.2. *N*-Alkyl-2-deoxy-D-*arabino*-hexosylamines

In reaction solutions containing *N*-alkyl-2-deoxy-D-*arabino*-hexosylamines, Pd-en and iodic acid in the molar ratios 1:1:1 and 1:2:1 the in figure 2.35 depicted complex species could be identified.

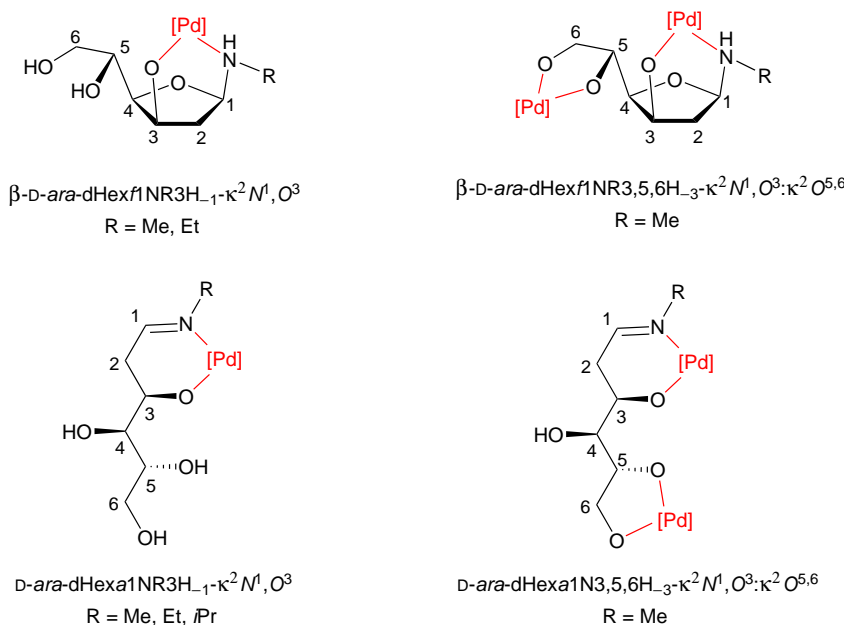


Figure 2.35. Complex species detected in reaction solutions resulting from the treatment of *N*-alkyl-2-deoxy-D-*arabino*-hexosylamines with Pd-en and iodic acid.

The only coordination mode detected for all three investigated *N*-alkyl-2-deoxy-D-*arabino*-hexosylamine derivatives featured a $\kappa^2\text{N}^1, \text{O}^3$ chelation of the ligand as acyclic imine. A corresponding metalation of a cyclic form was only observed for the methyl derivative and, to a smaller extent, for the ethyl derivative. In these complex species the ligand adapts its β -furanosyl form. As strikingly becomes evident from table 2.101, a double metalation was only observed in the

experiment featuring D-*ara*-dHex1NMe with two equivalents of palladium(II) probe. The respective NMR spectrum indicates the presence of two binuclear complex species. Both complex species exhibit a $\kappa^2O^{5,6}$ binding of the second PdN₂-fragment to the acyclic imine form and β -furanosylamine form, respectively. Surprisingly, all dimolar reaction attempts with the ethyl and *iso*-propyl derivative only led to the formation of the same monometalated species already identified in the aforementioned equimolar reaction solutions.

Table 2.101. Percentage distribution of the metalated species resulting from the treatment of *N*-alkyl-2-deoxy-D-*arabino*-hexosylamines with Pd-en and iodic acid in the molar ratio 1:1:1 and 1:2:1 at 4 °C.

	1:1:1			1:2:1		
	Me	Et	<i>i</i> Pr	Me	Et	<i>i</i> Pr
β -D- <i>ara</i> -dHexf1NR3H ₋₁ - κ^2N^1,O^3	57	27	75	0	14	0
D- <i>ara</i> -dHexa1NR3H ₋₁ - κ^2N^1,O^3	17	67	0	0	60	64
β -D- <i>ara</i> -dHexf1NR3,5,6H ₋₃ - $\kappa^2N^1,O^3;\kappa^2O^{5,6}$	0	0	0	41	0	0
D- <i>ara</i> -dHexa1NR3,5,6H ₋₃ - $\kappa^2N^1,O^3;\kappa^2O^{5,6}$	0	0	0	39	0	0
other species	26	6	25	20	26	36

Since, as described in chapter 2.1.3.2, no traces of *N*-alkyl-2-deoxy-D-*arabino*-hexofuranosylamines were detected for the free ligands in aqueous solutions, a determination of CIS values was not possible due to the lack of reference values. The presence of the furanoid form for all investigated ligands in cyclic complex species was indicated by the significantly downfield shifted NMR signals assigned to the respective C4 atoms. The assumed β -configuration was primarily derived from the fact that a reasonable coordination pattern can only be constructed for the β -furanosylamine isomer. Another thinkable coordination mode would feature the β -pyranosylamine isomer in the ¹C₄ conformation as ligand, but seems highly unlikely due to the energetically unfavorable axial position of the hydroxymethyl moiety.

The cyclic doubly metalated complex species found for D-*ara*-dHex1NMe was characterized by the observed shift differences of about 10 ppm at the C5 and C6 atom in comparison to the corresponding monometalated species. This distinctive shift is a result of the exocyclic coordination of a second PdN₂-fragment to the respective alkoxide functions. An overview of the determined ¹³C{¹H} NMR chemical shifts for all complex species featuring the ligands in their furanoid form is given in table 2.102.

Table 2.102. Selected ¹³C{¹H} NMR chemical shifts (δ /ppm) of the detected metalated *N*-alkyl-2-deoxy-D-*arabino*-hexofuranosylamines with Pd-en in D₂O at 4 °C.

		C1	C2	C3	C4	C5	C6	C α
β -D- <i>ara</i> -dHexf1NMe3H ₋₁	δ	89.6	38.6	70.1	84.9	70.3	64.6	37.0
β -D- <i>ara</i> -dHexf1NMe3,5,6H ₋₃	δ	89.5	38.4	78.3	87.5	80.9	75.0	36.7
β -D- <i>ara</i> -dHexf1NEt3H ₋₁	δ	91.9	38.1	74.1	88.7	72.3	63.3	40.7

The ¹³C{¹H} NMR chemical shifts listed in table 2.103 were assigned to the metalated open-chain species of the investigated *N*-alkyl-2-deoxy-D-*arabino*-hexosylamine. Most notably for the formation of the imine species are the chemical shifts assigned to the C1 atom in the downfield

region of the respective $^{13}\text{C}\{^1\text{H}\}$ NMR spectra. The associated ^1H NMR shifts were detected between 7.80 ppm to 7.88 ppm for the monometalated species and at 7.67 ppm for the sole identified doubly metalated imine species. The acyclic binuclear complex unexpectedly features a $\kappa^2\text{O}^{5,6}$ chelation instead of $\kappa^2\text{O}^{4,5}$ chelation, which was identified by the significant downfield shift of the terminal hydroxymethyl moiety in the DEPT 135 NMR experiment.

Table 2.103. Selected $^{13}\text{C}\{^1\text{H}\}$ NMR chemical shifts (δ/ppm) of the detected metalated open-chain species of *N*-alkyl-2-deoxy-*D*-arabino-hexosylamines with Pd-en in D_2O at 4°C .

		C1	C2	C3	C4	C5	C6	C α
<i>D</i> -ara-dHexa1NMe2H $_{-1}$ - $\kappa^2\text{N}^1, \text{O}^2$	δ	175.3	41.1	73.6	67.1	73.4	63.3	50.7
<i>D</i> -ara-dHexa1NMe2H $_{-1}$ - $\kappa^2\text{N}^1, \text{O}^2; \kappa^2\text{O}^{5,6}$	δ	178.8	40.8	83.7	70.5	86.7	76.0	50.9
<i>D</i> -ara-dHexa1NEt2H $_{-1}$ - $\kappa^2\text{N}^1, \text{O}^2$	δ	173.9	41.7	73.7	66.6	73.2	63.4	57.6
<i>D</i> -ara-dHexa1N <i>i</i> Pr2H $_{-1}$ - $\kappa^2\text{N}^1, \text{O}^2$	δ	171.3	42.4	73.9	66.5	73.3	63.5	61.1

2.2.3.3. *N*-Alkyl-2-deoxy-*D*-lyxo-hexosylamines

The treatment of *N*-methyl- and *N*-ethyl-2-deoxy-*D*-lyxo-hexosylamine with Pd-en and iodic acid in molar ratios 1:1:1 and 1:2:1 led to the formation of various species of which four complex species could be characterized with certainty. These species are depicted in figure 2.36.

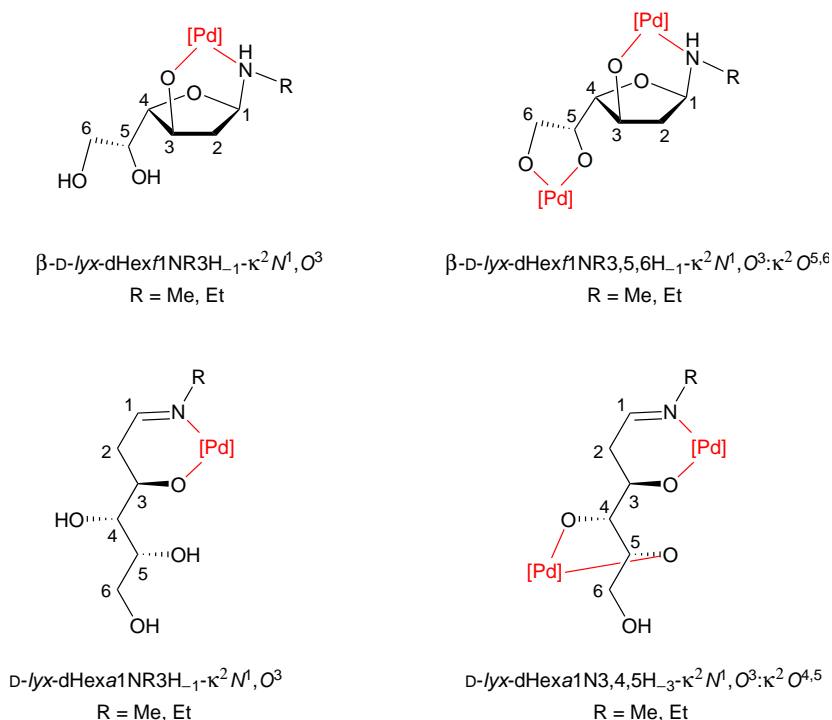


Figure 2.36. Complex species detected in reaction solutions resulting from the treatment of *N*-alkyl-2-deoxy-*D*-lyxo-hexosylamines with Pd-en and iodic acid.

The NMR spectra obtained from the reaction solutions show a metalation of the α -furanosyl isomers as well as the open-chain imine form for both investigated ligands. As can be seen

in table 2.104, a prevalence of the furanoid species over the open-chain species was detected in all equimolar experiments. In the case of the methyl derivative an additional species with comparable $^{13}\text{C}\{^1\text{H}\}$ NMR chemical shifts to those found for the furanoid species was observed, but could not be further identified. This unidentified species was also not present in the equimolar reaction including the ethyl derivative, but therefore significant amounts of hydrolysis products and reactant were detected in the reaction solution.

If two equivalents of Pd-en were used, the double metalation of the open-chain form prevailed over the double metalation of the furanoid isomer in the case of D-*lyx*-dHex1NMe and D-*lyx*-dHex1NEt. For the methyl derivative also traces of the aforementioned mononuclear species were detected in the corresponding NMR spectra.

Table 2.104. Percentage distribution of the metalated species resulting from the treatment of *N*-alkyl-2-deoxy-D-*lyxo*-hexosylamines with Pd-en and iodic acid in the molar ratio 1:1:1 and 1:2:1 at 4 °C.

	1:1:1		1:2:1	
	Me	Et	Me	Et
β -D- <i>lyx</i> -dHexf1NR3H ₋₁ - κ^2N^1,O^3	63	28	22	0
D- <i>lyx</i> -dHexa1NR3H ₋₁ - κ^2N^1,O^3	11	23	0	0
D- <i>lyx</i> -dHexa1NR3,4,5H ₋₃ - $\kappa^2N^1,O^3:\kappa^2O^{4,5}$	0	3	35	92
β -D- <i>lyx</i> -dHexf1NR3,5,6H ₋₃ - $\kappa^2N^1,O^3:\kappa^2O^{5,6}$	0	0	32	8
other species	26	46	11	0

The metalation of the β -furanosyl isomers was primarily characterized by the $^{13}\text{C}\{^1\text{H}\}$ NMR chemical shift assigned to the C4 atom. A 1,3-diaxial coordination of a corresponding pyranoid isomer would only be possible for the β -anomer in the 1C_4 conformation, but is highly unlikely due to the energetically unfavorable axial orientation of the hydroxymethyl function. The $^{13}\text{C}\{^1\text{H}\}$ NMR chemical shifts and resulting CIS values are displayed in table 2.105. Although the CIS values resulting from the κ^2N^1,O^3 binding are exceptionally low, this coordination pattern was assumed as consequence of the aforementioned arguments. The CIS values caused by the binding of a second Pd₂N-fragment to the exocyclic alkoxide functions at C5 and C6 atom on the other hand are with 9.4 ppm to 11.6 ppm within the expected range.

2. Results

Table 2.105. Selected $^{13}\text{C}\{^1\text{H}\}$ NMR chemical shifts (δ/ppm) and shift differences ($\Delta\delta$) to the free ligand of the detected monometalated *N*-alkyl-2-deoxy-D-*lyxo*-hexofuranosylamines with Pd-en in D_2O at 4°C . The $\Delta\delta$ values indicating a CIS are printed bold.

		C1	C2	C3	C4	C5	C6	Cα
β -D- <i>lyx</i> -dHexf1NMe	δ	92.7	40.3	72.1	85.9	70.5	63.5	31.8
β -D- <i>lyx</i> -dHexf1NMe3H $_{-1}$	δ	92.0	38.0	73.9	90.9	72.2	63.2	36.9
$\kappa^2\text{N}^1, \text{O}^3$	$\Delta\delta$	-0.7	-2.3	1.8	5.0	1.7	-0.3	5.1
β -D- <i>lyx</i> -dHexf1NMe3,5,6H $_{-3}$	δ	92.7	37.5	72.3	90.3	82.0	74.0	36.8
$\kappa^2\text{N}^1, \text{O}^3; \kappa^2\text{O}^{5,6}$	$\Delta\delta$	0.0	-2.8	0.2	4.4	11.5	10.5	5.0
β -D- <i>lyx</i> -dHexf1NEt	δ	91.2	40.6	72.2	85.9	70.5	63.6	40.4
β -D- <i>lyx</i> -dHexf1NEt3H $_{-1}$	δ	91.9	38.1	74.1	88.7	72.3	63.3	40.7
$\kappa^2\text{N}^1, \text{O}^3$	$\Delta\delta$	0.7	-2.5	1.9	2.8	1.8	-0.3	0.3
β -D- <i>lyx</i> -dHexf1NEt3,5,6H $_{-3}$	δ	92.6	37.5	73.1	88.1	82.1	73.0	40.5
$\kappa^2\text{N}^1, \text{O}^3; \kappa^2\text{O}^{5,6}$	$\Delta\delta$	1.4	-3.1	0.9	2.2	11.6	9.4	0.1

Single and double metalation was also detected for the acyclic imine isomer of D-*lyx*-dHex1NMe and D-*lyx*-dHex1NEt. The distinct ^1H NMR signals for the respective imine hydrogen atoms are located at 7.76 ppm and 7.82 ppm for the mononuclear species and at 7.71 ppm and 7.77 ppm for the binuclear species. The corresponding $^{13}\text{C}\{^1\text{H}\}$ NMR chemical shifts and determined CIS values for the complex species are listed in table 2.105. The listed CIS values clearly validate the assumed $\kappa^2\text{N}^1, \text{O}^3$ and $\kappa^2\text{N}^1, \text{O}^3; \kappa^2\text{O}^{4,5}$ coordination pattern for these palladium-imine complexes.

Table 2.106. Selected $^{13}\text{C}\{^1\text{H}\}$ NMR chemical shifts (δ/ppm) and shift differences ($\Delta\delta$) to the free ligand in $\text{DMSO-}d_6$ of the detected open-chain species of *N*-alkyl-2-deoxy-D-*lyxo*-hexosylamines with Pd-en in D_2O at 4°C .

		C1	C2	C3	C4	C5	C6	Cα
D- <i>lyx</i> -dHexa1NMe	δ	165.5	39.9	68.6	69.9	72.9	63.0	47.4
D- <i>lyx</i> -dHexa1NMe3H $_{-1}$	δ	174.3	39.8	71.6	67.2	73.8	63.7	51.4
$\kappa^2\text{N}^1, \text{O}^3$	$\Delta\delta$	8.8	-0.1	3.0	-2.7	0.9	0.7	4.0
D- <i>lyx</i> -dHexa1NMe3,4,5H $_{-3}$	δ	174.4	39.6	68.9	85.0	87.2	64.2	51.6
$\kappa^2\text{N}^1, \text{O}^3; \kappa^2\text{O}^{4,5}$	$\Delta\delta$	8.9	-0.3	0.3	15.1	14.3	1.2	4.2
D- <i>lyx</i> -dHexa1NEt	δ	163.2	36.2	68.7	69.1	72.9	63.0	54.8
D- <i>lyx</i> -dHexa1NEt3H $_{-1}$	δ	173.3	39.5	71.9	67.2	73.8	63.7	57.9
$\kappa^2\text{N}^1, \text{O}^3$	$\Delta\delta$	10.1	3.3	3.2	-1.9	0.9	0.7	3.1
D- <i>lyx</i> -dHexa1NEt3,4,5H $_{-3}$	δ	173.2	39.9	68.6	84.8	87.3	64.5	58.1
$\kappa^2\text{N}^1, \text{O}^3; \kappa^2\text{O}^{4,5}$	$\Delta\delta$	10.0	3.3	-0.1	15.7	14.4	1.5	3.3

2.2.4. *N*-Phenylglycosylamines

For the investigation of the coordination behavior of *N*-phenylglycosylamines towards palladium(II) probes D-Ara1NPh, D-Lyx1NPh, D-Rib1NPh, D-Xyl1NPh, D-Glc1NPh, D-Gul1NPh and D-Man1NPh were treated with Pd-en or Pd-tmeda and iodic acid in various molar ratios. All applied ligands were synthesized using aniline- ^{15}N and thus included a ^{15}N enriched aminophenyl moiety. This approach allows the measurement of meaningful ^{15}N NMR spectra from the resulting reaction solutions, which allow a more lucid overview of the formed species.

2.2.4.1. *N*-Phenylpentosylamines

In the respective experiments including *N*-phenyl-D-pentosylamines as ligand the pyranoid form prevailed in all detected complex species. The corresponding complexes are depicted in figure 2.37. A double metalation of a cyclic isomer was only observed in the case of D-Lyx1NPh and D-Rib1NPh. Furthermore, it is noteworthy that in all experiments no indications for the coordination of the corresponding other pyranoid anomer were found.

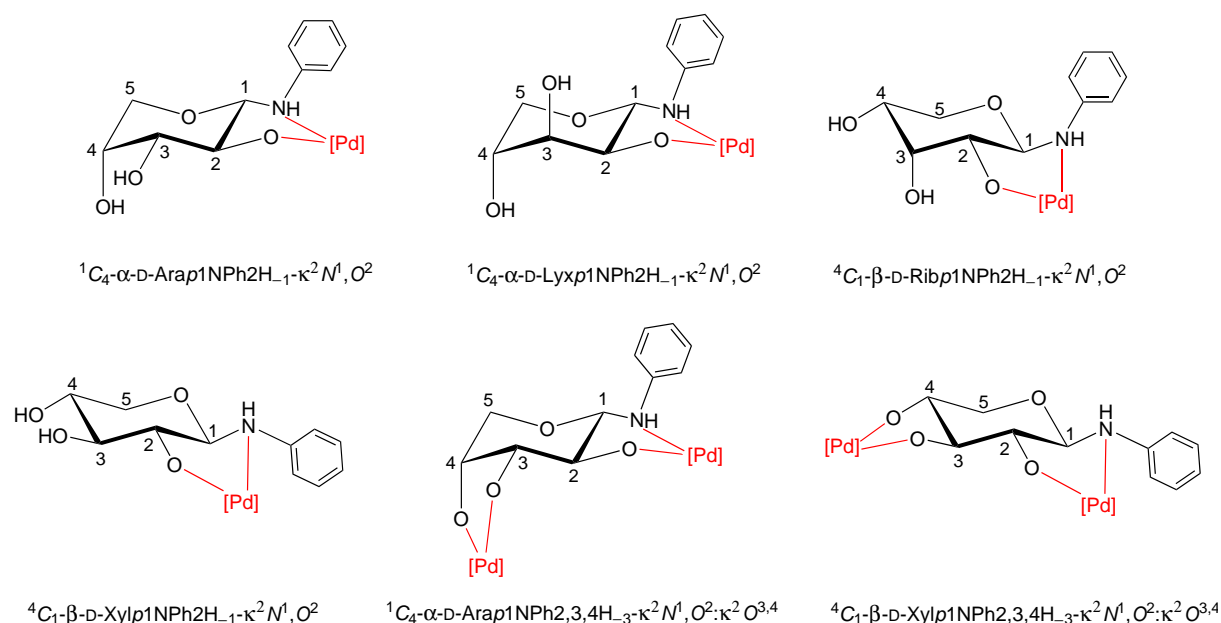


Figure 2.37. Pyranoid complex species detected in reaction solutions resulting from the treatment of *N*-phenyl-D-pentosylamines with Pd-en and iodic acid.

The $\kappa^2\text{N}^1,\text{O}^2$ chelation in the aforementioned species was primarily characterized by the distinct CIS values determined for the C1 and C2 atom. The comparison of the NMR signals for the aminophenyl moiety in the free ligand and in the complexed ligand led to a rather unexpected finding. While the CIS for the aromatic carbon atom in the *ipso* position adapted negative values in all experiments, the carbon atom in the *ortho* and *para* position showed CIS values from about 7 ppm to 9 ppm. The carbon atom in the *meta* position on the other hand appeared to be largely unaffected by the coordination. The respective $^{13}\text{C}\{^1\text{H}\}$ NMR chemical shifts and CIS values are listed in table 2.107. The $^3J_{1,2}$ values and further coupling constants determined for the chelated *N*-phenyl-D-pentosylamines unanimously correlated to the coupling constants found

2. Results

for the complexes of their corresponding alkyl derivatives (see chapter 2.2.1). Each cyclic species exhibits one specific signal in the respective ^{15}N NMR spectrum and the determined ^{15}N NMR chemical shifts range from -340 ppm to -332 ppm.

Table 2.107. Selected $^{13}\text{C}\{^1\text{H}\}$ NMR chemical shifts (δ/ppm) and shift differences ($\Delta\delta$) to the free ligand of the detected metalated *N*-phenyl-D-pentopyranosylamines with Pd-en in D_2O at 4°C . The $\Delta\delta$ values indicating a CIS are printed bold.

		C1	C2	C3	C4	C5	C_i	C_o	C_m	C_p
$^1\text{C}_4\text{-}\alpha\text{-D-Arap1NPh}$	δ	86.1	70.9	73.9	69.5	67.6	146.3	115.1	130.2	120.3
$^1\text{C}_4\text{-}\alpha\text{-D-Arap1NPh2H}_{-1}$	δ	98.0	76.7	75.3	68.5	70.7	143.0	124.1	130.8	128.8
$\kappa^2\text{N}^1, \text{O}^2$	$\Delta\delta$	11.9	5.8	1.4	-1.0	0.9	-3.3	9.0	0.6	8.5
$^1\text{C}_4\text{-}\alpha\text{-D-Arap1NPh2,3,4H}_{-3}$	δ	97.9	81.3	85.2	78.8	69.7	143.5	124.9	131.6	128.9
$\kappa^2\text{N}^1, \text{O}^2; \kappa^2\text{O}^{3,4}$	$\Delta\delta$	11.8	10.4	11.3	9.3	0.9	-2.9	9.8	1.4	8.6
$^1\text{C}_4\text{-}\alpha\text{-D-Lyxp1NPh}$	δ	82.8	68.7	71.1	69.7	65.1	146.2	115.0	130.1	120.1
$^1\text{C}_4\text{-}\alpha\text{-D-Lyxp1NPh2H}_{-1}$	δ	90.9	74.6	72.5	69.4	68.2	142.9	122.3	130.8	128.2
$\kappa^2\text{N}^1, \text{O}^2$	$\Delta\delta$	8.1	5.9	1.4	-0.3	3.1	-3.3	7.3	0.7	8.1
$^4\text{C}_1\text{-}\beta\text{-D-Ribp1NPh}$	δ	81.5	70.5	69.8	66.7	62.9	145.0	114.3	129.5	119.4
$^4\text{C}_1\text{-}\beta\text{-D-Ribp1NPh2H}_{-1}$	δ	90.6	77.5	72.2	66.6	64.8	142.8	122.3	130.9	128.1
$\kappa^2\text{N}^1, \text{O}^2$	$\Delta\delta$	9.1	7.0	2.4	-0.1	1.9	-2.2	8.0	1.4	8.5
$^4\text{C}_1\text{-}\beta\text{-D-Xylp1NPh}$	δ	86.2	73.2	77.5	70.0	66.4	146.1	115.1	130.2	120.3
$^4\text{C}_1\text{-}\beta\text{-D-Xylp1NPh2H}_{-1}$	δ	94.4	79.7	78.0	69.5	68.5	142.5	122.3	130.9	128.2
$\kappa^2\text{N}^1, \text{O}^2$	$\Delta\delta$	8.2	6.5	0.5	-0.5	2.1	-3.6	7.2	0.7	7.9
$^4\text{C}_1\text{-}\beta\text{-D-Xylp1NPh2,3,4H}_{-3}$	δ	94.7	81.4	88.4	79.5	68.3	142.8	122.0	130.5	128.1
$\kappa^2\text{N}^1, \text{O}^2; \kappa^2\text{O}^{3,4}$	$\Delta\delta$	8.5	8.2	10.9	9.5	1.9	-3.3	6.9	0.3	7.8

In addition to the cyclic complex species, also $\kappa^2\text{N}^1, \text{O}^2$ metalation of the imine form was detected for all *N*-phenyl-D-pentosylamines. The resulting complexes are depicted in figure 2.38.

The $^{13}\text{C}\{^1\text{H}\}$ NMR chemical shifts assigned to these open-chain complex species are listed in table 2.108. The respective ^1H NMR signals of the imine hydrogen atom are located between 8.16 ppm and 8.28 ppm.

Table 2.108. Selected $^{13}\text{C}\{^1\text{H}\}$ NMR chemical shifts (δ/ppm) of the detected $\kappa^2\text{N}^1, \text{O}^2$ monometalated and $\kappa^2\text{N}^1, \text{O}^2; \kappa^2\text{O}^{3,4}$ dimetalated open-chain species of *N*-phenyl-D-pentosylamines with Pd-en in D_2O at 4°C . Dashes indicate that due to the superposition of signals no definite values could be determined.

		C1	C2	C3	C4	C5	C_i	C_o	C_m	C_p
D-Lyxa1NPh2H ₋₁	δ	190.0	87.3	74.9	71.2	63.3	148.5	123.4	130.5	129.4
D-Riba1NPh2H ₋₁	δ	188.3	87.8	74.1	71.7	63.5	148.2	123.4	130.8	129.3
D-Xyla1NPh2H ₋₁	δ	188.8	88.0	73.6	70.3	63.4	148.5	122.2	130.5	129.2
D-Xyla1NPh2,3,4H ₋₃	δ	190.2	88.9	85.7	79.8	65.9	148.6	–	–	–

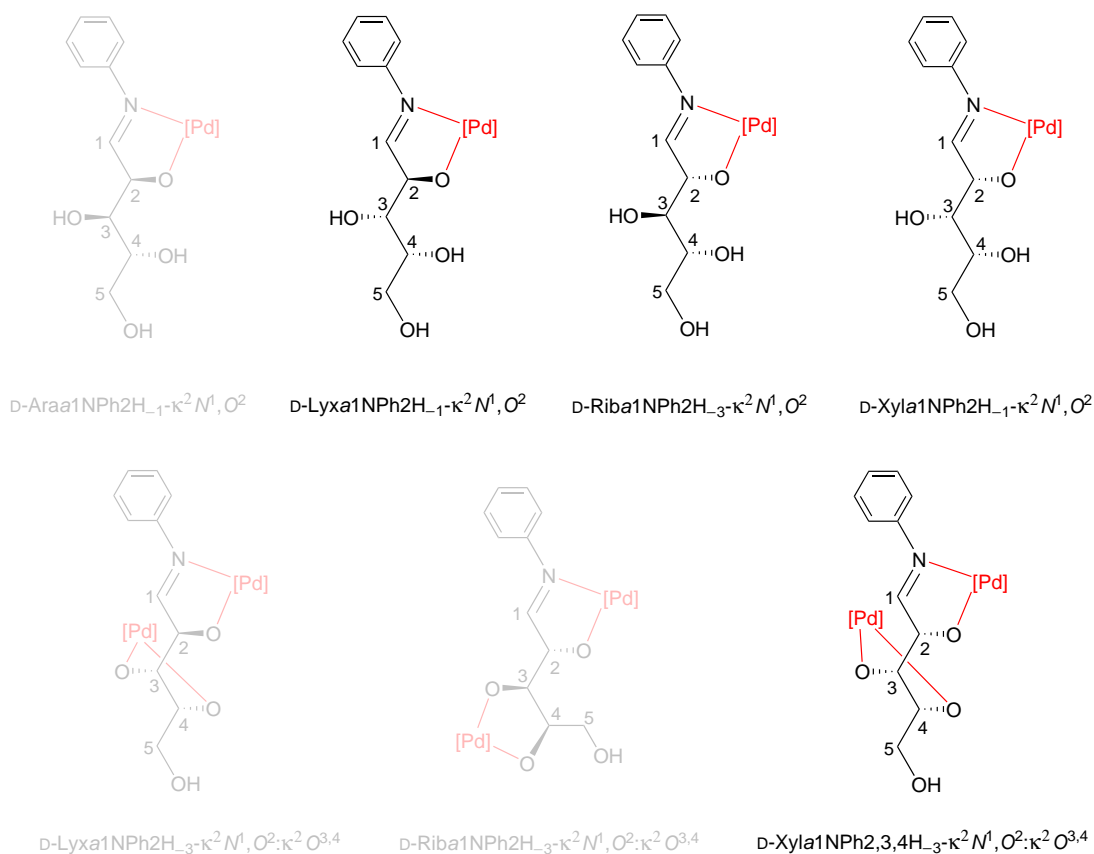


Figure 2.38. Imine complex species detected in reaction solutions resulting from the treatment of *N*-phenyl-D-pentosylamines with Pd-en and iodic acid. Complex species which were only detected in ^1H and ^{15}N NMR spectra are displayed grayed out.

Aside from the characteristic ^1H and $^{13}\text{C}\{^1\text{H}\}$ NMR values, the presence of the open-chain species became evident by the observed prominent ^{15}N NMR signals between -145.9 ppm and -137.4 ppm for monometalated species and between -153.4 ppm and -148.6 ppm for binuclear species. Due to the high sensitivity of the ^{15}N NMR-spectroscopic methods it was even possible to detect traces of the monometalated imine form of D-Ara1NPh, which was not observed in the corresponding $^{13}\text{C}\{^1\text{H}\}$ NMR spectrum because of the bad signal-to-noise ratio. All ^{15}N NMR chemical shifts and their assignment to the associated species are listed in table 2.108.

Table 2.109. ^{15}N NMR chemical shifts (δ /ppm) of the detected complex species of *N*-phenyl-D-pentosylamines with Pd-en in D_2O at 4°C . Values in parenthesis indicate that the species was not detected in the corresponding $^{13}\text{C}\{^1\text{H}\}$ NMR spectrum.

		D-Ara	D-Lyx	D-Rib	D-Xyl
Pent p 1NPh	δ	-302.5 (α)	-303.5 (α)	-303.8 (β)	-302.5 (β)
Pent p 1NPh2H ₋₁	δ	-324.4 (α)	-328.0 (α)	-330.2 (β)	-329.0 (β)
Pent p 1NPh2,3,4H ₋₃	δ	-322.8 (α)	–	–	-329.5 (β)
Pent a 1NPh2H ₋₁	δ	(-145.9)	-137.4	-142.4	-145.2
Pent a 1NPh2,3,4H ₋₃	δ	–	(-151.8)	(-153.4)	-148.6

2.2.4.2. *N*-Phenylhexosylamines

In comparison to their aforementioned pentosylamines analogues the investigated *N*-phenylhexosylamines exhibited a smaller variety of formed complex species. All species detected in the reaction solutions resulting from the treatment of the compounds with Pd-en and iodic acid are depicted in figure 2.39. An increase of the Pd-en concentration up to two equivalents yielded only in the case of D-Glc1NPh an analyzable NMR spectrum. The corresponding NMR-spectroscopic data indicate the formation of a doubly metalated cyclic complex species. Reaction solutions with L-Gul1NPh and D-Man1NPh and an excess of palladium(II) probe on the other hand showed visible signs of decomposition within minutes and the associated NMR spectra have a bad signal-to-noise ratio and mostly reveal signals that could be assigned to hydrolysis products.

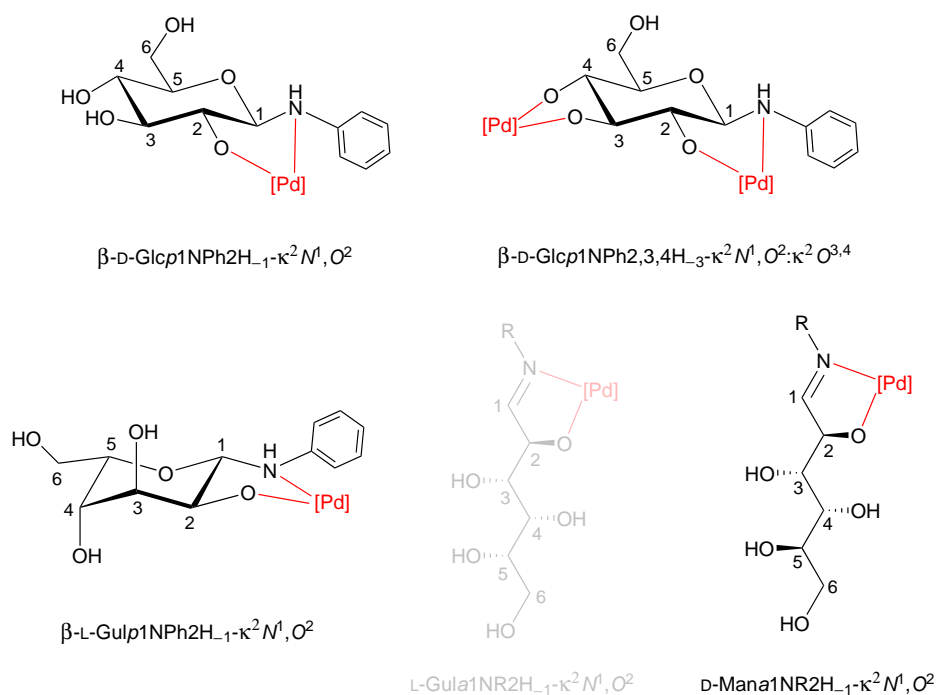


Figure 2.39. Complex species detected in reaction solutions resulting from the treatment of *N*-phenylhexosylamines with Pd-en and iodic acid. Complex species which were only detected in the ^1H and ^{15}N NMR spectra are displayed grayed out.

While D-Glc1NPh was only detected as ligand in its respective pyranoid form, solely the open-chain form of D-Man1NPh was metalated. For L-Gul1NPh the acyclic and one cyclic isomer were represented as ligand in the observed complex species, although it has to be noted that, due to the minimal amount of the open-chain species, the corresponding NMR signals were only detected in the respective ^1H and ^{15}N NMR spectra and not in the $^{13}\text{C}\{^1\text{H}\}$ NMR spectrum. An overview of the $^{13}\text{C}\{^1\text{H}\}$ NMR chemical shifts and determined CIS values is given in table 2.110. The obtained CIS values show similar trends as previously mentioned for the corresponding *N*-phenyl-D-pentosylamines complexes.

2. Results

Table 2.110. Selected $^{13}\text{C}\{^1\text{H}\}$ NMR chemical shifts (δ/ppm) and shift differences ($\Delta\delta$) to the free ligand of the detected metalated *N*-phenylhexopyranosylamines with Pd-en in D_2O at 4°C . The $\Delta\delta$ values indicating a CIS are printed bold.

		C1	C2	C3	C4	C5	C6	C_i	C_o	C_m	C_p
$\beta\text{-D-Glcp1NPh}$	δ	85.5	73.3	77.1	70.4	77.5	61.4	146.3	115.0	130.2	120.2
$\beta\text{-D-Glcp1NPh2H}_{-1}$	δ	93.6	79.8	79.2	69.3	77.9	60.6	142.8	122.3	130.8	128.1
$\kappa^2\text{N}^1,\text{O}^2$	$\Delta\delta$	8.1	6.5	2.1	-1.1	0.4	-0.8	-3.5	7.1	0.6	7.9
$^1\text{C}_4\text{-}\alpha\text{-D-Glcp1NPh2,3,4H}_{-3}$	δ	94.2	81.8	88.3	79.8	79.1	61.4	143.1	122.3	130.9	128.2
$\kappa^2\text{N}^1,\text{O}^2;\kappa^2\text{O}^{3,4}$	$\Delta\delta$	8.7	8.5	11.2	9.4	1.6	0.0	-3.2	7.3	0.6	7.9
$\beta\text{-L-Gulp1NPh}$	δ	82.6	68.2	71.5	70.0	74.2	61.5	146.4	114.7	130.2	120.0
$\beta\text{-L-Gulp1NPh2H}_{-1}$	δ	90.7	74.9	72.6	69.5	76.7	61.0	143.0	122.2	130.8	128.0
$\kappa^2\text{N}^1,\text{O}^2$	$\Delta\delta$	8.1	6.7	1.1	-0.5	1.5	-0.5	-3.3	8.0	0.6	8.0
$\beta\text{-D-Manp1NPh}$	δ	81.5	70.5	69.8	66.7	66.7	62.9	145.0	114.3	129.5	119.4
D-Mana1NPh2H_{-1}	δ	189.2	86.2	73.3	69.3	70.3	62.8	147.2	121.4	129.5	128.4

Table 2.111. ^{15}N NMR chemical shifts (δ/ppm) of the detected complex species of *N*-phenylhexosylamines with Pd-en in D_2O at 4°C . Values in parenthesis indicate that the species was not detected in the corresponding $^{13}\text{C}\{^1\text{H}\}$ NMR spectrum.

	Hex =	D-Glc	L-Gul	D-Man
Hexp1NPh	δ	-302.7 (β)	-302.2 (β)	-304.2 (β)
Hexp1NPh2H_{-1}	δ	-328.6 (β)	-329.0 (β)	-
$\text{Hexp1NPh2,3,4H}_{-3}$	δ	-329.0 (β)	-	-
Hexa1NPh2H_{-1}	δ	-	(-137.4)	-137.3

3. Discussion

3.1. Comparison of *N*-Substituted Glycosylamines to their corresponding Glycoses

Similar to their glucose analogues most glycosylamines show a vivid isomerization between their furanoid and pyranoid anomers in aqueous solution. Although it can be assumed that this isomerization proceeds *via* the hydrolysis of the glycosylamine to the corresponding reducing sugar, there are two clear indications highlighted in this work for the involvement of the acyclic imine form as intermediate product in the isomerization process. Firstly, this equilibrium between the different isomers is also present and temperature-dependent in anhydrous DMSO. In the case of some *N*-alkyl-D-ribosylamines, *N*-alkyl-2-deoxy-D-*erythro*-pentosylamines and *N*-alkyl-2-deoxy-D-*lyxo*-hexosylamines traces of the imine form are even detected in small concentrations in the respective NMR spectra. The imine function can be readily distinguished from a carbonyl function by the more upfield chemical shift of the associated NMR signals. Secondly, in many cases the imine form can be trapped and fixed in aqueous solution through the addition of a palladium(II) probe. These findings collectively support the reaction mechanism initially formulated by FRUSH and ISBELL.^[19]

When the determined anomeric ratios of the investigated *N*-alkyl-D-glycosylamines in aqueous solution are compared to the ratios listed for the corresponding glycoses in the literature,^[51] it stands out that configurations with the alkylamino function in the axial position are generally less favored. As can be seen in table 3.1 and 3.2, this preference becomes especially apparent for *N*-alkyl-D-lyxosylamines and *N*-alkyl-D-mannosylamines. In both cases the β -anomer prevails in aqueous solution while for D-lyxose and D-mannose the equilibrium favors the α -anomer. This observation can be attributed to the absence of the anomeric effect in pyranosides featuring an amino group at the anomeric center.^[24,52] Furthermore, the influence of a possible reverse anomeric effect can be considered,^[53] although it has been noted by MILJKOVIC that "the controversy about the existence of the reverse anomeric effect is practically impossible to resolve by using glycosylamine type of compounds due to solvent stabilization of the positive charge on the nitrogen".^[54] Thus, it is not possible to differentiate between the contribution of electronic and steric effects.

Table 3.1. Comparison of the anomeric ratios of *N*-methyl-D-pentosylamines with the corresponding D-aldopentoses. The percentages of the various cyclic forms of pentosylamines were determined from their ^1H or $^{13}\text{C}\{^1\text{H}\}$ NMR spectra in D_2O at room temperature or at 4°C^* . The percentages of the different forms of the pentoses were NMR spectroscopically determined by *Drew et al.* at 30°C .^[55]

	Ara	Ara1NMe	Lyx	Lyx1NMe	Rib	Rib1NMe*	Xyl	Xyl1NMe
αp	59	64	71	31	20	41	36	11
βp	32	18	27	69	59	42	62	87
$\alpha/\beta f$	9	18	2	0	21	17	2	2

Table 3.2. Comparison of the anomeric ratios of *N*-methylhexoosylamines with the corresponding D-aldohexoses. The percentages of the various cyclic forms of hexosylamines were determined from their ^1H or $^{13}\text{C}\{^1\text{H}\}$ NMR spectra in D_2O at room temperature or at 4°C^* . The percentages of the different forms of the hexoses were NMR spectroscopically determined by *Zhu et al.* at 30°C ^[16] and in the case of D-gulose by ANGYAL and PICKLES at 40°C .^[56]

	Gal	Gal1NMe	Glc	Glc1NMe	Gul	Gul1NMe*	Man	Man1NMe
αp	31	6	37	9	16	0	66	16
βp	63	90	62	91	78	100	33	84
$\alpha/\beta f$	6	4	1	0	6	0	1	0

Another finding associated to the absence of the anomeric effect is the detection of conformations for some *N*-alkyl-D-glycosylamines which are not adapted by their corresponding reducing sugar analogues. For example, in the case of *N*-alkyl-D-arabinosylamines the β -anomer shows a dynamic fluxional behavior between the 1C_4 and 4C_1 conformation while β -D-arabinose strictly sticks to the 4C_1 conformation in aqueous solution.^[55] This preference of the 4C_1 conformation is mainly attributed to the stabilization provided by the anomeric effect. This stabilization ceases when the hydroxy function at the anomeric center is replaced by an alkylamino function. In accordance to this finding, some sterically unfavorable conformations of glycoses, which are only relevant because their stabilization by the anomeric effect, are not observed for the corresponding glycosylamines. This, for example, is the case in the investigated *N*-alkyl-D-ribosylamines. Unlike in D-ribose, these compounds show no dynamic fluxional behavior for neither of the detected anomers. Generally speaking, the dynamic fluxional behavior between 1C_4 and 4C_1 conformation in glycosylamines is significantly shifted towards the conformation, which features no anomeric effect in the respective reducing sugar counterpart.

3.2. Effects of the Aglycon on the Configuration and Conformation of *N*-Substituted Glycosylamines

The nature of the featured aglycon has a detectable influence on the isomerization behavior, the anomeric ratio and the dynamic fluxional behavior between different conformations of glycosylamines. In general, it can be stated that the concentration of the anomer featuring the alkylamino moiety in axial position decreases with increasing bulkiness of the respective moiety in most *N*-alkyl-D-glycosylamines.

For *N*-alkyl-D-pentosylamines the axial orientation of the alkylamino moiety can be avoided by an alteration of the conformation *via* ring inversion. This behavior is detected for the investigated *N*-alkyl-D-arabino- and *N*-alkyl-D-lyxosylamines. With an increasing steric demand of the alkylamino moiety in these compounds, the determined $^3J_{1,2}$ values indicate a shift of the conformational equilibrium towards the conformation featuring the alkylamino moiety in equatorial position. In the case of *N*-alkyl-D-ribosylamines a conformation featuring an axial orientation of the alkylamino moiety is not realized at all. As can be seen in table 3.3, only in the case of *N*-alkyl-D-xylosylamines the potential ring inversion is sterically unfavored to such an extent that an actual decrease of the amount of α -anomer veritably occurs.

A similar decrease of the amount of anomer featuring an axial substitution with increasing steric demand of the alkyl group is observed for all investigated *N*-alkyl-D-hexosylamines. This tendency derives from the fact that a ring inversion in the respective compounds is highly unlikely due to the energetically unfavorable axial orientation of the hydroxymethyl moiety at the C6 atom upon ring inversion. This barrier hinders the system to evade the also energetically unfavorable axial orientation of the bulky anomeric substituent by ring inversion as in the case of the aforementioned *N*-alkyl-D-pentosylamines. As a consequence for the respective *tert*-butyl derivatives not even traces of the anomer featuring the *tert*-butylamino moiety in axial position are detected (see table 3.3).

Table 3.3. Percentage of the anomer featuring a axial orientation or a conceivable conformation with axial orientation for the investigated *N*-alkyl-D-glycosylamines in relation to their alkylamino substitution. The values were determined from the respective ^1H or $^{13}\text{C}\{^1\text{H}\}$ NMR spectra in D_2O .

	Ara1NR	Lyx1NR	Rib1NR	Xyl1NR	Gal1NR	Glc1NR	Gul1NR	Man1NR
Me	18	31	41	11	6	9	0	16
Et	15	27	34	11	4	6	0	13
Pr	18	26	44	10	5	5	0	15
<i>i</i> Pr	14	23	38	6	0	8	0	10
<i>t</i> Bu	0	36	39	2	0	0	0	0

3.3. The Chelation Preferences of *N*-Substituted Glycosylamines

The most striking principal found for the chelation of *N*-substituted glycosylamines is the preference to always incorporate the neutral alkylamino or arylamino function at the anomeric center in the binding of the first PdN₂-fragment. This increased affinity of palladium towards the nitrogen-containing function in comparison to the remaining alkoxide functions is in accordance with the HSAB concept. There are no reactions described in this work in which the addition of one equivalent palladium leads to a favored κ^2O,O metalation instead of a κ^2N,O metalation, even at higher pH values. This observation was already described for non-substituted glycosylamines by SCHWARZ and LINDNER.^[21,22]

If the complex formation with palladium probes is regarded individually for each group of *N*-substituted glycosylamines, a clear preference of a *trans*-vicinal chelation of the first PdN₂ fragment becomes apparent. In the case of *N*-alkyl-D-lyxosylamines for example, the β -anomer in the ⁴C₁ conformation is sterically favored due to the lower number of axial functional groups, and hence also prevails in aqueous solution. Upon addition of one equivalent palladium probe, an accumulation of the α -anomer in the ¹C₄ conformation is observed as a consequence of the preferred *trans*-vicinal κ^2N^1,O^2 metalation. A similar shift in the respective percentage distribution is observed for all *N*-alkyl-D-pentosylamines.

In the case of *N*-alkyl-D-mannosylamines and *N*-alkyl-L-rhamnosylamines, the impact of the preference of a *trans*-vicinal coordination mode becomes even more obvious. For both compound classes the β -anomer clearly prevails for the free ligand in aqueous solution, but after the treatment with a palladium probe a mixture of various complex species is detected. Surprisingly, the β -anomer featuring a *cis*-vicinal κ^2N^1,O^2 -metalation is only partially present in the obtained reaction solutions. Further detected species include significant amounts of the metalated acyclic imine form and even the corresponding α -anomers after ring inversion. The latter enables a *trans*-vicinal chelation of the metal ion. This alteration of the conformation was considered as highly unlikely for the *N*-alkyl- α -D-mannosylamines as the ring inversion leads to an axial orientation of the hydroxymethyl moiety located at the C5 atom, but could be verified through the comparison of the coordination behavior observed for its 6-deoxy analogues *N*-alkyl- α -L-rhamnosylamines. As shown in table 3.4, a *cis*-vicinal chelation is also observed for the following *N*-substituted glycosylamines, but only to a minimal extent: Lyx1NR, Rib1NR, Xyl1NR, Glc1NR, Gul1NR. The amount of the species coordinated in a *cis*-vicinal fashion seems to also correlate with the featured alkylamino moiety. While this coordination mode is more commonly detected for methyl derivatives, it is rarely observed for the respective *iso*-propyl and *tert*-butyl derivatives.

Table 3.4. Percentage of complex species featuring a *cis*-vicinal κ^2N^1,O^2 metalation determined from the ¹³C{¹H} NMR spectra of the reaction solutions resulting from the equimolar treatment of *N*-alkyl-D-glycosylamines with Pd-en and iodic acid in D₂O at 4 °C.

	Lyx1NR	Rib1NR	Xyl1NR	Glc1NR	Gul1NR	Man1NR	Rha1NR
Me	17	25	3	12	16	40	52
Et	18	0	0	0	14	38	42
Pr	8	0	0	0	5	38	–
<i>i</i> Pr	0	0	8	0	6	24	42
<i>t</i> Bu	0	0	0	0	0	28	–

Investigations conducted by ALLSCHER on the chelation of aldopentoses and aldohexoses by various PdN₂-fragments demonstrated a favored $\kappa^2O^{1,2}$ metalation of *cis*-vicinal diolato functions and in many cases an additional $\kappa^2O^{1,2}$ metalation of furanoid isomers.^[49] Both observations are apparently not valid for *N*-alkylpentosylamines and *N*-alkylhexosylamines.

While the absence of metalated furanoid glycosylamines can be attributed to the enhanced steric demand of the anomeric alkylamino moiety in comparison to a hydroxy function, the preference of the *trans*-vicinal coordination mode is harder to clarify. When only the *N*-alkyl-D-hexosylamines are taken into account, a *cis*-vicinal κ^2N^1,O^2 metalation, under the assumption of a fixed 4C_1 conformation, is only conceivable for selected α -anomers. In these anomers the alkylamino function is oriented in axial position, which is energetically unfavorable, especially in the case of more bulky moieties. Furthermore, as previously discussed in chapter 3.1, the axial orientation of the aminoalkyl function leads to no stabilization of the respective α -anomer due to the absence of the anomeric effect. Conversely, a reverse anomeric effect, enhanced by the coordination of the Pd²⁺ ion to the nitrogen atom and resembling a protonation, could be discussed.

For the investigated *N*-alkyl-D-pentosylamines on the other hand, the aforementioned explanations are not sufficient as these compounds can easily adapt another chair conformation without encountering significant steric hindrances. Through this conformational change, the axial orientation of the alkylamino function can be avoided in the *cis*-vicinal κ^2N^1,O^2 -metalated species. As shown in table 3.4, this coordination mode and the associated dynamic fluxional behavior is observed for all *N*-methyl-D-pentosylamines except the arabinose derivatives. A similar conformational fluxional behavior within complex species featuring a $\kappa^2O^{1,2}$ metalation was already described by ALLSCHER for palladium(II)-arabinose and -xylose complexes.^[49]

Structural evidence for the preference of the *trans*-vicinal coordination mode in *N*-alkylglycosylamines is provided by the crystal structure of [Pd(en)(4C_1 - β -D-Xylp1NMe2H₋₁- κ^2N^1,O^2)]-IO₃-tetrahydrate (**8**) described in this work. A crystal structure for an analogous palladium(II)-xylose complex was previously published by ARENDT *et al.* with [Pd(chxn)(4C_1 - α -D-Xylp1,2H₋₂- κ^2N^1,O^2)]-monohydrate.^[48] Since this structure features the xylose ligand in the α -configuration and thus a *cis*-vicinal metalation, the comparison of these structures exemplifies the significantly differing coordination patterns in palladium(II)-glycosylamine and -aldoglycose complexes.

3.4. Influencing Factors for the Chelation of the Imine Form

A chelation of the open-chain form is observed for the majority of the investigated *N*-substituted glycosylamines, but the percentage of the acyclic imine species in the total species distribution seems to relate to various factors.

Firstly, and probably most important, the affinity to form a palladium(II)-imine complex depends on the glycosylamine applied as ligand. As previously discussed in chapter 3.3, the palladium(II)-glycosylamine complexes investigated in this work tend to favor a *trans*-vicinal binding mode. If this coordination mode cannot be realized in the regarded system, it avoids a *cis*-vicinal metalation or axial substitution at the anomeric center by, *inter alia*, the chelation of the open-chain form of the respective glycosylamine. This is especially the case for glycosylamines which feature an axial oriented hydroxy function at the C2 atom as the investigated lyxosylamine and mannosylamine derivatives.

But imine metalation is also detected for *N*-alkyl-D-glycosylamines which allow a facile *trans*-vicinal binding of the PdN₂-fragment in their preferred configuration and conformation. The extent of the chelation of the open-chain form seems to be essentially dependent from the featured alkyl moiety at the alkylamino function. As can be derived from the percentages listed in table 3.5 and 3.6, the affinity to form acyclic imine species increases in the following order: Me < Et < Pr ≈ *i*Pr < *t*Bu. The striking question if this tendency is attributed to electronic or steric effects, could not be answered with definite certainty in this work.

Table 3.5. Percentage of complexed imine species in reaction solutions containing *N*-alkyl-D-pentosylamine, Pd-en and iodic acid in the molar ratios 1:1:1 and 1:2:1 in D₂O at 4 °C.

R	Ara1NR		Lyx1NR		Rib1NR		Xyl1NR	
	1:1:1	1:2:1	1:1:1	1:2:1	1:1:1	1:2:1	1:1:1	1:2:1
Me	0	0	35	48	14	15	4	24
Et	10	4	27	82	12	34	2	13
Pr	12	7	82	100	31	56	24	41
<i>i</i> -Pr	12	20	64	100	29	56	14	33
<i>t</i> -Bu	–	–	100	100	81	100	67	100

Table 3.6. Percentage of complexed imine species in reaction solutions containing *N*-alkylhexosylamine, Pd-en and iodic acid in the molar ratios 1:1:1 and 1:2:1 in D₂O at 4 °C.

R	Gal1NR		Glc1NR		Gul1NR		Man1NR		Rha1NR	
	1:1:1	1:2:1	1:1:1	1:2:1	1:1:1	1:2:1	1:1:1	1:2:1	1:1:1	1:2:1
Me	2	0	12	0	8	43	18	–	14	–
Et	5	0	5	7	6	46	36	88	20	–
Pr	9	0	0	11	17	–	40	92	–	–
<i>i</i> -Pr	7	12	0	12	27	96	62	–	46	–
<i>t</i> -Bu	29	20	12	36	67	100	62	100	–	–

Another factor influencing the extent of the emergence of imine complex species is the amount of palladium(II) probe in the reaction solution. As shown in table 3.5 and 3.6, in most cases an increase of the palladium concentration results in an enhanced formation of acyclic complex

species, when compared to the percentages determined for the corresponding reactions with stoichiometric amounts of palladium(II) probe and iodic acid.

This increase becomes particularly apparent when a $\kappa^2O^{3,4}$ binding of the second PdN₂ fragment is not feasible due to the *anti*-orientation of the respective hydroxy functions at the C3 and C4 atom of a species already boasting a *trans*-vicinal κ^2N^1,O^2 metalation. From all ligands investigated in this work, this is the case for *N*-alkyl-D-lyxosylamines, *N*-alkyl-L-gulosylamines, *N*-alkyl-D-mannosylamines and *N*-alkyl-L-rhamnosylamines. It has to be noted, that the reactions involving these compounds and two equivalents palladium probe also showed rapid and immediate signs of the formation of elementary palladium. In many cases these side reactions hinder a comprehensive NMR-spectroscopic investigation.

For the successful binding of a second PdN₂ fragment to a *N*-alkylglycosylamines in its respective open-chain form a *cis*-vicinal diolato function has to be present in the structure. This is not the case in *N*-alkylarabinosylamines and *N*-alkylgalactosylamines which thus exhibit no double metalation of their respective acyclic imine species. Alternatively, an energetically unfavorable deviation from the imine's zigzag conformation through the rotation around a C–C bond in order to facilitate the binding of a second PdN₂ fragment is possible. This is realized for *N*-alkylribosylamines in which through the rotation around the C3–C4 bond a $\kappa^2O^{3,4}$ binding is enabled. At the same time, due to the energetic downside of the aforementioned approach, almost the same degree of $\kappa^2O^{4,5}$ binding to the respective zigzag conformer is observed. This coordination mode features a less adverse structural alteration as a rotation around the C4–C5 bond has no effect on the zigzag conformation of the carbon scaffold, but it is also unfavorable since the hydroxy atom at terminal C5 atom is less acidic than the other hydroxy functions. A similar vivid competition between different coordination sites is observed for *N*-alkylgulosylamines for which $\kappa^2O^{3,4}$, $\kappa^2O^{4,5}$ and $\kappa^2O^{5,6}$ binding modes are realized.

3.5. The exceptional Coordination Behavior of *N*-Alkyl-2-deoxyglycosylamines

The trends established and discussed in chapter 3.3 and 3.4 for the chelation and imine formation of glycosylamines, raise the question which coordination mode is preferably realized when no hydroxy function is present at the C2 atom.

The reactions of the investigated *N*-alkyl-2-deoxy-D-glycosylamines with palladium(II) probes show a clear preference of their respective furanoid and acyclic imine forms when featured as ligand. In the case of both investigated *N*-alkyl-2-deoxy-D-hexosylamines this observation comes as no surprise as the 1,3-diaxial orientation of two functional groups, one of them being the alkylamino moiety, required for a chelation is only realized for the respective β -anomers in the ¹C₄ conformation. In this conformation the hydroxymethyl at C5 atom would adopt the energetically unfavorable axial position, and hence the system avoids this conceivable coordination mode. The resulting preferred κ^2N^1,O^3 metalation of the furanoid forms for the corresponding non-substituted 2-deoxy-D-hexosylamines was already described by SCHWARZ.^[21,57] It is also noteworthy that SCHWARZ has found no indication for a metalation of the respective open-chain forms in his studies.

Unexpectedly, the investigated *N*-alkyl-2-deoxy-D-*erythro*-pentosylamines showed no signs for

a 1,3-diaxial metalation of their respective pyranoid α -anomer as well, although no substantial steric hindrances would be present in the 4C_1 conformation. This observation indicates a clear preference of the metalation of furanosylamine structures over pyranosylamines when the formation of a six-membered chelate ring is mandatory.

The κ^2N^1,O^3 metalation of the open-chain species also comes with some energetic disadvantages since an alteration from the zigzag conformation in form of a C1–C2 bond rotation is required to facilitate the formation of a six-membered chelate ring. The percentage of metalated imine species detected in the respective reaction solutions increases with increasing steric demand of the alkylamino moiety in the featured *N*-alkyl-2-deoxy-D-glycosylamine. The preference of *N*-alkylglycosylamines with bulky alkyl substituents to avoid the formation of furanoid isomers already becomes obvious from the percentage distributions for the free ligands in aqueous solution listed in chapter 2.1. This tendency also seems to apply for the respective complex species as, for example, in the case of D-*ara*-dHex1N*i*Pr solely a chelation of the imine form is observed (aside from the formation of hydrolysis products).

The affinity of *N*-alkyl-2-deoxy-D-glycosylamines to reside as ligand in their respective open-chain form further increases when two equivalents of palladium probe are used in the reaction. This is especially the case for *N*-alkyl-2-deoxy-D-*erythro*-pentosylamines which lack additional functional groups for the chelation of a second PdN₂-fragment in the respective furanoid form. For the investigated *N*-alkyl-2-deoxy-D-hexosylamines a exocyclic coordination of the second Pd²⁺ ion by the α -furanosylamine form is observed but always in an equilibrium with the corresponding binuclear acyclic imine complex species.

For the imine form of *N*-alkyl-2-deoxy-D-*erythro*-pentosylamines the less acidic terminal hydroxy group is involved in the $\kappa^2O^{4,5}$ coordination of the second PdN₂-fragment due to the fact that there are no alternative binding sites present in this species. Despite featuring an additional hydroxy function, the same behavior is observed for open-chain *N*-alkyl-2-deoxy-D-*arabino*-hexosylamines, which boast a $\kappa^2O^{5,6}$ chelation of the second Pd²⁺ ion. This observation can be primarily attributed to the unfavorable *trans*-orientation of the hydroxy functions at the C4 and C5 atom. In order to provide a sufficient binding site a rotation around the C4–C5 bond, and thus a further deviation from the ideal zigzag conformation, would be required. This seems to be disadvantageous to such an extent that the involvement of the terminal hydroxy function in the chelation as alternative binding mode is clearly preferred. Conversely, in the C4 epimeric *N*-alkyl-2-deoxy-D-*lyxo*-hexosylamines a $\kappa^2O^{4,5}$ chelation is feasibly realized due to the favorable *cis*-orientation of the respective functional groups.

4. Summary

In order to gain a better understanding of the chelation properties of *N*-substituted glycosylamines and the associated uncommon affinity of some representatives to bind Pd²⁺ ions in their respective open-chain form, a large variety of *N*-substituted glycosylamines was synthesized and subsequently treated with various palladium(II) probes.

The synthesis of *N*-substituted glycosylamines was achieved through the reaction of aldoses with primary amines. The applied aldoses include D-arabinose, D-lyxose, D-ribose, D-xylose, D-galactose, D-glucose, L-gulose, D-mannose, L-rhamnose, 2-Deoxy-*erythro*-D-pentose, 2-Deoxy-*arabino*-D-hexose and 2-Deoxy-*lyxo*-D-hexose while methyl, ethyl, propyl, *iso*-propyl and *tert*-butyl as well as aniline were used as amines. The thereby obtained compounds were characterized by NMR spectroscopy, elemental analysis, mass spectrometry and single crystal X-ray diffraction. Crystal structures which have not yet been described in the literature could be obtained for two *N*-alkyl- and five *N*-phenyl-D-glycosylamines: ⁴C₁-β-D-Glcp1NMe·MeNH₂ (**1**), ¹C₄-β-L-Rhap1NEt (**2**), ⁴C₁-β-D-Lyxp1NPh (**3**), ⁴C₁-α-D-Ribp1NPh·0.5H₂O (**4**), ⁴C₁-β-D-Xylp1NPh (**5**), ⁴C₁-β-D-*ara*-dHexp1NPh (**6**) and ⁴C₁-β-D-*lyx*-dHexp1NPh·0.33H₂O (**7**). These structures represent in most cases the prevailing isomer of the respective compound in aqueous solution.

It was shown that for *N*-substituted glycosylamines the equilibrium in solution between the cyclic isomers and the open-chain form is, aside from the structure of the glycon, primarily influenced by the steric and electronic properties of the amino substituent. Furthermore, the comparison of the determined percentages with those known for the corresponding aldose analogues are in accordance with the inexistence of an anomeric effect for amino functions.

In contrast to their non-substituted counterparts, *N*-alkyl-D-glycosylamines show a substantial higher susceptibility to hydrolysis. This complicates the investigation of chelation reactions as there is always a competition between the hydrolysis and the metalation of the ligand. A rapid hydrolysis is characterized by the accompanying formation of elemental palladium induced by the presence of a reducing sugar. A rapid metalation on the other hand seems to reduce the potential of the ligand to hydrolyze. Thus, some reaction solutions could be stored for few days before showing signs of decomposition.

Taking advantage of this stabilization, crystallization occurred in one reaction attempt. The determined crystal structure of [Pd(en)(⁴C₁-β-D-Xylp1NMe2H_{-1-κN¹,κO²)]IO₃·4H₂O (**8**) represents the first molecular structure of an alkylglycosylamine-palladium complex. The found structure displays the clearly prevailing species in the reaction solution, which should be, alongside with the featured hydrogen bond network, a beneficial factor for the crystallization. Unfortunately, the majority of the reaction attempts showed more diverse species distributions or higher affinity towards hydrolysis, so that only a NMR spectroscopic characterization of most complex species was feasible.}

The following rules for the formation of glycosylamine-palladium complexes could be derived from the results of the NMR spectroscopic investigations described in this work. Firstly, the amino function always participates in the chelation of the first PdN₂-fragment. Secondly, for this binding a *trans*-vicinal coordination pattern is always favored over a *cis*-vicinal metalation. Thirdly, for the binding of a second PdN₂-fragment there is no preference between a *trans*- and *cis*-orientation of the hydroxy groups at the C3 and C4 atom. Additionally, a formation of six-membered chelate rings and metalation of furanoid isomers is only observed for *N*-substituted 2-deoxyglycosylamines.

If one of the above mentioned criteria cannot be met, the chelation of the open-chain form becomes significantly favored. As, for example, in *N*-substituted lyxosylamines, where the *trans*-vicinal chelation is linked to an energetically unfavorable all-axial orientation of the remaining functional groups. Or even worse in mannosylamine, the hexosyl analogue of lyxosylamine, in which a *trans*-vicinal chelation is only possible in a conformation with the terminal hydroxymethyl function occupying the axial position. Additionally, the *anti* orientation of the hydroxy groups at the C3 and C4 atom in both ligand groups leads to the observation that only acyclic binuclear complex species are formed.

But aside from the configuration of the glycon, there are more factors favoring a chelation of the open-chain form. One is the type of amino group featured in the regarded *N*-substituted glycosylamine. For *N*-alkyl-D-glycosylamines the trend for a higher amount of imine chelation is as follows: Me < Et < Pr \approx *i*Pr < *t*Bu. This tendency is reflected in the detection of at least minimal amounts of imine-palladium complex for the *iso*-propyl and *tert*-butyl derivatives of all investigated *N*-alkyl-D-glycosylamines. The corresponding *N*-phenyl-D-glycosylamines show a rather low tendency towards the metalation of the open-chain form, quantitatively comparable to the affinity of *N*-methyl-D-glycosylamines.

In the case of *N*-phenyl-D-glycosylamines the availability of ¹⁵N-enriched aniline provided the opportunity for the establishment of an additional analytical approach for the investigation of phenylglycosylamine-palladium complexes. With the use of ¹⁵N NMR spectroscopic methods more lucid insights in the species distribution are enabled as each species can be assigned to one particular NMR signal. Furthermore, this analytical method provides further evidence for the presence of the imine form in respective acyclic complex species: Firstly, the distinct ¹⁵N NMR shift for Schiff base compounds and associated complexes and secondly the spin-spin splitting observed for the ¹³C{¹H} NMR signals assigned to the imine group as a result of its vicinity to the ¹⁵N-enriched nitrogen atom.

5. Experimental Section

5.1. Methods and Materials

Unless not specifically stated otherwise, all syntheses were carried out in oven-dried glassware in an atmosphere of argon (purity 5.0, Air Liquide) and with exclusion of water using standard Schlenk techniques. Filtrations were performed using Schlenk-frits (pore size G4), and in some cases pressure in the bottom part of the filter was lowered in order to accelerate the filtration. Alkaline solutions containing palladium precursors were stored at $-25\text{ }^{\circ}\text{C}$ in Schlenk tubes guaranteeing the exclusion of air and therefore minimizing the uptake of carbon dioxide and the formation of elemental palladium. *N*-Substituted glycosylamines were stored in the same manner to prevent their hydrolysis.

Reactions solutions containing glycosylamine palladium complexes were slowly covered with the same amount of acetone and stored at $4\text{ }^{\circ}\text{C}$ in order to obtain crystals at the boundary layer between both liquids.

5.2. NMR Spectroscopy

NMR spectra were recorded at room temperature or at $4\text{ }^{\circ}\text{C}$ on a Bruker AV400 spectrometer (^1H : 400 MHz, ^{13}C : 101 MHz, ^{15}N : 41 MHz). Measurements at $4\text{ }^{\circ}\text{C}$ were performed utilizing a BCU-I (Bruker Cooling Unit I). All ^{13}C NMR spectra were recorded broadband proton decoupled, ^{15}N NMR spectra were measured broadband proton decoupled and coupled. When necessary, the ^1H and $^{13}\text{C}\{^1\text{H}\}$ signals were assigned by means of ^1H , ^1H -COSY, ^1H , ^{13}C -HMQC, ^1H , ^{13}C -HMBC and DEPT135 NMR experiments in D_2O . NMR data were processed and visualized using the MestReNova software by the company Mestrelab Research.

The signals of the deuterated solvent and the residual protons therein were used as internal secondary reference for the chemical shift (^1H : D_2O 4.79 ppm, $\text{DMSO-}d_6$: 2.50 ppm; ^{13}C : $\text{DMSO-}d_6$ 39.52 ppm). When D_2O was used as solvent, one drop of methanol was added to the sample tube in order to obtain a reference signal in the $^{13}\text{C}\{^1\text{H}\}$ spectra. The position of this signal was defined to 49.5 ppm, as suggested by GOTTlieb *et al.*^[58] Since the chemical shift of the HDO signal is highly temperature dependent, this signal is not suitable as an internal secondary reference in ^1H NMR measurements in D_2O not performed at room temperature. The value of the HDO reference signal can be corrected by the equation $\delta = 5.051 - 0.0111T$ (T in $^{\circ}\text{C}$) for the $0\text{--}50\text{ }^{\circ}\text{C}$ range and, thus, is set to 5.00 ppm for all measurements at $4\text{ }^{\circ}\text{C}$.^[58,59] ^{15}N NMR spectra were recorded for samples containing ^{15}N labeled *N*-phenylglycosylamines and no secondary internal reference was added. All shifts are given in regard to Nitromethane as internal standard and reference sample, although liquid ammonia is commonly used as reference compound in the literature.^[60,61]

5.3. Reagents and Solvents

All reagents were purchased in high quality and used without further purification. Anhydrous solvents over molecular sieves were purchased from Acros and not further dried.

Table 5.1. List of reagents.

Chemikalie	Reinheit	Hersteller
2-deoxy- <i>arabino</i> -D-hexose	98%	ABCR
2-deoxy- <i>erythro</i> -D-hexose	≥ 99.0%	Sigma-Aldrich
2-deoxy- <i>lyxo</i> -D-pentose	98%	Sigma-Aldrich
aniline	≥ 99.5%	Merck
aniline- ¹⁵ N	98 atom % ¹⁵ N	Merck
D-arabinose	≥ 99.0%	Merck
<i>tert</i> -butylamine	≥ 99.5%	Sigma-Aldrich
deuterium oxide	99.9%D	Euriso-Top
diethyl ether	99.9%	VWR
dimethyl sulfoxide- <i>d</i> ₆	99.8%D	Euriso-Top
ethan-1,2-diamine	≥ 99.5%	Sigma-Aldrich
ethylamine	2 M in MeOH	Sigma-Aldrich
D-galactose	≥ 99.5%	Sigma-Aldrich
D-glucose	≥ 99.5%	Merck
L-gulose	≥ 98.0%	TCI
hydrochloric acid	37%	Biesterfeld Graen
iodic acid	≥ 99.5%	Fluka
D-lyxose	≥ 99.0%	ABCR
methanol	≥ 99.8%	Acros Organics
methylamine	33 wt. % in EtOH	Acros Organics
D-mannose	99%	ABCR
palladium(II) chloride	99.9%	ABCR
potassium hydroxide	p.a.	Bernd Kraft
potassium tetrachloropalladate(II)	99%	ABCR
propylamine	≥ 99.0%	Sigma-Aldrich
<i>iso</i> -propylamine	≥ 99.5%	Sigma-Aldrich
L-rhamnose monohydrate	99.0%	ABCR
D-ribose	98%	ABCR
silver(I) oxide	99.9%	Sigma-Aldrich
sulfuric acid	p.a.	Fluka
water	deionized	house installation
D-xylose	> 99.0%	Glycon Biochemicals

5.4. Preparation of Palladium Precursor Compounds

Dichlorido(ethylenediamine)palladium(II), [Pd(en)Cl₂]^[62]

To a suspension of palladium(II) chloride (5.02 g, 28.3 mmol, 1.00 eq.) in 25 mL water, hydrochloric acid (37 %, 5 mL) was added upon stirring. After 5 min a brown solution was obtained. A mixture of ethan-1,2-diamine (7.00 mL, 6.29 g, 105 mmol, 3.70 eq.) in water (15 mL) was added dropwise to the reaction mixture and a pink precipitate formed. After the addition of two-thirds of the ethan-1,2-diamine solution the reaction mixture was heated to 45 °C and the remaining ethan-1,2-diamine solution was added subsequently, causing the pink precipitate to dissolve and a pale yellow solution formed. The solution was acidified to pH 2 with hydrochloric acid (semi-conc.) to precipitate the yellow product. After cooling the suspension to 4 °C, the precipitate was filtered off, washed with cold water (5 × 20 mL) dried *in vacuo*, yielding 5.95 g (25.1 mmol, 89.0 % of theory) of the product.

EA: calcd.: C 10.12 %, H 3.40 %, N 11.80 %, Cl 29.89 %
found: C 10.18 %, H 3.37 %, N 11.88 %, Cl 29.88 %

Dihydroxido(ethylenediamine)palladium(II), [Pd(en)(OD)₂]^[47]

[Pd(en)Cl₂] (5.34 g, 22.5 mmol, 1.00 eq.), silver(I) oxide (5.63 g, 24.3 mmol, 1.08 eq.) and deuterium oxide (50 mL) were stirred in the dark for 30 min at 40 °C. The precipitated silver chloride was removed from the resulting suspension *via* filtration, yielding a yellow, alkaline solution of Dichloro(ethylenediamine)palladium(II) (0.45 M).

¹H NMR (400 MHz, D₂O, 13OR10-2017): δ /ppm = 2.61 (CH₂).

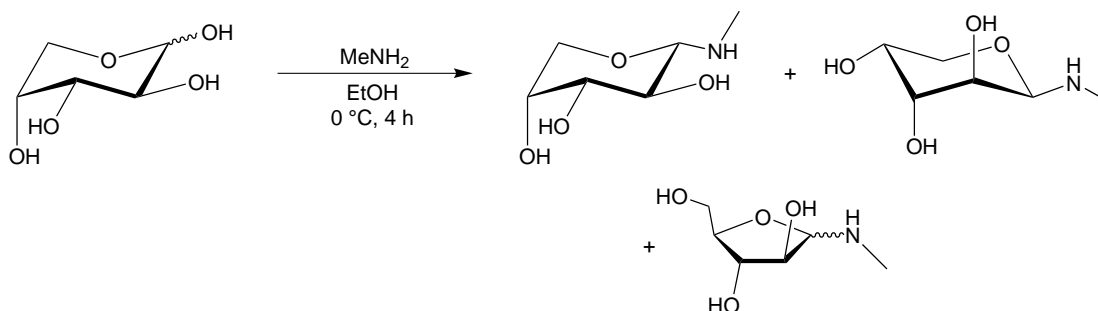
¹³C{¹H} NMR (101 MHz, D₂O, 13OR11-2017): δ /ppm = 46.4 (CH₂).

5.5. Preparation of *N*-Substituted Alkylglycosylamines

5.5.1. Preparation of *N*-Alkylpentosylamines

5.5.1.1. Preparation of *N*-Alkylarabinosylamines

N-Methyl-*D*-arabinosylamin (D-Ara1NMe)



D-Arabinose (4.00 g, 26.6 mmol, 1.00 eq.) was dried and subsequently stirred with a solution of methylamine in ethanol (33 %, 10.0 mL, 74.5 mmol, 2.80 eq.) for 4 h under ice cooling. The reaction solution was stored at 4 °C overnight, whereupon colorless crystals were obtained. The crystals were filtered off, washed with ethanol (1 × 10 mL) and diethyl ether (2 × 10 mL), and dried *in vacuo*. The product was obtained as a colorless powder in a yield of 3.23 g (19.8 mmol, 49.6 % of theory).

EA: calcd.: C 44.17 %, H 8.03 %, N 8.58 %
found: C 44.13 %, H 8.05 %, N 8.56 %

MS (FAB+): calcd.: 164.2 ([M+H]⁺)
found: 164.2

N-Methyl- α -*D*-arabinopyranosylamine – D₂O: 64 % (RT), 95 % (4 °C) – DMSO-*d*₆: 36 %

¹H NMR (400 MHz, D₂O, 41OR1-2015): δ /ppm = 3.91 (dd, 1H, H4, ³*J*_{4,5eq} = 2.3 Hz, ³*J*_{4,5ax} = 1.2 Hz), 3.83 (dd, 1H, H5eq, ²*J*_{5eq,5ax} = -13.0 Hz), 3.78 (d, 1H, H1, ³*J*_{1,2} = 8.6 Hz), 3.61 (dd, 1H, H5ax), 3.60 (dd, 1H, H3, ³*J*_{3,4} = 3.6 Hz), 3.44 (d, 1H, H2, ³*J*_{2,3} = 9.5 Hz), 2.43 (s, 3H, CH₃).

¹³C{¹H} NMR (101 MHz, D₂O, 41OR2-2015): δ /ppm = 92.2 (C1), 73.8 (C3), 70.9 (C2), 69.4 (C4), 67.7 (C5), 31.5 (CH₃).

¹³C{¹H} NMR (101 MHz, DMSO-*d*₆, 41OR5-2015): δ /ppm = 91.8 (C1), 73.0 (C3), 70.7 (C2), 70.6 (C4), 67.5 (C5), 31.8 (CH₃).

N-Methyl- β -*D*-arabinopyranosylamine – D₂O: 18 % (RT), 4 % (4 °C) – DMSO-*d*₆: 32 %

¹H NMR (400 MHz, D₂O, 41OR1-2015): δ /ppm = 4.30 (d, H1, ³*J*_{1,2} = 2.6 Hz), 2.36 (s, 3H, CH₃).

¹³C{¹H} NMR (101 MHz, D₂O, 41OR2-2015): δ /ppm = 87.1 (C1), 70.4 (C3), 70.3 (C2), 66.1 (C4), 63.6 (C5), 31.7 (CH₃).

¹³C{¹H} NMR (101 MHz, DMSO-*d*₆, 41OR5-2015): δ /ppm = 86.2 (C1), 71.0 (C3), 70.7 (C2), 64.9 (C5), 64.8 (C4), 32.2 (CH₃).

N-Methyl- α -D-arabinofuranosylamine – D₂O: 10 % (RT), 1 % (4 °C) – DMSO-*d*₆: 20 %

¹H NMR (400 MHz, D₂O, 41OR1-2015): δ /ppm = 4.44 (d, H1, ³*J*_{1,2}=5.1 Hz), 2.43 (s, 3H, CH₃).

¹³C{¹H} NMR (101 MHz, D₂O, 41OR2-2015): δ /ppm = 95.1 (C1), 81.9 (C4), 79.9 (C2), 76.0 (C3), 61.8 (C5), 31.1 (CH₃).

¹³C{¹H} NMR (101 MHz, DMSO-*d*₆, 41OR5-2017): δ /ppm = 96.1 (C1), 82.6 (C4), 80.2 (C2), 76.4 (C3), 62.0 (C5), 31.6 (CH₃).

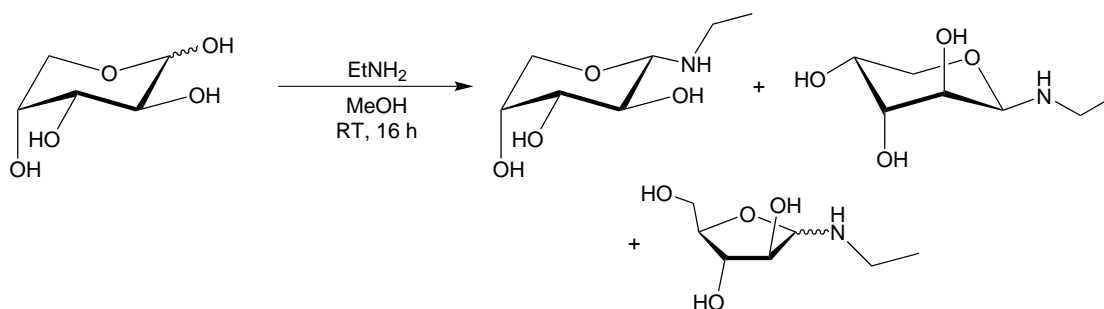
N-Methyl- β -D-arabinofuranosylamine – D₂O: 8 % (RT), >1 % (4 °C) – DMSO-*d*₆: 12 %

¹H NMR (400 MHz, D₂O, 41OR1-2015): δ /ppm = 4.64 (d, H1, ³*J*_{1,2}=3.7 Hz).

¹³C{¹H} NMR (101 MHz, D₂O, 41OR2-2017): δ /ppm = 92.8 (C1), 83.1 (C3), 77.2 (C2), 76.3 (C4), 62.5 (C5), 32.3 (CH₃).

¹³C{¹H} NMR (101 MHz, DMSO-*d*₆, 41OR5-2017): δ /ppm = 92.8 (C1), 83.5 (C4), 77.0 (C2), 76.3 (C3), 62.3 (C5), 32.7 (CH₃).

N-Ethyl-D-arabinosylamin (*D*-Ara1NEt)



D-Arabinose (1.50 g, 9.99 mmol, 1.00 eq.) was dried and subsequently stirred with a solution of ethylamine in methanol (2 M, 10.0 mL, 20.0 mmol, 2.00 eq.) for 16 h at room temperature. The reaction mixture was concentrated by evaporation of the solvent until a colorless precipitate formed, which was filtered off, washed with cold methanol (2 × 10 mL) and dried *in vacuo*. The product was obtained as a yellowish powder in a yield of 1.58 g (8.96 mmol, 89.7 % of theory).

EA: calcd.: C 47.45 %, H 8.53 %, N 7.90 %

found: C 46.99 %, H 8.55 %, N 7.64 %

MS (FAB+): calcd.: 178.2 ([M+H]⁺)

found: 178.2

N-Ethyl- α -D-arabinopyranosylamine – D₂O: 66 %, 85 % (4 °C) – DMSO-*d*₆: 60 %

¹H NMR (400 MHz, D₂O, 4 °C, 45OR1-2018): δ /ppm = 3.91 (ddd, 1H, H4), 3.87 (d, 1H, H1, ³*J*_{1,2}=8.6 Hz) 3.80 (dd, 1H, H5_{eq}, ³*J*_{4,5_{eq}}=2.3 Hz, ²*J*_{5_{eq},5_{ax}}=-13.0 Hz), 3.62 (dd, 1H, H3, ³*J*_{3,4}=3.5 Hz), 3.59 (dd, 1H, H5_{ax}), 3.44 (d, 1H, H2, ³*J*_{2,3}=9.5 Hz), 2.87–2.82 (m, 1H, CH₂), 2.64–2.54 (m, 1H, CH₂), 1.04 (t, 3H, CH₃).

¹³C{¹H} NMR (101 MHz, D₂O, 43OR20-2015): δ /ppm = 90.8 (C1), 73.8 (C3), 71.2 (C2), 69.4 (C4), 67.7 (C5), 39.9 (CH₂), 14.5 (CH₃).

$^{13}\text{C}\{^1\text{H}\}$ NMR (101 MHz, DMSO- d_6 , 43OR5-2018): δ/ppm = 90.3 (C1), 72.9 (C3), 70.8 (C2), 67.4 (C4), 65.7 (C5), 39.3 (CH₂), 15.4 (CH₃).

N-Ethyl- β -D-arabinopyranosylamine – D₂O: 15 %, 7 % (4 °C) – DMSO- d_6 : 19 %

^1H NMR (400 MHz, D₂O, 4 °C, 45OR1-2018): δ/ppm = 4.39 (d, H1, $^3J_{1,2}=2.2$ Hz), 2.36 (s, 3H, CH₃).

$^{13}\text{C}\{^1\text{H}\}$ NMR (101 MHz, D₂O, 45OR1-2018): δ/ppm = 85.1 (C1), 71.1 (C3), 70.7 (C2), 64.6 (C4), 63.6 (C5), 39.0 (CH₃), 15.4 (CH₃).

$^{13}\text{C}\{^1\text{H}\}$ NMR (101 MHz, DMSO- d_6 , 43OR5-2018): δ/ppm = 84.3 (C1), 70.7 (C3), 70.5 (C2), 65.7 (C4), 63.8 (C5), 39.8 (CH₃), 14.2 (CH₃).

N-Ethyl- α -D-arabinofuranosylamine – D₂O: 12 %, 6 % (4 °C) – DMSO- d_6 : 13 %

^1H NMR (400 MHz, D₂O, 4 °C, 45OR1-2018): δ/ppm = 4.51 (d, H1, $^3J_{1,2}=5.2$ Hz), 2.43 (s, 3H, CH₃).

$^{13}\text{C}\{^1\text{H}\}$ NMR (101 MHz, D₂O, 43OR20-2015): δ/ppm = 93.8 (C1), 81.9 (C4), 80.4 (C2), 76.1 (C3), 61.8 (C5), 39.7 (CH₂), 14.4 (CH₃).

$^{13}\text{C}\{^1\text{H}\}$ NMR (101 MHz, DMSO- d_6 , 43OR5-2018): δ/ppm = 94.7 (C1), 82.6 (C4), 80.6 (C2), 76.4 (C3), 62.0 (C5), 39.9 (CH₂), 15.5 (CH₃).

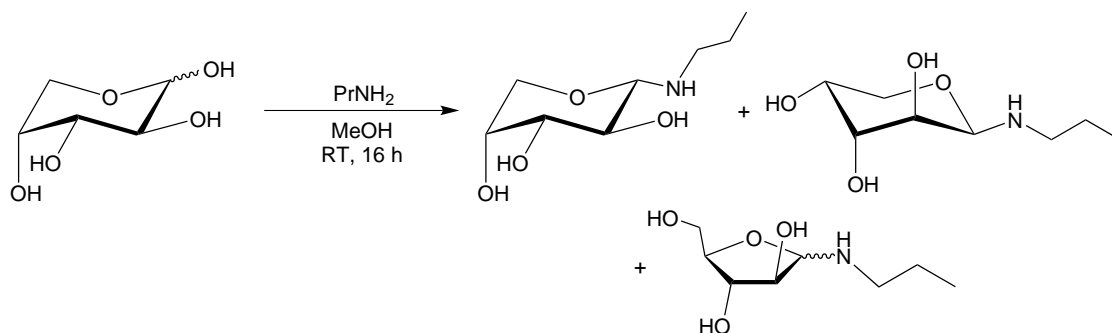
N-Ethyl- β -D-arabinofuranosylamine – D₂O: 7 %, 2 % (4 °C) – DMSO- d_6 : 8 %

^1H NMR (400 MHz, D₂O, 4 °C, 45OR1-2018): δ/ppm = 4.74 (d, H1, $^3J_{1,2}=3.8$ Hz).

$^{13}\text{C}\{^1\text{H}\}$ NMR (101 MHz, D₂O, 43OR20-2015): δ/ppm = 91.2 (C1), 83.3 (C3), 77.3 (C2), 76.4 (C4), 62.5 (C5), 40.7 (CH₂), 14.5 (CH₃).

$^{13}\text{C}\{^1\text{H}\}$ NMR (101 MHz, DMSO- d_6 , 43OR5-2018): δ/ppm = 90.8 (C1), 83.6 (C3), 76.9 (C2), 76.4 (C4), 62.3 (C5), 39.9 (CH₂), 15.5 (CH₃).

N-Propyl-D-arabinosylamin (D-Ara1NPr)



D-Arabinose (1.50 g, 9.99 mmol, 1.00 eq.) was dried and subsequently solved in 5 mL dry methanol. Propylamine (2.10 mL, 1.51 g, 25.6 mmol, 2.56 eq.) was added and the reaction mixture stirred for 16 h at room temperature. The resulting yellow solution was evaporated until it reached dryness and the obtained yellowish solid further dried *in vacuo*. Due to the high hygroscopy of the compound no yield was determined.

EA: calcd.: C 50.25 %, H 8.96 %, N 7.32 %
found: C 49.15 %, H 8.71 %, N 7.26 %

MS (FAB+): calcd.: 192.2 ([M+H]⁺)
found: 192.4

N-Propyl- α -D-arabinopyranosylamine – D₂O: 70 % – DMSO-*d*₆: 55 %

¹H NMR (400 MHz, D₂O, 4 °C, 37OR6-2017): δ /ppm = 3.91–3.89 (sp, 1H, H4), 3.87 (d, 1H, H1, ³*J*_{1,2}=8.6 Hz), 3.80 (dd, 1H, H5a, ³*J*_{4,5a}=2.3 Hz, ²*J*_{5a,5b}=–12.9 Hz), 3.60 (dd, 1H, H3, ³*J*_{2,3}=9.4 Hz ³*J*_{3,4}=3.6 Hz), 3.59 (dd, 1H, H5b, ³*J*_{4,5b}=1.2 Hz), 3.42 (dd, 1H, H2), 2.78–2.72 (s, 1H, NH–CH₂), 2.59–2.51 (s, 1H, NH–CH₂), 1.52–1.39 (sp, 2H, CH₂), 1.52–1.39 (sp, 2H, CH₂), 0.86 (t, 3H, CH₃).

¹³C{¹H} NMR (101 MHz, D₂O, 4 °C, 37OR7-2017): δ /ppm = 91.1 (C1), 73.8 (C3), 71.1 (C2), 69.4 (C4), 67.7 (C5), 47.6 (NH–CH₂), 22.9 (CH₂), 11.8 (CH₃).

¹³C{¹H} NMR (101 MHz, DMSO-*d*₆, 37OR2-2017): δ /ppm = 90.5 (C1), 72.9 (C3), 70.8 (C2), 67.4 (C4), 64.6 (C5), 47.1 (NH–CH₂), 23.1 (CH₂), 11.8 (CH₃).

N-Propyl- β -D-arabinopyranosylamine – D₂O: 18 % – DMSO-*d*₆: 23 %

¹H NMR (400 MHz, D₂O, 4 °C, 37OR6-2017): δ /ppm = 4.38 (d, H1, ³*J*_{1,2}=2.1 Hz).

¹³C{¹H} NMR (101 MHz, D₂O, 4 °C, 37OR7-2017): δ /ppm = 85.3 (C1), 70.8 (C3), 70.8 (C2), 65.6 (C4), 63.9 (C5), 47.5 (NH–CH₂), 22.7 (CH₂), 11.8 (CH₃).

¹³C{¹H} NMR (101 MHz, DMSO-*d*₆, 37OR2-2017): δ /ppm = 84.7 (C1), 71.1 (C3), 70.7 (C2), 64.7 (C4), 63.6 (C5), 47.1 (NH–CH₂), 23.1 (CH₂), 11.8 (CH₃).

N-Propyl- α -D-arabinofuranosylamine – D₂O: 8 % – DMSO-*d*₆: 13 %

¹H NMR (400 MHz, D₂O, 4 °C, 37OR6-2017): δ /ppm = 4.51 (d, H1, ³*J*_{1,2}=5.1 Hz).

¹³C{¹H} NMR (101 MHz, D₂O, 4 °C, 37OR7-2017): δ /ppm = 94.1 (C1), 81.9 (C4), 80.2 (C2), 75.9 (C3), 61.7 (C5), 47.3 (NH–CH₂), 22.9 (CH₂), 11.8 (CH₃).

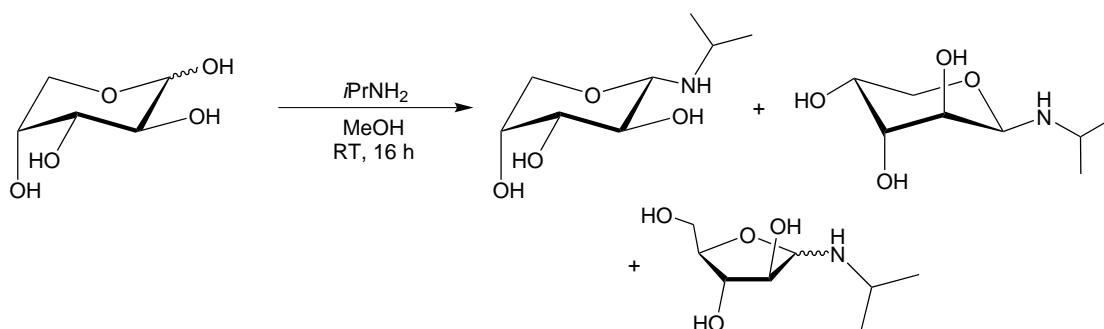
¹³C{¹H} NMR (101 MHz, DMSO-*d*₆, 37OR2-2017): δ /ppm = 96.1 (C1), 82.6 (C4), 80.2 (C2), 76.4 (C3), 62.0 (C5), 47.0 (NH–CH₂), 23.2 (CH₂), 11.7 (CH₃).

N-Propyl- β -D-arabinofuranosylamine – D₂O: 4 % – DMSO-*d*₆: 9 %

¹H NMR (400 MHz, D₂O, 4 °C, 37OR6-2017): δ /ppm = 4.74 (d, H1, ³*J*_{1,2}=3.7 Hz).

¹³C{¹H} NMR (101 MHz, D₂O, 4 °C, 37OR7-2017): δ /ppm = 91.7 (C1), 83.1 (C3), 77.2 (C2), 76.3 (C4), 62.5 (C5), 48.3 (NH–CH₂), 23.0 (CH₂), 11.8 (CH₃).

¹³C{¹H} NMR (101 MHz, DMSO-*d*₆, 37OR2-2017): δ /ppm = 92.8 (C1), 83.5 (C4), 77.0 (C2), 76.3 (C3), 62.3 (C5), 47.9 (NH–CH₂), 23.2 (CH₂), 11.7 (CH₃).

***N*-(*iso*-Propyl)-D-arabinosylamin (D-Ara1NiPr)**

D-Arabinose (1.50 g, 9.99 mmol, 1.00 eq.) was dried and subsequently solved in 2.5 mL dry methanol. *iso*-Propylamine (2.10 mL, 1.44 g, 24.4 mmol, 2.45 eq.) was added and the reaction mixture stirred for 16 h at room temperature. The resulting yellow solution was evaporated until it reached dryness and the obtained beige powder further dried *in vacuo*. Due to the high hygroscopy of the compound no yield was determined.

N-(*iso*-Propyl)- α -D-arabinopyranosylamine – D₂O: 78 % – DMSO-*d*₆: 56 %

¹H NMR (400 MHz, D₂O, 4 °C, 37OR8-2017): δ /ppm = 3.95 (d, 1H, H1, ³*J*_{1,2}=8.5 Hz), 3.91 (td, 1H, H4) 3.79 (dd, 1H, H5a, ³*J*_{4,5a}=2.3 Hz, ²*J*_{5a,5b}=−13.0 Hz), 3.61 (dd, 1H, H3, ³*J*_{2,3}=9.4 Hz, ³*J*_{3,4}=3.6 Hz), 3.60 (dd, 1H, H5b, ³*J*_{4,5b}=1.2 Hz), 3.37 (dd, 1H, H2), 3.12–3.01 (sp, 1H, CH), 1.02 (sp, 6H, CH₃).

¹³C{¹H} NMR (101 MHz, D₂O, 4 °C, 37OR9-2017): δ /ppm = 91.1 (C1), 73.8 (C3), 71.1 (C2), 69.4 (C4), 67.7 (C5), 47.6 (CH), 23.3 (CH₃), 21.2 (CH₃).

¹³C{¹H} NMR (101 MHz, DMSO-*d*₆, 37OR10-2017): δ /ppm = 88.2 (C1), 72.8 (C3), 71.0 (C2), 67.3 (C4), 64.4 (C5), 43.9 (CH), 24.4 (CH₃), 22.1 (CH₃).

N-(*iso*-Propyl)- β -D-arabinopyranosylamine – D₂O: 14 % – DMSO-*d*₆: 22 %

¹H NMR (400 MHz, D₂O, 4 °C, 37OR8-2017): δ /ppm = 4.47 (d, H1, ³*J*_{1,2}=1.8 Hz).

¹³C{¹H} NMR (101 MHz, D₂O, 4 °C, 37OR9-2017): δ /ppm = 85.3 (C1), 70.8 (C3), 70.8 (C2), 65.6 (C4), 63.9 (C5), 47.5 (CH₂), 23.4 (CH₃), 20.3 (CH₃).

¹³C{¹H} NMR (101 MHz, DMSO-*d*₆, 37OR10-2017): δ /ppm = 81.9 (C1), 71.3 (C3), 70.8 (C2), 64.6 (C4), 63.6 (C5), 43.1 (CH), 24.4 (CH₃), 22.1 (CH₃).

N-(*iso*-Propyl)- α -D-arabinofuranosylamine – D₂O: 6 % – DMSO-*d*₆: 15 %

¹H NMR (400 MHz, D₂O, 4 °C, 37OR8-2017): δ /ppm = 4.62 (d, H1, ³*J*_{1,2}=4.9 Hz).

¹³C{¹H} NMR (101 MHz, D₂O, 4 °C, 37OR9-2017): δ /ppm = 94.1 (C1), 81.9 (C4), 80.2 (C2), 75.9 (C3), 61.7 (C5), 47.3 (CH), 23.5 (CH₃), 20.4 (CH₃).

¹³C{¹H} NMR (101 MHz, DMSO-*d*₆, 37OR10-2017): δ /ppm = 92.7 (C1), 82.9 (C4), 80.9 (C2), 76.6 (C3), 62.1 (C5), 43.7 (CH), 24.4 (CH₃), 21.9 (CH₃).

N-(*iso*-Propyl)- β -D-arabinofuranosylamine – D₂O: 2 % – DMSO-*d*₆: 7 %

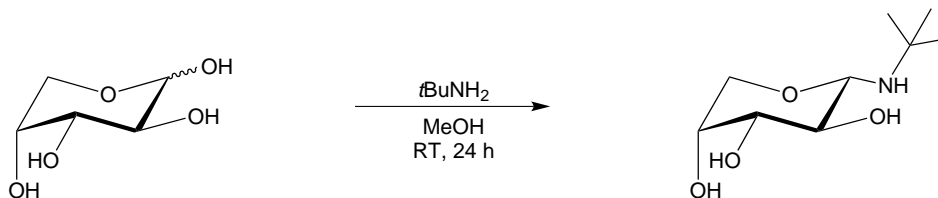
¹H NMR (400 MHz, D₂O, 4 °C, 37OR8-2017): δ /ppm = 4.87 (d, H1, ³*J*_{1,2}=3.6 Hz).

¹³C{¹H} NMR (101 MHz, D₂O, 4 °C, 37OR9-2017): δ /ppm = 91.7 (C1), 83.1 (C3), 77.2 (C2),

76.3 (C4), 62.5 (C5), 48.3 (CH), 23.6 (CH₃), 20.5 (CH₃).

¹³C{¹H} NMR (101 MHz, DMSO-*d*₆, 37OR10-2017): δ/ppm = 88.5 (C1), 83.6 (C4), 76.9 (C2), 76.5 (C3), 62.3 (C5), 44.7 (CH), 24.5 (CH₃), 22.2 (CH₃).

N-(*tert*-Butyl)-D-arabinosylamin (*D*-Ara1*N*tBu)



D-Arabinose (1.50 g, 9.99 mmol, 1.00 eq.) was dried and subsequently solved in 8 mL dry methanol. *tert*-Butylamine (2.10 mL, 1.47 g, 20.1 mmol, 2.01 eq.) was added and the reaction mixture stirred for 24 h at room temperature. The resulting yellow solution was evaporated until it reached dryness and the obtained beige powder further dried *in vacuo*. Due to the high hygroscopy of the compound no yield was determined.

N-(*tert*-Butyl)-α-D-arabinopyranosylamine – D₂O: 100 % (4 °C) – DMSO-*d*₆ 30 %

¹H NMR (400 MHz, D₂O, 4 °C, 37OR10-2017): δ/ppm = 3.97 (d, 1H, H1, ³*J*_{1,2}=8.7 Hz), 3.85–3.83 (sp, 1H, H4) 3.70 (sp, H5a, ³*J*_{4,5a}=1.9 Hz, ²*J*_{5a,5b}=–13.0 Hz), 3.60–3.58 (sp, 1H, H3), 3.57–3.55 (sp, 1H, H5b), 3.28–3.24 (sp, 1H, H2), 1.04 (sp, 9H, (9×CH₃)).

¹³C{¹H} NMR (101 MHz, D₂O, 4 °C, 37OR11-2017): δ/ppm = 87.6 (C1), 73.9 (C3), 71.3 (C2), 69.6 (C4), 67.3 (C5), 51.2 (C_q), 29.4 (CH₃).

¹³C{¹H} NMR (101 MHz, DMSO-*d*₆, 37OR2-2017): δ/ppm = 87.1 (C1), 73.1 (C3), 71.1 (C2), 68.0 (C4), 65.2 (C5), 49.5 (C_q), 30.3 (3×CH₃).

N-(*tert*-Butyl)-β-D-arabinopyranosylamine – D₂O: 0 % (4 °C) – DMSO-*d*₆ 27 %

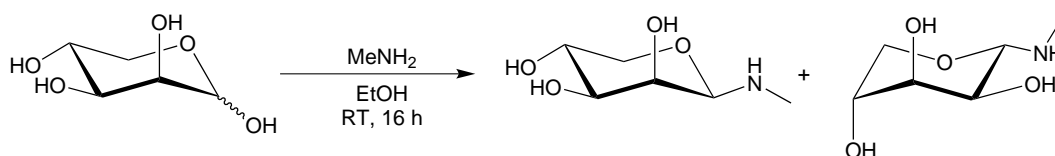
¹³C{¹H} NMR (101 MHz, DMSO-*d*₆, 37OR2-2017): δ/ppm = 81.2 (C1), 71.3 (C3), 70.8 (C2), 64.6 (C4), 63.6 (C5), 49.3 (C_q), 30.6 (3×CH₃).

N-(*tert*-Butyl)-α-D-arabinofuranosylamine – D₂O: 0 % (4 °C) – DMSO-*d*₆: 22 %

¹³C{¹H} NMR (101 MHz, DMSO-*d*₆, 37OR2-2017): δ/ppm = 91.4 (C1), 82.3 (C4), 81.6 (C2), 76.3 (C3), 62.1 (C5), 49.4 (C_q), 30.2 (3×CH₃).

N-(*tert*-Butyl)-β-D-arabinofuranosylamine – D₂O: 0 % (4 °C) – DMSO-*d*₆: 21 %

¹³C{¹H} NMR (101 MHz, DMSO-*d*₆, 37OR2-2017): δ/ppm = 86.3 (C1), 83.4 (C4), 77.0 (C2), 76.4 (C3), 62.3 (C5), 49.5 (C_q), 30.5 (3×CH₃).

5.5.1.2. Preparation of *N*-Alkyllyxosylamines*N*-Methyl-D-lyxosylamin (D-Lyx1NMe)

D-Lyxose (1.00 g, 6.66 mmol, 1.00 eq.) was dried and subsequently stirred with a solution of methylamine in ethanol (33 %, 12.0 mL, 89.2 mmol, 13.4 eq.) for 16 h at room temperature. The resulting solution was evaporated *in vacuo* until it reached dryness. The product was obtained as a colorless powder in a yield of 1.06 g (6.47 mmol, 97.2 % of theory).

EA: calcd.: C 44.17 %, H 8.03 %, N 8.58 %
found: C 44.05 %, H 8.16 %, N 8.65 %

MS (FAB+): calcd.: 164.2 ([M+H]⁺)
found: 164.2

N-Methyl-β-D-lyxopyranosylamine – D₂O: 69 % – DMSO-*d*₆: 56 %

¹H NMR (400 MHz, D₂O, 19OR15-2016): δ/ppm = 4.07 (d, 1H, H1, ³J_{1,2}=1.2 Hz), 3.90 (dd, 1H, H5a, ³J_{4,5a}=5.5 Hz, ²J_{5a,5b}=-11.3 Hz), 3.84 (dd, 1H, H2, ³J_{2,3}=3.3 Hz), 3.77 (dd, 1H, H4), 3.55 (dd, 1H, H3, ³J_{3,4}=9.6 Hz), 3.18 (dd, 1H, H5b, ³J_{4,5b}=10.4 Hz), 2.41 (s, 3H, CH₃).

¹³C{¹H} NMR (101 MHz, D₂O, 19OR16-2016): δ/ppm = 89.7 (C1), 74.4 (C3), 71.4 (C2), 67.2 (C4), 67.0 (C5), 31.6 (CH₃).

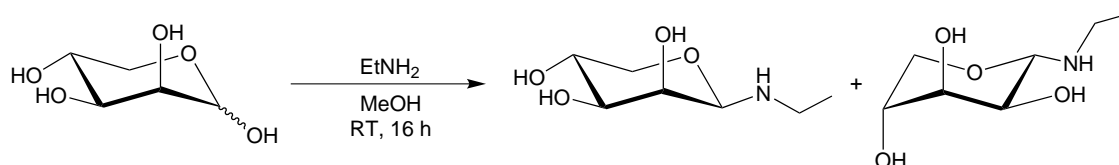
¹³C{¹H} NMR (101 MHz, DMSO-*d*₆, 19OR8-2016): δ/ppm = 89.4 (C1), 74.5 (C3), 70.9 (C2), 67.0 (C4), 66.1 (C5), 31.8 (CH₃).

N-Methyl-α-D-lyxopyranosylamine – D₂O: 31 % – DMSO-*d*₆: 44 % :

¹H NMR (400 MHz, D₂O, 19OR15-2016): δ/ppm = 4.19 (d, 1H, H1, ³J_{1,2}=6.8 Hz), 3.92–3.88 (sp, 1H, H3), 3.84–3.76 (sp, 2H, H4/H5a), 3.69 (dd, 1H, H2, ³J_{2,3}=3.3 Hz), 3.60 (dd, 1H, H5b, ³J_{4,5b}=4.7 Hz, ²J_{5a,5b}=-13.3 Hz), 2.39 (s, 3H, CH₃).

¹³C{¹H} NMR (101 MHz, D₂O, 19OR16-2016): δ/ppm = 89.1 (C1), 71.1 (C3), 69.3 (C2), 69.2 (C4), 64.7 (C5), 31.2 (CH₃).

¹³C{¹H} NMR (101 MHz, DMSO-*d*₆, 19OR8-2016): δ/ppm = 88.9 (C1), 70.6 (C3), 69.0 (C2), 68.9 (C4), 64.3 (C5), 31.8 (CH₃).

N-Ethyl-D-lyxosylamin (D-Lyx1NEt)

D-Lyxose (1.00 g, 6.66 mmol, 1.00 eq.) was dried and subsequently stirred with a solution of ethylamine in methanol (2 M, 13.6 mL, 40.0 mmol, 6.00 eq.) for 16 h at room temperature. After subsequent storage at 4 °C for 48 h a precipitate formed, which was filtered off, washed with cold methanol (2 × 10 mL) and dried *in vacuo*. The product was obtained as a slightly yellowish powder in a yield of 278 mg (1.57 mmol, 23.6 % of theory).

EA: calcd.: C 47.45 %, H 8.53 %, N 7.90 %
found: C 47.42 %, H 8.56 %, N 7.88 %

MS (FAB+): calcd.: 178.2 ([M+H]⁺)
found: 178.2

N-Ethyl-β-D-lyxopyranosylamine – D₂O: 74 % – DMSO-*d*₆: 57 %

¹H NMR (400 MHz, D₂O, 19OR19-2016): δ/ppm = 4.17 (d, 1H, H1, ³J_{1,2}=1.1 Hz), 3.89 (dd, 1H, H5a, ³J_{4,5a}=5.5 Hz, ²J_{5a,5b}=-11.3 Hz), 3.84 (dd, 1H, H2, ³J_{2,3}=3.4 Hz), 3.78 (dd, 1H, H4), 3.56 (dd, 1H, H3, ³J_{3,4}=9.6 Hz), 3.18 (dd, 1H, H5b, ³J_{4,5b}=10.4 Hz), 2.92–2.82 (sp, 1H, CH₂), 2.69–2.61 (sp, 1H, CH₂), 1.06 (t, 3H, CH₃).

¹³C{¹H} NMR (101 MHz, D₂O, 20OR2-2016): δ/ppm = 87.8 (C1), 74.4 (C3), 71.6 (C2), 67.2 (C4), 67.0 (C5), 39.5 (CH₂), 14.2 (CH₃).

¹³C{¹H} NMR (101 MHz, DMSO-*d*₆, 19OR11-2016): δ/ppm = 87.7 (C1), 74.5 (C3), 70.9 (C2), 66.9 (C4), 66.3 (C5), 39.0 (CH₂), 15.4 (CH₃).

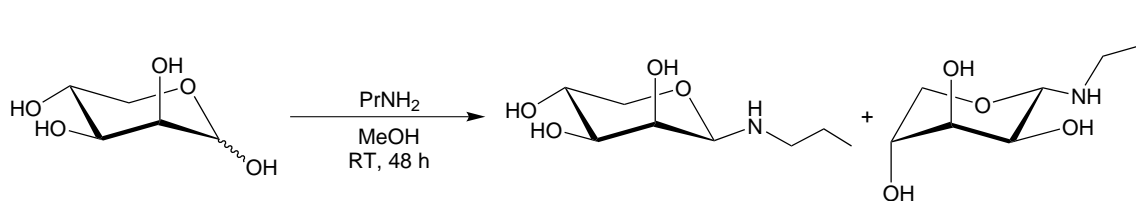
N-Ethyl-α-D-lyxopyranosylamine – D₂O: 26 % – DMSO-*d*₆: 43 %

¹H NMR (400 MHz, D₂O, 19OR19-2016): δ/ppm = 4.29 (d, 1H, H1, ³J_{1,2}=6.8 Hz), 3.90–3.85 (sp, 1H, H3), 3.82–3.76 (sp, 2H, H4/H5a), 3.69 (dd, 1H, H2, ³J_{2,3}=3.3 Hz), 3.62–3.58 (dd, 1H, H5b) 2.92–2.82 (sp, 1H, CH₂), 2.69–2.61 (sp, 1H, CH₂), 1.07 (t, 3H, CH₃).

¹³C{¹H} NMR (101 MHz, D₂O, 20OR2-2016): δ/ppm = 87.6 (C1), 71.1 (C3), 69.4 (C2), 69.2 (C4), 64.6 (C5), 39.6 (CH₂), 14.3 (CH₃).

¹³C{¹H} NMR (101 MHz, DMSO-*d*₆, 19OR11-2016): δ/ppm = 87.5 (C1), 70.7 (C3), 69.1 (C2), 69.0 (C4), 64.4 (C5), 39.4 (CH₂), 15.4 (CH₃).

N-Propyl-D-lyxosylamin (D-Lyx1NPr)



D-Lyxose (1.00 g, 6.66 mmol, 1.00 eq.) was dried and subsequently solved in 6 mL dry methanol. Propylamine (4.80 mL, 3.46 g, 58.5 mmol, 8.78 eq.) was added and the reaction mixture stirred for 48 h at room temperature. Half of the solvent was evaporated and the formed precipitate was filtered off, washed with cold methanol (2 × 10 mL) and dried *in vacuo*. The product was

obtained as a slightly rose powder in a yield of 1.17 g (6.12 mmol, 91.9 % of theory).

EA: calcd.: C 50.25 %, H 8.96 %, N 7.32 %

found: C 50.25 %, H 9.04 %, N 7.27 %

MS (FAB+): calcd.: 192.2 ([M+H]⁺)

found: 192.4

N-Propyl-β-D-lyxopyranosylamine – D₂O: 73 % – DMSO-*d*₆: 59 %

¹H NMR (400 MHz, D₂O, 22OR4-2016): δ/ppm = 4.17 (d, 1H, H1, ³J_{1,2}=1.1 Hz), 3.90 (dd, 1H, H5a, ³J_{4,5a}=5.6 Hz, ²J_{5a,5b}=-11.3 Hz), 3.86 (dd, 1H, H2, ³J_{2,3}=3.4 Hz), 3.78 (dd, 1H, H4), 3.56 (dd, 1H, H3, ³J_{3,4}=9.6 Hz), 3.18 (dd, 1H, H5b, ³J_{4,5b}=10.4 Hz), 2.83–2.71 (sp, 1H, CH₂), 2.83–2.71 (sp, 2H, CH₂), 1.55–1.41 (sp, 1H, CH₂), 0.89 (t, 3H, CH₃).

¹³C{¹H} NMR (101 MHz, D₂O, 22OR5-2016): δ/ppm = 88.2 (C1), 74.5 (C3), 71.6 (C2), 67.2 (C4), 67.0 (C5), 47.1 (NH–CH₂), 22.7 (CH₂), 11.6 (CH₃).

¹³C{¹H} NMR (101 MHz, DMSO-*d*₆, 19OR11-2016): δ/ppm = 88.1 (C1), 74.5 (C3), 70.9 (C2), 66.9 (C4), 66.2 (C5), 46.8 (NH–CH₂), 23.1 (CH₂), 11.8 (CH₃).

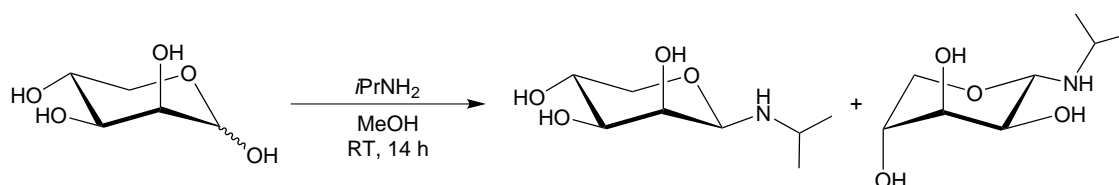
N-Propyl-α-D-lyxopyranosylamine – D₂O: 27 % – DMSO-*d*₆: 31 %

¹H NMR (400 MHz, D₂O, 22OR4-2016): δ/ppm = 4.28 (d, 1H, H1, ³J_{1,2}=6.9 Hz), 3.90–3.85 (sp, 1H, H3), 3.82–3.76 (sp, 2H, H4/H5a), 3.70 (dd, 1H, H2, ³J_{2,3}=3.1 Hz), 3.62 (dd, 1H, H5b) 2.92–2.82 (sp, 1H, CH₂), 2.83–2.71 (sp, 1H, CH₂), 2.83–2.71 (sp, 2H, CH₂), 1.55–1.41 (sp, 1H, CH₂), 0.89 (t, 3H, CH₃).

¹³C{¹H} NMR (101 MHz, D₂O, 22OR5-2016): δ/ppm = 87.9 (C1), 71.2 (C3), 69.4 (C2), 69.2 (C4), 64.7 (C5), 47.3 (NH–CH₂), 22.7 (CH₂), 11.6 (CH₃).

¹³C{¹H} NMR (101 MHz, DMSO-*d*₆, 19OR11-2016): δ/ppm = 87.7 (C1), 70.7 (C3), 69.11 (C2), 69.06 (C4), 64.4 (C5), 47.2 (NH–CH₂), 23.1 (CH₂), 11.8 (CH₃).

N-(*iso*-Propyl)-D-lyxosylamin (*D*-Lyx1NiPr)



D-Lyxose (800 mg, 5.33 mmol, 1.00 eq.) was dried and subsequently solved in 10 mL dry methanol. *iso*-Propylamine (1.37 mL, 945 mg, 16.0 mmol, 3.00 eq.) was added and the reaction mixture stirred for 14 h at room temperature. Upon evaporation of the solvent a precipitate formed, which was filtered off, washed with cold methanol (2 × 5 mL) and dried *in vacuo*. The product was obtained as a slightly yellow powder in a yield of 734 mg (3.89 mmol, 72.9 % of theory).

EA: calcd.: C 50.25 %, H 8.96 %, N 7.32 %

found: C 50.16 %, H 8.95 %, N 7.24 %

MS (FAB+): calcd.: 192.2 ([M+H]⁺)
found: 192.4

N-(*iso*-Propyl)- β -D-lyxopyranosylamine – D₂O: 77 % – DMSO-*d*₆: 62 %

¹H NMR (400 MHz, D₂O, 19OR22-2016): δ /ppm = 4.26 (d, 1H, H1, ³*J*_{1,2}=1.1 Hz), 3.87 (dd, 1H, H5a, ³*J*_{4,5a}=5.6 Hz, ²*J*_{5a,5b}=-11.2 Hz), 3.82 (dd, 1H, H2, ³*J*_{2,3}=3.4 Hz), 3.77 (dd, 1H, H4), 3.56 (dd, 1H, H3, ³*J*_{3,4}=9.6 Hz), 3.17 (dd, 1H, H5b, ³*J*_{4,5b}=11.3 Hz), 3.18–3.05 (sp, 1H, CH), 1.07–1.00 (sp, 6H, 2×CH₃).

¹³C{¹H} NMR (101 MHz, D₂O, 19OR23-2016): δ /ppm = 85.4 (C1), 74.5 (C3), 71.8 (C2), 67.2 (C4), 67.1 (C5), 43.8 (CH), 23.3 (CH₃), 20.3 (CH₃).

¹³C{¹H} NMR (101 MHz, DMSO-*d*₆, 28OR2-2015): δ /ppm = 85.3 (C1), 74.6 (C3), 70.9 (C2), 66.9 (C4), 66.4 (C5), 42.7 (CH), 24.4 (CH₃), 21.7 (CH₃).

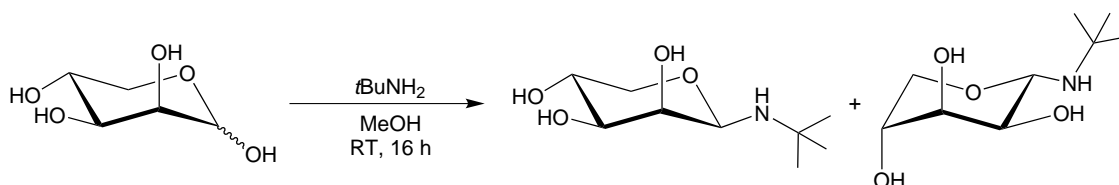
N-(*iso*-Propyl)- α -D-lyxopyranosylamine – D₂O: 23 % – DMSO-*d*₆: 38 %

¹H NMR (400 MHz, D₂O, 19OR22-2016): δ /ppm = 4.36 (d, 1H, H1, ³*J*_{1,2}=6.9 Hz), 3.90–3.85 (sp, 1H, H3), 3.82–3.76 (sp, 2H, H4/H5a), 3.70 (dd, 1H, H2, ³*J*_{2,3}=3.1 Hz), 3.62 (dd, 1H, H5b), 2.92–2.82 (sp, 1H, CH₂), 2.83–2.71 (sp, 1H, CH₂), 3.18–3.05 (sp, 1H, CH), 1.07–1.00 (sp, 6H, 2×CH₃).

¹³C{¹H} NMR (101 MHz, D₂O, 19OR23-2016): δ /ppm = 85.7 (C1), 71.1 (C3), 69.7 (C2), 69.4 (C4), 64.7 (C5), 45.0 (CH), 23.3 (CH₃), 21.1 (CH₃).

¹³C{¹H} NMR (101 MHz, DMSO-*d*₆, 28OR2-2015): δ /ppm = 85.5 (C1), 70.9 (C3), 69.24 (C2), 69.17 (C4), 64.4 (C5), 44.3 (CH), 24.4 (CH₃), 22.4 (CH₃).

N-(*tert*-Butyl)-D-lyxosylamin (*D*-Lyx1*Nt*Bu)



D-Lyxose (1.00 g, 6.66 mmol, 1.00 eq.) was dried and subsequently solved in 2 mL dry methanol. *tert*-Butylamine (1.50 mL, 1.05 g, 14.4 mmol, 2.16 eq.) was added and the reaction mixture stirred for 16 h at room temperature. The resulting yellow solution was evaporated until it reached dryness and the obtained beige powder further dried *in vacuo*. The compound showed immediate signs of hydrolysis, when exposed to air and no yield was determined.

EA: calcd.: C 52.67 %, H 9.33 %, N 6.28 %
found: C 54.09 %, H 10.00 %, N 8.28 %

N-(*tert*-Butyl)- β -D-lyxopyranosylamine – D₂O: 76 % – DMSO-*d*₆: 46 %

¹H NMR (400 MHz, D₂O, 4 °C, 17OR13-2019): δ /ppm = 4.31 (d, 1H, H1, ³*J*_{1,2}=1.1 Hz).

¹³C{¹H} NMR (101 MHz, D₂O, 4 °C, 17OR14-2019): δ /ppm = 85.3 (C1), 74.7 (C3), 71.1 (C2), 67.2 (C4), 66.6 (C5), 51.1 (C_q), 29.8 (3×CH₃).

$^{13}\text{C}\{^1\text{H}\}$ NMR (101 MHz, DMSO- d_6 , 32OR8-2015): $\delta/\text{ppm} = 84.7$ (C1), 74.6 (C3), 70.8 (C2), 66.9 (C4), 65.8 (C5), 49.6 (C_q), 30.7 ($3\times\text{CH}_3$).

N-(*tert*-Butyl)- α -D-lyxopyranosylamine – D₂O: 24 % – DMSO- d_6 : 54 % :

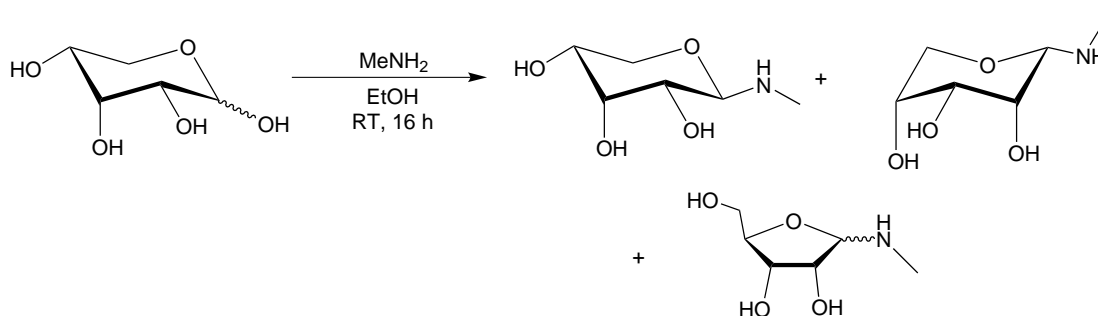
^1H NMR (400 MHz, D₂O, 4 °C, 17OR13-2019): $\delta/\text{ppm} = 4.39$ (d, 1H, H1, $^3J_{1,2}=7.6$ Hz).

$^{13}\text{C}\{^1\text{H}\}$ NMR (101 MHz, D₂O, 4 °C, 17OR14-2019): $\delta/\text{ppm} = 84.3$ (C1), 71.1 (C3), 69.8 (C2), 69.4 (C4), 64.7 (C5), 51.2 (C_q), 29.5 ($3\times\text{CH}_3$).

$^{13}\text{C}\{^1\text{H}\}$ NMR (101 MHz, DMSO- d_6 , 32OR8-2015): $\delta/\text{ppm} = 83.6$ (C1), 70.8 (C3), 69.3 (C2), 69.3 (C4), 64.3 (C5), 49.3 (C_q), 30.3 ($3\times\text{CH}_3$).

5.5.1.3. Preparation of *N*-Alkylribosylamines

N-Methyl-D-ribosylamin (D-Rib1NMe)



D-Ribose (1.00 g, 6.66 mmol, 1.00 eq.) was dried and subsequently stirred with a solution of methylamine in ethanol (33 %, 3.0 mL, 22.3 mmol, 3.35 eq.) for 16 h at room temperature. The resulting solution was evaporated until it reached dryness. The brownish syrup-like residue was frozen, crushed and further dried *in vacuo* several times to remove remnants of solvent and amine. Due to the significant hydrolysis sensitivity of the product no yield was determined.

N-Methyl- β -D-ribopyranosylamine – D₂O: 43 % (4 °C) – DMSO- d_6 : 44 %

^1H NMR (400 MHz, D₂O, 4 °C, 26OR10-2019): $\delta/\text{ppm} = 4.08$ (d, 1H, H1, $^3J_{1,2}=8.5$ Hz), 4.07 (t, 1H, H3, $^3J_{2,3}=2.8$ Hz, $^3J_{3,4}=2.8$ Hz), 3.87 (dd, 1H, H4, $^3J_{4,5eq}=4.9$ Hz, $J_{4,5ax}=11.1$ Hz), 3.73 (ddd, 1H, H5eq), 3.64 (dd, 1H, H5ax, $^2J_{5ax,5eq}=-11.1$ Hz), 3.38 (dd, 1H, H2), 2.37 (s, 3H, CH₃).

$^{13}\text{C}\{^1\text{H}\}$ NMR (101 MHz, D₂O, 4 °C, 26OR11-2019): $\delta/\text{ppm} = 88.4$ (C1), 72.2 (C2), 70.6 (C3), 67.6 (C4), 63.9 (C5), 31.4 (CH₃).

$^{13}\text{C}\{^1\text{H}\}$ NMR (101 MHz, DMSO- d_6 , 26OR2-2019): $\delta/\text{ppm} = 88.4$ (C1), 71.4 (C2), 70.6 (C3), 67.7 (C4), 63.7 (C5), 31.9 (CH₃).

N-Methyl- α -D-ribopyranosylamine – D₂O: 41 % (4 °C) – DMSO- d_6 : 32 %

^1H NMR (400 MHz, D₂O, 4 °C, 26OR10-2019): $\delta/\text{ppm} = 4.00$ (d, H1, $^3J_{1,2}=1.1$ Hz), 2.41 (s, 3H, CH₃).

$^{13}\text{C}\{^1\text{H}\}$ NMR (101 MHz, D₂O, 4 °C, 26OR11-2019): $\delta/\text{ppm} = 89.4$ (C1), 71.2 (C2), 69.3 (C3), 69.2 (C4), 63.5 (C5), 31.6 (CH₃).

$^{13}\text{C}\{^1\text{H}\}$ NMR (101 MHz, DMSO- d_6 , 26OR2-2019): $\delta/\text{ppm} = 88.8$ (C1), 70.1 (C2), 69.6 (C3),

68.6 (C4), 63.7 (C5), 32.0 (CH₃).

N-Methyl-β-D-ribofuranosylamine – D₂O: 9 % (4 °C) – DMSO-*d*₆: 17 %

¹H NMR (400 MHz, D₂O, 4 °C, 26OR10-2019): δ/ppm = 4.44 (d, H1, ³*J*_{1,2}=4.8 Hz), 2.31 (s, 3H, CH₃).

¹³C{¹H} NMR (101 MHz, D₂O, 4 °C, 26OR11-2019): δ/ppm = 95.5 (C1), 82.9 (C4), 74.5 (C3), 71.2 (C2), 62.4 (C5), 31.7 (CH₃).

¹³C{¹H} NMR (101 MHz, DMSO-*d*₆, 26OR2-2019): δ/ppm = 95.7 (C1), 82.7 (C4), 73.7 (C3), 70.8 (C2), 62.5 (C5), 31.7 (CH₃).

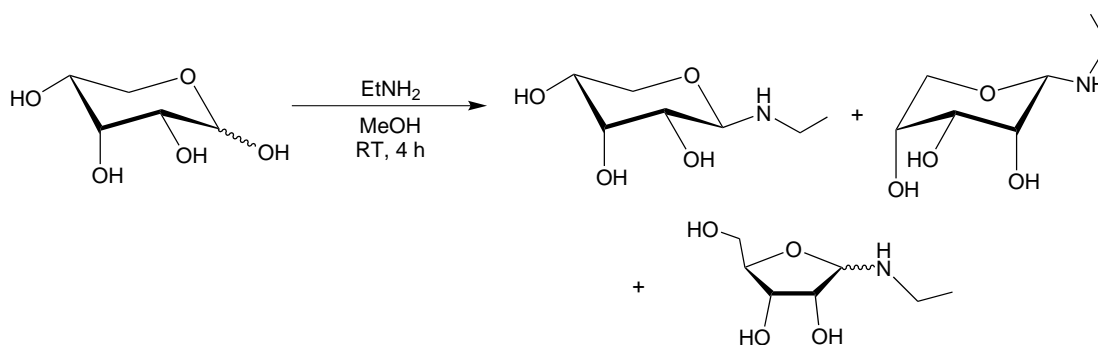
N-Methyl-α-D-ribofuranosylamine – D₂O: 7 % (4 °C) – DMSO-*d*₆: 7 %

¹H NMR (400 MHz, D₂O, 4 °C, 26OR11-2019): δ/ppm = 4.67 (d, H1, ³*J*_{1,2}=3.3 Hz), 2.40 (s, 3H, CH₃).

¹³C{¹H} NMR (101 MHz, D₂O, 4 °C, 41OR2-2017): δ/ppm = 92.5 (C1), 81.0 (C4), 72.1 (C2), 71.8 (C3), 61.8 (C5), 31.8 (CH₃).

¹³C{¹H} NMR (101 MHz, DMSO-*d*₆, 26OR2-2019): δ/ppm = 91.6 (C1), 81.3 (C4), 71.4 (C2), 71.1 (C3), 61.8 (C5), 31.7 (CH₃).

N-Ethyl-D-ribosylamin (D-Rib1NEt)



D-Ribose (1.00 g, 6.66 mmol, 1.00 eq.) was dried and subsequently stirred with a solution of ethylamine in methanol (2 M, 7.00 mL, 14.0 mmol, 2.10 eq.) for 4 h at room temperature. The resulting yellow reaction solution was concentrated by evaporation until the product was obtained as a syrup-like liquid. The brownish residue was frozen, crushed and further dried *in vacuo* several times to remove remnants of solvent and amine. Due to the significant hydrolysis sensitivity of the product no yield was determined.

N-Ethyl-β-D-ribopyranosylamine – D₂O: 62 % (4 °C) – DMSO-*d*₆: 42 %

¹H NMR (400 MHz, D₂O, 4 °C, 26OR13-2019): δ/ppm = 4.17 (d, 1H, H1, ³*J*_{1,2}=8.4 Hz), 4.07 (t, 1H, H3, ³*J*_{2,3}=3.0 Hz, ³*J*_{3,4}=3.0 Hz), 3.87 (dd, 1H, H4, ³*J*_{4,5eq}=4.9 Hz, *J*_{4,5ax}=11.1 Hz), 3.73 (ddd, 1H, H5eq), 3.66 (dd, 1H, H5ax, ²*J*_{5ax,5eq}=-11.5 Hz), 3.38 (dd, 1H, H2), 2.82 (dq, 1H, CH₂), 2.60 (dq, 1H, CH₂), 1.05 (t, 2H, CH₃).

¹³C{¹H} NMR (101 MHz, D₂O, 4 °C, 26OR14-2019): δ/ppm = 86.9 (C1), 72.5 (C2), 70.8 (C3), 67.6 (C4), 63.9 (C5), 40.0 (CH₂), 14.4 (CH₃).

$^{13}\text{C}\{^1\text{H}\}$ NMR (101 MHz, DMSO- d_6 , 26OR05-2019): δ/ppm = 87.0 (C1), 71.5 (C2), 70.8 (C3), 67.7 (C4), 63.7 (C5), 39.8 (CH₂), 15.5 (CH₃).

N-Ethyl- α -D-ribofuranosylamine – D₂O: 25 % (4 °C) – DMSO- d_6 : 35 %

^1H NMR (400 MHz, D₂O, 4 °C, 26OR13-2019): δ/ppm = 4.10 (d, H1, $^3J_{1,2}=1.0$ Hz).

$^{13}\text{C}\{^1\text{H}\}$ NMR (101 MHz, D₂O, 4 °C, 26OR14-2019): δ/ppm = 87.6 (C1), 70.9 (C2), 69.4 (C3), 69.2 (C4), 63.5 (C5), 39.5 (CH₂), 14.5 (CH₃).

$^{13}\text{C}\{^1\text{H}\}$ NMR (101 MHz, DMSO- d_6 , 26OR05-2019): δ/ppm = 87.1 (C1), 70.0 (C2), 69.6 (C3), 68.6 (C4), 63.7 (C5), 38.9 (CH₂), 15.4 (CH₃).

N-Ethyl- β -D-ribofuranosylamine – D₂O: 8 % (4 °C) – DMSO- d_6 : 16 %

^1H NMR (400 MHz, D₂O, 4 °C, 26OR13-2019): δ/ppm = 4.52 (d, H1, $^3J_{1,2}=4.6$ Hz).

$^{13}\text{C}\{^1\text{H}\}$ NMR (101 MHz, D₂O, 4 °C, 26OR14-2019): δ/ppm = 94.1 (C1), 82.9 (C4), 74.9 (C3), 71.2 (C2), 62.4 (C5), 40.3 (CH₃), 14.5 (CH₃).

$^{13}\text{C}\{^1\text{H}\}$ NMR (101 MHz, DMSO- d_6 , 26OR05-2019): δ/ppm = 94.3 (C1), 82.7 (C4), 74.1 (C3), 70.7 (C2), 62.4 (C5), 39.4 (CH₃), 15.6 (CH₃).

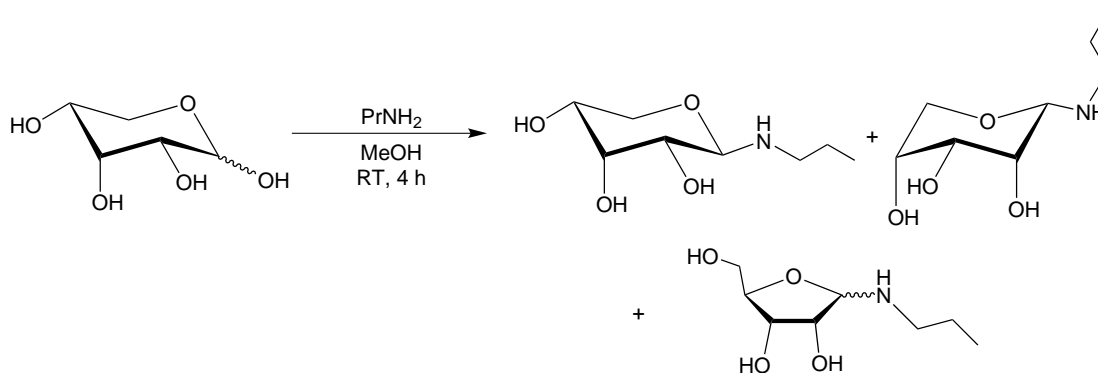
N-Ethyl- α -D-ribofuranosylamine – D₂O: 4 % (4 °C) – DMSO- d_6 : 7 %

^1H NMR (400 MHz, D₂O, 4 °C, 26OR13-2019): δ/ppm = 4.77 (d, H1, $^3J_{1,2}=3.2$ Hz).

$^{13}\text{C}\{^1\text{H}\}$ NMR (101 MHz, D₂O, 4 °C, 41OR14-2017): δ/ppm = 90.8 (C1), 80.9 (C4), 72.1 (C2), 72.0 (C3), 61.8 (C5), 40.1 (CH₃), 14.2 (CH₃).

$^{13}\text{C}\{^1\text{H}\}$ NMR (101 MHz, DMSO- d_6 , 26OR05-2019): δ/ppm = 90.0 (C1), 81.2 (C4), 71.45 (C2), 71.1 (C3), 61.8 (C5), 40.2 (CH₃), 15.4 (CH₃).

N-Propyl-D-ribosylamin (D-Rib1NPr)



D-Ribose (1.00 g, 6.66 mmol, 1.00 eq.) was dried and subsequently suspended in 2.5 mL dry methanol. Propylamine (1.50 mL, 1.08 g, 18.3 mmol, 2.74 eq.) was slowly added and the reaction mixture was stirred for 4 h at room temperature. The resulting yellowish solution was concentrated by evaporation until an orange syrup-like liquid was obtained. The residue was frozen, crushed and further dried *in vacuo* to remove all remains of the solvent and amine. Due to the immense hydrolysis sensitivity of the viscous product no yield was determined.

N-Propyl- β -D-ribofuranosylamine – D₂O: 44 % (4 °C) – DMSO-*d*₆: 40 %

¹H NMR (400 MHz, D₂O, 4 °C, 38OR16-2019): δ /ppm = 4.16 (d, 1H, H1, ³*J*_{1,2}=8.5 Hz, 4.07 (t, 1H, H3, ³*J*_{3,4}=3.0 Hz), 3.87 (dd, 1H, H4, ³*J*_{4,5eq}=4.8 Hz, *J*_{4,5ax}=11.1 Hz), 3.73 (m, 1H, H5eq), 3.66 (dd, 1H, H5ax, ²*J*_{5ax,5eq}=-11.5 Hz), 3.38 (dd, 1H, H2, ³*J*_{2,3}=3.0 Hz), 2.81 (m, 1H, NH-CH₂), 2.72 (m, 1H, NH-CH₂), 1.47 (sp, 2H, CH₂), 0.85 (t, 3H, CH₃).

¹³C{¹H} NMR (101 MHz, D₂O, 4 °C, 38OR17-2019): δ /ppm = 87.2 (C1), 72.4 (C2), 70.7 (C3), 67.6 (C4), 63.8 (C5), 47.6 (NH-CH₂), 22.8 (CH₂), 11.7 (CH₃).

¹³C{¹H} NMR (101 MHz, DMSO-*d*₆, 37OR11-2019): δ /ppm = 87.4 (C1), 71.4 (C2), 70.8 (C3), 67.7 (C4), 63.8 (C5), 47.4 (NH-CH₂), 23.2 (CH₂), 11.8 (CH₃).

N-Propyl- α -D-ribofuranosylamine – D₂O: 44 % (4 °C) – DMSO-*d*₆: 35 %

¹H NMR (400 MHz, D₂O, 4 °C, 38OR16-2019): δ /ppm = 4.08 (d, H1, ³*J*_{1,2}=0.9 Hz).

¹³C{¹H} NMR (101 MHz, D₂O, 4 °C, 38OR17-2019): δ /ppm = 87.9 (C1), 71.0 (C2), 69.4 (C3), 69.2 (C4), 63.5 (C5), 47.1 (NH-CH₂), 22.9 (CH₂), 11.7 (CH₃).

¹³C{¹H} NMR (101 MHz, DMSO-*d*₆, 37OR11-2019): δ /ppm = 87.4 (C1), 70.1 (C2), 69.7 (C3), 68.6 (C4), 63.7 (C5), 46.7 (NH-CH₂), 23.1 (CH₂), 11.7 (CH₃).

N-Propyl- β -D-ribofuranosylamine – D₂O: 8 % (4 °C) – DMSO-*d*₆: 15 %

¹H NMR (400 MHz, D₂O, 4 °C, 38OR16-2019): δ /ppm = 4.51 (d, H1, ³*J*_{1,2}=4.6 Hz).

¹³C{¹H} NMR (101 MHz, D₂O, 4 °C, 38OR17-2019): δ /ppm = 94.5 (C1), 82.8 (C4), 74.8 (C3), 71.2 (C2), 62.3 (C5), 47.8 (NH-CH₂), 22.9 (CH₂), 11.7 (CH₃).

¹³C{¹H} NMR (101 MHz, DMSO-*d*₆, 37OR11-2019): δ /ppm = 94.6 (C1), 82.7 (C4), 74.1 (C3), 70.7 (C2), 62.4 (C5), 47.6 (NH-CH₂), 23.2 (CH₂), 11.8 (CH₃).

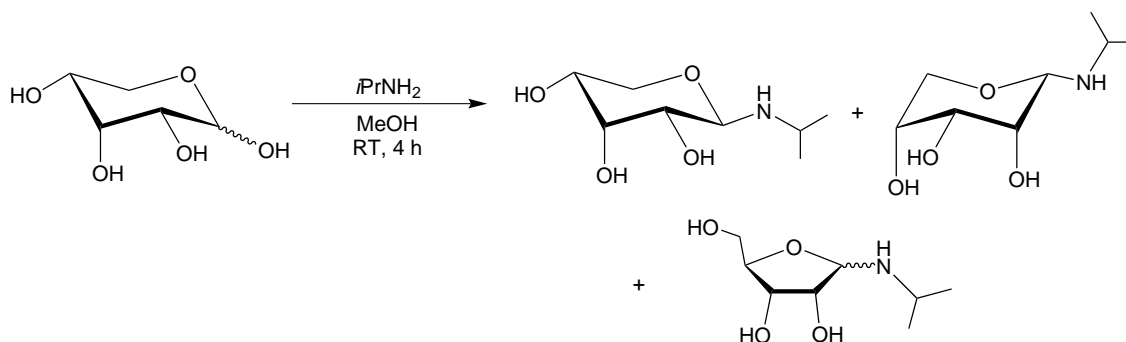
N-Propyl- α -D-ribofuranosylamine – D₂O: 4 % (4 °C) – DMSO-*d*₆: 10 %

¹H NMR (400 MHz, D₂O, 4 °C, 38OR16-2019): δ /ppm = 4.76 (d, H1, ³*J*_{1,2}=3.2 Hz).

¹³C{¹H} NMR (101 MHz, D₂O, 4 °C, 38OR17-2017): δ /ppm = 91.1 (C1), 80.9 (C4), 72.1 (C2), 72.0 (C3), 61.8 (C5), 47.6 (NH-CH₂), 22.9 (CH₂), 11.6 (CH₃).

¹³C{¹H} NMR (101 MHz, DMSO-*d*₆, 37OR11-2019): δ /ppm = 90.3 (C1), 81.3 (C4), 71.5 (C2), 71.1 (C3), 61.9 (C5), 47.2 (NH-CH₂), 23.3 (CH₂), 11.8 (CH₃).

N-(*iso*-Propyl)-D-ribosylamin (D-Rib1NiPr)



D-Ribose (1.00 g, 6.66 mmol, 1.00 eq.) was dried and subsequently suspended in 5 mL dry

methanol. *iso*-Propylamine (1.50 mL, 1.03 g, 17.5 mmol, 2.62 eq.) was slowly added and the reaction mixture was stirred for 4 h at room temperature. The resulting solution was concentrated *in vacuo* to about one third of its previous volume, leading to precipitation of a white solid. The precipitate was filtered off, washed with cold methanol (2 × 5 mL) and dried *in vacuo*. The product was obtained as an off-white powder in a yield of 877 mg (4.59 mmol, 68.9 % of theory).

EA: calcd.: C 50.25 %, H 8.96 %, N 7.32 %

found: C 49.98 %, H 9.17 %, N 7.28 %

N-(*iso*-Propyl)-β-D-ribosepyranosylamine – D₂O: 50 % (4 °C) – DMSO-*d*₆: 40 %

¹H NMR (400 MHz, D₂O, 4 °C, 26OR16-2019): δ/ppm = 4.26 (d, 1H, H1, ³*J*_{1,2}=8.4 Hz), 4.08 (t, 1H, H3, ³*J*_{2,3}=2.7 Hz, ³*J*_{3,4}=2.7 Hz), 3.87 (dd, 1H, H4, ³*J*_{4,5eq}=4.9 Hz, *J*_{4,5ax}=11.1 Hz), 3.73 (ddd, 1H, H5eq), 3.64 (dd, 1H, H5ax, ²*J*_{5ax,5eq}=−11.1 Hz), 3.34 (dd, 1H, H2), 3.09 (m, 1H, CH), 1.00 (s, 6H, 2×CH₃).

¹³C{¹H} NMR (101 MHz, D₂O, 4 °C, 26OR17-2019): δ/ppm = 85.1 (C1), 72.7 (C2), 71.0 (C3), 67.6 (C4), 63.7 (C5), 45.2 (CH), 23.8 (CH₃), 20.5 (CH₃).

¹³C{¹H} NMR (101 MHz, DMSO-*d*₆, 34OR02-2015): δ/ppm = 85.0 (C1), 71.7 (C2), 71.1 (C3), 67.7 (C4), 63.6 (C5), 44.5 (CH), 24.4 (CH₃), 22.4 (CH₃).

N-(*iso*-Propyl)-α-D-ribosepyranosylamine – D₂O: 38 % (4 °C) – DMSO-*d*₆: 36 %

¹H NMR (400 MHz, D₂O, 4 °C, 26OR16-2019): δ/ppm = 4.21 (d, H1, ³*J*_{1,2}=1.2 Hz).

¹³C{¹H} NMR (101 MHz, D₂O, 4 °C, 26OR17-2019): δ/ppm = 85.0 (C1), 71.0 (C2), 69.4 (C3), 69.2 (C4), 63.5 (C5), 44.5 (CH), 23.5 (CH₃), 20.4 (CH₃).

¹³C{¹H} NMR (101 MHz, DMSO-*d*₆, 34OR02-2015): δ/ppm = 84.7 (C1), 71.0 (C2), 69.6 (C3), 68.7 (C4), 63.6 (C5), 42.8 (CH), 24.4 (CH₃), 21.8 (CH₃).

N-(*iso*-Propyl)-β-D-ribofuranosylamine – D₂O: 8 % (4 °C) – DMSO-*d*₆: 13 %

¹H NMR (400 MHz, D₂O, 4 °C, 26OR16-2019): δ/ppm = 4.62 (d, H1, ³*J*_{1,2}=4.7 Hz).

¹³C{¹H} NMR (101 MHz, D₂O, 4 °C, 26OR17-2019): δ/ppm = 91.7 (C1), 82.9 (C4), 75.3 (C3), 71.2 (C2), 62.3 (C5), 43.6 (CH), 23.4 (CH₃), 20.2 (CH₃).

¹³C{¹H} NMR (101 MHz, DMSO-*d*₆, 34OR02-2015): δ/ppm = 92.1 (C1), 82.7 (C4), 74.7 (C3), 70.6 (C2), 62.4 (C5), 44.7 (CH), 24.4 (CH₃), 22.2 (CH₃).

N-(*iso*-Propyl)-α-D-ribofuranosylamine – D₂O: 4 % (4 °C) – DMSO-*d*₆: 9 %

¹H NMR (400 MHz, D₂O, 4 °C, 26OR16-2019): δ/ppm = 4.84 (d, H1, ³*J*_{1,2}=3.7 Hz).

¹³C{¹H} NMR (101 MHz, D₂O, 4 °C, 41OR17-2017): δ/ppm = 88.1 (C1), 80.9 (C4), 72.2 (C2), 72.1 (C3), 61.8 (C5), 45.3 (CH), 23.3 (CH₃), 21.2 (CH₃).

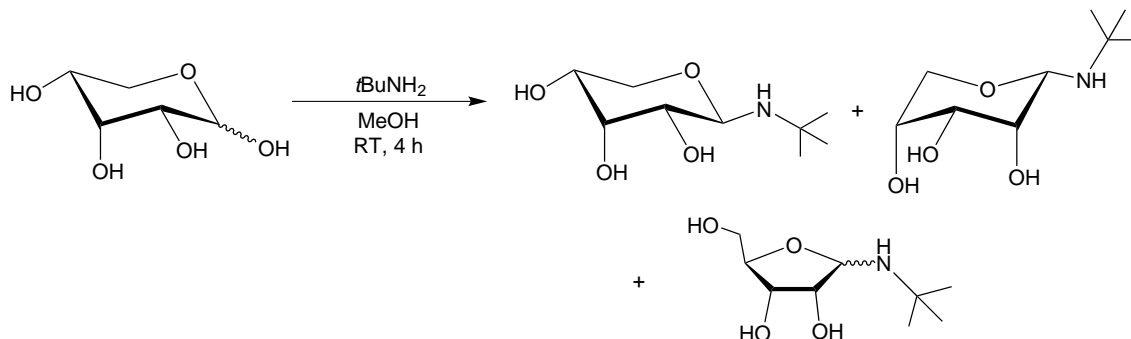
¹³C{¹H} NMR (101 MHz, DMSO-*d*₆, 34OR02-2015): δ/ppm = 87.7 (C1), 81.2 (C4), 71.7 (C2), 71.1 (C3), 61.9 (C5), 45.8 (CH), 24.6 (CH₃), 22.1 (CH₃).

N-(*iso*-Propyl)-D-ribosylamine (imine form) – D₂O: 0 % (4 °C) – DMSO-*d*₆: 2 %

¹H NMR (400 MHz, D₂O, 4 °C, 34OR1-2015): δ/ppm = 7.70 (d, H1, ³*J*_{1,2}=4.1 Hz).

$^{13}\text{C}\{^1\text{H}\}$ NMR (101 MHz, DMSO- d_6 , 34OR2-2015): $\delta/\text{ppm} = 162.8$ (C1), 74.4 (C3), 72.9 (C4), 72.0 (C3), 63.2 (C5), 59.6 (CH), 24.0 (CH₃), 22.8 (CH₃).

N-(*tert*-Butyl)-D-ribosylamin (*D*-Rib1*Nt*Bu)



D-Ribose (500 mg, 3.33 mmol, 1.00 eq.) was dried and subsequently suspended in 2 mL dry methanol. *tert*-Butylamine (1.00 mL, 700 mg, 9.57 mmol, 2.87 eq.) was slowly added and the reaction mixture was stirred for 4 h at room temperature. The resulting solution was concentrated *in vacuo* until a white, foam-like residue formed. The residue was frozen, crushed and further dried *in vacuo* to remove all remains of the solvent and amine. After repeating this procedure three times the product was obtained as an off-white powder. Due to the significant hydrolysis sensitivity of the product no yield was determined.

N-(*tert*-Butyl)- β -D-ribofuranosylamine – D₂O: 52 % (4 °C) – DMSO- d_6 : 42 %

^1H NMR (400 MHz, D₂O, 4 °C, 38OR13-2019): $\delta/\text{ppm} = 4.32$ (d, 1H, H1, $^3J_{1,2}=8.6$ Hz), 4.08 (dd, 1H, H3, $^3J_{3,4}=2.7$ Hz), 3.90–3.52 (sp, H4/H5_{ax}/H5_{eq}), 3.27 (dd, 1H, H2, $^3J_{2,3}=2.4$ Hz), 1.08 (9H, 3 \times CH₃).

$^{13}\text{C}\{^1\text{H}\}$ NMR (101 MHz, D₂O, 4 °C, 38OR14-2019): $\delta/\text{ppm} = 83.5$ (C1), 73.7 (C2), 71.1 (C3), 67.6 (C4), 63.5 (C5), 51.1 (C_q), 30.3 (3 \times CH₃).

$^{13}\text{C}\{^1\text{H}\}$ NMR (101 MHz, DMSO- d_6 , 37OR8-2019): $\delta/\text{ppm} = 83.1$ (C1), 71.6 (C2), 71.1 (C3), 67.7 (C4), 63.5 (C5), 49.5 (C_q), 30.4 (3 \times CH₃).

N-(*tert*-Butyl)- α -D-ribofuranosylamine – D₂O: 39 % (4 °C) – DMSO- d_6 : 23 %

^1H NMR (400 MHz, D₂O, 4 °C, 38OR13-2019): $\delta/\text{ppm} = 4.26$ (d, H1, $^3J_{1,2}=0.9$ Hz).

$^{13}\text{C}\{^1\text{H}\}$ NMR (101 MHz, D₂O, 4 °C, 38OR14-2019): $\delta/\text{ppm} = 85.1$ (C1), 72.4 (C2), 69.4 (C3), 69.3 (C4), 63.3 (C5), 50.9 (C_q), 29.6 (3 \times CH₃).

$^{13}\text{C}\{^1\text{H}\}$ NMR (101 MHz, DMSO- d_6 , 37OR8-2019): $\delta/\text{ppm} = 83.7$ (C1), 71.8 (C2), 69.9 (C3), 68.4 (C4), 63.5 (C5), 49.2 (C_q), 30.7 (3 \times CH₃).

N-(*tert*-Butyl)- β -D-ribofuranosylamine – D₂O: 9 % (4 °C) – DMSO- d_6 : 19 %

^1H NMR (400 MHz, D₂O, 4 °C, 38OR13-2019): $\delta/\text{ppm} = 4.69$ (d, H1, $^3J_{1,2}=5.0$ Hz).

$^{13}\text{C}\{^1\text{H}\}$ NMR (101 MHz, D₂O, 4 °C, 38OR14-2019): $\delta/\text{ppm} = 90.6$ (C1), 82.9 (C4), 76.1 (C3), 71.2 (C2), 62.4 (C5), 51.1 (C_q), 29.9 (3 \times CH₃).

$^{13}\text{C}\{^1\text{H}\}$ NMR (101 MHz, DMSO- d_6 , 37OR8-2019): $\delta/\text{ppm} = 90.6$ (C1), 82.7 (C4), 75.3 (C3),

70.4 (C2), 62.4 (C5), 49.6 (C_q), 30.4 (3×CH₃).

N-(*tert*-Butyl)- α -D-ribofuranosylamine – D₂O: 0 % (4 °C) – DMSO-*d*₆: 14 %

¹³C{¹H} NMR (101 MHz, DMSO-*d*₆, 37OR8-2019): δ /ppm = 86.2 (C1), 81.4 (C4), 71.3 (C2), 71.0 (C3), 62.0 (C5), 49.3 (C_q), 30.6 (3×CH₃).

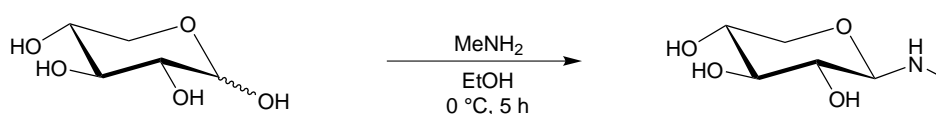
N-(*tert*-Butyl)-D-ribosylamine (imine form) – D₂O: 0 % (4 °C) – DMSO-*d*₆: 2 %

¹H NMR (400 MHz, D₂O, 4 °C, 37OR7-2019): δ /ppm = 7.69 (d, H1, ³*J*_{1,2}=3.5 Hz).

¹³C{¹H} NMR (101 MHz, DMSO-*d*₆, 37OR8-2019): δ /ppm = 159.7 (C1).

5.5.1.4. Preparation of *N*-Alkylxylosylamines

N-Methyl-D-xylosylamin (D-Xyl1NMe)



D-Xylose (1.97 g, 13.1 mmol, 1.00 eq.) was dried and subsequently stirred with a solution of methylamine in ethanol (33 %, 9.00 mL, 72.3 mmol, 5.52 eq.) for 5 h under ice cooling. The reaction mixture was concentrated by evaporation of the solvent until a colorless precipitate formed. The precipitate was filtered off, washed with cold methanol (2 × 10 mL) and dried *in vacuo*. The product was obtained as a slightly yellowish, moisture sensitive powder in a yield of 816 mg (5.00 mmol, 38.2 % of theory).

EA: calcd.: C 44.17 %, H 8.03 %, N 8.58 %

found: C 43.44 %, H 8.14 %, N 8.46 %

MS (FAB+): calcd.: 164.1 ([M+H]⁺)

found: 164.1

N-Methyl- β -D-xylopyranosylamine – D₂O: 87 % (RT), 94 % (4 °C) – DMSO-*d*₆: 72 %

¹H NMR (400 MHz, D₂O, 48OR15-2016): δ /ppm = 3.89 (dd, 1H, H5a, ²*J*_{5a,5b}=−11.4 Hz), 3.85 (d, 1H, H1, ³*J*_{1,2}=8.8 Hz), 3.57 (dd, 1H, H4, ³*J*_{4,5a}=5.4 Hz), 3.40 (t, 1H, H3, ³*J*_{3,4}=9.1 Hz), 3.26 (t, 1H, H5b, ³*J*_{4,5b}=10.6 Hz), 3.13 (t, 1H, H2, ³*J*_{2,3}=9.0 Hz), 2.40 (s, 3H, CH₃).

¹³C{¹H} NMR (101 MHz, D₂O, 4 °C, 48OR16-2016): δ /ppm = 92.2 (C1), 77.4 (C3), 73.3 (C2), 70.0 (C4), 66.7 (C5), 31.5 (CH₃).

¹³C{¹H} NMR (101 MHz, DMSO-*d*₆, 48OR19-2016): δ /ppm = 92.8 (C1), 77.4 (C3), 73.3 (C2), 70.0 (C4), 66.7 (C5), 32.0 (CH₃).

N-Methyl- α -D-xylopyranosylamine – D₂O: 11 % (RT), 6 % (4 °C) – DMSO-*d*₆: 23 %

¹H NMR (400 MHz, D₂O, 48OR15-2016): δ /ppm = 4.37 (d, H1, ³*J*_{1,2}=3.7 Hz), 2.37 (s, 3H, CH₃).

¹³C{¹H} NMR (101 MHz, D₂O, 4 °C, 48OR16-2016): δ /ppm = 87.8 (C1), 72.0 (C3), 71.1 (C2),

69.6 (C4), 63.1 (C5), 31.4 (CH₃).

¹³C{¹H} NMR (101 MHz, DMSO-*d*₆, 48OR19-2016): δ /ppm = 87.6 (C1), 71.6 (C3), 71.5 (C2), 69.5 (C4), 63.1 (C5), 32.3 (CH₃).

N-Methyl- β -D-xylofuranosylamine – D₂O: 2 % (RT), 0 % (4 °C) – DMSO-*d*₆: 3 %

¹H NMR (400 MHz, D₂O, 48OR15-2016): δ /ppm = 4.40 (d, 1H, ³*J*_{1,2}=3.0 Hz), 2.38 (s, 3H, CH₃).

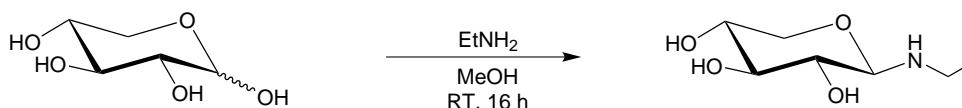
¹³C{¹H} NMR (101 MHz, D₂O, 4 °C, 48OR16-2016): δ /ppm = 96.7 (C1), 80.5 (C4), 80.2 (C2), 76.1 (C3), 61.2 (C5), 31.7 (CH₃).

¹³C{¹H} NMR (101 MHz, DMSO-*d*₆, 48OR19-2016): δ /ppm = 97.5 (C1), 80.6 (C4), 80.5 (C2), 75.6 (C3), 60.4 (C5), 32.1 (CH₃).

N-Methyl- α -D-xylofuranosylamine – D₂O: 0 % (RT), 0 % (4 °C) – DMSO-*d*₆: 2 %

¹³C{¹H} NMR (101 MHz, DMSO-*d*₆, 48OR19-2016): δ /ppm = 92.2 (C1), 79.0 (C4), 75.8 (C2/C3), 60.2 (C5), 32.8 (CH₃).

N-Ethyl-D-xylosylamin (D-Xyl1NEt)



D-Xylose (1.00 g, 6.66 mmol, 1.00 eq.) was dried and subsequently stirred with a solution of ethylamine in methanol (2 M, 20.0 mL, 40.0 mmol, 6.01 eq.) for 16 h at room temperature. The reaction mixture was concentrated by evaporation of the solvent until a colorless precipitate formed, which was filtered off, washed with cold methanol (2 × 10 mL) and dried *in vacuo*. The product was obtained as a yellowish, moisture sensitive powder in a yield of 1.02 g (5.72 mmol, 86.0 % of theory).

EA: calcd.: C 47.45 %, H 8.53 %, N 7.90 %

found: C 46.82 %, H 8.50 %, N 7.73 %

MS (FAB+): calcd.: 178.2 ([M+H]⁺)

found: 178.2

N-Ethyl- β -D-xylopyranosylamine – D₂O: 87 % (RT), 97 % (4 °C) – DMSO-*d*₆: 84 %

¹H NMR (400 MHz, D₂O, 4 °C, 33OR1-2017): δ /ppm = 3.91 (d, 1H, H1, ³*J*_{1,2}=8.8 Hz), 3.84 (dd, 1H, H5a, ³*J*_{4,5a}=5.5 Hz, ²*J*_{5a,5b}=-11.4 Hz), 3.53 (dd, 1H, H4), 3.36 (t, 1H, H3, ³*J*_{3,4}=9.1 Hz), 3.23 (t, 1H, H5b, ³*J*_{4,5b}=11.0 Hz), 3.12 (t, 1H, H2, ³*J*_{2,3}=8.9 Hz), 2.89-2.75 (m, 1H, CH₂), 2.68-2.54 (m, 1H, CH₂), 1.03 (t, 3H, CH₃).

¹³C{¹H} NMR (101 MHz, D₂O, 48OR22-2016): δ /ppm = 90.7 (C1), 77.5 (C3), 73.5 (C2), 70.1 (C4), 66.8 (C5), 39.9 (CH₂), 14.6 (CH₃).

¹³C{¹H} NMR (101 MHz, DMSO-*d*₆, 48OR25-2016): δ /ppm = 91.2 (C1), 77.2 (C3), 73.3 (C2), 69.9 (C4), 66.5 (C5), 39.4 (CH₂), 15.3 (CH₃).

N-Ethyl- α -D-xylopyranosylamine – D₂O: 11 % (RT), 3 % (4 °C) – DMSO-*d*₆: 12 %

¹H NMR (400 MHz, D₂O, 4 °C, 33OR1-2017): δ /ppm = 4.45 (d, H1, ³*J*_{1,2}=3.5 Hz).

¹³C{¹H} NMR (101 MHz, D₂O, 48OR22-2016): δ /ppm = 85.9 (C1), 71.6 (C3), 71.1 (C2), 69.4 (C4), 63.1 (C5), 39.8 (CH₂), 14.3 (CH₃).

¹³C{¹H} NMR (101 MHz, DMSO-*d*₆, 48OR25-2016): δ /ppm = 85.6 (C1), 71.3 (C2/C3), 69.3 (C4), 63.1 (C5), 39.9 (CH₂), 15.3 (CH₃).

N-Ethyl- β -D-xylofuranosylamine – D₂O: 2 % (RT), 0 % (4 °C) – DMSO-*d*₆: <2 %

¹H NMR (400 MHz, D₂O, 48OR21-2016): δ /ppm = 4.46 (d, H1, ³*J*_{1,2}=2.9 Hz).

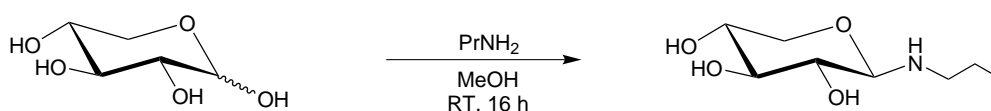
¹³C{¹H} NMR (101 MHz, D₂O, 48OR22-2016): δ /ppm = 95.2 (C1), 80.7 (C4), 80.6 (C2), 76.1 (C3), 61.1 (C5), 40.1 (CH₂), 14.4 (CH₃).

¹³C{¹H} NMR (101 MHz, DMSO-*d*₆, 48OR25-2016): δ /ppm = 95.7 (C1), 80.6 (C4), 80.4 (C2), 75.7 (C3), 60.3 (C5), 15.5 (CH₃).

N-Ethyl- α -D-xylofuranosylamine – D₂O: 0 % (RT), 0 % (4 °C) – DMSO-*d*₆: <2 %

¹³C{¹H} NMR (101 MHz, DMSO-*d*₆, 48OR25-2016): δ /ppm = 90.3 (C1), 78.9 (C4), 75.4 (C2/C3), 60.1 (C5), 15.2 (CH₃).

N-Propyl-D-xylosylamin (D-Xyl1NPr)



D-Xylose (1.00 g, 6.66 mmol, 1.00 eq.) was dried and subsequently solved in 20.0 mL dry methanol. Propylamine (4.00 mL, 2.88 g, 48.7 mmol, 7.32 eq.) was added and the reaction mixture stirred for 16 h at room temperature. The resulting solution was evaporated until it reached dryness and the obtained colorless solid further dried *in vacuo*. Due to the high hygroscopy of the compound no yield was determined.

EA: calcd.: C 50.25 %, H 8.96 %, N 7.32 %

found: C 50.18 %, H 8.96 %, N 7.59 %

MS (FAB+): calcd.: 192.2 ([M+H]⁺)

found: 192.2

N-Propyl- β -D-xylopyranosylamine – D₂O: 90 % (RT), 98 % (4 °C) – DMSO-*d*₆: 85 %

¹H NMR (400 MHz, D₂O, 11OR27-2016): δ /ppm = 3.93 (d, 1H, H1, ³*J*_{1,2}=8.8 Hz), 3.87 (dd, 1H, H5a, ³*J*_{4,5a}=5.5 Hz, ²*J*_{5a,5b}=-11.4 Hz), 3.56 (dd, 1H, H4), 3.39 (t, 1H, H3, ³*J*_{3,4}=9.1 Hz), 3.25 (dd, 1H, H5b, ³*J*_{4,5b}=11.0 Hz), 3.17 (t, 1H, H2, ³*J*_{2,3}=8.9 Hz), 2.65–2.51 (sp, 2H, NH–CH₂) 1.63–1.30 (sp, 2H, CH₂), 0.87 (t, 3H, CH₃).

¹³C{¹H} NMR (101 MHz, D₂O, 11OR28-2016): δ /ppm = 91.1 (C1), 77.4 (C3), 73.5 (C2), 70.1 (C4), 66.8 (C5), 47.5 (NH–CH₂), 22.9 (CH₂), 11.6 (CH₃).

¹³C{¹H} NMR (101 MHz, DMSO-*d*₆, 11OR31-2016): δ /ppm = 91.6 (C1), 77.3 (C3), 73.4 (C2),

70.0 (C4), 66.6 (C5), 47.5 (NH-CH₂), 23.1 (CH₂), 11.8 (CH₃).

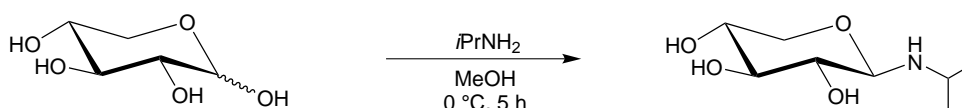
N-Propyl- α -D-xylopyranosylamine – D₂O: 10 % (RT), 2 % (4 °C) – DMSO-*d*₆: 15 %

¹H NMR (400 MHz, D₂O, 11OR27-2016): δ /ppm = 4.46 (d, H1, ³*J*_{1,2}=3.4 Hz).

¹³C{¹H} NMR (101 MHz, D₂O, 11OR28-2016): δ /ppm = 86.2 (C1), 71.7 (C3), 71.2 (C2), 69.5 (C4), 63.6 (C5), 47.4 (NH-CH₂), 22.6 (CH₂), 11.7 (CH₃).

¹³C{¹H} NMR (101 MHz, DMSO-*d*₆, 11OR31-2016): δ /ppm = 86.1 (C1), 71.4 (C3), 71.4 (C2), 69.4 (C4), 63.1 (C5), 47.8 (NH-CH₂), 23.0 (CH₂), 11.8 (CH₃).

N-(*iso*-Propyl)-D-xylosylamin (D-Xyl1NiPr)



D-Xylose (1.00 g, 6.66 mmol, 1.00 eq.) was dried and subsequently solved in 4.0 mL dry methanol. *iso*-Propylamine (4.00 mL, 2.75 g, 46.6 mmol, 6.99 eq.) was added and the reaction mixture stirred for 5 h under ice cooling. The resulting solution was evaporated until it reached dryness. Upon further drying *in vacuo* a highly viscous sirup, which showed significant signs of hydrolysis, was obtained in a yield of 753 mg (5.73 mmol, 57.7 % of theory).

EA: calcd.: C 50.25 %, H 8.96 %, N 7.32 %

found: C 50.45 %, H 9.34 %, N 8.44 %

N-(*iso*-Propyl)- β -D-xylopyranosylamine – D₂O: 94 % (RT), 94 % (4 °C) – DMSO-*d*₆: 88 %

¹H NMR (400 MHz, D₂O, 4 °C, 32OR4-2017): δ /ppm = 4.00 (d, 1H, H1, ³*J*_{1,2}=8.7 Hz), 3.83 (dd, 1H, H5a, ³*J*_{4,5a}=5.3 Hz, ²*J*_{5a,5b}=-11.3 Hz), 3.57–3.50 (m, 1H, H4), 3.37 (t, 1H, H3, ³*J*_{3,4}=9.1 Hz), 3.24 (t, 1H, H5b, ³*J*_{4,5b}=11.0 Hz), 3.11–3.03 (sp, 2H, H2/CH), 1.07–0.96 (sp, 6H, 2×CH₃).

¹³C{¹H} NMR (101 MHz, D₂O, 4 °C, 32OR5-2017): δ /ppm = 89.0 (C1), 77.6 (C3), 73.9 (C2), 70.1 (C4), 66.8 (C5), 45.5 (CH), 23.3 (CH₃), 21.3 (CH₃).

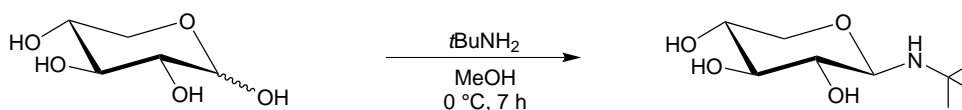
¹³C{¹H} NMR (101 MHz, DMSO-*d*₆, 10OR48-2016): δ /ppm = 89.5 (C1), 77.3 (C3), 73.6 (C2), 70.0 (C4), 66.5 (C5), 44.6 (CH), 24.4 (CH₃), 22.4 (CH₃).

N-(*iso*-Propyl)- α -D-xylopyranosylamine – D₂O: 6 % (RT), 6 % (4 °C) – DMSO-*d*₆: 12 %

¹H NMR (400 MHz, D₂O, 4 °C, 32OR4-2017): δ /ppm = 4.52 (d, H1, ³*J*_{1,2}=2.8 Hz).

¹³C{¹H} NMR (101 MHz, D₂O, 4 °C, 32OR5-2017): δ /ppm = 83.4 (C1), 71.2 (C3), 71.0 (C2), 69.2 (C4), 64.7 (C5), 44.5 (CH), 23.3 (CH₃), 20.6 (CH₃).

¹³C{¹H} NMR (101 MHz, DMSO-*d*₆, 10OR48-2016): δ /ppm = 83.7 (C1), 71.4 (C3), 71.2 (C2), 69.4 (C4), 63.3 (C5), 44.4 (CH), 24.4 (CH₃), 22.2 (CH₃).

***N*-(*tert*-Butyl)-D-xylosylamin (D-Xyl1N*t*Bu)**

D-Xylose (1.00 g, 6.66 mmol, 1.00 eq.) was dried and subsequently solved in 11.5 mL dry methanol. *tert*-Butylamine (3.50 mL, 2.45 g, 33.5 mmol, 5.03 eq.) was added and the reaction mixture stirred for 7 h under ice cooling. The resulting suspension was filtered and the filtrate evaporated until it reached dryness. Upon further drying *in vacuo* a highly viscous sirup, which showed significant signs of hydrolysis, was obtained in a yield of 326 mg (1.59 mmol, 23.8 % of theory).

EA: calcd.: C 52.67 %, H 9.33 %, N 6.82 %

found: C 53.16 %, H 10.04 %, N 8.02 %

N-(*tert*-Butyl)- β -D-xylopyranosylamine – D₂O: >98 % (RT, 4 °C) – DMSO-*d*₆: 67 %

¹H NMR (400 MHz, D₂O, 4 °C, 32OR7-2017): δ /ppm = 4.06 (d, 1H, H1, ³*J*_{1,2}=8.7 Hz), 3.78 (dd, 1H, H5a, ³*J*_{4,5a}=5.4 Hz, ²*J*_{5a,5b}=-11.4 Hz), 3.52 (m, 1H, H4), 3.38 (t, 1H, H3, ³*J*_{3,4}=9.1 Hz), 3.24 (t, 1H, H5b, ³*J*_{4,5b}=11.0 Hz), 3.03 (t, 1H, H2, ³*J*_{2,3}=8.9 Hz), 1.08 (s, 9H, 3×CH₃).

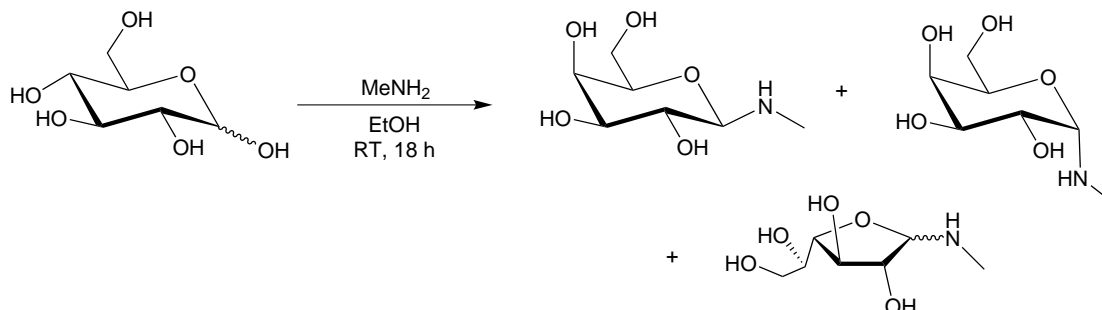
¹³C{¹H} NMR (101 MHz, D₂O, 4 °C, 32OR8-2017): δ /ppm = 87.5 (C1), 77.5 (C3), 73.8 (C2), 70.3 (C4), 66.2 (C5), 51.1 (C_q), 29.5 (3×CH₃).

¹³C{¹H} NMR (101 MHz, DMSO-*d*₆, 10OR53-2016): δ /ppm = 87.7 (C1), 77.3 (C3), 73.5 (C2), 70.0 (C4), 66.4 (C5), 49.6 (C_q), 30.3 (3×CH₃).

N-(*tert*-Butyl)- α -D-xylopyranosylamine – D₂O: <2 % (RT, 4 °C) – DMSO-*d*₆: 33 %

¹H NMR (400 MHz, D₂O, 4 °C, 32OR7-2017): δ /ppm = 4.68 (d, H1, ³*J*_{1,2}=3.7 Hz).

¹³C{¹H} NMR (101 MHz, DMSO-*d*₆, 10OR53-2016): δ /ppm = 82.0 (C1), 72.1 (C3), 71.6 (C2), 69.7 (C4), 62.1 (C5), 49.4 (C_q), 30.1 (3×CH₃).

5.5.2. Preparation of *N*-Alkylhexosylamines**5.5.2.1. Preparation of *N*-Alkylgalactosylamines*****N*-Methyl-D-galactosylamin (D-Gal1NMe)**

D-Galactose (2.00 g, 11.1 mmol, 1.00 eq.) was dried and suspended in a solution of methylamine in ethanol (33 %, 12.0 mL, 89.2 mmol, 8.04 eq.). In order to obtain a clear solution 20.0 mL methanol

were added and the reaction mixture was stirred for 18 h at room temperature. The during the reaction formed white precipitate was filtered off, washed with cold methanol (2×10 mL) and dried *in vacuo*. The product was obtained as a white powder in a yield of 1.25 g (6.50 mmol, 58.5 % of theory).

EA: calcd.: C 43.52 %, H 7.83 %, N 7.25 %
found: C 43.26 %, H 7.86 %, N 7.23 %

MS (FAB+): calcd.: 194.1 ([M+H]⁺)
found: 194.3

N-Methyl- β -D-galactopyranosylamine – D₂O: 90 % – DMSO-*d*₆: 52 %

¹H NMR (400 MHz, D₂O, 37OR1-2016): δ /ppm = 3.88 (dd, 1H, H4, ³*J*_{3,4}=3.5 Hz, ³*J*_{4,5}=1.0 Hz), 3.82 (d, 1H, H1, ³*J*_{1,2}=8.5 Hz), 3.70 (m, 2H, H6/H6'), 3.60 (dd, 1H, H5), 3.57 (dd, 1H, H3), 3.39 (dd, 1H, H2, ³*J*_{2,3}=9.7 Hz), 2.41 (s, 3H, CH₃).

¹³C{¹H} NMR (101 MHz, D₂O, 37OR2-2016): δ /ppm = 91.8 (C1), 76.5 (C5), 74.3 (C3), 71.0 (C2), 69.7 (C4), 61.8 (C6), 31.5 (CH₃).

¹³C{¹H} NMR (101 MHz, DMSO-*d*₆, 37OR11-2016): δ /ppm = 92.4 (C1), 75.8 (C5), 74.2 (C3), 70.6 (C2), 68.5 (C4), 60.6 (C6), 32.0 (CH₃).

N-Methyl- α -D-galactopyranosylamine – D₂O: 6 % – DMSO-*d*₆: 11 %

¹H NMR (400 MHz, D₂O, 37OR1-2016): δ /ppm = 4.49 (d, H1, ³*J*_{1,2}=5.3 Hz).

¹³C{¹H} NMR (101 MHz, D₂O, 37OR2-2016): δ /ppm = 88.4 (C1), 69.9 (C5), 69.7 (C4), 69.4 (C3), 68.3 (C4), 61.6 (C6), 31.0 (CH₃).

¹³C{¹H} NMR (101 MHz, DMSO-*d*₆, 37OR11-2016): δ /ppm = 88.5 (C1), 70.0 (C5), 69.6 (C4), 68.9 (C3), 68.3 (C2), 60.7 (C6), 32.6 (CH₃).

N-Methyl- β -D-galactofuranosylamine – D₂O: 4 % – DMSO-*d*₆: 21 %

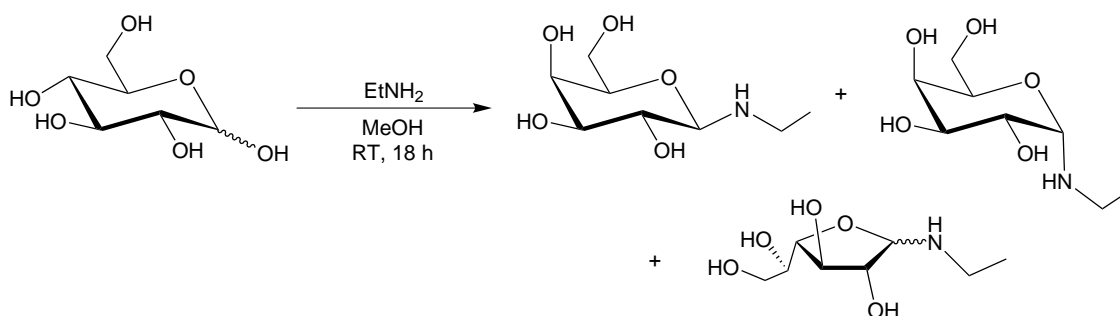
¹H NMR (400 MHz, D₂O, 37OR1-2016): δ /ppm = 4.42 (d, 1H, H1, ³*J*_{1,2}=5.7 Hz).

¹³C{¹H} NMR (101 MHz, D₂O, 37OR2-2016): δ /ppm = 94.9 (C1), 80.9 (C4), 79.5 (C2), 76.3 (C3), 71.6 (C5), 63.4 (C6), 31.5 (CH₃).

¹³C{¹H} NMR (101 MHz, DMSO-*d*₆, 37OR11-2016): δ /ppm = 95.8 (C1), 80.9 (C4), 79.6 (C2), 76.6 (C3), 71.1 (C5), 62.8 (C6), 31.3 (CH₃).

N-Methyl- α -D-galactofuranosylamine – D₂O: 0 % – DMSO-*d*₆: 16 %

¹³C{¹H} NMR (101 MHz, DMSO-*d*₆, 37OR11-2016): δ /ppm = 91.9 (C1), 82.4 (C4), 76.7 (C2), 76.3 (C3), 70.8 (C5), 62.7 (C5), 32.7 (CH₃).

N-Ethyl-D-galactosylamin (D-Gal1NEt)

D-Galactose (1.00 g, 5.55 mmol, 1.00 eq.) was dried and subsequently stirred for 18 h at room temperature with a solution of ethylamine in methanol (2 M, 22.2 mL, 44.4 mmol, 4.00 eq.). During the reaction 10 mL methanol were added. The resulting colorless precipitate was filtered off, washed with cold methanol (2 × 10 mL) and dried *in vacuo*. The product was obtained as a white powder in a yield of 553 mg (2.67 mmol, 24.0 % of theory).

EA: calcd.: C 46.37 %, H 8.27 %, N 6.79 %
found: C 46.01 %, H 8.29 %, N 6.73 %

MS (FAB+): calcd.: 208.2 ([M+H]⁺)
found: 208.4

N-Ethyl-β-D-galactopyranosylamine – D₂O: 92 % – DMSO-*d*₆: 44 %

¹H NMR (400 MHz, D₂O, 11OR19-2016): δ/ppm = 3.90 (d, 1H, H1, ³J_{1,2}=8.8 Hz), 3.88 (dd, 1H, H4, ³J_{3,4}=3.6 Hz, ³J_{4,5}=1.0 Hz), 3.70 (m, 2H, H6/H6'), 3.59 (dd, 1H, H5), 3.57 (dd, 1H, H3), 3.39 (dd, 1H, H2, ³J_{2,3}=9.7 Hz), 2.89 (dq, 1H, CH₂), 2.68–2.62 (sp, 1H, CH₂), 1.04 (t, 3H, CH₃).

¹³C{¹H} NMR (101 MHz, D₂O, 37OR5-2016): δ/ppm = 90.4 (C1), 76.5 (C5), 74.3 (C3), 71.2 (C2), 69.6 (C4), 61.8 (C6), 39.9 (CH₂), 14.5 (CH₃).

¹³C{¹H} NMR (101 MHz, DMSO-*d*₆, 37OR13-2016): δ/ppm = 91.1 (C1), 75.8 (C5), 74.2 (C3), 70.8 (C2), 68.5 (C4), 60.6 (C6), 39.5 (CH₂), 15.3 (CH₃).

N-Ethyl-α-D-galactopyranosylamine – D₂O: 4 % – DMSO-*d*₆: 14 %

¹H NMR (400 MHz, D₂O, 11OR19-2016): δ/ppm = 4.62 (d, H1, ³J_{1,2}=5.3 Hz).

¹³C{¹H} NMR (101 MHz, D₂O, 37OR5-2016): δ/ppm = 86.9 (C1), 70.4 (C5), 69.6 (C4), 69.4 (C3), 68.3 (C4), 61.6 (C6), 39.6 (CH₂), 14.2 (CH₃).

¹³C{¹H} NMR (101 MHz, DMSO-*d*₆, 37OR13-2016): δ/ppm = 87.1 (C1), 70.0 (C5), 69.8 (C4), 68.9 (C3), 68.2 (C2), 60.6 (C6), 40.1 (CH₂), 15.3 (CH₃).

N-Ethyl-β-D-galactofuranosylamine – D₂O: 4 % – DMSO-*d*₆: 21 %

¹H NMR (400 MHz, D₂O, 11OR19-2016): δ/ppm = 4.49 (d, 1H, H1, ³J_{1,2}=5.6 Hz).

¹³C{¹H} NMR (101 MHz, D₂O, 37OR5-2016): δ/ppm = 93.6 (C1), 80.9 (C4), 80.1 (C2), 76.4 (C3), 71.6 (C5), 63.4 (C6), 40.1 (CH₂), 14.5 (CH₃).

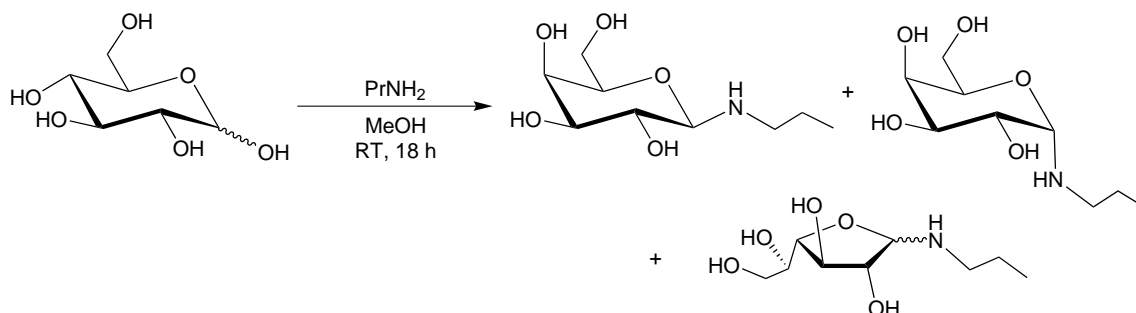
¹³C{¹H} NMR (101 MHz, DMSO-*d*₆, 37OR13-2016): δ/ppm = 94.5 (C1), 80.8 (C4), 80.1 (C2),

76.5 (C3), 71.1 (C5), 62.8 (C6), 39.0 (CH₂), 15.3 (CH₃).

N-Ethyl- α -D-galactofuranosylamine – D₂O: 0 % – DMSO-*d*₆: 21 %

¹³C{¹H} NMR (101 MHz, DMSO-*d*₆, 37OR13-2016): δ /ppm = 90.0 (C1), 82.4 (C4), 76.7 (C2), 76.3 (C3), 70.8 (C5), 62.7 (C6), 40.1 (CH₂), 15.1 (CH₃).

N-Propyl-D-galactosylamin (β -Gal1NPr)



D-Galactose (2.00 g, 11.1 mmol, 1.00 eq.) was dried and subsequently solved in 26.5 mL dry methanol. Propylamine (5.47 mL, 3.94 g, 66.6 mmol, 6.00 eq.) was added and the reaction mixture stirred for 18 h at room temperature. The reaction solution was concentrated by evaporation until a white precipitate formed. The solid was filtered off, washed with cold methanol (2 \times 10 mL) and dried *in vacuo*. The product was obtained as a yellowish powder in a yield of 1.12 g (5.07 mmol, 91.4 % of theory).

EA: calcd.: C 48.86 %, H 8.66 %, N 6.33 %

found: C 48.66 %, H 8.68 %, N 6.34 %

MS (FAB+): calcd.: 222.3 ([M+H]⁺)

found: 222.4

N-Propyl- β -D-galactopyranosylamine – D₂O: 90 % – DMSO-*d*₆: 49 %

¹H NMR (400 MHz, D₂O, 37OR7-2016): δ /ppm = 3.90 (d, 1H, H1, ³J_{1,2}=8.8 Hz), 3.87 (dd, 1H, H4, ³J_{3,4}=3.5 Hz, ³J_{4,5}=1.0 Hz), 3.69 (m, 2H, H6/H6'), 3.59 (dd, 1H, H5), 3.57 (dd, 1H, H3), 3.39 (dd, 1H, H2, ³J_{2,3}=9.7 Hz), 2.80 (m, 1H, NH-CH₂), 2.62–2.54 (sp, 1H, NH-CH₂), 1.53–1.37 (sp, 2H, CH₂), 0.86 (t, 3H, CH₃).

¹³C{¹H} NMR (101 MHz, D₂O, 37OR8-2016): δ /ppm = 90.7 (C1), 76.5 (C5), 74.3 (C3), 71.2 (C2), 69.6 (C4), 61.7 (C6), 47.5 (NH-CH₂), 22.9 (CH₂), 11.6 (CH₃).

¹³C{¹H} NMR (101 MHz, DMSO-*d*₆, 37OR15-2016): δ /ppm = 91.4 (C1), 75.8 (C5), 74.1 (C3), 70.8 (C2), 68.5 (C4), 60.6 (C6), 47.5 (NH-CH₂), 23.2 (CH₂), 11.7 (CH₃).

N-Propyl- α -D-galactopyranosylamine – D₂O: 5 % – DMSO-*d*₆: 11 %

¹H NMR (400 MHz, D₂O, 37OR7-2016): δ /ppm = 4.61 (d, H1, ³J_{1,2}=5.3 Hz).

¹³C{¹H} NMR (101 MHz, D₂O, 37OR8-2016): δ /ppm = 87.1 (C1), 70.3 (C5), 69.8 (C4), 69.4 (C3), 68.3 (C4), 61.6 (C6), 47.1 (NH-CH₂), 22.5 (CH₂), 11.7 (CH₃).

$^{13}\text{C}\{^1\text{H}\}$ NMR (101 MHz, DMSO- d_6 , 37OR15-2016): δ/ppm = 87.1 (C1), 70.0 (C5), 69.5 (C4), 68.8 (C3), 68.2 (C2), 60.6 (C6), 48.0 (NH-CH₂), 22.8 (CH₂), 11.7 (CH₃).

N-Propyl- β -D-galactofuranosylamine – D₂O: 5 % – DMSO- d_6 : 21 %

^1H NMR (400 MHz, D₂O, 37OR7-2016): δ/ppm = 4.49 (d, 1H, H1, $^3J_{1,2}=5.5$ Hz).

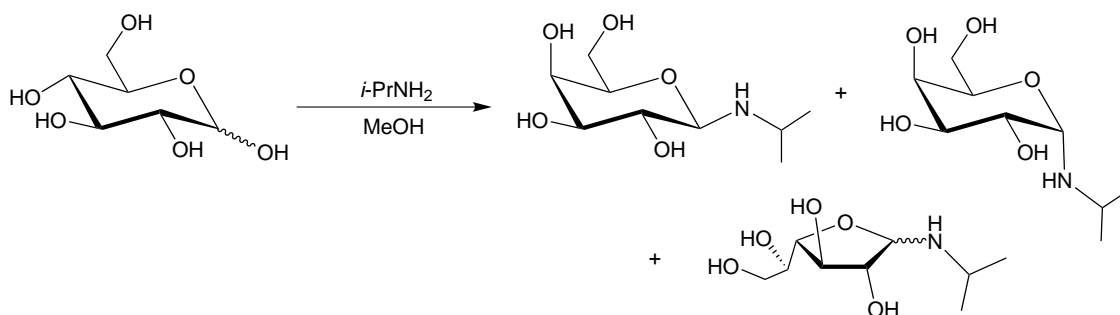
$^{13}\text{C}\{^1\text{H}\}$ NMR (101 MHz, D₂O, 37OR8-2016): δ/ppm = 94.0 (C1), 80.9 (C4), 79.9 (C2), 76.4 (C3), 71.6 (C5), 63.4 (C6), 47.8 (NH-CH₂), 22.9 (CH₂), 11.6 (CH₃).

$^{13}\text{C}\{^1\text{H}\}$ NMR (101 MHz, DMSO- d_6 , 37OR15-2016): δ/ppm = 94.8 (C1), 81.0 (C4), 80.0 (C2), 76.5 (C3), 71.1 (C5), 62.8 (C6), 47.0 (NH-CH₂), 23.2 (CH₂), 11.8 (CH₃).

N-Propyl- α -D-galactofuranosylamine – D₂O: 0 % – DMSO- d_6 : 19 %

$^{13}\text{C}\{^1\text{H}\}$ NMR (101 MHz, DMSO- d_6 , 37OR15-2016): δ/ppm = 90.5 (C1), 82.4 (C4), 76.7 (C2), 76.4 (C3), 70.9 (C5), 62.7 (C6), 48.1 (NH-CH₂), 22.9 (CH₂), 11.7 (CH₃).

N-(*iso*-Propyl)-D-galactosylamin (D-Gal1NiPr)



D-Galactose (501 mg, 2.78 mmol, 1.00 eq.) was dried and subsequently suspended in 16.5 mL dry methanol. *iso*-Propylamine (1.50 mL, 1.03 g, 17.5 mmol, 6.28 eq.) was added and the reaction mixture stirred for 16 h. The resulting solution was concentrated by evaporation until it reached dryness. Upon further drying *in vacuo* the product was obtained as a yellowish powder in a yield of 547 mg (5.47 mmol, 88.9 % of theory).

EA: calcd.: C 48.86 %, H 8.66 %, N 6.33 %

found: C 47.28 %, H 8.88 %, N 6.27 %

MS (FAB+): calcd.: 222.3 ([M+H]⁺)

found: 222.4

N-(*iso*-Propyl)- β -D-galactopyranosylamine – D₂O: >98 % – DMSO- d_6 : 45 %

^1H NMR (400 MHz, D₂O, 18OR16-2016): δ/ppm = 3.97 (d, 1H, H1, $^3J_{1,2}=8.7$ Hz), 3.87 (dd, 1H, H4, $^3J_{3,4}=3.8$ Hz, $^3J_{4,5}=1.0$ Hz), 3.74 – 3.63 (sp, 3H, H5/H6/H6'), 3.59 (dd, 1H, H3, $^3J_{2,3}=9.9$ Hz), 3.42 (dd, 1H, H2), 3.15 (m, 1H, CH), 1.05–1.00 (sp, 6H, 2×CH₃).

$^{13}\text{C}\{^1\text{H}\}$ NMR (101 MHz, D₂O, 18OR17-2016): δ/ppm = 88.6 (C1), 76.4 (C5), 74.5 (C3), 71.6 (C2), 69.6 (C4), 61.8 (C6), 45.5 (CH), 23.2 (CH₃), 21.4 (CH₃).

$^{13}\text{C}\{^1\text{H}\}$ NMR (101 MHz, DMSO- d_6 , 37OR17-2016): δ/ppm = 89.2 (C1), 75.8 (C5), 74.1 (C3),

71.1 (C2), 68.4 (C4), 60.5 (C6), 44.6 (CH), 24.4 (CH₃), 22.5 (CH₃).

N-(*iso*-Propyl)- α -D-galactopyranosylamine – D₂O: 0 % – DMSO-*d*₆: 11 %

¹³C{¹H} NMR (101 MHz, DMSO-*d*₆, 37OR17-2016): δ /ppm = 85.5 (C1), 70.0 (C5), 69.4 (C4), 68.7 (C3), 68.0 (C2), 60.4 (C6), 46.3 (CH), 24.3 (CH₃), 22.7 (CH₃).

N-(*iso*-Propyl)- β -D-galactofuranosylamine – D₂O: <2 % – DMSO-*d*₆: 21 %

¹H NMR (400 MHz, D₂O, 18OR16-2016): δ /ppm = 4.58 (d, 1H, H1, ³J_{1,2}=5.3 Hz).

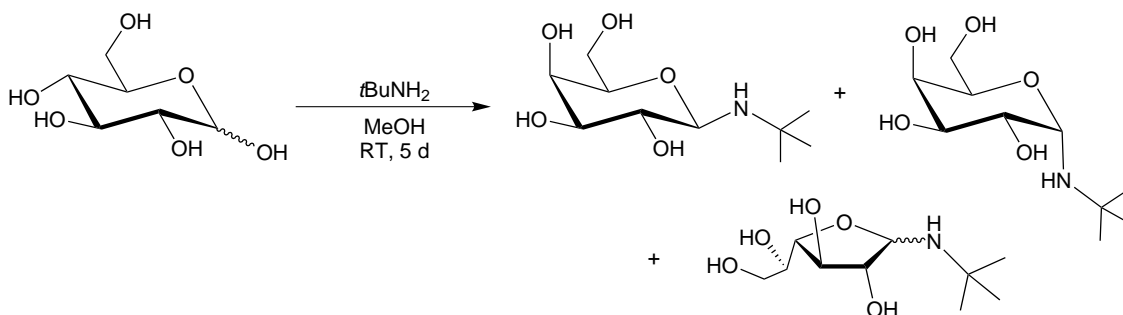
¹³C{¹H} NMR (101 MHz, D₂O, 18OR17-2016): δ /ppm = 91.6 (C1), 80.9 (C4), 80.7 (C2), 76.5 (C3), 70.3 (C5), 63.4 (C6), 46.0 (CH), 23.3 (CH₃), 20.9 (CH₃).

¹³C{¹H} NMR (101 MHz, DMSO-*d*₆, 37OR17-2016): δ /ppm = 92.7 (C1), 81.1 (C4), 80.5 (C2), 76.6 (C3), 71.2 (C5), 62.7 (C6), 44.0 (CH), 24.5 (CH₃), 22.4 (CH₃).

N-(*iso*-Propyl)- α -D-galactofuranosylamine – D₂O: 0 % – DMSO-*d*₆: 23 %

¹³C{¹H} NMR (101 MHz, DMSO-*d*₆, 37OR17-2016): δ /ppm = 88.3 (C1), 82.3 (C4), 76.6 (C2), 76.4 (C3), 70.8 (C5), 62.7 (C6), 45.6 (CH), 23.9 (CH₃), 22.4 (CH₃).

N-(*tert*-Butyl)-D-galactosylamin (D-Gal1N*t*Bu)



D-Galactose (600 mg, 3.33 mmol, 1.00 eq.) was dried and subsequently suspended in 40 mL dry methanol. *tert*-Butylamine (1.00 mL, 700 mg, 9.57 mmol, 2.87 eq.) was added and the reaction mixture stirred for 5 d. The resulting yellowish solution was concentrated by evaporation until it reached dryness. The foam-like residue was frozen, crushed and further dried *in vacuo*. The product was obtained as a hygroscopic, off-white powder in a yield of 679 mg (2.89 mmol, 86.7 % of theory).

N-(*tert*-Butyl)- β -D-galactopyranosylamine – D₂O: 100 % (4 °C) – DMSO-*d*₆: 40 %

¹H NMR (400 MHz, D₂O, 4 °C, 38OR18-2019): δ /ppm = 4.03 (d, 1H, H1, ³J_{1,2}=8.8 Hz), 1.13 (s, 9H, 3×CH₃).

¹³C{¹H} NMR (101 MHz, D₂O, 4 °C, 38OR19-2019): δ /ppm = 87.1 (C1), 76.1 (C5), 74.4 (C3), 71.4 (C2), 69.8 (C4), 61.9 (C6), 51.1 (C_q), 30.4 (3×CH₃).

¹³C{¹H} NMR (101 MHz, DMSO-*d*₆, 38OR11-2019): δ /ppm = 87.4 (C1), 75.5 (C5), 74.1 (C3), 71.0 (C2), 68.4 (C4), 60.5 (C6), 49.0 (C_q), 30.4 (3×CH₃).

N-(*tert*-Butyl)- α -D-galactopyranosylamine – D₂O: 0 % (4 °C) – DMSO-*d*₆: 12 %

$^{13}\text{C}\{^1\text{H}\}$ NMR (101 MHz, DMSO- d_6 , 38OR11-2019): δ/ppm = 82.5 (C1), 70.0 (C5), 69.8 (C4), 68.6 (C3), 68.1 (C2), 60.3 (C6), 49.4 (C_q), 29.8 (3 \times CH₃).

N-(*tert*-Butyl)- β -D-galactofuranosylamine – D₂O: 0 % (4 °C) – DMSO- d_6 : 15 %

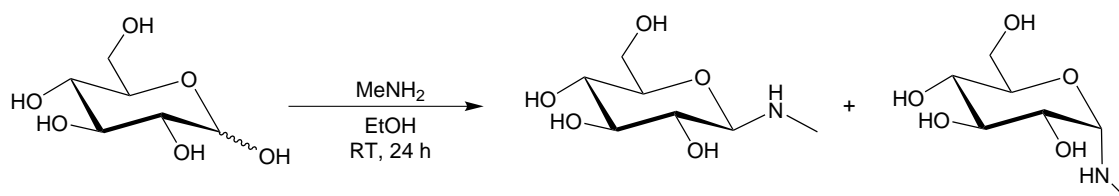
$^{13}\text{C}\{^1\text{H}\}$ NMR (101 MHz, DMSO- d_6 , 38OR11-2019): δ/ppm = 90.9 (C1), 81.1 (C4), 80.3 (C2), 76.0 (C3), 71.0 (C5), 63.1 (C6), 49.6 (C_q), 30.3 (3 \times CH₃).

N-(*tert*-Butyl)- α -D-galactofuranosylamine – D₂O: 0 % (4 °C) – DMSO- d_6 : 33 %

$^{13}\text{C}\{^1\text{H}\}$ NMR (101 MHz, DMSO- d_6 , 38OR11-2019): δ/ppm = 85.2 (C1), 82.1 (C4), 76.5 (C2), 76.2 (C3), 70.4 (C5), 62.9 (C6), 49.6 (C_q), 29.6 (3 \times CH₃).

5.5.2.2. Preparation of *N*-Alkylglucosylamines

N-Methyl-D-glucosylamin (D-Glc1NMe)



D-Glucose (1.00 g, 5.55 mmol, 1.00 eq.) was dried and subsequently stirred for 24 h at room temperature with a solution of methylamine in ethanol (33 %, 10.00 mL, 74.4 mmol, 13.4 eq.). The reaction mixture was concentrated by evaporation of the solvent until a colorless precipitate formed. The precipitate was filtered off, washed with cold methanol (2 \times 5 mL) and dried *in vacuo*. The product was obtained as a slightly yellowish, moisture sensitive powder in a yield of 995 mg (5.15 mmol, 92.8 % of theory).

EA: calcd.: C 43.52 %, H 7.83 %, N 7.25 %

found: C 43.36 %, H 8.07 %, N 6.98 %

MS (FAB+): calcd.: 194.1 ([M+H]⁺)

found: 194.1

N-Methyl- β -D-glucopyranosylamine – D₂O: 91 % – DMSO- d_6 : 85 %

^1H NMR (400 MHz, D₂O, 07OR41-2016): δ/ppm = 3.92 (d, 1H, H1, $^3J_{1,2}$ =8.9 Hz), 3.90 (dd, 1H, H6a, $^3J_{5,6a}$ =2.0 Hz, $^2J_{6a,6b}$ =-12.3 Hz), 3.71 (dd, 1H, H6b, $^3J_{5,6a}$ =5.5 Hz), 3.47 (t, 1H, H3, $^3J_{3,4}$ =8.9 Hz), 3.38 (dd, 1H, H5), 3.36 (sp, H4), 3.20 (t, 1H, H2, $^3J_{2,3}$ =9.0 Hz), 2.44 (s, 3H, CH₃).

$^{13}\text{C}\{^1\text{H}\}$ NMR (101 MHz, D₂O, 21OR11-2016): δ/ppm = 91.3 (C1), 77.44 (C5), 77.42 (C3), 73.4 (C2), 70.6 (C4), 61.5 (C6), 31.5 (CH₃).

$^{13}\text{C}\{^1\text{H}\}$ NMR (101 MHz, DMSO- d_6 , 21OR11-2016): δ/ppm = 91.9 (C1), 77.6 (C5), 77.5 (C3), 73.3 (C2), 70.6 (C4), 61.5 (C6), 32.0 (CH₃).

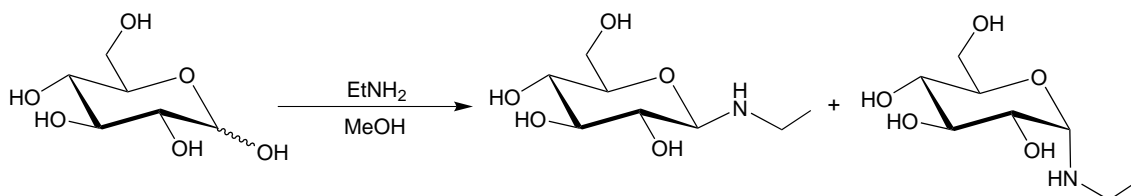
N-Methyl- α -D-glucopyranosylamine – D₂O: 9 % – DMSO- d_6 : 15 %

^1H NMR (400 MHz, D₂O, 07OR41-2016): δ/ppm = 4.50 (d, H1, $^3J_{1,2}$ =4.9 Hz), 2.34 (s, CH₃).

$^{13}\text{C}\{^1\text{H}\}$ NMR (101 MHz, D_2O , 21OR11-2016): δ/ppm = 88.2 (C1), 73.6 (C3), 71.4 (C2), 71.2 (C5), 70.6 (C4), 61.4 (C6), 31.4 (CH_3).

$^{13}\text{C}\{^1\text{H}\}$ NMR (101 MHz, $\text{DMSO-}d_6$, 21OR2-2016): δ/ppm = 88.3 (C1), 73.8 (C3), 71.8 (C2), 71.0 (C5), 70.8 (C4), 61.3 (C6), 32.4 (CH_3).

N-Ethyl-D-glucosylamin (D-Glc1NEt)



D-Glucose (1.00 g, 5.55 mmol, 1.00 eq.) was dried and subsequently stirred for 16 h at room temperature with a solution of ethylamine in methanol (2 M, 20.0 mL, 40.0 mmol, 7.21 eq.). The reaction mixture was concentrated by evaporation of the solvent until a colorless precipitate formed, which was filtered off, washed with cold methanol ($2 \times 10 \text{ mL}$) and dried *in vacuo*. The product was obtained as a colorless powder in a yield of 855 mg (4.27 mmol, 76.9 % of theory).

EA: calcd.: C 46.37 %, H 8.27 %, N 6.79 %

found: C 46.07 %, H 8.65 %, N 6.97 %

MS (FAB+): calcd.: 208.2 ($[\text{M}+\text{H}]^+$)

found: 208.2

N-Ethyl- β -D-glucopyranosylamine – D_2O : 94 % – $\text{DMSO-}d_6$: 93 %

^1H NMR (400 MHz, D_2O , 4 °C, 09OR4-2016): δ/ppm = 3.97 (d, 1H, H1, $^3J_{1,2}=8.8 \text{ Hz}$), 3.86 (dd, 1H, H6a, $^3J_{5,6a}=1.9 \text{ Hz}$), 3.64 (dd, 1H, H6b, $^3J_{5,6b}=5.5 \text{ Hz}$, $^2J_{6a,6b}=-12.3 \text{ Hz}$), 3.44 (t, 1H, H3, $^3J_{3,4}=8.8 \text{ Hz}$), 3.38–3.29 (m, 2H, H4/H5), 3.15 (t, 1H, H2, $^3J_{2,3}=9.0 \text{ Hz}$), 2.88 (dd, 1H, CH_2), 2.66 (dd, 1H, CH_2), 1.05 (t, 3H, CH_3).

$^{13}\text{C}\{^1\text{H}\}$ NMR (101 MHz, D_2O , 09OR5-2016): δ/ppm = 89.7 (C1), 77.5 (C5), 77.4 (C3), 73.6 (C2), 70.5 (C4), 61.5 (C6), 39.9 (CH_2), 14.5 (CH_3).

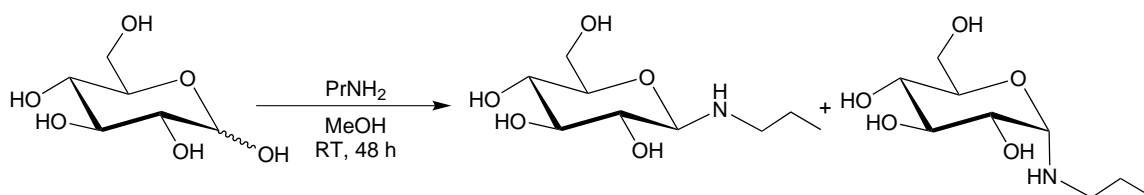
$^{13}\text{C}\{^1\text{H}\}$ NMR (101 MHz, $\text{DMSO-}d_6$, 09OR14-2016): δ/ppm = 90.6 (C1), 77.6 (C5), 77.5 (C3), 73.6 (C2), 70.6 (C4), 61.4 (C6), 39.7 (CH_2), 15.5 (CH_3).

N-Ethyl- α -D-glucopyranosylamine – D_2O : 6 % – $\text{DMSO-}d_6$: 7 %

^1H NMR (400 MHz, D_2O , 4 °C, 09OR4-2016): δ/ppm = 4.60 (d, H1, $^3J_{1,2}=4.5 \text{ Hz}$).

$^{13}\text{C}\{^1\text{H}\}$ NMR (101 MHz, D_2O , 09OR5-2016): δ/ppm = 86.8 (C1), 73.6 (C3), 71.3 (C2), 71.2 (C5), 69.5 (C4), 61.4 (C6), 39.7 (CH_2), 14.2 (CH_3).

$^{13}\text{C}\{^1\text{H}\}$ NMR (101 MHz, $\text{DMSO-}d_6$, 09OR14-2016): δ/ppm = 86.8 (C1), 73.6 (C3), 71.6 (C2), 71.0 (C5), 70.8 (C4), 61.3 (C6), 40.2 (CH_2), 15.3 (CH_3).

***N*-Propyl-D-glucosylamin (D-Glc1NPr)**

D-Glucose (1.00 g, 5.55 mmol, 1.00 eq.) was dried and subsequently solved in 6 mL dry methanol. Propylamine (4.00 mL, 2.88 g, 48.7 mmol, 8.78 eq.) was added and the reaction mixture stirred for 48 h at room temperature. The resulting solution was evaporated until it reached dryness and the solid residue further dried *in vacuo*. The product was obtained as a yellowish powder in a yield of 1.18 g (5.33 mmol, 96.1 % of theory).

EA: calcd.: C 48.86 %, H 8.66 %, N 6.33 %
found: C 48.71 %, H 9.14 %, N 6.66 %

MS (FAB+): calcd.: 222.2 ([M+H]⁺)
found: 222.2

N-Propyl-β-D-glucopyranosylamine – D₂O: 95 % – DMSO-*d*₆: 95 %

¹H NMR (400 MHz, D₂O, 22OR1-2016): δ/ppm = 3.98 (d, 1H, H1, ³J_{1,2}=8.8 Hz), 3.88 (dd, 1H, H6a, ³J_{5,6a}=1.9 Hz), 3.70 (dd, 1H, H6b, ³J_{5,6b}=5.5 Hz, ²J_{6a,6b}=-12.3 Hz), 3.46 (t, 1H, H3, ³J_{3,4}=9.0 Hz), 3.41–3.28 (m, 2H, H4/H5), 3.18 (t, 1H, H2, ³J_{2,3}=9.0 Hz), 2.81 (dd, 1H, NH–CH₂), 2.61 (dd, 1H, NH–CH₂), 1.52–1.42 (sp, 2H, CH₂), 0.89 (t, 3H, CH₃).

¹³C{¹H} NMR (101 MHz, D₂O, 22OR2-2016): δ/ppm = 90.2 (C1), 77.5 (C5), 77.4 (C3), 73.6 (C2), 70.5 (C4), 61.5 (C6), 47.6 (NH–CH₂), 22.8 (CH₂), 11.6 (CH₃).

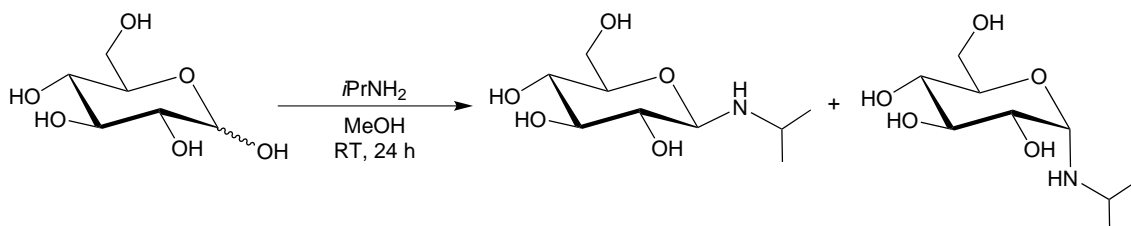
¹³C{¹H} NMR (101 MHz, DMSO-*d*₆, 22OR14-2016): δ/ppm = 90.8 (C1), 77.6 (C5), 77.5 (C3), 73.5 (C2), 70.6 (C4), 61.4 (C6), 47.5 (NH–CH₂), 23.1 (CH₂), 11.8 (CH₃).

N-Propyl-α-D-glucopyranosylamine – D₂O: 5 % – DMSO-*d*₆: 5 %

¹H NMR (400 MHz, D₂O, 22OR1-2016): δ/ppm = 4.42 (d, H1, ³J_{1,2}=4.9 Hz).

¹³C{¹H} NMR (101 MHz, D₂O, 22OR2-2016): δ/ppm = 87.0 (C1), 73.5 (C3), 71.4 (C2), 71.2 (C5), 70.6 (C4), 61.5 (C5), 47.7 (NH–CH₂), 22.5 (CH₂), 11.7 (CH₃).

¹³C{¹H} NMR (101 MHz, DMSO-*d*₆, 22OR14-2016): δ/ppm = 86.9 (C1), 73.7 (C3), 71.6 (C2), 71.0 (C5), 70.8 (C4), 61.2 (C6), 47.9 (NH–CH₂), 22.7 (CH₂), 11.4 (CH₃).

***N*-(*iso*-Propyl)-D-glucosylamin (D-Glc1NiPr)**

D-Glucose (1.00 g, 5.55 mmol, 1.00 eq.) was dried and subsequently solved in 6 mL dry methanol. *iso*-Propylamine (4.00 mL, 2.75 g, 46.6 mmol, 8.39 eq.) was added and the reaction mixture stirred for 24 h at room temperature. The resulting solution was concentrated by evaporation until it reached dryness. Upon further drying *in vacuo* the product was obtained as a yellow powder, showing eminent signs of spontaneous hydrolysis. Due to the high hygroscopy of the compound no yield was determined.

EA: calcd.: C 48.86 %, H 8.66 %, N 6.33 %
found: C 49.29 %, H 9.19 %, N 7.65 %

MS (FAB+): calcd.: 222.3 ([M+H]⁺)
found: 222.3

N-(*iso*)-Propyl- β -D-glucopyranosylamine – D₂O: 92 % – DMSO-*d*₆: 85 %

¹H NMR (400 MHz, D₂O, 4 °C, 21OR43-2016): δ /ppm = 4.05 (d, 1H, H1, ³J_{1,2}=8.8 Hz), 3.86 (dd, 1H, H6a, ³J_{5,6a}=1.9 Hz), 3.67 (dd, 1H, H6b, ³J_{5,6b}=5.5 Hz, ²J_{6a,6b}=–12.3 Hz), 3.46 (t, 1H, H3, ³J_{3,4}=9.0 Hz), 3.37–3.31 (m, 2H, H4/H5), 3.19–3.11 (m, 1H, H2), 3.05 (q, 1H, CH), 1.04 (d, 6H, 2×CH₃).

¹³C{¹H} NMR (101 MHz, D₂O, 4 °C, 21OR44-2016): δ /ppm = 88.2 (C1), 77.6 (C5), 77.3 (C3), 74.0 (C2), 70.6 (C4), 61.6 (C6), 45.5 (CH), 23.2 (CH₃), 21.4 (CH₃).

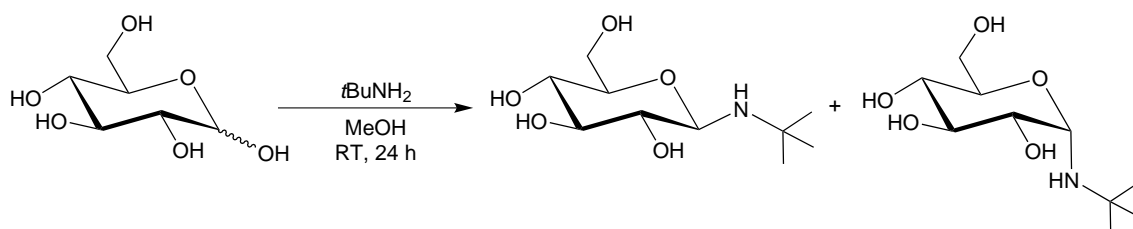
¹³C{¹H} NMR (101 MHz, DMSO-*d*₆, 4 °C, 21OR47-2016): δ /ppm = 88.7 (C1), 77.6 (C5), 77.5 (C3), 73.8 (C2), 70.6 (C4), 61.4 (C6), 44.6 (CH), 24.4 (CH₃), 22.5 (CH₃).

N-(*iso*)-Propyl- α -D-glucopyranosylamine – D₂O: 8 % – DMSO-*d*₆: 15 %

¹H NMR (400 MHz, DMSO-*d*₆, 21OR46-2016): δ /ppm = 4.52 (d, H1, ³J_{1,2}=2.8 Hz).

¹³C{¹H} NMR (101 MHz, DMSO-*d*₆, 21OR47-2016): δ /ppm = 85.7 (C1), 73.7 (C3), 71.4 (C5), 70.8 (C2/C4), 61.2 (C6), 46.4 (CH), 24.3 (CH₃), 22.7 (CH₃).

N-(*tert*-Butyl)-D-glucosylamin (D-Glc1N*t*Bu)



D-Glucose (2.40 g, 13.3 mmol, 1.00 eq.) was dried and subsequently solved in 50 mL dry methanol. *tert*-Propylamine (9.73 mL, 6.81 g, 93.1 mmol, 7.00 eq.) was added and the reaction mixture stirred for 24 h at room temperature. The resulting solution was concentrated by evaporation until it reached dryness. The colorless residue was crushed and further dried *in vacuo*. Due to the high hygroscopy of the obtained product no yield was determined.

EA: calcd.: C 51.05 %, H 9.00 %, N 5.95 %
found: C 51.67 %, H 9.77 %, N 7.55 %

MS (FAB+): calcd.: 236.3 ([M+H]⁺)
found: 236.3

N-(*tert*)-Butyl-β-D-glucopyranosylamine – D₂O: 100 % – DMSO-*d*₆ 78 %

¹H NMR (400 MHz, D₂O, 27OR4-2018): δ/ppm = 4.14 (d, 1H, H1, ³J_{1,2}=8.8 Hz), 3.86 (dd, 1H, H6a, ²J_{6a,6b}=-12.7 Hz), 3.70 (dd, 1H, H6b, ³J_{5,6b}=5.5 Hz), 3.49 (t, 1H, H3, ³J_{3,4}=8.6 Hz), 3.37–3.31 (m, 2H, H4/H5), 3.10 (t, 1H, H2, ³J_{2,3}=8.9 Hz), 1.13 (d, 9H, 3×CH₃).

¹³C{¹H} NMR (101 MHz, D₂O, 27OR4-2018): δ/ppm = 86.6 (C1), 77.6 (C5), 76.9 (C3), 73.8 (C2), 70.7 (C4), 61.7 (C6), 50.9 (C_q), 29.5 (3×CH₃).

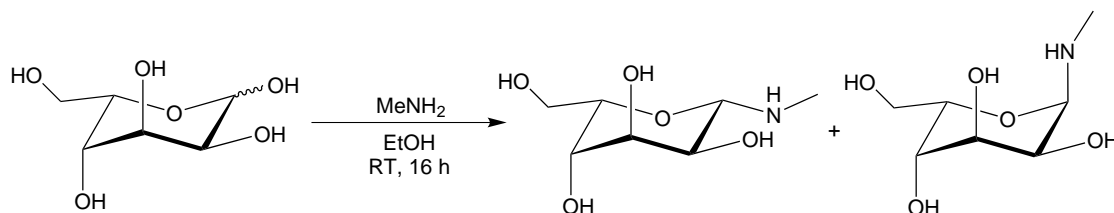
¹³C{¹H} NMR (101 MHz, DMSO-*d*₆, 27OR11-2018): δ/ppm = 86.9 (C1), 77.5 (C5), 77.3 (C3), 73.6 (C2), 70.7 (C4), 61.5 (C6), 49.7 (C_q), 30.3 (3×CH₃).

N-(*tert*)-Butyl-α-D-glucopyranosylamine – D₂O: 0 % – DMSO-*d*₆ 22 %

¹³C{¹H} NMR (101 MHz, DMSO-*d*₆, 27OR11-2018): δ/ppm = 82.2 (C1), 73.8 (C3), 71.2 (C2), 70.8 (C5), 70.1 (C4), 61.2 (C6), 49.6 (C_q), 29.8 (3×CH₃).

5.5.2.3. Preparation of *N*-Alkylgulosylamines

N-Methyl-L-gulosylamin (L-Gul1NMe)



L-Gulose (500 mg, 2.78 mmol, 1.00 eq.) was dried and subsequently stirred for 16 h at room temperature with a solution of methylamine in ethanol (33 %, 5.00 mL, 37.2 mmol, 13.4 eq.). The reaction mixture was concentrated by evaporation of the solvent until a syrup-like residue was obtained. The residue was frozen in liquid nitrogen, crushed and dried *in vacuo* several times until the product was obtained as a colorless, moisture sensitive powder. Due to the hygroscopy of the product no yield was determined.

EA: calcd.: C 43.52 %, H 7.83 %, N 7.25 %
found: C 42.76 %, H 8.34 %, N 6.60 %

MS (FAB+): calcd.: 194.1 ([M+H]⁺)
found: 194.1

N-Methyl-β-L-gulopyranosylamine – D₂O: 100 % – DMSO-*d*₆: 86 %

¹H NMR (400 MHz, D₂O, 13OR30-2017): δ/ppm = 4.14 (d, 1H, H1, ³J_{1,2}=9.3 Hz), 4.01 (t, 1H,

H3), 3.89 (ddd, 1H, H5, $^3J_{4,5}=1.8$ Hz, $^3J_{5,6}=4.4$ Hz, $^3J_{5,6'}=8.7$ Hz), 3.78 (d, 1H, H4, $^3J_{3,4}=3.3$ Hz), 3.71 (sp, 2H, H6/H6'), 3.58 (dd, 1H, H2, $^3J_{2,3}=3.5$ Hz), 2.43 (s, 3H, CH₃).

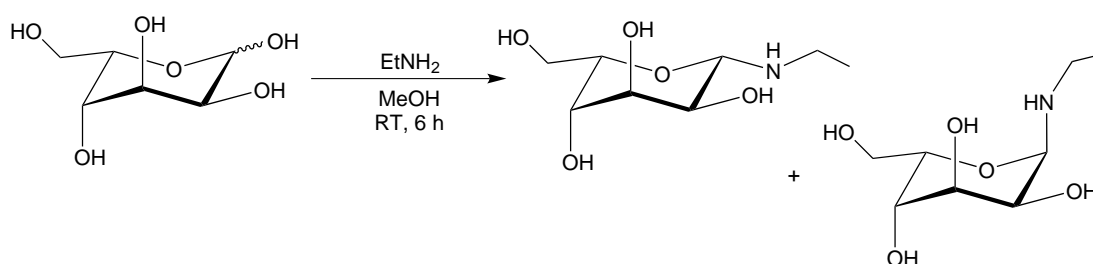
$^{13}\text{C}\{^1\text{H}\}$ NMR (101 MHz, D₂O, 13OR31-2017): $\delta/\text{ppm} = 88.4$ (C1), 74.5 (C5), 71.7 (C3), 70.3 (C4), 68.2 (C2), 61.8 (C6), 31.3 (CH₃).

$^{13}\text{C}\{^1\text{H}\}$ NMR (101 MHz, DMSO-*d*₆, 13OR5-2017): $\delta/\text{ppm} = 88.4$ (C1), 73.5 (C5), 71.2 (C3), 69.2 (C4), 68.0 (C2), 60.6 (C6), 31.8 (CH₃).

N-Methyl- α -L-gulopyranosylamine – D₂O: 0 % – DMSO-*d*₆: 14 %

$^{13}\text{C}\{^1\text{H}\}$ NMR (101 MHz, DMSO-*d*₆, 13OR5-2017): $\delta/\text{ppm} = 87.7$ (C1), 72.0 (C3), 69.5 (C4), 65.2 (C5), 64.8 (C2), 60.6 (C6), 31.4 (CH₃).

N-Ethyl-D-gulosylamin (D-Gul1NEt)



L-Gulose (1.00 g, 5.55 mmol, 1.00 eq.) was dried and subsequently stirred for 6 h at room temperature with a solution of ethylamine in methanol (2 M, 15.0 mL, 30.0 mmol, 5.41 eq.). The reaction mixture was concentrated by evaporation of the solvent until a syrup-like liquid was obtained. The residue was frozen in liquid nitrogen, crushed and dried *in vacuo* several times until the product was obtained as a yellowish, moisture sensitive powder. Due to the hygroscopy of the product no yield was determined.

EA: calcd.: C 46.37 %, H 8.27 %, N 6.79 %

found: C 46.16 %, H 8.54 %, N 7.60 %

MS (FAB+): calcd.: 208.2 ([M+H]⁺)

found: 208.2

N-Ethyl- β -L-gulopyranosylamine – D₂O: 100 % – DMSO-*d*₆: 82 %

^1H NMR (400 MHz, D₂O, 4 °C, 13OR16-2017): $\delta/\text{ppm} = 4.20$ (d, 1H, H1, $^3J_{1,2}=9.3$ Hz), 3.98 (t, 1H, H3), 3.86 (ddd, 1H, H5, $^3J_{4,5}=1.3$ Hz, $^3J_{5,6}=5.1$ Hz, $^3J_{5,6'}=7.3$ Hz), 3.76 (dd, 1H, H4, $^3J_{3,4}=3.6$ Hz), 3.69–3.66 (sp, 2H, H6/H6'), 3.55 (dd, 1H, H2, $^3J_{2,3}=3.4$ Hz), 2.89 (m, 1H, CH₂), 2.66 (m, 1H, CH₂), 1.05 (t, 3H, CH₃).

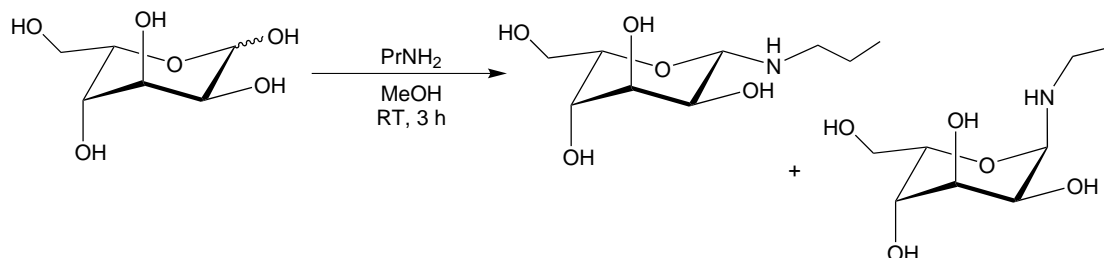
$^{13}\text{C}\{^1\text{H}\}$ NMR (101 MHz, D₂O, 13OR17-2017): $\delta/\text{ppm} = 87.0$ (C1), 74.5 (C5), 71.7 (C3), 70.3 (C4), 68.4 (C2), 61.8 (C6), 39.7 (CH₂), 14.5 (CH₃).

$^{13}\text{C}\{^1\text{H}\}$ NMR (101 MHz, DMSO-*d*₆, 09OR14-2016): $\delta/\text{ppm} = 87.1$ (C1), 73.5 (C5), 71.2 (C3), 69.2 (C4), 68.2 (C2), 60.6 (C6), 39.4 (CH₂), 15.6 (CH₃).

N-Ethyl- α -L-gulopyranosylamine – D₂O: 0 % – DMSO-*d*₆: 18 %

¹³C{¹H} NMR (101 MHz, DMSO-*d*₆, 13OR8-2017): δ /ppm = 86.2 (C1), 72.0 (C3), 69.4 (C4), 65.2 (C5), 64.7 (C2), 60.5 (C6), 38.9 (CH₂), 15.5 (CH₃).

N-Propyl-D-gulosylamin (D-Gul1NPr)



L-Gulose (1.00 g, 5.55 mmol) was dried and subsequently suspended in 2 mL dry methanol. Propylamine (1.25 mL, 900 mg, 15.2 mmol, 2.74 eq.) was added and the reaction mixture stirred for 3 h at room temperature. The resulting solution was concentrated by evaporation until it reached dryness. The thereby obtained residue was frozen in liquid nitrogen, crushed and further dried *in vacuo* to give the product as a yellowish, moisture sensitive powder in a yield of 1.01 g (4.57 mmol, 82.3 % of theory).

N-Propyl- β -L-gulopyranosylamine – D₂O: 100 % – DMSO-*d*₆: 80 %

¹H NMR (400 MHz, D₂O, 4 °C, 35OR1-2019): δ /ppm = 4.20 (d, 1H, H1, ³*J*_{1,2}=9.4 Hz), 3.98 (t, 1H, H3), 3.86 (ddd, 1H, H5, ³*J*_{4,5}=1.3 Hz, ³*J*_{5,6}=5.1 Hz, ³*J*_{5,6'}=7.3 Hz), 3.76 (dd, 1H, H4, ³*J*_{3,4}=3.7 Hz), 3.69–3.66 (sp, 2H, H6/H6'), 3.56 (dd, 1H, H2, ³*J*_{2,3}=3.4 Hz), 2.82 (m, 1H, NH–CH₂), 2.55 (sp, 1H, NH–CH₂), 1.42 (m, 2H, CH₂) 0.86 (t, 3H, CH₃).

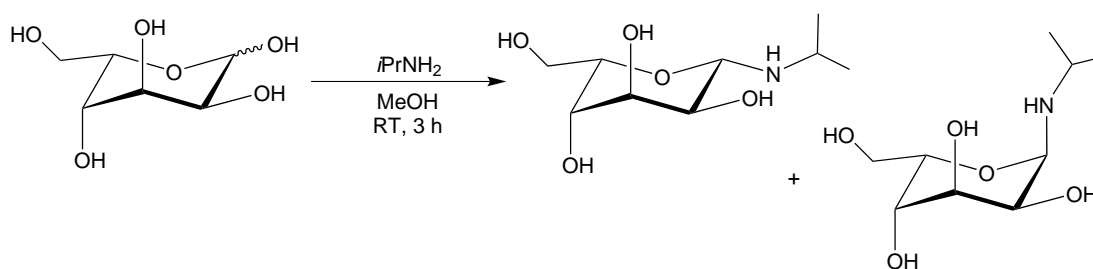
¹³C{¹H} NMR (101 MHz, D₂O, 4 °C, 35OR2-2019): δ /ppm = 87.3 (C1), 74.6 (C5), 71.8 (C3), 70.3 (C4), 68.4 (C2), 61.8 (C6), 47.4 (NH–CH₂), 23.0 (CH₂), 11.8 (CH₃).

¹³C{¹H} NMR (101 MHz, DMSO-*d*₆, 35OR2BT-2019): δ /ppm = 87.4 (C1), 73.5 (C5), 71.2 (C3), 69.2 (C4), 68.2 (C2), 60.6 (C6), 47.3 (NH–CH₂), 23.3 (CH₂), 11.8 (CH₃).

N-Propyl- α -L-gulopyranosylamine – D₂O: 0 % – DMSO-*d*₆: 20 %

¹³C{¹H} NMR (101 MHz, DMSO-*d*₆, 35OR2BT-2019): δ /ppm = 86.5 (C1), 72.0 (C3), 69.4 (C4), 65.2 (C5), 64.7 (C2), 60.5 (C6), 46.7 (NH–CH₂), 23.0 (CH₂), 11.8 (CH₃).

N-*iso*-Propyl-D-gulosylamin (D-Gul1NiPr)



L-Gulose (1.00 g, 5.55 mmol, 1.00 eq.) was dried and subsequently suspended in 2 mL dry methanol. *iso*-Propylamine (1.25 mL, 860 mg, 14.5 mmol, 2.62 eq.) was slowly added and the reaction mixture stirred for 3 h at room temperature. The resulting solution was concentrated by evaporation of the solvent until it reached dryness. The obtained residue was frozen in liquid nitrogen, crushed and further dried *in vacuo* to give the product as a yellowish, moisture sensitive powder in a yield of 747 mg (3.38 mmol, 60.8 % of theory).

N-(*iso*-Propyl)- β -L-gulopyranosylamine – D₂O: 100 % – DMSO-*d*₆: 80 %

¹H NMR (400 MHz, D₂O, 4 °C, 35OR5-2019): δ /ppm = 4.28 (d, 1H, H1, ³*J*_{1,2}=9.3 Hz), 3.98 (t, 1H, H3), 3.85 (ddd, 1H, H5, ³*J*_{4,5}=1.3 Hz, ³*J*_{5,6}=5.1 Hz, ³*J*_{5,6'}=7.3 Hz), 3.76 (dd, 1H, H4, ³*J*_{3,4}=3.6 Hz), 3.69–3.66 (sp, 2H, H6/H6'), 3.51 (dd, 1H, H2, ³*J*_{2,3}=3.3 Hz), 3.19 (m, 1H, CH), 1.01 (t, 6H, 2×CH₃).

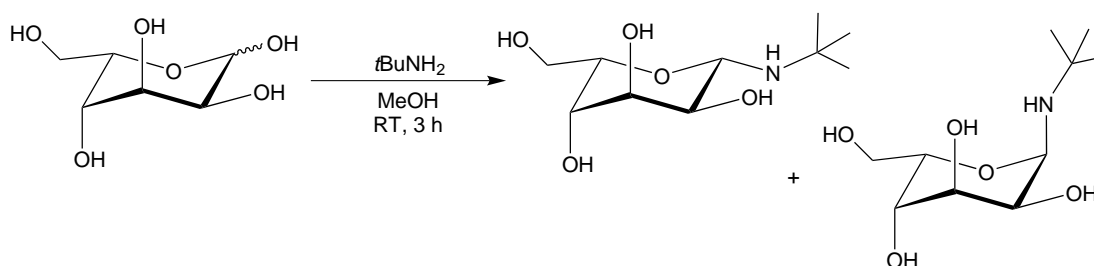
¹³C{¹H} NMR (101 MHz, D₂O, 4 °C, 35OR6-2019): δ /ppm = 85.2 (C1), 74.5 (C5), 71.8 (C3), 70.4 (C4), 68.8 (C2), 61.8 (C6), 45.2 (CH), 23.3 (CH₃), 21.3 (CH₃).

¹³C{¹H} NMR (101 MHz, DMSO-*d*₆, 35OR5BT-2019): δ /ppm = 85.1 (C1), 73.4 (C5), 71.2 (C3), 69.2 (C4), 68.4 (C2), 60.6 (C6), 44.3 (CH), 24.4 (CH₃), 22.6 (CH₃).

N-(*iso*-Propyl)- α -L-gulopyranosylamine – D₂O: 0 % – DMSO-*d*₆: 20 %

¹³C{¹H} NMR (101 MHz, DMSO-*d*₆, 35OR5BT-2019): δ /ppm = 84.1 (C1), 71.9 (C3), 69.3 (C4), 65.3 (C5), 64.6 (C2), 60.4 (C6), 43.5 (CH), 24.5 (CH₃), 21.9 (CH₃).

N-*tert*-Butyl-D-gulosylamin (D-Gul1N*t*Bu)



L-Gulose (600 mg, 6.66 mmol, 1.00 eq.) was dried and subsequently suspended in 10 mL dry methanol. *tert*-Butylamine (1.00 mL, 700 mg, 9.57 mmol, 2.87 eq.) was slowly added and the reaction mixture stirred for 3 h at room temperature. The resulting solution was concentrated by evaporation of the solvent until it reached dryness. The obtained residue was frozen in liquid nitrogen, crushed and further dried *in vacuo* to give the product as a white, slightly hygroscopic powder in a yield of 668 mg (2.84 mmol, 85.3 % of theory).

N-(*tert*-Butyl)- β -L-gulopyranosylamine – D₂O: 100 % – DMSO-*d*₆: 78 %

¹H NMR (400 MHz, D₂O, 4 °C, 38OR7-2019): δ /ppm = 4.20 (d, 1H, H1, ³*J*_{1,2}=9.2 Hz), 1.10 (s, 9H, 3×CH₃).

¹³C{¹H} NMR (101 MHz, D₂O, 4 °C, 38OR8-2019): δ /ppm = 83.7 (C1), 74.2 (C5), 71.7 (C3), 70.6 (C4), 68.5 (C2), 61.8 (C6), 51.1 (C_q), 30.8 (3×CH₃).

¹³C{¹H} NMR (101 MHz, DMSO-*d*₆, 35OR7-2019): δ /ppm = 83.4 (C1), 73.3 (C5), 71.1 (C3),

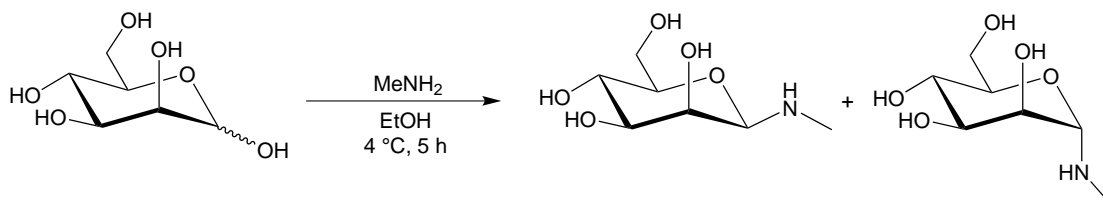
69.1 (C4), 68.3 (C2), 60.5 (C6), 49.6 (C_q), 30.5 (3×CH₃).

N-(*tert*-Butyl)- α -L-gulopyranosylamine – D₂O: 0 % – DMSO-*d*₆: 18 %

¹³C{¹H} NMR (101 MHz, DMSO-*d*₆, 37OR2-2019): δ /ppm = 82.6 (C1), 71.9 (C3), 69.1 (C4), 64.5 (C2), 64.2 (C5), 60.3 (C6), 49.1 (C_q), 30.3 (3×CH₃).

5.5.2.4. Preparation of *N*-Alkylmannosylamines

N-Methyl-D-mannosylamin (D-Man1NMe)



D-Mannose (1.96 g, 10.9 mmol, 1.00 eq.) was dried and subsequently stirred with a solution of methylamine in ethanol (33 %, 9.00 mL, 66.9 mmol, 6.14 eq.) for 5 h at 4 °C. Upon storage of the resulting solution at 4 °C for 48 h a white precipitate formed. The product was filtered off, washed with cold methanol (2 × 5 mL) and dried *in vacuo*. The product was obtained as a colorless powder in a yield of 1.85 g (9.65 mmol, 87.7 % of theory).

EA: calcd.: C 43.52 %, H 7.83 %, N 7.25 %

found: C 42.69 %, H 8.46 %, N 8.26 %

MS (FAB+): calcd.: 194.2 ([M+H]⁺)

found: 194.2

N-Methyl- β -D-mannopyranosylamine – D₂O: 84 % – DMSO-*d*₆: 86 %

¹H NMR (400 MHz, D₂O, 07OR44-2016): δ /ppm = 4.12 (d, 1H, H1, ³J_{1,2}=1.0 Hz), 3.92 (dd, 1H, H6a, ³J_{5,6a}=2.4 Hz, ²J_{6a,6b}=−12.2 Hz), 3.86 (dd, 1H, H2, ³J_{2,3}=3.4 Hz), 3.70 (dd, 1H, H6b, ³J_{5,6b}=6.6 Hz), 3.63 (dd, 1H, H3, ³J_{3,4}=9.6 Hz), 3.52 (t, 1H, H4, ³J_{4,5}=9.7 Hz), 3.32 (dd, 1H, H5), 2.45 (s, 3H, CH₃).

¹³C{¹H} NMR (101 MHz, D₂O, 07OR45-2016): δ /ppm = 88.7 (C1), 77.9 (C5), 74.5 (C3), 71.5 (C2), 67.9 (C4), 61.9 (C6), 31.6 (CH₃).

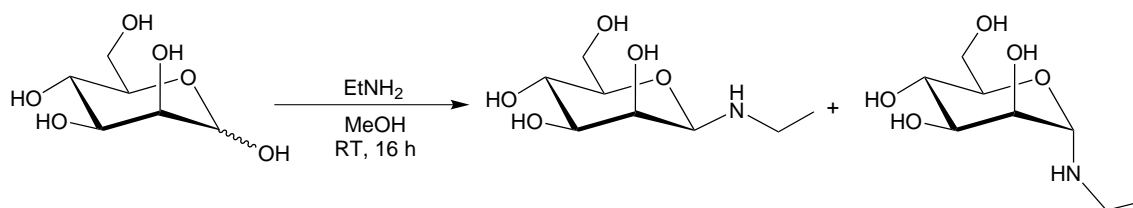
¹³C{¹H} NMR (101 MHz, DMSO-*d*₆, 39OR34-2015): δ /ppm = 88.6 (C1), 77.9 (C5), 74.7 (C3), 71.4 (C2), 67.6 (C4), 61.7 (C6), 31.9 (CH₃).

N-Methyl- α -D-mannopyranosylamine – D₂O: 16 % – DMSO-*d*₆: 14 % :

¹H NMR (400 MHz, D₂O, 07OR44-2016): δ /ppm = 4.40 (d, 1H, H1, ³J_{1,2}=1.6 Hz), 2.33 (s, 3H, CH₃).

¹³C{¹H} NMR (101 MHz, D₂O, 07OR45-2016): 89.8 (C1), 72.4 (C5), 71.5 (C2), 71.2 (C3), 67.6 (C4), 61.7 (C6), 31.0 (CH₃).

¹³C{¹H} NMR (101 MHz, DMSO-*d*₆, 39OR34-2015): δ /ppm = 89.6 (C1), 72.1 (C5), 71.3 (C2), 71.3 (C3), 67.9 (C4), 61.6 (C6), 31.6 (CH₃).

N-Ethyl-D-mannosylamin (D-Man1NEt)

D-Mannose (2.00 g, 11.1 mmol, 1.00 eq.) was dried and subsequently stirred with a solution of ethylamine in methanol (2 M, 20.0 mL, 40.0 mmol, 3.60 eq.) for 16 h at room temperature. Upon storage of the resulting solution at 4 °C for 48 h a white precipitate formed. The product was filtered off, washed with cold methanol (2 × 5 mL) and dried *in vacuo*. The product was obtained as a white powder in a yield of 942 mg (4.55 mmol, 41.0 % of theory).

EA: calcd.: C 46.37 %, H 8.27 %, N 6.76 %
found: C 46.23 %, H 8.36 %, N 6.66 %

MS (FAB+): calcd.: 206.2 ([M+H]⁺)
found: 206.2

N-Ethyl-β-D-mannopyranosylamine – D₂O: 87 % – DMSO-*d*₆: 81 %

¹H NMR (400 MHz, D₂O, 09OR7-2016): δ/ppm = 4.21 (d, 1H, H1, ³J_{1,2}=1.1 Hz), 3.90 (dd, 1H, H6a, ³J_{5,6a}=2.3 Hz, ²J_{6a,6b}=−12.2 Hz), 3.84 (dd, 1H, H2, ³J_{2,3}=3.4 Hz), 3.68 (dd, 1H, H6b, ³J_{5,6b}=6.6 Hz), 3.62 (dd, 1H, H3, ³J_{3,4}=9.6 Hz), 3.51 (t, 1H, H4, ³J_{4,5}=9.7 Hz), 3.32 (sp, 1H, H5), 2.99–2.90 (m, 1H, CH₂), 2.73–2.63 (m, 1H, CH₂), 1.07 (s, 3H, CH₃).

¹³C{¹H} NMR (101 MHz, D₂O, 41OR11-2017): δ/ppm = 86.9 (C1), 77.9 (C5), 74.5 (C3), 71.8 (C2), 67.9 (C4), 61.9 (C6), 39.5 (CH₂), 14.2 (CH₃).

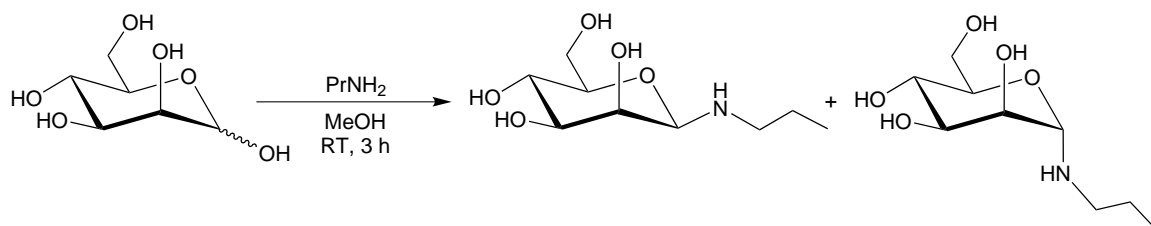
¹³C{¹H} NMR (101 MHz, DMSO-*d*₆, 09OR17-2017): δ/ppm = 86.9 (C1), 77.9 (C5), 74.7 (C3), 71.5 (C2), 67.6 (C4), 61.7 (C6), 39.0 (CH₂), 15.4 (CH₃).

N-Ethyl-α-D-mannopyranosylamine – D₂O: 13 % – DMSO-*d*₆: 19 % :

¹H NMR (400 MHz, D₂O, 09OR7-2016): δ/ppm = 4.50 (d, 1H, H1, ³J_{1,2}=1.5 Hz).

¹³C{¹H} NMR (101 MHz, D₂O, 41OR11-2017): 88.3 (C1), 72.4 (C5), 71.6 (C2), 71.2 (C3), 67.6 (C4), 61.7 (C6), 39.2 (CH₂), 13.9 (CH₃).

¹³C{¹H} NMR (101 MHz, DMSO-*d*₆, 09OR17-2017): δ/ppm = 87.9 (C1), 72.0 (C5), 71.3 (C2), 71.2 (C3), 67.9 (C4), 61.6 (C6), 39.0 (CH₂), 15.0 (CH₃).

N-Propyl-D-mannosylamin (D-Man1NPr)

D-Mannose (2.00 g, 11.1 mmol) was dried and subsequently suspended in 4 mL dry methanol. Propylamine (5.40 mL, 3.87 g, 65.5 mmol, 5.90 eq.) was added and the reaction mixture stirred for 3 h at room temperature. The resulting yellowish solution was concentrated by evaporation of half of the solvent and 20 mL diethyl ether were added. The reaction mixture was stored at 4 °C for 24 h and the thereby formed white precipitate was filtered off, washed with isopropanol (1 × 10 mL) and diethyl ether (1 × 20 mL) and dried *in vacuo*. The product was obtained as a white powder in a yield of 2.36 g (10.7 mmol, 96.3 % of theory).

EA: calcd.: C 48.86 %, H 8.66 %, N 6.33 %
found: C 47.55 %, H 8.96 %, N 6.15 %

MS (FAB+): calcd.: 222.3 ([M+H]⁺)
found: 222.4

N-Propyl-β-D-mannopyranosylamine – D₂O: 85 % – DMSO-*d*₆: 90 %

¹H NMR (400 MHz, D₂O, 39OR7-2015): δ/ppm = 4.19 (d, 1H, H1, ³J_{1,2}=1.1 Hz), 3.89 (dd, 1H, H6a, ³J_{5,6a}=2.3 Hz, ²J_{6a,6b}=-12.2 Hz), 3.84 (dd, 1H, H2, ³J_{2,3}=3.4 Hz), 3.68 (dd, 1H, H6b, ³J_{5,6b}=6.5 Hz), 3.61 (dd, 1H, H3, ³J_{3,4}=9.6 Hz), 3.51 (t, 1H, H4, ³J_{4,5}=9.6 Hz), 3.32 (sp, 1H, H5), 2.85 (dd, 1H, NH-CH₂), 2.60 (dd, 1H, NH-CH₂), 1.55–1.39 (sp, 2H, CH₂), 0.87 (t, 3H, CH₃).

¹³C{¹H} NMR (101 MHz, D₂O, 39OR8-2015): δ/ppm = 87.2 (C1), 77.9 (C5), 74.5 (C3), 71.8 (C2), 67.9 (C4), 61.9 (C6), 47.1 (CH₂), 22.7 (CH₂), 11.6 (CH₃).

¹³C{¹H} NMR (101 MHz, DMSO-*d*₆, 40OR2-2015): δ/ppm = 87.3 (C1), 77.9 (C5), 74.7 (C3), 71.5 (C2), 67.6 (C4), 61.7 (C6), 46.8 (CH₂), 23.2 (CH₂), 11.8 (CH₃).

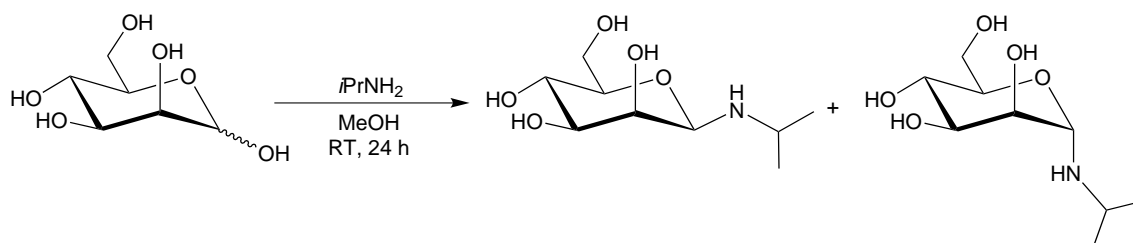
N-Propyl-α-D-mannopyranosylamine – D₂O: 15 % – DMSO-*d*₆: 10 % :

¹H NMR (400 MHz, D₂O, 39OR7-2015): δ/ppm = 4.48 (d, 1H, H1, ³J_{1,2}=1.6 Hz).

¹³C{¹H} NMR (101 MHz, D₂O, 39OR8-2015): 88.6 (C1), 72.4 (C5), 71.6 (C2), 71.2 (C3), 67.6 (C4), 61.7 (C6), 47.1 (CH₂), 22.4 (CH₂), 11.7 (CH₃).

¹³C{¹H} NMR (101 MHz, DMSO-*d*₆, 40OR2-2015): δ/ppm = 88.2 (C1), 72.0 (C5), 71.3 (C2), 71.2 (C3), 67.9 (C4), 61.6 (C6), 46.9 (CH₂), 22.6 (CH₂), 11.9 (CH₃).

N-(*iso*-Propyl)-D-mannosylamin (D-Man1NiPr)



D-Mannose (2.88 g, 16.0 mmol, 1.00 eq.) was dried and subsequently suspended in 10 mL dry methanol. *iso*-Propylamine (1.65 mL, 1.13 g, 19.2 mmol, 1.20 eq.) was added and the reaction

mixture stirred for 24 h at room temperature. The resulting yellowish solution was concentrated by evaporation of the solvent until a white precipitate formed. The precipitate was filtered off, washed with cold methanol (1 × 10 mL) and diethyl ether (1 × 20 mL) and dried *in vacuo*. The product was obtained as a white powder in a yield of 2.86 g (12.9 mmol, 80.9 % of theory).

EA: calcd.: C 48.86 %, H 8.66 %, N 6.33 %
found: C 47.63 %, H 8.98 %, N 6.13 %

MS (FAB+): calcd.: 222.3 ([M+H]⁺)
found: 222.3

N-(*iso*-Propyl)-β-D-mannopyranosylamine – D₂O: 90 % – DMSO-*d*₆: 88 %

¹H NMR (400 MHz, D₂O, 41OR32-2017): δ/ppm = 4.27 (d, 1H, H1, ³J_{1,2}=1.1 Hz), 3.86 (dd, 1H, H6, ³J_{5,6}=2.3 Hz, ²J_{6,6'}=−12.1 Hz), 3.79 (dd, 1H, H2, ³J_{2,3}=3.1 Hz), 3.65 (ddd, 1H, H6', ³J_{5,6'}=6.5 Hz), 3.60 (dd, 1H, H3, ³J_{3,4}=9.6 Hz), 3.49 (t, 1H, H4, ³J_{4,5}=9.8 Hz), 3.32 (sp, 1H, H5), 3.06–3.01 (m, 1H, CH), 1.02 (dd, 6H, 2 × CH₃).

¹³C{¹H} NMR (101 MHz, D₂O, 41OR31-2017): δ/ppm = 84.5 (C1), 77.9 (C5), 74.7 (C3), 72.0 (C2), 67.9 (C4), 61.9 (C6), 43.8 (CH), 23.3 (CH₃), 20.4 (CH₃).

¹³C{¹H} NMR (101 MHz, DMSO-*d*₆, 33OR22-2015): δ/ppm = 84.5 (C1), 77.9 (C5), 74.8 (C3), 71.7 (C2), 67.7 (C4), 61.7 (C6), 42.6 (CH), 24.4 (CH₃), 21.9 (CH₃).

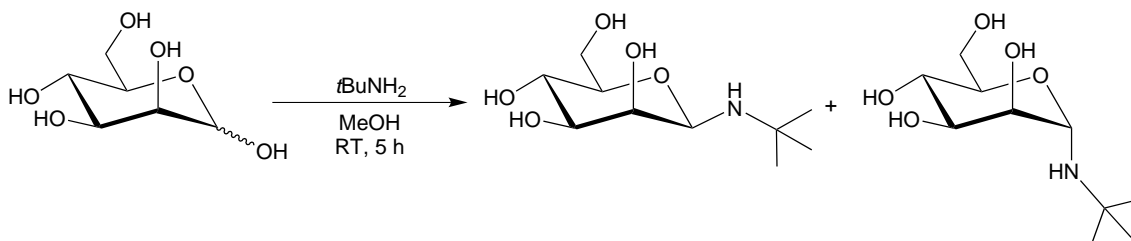
N-(*iso*-Propyl)-α-D-mannopyranosylamine – D₂O: 10 % – DMSO-*d*₆: 12 % :

¹H NMR (400 MHz, D₂O, 41OR31-2017): δ/ppm = 4.58 (d, 1H, H1, ³J_{1,2}=1.8 Hz).

¹³C{¹H} NMR (101 MHz, D₂O, 41OR32-2017): 86.1 (C1), 72.4 (C5), 71.9 (C2), 71.2 (C3), 67.7 (C4), 61.7 (C6), 44.3 (CH), 23.1 (CH₃), 20.4 (CH₃).

¹³C{¹H} NMR (101 MHz, DMSO-*d*₆, 33OR22-2015): δ/ppm = 86.1 (C1), 72.0 (C5), 71.6 (C2), 71.2 (C3), 68.0 (C4), 61.6 (C6), 44.1 (CH), 24.1 (CH₃), 22.0 (CH₃).

N-(*tert*-Butyl)-D-mannosylamin (D-Man1N*t*Bu)



D-Mannose (4.00 g, 2.22 mmol, 1.00 eq.) was dried and subsequently suspended in 60 mL dry methanol. *tert*-Butylamine (16.7 mL, 11.7 g, 160 mmol, 7.20 eq.) was added and the reaction mixture stirred for 5 h at room temperature. The resulting slightly brown solution was concentrated *in vacuo* until an orange syrup-like residue was obtained. The residue was solved in 50 mL diethyl ether and stored for a week at 4 °C. Since no precipitation of the desired product occurred, the diethyl ether was removed *in vacuo*. Thereby the product was obtained as a highly

hygroscopic white powder in a yield of 4.70 g (20.0 mmol, 90.0 % of theory).

EA: calcd.: C 51.05 %, H 9.00 %, N 5.95 %
found: C 51.59 %, H 9.75 %, N 7.31 %

MS (FAB+): calcd.: 236.3 ([M+H]⁺)
found: 236.4

N-(*tert*-Butyl)- β -D-mannopyranosylamine – D₂O: 100 % – DMSO-*d*₆: 76 %

¹H NMR (400 MHz, D₂O, 43OR39-2015): δ /ppm = 4.34 (d, H1, ³J_{1,2}=1.0 Hz).

¹³C{¹H} NMR (101 MHz, D₂O, 43OR40-2015): δ /ppm = 84.4 (C1), 77.6 (C5), 74.8 (C3), 73.1 (C2), 67.8 (C4), 61.9 (C6), 51.0 (C_q), 29.8 (3×CH₃).

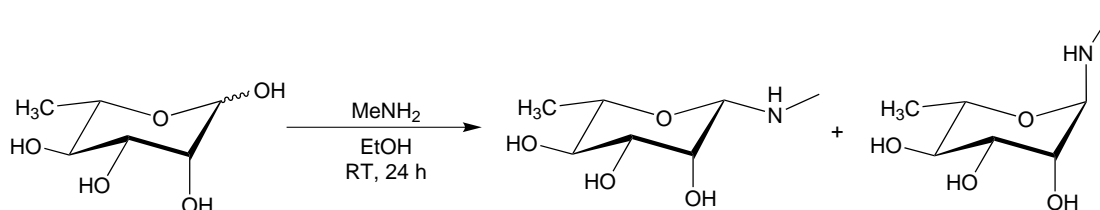
¹³C{¹H} NMR (101 MHz, DMSO-*d*₆, 43OR43-2015): δ /ppm = 84.0 (C1), 77.6 (C5), 74.9 (C3), 72.6(C2), 67.7 (C4), 61.9 (C6), 49.4 (C_q), 30.8 (3×CH₃).

N-(*tert*-Butyl)- α -D-mannopyranosylamine – D₂O: 0 % – DMSO-*d*₆: 24 % :

¹³C{¹H} NMR (101 MHz, DMSO-*d*₆, 43OR43-2015): δ /ppm = 84.2 (C1), 72.4 (C5), 71.4 (C2), 71.1 (C3), 68.1 (C4), 61.5 (C6), 49.7 (C_q), 29.9 (3×CH₃).

5.5.2.5. Preparation of *N*-Alkylrhamnosylamines

N-Methyl-L-rhamnosylamin (L-Rha1NMe)



L-Rhamnose (500 mg, 2.74 mmol, 1.00 eq.) was dried and subsequently suspended in a solution of methylamine in ethanol (33 %, 5.00 mL, 37.2 mmol, 13.4 eq.). After stirring the clear reaction solution for 16 h a white precipitate formed. The reaction solution was stored for 24 h at 4 °C to increase the precipitation of the product. The white solid was separated from the reaction solution by filtration, washed with cold methanol (2 × 10 mL) and dried *in vacuo*. The product was obtained as a white powder in a yield of 418 mg (2.36 mmol, 86.1 % of theory).

EA: calcd.: C 47.45 %, H 8.53 %, N 7.90 %
found: C 47.21 %, H 8.71 %, N 7.76 %

MS (FAB+): calcd.: 178.2 ([M+H]⁺)
found: 178.2

N-Methyl- β -L-rhamnopyranosylamine – D₂O: 86 % – DMSO-*d*₆: 80 %

¹H NMR (400 MHz, D₂O, 16OR13-2017): δ /ppm = 4.06 (d, 1H, H1, ³J_{1,2}=1.1 Hz), 3.81 (dd, 1H,

H2, $^3J_{2,3}=3.4$ Hz), 3.54 (dd, 1H, H3, $^3J_{3,4}=9.4$ Hz), 3.31–3.29 (dd, H4/H5), 2.43 (s, 3H, CH₃), 1.25 (d, 3H, 3×H6).

$^{13}\text{C}\{^1\text{H}\}$ NMR (101 MHz, D₂O, 16OR14-2017): δ/ppm = 88.7 (C1), 74.2 (C3), 73.8 (C5), 73.0 (C4), 71.8 (C2), 31.6 (CH₃), 17.4 (C6).

$^{13}\text{C}\{^1\text{H}\}$ NMR (101 MHz, DMSO-*d*₆, 17OR5-2017): δ/ppm = 88.5 (C1), 74.4 (C3), 72.5 (C5), 72.4 (C4), 71.5 (C2), 31.9 (CH₃), 18.1 (C6).

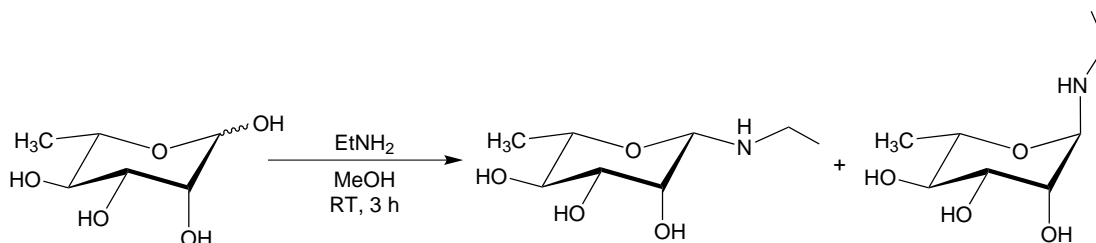
N-Methyl- α -L-rhamnopyranosylamine – D₂O: 14 % – DMSO-*d*₆: 20 %

^1H NMR (400 MHz, D₂O, 16OR13-2017): δ/ppm = 4.29 (d, 1H, H1, $^3J_{1,2}=1.6$ Hz), 2.29 (s, 3H, CH₃).

$^{13}\text{C}\{^1\text{H}\}$ NMR (101 MHz, D₂O, 16OR14-2017): δ/ppm = 89.9 (C1), 72.8 (C4), 71.6 (C2), 70.9 (C4), 68.1 (C2), 31.0 (CH₃), 17.3 (C6).

$^{13}\text{C}\{^1\text{H}\}$ NMR (101 MHz, DMSO-*d*₆, 17OR5-2017): δ/ppm = 89.7 (C1), 72.7 (C4), 71.4 (C2), 71.0 (C4), 66.5 (C2), 31.7 (CH₃), 18.1 (C6).

N-Ethyl-D-rhamnosylamin (D-Rha1NEt)



L-Rhamnose (1.00 g, 5.79 mmol, 1.00 eq.) was dried and subsequently suspended in a solution of ethylamine in methanol (2 M, 15.0 mL, 30.0 mmol, 5.46 eq.). After stirring the clear reaction solution for 3 h a white precipitate formed. The reaction solution was stored for 24 h at 4 °C to increase the precipitation of the product. The white solid was separated from the reaction solution by filtration, washed with cold methanol (2 × 10 mL) and dried *in vacuo*. The product was obtained as a white powder in a yield of 939 mg (4.91 mmol, 89.4 % of theory).

EA: calcd.: C 50.25 %, H 8.96 %, N 7.32 %
found: C 50.33 %, H 9.26 %, N 7.34 %

MS (FAB+): calcd.: 192.2 ([M+H]⁺)
found: 192.3

N-Ethyl- β -L-rhamnopyranosylamine – D₂O: 87 % – DMSO-*d*₆: 80 %

^1H NMR (400 MHz, D₂O, 16OR10-2017): δ/ppm = 4.16 (d, 1H, H1, $^3J_{1,2}=1.1$ Hz), 3.81 (dd, 1H, H2, $^3J_{2,3}=3.4$ Hz), 3.54 (dd, 1H, H3, $^3J_{3,4}=9.5$ Hz), 3.31–3.29 (dd, H4/H5), 2.89 (m, 1H, CH₂), 2.63 (m, 1H, CH₂), 1.24 (d, 3H, 3×H6), 1.04 (td, 3H, CH₃).

$^{13}\text{C}\{^1\text{H}\}$ NMR (101 MHz, D₂O, 16OR11-2017): δ/ppm = 86.8 (C1), 74.2 (C3), 73.8 (C5), 73.1 (C4), 71.9 (C2), 39.5 (CH₂), 17.4 (C6), 14.2 (CH₃).

$^{13}\text{C}\{^1\text{H}\}$ NMR (101 MHz, DMSO- d_6 , 17OR8-2017): δ/ppm = 86.8 (C1), 74.4 (C3), 72.5 (C5), 72.4 (C4), 71.6 (C2), 39.0 (CH₂), 18.1 (C6), 15.4 (CH₃).

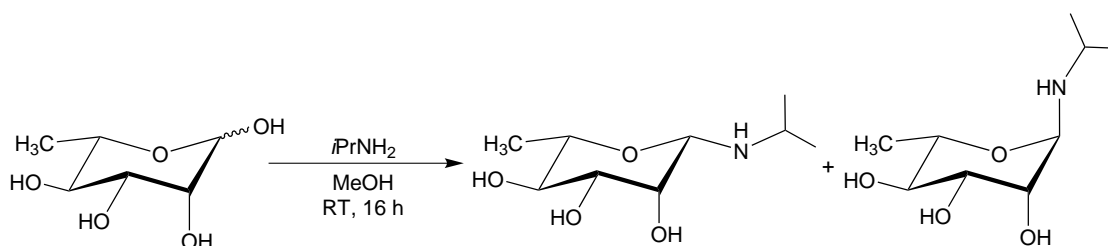
N-Ethyl- α -L-rhamnopyranosylamine – D₂O: 13 % – DMSO- d_6 : 20 %

^1H NMR (400 MHz, D₂O, 16OR10-2017): δ/ppm = 4.41 (d, H1, $^3J_{1,2}=1.6$ Hz).

$^{13}\text{C}\{^1\text{H}\}$ NMR (101 MHz, D₂O, 16OR11-2017): δ/ppm = 88.3 (C1), 72.8 (C4), 71.8 (C2), 70.9 (C4), 68.1 (C2), 39.5 (CH₂), 17.3 (C6), 13.8 (CH₃).

$^{13}\text{C}\{^1\text{H}\}$ NMR (101 MHz, DMSO- d_6 , 17OR8-2017): δ/ppm = 88.1 (C1), 72.8 (C4), 71.5 (C2), 71.1 (C4), 66.5 (C2), 39.3 (CH₂), 18.0 (C6), 15.1 (CH₃).

N-(*iso*-Propyl)-D-rhamnosylamin (D-Rha1NiPr)



D-Rhamnose monohydrate (1.00 g, 3.29 mmol, 1.00 eq.) was dried and subsequently suspended in 5 mL dry methanol. *iso*-Propylamine (1.50 mL, 1.03 g, 17.5 mmol, 5.31 eq.) was added and the reaction mixture stirred for 16 h at room temperature. Subsequent storage at 4 °C for 24 h resulted in the precipitation of a white solid. The solid was separated from the reaction solution by filtration, washed with cold methanol (2 × 5 mL) and dried *in vacuo*. The product was obtained as a white powder in a yield of 175 mg (853 μmol , 25.9 % of theory).

N-(*iso*-Propyl)- β -L-rhamnopyranosylamine – D₂O: 90 % – DMSO- d_6 : 88 %

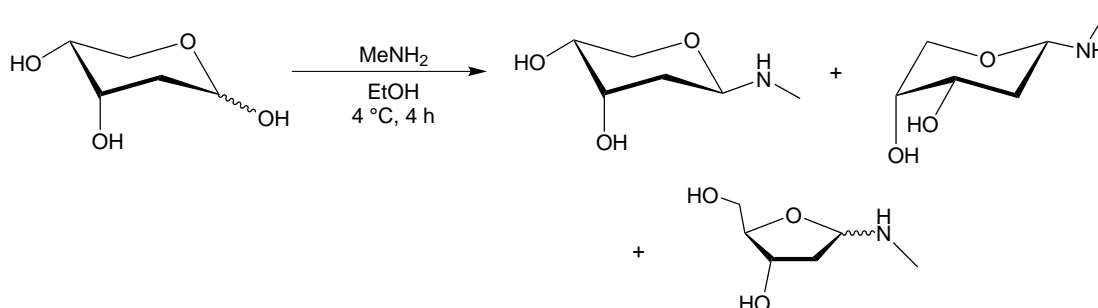
^1H NMR (400 MHz, D₂O, 39OR3-2017): δ/ppm = 4.26 (d, 1H, H1, $^3J_{1,2}=1.1$ Hz), 3.79 (dd, 1H, H2, $^3J_{2,3}=3.4$ Hz), 3.54 (dd, 1H, H3, $^3J_{3,4}=8.8$ Hz), 3.31–3.29 (dd, H4/H5), 3.16 (m, 1H, CH), 1.24 (d, 3H, 3×H6), 1.01 (dd, 6H, 2×CH₃).

$^{13}\text{C}\{^1\text{H}\}$ NMR (101 MHz, D₂O, 39OR4-2017): δ/ppm = 84.3 (C1), 74.3 (C3), 73.8 (C5), 73.1 (C4), 72.1 (C2), 43.7 (CH), 22.3 (CH₃), 20.3 ((CH₃), 17.4 (C6).

N-(*iso*-Propyl)- α -L-rhamnopyranosylamine – D₂O: 10 % – DMSO- d_6 : 12 % :

^1H NMR (400 MHz, D₂O, 39OR3-2017): δ/ppm = 4.57 (d, H1, $^3J_{1,2}=1.6$ Hz).

$^{13}\text{C}\{^1\text{H}\}$ NMR (101 MHz, D₂O, 39OR4-2017): δ/ppm = 86.2 (C1), 72.9 (C4), 72.0 (C2), 70.8 (C4), 68.1 (C2), 44.4 (CH), 23.0 (CH₃), 20.4 (CH₃), 17.3 (C6).

5.5.3. Preparation of *N*-Alkyl-2-deoxy-D-glycoamines5.5.3.1. Preparation of *N*-Alkyl-2-deoxy-D-erythro-pentosylamines*N*-Methyl-2-deoxy-D-erythro-pentosylamine (D-ery-dPent1NMe)

2-Deoxy-D-erythro-pentose (614 mg, 4.58 mmol, 1.00 eq.) was dried and subsequently stirred for 4 h at 4 °C with a solution of methylamine in ethanol (33 %, 4.50 mL, 33.5 mmol, 7.31 eq.). The reaction mixture was concentrated by evaporation until a syrup-like residue was obtained. The residue was frozen, crushed and dried *in vacuo*. This procedure was repeated three times until the product was obtained as an orange gelatinous substance in a yield of 727 mg (4.94 mmol, 93.2 % of theory).

EA: calcd.: C 48.97 %, H 8.90 %, N 9.52 %

found: C 48.53 %, H 9.05 %, N 8.70 %

MS (FAB+): calcd.: 148.2 ([M+H]⁺)

found: 148.3

N-Methyl-2-deoxy-β-D-erythro-pentopyranosylamine – D₂O: 53 % – DMSO-*d*₆: 30 %

¹³C{¹H} NMR (101 MHz, D₂O, 45OR21-2015): δ/ppm = 88.0 (C1), 68.5 (C4), 67.9 (C5), 67.6 (C3), 34.1 (C2), 31.1 (CH₃).

¹³C{¹H} NMR (101 MHz, DMSO-*d*₆, 45OR30-2015): δ/ppm = 87.2 (C1), 68.1 (C4), 67.0 (C3), 65.6 (C5), 35.5 (C2), 31.8 (CH₃).

N-Methyl-2-deoxy-α-D-erythro-pentopyranosylamine – D₂O: 24 % – DMSO-*d*₆: 35 %

¹³C{¹H} NMR (101 MHz, D₂O, 45OR21-2015): δ/ppm = 85.1 (C1), 67.6 (C4), 66.5 (C3), 63.6 (C5), 35.6 (C2), 31.2 (CH₃).

¹³C{¹H} NMR (101 MHz, DMSO-*d*₆, 45OR30-2015): δ/ppm = 84.4 (C1), 67.5 (C4), 66.4 (C3), 63.8 (C5), 37.7 (C2), 31.5 (CH₃).

N-Methyl-2-deoxy-β-D-erythro-pentofuranosylamine – D₂O: 14 % – DMSO-*d*₆: 16 %

¹³C{¹H} NMR (101 MHz, D₂O, 45OR21-2015): δ/ppm = 92.5 (C1), 85.9 (C4), 72.2 (C3), 62.9 (C5), 39.3 (C2), 31.5 (CH₃).

¹³C{¹H} NMR (101 MHz, DMSO-*d*₆, 45OR30-2015): δ/ppm = 91.7 (C1), 85.7 (C4), 71.1 (C3),

62.8 (C5), 40.1 (C2), 31.9 (CH₃).

N-Methyl-2-deoxy- α -D-*erythro*-pentofuranosylamine – D₂O: 9 % – DMSO-*d*₆: 13 %

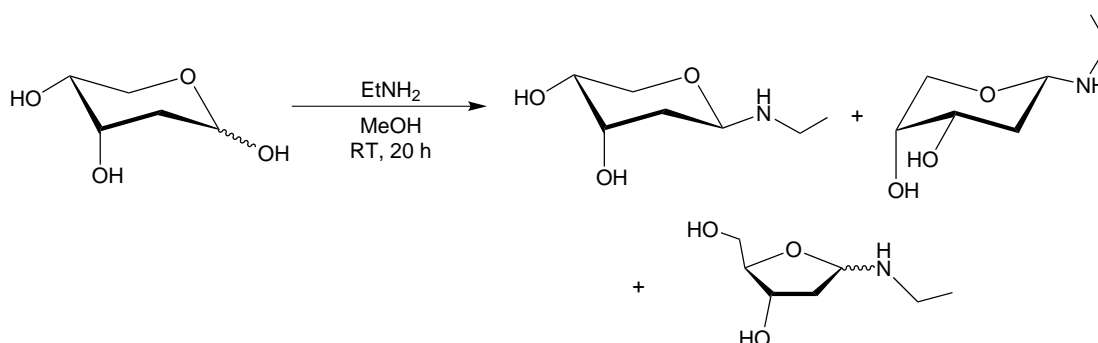
¹³C{¹H} NMR (101 MHz, D₂O, 45OR21-2015): δ /ppm = 91.9 (C1), 84.5 (C4), 71.5 (C3), 62.1 (C5), 39.3 (C2), 31.5 (CH₃).

¹³C{¹H} NMR (101 MHz, DMSO-*d*₆, 45OR30-2015): δ /ppm = 91.2 (C1), 84.5 (C4), 70.9 (C3), 62.1 (C5), 40.0 (C2), 31.7 (CH₃).

N-Methyl-2-deoxy-*erythro*-D-pentosylamine (imine form) – D₂O: 0 % – DMSO-*d*₆: 6 %

¹³C{¹H} NMR (101 MHz, DMSO-*d*₆, 45OR30-2015): δ /ppm = 165.3 (C1), 74.6 (C4), 69.5 (C3), 63.2 (C5), 47.4 (CH₃), 39.0 (C2).

N-Ethyl-2-deoxy-D-*erythro*-pentosylamine (D-*ery*-dPent1NEt)



2-Deoxy-D-*erythro*-pentose (402 mg, 3.00 mmol, 1.00 eq.) was dried, suspended in a solution of ethylamine in methanol (2 M, 9.00 mL, 18.0 mmol, 6.00 eq.) and stirred for 20 h at room temperature. The resulting clear reaction solution was concentrated by evaporation until it reached dryness. The obtained syrup-like residue was frozen, crushed and further dried *in vacuo*. The product was obtained as a orange gelatinous substance in a yield of 448 mg (2.78 mmol, 92.7 % of theory).

EA: calcd.: C 52.16 %, H 9.38 %, N 8.69 %

found: C 50.81 %, H 9.26 %, N 7.85 %

MS (FAB+): calcd.: 162.2 ([M+H]⁺)

found: 162.3

N-Ethyl-2-deoxy- β -D-*erythro*-pentopyranosylamine – D₂O: 64 % – DMSO-*d*₆: 30 %

¹³C{¹H} NMR (101 MHz, D₂O, 45OR24-2015): δ /ppm = 86.5 (C1), 68.5 (C4), 67.9 (C5), 67.5 (C3), 39.4 (CH₂), 34.3 (C2), 14.3 (CH₃).

¹³C{¹H} NMR (101 MHz, DMSO-*d*₆, 44OR26-2015): δ /ppm = 85.6 (C1), 68.1 (C4), 67.0 (C3), 65.5 (C5), 38.9 (CH₂), 35.6 (C2), 15.4 (CH₃).

N-Ethyl-2-deoxy- α -D-*erythro*-pentopyranosylamine – D₂O: 24 % – DMSO-*d*₆: 33 %

¹³C{¹H} NMR (101 MHz, D₂O, 45OR24-2015): δ /ppm = 83.4 (C1), 67.5 (C4), 66.7 (C3), 63.7 (C5), 39.5 (CH₂), 35.9 (C2), 14.2 (CH₃).

¹³C{¹H} NMR (101 MHz, DMSO-*d*₆, 44OR26-2015): δ /ppm = 82.8 (C1), 67.5 (C4), 66.4 (C3), 63.8 (C5), 39.1 (CH₂), 37.9 (C2), 15.4 (CH₃).

N-Ethyl-2-deoxy- β -D-*erythro*-pentofuranosylamine – D₂O: 8 % – DMSO-*d*₆: 17 %

¹³C{¹H} NMR (101 MHz, D₂O, 45OR24-2015): δ /ppm = 91.0 (C1), 86.0 (C4), 72.2 (C3), 62.9 (C5), 39.2 (CH₂), 14.4 (CH₃).

¹³C{¹H} NMR (101 MHz, DMSO-*d*₆, 44OR26-2015): δ /ppm = 90.3 (C1), 85.7 (C4), 71.1 (C3), 62.8 (C5), 40.6 (C2), 39.7 (CH₂), 15.5 (CH₃).

N-Ethyl-2-deoxy- α -D-*erythro*-pentofuranosylamine – D₂O: 4 % – DMSO-*d*₆: 14 %

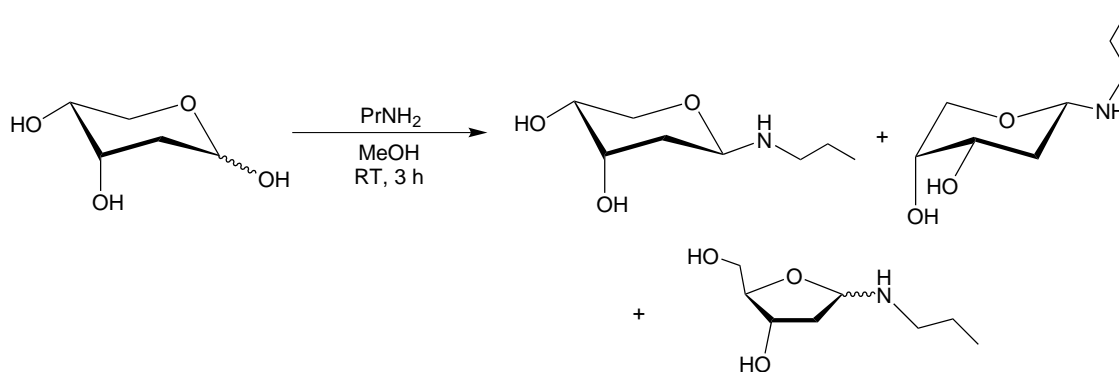
¹³C{¹H} NMR (101 MHz, D₂O, 45OR24-2015): δ /ppm = 90.3 (C1), 84.4 (C4), 71.4 (C3), 62.1 (C5), 39.7 (CH₂), 14.5 (CH₃).

¹³C{¹H} NMR (101 MHz, DMSO-*d*₆, 44OR26-2015): δ /ppm = 89.7 (C1), 84.5 (C4), 71.0 (C3), 62.1 (C5), 40.2 (C2), 39.2 (CH₂), 15.5 (CH₃).

N-Ethyl-2-deoxy-*erythro*-D-pentosylamine (imine form) – D₂O: 0 % – DMSO-*d*₆: 6 %

¹³C{¹H} NMR (101 MHz, DMSO-*d*₆, 44OR26-2015): δ /ppm = 163.2 (C1), 74.6 (C4), 69.6 (C3), 63.2 (C5), 54.7 (CH₂), 38.9 (C2), 16.3 (CH₃).

***N*-Propyl-2-deoxy-D-*erythro*-pentosylamine (D-*ery*-dPent1NPr)**



2-Deoxy-D-*erythro*-pentose (496 mg, 3.70 mmol, 1.00 eq.) was dried and subsequently suspended in 1 mL dry methanol. After the addition of propylamine (1.79 mL, 1.29 g, 21.8 mmol, 5.90 eq.) the resulting yellowish solution was stirred for 3 h at room temperature. The reaction mixture was concentrated by evaporation of the solvent until it reached dryness and the obtained residue solved in diethyl ether (10 mL). Concentration of the solution to about one third of its previous volume and subsequent storage at 4 °C for 3 d resulted in the precipitation of a white solid. The precipitate was separated by filtration, washed with diethyl ether (2 \times 5 mL) and dried *in vacuo*. The product was obtained as a white powder in a yield of 254 mg (1.45 mmol, 39.2 % of theory).

EA: calcd.: C 54.84 %, H 9.78 %, N 7.99 %

found: C 53.33 %, H 9.46 %, N 7.81 %

MS (FAB+): calcd.: 176.2 ($[M+H]^+$)

found: 176.3

N-Propyl-2-deoxy- β -D-*erythro*-pentopyranosylamine – D₂O: 65 % – DMSO-*d*₆: 76 %

¹³C{¹H} NMR (101 MHz, D₂O, 47OR2-2015): δ /ppm = 86.9 (C1), 68.5 (C4), 67.9 (C5), 67.5 (C3), 39.4 (NH–CH₂), 34.2 (C2), 22.8 (CH₂), 11.7 (CH₃).

¹³C{¹H} NMR (101 MHz, DMSO-*d*₆, 46OR14-2015): δ /ppm = 85.9 (C1), 68.1 (C4), 67.0 (C3), 65.4 (C5), 46.7 (NH–CH₂), 35.6 (C2), 23.1 (CH₂), 11.8 (CH₃).

N-Propyl-2-deoxy- α -D-*erythro*-pentopyranosylamine – D₂O: 22 % – DMSO-*d*₆: 6 %

¹³C{¹H} NMR (101 MHz, D₂O, 47OR2-2015): δ /ppm = 83.8 (C1), 67.5 (C4), 66.7 (C3), 63.7 (C5), 47.1 (NH–CH₂), 36.0 (C2), 22.1 (CH₂), 11.7 (CH₃).

¹³C{¹H} NMR (101 MHz, DMSO-*d*₆, 46OR14-2015): δ /ppm = 83.1 (C1), 67.5 (C4), 66.4 (C3), 63.8 (C5), 47.0 (NH–CH₂), 38.0 (C2), 23.0 (CH₂), 11.8 (CH₃).

N-Propyl-2-deoxy- β -D-*erythro*-pentofuranosylamine – D₂O: 11 % – DMSO-*d*₆: 8 %

¹³C{¹H} NMR (101 MHz, D₂O, 47OR2-2015): δ /ppm = 91.4 (C1), 85.9 (C4), 72.2 (C3), 62.9 (C5), 47.7 (NH–CH₂), 22.9 (CH₂), 11.7 (CH₃).

¹³C{¹H} NMR (101 MHz, DMSO-*d*₆, 46OR14-2015): δ /ppm = 90.7 (C1), 85.7 (C4), 71.1 (C3), 62.8 (C5), 47.6 (NH–CH₂), 40.5 (C2), 23.2 (CH₂), 11.8 (CH₃).

N-Propyl-2-deoxy- α -D-*erythro*-pentofuranosylamine – D₂O: 2 % – DMSO-*d*₆: 6 %

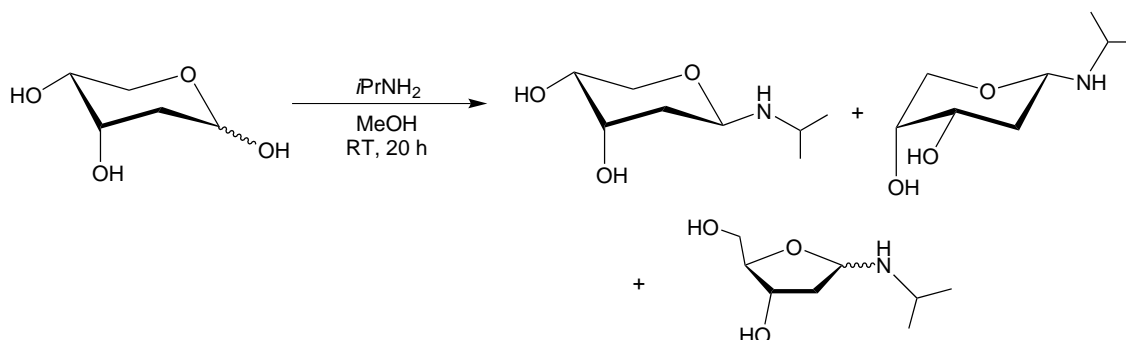
¹³C{¹H} NMR (101 MHz, D₂O, 47OR2-2015): δ /ppm = 90.6 (C1), 84.4 (C4), 71.5 (C3), 62.1 (C5), 47.2 (NH–CH₂), 23.0 (CH₂), 11.7 (CH₃).

¹³C{¹H} NMR (101 MHz, DMSO-*d*₆, 46OR14-2015): δ /ppm = 90.0 (C1), 84.5 (C4), 71.0 (C3), 62.1 (C5), 47.2 (NH–CH₂), 40.2 (C2), 23.0 (CH₂), 11.8 (CH₃).

N-Propyl-2-deoxy-*erythro*-D-pentosylamine (imine form) – D₂O: 0 % – DMSO-*d*₆: 4 %

¹³C{¹H} NMR (101 MHz, DMSO-*d*₆, 46OR14-2015): δ /ppm = 163.7 (C1), 74.6 (C4), 69.6 (C3), 63.2 (C5), 62.3 (NH–CH₂), 38.8 (C2), 23.5 (CH₂), 11.6 (CH₃).

N-(*iso*-Propyl)-2-deoxy-D-*erythro*-pentosylamine (D-*ery*-dPent1NiPr)



2-Deoxy-D-*erythro*-pentose (402 mg, 3.00 mmol, 1.00 eq.) was dried and subsequently suspended in 5 mL dry methanol. Upon addition of *iso*-propylamine (1.50 mL, 1.03 g, 17.5 mmol, 5.72 eq.) a clear solution formed within 15 min. The reaction mixture was stirred for 20 h at room temperature and afterwards the solution was concentrated until it reached dryness. The resulting residue was frozen, crushed and dried *in vacuo* three times. The product was obtained as a yellowish solid in a yield of 124 mg (0.71 mmol, 23.6 % of theory).

EA: calcd.: C 52.67 %, H 9.33 %, N 6.82 %
found: C 52.22 %, H 9.41 %, N 6.85 %

MS (FAB+): calcd.: 205.3 ([M+H]⁺)
found: 206.3

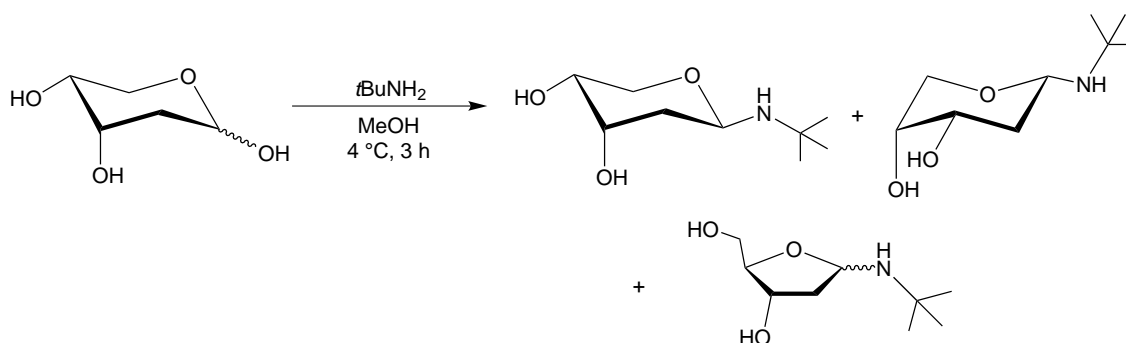
N-(*iso*-Propyl)-2-deoxy-β-D-*erythro*-pentopyranosylamine – D₂O: 62 % – DMSO-*d*₆: 31 %
¹³C{¹H} NMR (101 MHz, D₂O, 47OR2-2015): δ/ppm = 84.0 (C1), 68.6 (C4), 67.9 (C5), 67.6 (C3), 44.0 (CH), 34.2 (C2), 23.4 (CH₃), 20.5 (CH₃).
¹³C{¹H} NMR (101 MHz, DMSO-*d*₆, 46OR14-2015): δ/ppm = 83.1 (C1), 68.1 (C4), 67.1 (C3), 65.4 (C5), 43.7 (CH), 35.8 (C2), 24.4 (CH₃), 21.8 (CH₃).

N-(*iso*-Propyl)-2-deoxy-α-D-*erythro*-pentopyranosylamine – D₂O: 24 % – DMSO-*d*₆: 39 %
¹³C{¹H} NMR (101 MHz, D₂O, 47OR2-2015): δ/ppm = 80.9 (C1), 67.5 (C4), 66.9 (C3), 63.6 (C5), 44.1 (CH), 36.7 (C2), 23.4 (CH₃), 20.5 (CH₃).
¹³C{¹H} NMR (101 MHz, DMSO-*d*₆, 46OR14-2015): δ/ppm = 80.4 (C1), 67.5 (C4), 66.6 (C3), 63.9 (C5), 43.3 (CH), 38.4 (C2), 24.3 (CH₃), 22.0 (CH₃).

N-(*iso*-Propyl)-2-deoxy-β-D-*erythro*-pentofuranosylamine – D₂O: 12 % – DMSO-*d*₆: 13 %
¹³C{¹H} NMR (101 MHz, D₂O, 47OR2-2015): δ/ppm = 88.6 (C1), 86.1 (C4), 72.2 (C3), 62.9 (C5), 45.3 (CH), 23.6 (CH₃), 20.6 (CH₃).
¹³C{¹H} NMR (101 MHz, DMSO-*d*₆, 46OR14-2015): δ/ppm = 88.2 (C1), 85.9 (C4), 71.2 (C3), 62.8 (C5), 44.7 (CH), 40.5 (C2), 24.5 (CH₃), 21.9 (CH₃).

N-(*iso*-Propyl)-2-deoxy-α-D-*erythro*-pentofuranosylamine – D₂O: 2 % – DMSO-*d*₆: 11 %
¹³C{¹H} NMR (101 MHz, D₂O, 47OR2-2015): δ/ppm = 87.7 (C1), 84.4 (C4), 71.5 (C3), 62.2 (C5), 44.5 (CH), 23.6 (CH₃), 20.6 (CH₃).
¹³C{¹H} NMR (101 MHz, DMSO-*d*₆, 46OR14-2015): δ/ppm = 87.7 (C1), 84.4 (C4), 71.5 (C3), 62.2 (C5), 44.5 (CH), 40.5 (C2), 24.6 (CH₃), 22.2 (CH₃).

N-(*iso*-Propyl)-2-deoxy-*erythro*-D-pentosylamine (imine form) – D₂O: 0 % – DMSO-*d*₆: 6 %
¹³C{¹H} NMR (101 MHz, DMSO-*d*₆, 46OR14-2015): δ/ppm = 161.1 (C1), 74.6 (C4), 69.6 (C3), 63.9 (CH), 63.2 (C5), 42.2 (C2), 24.2 (CH₃), 21.9 (CH₃).

***N*-(*tert*-Butyl)-2-deoxy-*erythro*-D-pentosylamine (D-*ery*-dPent1N*t*Bu)**

2-Deoxy-*erythro*-D-pentose (499 mg, 3.72 mmol, 1.00 eq.) was dried and subsequently suspended in 10 mL dry methanol. *tert*-Butylamine (2.80 mL, 1.96 g, 26.8 mmol, 7.20 eq.) was added and the reaction mixture stirred for 3 h at 4 °C. The reaction mixture was concentrated until reached dryness and the obtained residue was resolved in diethyl ether (20 mL). Storage at 4 °C for 3 d resulted in the precipitation of a white solid. The precipitate was separated by filtration, washed with diethyl ether (2 × 10 mL) and dried *in vacuo*. The product was obtained as a white solid in a yield of 290 mg (1.53 mmol, 41.2 % of theory).

MS (FAB+): calcd.: 176.2 ([M+H]⁺)
found: 176.3

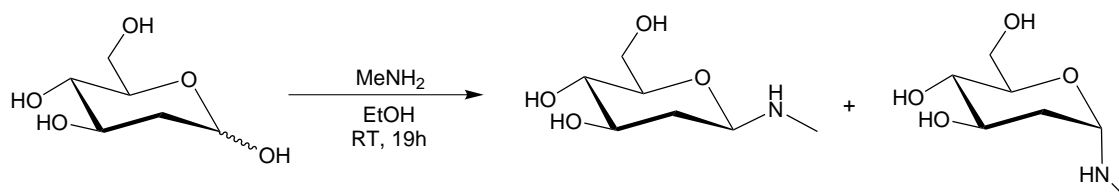
N-(*tert*-Butyl)-2-deoxy-β-D-*erythro*-pentopyranosylamine – D₂O: 100 % – DMSO-*d*₆: 50 %
¹³C{¹H} NMR (101 MHz, D₂O, 48OR11-2015): δ/ppm = 82.4 (C1), 68.3 (C4), 66.9 (C5), 65.4 (C3), 49.6 (C_q), 36.8 (C2), 30.6 (3 × CH₃).
¹³C{¹H} NMR (101 MHz, DMSO-*d*₆, 50OR5-2015): δ/ppm = 82.4 (C1), 68.3 (C4), 67.0 (C3), 65.4 (C5), 49.5 (C_q), 36.9 (C2), 30.6 (3 × CH₃).

N-(*tert*-Butyl)-2-deoxy-α-D-*erythro*-pentopyranosylamine – D₂O: 0 % – DMSO-*d*₆: 11 %
¹³C{¹H} NMR (101 MHz, DMSO-*d*₆, 50OR5-2015): δ/ppm = 79.4 (C1), 67.3 (C4), 66.7 (C3), 63.6 (C5), 49.6 (C_q), 39.1 (C2), 30.5 (3 × CH₃).

N-(*tert*-Butyl)-2-deoxy-β-D-*erythro*-pentofuranosylamine – D₂O: 0 % – DMSO-*d*₆: 17 %
¹³C{¹H} NMR (101 MHz, DMSO-*d*₆, 50OR5-2015): δ/ppm = 86.5 (C1), 85.9 (C4), 71.1 (C3), 62.9 (C5), 49.5 (C_q), 42.1 (C2), 30.5 (3 × CH₃).

N-(*tert*-Butyl)-2-deoxy-α-D-*erythro*-pentofuranosylamine – D₂O: 0 % – DMSO-*d*₆: 11 %
¹³C{¹H} NMR (101 MHz, DMSO-*d*₆, 50OR5-2015): δ/ppm = 86.3 (C1), 84.1 (C4), 70.8 (C3), 62.1 (C5), 49.7 (C_q), 41.5 (C2), 30.5 (3 × CH₃).

N-(*tert*-Butyl)-2-deoxy-*erythro*-D-pentosylamine (imine form) – D₂O: 0 % – DMSO-*d*₆: 11 %
¹³C{¹H} NMR (101 MHz, DMSO-*d*₆, 50OR5-2015): δ/ppm = 158.0 (C1), 74.6 (C4), 69.7 (C3), 63.1 (C5), 56.4 (C_q), 39.2 (C2), 29.5 (3 × CH₃).

5.5.3.2. Preparation of *N*-Alkyl-2-deoxy-*D*-*arabino*-hexosylamines*N*-Methyl-2-deoxy-*D*-*arabino*-hexosylamine (*D*-*ara*-dHex1NMe)

2-Deoxy-*D*-*arabino*-hexose (1.00 g, 6.09 mmol, 1.00 eq.) was dried and subsequently stirred for 19 h at room temperature with a solution of methylamine in ethanol (33 %, 5.00 mL, 37.2 mmol, 6.10 eq.). The reaction mixture was concentrated by evaporation of the solvent until a colorless precipitate formed, which was filtered off, washed with cold methanol (2 × 10 mL) and dried *in vacuo*. The product was obtained as a colorless solid in a yield of 967 mg (5.46 mmol, 89.6 % of theory).

EA: calcd.: C 47.45 %, H 8.53 %, N 7.90 %

found: C 47.44 %, H 8.43 %, N 7.79 %

MS (FAB+): calcd.: 178.2 ([M+H]⁺)

found: 178.2

N-Methyl-2-deoxy- β -*D*-*arabino*-hexopyranosylamine – D₂O: 85 % – DMSO-*d*₆: 81 %

¹³C{¹H} NMR (101 MHz, D₂O, 43OR2-2016): δ /ppm = 87.5 (C1), 77.6 (C5), 71.9 (C3), 71.9 (C4), 61.7 (C6), 38.6 (C2), 31.1 (CH₃).

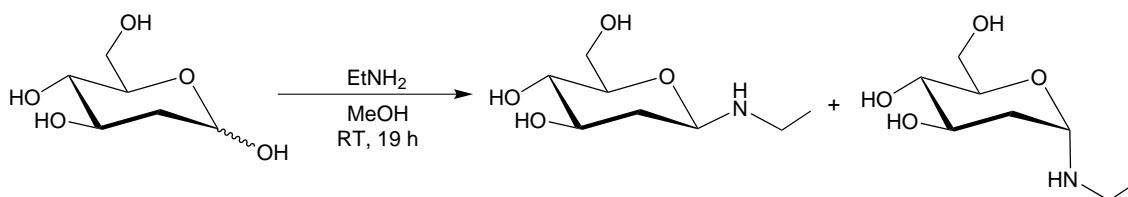
¹³C{¹H} NMR (101 MHz, DMSO-*d*₆, 07OR35-2016): δ /ppm = 87.3 (C1), 77.7 (C5), 72.2 (C3), 71.8 (C4), 61.6 (C6), 40.0 (C2), 31.6 (CH₃).

N-Methyl-2-deoxy- α -*D*-*arabino*-hexopyranosylamine – D₂O: 15 % – DMSO-*d*₆: 19 %

¹H NMR (400 MHz, D₂O, 43OR1-2016): δ /ppm = 4.51 (d, H1, ³J_{1,2}=4.8 Hz).

¹³C{¹H} NMR (101 MHz, D₂O, 4 °C, 43OR2-2016): δ /ppm = 85.2 (C1), 72.0 (C5), 71.8 (C4), 68.8 (C3), 61.5 (C6), 36.4 (C2), 30.8 (CH₃).

¹³C{¹H} NMR (101 MHz, DMSO-*d*₆, 07OR35-2016): δ /ppm = 84.6 (C1), 72.6 (C5), 71.1 (C4), 68.2 (C3), 61.4 (C6), 37.8 (C2), 31.5 (CH₃).

N-Ethyl-2-deoxy-*D*-*arabino*-hexosylamine (*D*-*ara*-dHex1NEt)

2-Deoxy-D-*arabino*-hexose (860 mg, 5.24 mmol, 1.00 eq.) was dried, subsequently suspended in a solution of ethylamine in methanol (2 M, 13.0 mL, 26.0 mmol, 5.00 eq.) and stirred for 19 h at room temperature. The resulting reaction solution was concentrated by evaporation of the solvent until it reached dryness. The thereby formed white solid was crushed and further dried *in vacuo*. The product was obtained as a white solid in a yield of 912 mg (4.77 mmol, 91.0 % of theory).

EA: calcd.: C 50.25 %, H 8.96 %, N 7.32 %
found: C 50.19 %, H 8.90 %, N 7.20 %

MS (FAB+): calcd.: 192.2 ([M+H]⁺)
found: 192.3

N-Ethyl-2-deoxy-β-D-*arabino*-hexopyranosylamine – 83 %:

¹³C{¹H} NMR (101 MHz, D₂O, 07OR32-2016): δ/ppm = 86.0 (C1), 77.7 (C5), 72.0 (C3), 71.9 (C4), 61.8 (C6), 39.5 (CH₂), 38.8 (C2), 14.3 (CH₃).

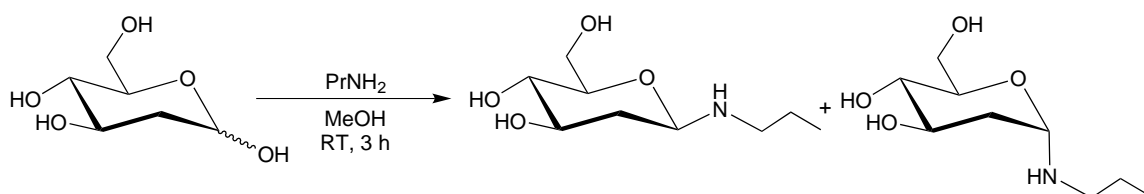
¹³C{¹H} NMR (101 MHz, DMSO-*d*₆, 07OR35-2016): δ/ppm = 85.8 (C1), 77.7 (C5), 72.3 (C3), 71.8 (C4), 61.6 (C6), 40.2 (C2), 39.0 (CH₂), 15.4 (CH₃).

N-Ethyl-2-deoxy-α-D-*arabino*-hexopyranosylamine – 17 %:

¹³C{¹H} NMR (101 MHz, D₂O, 07OR32-2016): δ/ppm = 83.6 (C1), 72.1 (C5), 71.8 (C4), 68.8 (C3), 61.5 (C6), 37.6 (CH₂), 37.6 (C2), 13.9 (CH₃).

¹³C{¹H} NMR (101 MHz, DMSO-*d*₆, 07OR35-2016): δ/ppm = 83.0 (C1), 72.6 (C5), 71.1 (C4), 68.2 (C3), 61.4 (C6), 39.0 (CH₂), 37.9 (C2), 15.0 (CH₃).

N-Propyl-2-deoxy-D-*arabino*-hexosylamine (D-*ara*-dHex1NPr)



2-Deoxy-D-*arabino*-hexose (500 mg, 3.04 mmol, 1.00 eq.) was dried and subsequently suspended in 1 mL dry methanol. After the addition of propylamine (1.50 mL, 1.06 g, 18.0 mmol, 5.90 eq.) the resulting solution was stirred for 3 h at room temperature. The reaction mixture was concentrated by evaporation of the solvent to about one third of its previous volume and diethyl ether (20 mL) was added. Storage at 4 °C for 3 d resulted in the precipitation of a white solid. The precipitate was separated by filtration, washed with diethyl ether (2 × 5 mL) and dried *in vacuo*. The product was obtained as a white solid in a yield of 548 mg (2.67 mmol, 87.7 % of theory).

EA: calcd.: C 52.67 %, H 9.33 %, N 6.82 %
found: C 52.22 %, H 9.41 %, N 6.85 %

MS (FAB+): calcd.: 206.3 ($[M+H]^+$)
found: 206.4

N-Propyl-2-deoxy- β -D-*arabino*-hexopyranosylamine – D₂O: 88 % – DMSO-*d*₆: 83 %

¹³C{¹H} NMR (101 MHz, D₂O, 42OR8-2015): δ /ppm = 86.4 (C1), 77.7 (C5), 72.0 (C3), 71.9 (C4), 61.8 (C6), 47.2 (CH), 38.9 (C2), 22.9 (CH₂), 11.7 (CH₃).

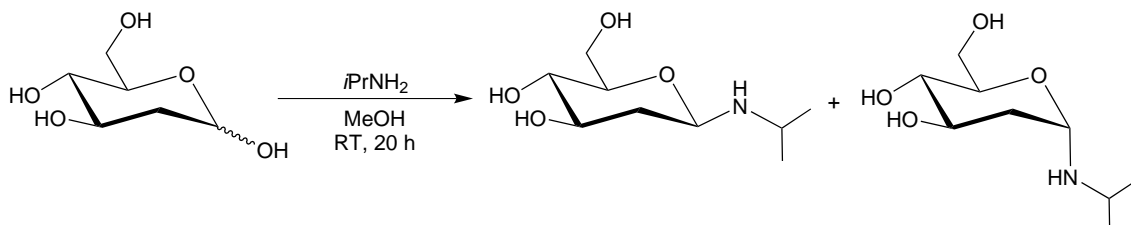
¹³C{¹H} NMR (101 MHz, DMSO-*d*₆, 42OR11-2015): δ /ppm = 86.2 (C1), 77.7 (C5), 72.3 (C3), 71.8 (C4), 61.6 (C6), 46.9 (CH), 40.2 (C2), 23.1 (CH₂), 11.8 (CH₃).

N-Propyl-2-deoxy- α -D-*arabino*-hexopyranosylamine – D₂O: 12 % – DMSO-*d*₆: 17 %

¹³C{¹H} NMR (101 MHz, D₂O, 42OR8-2015): δ /ppm = 83.8 (C1), 72.1 (C5), 71.9 (C4), 68.9 (C3), 61.5 (C6), 46.9 (CH), 37.7 (C2), 22.4 (CH₂), 11.8 (CH₃).

¹³C{¹H} NMR (101 MHz, DMSO-*d*₆, 42OR11-2015): δ /ppm = 83.2 (C1), 72.6 (C5), 71.1 (C4), 68.2 (C3), 61.4 (C6), 46.9 (CH), 37.9 (C2), 22.6 (CH₂), 11.9 (CH₃).

N-(*iso*-Propyl)-2-deoxy-D-*arabino*-hexosylamine (D-*ara*-dHex1NiPr)



2-Deoxy-D-*arabino*-hexose (501 mg, 3.05 mmol, 1.00 eq.) was dried and subsequently suspended in 5 mL dry methanol. Upon addition of *iso*-propylamine (1.50 mL, 1.03 g, 17.5 mmol, 5.72 eq.) a clear solution formed within 15 min. The reaction mixture was stirred for 20 h at room temperature. The solution was concentrated by evaporation of the solvent until the precipitation of a white solid was observed. After storage for a day at -20°C , the precipitate was separated from the reaction solution by filtration, washed with cold methanol ($2 \times 5\text{ mL}$) and dried *in vacuo*. The product was obtained as a white solid in a yield of 351 mg (1.71 mmol, 56.1 % of theory).

EA: calcd.: C 52.67 %, H 9.33 %, N 6.82 %
found: C 52.22 %, H 9.41 %, N 6.85 %

MS (FAB+): calcd.: 205.3 ($[M+H]^+$)
found: 206.3

N-(*iso*-Propyl)-2-deoxy- β -D-*arabino*-hexopyranosylamine – D₂O: 89 % – DMSO-*d*₆: 85 %

¹³C{¹H} NMR (101 MHz, D₂O, 38OR37-2016): δ /ppm = 83.6 (C1), 77.7 (C5), 72.1 (C3), 72.0 (C4), 61.8 (C6), 44.2 (CH), 39.4 (C2), 23.3 (CH₃), 20.7 (CH₃).

¹³C{¹H} NMR (101 MHz, DMSO-*d*₆, 39OR17-2016): δ /ppm = 83.5 (C1), 77.7 (C5), 72.3 (C3), 72.0 (C4), 61.8 (C6), 43.1 (CH), 40.5 (C2), 24.3 (CH₃), 22.1 (CH₃).

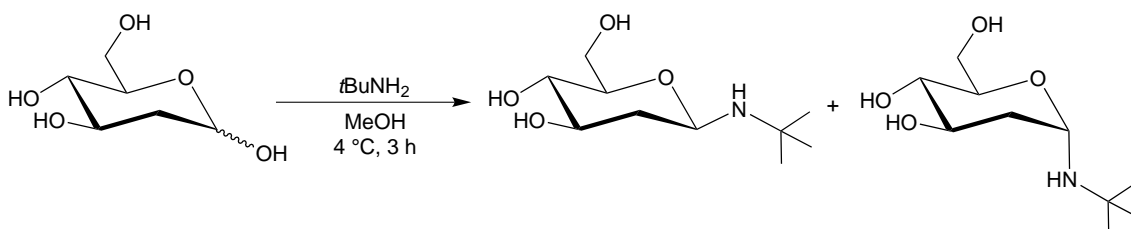
N-(*iso*-Propyl)-2-deoxy- α -D-*arabino*-hexopyranosylamine – D₂O: 11 % – DMSO-*d*₆: 15 %

¹H NMR (400 MHz, D₂O, 38OR36-2016): δ /ppm = 4.51 (d, H1, ³J_{1,2}=4.8 Hz).

¹³C{¹H} NMR (101 MHz, D₂O, 4 °C, 38OR37-2016): δ /ppm = 81.1 (C1), 72.1 (C5), 71.9 (C4), 68.8 (C3), 61.6 (C6), 43.8 (CH), 37.8 (C2), 23.1 (CH₃), 20.2 (CH₃).

¹³C{¹H} NMR (101 MHz, DMSO-*d*₆, 39OR17-2016): δ /ppm = 81.0 (C1), 72.6 (C5), 71.1 (C4), 68.2 (C3), 61.4 (C6), 43.9 (CH), 38.0 (C2), 24.1 (CH₃), 21.9 (CH₃).

***N*-(*tert*-Butyl)-2-deoxy-D-*arabino*-hexosylamine (D-*ara*-dHex1N*t*Bu)**



2-Deoxy-*arabino*-D-hexose (501 mg, 3.05 mmol, 1.00 eq.) was dried and subsequently suspended in 20 mL dry methanol. *tert*-Butylamine (2.29 mL, 1.61 g, 22.0 mmol, 7.20 eq.) was added and the reaction mixture stirred for 3 h at room temperature. The clear reaction mixture was concentrated by evaporation of the solvent to about one third of its previous volume and diethyl ether (20 mL) was added. Storage at 4 °C for 3 d resulted in the precipitation of white solid. The precipitate was separated by filtration, washed with diethyl ether (2 × 10 mL) and dried *in vacuo*. The product was obtained as a white solid in a yield of 460 mg (2.10 mmol, 68.8 % of theory).

EA: calcd.: C 54.77 %, H 9.65 %, N 6.39 %

found: C 54.22 %, H 9.64 %, N 6.23 %

MS (FAB+): calcd.: 220.3 ([M+H]⁺)

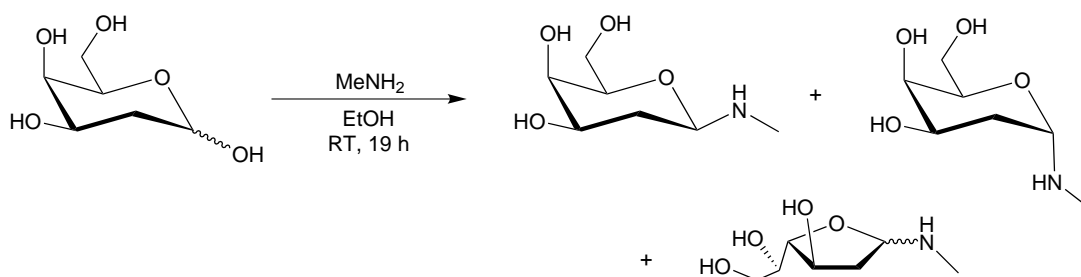
found: 220.4

N-(*tert*-Butyl)-2-deoxy- β -D-*arabino*-hexopyranosylamine – DMSO-*d*₆: 88 %:

¹³C{¹H} NMR (101 MHz, DMSO-*d*₆ 43OR2-2016): δ /ppm = 82.6 (C1), 77.4 (C5), 72.3 (C3), 72.0 (C4), 61.8 (C6), 49.6 (C_q), 41.4 (C2), 30.6 (3 × CH₃).

N-(*tert*-Butyl)-2-deoxy- α -D-*arabino*-hexopyranosylamine – DMSO-*d*₆: 12 %:

¹³C{¹H} NMR (101 MHz, DMSO-*d*₆, 48OR8-2015): δ /ppm = 79.2 (C1), 72.8 (C5), 70.4 (C4), 68.2 (C3), 61.4 (C6), 49.6 (C_q), 39.1 (C2), 29.9 (3 × CH₃).

5.5.3.3. Preparation of *N*-Alkyl-2-deoxy-*D*-*lyxo*-hexosylamines*N*-Methyl-2-deoxy-*D*-*lyxo*-hexosylamine (*D*-*lyx*-dHex1NMe)

2-Deoxy-*D*-*lyxo*-hexose (5.01 mg, 3.05 mmol, 1.00 eq.) was dried and subsequently stirred for 19 h at room temperature with a solution of methylamine in ethanol (33 %, 4.10 mL, 30.5 mmol, 10.0 eq.). The reaction mixture was concentrated by evaporation of the solvent until a syrup-like residue formed. The residue was frozen in liquid nitrogen, crushed and dried *in vacuo* three times to obtain the product as a colorless solid. Due to the immense hygroscopy of the product no yield was determined.

N-Methyl-2-deoxy- β -*D*-*lyxo*-hexopyranosylamine – D₂O: 62 % – DMSO-*d*₆: 52 %

¹³C{¹H} NMR (101 MHz, D₂O, 45OR21-2015): δ /ppm = 87.9 (C1), 76.8 (C5), 69.2 (C4), 67.7 (C3), 62.2 (C6), 34.2 (C2), 31.1 (CH₃).

¹³C{¹H} NMR (101 MHz, DMSO-*d*₆, 45OR30-2015): 87.7 (C1), 76.1 (C5), 69.0 (C4), 66.8 (C3), 60.9 (C6), 35.3 (C2), 31.6 (CH₃).

N-Methyl-2-deoxy- α -*D*-*lyxo*-hexopyranosylamine – D₂O: 16 % – DMSO-*d*₆: 12 %

¹³C{¹H} NMR (101 MHz, D₂O, 45OR21-2015): δ /ppm = 85.3 (C1), 69.1 (C5), 68.2 (C4), 65.5 (C3), 62.3 (C6), 31.7 (C2), 31.0 (CH₃).

¹³C{¹H} NMR (101 MHz, DMSO-*d*₆, 45OR30-2015): δ /ppm = 84.8 (C1), 69.4 (C5), 67.7 (C4), 64.8 (C3), 61.2 (C6), 32.8 (C2), 31.7 (CH₃).

N-Methyl-2-deoxy- β -*D*-*lyxo*-hexofuranosylamine – D₂O: 14 % – DMSO-*d*₆: 20 %

¹³C{¹H} NMR (101 MHz, D₂O, 45OR21-2015): δ /ppm = 92.7 (C1), 85.9 (C4), 72.1 (C3), 70.5 (C5), 63.5 (C6), 40.3 (C2), 31.8 (CH₃).

¹³C{¹H} NMR (101 MHz, DMSO-*d*₆, 45OR30-2015): δ /ppm = 92.0 (C1), 85.4 (C4), 72.0 (C3), 71.4 (C5), 63.1 (C6), 41.7 (C2), 32.3 (CH₃).

N-Methyl-2-deoxy- α -*D*-*lyxo*-hexofuranosylamine – D₂O: 8 % – DMSO-*d*₆: 12 %

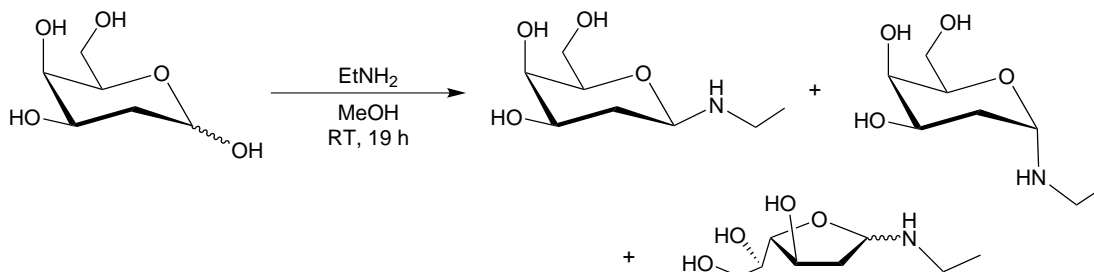
¹³C{¹H} NMR (101 MHz, D₂O, 45OR21-2015): δ /ppm = 92.2 (C1), 84.0 (C4), 73.1 (C3), 72.0 (C5), 63.6 (C6), 39.8 (C2), 31.1 (CH₃).

¹³C{¹H} NMR (101 MHz, DMSO-*d*₆, 45OR30-2015): δ /ppm = 91.5 (C1), 83.5 (C4), 71.6 (C3), 71.2 (C5), 63.1 (C6), 40.5 (C2), 31.5 (CH₃).

N-Methyl-2-deoxy-*lyxo*-*D*-hexosylamine (imine form) – D₂O: 0 % – DMSO-*d*₆: 4 %

$^{13}\text{C}\{^1\text{H}\}$ NMR (101 MHz, $\text{DMSO-}d_6$, 45OR30-2015): $\delta/\text{ppm} = 165.5$ (C1), 72.9 (C5), 69.9 (C3), 68.7 (C4), 63.0 (C6), 47.4 (CH_3), 39.9 (C2).

N-Ethyl-2-deoxy- β -D-*lyxo*-hexosylamine (β -*lyx*-dHex1NEt)



2-Deoxy- β -D-*lyxo*-hexose (860 mg, 5.24 mmol, 1.00 eq.) was dried, subsequently suspended in a solution of ethylamine in methanol (2 M, 7.00 mL, 14.0 mmol, 4.59 eq.) and stirred for 19 h at room temperature. The reaction mixture was concentrated by evaporation of the solvent until a syrup-like residue formed. The residue was frozen in liquid nitrogen, crushed and dried *in vacuo* three times to obtain the product as a colorless solid. Due to the immense hygroscopy of the product no yield was determined.

N-Ethyl-2-deoxy- β -D-*lyxo*-hexopyranosylamine – D_2O : 75 % – $\text{DMSO-}d_6$: 54 %

$^{13}\text{C}\{^1\text{H}\}$ NMR (101 MHz, D_2O , 45OR21-2015): $\delta/\text{ppm} = 86.3$ (C1), 76.8 (C5), 69.2 (C4), 67.7 (C3), 62.2 (C6), 39.4 (CH_2), 34.4 (C2), 14.3 (CH_3).

$^{13}\text{C}\{^1\text{H}\}$ NMR (101 MHz, $\text{DMSO-}d_6$, 45OR30-2015): 86.3 (C1), 76.1 (C5), 68.0 (C4), 66.8 (C3), 60.9 (C6), 39.1 (CH_2), 35.6 (C2), 15.5 (CH_3).

N-Ethyl-2-deoxy- α -D-*lyxo*-hexopyranosylamine – D_2O : 13 % – $\text{DMSO-}d_6$: 12 %

$^{13}\text{C}\{^1\text{H}\}$ NMR (101 MHz, D_2O , 45OR21-2015): $\delta/\text{ppm} = 83.7$ (C1), 69.2 (C5), 68.2 (C4), 65.4 (C3), 62.3 (C6), 39.3 (CH_2), 31.7 (C2), 13.9 (CH_3).

$^{13}\text{C}\{^1\text{H}\}$ NMR (101 MHz, $\text{DMSO-}d_6$, 45OR30-2015): $\delta/\text{ppm} = 83.3$ (C1), 69.4 (C5), 67.7 (C4), 64.8 (C3), 61.1 (C6), 39.2 (CH_2), 32.9 (C2), 15.1 (CH_3).

N-Ethyl-2-deoxy- β -D-*lyxo*-hexofuranosylamine – D_2O : 9 % – $\text{DMSO-}d_6$: 20 %

$^{13}\text{C}\{^1\text{H}\}$ NMR (101 MHz, D_2O , 45OR21-2015): $\delta/\text{ppm} = 91.2$ (C1), 85.9 (C4), 72.2 (C3), 70.5 (C5), 63.6 (C6), 40.6 (C2), 40.4 (CH_2), 14.4 (CH_3).

$^{13}\text{C}\{^1\text{H}\}$ NMR (101 MHz, $\text{DMSO-}d_6$, 45OR30-2015): $\delta/\text{ppm} = 90.4$ (C1), 85.4 (C4), 72.0 (C3), 71.4 (C5), 63.1 (C6), 41.7 (C2), 40.1 (CH_2), 14.4 (CH_3).

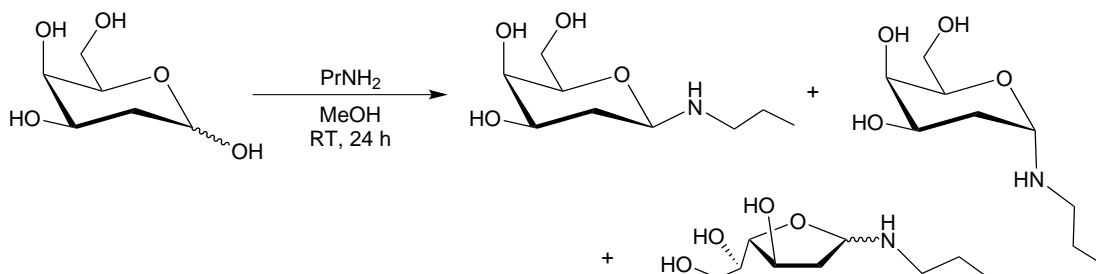
N-Ethyl-2-deoxy- α -D-*lyxo*-hexofuranosylamine – D_2O : 3 % – $\text{DMSO-}d_6$: 10 %

$^{13}\text{C}\{^1\text{H}\}$ NMR (101 MHz, D_2O , 45OR21-2015): $\delta/\text{ppm} = 90.6$ (C1), 83.8 (C4), 73.1 (C3), 72.0 (C5), 63.6 (C6), 40.4 (CH_2), 40.0 (C2), 14.4 (CH_3).

$^{13}\text{C}\{^1\text{H}\}$ NMR (101 MHz, $\text{DMSO-}d_6$, 45OR30-2015): $\delta/\text{ppm} = 90.1$ (C1), 83.5 (C4), 71.6 (C3), 71.2 (C5), 63.1 (C6), 40.8 (C2), 39.2 (CH_2), 14.4 (CH_3).

N-Ethyl-2-deoxy-*lyxo*-D-hexosylamine (imine form) – D₂O: 0 % – DMSO-*d*₆: 4 %
¹³C{¹H} NMR (101 MHz, DMSO-*d*₆, 45OR30-2015): δ/ppm = 163.4 (C1), 72.9 (C5), 69.1 (C3), 68.7 (C4), 63.0 (C6), 54.8 (CH₂), 36.2 (C2), 16.3 (CH₃).

***N*-Propyl-2-deoxy-D-*lyxo*-hexosylamine (D-*lyx*-dHex1NPr)**



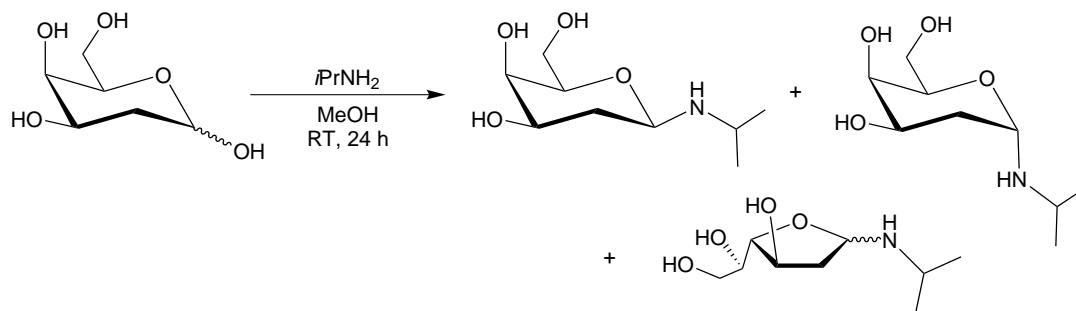
2-Deoxy-D-*lyxo*-hexose (1.09 g, 6.66 mmol, 1.00 eq.) was dried and subsequently suspended in 2.5 mL dry methanol. After the addition of propylamine (1.50 mL, 1.08 g, 18.3 mmol, 2.74 eq.) the resulting solution was stirred for 24 h at room temperature. The reaction mixture was concentrated by evaporation of the solvent until a syrup-like residue formed. The residue was frozen in liquid nitrogen, crushed and dried *in vacuo* three times to obtain the product as a colorless solid. Due to the immense hygroscopy of the product no yield was determined.

N-Propyl-2-deoxy-β-D-*lyxo*-hexopyranosylamine – D₂O: 85 % – DMSO-*d*₆: 48 %
¹³C{¹H} NMR (101 MHz, D₂O, 38OR37-2019): δ/ppm = 86.8 (C1), 76.9 (C5), 69.3 (C4), 67.7 (C3), 62.3 (C6), 47.1 (NH–CH₂), 34.4 (C2), 22.9 (CH₂), 11.8 (CH₃).
¹³C{¹H} NMR (101 MHz, DMSO-*d*₆, 37OR11-2019): 86.3 (C1), 76.1 (C5), 68.0 (C4), 66.8 (C3), 60.9 (C6), 39.1 (NH–CH₂), 35.6 (C2), 39.1 (CH₂), 15.5 (CH₃).

N-Propyl-2-deoxy-α-D-*lyxo*-hexopyranosylamine – D₂O: 11 % – DMSO-*d*₆: 18 %
¹³C{¹H} NMR (101 MHz, D₂O, 38OR37-2019): δ/ppm = 84.0 (C1), 69.3 (C5), 68.2 (C4), 65.5 (C3), 62.3 (C6), 47.1 (NH–CH₂), 31.7 (C2), 23.0 (CH₂), 11.9 (CH₃).
¹³C{¹H} NMR (101 MHz, DMSO-*d*₆, 37OR11-2019): δ/ppm = 85.3 (C1), 69.4 (C5), 67.6 (C4), 64.8 (C3), 61.0 (C6), 47.0 (NH–CH₂), 32.0 (C2), 23.0 (CH₂), 11.4 (CH₃).

N-Propyl-2-deoxy-β-D-*lyxo*-hexofuranosylamine – D₂O: 4 % – DMSO-*d*₆: 21 %
¹³C{¹H} NMR (101 MHz, D₂O, 38OR37-2019): δ/ppm = 91.8 (C1), 86.1 (C4), 72.3 (C3), 70.6 (C5), 63.6 (C6), 48.2 (NH–CH₂), 40.6 (C2), 23.0 (CH₂), 11.8 (CH₃).
¹³C{¹H} NMR (101 MHz, DMSO-*d*₆, 37OR11-2019): δ/ppm = 90.8 (C1), 85.3 (C4), 72.0 (C3), 71.4 (C5), 63.1 (C6), 47.9 (NH–CH₂), 41.6 (C2), 23.0 (CH₂), 11.8 (CH₃).

N-Propyl-2-deoxy-α-D-*lyxo*-hexofuranosylamine – D₂O: 0 % – DMSO-*d*₆: 13 %
¹³C{¹H} NMR (101 MHz, DMSO-*d*₆, 37OR11-2019): δ/ppm = 90.1 (C4), 83.5 (C4), 71.6 (C3), 71.2 (C5), 63.1 (C6), 47.1 (NH–CH₂), 40.8 (C2), 23.0 (CH₂), 11.8 (CH₃).

***N*-(*iso*-Propyl)-2-deoxy-D-*lyxo*-hexosylamine (D-*lyx*-dHex1NiPr)**

2-Deoxy-D-*lyxo*-hexose (501 mg, 3.05 mmol, 1.00 eq.) was dried and subsequently suspended in 2 mL dry methanol. After the addition of *iso*-propylamine (1.00 mL, 688 mg, 11.6 mmol, 3.82 eq.) the resulting solution was stirred for 24 h at room temperature. The reaction mixture was concentrated by evaporation of the solvent until a syrup-like residue formed. The residue was frozen in liquid nitrogen, crushed and dried *in vacuo* three times to obtain the product as a colorless solid. Due to the immense hygroscopy of the product no yield was determined.

N-(*iso*-Propyl)-2-deoxy- β -D-*lyxo*-hexopyranosylamine – D₂O: 96 % – DMSO-*d*₆: 48 %

¹³C{¹H} NMR (101 MHz, D₂O, 35OR4-2019): δ /ppm = 83.8 (C1), 76.9 (C5), 69.3 (C4), 67.8 (C3), 62.3 (C6), 43.7 (CH), 34.9 (C2), 23.3 (CH₃), 20.3 (CH₃).

¹³C{¹H} NMR (101 MHz, DMSO-*d*₆, 35OR8-2019): 83.9 (C1), 76.0 (C5), 69.0 (C4), 66.8 (C3), 60.8 (C6), 43.1 (CH₂), 35.9 (C2), 24.3 (CH₃), 22.1 (CH₃).

N-(*iso*-Propyl)-2-deoxy- α -D-*lyxo*-hexopyranosylamine – D₂O: 2 % – DMSO-*d*₆: 12 %

¹³C{¹H} NMR (101 MHz, D₂O, 35OR4-2019): δ /ppm = 81.0 (C1), 69.3 (C5), 68.2 (C4), 65.3 (C3), 62.4 (C6), 43.6 (CH₂), 32.8 (C2), 23.6 (CH₃), 20.4 (CH₃).

¹³C{¹H} NMR (101 MHz, DMSO-*d*₆, 35OR8-2019): δ /ppm = 81.2 (C1), 69.3 (C5), 67.6 (C4), 64.7 (C3), 60.9 (C6), 44.0 (CH₂), 33.0 (C2), 24.0 (CH₃), 22.0 (CH₃).

N-(*iso*-Propyl)-2-deoxy- β -D-*lyxo*-hexofuranosylamine – D₂O: 2 % – DMSO-*d*₆: 22 %

¹³C{¹H} NMR (101 MHz, D₂O, 35OR4-2019): δ /ppm = 88.8 (C1), 86.1 (C4), 72.3 (C3), 70.6 (C5), 63.6 (C6), 45.3 (CH), 41.1 (C2), 23.1 (CH₃), 19.9 (CH₃).

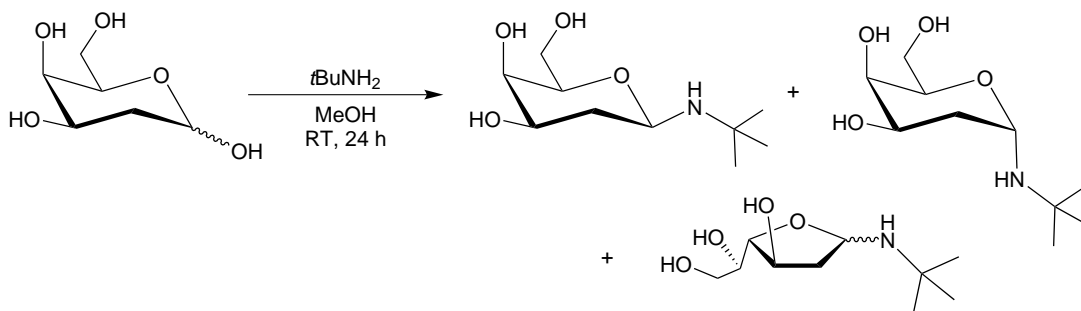
¹³C{¹H} NMR (101 MHz, DMSO-*d*₆, 35OR8-2019): δ /ppm = 88.3 (C1), 85.3 (C4), 72.0 (C3), 71.4 (C5), 63.1 (C6), 45.0 (CH), 42.0 (C2), 24.2 (CH₃), 22.4 (CH₃).

N-(*iso*-Propyl)-2-deoxy- α -D-*lyxo*-hexofuranosylamine – D₂O: 0 % – DMSO-*d*₆: 14 %

¹³C{¹H} NMR (101 MHz, DMSO-*d*₆, 35OR8-2019): δ /ppm = 87.9 (C1), 83.4 (C4), 71.6 (C3), 71.3 (C5), 63.1 (C6), 43.8 (CH), 41.2 (C2), 24.6 (CH₃), 22.1 (CH₃).

N-(*iso*-Propyl)-2-deoxy-*lyxo*-D-hexosylamine (imine form) – D₂O: 0 % – DMSO-*d*₆: 4 %

¹³C{¹H} NMR (101 MHz, DMSO-*d*₆, 35OR8-2019): δ /ppm = 161.2 (C1), 72.9 (C5), 69.9 (C3), 68.7 (C4), 63.0 (C6), 60.5 (CH), 40.0 (C2), 24.4 (CH₃), 22.3 (CH₃).

***N*-(*tert*-Butyl)-2-deoxy-*D*-lyxo-hexosylamine (*D*-lyx-dHex1NtBu)**

2-Deoxy-*lyxo*-*D*-hexose (547 mg, 3.33 mmol, 1.00 eq.) was dried and subsequently suspended in 5 mL dry methanol. *tert*-Butylamine (1.00 mL, 700 mg, 9.57 mmol, 2.87 eq.) was added and the reaction mixture stirred for 24 h at room temperature. The reaction mixture was concentrated by evaporation of the solvent until a syrup-like residue formed. The residue was frozen in liquid nitrogen, crushed and dried *in vacuo* three times to obtain the product as a colorless solid. Due to the immense hygroscopy of the product no yield was determined.

N-(*tert*-Butyl)-2-deoxy- β -*D*-*lyxo*-hexopyranosylamine – DMSO- d_6 : 36 %

$^{13}\text{C}\{^1\text{H}\}$ NMR (101 MHz, DMSO- d_6 , 37OR5-2019): 83.4 (C1), 76.3 (C5), 69.6 (C4), 67.0 (C3), 61.3 (C6), 50.1 (C), 37.2 (C2), 31.1 (3 \times CH $_3$).

N-(*tert*-Butyl)-2-deoxy- α -*D*-*lyxo*-hexopyranosylamine – DMSO- d_6 : 15 %

$^{13}\text{C}\{^1\text{H}\}$ NMR (101 MHz, DMSO- d_6 , 37OR5-2019): δ /ppm = 80.0 (C1), 69.1 (C5), 68.0 (C4), 65.4 (C3), 61.1 (C6), 50.0 (C), 34.6 (C2), 31.0 (3 \times CH $_3$).

N-(*tert*-Butyl)-2-deoxy- β -*D*-*lyxo*-hexofuranosylamine – DMSO- d_6 : 25 %

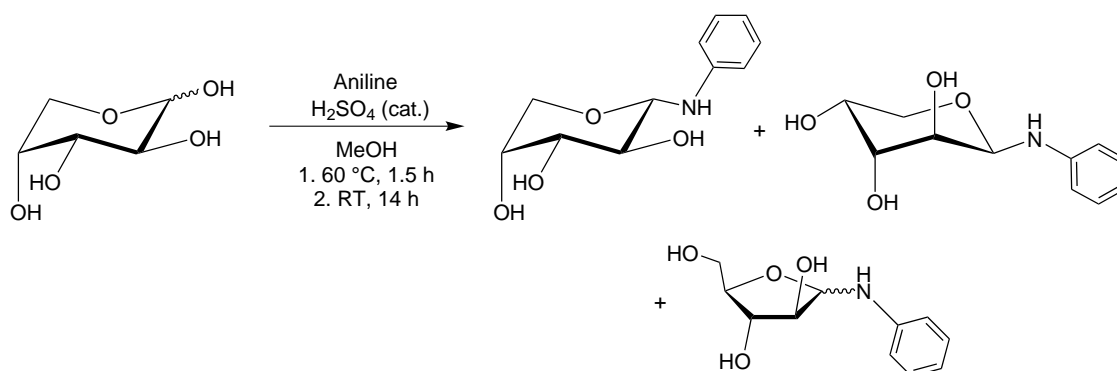
$^{13}\text{C}\{^1\text{H}\}$ NMR (101 MHz, DMSO- d_6 , 37OR5-2019): δ /ppm = 86.7 (C1), 85.7 (C4), 72.3 (C3), 71.8 (C5), 63.8 (C6), 50.2 (C), 43.3 (C2), 30.6 (3 \times CH $_3$).

N-(*tert*-Butyl)-2-deoxy- α -*D*-*lyxo*-hexofuranosylamine – DMSO- d_6 : 15 %

$^{13}\text{C}\{^1\text{H}\}$ NMR (101 MHz, DMSO- d_6 , 37OR5-2019): δ /ppm = 87.0 (C1), 83.4 (C4), 71.9 (C3), 71.2 (C5), 63.8 (C6), 50.2 (C), 42.8 (C2), 30.4 (3 \times CH $_3$).

N-(*tert*-Butyl)-2-deoxy-*lyxo*-*D*-hexosylamine (imine form) – DMSO- d_6 : 9 %

$^{13}\text{C}\{^1\text{H}\}$ NMR (101 MHz, DMSO- d_6 , 37OR5-2019): δ /ppm = 158.6 (C1), 73.4 (C5), 70.3 (C3), 69.3 (C4), 63.5 (C6), 56.8 (C), 40.5 (C2), 30.0 (3 \times CH $_3$).

5.5.4. Preparation of *N*-Phenylglycosylamines*N*-Phenyl-D-arabinosylamine (D-Ara1NPh)

To a solution of aniline (304 μL , 310 mg, 3.33 mmol, 1.00 eq.) in 2.5 mL dry methanol D-arabinose (500 mg, 3.33 mmol, 1.00 eq.) and sulfuric acid (0.1 N, 30.0 μL) were added. The resulting suspension was stirred for 1.5 h at 60 $^{\circ}\text{C}$ and for another 14 h at room temperature. The resulting solution was concentrated by evaporation of the solvent until it reach dryness. The residue was frozen, crushed, washed with cold methanol ($3 \times 5 \text{ mL}$) and dried *in vacuo*. The product was obtained as a slight beige powder in yield of 628 mg (2.79 mmol, 83.7% of theory).

N-Phenyl- α -D-arabinopyranosylamine – D_2O : 100 % – $\text{DMSO-}d_6$: 37 %

^1H NMR (400 MHz, D_2O , 41OR5-2018): $\delta/\text{ppm} = 7.27$ (t, 2H, H_m), 6.90–6.86 (sp, 3H, H_o/H_p), 4.67 (d, 1H, H_1 , $^3J_{1,2}=8.6 \text{ Hz}$), 3.91 (m, 1H, H_4), 3.84–3.65 (sp, 4H, $\text{H}_2/\text{H}_3/\text{H}5_{\text{ax}}/\text{H}5_{\text{eq}}$).

$^{13}\text{C}\{^1\text{H}\}$ NMR (101 MHz, D_2O , 41OR6-2018): $\delta/\text{ppm} = 146.3$ (C_i), 130.3 (C_m), 120.3 (C_p), 115.1 (C_o), 86.1 (C_1), 73.9 (C_3), 70.9 (C_2), 69.5 (C_4), 67.6 (C_5).

$^{13}\text{C}\{^1\text{H}\}$ NMR (101 MHz, $\text{DMSO-}d_6$, 40OR8-2018): $\delta/\text{ppm} = 147.0$ (C_i), 128.8 (C_m), 117.0 (C_p), 113.7 (C_o), 85.3 (C_1), 73.4 (C_3), 70.2 (C_2), 68.0 (C_4), 65.6 (C_5).

^{15}N NMR (41 MHz, D_2O , 41OR7-2018): $\delta/\text{ppm} = -302.5$.

^{15}N NMR (41 MHz, $\text{DMSO-}d_6$, 40OR11-2018): $\delta/\text{ppm} = -298.8$ (d, $^2J=88.3 \text{ Hz}$).

N-Phenyl- β -D-arabinopyranosylamine – D_2O : 0 % – $\text{DMSO-}d_6$: 31 %

$^{13}\text{C}\{^1\text{H}\}$ NMR (101 MHz, $\text{DMSO-}d_6$, 40OR8-2018): $\delta/\text{ppm} = 146.6$ (C_i), 128.8 (C_m), 117.4 (C_p), 113.2 (C_o), 79.6 (C_1), 70.6 (C_3), 70.4 (C_2), 64.8 (C_4), 63.3 (C_5).

^{15}N NMR (41 MHz, $\text{DMSO-}d_6$, 40OR11-2018): $\delta/\text{ppm} = -304.8$ (d, $^2J=88.0 \text{ Hz}$).

N-Phenyl- α -D-arabinofuranosylamine – D_2O : 0 % – $\text{DMSO-}d_6$: 21 %

$^{13}\text{C}\{^1\text{H}\}$ NMR (101 MHz, $\text{DMSO-}d_6$, 40OR8-2018): $\delta/\text{ppm} = 147.0$ (C_i), 128.8 (C_m), 117.2 (C_p), 113.7 (C_o), 88.2 (C_1), 81.9 (C_4), 80.9 (C_2), 76.0 (C_3), 61.6 (C_5).

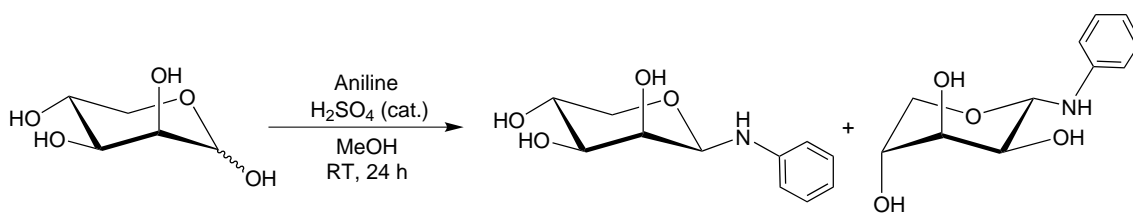
^{15}N NMR (41 MHz, $\text{DMSO-}d_6$, 40OR11-2018): $\delta/\text{ppm} = -295.4$ (d, $^2J=87.8 \text{ Hz}$).

N-Phenyl- β -D-arabinofuranosylamine – D_2O : 0 % – $\text{DMSO-}d_6$: 11 %

$^{13}\text{C}\{^1\text{H}\}$ NMR (101 MHz, $\text{DMSO-}d_6$, 40OR8-2018): $\delta/\text{ppm} = 146.4$ (C_i), 128.8 (C_m), 117.4 (C_p), 114.0 (C_o), 84.5 (C_1), 83.6 (C_4), 77.1 (C_2), 76.2 (C_3), 62.4 (C_5).

^{15}N NMR (41 MHz, $\text{DMSO-}d_6$, 40OR11-2018): $\delta/\text{ppm} = -303.6$ (d, $^2J=88.4$ Hz).

N-Phenyl- β -D-lyxosylamine (β -Lyx1NPh)



To a solution of aniline (1.44 mL, 1.47 mg, 15.8 mmol, 1.00 eq.) in 25 mL dry methanol β -lyxose (2.37 g, 15.8 mmol) and sulfuric acid (0.1 N, 300 μL) were added. The resulting solution was stirred for 24 h at room temperature, leading to the precipitation of a white solid. The precipitate was filtered off, washed with cold methanol (3×5 mL) and dried *in vacuo*, yielding 1.55 g (6.88 mmol, 43.7% of theory) of the product as a white powder. In addition, colorless crystals were obtained from the filtrate after storage at 4 $^{\circ}\text{C}$ for a few days.

EA: calcd.: C 58.66 %, H 6.71 %, N 6.22 %

found: C 58.65 %, H 6.69 %, N 6.18 %

MS (FAB+): calcd.: 226.2 ($[\text{M}+\text{H}]^+$)

found: 226.0

N-Phenyl- β -D-lyxoopyranosylamine – D_2O : 58 % – $\text{DMSO-}d_6$: 55 %

^1H NMR (400 MHz, D_2O , 02OR16-2018): $\delta/\text{ppm} = 7.25$ (t, 2H, H_m), 6.88–6.85 (sp, 3H, H_o/H_p), 4.96 (d, 1H, H_1 , $^3J_{1,2}=1.3$ Hz).

$^{13}\text{C}\{^1\text{H}\}$ NMR (101 MHz, D_2O , 02OR18-2018): $\delta/\text{ppm} = 145.3$ (C_i), 130.2 (C_m), 120.6 (C_p), 115.6 (C_o), 83.7 (C_1), 74.3 (C_3), 71.1 (C_2), 67.1 (C_4), 66.3 (C_5).

$^{13}\text{C}\{^1\text{H}\}$ NMR (101 MHz, $\text{DMSO-}d_6$, 27OR33-2015): $\delta/\text{ppm} = 146.3$ (C_i), 128.8 (C_m), 117.4 (C_p), 113.6 (C_o), 82.1 (C_1), 73.9 (C_3), 69.6 (C_2), 67.1 (C_4), 65.1 (C_5).

^{15}N NMR (41 MHz, D_2O , 02OR17-2018): $\delta/\text{ppm} = -304.7$.

^{15}N NMR (41 MHz, $\text{DMSO-}d_6$, 02OR21-2018): $\delta/\text{ppm} = -299.8$ (d, $^2J=87.8$ Hz).

N-Phenyl- α -D-lyxoopyranosylamine – D_2O : 42 % – $\text{DMSO-}d_6$: 45 %

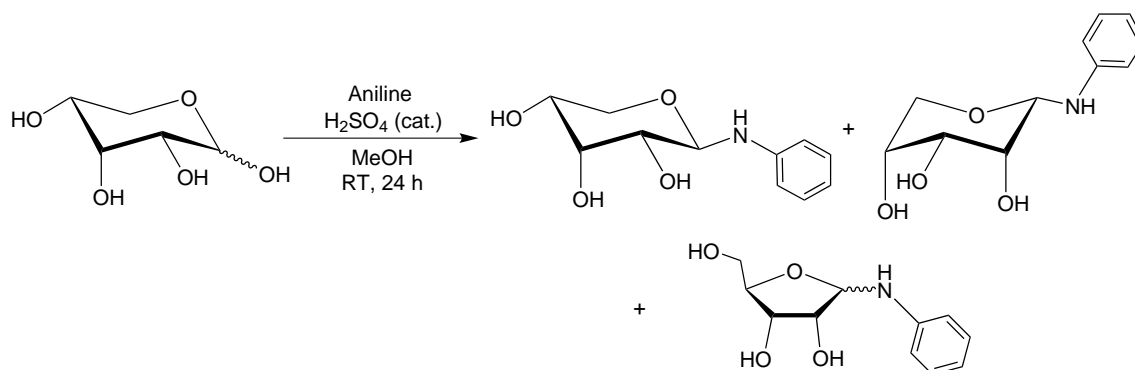
^1H NMR (400 MHz, D_2O , 02OR16-2018): $\delta/\text{ppm} = 7.26$ (t, 2H, H_m), 6.88–6.85 (sp, 3H, H_o/H_p), 4.98 (d, 1H, H_1 , $^3J_{1,2}=8.0$ Hz).

$^{13}\text{C}\{^1\text{H}\}$ NMR (101 MHz, D_2O , 02OR18-2018): $\delta/\text{ppm} = 146.2$ (C_i), 130.1 (C_m), 120.1 (C_p), 115.0 (C_o), 82.8 (C_1), 71.1 (C_3), 69.7 (C_4), 68.7 (C_2), 65.1 (C_5).

$^{13}\text{C}\{^1\text{H}\}$ NMR (101 MHz, $\text{DMSO-}d_6$, 27OR33-2015): $\delta/\text{ppm} = 147.3$ (C_i), 128.7 (C_m), 116.9 (C_p), 113.21 (C_o), 82.3 (C_1), 71.0 (C_3), 69.2 (C_4), 68.2 (C_2), 64.4 (C_5).

^{15}N NMR (41 MHz, D_2O , 02OR17-2018): $\delta/\text{ppm} = -303.5$.

^{15}N NMR (41 MHz, $\text{DMSO-}d_6$, 02OR21-2018): $\delta/\text{ppm} = -298.0$ (d, $^2J=88.5$ Hz).

***N*-Phenyl-D-ribosylamine (D-Rib1NPh)**

To a solution of aniline (905 μ L, 923 mg, 9.91 mmol, 1.00 eq.) in 10 mL dry methanol D-ribose (1.49 g, 9.91 mmol, 1.00 eq.) and sulfuric acid (0.1 N, 100 μ L) were added. After stirring for 24 h at room temperature a white precipitate formed in the reaction solution. The precipitate was filtered off, washed with cold methanol (2×5 mL) and dried *in vacuo*, yielding 894 mg (3.97 mmol, 40.1 % of theory) of the product as a white powder. In addition, colorless crystals were obtained from the filtrate after further storage at 4 °C for a few days.

EA: calcd.: C 58.66 %, H 6.71 %, N 6.22 %
found: C 58.28 %, H 6.71 %, N 6.19 %

MS (FAB+): calcd.: 226.2 ([M+H]⁺)
found: 226.4

N-Phenyl-β-D-ribopyranosylamine – D₂O: 100 % – DMSO-*d*₆: 37 %

¹H NMR (400 MHz, D₂O, 21OR4-2018): δ /ppm = 4.92 (d, H1, ³*J*_{1,2}=8.9 Hz).

¹³C{¹H} NMR (101 MHz, D₂O, 21OR5-2018): δ /ppm = 145.0 (C_i), 129.5 (C_m), 119.4 (C_p), 114.3 (C_o), 81.5 (C1), 70.5 (C2), 69.8 (C3), 66.7 (C4), 62.9 (C5).

¹³C{¹H} NMR (101 MHz, DMSO-*d*₆, 32OR5-2015): δ /ppm = 146.3 (C_i), 128.8 (C_m), 117.3 (C_p), 114.3 (C_o), 81.4 (C1), 70.5 (C2), 70.2 (C2), 67.5 (C4), 63.3 (C5).

¹⁵N NMR (41 MHz, D₂O, 21OR6-2018): δ /ppm = –303.8.

¹⁵N NMR (41 MHz, DMSO-*d*₆, 21OR19-2018): δ /ppm = –300.0 (d, ²*J*=88.6 Hz).

N-Phenyl-α-D-ribopyranosylamine – D₂O: 0 % – DMSO-*d*₆: 31 %

¹³C{¹H} NMR (101 MHz, DMSO-*d*₆, 32OR5-2015): δ /ppm = 147.3 (C_i), 128.7 (C_m), 117.7 (C_p), 113.1 (C_o), 81.7 (C1), 70.1 (C2), 69.8 (C3), 67.8 (C4), 62.9 (C5).

¹⁵N NMR (41 MHz, DMSO-*d*₆, 21OR19-2018): δ /ppm = –296.9 (d, ²*J*=86.7 Hz).

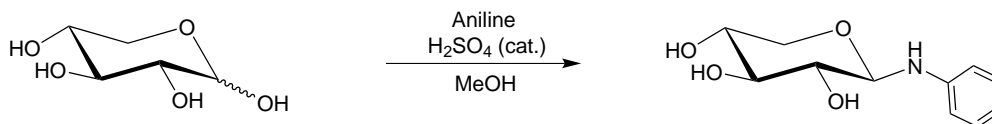
N-Phenyl-β-D-ribofuranosylamine – D₂O: 0 % – DMSO-*d*₆: 21 %

¹³C{¹H} NMR (101 MHz, DMSO-*d*₆, 32OR5-2015): δ /ppm = 147.2 (C_i), 128.8 (C_m), 117.1 (C_p), 113.3 (C_o), 88.1 (C1), 83.2 (C4), 74.1 (C3), 70.3 (C2), 62.4 (C5).

N-Phenyl- α -D-ribofuranosylamine – D₂O: 0 % – DMSO-*d*₆: 11 %

¹³C{¹H} NMR (101 MHz, DMSO-*d*₆, 32OR5-2015): δ /ppm = 146.3 (*C_i*), 128.8 (*C_m*), 117.3 (*C_p*), 113.7 (*C_o*), 83.9 (*C₁*), 81.7 (*C₄*), 70.9 (*C₃*), 70.5 (*C₂*), 62.4 (*C₅*).

N-Phenyl-D-xylosylamine (D-Xyl1NPh)



To a solution of aniline (2.68 mL, 2.73 g, 29.4 mmol, 1.00 eq.) in 12 mL dry methanol D-xylose (4.41 g, 29.4 mmol, 1.00 eq.) and sulfuric acid (0.1 N, 0.12 mL) were added. The resulting suspension was stirred for 24 h at room temperature. The formed precipitate was filtered off, washed with cold methanol (5 × 20 mL) and dried *in vacuo*, yielding 3.03 g (13.5 mmol, 45.9 % of theory) of the product as a white powder. In addition, colorless crystals were obtained from the filtrate after storage at 4 °C for a few days.

EA: calcd.: C 58.66 %, H 6.71 %, N 6.22 %

found: C 58.64 %, H 6.74 %, N 6.17 %

MS (FAB+): calcd.: 226.3 ([M+H]⁺)

found: 226.3

N-Phenyl- β -D-xylopyranosylamine – D₂O: 92 % (RT) 100 % (4 °C) – DMSO-*d*₆: 100 %

¹H NMR (400 MHz, D₂O, 37OR2-2017): δ /ppm = 7.31 (t, 2H, *H_m*), 6.97–6.81 (m, 3H, *H_o*/*H_p*), 4.73 (d, 1H, *H₁*, ³*J*_{1,2}=8.7 Hz), 3.91 (dd, 1H, *H_{5a}*, ³*J*_{4,5a}=5.3 Hz, ²*J*_{5a,5b}=–11.4 Hz), 3.73–3.61 (m, 1H, *H₄*), 3.55 (t, 1H, *H₃*, ³*J*_{3,4}=9.0 Hz), 3.49–3.34 (sp, 2H, *H_{5b}*/*H₂*).

¹³C{¹H} NMR (101 MHz, D₂O, 28OR17-2015): δ /ppm = 146.1 (*C_i*), 130.2 (*C_m*), 120.3 (*C_p*), 115.1 (*C_o*), 86.2 (*C₁*), 77.5 (*C₃*), 73.2 (*C₂*), 70.0 (*C₄*), 66.4 (*C₅*).

¹³C{¹H} NMR (101 MHz, DMSO-*d*₆, 28OR47-2015): δ /ppm = 147.1 (*C_i*), 128.7 (*C_m*), 117.1 (*C_p*), 113.2 (*C_o*), 85.7 (*C₁*), 77.6 (*C₃*), 72.9 (*C₂*), 69.9 (*C₄*), 66.3 (*C₅*).

¹⁵N NMR (41 MHz, D₂O, 50OR10-2017): δ /ppm = –302.5.

¹⁵N NMR (41 MHz, DMSO-*d*₆, 50OR15-2017): δ /ppm = –298.3 (d, ²*J*=90.1 Hz).

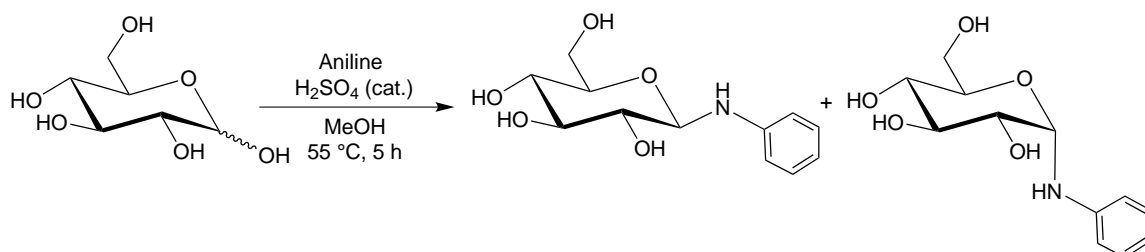
N-Phenyl- α -D-xylopyranosylamine – D₂O: 8 % (RT) 0 % (4 °C) – DMSO-*d*₆: 0 %

¹H NMR (400 MHz, D₂O, 28OR16-2015): δ /ppm = 5.24 (d, *H₁*, ³*J*_{1,2}=4.2 Hz).

¹³C{¹H} NMR (101 MHz, D₂O, 28OR17-2015): δ /ppm = 146.0 (*C_i*), 130.1 (*C_m*), 120.1 (*C_p*), 115.0 (*C_o*), 82.1 (*C₁*), 72.6 (*C₃*), 70.8 (*C₂*), 69.7 (*C₄*), 62.3 (*C₅*).

¹⁵N NMR (41 MHz, D₂O, 50OR10-2017): δ /ppm = –310.8.

¹⁵N NMR (41 MHz, DMSO-*d*₆, 50OR15-2017): δ /ppm = –298.3 (d, ²*J*=90.1 Hz).

***N*-Phenyl- β -D-glucosylamine (β -Glc1NPh)**

To a solution of aniline (224 μ L, 226 mg, 2.43 mmol, 1.00 eq.) in 5 mL dry methanol D-glucose (438 mg, 2.43 mmol, 1.00 eq.) and sulfuric acid (0.1 N, 0.05 mL) were added. The resulting suspension was stirred for 5 h at 55 $^{\circ}$ C. The clear solution was stored for a week at -25° C resulting in precipitation of the desired product. The colorless solid was filtered off, washed with cold methanol (2×5 mL) and dried *in vacuo*, yielding 288 mg (2.43 mmol, 46.4 % of theory) of the product as a white powder.

EA: calcd.: C 56.46 %, H 6.71 %, N 5.49 %
found: C 55.78 %, H 6.71 %, N 5.56 %

MS (FAB+): calcd.: 256.3 ($[M+H]^+$)
found: 256.4

N-Phenyl- β -D-glucopyranosylamine – D₂O: 86 % – DMSO-*d*₆: 72 %

¹H NMR (400 MHz, D₂O, 28OR13-2015): δ /ppm = 7.29 (t, 2H, H_m), 6.90–6.87 (m, 3H, H_o/H_p), 4.73 (d, 1H, H1, ³J_{1,2}=8.7 Hz), 3.86 (dd, 1H, H6a, ³J_{5,6a}=2.3 Hz, ²J_{6a,6b}=–12.4 Hz), 3.70 (dd, 1H, H6b, ³J_{5,6a}=5.5 Hz), 3.58 (t, 1H, H3, ³J_{3,4}=9.1 Hz), 3.52 (dd, 1H, H5), 3.45–3.40 (sp, 2H, H4, H2).

¹³C{¹H} NMR (101 MHz, D₂O, 28OR14-2015): δ /ppm = 146.3 (C_i), 130.2 (C_m), 120.2 (C_p), 115.0 (C_o), 85.5 (C1), 77.5 (C5), 77.1 (C3), 73.3 (C2), 70.4 (C4), 61.4 (C6).

¹³C{¹H} NMR (101 MHz, DMSO-*d*₆, 28OR23-2015): 147.3 (C_i), 128.8 (C_m), 117.1 (C_p), 113.2 (C_o), 85.1 (C1), 77.7 (C5), 77.3 (C3), 73.1 (C2), 70.3 (C4), 61.0 (C6).

¹⁵N NMR (41 MHz, D₂O, 03OR2-2018): δ /ppm = –302.7.

¹⁵N NMR (41 MHz, DMSO-*d*₆, 03OR6-2018): δ /ppm = –298.4 (d, ²J=89.4 Hz).

N-Phenyl- α -D-glucopyranosylamine – D₂O: 14 % – DMSO-*d*₆: 28 %

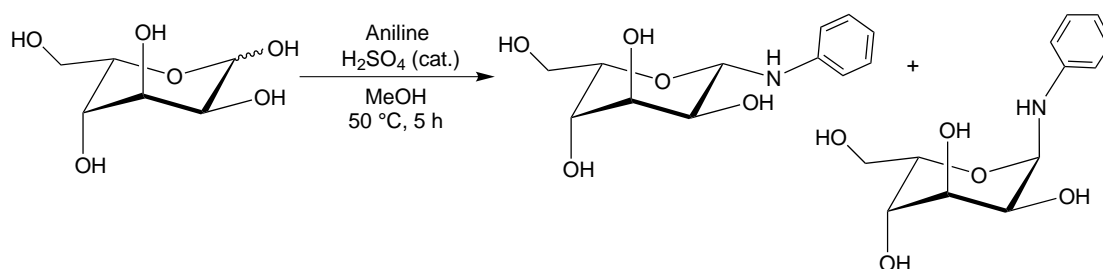
¹H NMR (400 MHz, D₂O, 28OR13-2015): δ /ppm = 5.24 (d, H1, ³J_{1,2}=4.2 Hz).

¹³C{¹H} NMR (101 MHz, D₂O, 28OR14-2015): δ /ppm = 146.6 (C_i), 130.1 (C_m), 119.9 (C_p), 114.9 (C_o), 82.7 (C1), 73.9 (C3), 71.1 (C2), 71.0 (C5), 70.6 (C4), 61.2 (C6).

¹³C{¹H} NMR (101 MHz, DMSO-*d*₆, 28OR23-2015): δ /ppm = 147.7 (C_i), 128.7 (C_m), 117.4 (C_p), 113.7 (C_o), 82.7 (C1), 73.5 (C3), 71.3 (C2), 71.2 (C5), 70.7 (C4), 61.1 (C6).

¹⁵N NMR (41 MHz, D₂O, 03OR2-2018): δ /ppm = –312.6.

¹⁵N NMR (41 MHz, DMSO-*d*₆, 03OR6-2018): δ /ppm = –308.7 (d, ²J=87.8 Hz).

N-Phenyl-L-gulosylamine (L-Gul1NPh)

To a solution of aniline (154 μ L, 157 mg, 1.67 mmol, 1.00 eq.) in 5 mL dry methanol L-gulose (301 mg, 1.67 mmol, 1.00 eq.) and sulfuric acid (0.1 N, 25.0 μ L) were added. The resulting suspension was stirred for 5 h at 50 $^{\circ}$ C. Since subsequent storage at 4 $^{\circ}$ C led to no precipitation of the desired product, the reaction solution was concentrated *in vacuo* until it reached dryness. After repeating this procedure three times, the product was obtained as an off-white powder in a yield of 320 mg (1.25 mmol, 75.1 % of theory).

N-Phenyl- β -L-gulopyranosylamine – D₂O: 100 % – DMSO-*d*₆: 84 %

¹H NMR (400 MHz, D₂O, 13OR1-2018): δ /ppm = 7.25 (dd, 2H, H_m), 6.85–6.82 (m, 3H, H_o/H_p), 5.04 (d, 1H, H1, ³J_{1,2}=9.2 Hz), 4.08 (t, 1H, H3), 4.03 (td, 1H, H5), 3.83 (dd, 1H, H4, ³J_{3,4}=3.7 Hz, ³J_{4,5}=1.2 Hz), 3.80 (sp, 2H, H6/H6'), 3.66 (dd, 1H, H2, ³J_{2,3}=6.2 Hz).

¹³C{¹H} NMR (101 MHz, D₂O, 13OR3-2018): δ /ppm = 146.4 (C_i), 130.2 (C_m), 120.0 (C_p), 114.7 (C_o), 82.6 (C1), 74.2 (C5), 71.5 (C3), 70.0 (C4), 68.2 (C2), 61.5 (C6).

¹³C{¹H} NMR (101 MHz, DMSO-*d*₆, 13OR10-2018): 147.5 (C_i), 128.7 (C_m), 116.7 (C_p), 113.1 (C_o), 81.8 (C1), 73.2 (C5), 71.4 (C3), 69.3 (C4), 67.4 (C2), 60.6 (C6).

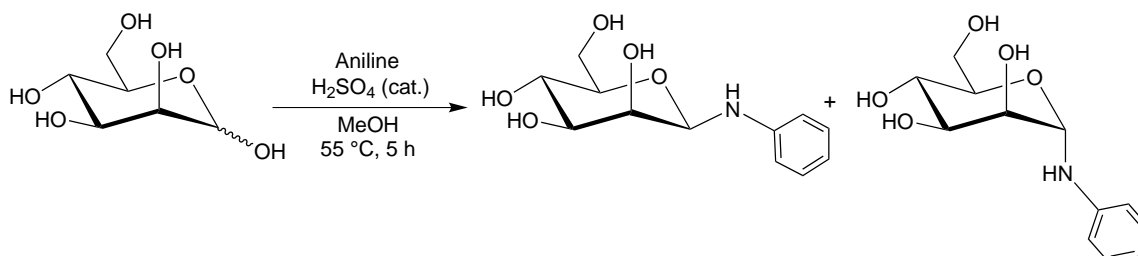
¹⁵N NMR (41 MHz, D₂O, 13OR2-2018): δ /ppm = –302.2.

¹⁵N NMR (41 MHz, DMSO-*d*₆, 13OR8-2018): δ /ppm = –298.2 (d, ²J=88.9 Hz).

N-Phenyl- α -L-gulopyranosylamine – D₂O: 0 % – DMSO-*d*₆: 16 %

¹³C{¹H} NMR (101 MHz, DMSO-*d*₆, 13OR10-2018): δ /ppm = 146.8 (C_i), 128.9 (C_m), 116.9 (C_p), 112.9 (C_o), 81.6 (C1), 71.8 (C3), 69.0 (C4), 65.9 (C5), 64.1 (C2), 60.1 (C6).

¹⁵N NMR (41 MHz, DMSO-*d*₆, 13OR8-2018): δ /ppm = –306.1 (d, ²J=90.7 Hz).

N-Phenyl-D-mannosylamine (D-Man1NPh)

To a solution of aniline (1.33 mL, 1.36 g, 14.6 mmol, 1.00 eq.) in 25 mL dry methanol D-mannose (2.63 g, 14.6 mmol, 1.00 eq.) and sulfuric acid (0.1 N, 0.1 mL) were added. The resulting suspen-

sion was stirred for 5 h at 55 °C. The clear solution was stored for a week at 4 °C resulting in the crystallization of the desired product. The colorless plate-like crystals were filtered off, washed with cold methanol (3 × 5 mL) and dried *in vacuo*, yielding 3.04 g (11.9 mmol, 81.5 % of theory) of the product.

EA: calcd.: C 56.46 %, H 6.71 %, N 5.49 %
found: C 55.16 %, H 6.68 %, N 5.46 %

MS (FAB+): calcd.: 256.3 ([M+H]⁺)
found: 256.4

N-Phenyl-β-D-mannopyranosylamine – D₂O: 100 % – DMSO-*d*₆: 74 %

¹H NMR (400 MHz, D₂O, 50OR1-2017): δ/ppm = 7.26 (t, 2H, H_m), 6.89–6.87 (m, 3H, H_o/H_p), 4.99 (d, 1H, H1, ³J_{1,2}=1.1 Hz), 4.01 (dd, 1H, H2, ³J_{2,3}=3.5 Hz), 3.84 (dd, 1H, H6a, ³J_{5,6a}=2.3 Hz, ²J_{6a,6b}=–12.3 Hz), 3.68 (dd, 1H, H6b, ³J_{5,6b}=6.6 Hz), 3.65 (dd, 1H, H3, ³J_{3,4}=9.6 Hz), 3.58 (t, 1H, H4, ³J_{4,5}=9.7 Hz).

¹³C{¹H} NMR (101 MHz, D₂O, 50OR3-2017): δ/ppm = 145.5 (C_i), 130.2 (C_m), 120.5 (C_p), 115.5 (C_o), 83.0 (C1), 77.6 (C5), 74.5 (C3), 71.6 (C2), 67.6 (C4), 61.7 (C6).

¹³C{¹H} NMR (101 MHz, DMSO-*d*₆, 50OR17-2017): 147.3 (C_i), 128.8 (C_m), 117.1 (C_p), 113.2 (C_o), 85.1 (C1), 77.7 (C5), 77.3 (C3), 73.1 (C2), 70.3 (C4), 61.0 (C6).

¹⁵N NMR (41 MHz, D₂O, 03OR2-2018): δ/ppm = –304.2.

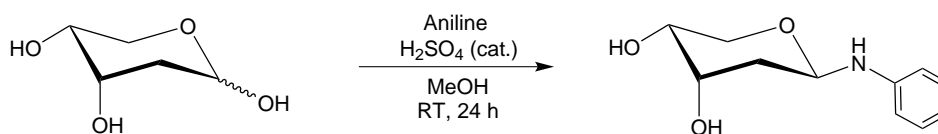
¹⁵N NMR (41 MHz, DMSO-*d*₆, 50OR20-2017): δ/ppm = –306.1 (d, ²J=88.5 Hz).

N-Phenyl-α-D-mannopyranosylamine – D₂O: 0 % – DMSO-*d*₆: 26 %

¹³C{¹H} NMR (101 MHz, DMSO-*d*₆, 50OR17-2017): δ/ppm = 147.7 (C_i), 128.7 (C_m), 117.4 (C_p), 113.7 (C_o), 82.7 (C1), 73.5 (C3), 71.3 (C2), 71.2 (C5), 70.7 (C4), 61.1 (C6).

¹⁵N NMR (41 MHz, DMSO-*d*₆, 50OR20-2017): δ/ppm = –305.9 (d, ²J=88.4 Hz).

N-Phenyl-2-deoxy-D-*erythro*-pentosylamine (D-*ery*-dPent1NPh)



2-Deoxy-D-*erythro*-pentose (708 mg, 5.28 mmol, 1.00 eq.) was solved in 5 mL dry methanol and subsequently aniline (492 μL, 492 mg, 5.28 mmol, 1.00 eq.) and sulfuric acid (0.1 N, 0.05 mL) were added. The reaction solution was stirred for 24 h at room temperature. The obtained clear solution was stored overnight at 4 °C resulting in the precipitation of the desired product. The colorless solid was filtered off, washed with cold methanol (3 × 5 mL) and dried *in vacuo*, yielding 497 mg (2.38 mmol, 45.0 % of theory) of the product.

EA: calcd.: C 63.14 %, H 7.23 %, N 6.69 %
found: C 62.97 %, H 7.28 %, N 6.58 %

MS (FAB+): calcd.: 210.3 ($[M+H]^+$)
found: 210.1

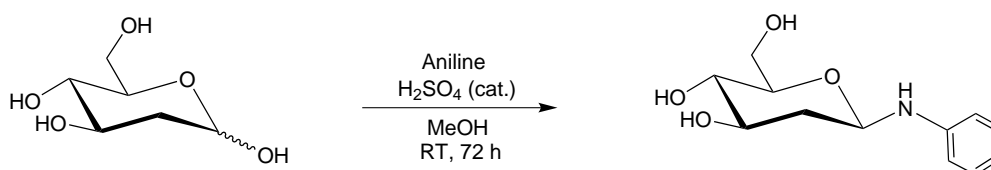
N-Phenyl-2-deoxy- β -D-*erythro*-pentopyranosylamine

$^{13}\text{C}\{^1\text{H}\}$ NMR (101 MHz, D_2O , 43OR34-2015): 130.1 (C_m), 120.1 (C_p), 115.4 (C_o), 82.3 (C_1), 68.6 (C_4), 67.4 (C_3), 63.4 (C_5), 35.6 (C_2).

$^{13}\text{C}\{^1\text{H}\}$ NMR (101 MHz, $\text{DMSO-}d_6$, 43OR37-2015): 146.5 (C_i), 128.7 (C_m), 117.0 (C_p), 113.3 (C_o), 80.0 (C_1), 68.0 (C_4), 66.8 (C_3), 65.8 (C_5), 34.7 (C_2).

^{15}N NMR (41 MHz, $\text{DMSO-}d_6$, 21OR24-2018): $\delta/\text{ppm} = -294.7$ (d, $^2J=88.5$ Hz).

N-Phenyl-2-deoxy-D-*arabino*-hexosylamine (D-*ara*-dHex1NPh)



To a solution of aniline (588 μL , 600 mg, 6.44 mmol, 1.00 eq.) in 40 mL dry methanol 2-Deoxy-D-*arabino*-hexose (1.06 g, 6.44 mmol, 1.00 eq.) and sulfuric acid (0.1 N, 0.13 mL) were added. The resulting suspension was stirred for 72 h at room temperature. The clear solution was stored for a week at 4 $^\circ\text{C}$ resulting in the crystallization of the desired product. The brownish plate-like crystals were filtered off, washed with cold methanol (3×5 mL) and dried *in vacuo*, yielding 519 mg (2.17 mmol, 33.7% of theory) of the product.

EA: calcd.: C 60.24 %, H 7.16 %, N 5.85 %
found: C 59.97 %, H 7.06 %, N 5.79 %

MS (FAB+): calcd.: 240.3 ($[M+H]^+$)
found: 240.1

N-Methyl-2-deoxy- β -D-*arabino*-hexopyranosylamine

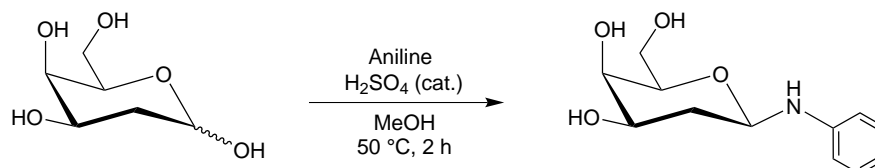
$^{13}\text{C}\{^1\text{H}\}$ NMR (101 MHz, D_2O , 44OR13-2015): $\delta/\text{ppm} = 146.3$ (C_i), 130.2 (C_m), 120.3 (C_p), 115.2 (C_o), 82.0 (C_1), 77.3 (C_5), 72.0 (C_4), 71.8 (C_3), 61.7 (C_6), 38.7 (C_2).

$^{13}\text{C}\{^1\text{H}\}$ NMR (101 MHz, $\text{DMSO-}d_6$, 44OR16-2015): 146.7 (C_i), 128.7 (C_m), 116.9 (C_p), 113.2 (C_o), 80.1 (C_1), 77.5 (C_5), 71.7 (C_4), 71.6 (C_3), 61.1 (C_6), 39.0 (C_2).

^{15}N NMR (41 MHz, D_2O , 06OR6-2018): $\delta/\text{ppm} = -298.5$.

^{15}N NMR (41 MHz, $\text{DMSO-}d_6$, 05OR17-2018): $\delta/\text{ppm} = -294.5$ (d, $^2J=89.2$ Hz).

N-Phenyl-2-deoxy-D-*lyxo*-hexosylamine (D-*lyx*-dHex1NPh)



2-Deoxy-D-*lyxo*-hexose (300 mg, 1.83 mmol, 1.00 eq.) was solved in 5 mL dry methanol and subsequently aniline (169 μ L, 172 mg, 1.83 mmol, 1.00 eq.) and sulfuric acid (0.1 N, 250 μ L) were added. The reaction solution was stirred for 2 h at 50 °C. The obtained clear solution was reduced to about one third of its previous volume by evaporation and stored overnight at 4 °C, resulting in the crystallization of the desired product. The colorless block-like crystals were filtered off, washed with cold methanol (3 \times 5 mL) and dried *in vacuo*, yielding 185 mg (1.83 mmol, 42.3 % of theory) of the product.

N-Methyl-2-deoxy- β -D-*lyxo*-hexopyranosylamine

$^{13}\text{C}\{^1\text{H}\}$ NMR (101 MHz, D₂O, 12OR15-2018): δ /ppm = 146.0 (C_i), 130.1 (C_m), 120.1 (C_p), 115.1 (C_o), 82.2 (C1), 76.2 (C5), 69.2 (C4), 67.5 (C3), 61.9 (C6), 33.7 (C2).

$^{13}\text{C}\{^1\text{H}\}$ NMR (101 MHz, DMSO-*d*₆, 11OR22-2018): 146.0 (C_i), 128.7 (C_m), 116.8 (C_p), 113.2 (C_o), 80.4 (C1), 75.8 (C5), 68.8 (C4), 66.8 (C3), 60.8 (C6), 34.5 (C2).

^{15}N NMR (41 MHz, D₂O, 12OR14-2018): δ /ppm = -297.6.

^{15}N NMR (41 MHz, DMSO-*d*₆, 11OR20-2018): δ /ppm = -294.2 (d, $^2J=89.0$ Hz).

5.6. Preparation of Complexes with Palladium(II)

General reaction procedure: Unless not specifically noted otherwise, a 0.45 M solution of the palladium(II) reagent [Pd(en)(OD)₂] in deuterium oxide was treated with iodic acid. Subsequently the glycosylamine was added and the solution stirred for 3 h at 4 °C. All steps were performed in an atmosphere of argon to avoid the uptake of carbon dioxide. Since the NMR-spectroscopic investigations focus on the shifts of the hydrogen and carbon atoms of the carbohydrate ligands, all NMR signals deriving from the Pd-en fragment are not explicitly listed in the following chapters. In all cases the peaks for the ethylene moiety of the ethylenediamine are located around 2.5 ppm in the ^1H NMR spectra and around 46 ppm in the $^{13}\text{C}\{^1\text{H}\}$ NMR spectra.

5.6.1. Complexes featuring *N*-Alkyl-D-arabinosylamines

N-Methyl-D-arabinosylamine and Pd-en

	D-Ara1NMe	Pd-en	HIO ₃	Pd-en chelate	%
1:1:1	110 mg 675 μ mol	1.50 mL 675 μ mol	119 mg 675 μ mol	$^1\text{C}_4\text{-}\alpha\text{-D-Arap1NMe2H}_{-1}\text{-}\kappa^2\text{N}^1, \text{O}^2$	100
1:2:1	55.1 mg 338 μ mol	1.50 mL 675 μ mol	59.4 mg 338 μ mol	$^1\text{C}_4\text{-}\alpha\text{-D-Arap1NMe2,3,4H}_{-3}\text{-}\kappa^2\text{N}^1, \text{O}^2\text{:}\kappa^2\text{O}^{3,4}$ $^1\text{C}_4\text{-}\alpha\text{-D-Arap1NMe2H}_{-3}\text{-}\kappa^2\text{N}^1, \text{O}^2$ 2 n. i. species	73 19 8
1:2:2	110 mg 675 μ mol	1.50 mL 675 μ mol	119 mg 675 μ mol	$^1\text{C}_4\text{-}\alpha\text{-D-Arap1NMe2H}_{-1}\text{-}\kappa^2\text{N}^1, \text{O}^2$	100

[Pd(en)($^1\text{C}_4\text{-}\alpha\text{-D-Arap1NMe2H}_{-1}\text{-}\kappa^2\text{N}^1, \text{O}^2$)]⁺

^1H NMR (400 MHz, D₂O, 4 °C, 45OR4-2018): δ /ppm = 3.89 (dd, 1H, H5a, $^3J_{4,5a}=1.8$ Hz, $^2J_{5a,5b}=-13.1$ Hz), 3.72 (ddd, 1H, H4), 3.61 (d, 1H, H1, $^3J_{1,2}=8.7$ Hz), 3.57 (dd, 1H, H5b,

$J_{4,5b}=0.8$ Hz), 3.50 (dd, 1H, H3, $^3J_{2,3}=9.7$ Hz, $^3J_{3,4}=3.5$ Hz), 3.34 (dd, 1H, H2), 2.49 (s, 3H, CH₃).

$^{13}\text{C}\{^1\text{H}\}$ NMR (101 MHz, D₂O, 4 °C, 45OR5-2018): $\delta/\text{ppm} = 94.8$ (C1), 77.2 (C2), 75.3 (C3), 70.5 (C5), 69.0 (C4), 36.7 (CH₃).

$[\{\text{Pd}(\text{en})\}_2(^1\text{C}_4\text{-}\alpha\text{-D-Arap1NMe2,3,4H}_{-3}\text{-}\kappa^2\text{N}^1, \text{O}^2:2\kappa^2\text{O}^{3,4})]^+$

$^{13}\text{C}\{^1\text{H}\}$ NMR (101 MHz, D₂O, 4 °C, 45OR11-2018): $\delta/\text{ppm} = 94.7$ (C1), 85.1 (C3), 80.9 (C2), 79.2 (C4), 69.6 (C5), 37.0 (CH₃).

N-Ethyl-D-arabinosylamine and Pd-en

	D-Ara1NEt	Pd-en	HIO ₃	Pd-en chelate	%
1:1:1	120 mg	1.50 mL	119 mg	$^1\text{C}_4\text{-}\alpha\text{-D-Arap1NEt2H}_{-1}\text{-}\kappa^2\text{N}^1, \text{O}^2$	82
	675 μmol	675 μmol	675 μmol	D-Araa1NEt2H ₋₁ - $\kappa^2\text{N}^1, \text{O}^2$	10
				D-arabinose	8
1:2:1	59.8 mg	1.50 mL	59.4 mg	$^1\text{C}_4\text{-}\alpha\text{-D-Arap1NEt2,3,4H}_{-3}\text{-}\kappa^2\text{N}^1, \text{O}^2: \kappa^2\text{O}^{3,4}$	66
	338 μmol	675 μmol	338 μmol	$^1\text{C}_4\text{-}\alpha\text{-D-Arap1NEt2H}_{-1}\text{-}\kappa^2\text{N}^1, \text{O}^2$	21
				1 n. i. species	9
				D-Araa1NEt2H ₋₁ - $\kappa^2\text{N}^1, \text{O}^2$	4

$[\text{Pd}(\text{en})(^1\text{C}_4\text{-}\alpha\text{-D-Arap1NEt2H}_{-1}\text{-}\kappa^2\text{N}^1, \text{O}^2)]^+$

^1H NMR (400 MHz, D₂O, 4 °C, 45OR13-2018): $\delta/\text{ppm} = 3.87$ (dd, 1H, H5a, $^3J_{4,5a}=1.8$ Hz, $^2J_{5a,5b}=-13.0$ Hz), 3.72 (d, 1H, H4, $^3J_{3,4}=3.4$ Hz), 3.65 (d, 1H, H1, $^3J_{1,2}=8.9$ Hz), 3.59 (dd, 1H, H5b, $^3J_{4,5b}=1.3$ Hz), 3.49 (dd, 1H, H3, $^3J_{2,3}=9.6$ Hz), 3.49 (dd, 1H, H2), 2.88 (dq, 1H, CH₂), 2.52 (dq, 1H, CH₂), 1.36 (t, 3H, CH₃).

$^{13}\text{C}\{^1\text{H}\}$ NMR (101 MHz, D₂O, 4 °C, 45OR14-2018): $\delta/\text{ppm} = 89.9$ (C1), 77.0 (C2), 75.4 (C3), 70.5 (C5), 69.0 (C4), 42.2 (CH₂), 12.9 (CH₃).

$[\text{Pd}(\text{en})(\text{D-Araa1NEt2H}_{-1}\text{-}\kappa^2\text{N}^1, \text{O}^2)]^+$

^1H NMR (400 MHz, D₂O, 4 °C, 45OR13-2018): $\delta/\text{ppm} = 7.92$ (s, H1).

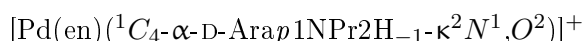
$^{13}\text{C}\{^1\text{H}\}$ NMR (101 MHz, D₂O, 4 °C, 45OR14-2018): $\delta/\text{ppm} = 186.1$ (C1), 85.8 (C2), 71.7 (C3), 71.5 (C4), 63.5 (C5), 55.6 (CH₂), 15.1 (CH₃).

$[\{\text{Pd}(\text{en})\}_2(^1\text{C}_4\text{-}\alpha\text{-D-Arap1NEt2,3,4H}_{-3}\text{-}\kappa^2\text{N}^1, \text{O}^2:2\kappa^2\text{O}^{3,4})]^+$

$^{13}\text{C}\{^1\text{H}\}$ NMR (101 MHz, D₂O, 4 °C, 45OR17-2018): $\delta/\text{ppm} = 89.6$ (C1), 85.2 (C3), 80.7 (C2), 79.1 (C4), 69.6 (C5), 42.2 (CH₂), 12.9 (CH₃).

N-Propyl-D-arabinosylamine and Pd-en

	D-Ara1NPr	Pd-en	HIO ₃	Pd-en chelate	%
1:1:1	129 mg	1.50 mL	119 mg	¹ C ₄ -α-D-Arap1NPr2H ₋₁ -κ ² N ¹ ,O ²	75
	675 μmol	675 μmol	675 μmol	D-Araa1NPr2H ₋₁ -κ ² N ¹ ,O ²	10
				D-arabinose	8
				1 n. i. species	7
1:2:1	64.5 mg	1.50 mL	59.4 mg	¹ C ₄ -α-D-Arap1NPr2,3,4H ₋₃ -κ ² N ¹ ,O ² :κ ² O ^{3,4}	64
	338 μmol	675 μmol	338 μmol	1 n. i. species	18
				¹ C ₄ -α-D-Arap1NPr2H ₋₁ -κ ² N ¹ ,O ²	12
				D-Araa1NPr2H ₋₁ -κ ² N ¹ ,O ²	6



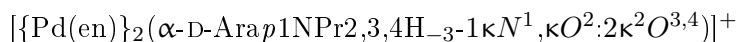
¹H NMR (400 MHz, D₂O, 4 °C, 41OR13-2018): δ/ppm = 3.86 (dd, 1H, H5a, ³J_{4,5a}=1.8 Hz, ²J_{5a,5b}=-13.1 Hz), 3.72 (d, 1H, H4, ³J_{3,4}=3.6 Hz), 3.65 (d, 1H, H1, ³J_{1,2}=8.8 Hz), 3.57 (dd, 1H, H5b, ³J_{4,5b}=1.3 Hz), 3.48 (dd, 1H, H3, ³J_{2,3}=9.7 Hz), 3.37 (dd, 1H, H2), 2.76 (dt, 1H, NH-CH₂), 2.45 (dt, 1H, NH-CH₂), 1.84-1.78 (m, 1H, CH₂), 0.91 (t, 3H, CH₃).

¹³C{¹H} NMR (101 MHz, D₂O, 4 °C, 41OR14-2018): δ/ppm = 91.1 (C1), 77.1 (C2), 75.4 (C3), 70.5 (C5), 69.0 (C4), 49.9 (NH-CH₂), 21.6 (CH₂), 11.4 (CH₃).



¹H NMR (400 MHz, D₂O, 4 °C, 41OR13-2018): δ/ppm = 7.91 (s, H1).

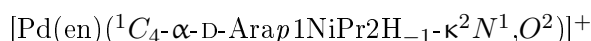
¹³C{¹H} NMR (101 MHz, D₂O, 4 °C, 41OR14-2018): δ/ppm = 187.2 (C1), 85.7 (C2), 71.7 (C3), 71.4 (C4), 63.4 (C5), 62.7 (NH-CH₂), 22.9 (CH₃), 11.6 (CH₃).



¹³C{¹H} NMR (101 MHz, D₂O, 4 °C, 41OR16-2018): δ/ppm = 90.8 (C1), 85.2 (C3), 80.9 (C2), 79.2 (C4), 69.6 (C5), 50.0 (NH-CH₂), 21.6 (CH₂), 11.4 (CH₃).

N-(iso-Propyl)-D-arabinosylamine and Pd-en

	D-Ara1NiPr	Pd-en	HIO ₃	Pd-en chelate	%
1:1:1	129 mg	1.50 mL	119 mg	¹ C ₄ -α-D-Arap1NiPr2H ₋₁ -κ ² N ¹ ,O ²	76
	675 μmol	675 μmol	675 μmol	1 n. i. species	14
				D-Araa1NiPr2H ₋₁ -κ ² N ¹ ,O ²	10
1:2:1	64.5 mg	1.50 mL	59.4 mg	¹ C ₄ -α-D-Arap1NiPr2,3,4H ₋₃ -κ ² N ¹ ,O ² :κ ² O ^{3,4}	52
	338 μmol	675 μmol	338 μmol	1 n. i. species	24
				D-Araa1NiPr2H ₋₁ -κ ² N ¹ ,O ²	15
				¹ C ₄ -α-D-Arap1NiPr2H ₋₁ -κ ² N ¹ ,O ²	9



¹H NMR (400 MHz, D₂O, 4 °C, 41OR17-2018): δ/ppm = 3.85 (dd, 1H, H5a, ³J_{4,5a}=1.8 Hz, ²J_{5a,5b}=-13.1 Hz), 3.71 (d, 1H, H4, ³J_{3,4}=2.8 Hz), 3.64 (d, 1H, H1, ³J_{1,2}=8.5 Hz), 3.58 (dd, 1H, H5b, ³J_{4,5b}=1.3 Hz), 3.44 (dd, 1H, H3, ³J_{2,3}=9.7 Hz), 3.37 (dd, 1H, H2), 3.06 (m, 1H, CH), 1.32

(t, 3H, CH₃), 1.24 (t, 3H, CH₃).

¹³C{¹H} NMR (101 MHz, D₂O, 4 °C, 41OR18-2018): δ/ppm = 90.8 (C1), 77.4 (C2), 75.5 (C3), 70.5 (C5), 68.9 (C4), 50.9 (CH), 22.5 (CH₃), 21.0 (CH₃).

[Pd(en)(D-Araa1NiPr2H₋₁-κ²N¹,O²)]⁺

¹H NMR (400 MHz, D₂O, 4 °C, 41OR17-2018): δ/ppm = 7.97 (s, H1).

¹³C{¹H} NMR (101 MHz, D₂O, 4 °C, 41OR14-2018): δ/ppm = 183.3 (C1), 86.1 (C2), 71.8 (C3), 71.6 (C4), 63.5 (C5), 60.0 (CH), 22.3 (CH₃), 21.1 (CH₃).

[{Pd(en)}₂(α-D-Arap1NiPr2,3,4H₋₃-κ²N¹,O²:2κ²O^{3,4})]⁺

¹³C{¹H} NMR (101 MHz, D₂O, 4 °C, 41OR20-2018): δ/ppm = 90.9 (C1), 85.4 (C3), 81.0 (C2), 79.2 (C4), 69.7 (C5), 50.6 (CH), 22.3 (CH₃), 21.1 (CH₃).

5.6.2. Complexes featuring *N*-Alkyl-D-lyxosylamines

N-Methyl-D-lyxosylamine and Pd-en

	D-Lyx1NMe	Pd-en	HIO ₃	species	%
1:1:1	110 mg	1.50 mL	119 mg	¹ C ₄ -α-D-Lyx p 1NMe2H ₋₁ -κ ² N ¹ ,O ²	36
	675 μmol	675 μmol	675 μmol	D-Lyx a 1NMe2H ₋₁ -κ ² N ¹ ,O ²	28
				β-D-Lyx p 1NMe2H ₋₁ -κ ² N ¹ ,O ²	17
				D-Lyx1NMe	15
				1 n. i. species	4
1:2:1	55.1 mg	1.50 mL	59.4 mg	2 n. i. species	41
	338 μmol	675 μmol	338 μmol	D-Lyx a 1NMe2,3,4H ₋₃ -κ ² N ¹ ,O ² :κ ² O ^{3,4}	33
				¹ C ₄ -α-D-Lyx p 1NMe2H ₋₁ -κ ² N ¹ ,O ²	26

[Pd(en)(¹C₄-α-D-Lyx p 1NMe2H₋₁-κ²N¹,O²)]⁺

¹H NMR (400 MHz, D₂O, 4 °C, 20OR7-2016): δ/ppm = 3.97 (t, 1H, H3, ³J_{3,4}=3.7 Hz), 3.91 (d, 1H, H1, ³J_{1,2}=9.4 Hz), 3.59 (dd, H4), 3.40 (dd, 1H, H2, ³J_{2,3}=3.1 Hz), 2.48 (s, 3H, CH₃).

¹³C{¹H} NMR (101 MHz, D₂O, 4 °C, 20OR8-2016): δ/ppm = 91.0 (C1), 75.3 (C2), 72.3 (C3), 69.6 (C4), 67.9 (C5), 36.8 (CH₃).

[Pd(en)(D-Lyx a 1NMe2H₋₁-κ²N¹,O²)]⁺

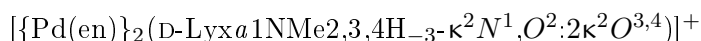
¹H NMR (400 MHz, D₂O, 4 °C, 20OR7-2016): δ/ppm = 8.09 (s, H1), 4.56 (m, H2), 3.32 (s, CH₃).

¹³C{¹H} NMR (101 MHz, D₂O, 4 °C, 20OR8-2016): δ/ppm = 187.8 (C1), 86.5 (C2), 74.6 (C3), 71.2 (C4), 63.3 (C5), 48.8 (CH₃).

[Pd(en)(¹C₄-β-D-Lyx p 1NMe2H₋₁-κ²N¹,O²)]⁺

¹H NMR (400 MHz, D₂O, 4 °C, 20OR7-2016): δ/ppm = 4.42 (d, H1, ³J_{1,2}=5.1 Hz), 2.38 (s, CH₃).

¹³C{¹H} NMR (101 MHz, D₂O, 4 °C, 20OR8-2016): δ/ppm = 93.0 (C1), 78.8 (C2), 72.6 (C3), 68.7 (C4), 61.0 (C5), 37.0 (CH₃).

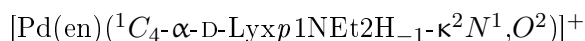


^1H NMR (400 MHz, D_2O , 4 °C, 20OR10-2016): $\delta/\text{ppm} = 8.11$ (s, H1).

$^{13}\text{C}\{^1\text{H}\}$ NMR (101 MHz, D_2O , 4 °C, 20OR11-2016): $\delta/\text{ppm} = 189.6$ (C1), 88.9 (C2), 87.5 (C3), 83.4 (C4), 64.6 (C5), 48.7 (CH_3).

N-Ethyl-D-lyxosylamine and Pd-en

	D-Lyx1NEt	Pd-en	HIO_3	species	%
1:1:1	120 mg	1.50 mL	119 mg	$^1\text{C}_4\text{-}\alpha\text{-D-Lyx}p\text{1NEt}2\text{H}_{-1-\kappa^2}\text{N}^1,\text{O}^2$	28
	675 μmol	675 μmol	675 μmol	D-lyxose	28
				D-Lyx α 1NEt2H $_{-1-\kappa^2}$ N 1 ,O 2	16
				β -D-Lyx p 1NMe2H $_{-1-\kappa^2}$ N 1 ,O 2	15
				1 n. i. species	13
1:2:1	59.8 mg	1.50 mL	59.4 mg	D-Lyx α 1NEt2,3,4H $_{-3-\kappa^2}$ N 1 ,O 2 : κ^2 O 3,4	58
	338 μmol	675 μmol	338 μmol	D-Lyx α 1NEt2H $_{-1-\kappa^2}$ N 1 ,O 2	24
				$^1\text{C}_4\text{-}\alpha\text{-D-Lyx}p\text{1NEt}2\text{H}_{-1-\kappa^2}\text{N}^1,\text{O}^2$	18



^1H NMR (400 MHz, D_2O , 4 °C, 20OR13-2016): $\delta/\text{ppm} = 3.97$ (d, 1H, H1, $^3J_{1,2}=9.4$ Hz), 3.45 (dd, 1H, H2, $^3J_{2,3}=3.1$ Hz).

$^{13}\text{C}\{^1\text{H}\}$ NMR (101 MHz, D_2O , 4 °C, 20OR14-2016): $\delta/\text{ppm} = 86.2$ (C1), 75.3 (C2), 72.4 (C3), 69.6 (C4), 67.9 (C5), 42.4 (CH_2), 13.0 (CH_3).



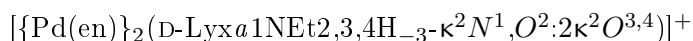
^1H NMR (400 MHz, D_2O , 4 °C, 20OR13-2016): $\delta/\text{ppm} = 8.07$ (s, H1).

$^{13}\text{C}\{^1\text{H}\}$ NMR (101 MHz, D_2O , 4 °C, 20OR14-2016): $\delta/\text{ppm} = 186.3$ (C1), 86.5 (C2), 74.6 (C3), 71.2 (C4), 63.3 (C5), 55.7 (CH_2), 15.1 (CH_3).



^1H NMR (400 MHz, D_2O , 4 °C, 20OR13-2016): $\delta/\text{ppm} = 4.49$ (d, H1, $^3J_{1,2}=4.6$ Hz).

$^{13}\text{C}\{^1\text{H}\}$ NMR (101 MHz, D_2O , 4 °C, 20OR14-2016): $\delta/\text{ppm} = 89.2$ (C1), 79.1 (C2), 71.5 (C3), 68.4 (C4), 62.0 (C5), 42.8 (CH_2), 12.7 (CH_3).



^1H NMR (400 MHz, D_2O , 4 °C, 33OR17-2017): $\delta/\text{ppm} = 8.13$ (s, H1).

$^{13}\text{C}\{^1\text{H}\}$ NMR (101 MHz, D_2O , 4 °C, 33OR18-2017): $\delta/\text{ppm} = 187.9$ (C1), 88.9 (C2), 87.6 (C3), 83.5 (C4), 64.6 (C5), 55.8 (CH_2), 15.2 (CH_3).

N-Propyl-D-lyxosylamine and Pd-en

	D-Lyx1NPr	Pd-en	HIO ₃	species	%
1:1:1	129 mg	1.50 mL	119 mg	D-Lyxa1NPr2H ₋₁ -κ ² N ¹ ,O ²	78
	675 μmol	675 μmol	675 μmol	¹ C ₄ -α-D-Lyxp1NPr2H ₋₁ -κ ² N ¹ ,O ²	10
				β-D-Lyxp1NPr2H ₋₁ -κ ² N ¹ ,O ²	8
				D-Lyxa1NPr2,3,4H ₋₃ -κ ² N ¹ ,O ² :κ ² O ^{3,4}	4
1:2:1	64.5 mg	1.50 mL	59.4 mg	D-Lyxa1NPr2,3,4H ₋₃ -κ ² N ¹ ,O ² :κ ² O ^{3,4}	50
	338 μmol	675 μmol	338 μmol	3 n. i. species	50



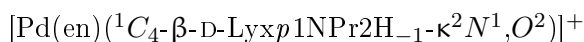
¹H NMR (400 MHz, D₂O, 4 °C, 22OR69-2016): δ/ppm = 8.08 (d, 1H, H1, ³J_{1,2}=1.2 Hz), 4.63 (dd, 1H, H2, ³J_{2,3}=6.3 Hz), 3.82 (ddd, 1H, H4), 3.76 (dd, 1H, H3, ³J_{3,4}=2.2 Hz), 3.65 (m, 2H, H5a/H5b), 2.66 (t, 2H, NH-CH₂), 1.60 (m, 2H, CH₂), 0.88 (t, 3H, NH-CH₃).

¹³C{¹H} NMR (101 MHz, D₂O, 4 °C, 22OR70-2016): δ/ppm = 187.3 (C1), 86.3 (C2), 74.7 (C3), 71.2 (C4), 63.3 (C5), 62.7 (NH-CH₂), 22.8 (CH₂), 10.7 (CH₃).



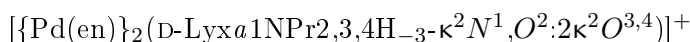
¹H NMR (400 MHz, D₂O, 4 °C, 22OR69-2016): δ/ppm = 4.01 (d, 1H, H1, ³J_{1,2}=9.3 Hz).

¹³C{¹H} NMR (101 MHz, D₂O, 4 °C, 22OR70-2016): δ/ppm = 87.4 (C1), 75.3 (C2), 72.4 (C3), 69.6 (C4), 67.9 (C5), 50.1 (NH-CH₂), 21.3 (CH₂), 11.1 (CH₃).



¹H NMR (400 MHz, D₂O, 4 °C, 22OR69-2016): δ/ppm = 4.49 (d, 1H, H1, ³J_{1,2}=4.3 Hz).

¹³C{¹H} NMR (101 MHz, D₂O, 4 °C, 22OR70-2016): δ/ppm = 91.0 (C1), 79.1 (C2), 72.6 (C3), 68.3 (C4), 67.5 (C5), 50.3 (NH-CH₂), 21.7 (CH₂), 11.4 (CH₃).



¹H NMR (400 MHz, D₂O, 4 °C, 23OR1-2016): δ/ppm = 8.11 (s, H1).

¹³C{¹H} NMR (101 MHz, D₂O, 4 °C, 23OR2-2016): δ/ppm = 188.8 (C1), 89.0 (C2), 87.4 (C3), 83.3 (C4), 64.6 (C5), 62.8 (NH-CH₂), 23.1 (CH₂), 10.8 (CH₃).

N-(iso-Propyl)-D-lyxosylamine and Pd-en

	D-Lyx1NiPr	Pd-en	HIO ₃	species	%
1:1:1	129 mg	1.50 mL	119 mg	D-Lyxa1NiPr2H ₋₁ -κ ² N ¹ ,O ²	64
	675 μmol	675 μmol	675 μmol	¹ C ₄ -α-D-Lyxp1NiPr2H ₋₁ -κ ² N ¹ ,O ²	36
1:2:1	64.5 mg	1.50 mL	59.4 mg	D-Lyxa1NiPr2,3,4H ₋₃ -κ ² N ¹ ,O ² :κ ² O ^{3,4}	100
	338 μmol	675 μmol	338 μmol		



¹H NMR (400 MHz, D₂O, 4 °C, 20OR1-2016): δ/ppm = 8.08 (s, 1H, H1), 4.56 (d, 1H, H2, ³J_{2,3}=6.2 Hz), 1.20 (t, 6H, 2×CH₃).

$^{13}\text{C}\{^1\text{H}\}$ NMR (101 MHz, D_2O , 4 °C, 20OR2-2016): δ/ppm = 183.5 (C1), 86.7 (C2), 74.7 (C3), 71.2 (C4), 63.3 (C5), 60.1 (CH), 22.2 (CH_3), 21.7 (CH_3).

$[\text{Pd}(\text{en})(^1\text{C}_4\text{-}\alpha\text{-D-Lyx}p1\text{NiPr}2\text{H}_{-1}\text{-}\kappa^2\text{N}^1, \text{O}^2)]^+$

^1H NMR (400 MHz, D_2O , 4 °C, 22OR69-2016): δ/ppm = 3.99 (d, 1H, H1, $^3J_{1,2}=9.6$ Hz).

$^{13}\text{C}\{^1\text{H}\}$ NMR (101 MHz, D_2O , 4 °C, 22OR70-2016): δ/ppm = 86.8 (C1), 75.5 (C2), 72.5 (C3), 69.6 (C4), 67.9 (C5), 50.8 (CH), 22.5 (CH_3), 21.2 (CH_3).

$[\{\text{Pd}(\text{en})\}_2(\text{D-Lyx}a1\text{NiPr}2,3,4\text{H}_{-3}\text{-}\kappa^2\text{N}^1, \text{O}^2:2\kappa^2\text{O}^{3,4})]^+$

^1H NMR (400 MHz, D_2O , 4 °C, 23OR4-2016): δ/ppm = 8.18 (s, H1).

$^{13}\text{C}\{^1\text{H}\}$ NMR (101 MHz, D_2O , 4 °C, 23OR5-2016): δ/ppm = 184.9 (C1), 88.5 (C2), 88.2 (C3), 83.6 (C4), 64.7 (C5), 60.4 (CH), 22.5 (CH_3), 21.7 (CH_3).

N-(*tert*-Butyl)-*D*-lyxosylamine and Pd-en

	D-Lyx1NtBu	Pd-en	HIO ₃	species	%
1:1:1	139 mg	1.50 mL	119 mg	D-lyxose	74
	675 μmol	675 μmol	675 μmol	D-Lyx $a1\text{NtBu}2\text{H}_{-1}\text{-}\kappa^2\text{N}^1, \text{O}^2$	36
				1 n. i. species	9
1:2:1	69.5 mg	1.50 mL	59.4 mg	D-Lyx $a1\text{NtBu}2,3,4\text{H}_{-3}\text{-}\kappa^2\text{N}^1, \text{O}^2:\kappa^2\text{O}^{3,4}$	73
	338 μmol	675 μmol	338 μmol	D-Lyx $a1\text{NtBu}2\text{H}_{-1}\text{-}\kappa^2\text{N}^1, \text{O}^2$	27

$[\text{Pd}(\text{en})(\text{D-Lyx}a1\text{NtBu}2\text{H}_{-1}\text{-}\kappa^2\text{N}^1, \text{O}^2)]^+$

^1H NMR (400 MHz, D_2O , 4 °C, 17OR7-2019): δ/ppm = 8.01 (d, 1H, H1), 4.49 (d, 1H, H2, $^3J_{1,2}=1.3$ Hz, $^3J_{2,3}=6.1$ Hz), 3.82 (d, 1H, H4), 3.77 (m, 1H, H3), 3.65 (m, 2H, H5a/H5b), 1.31 (s, 9H, 3 \times CH₃).

$^{13}\text{C}\{^1\text{H}\}$ NMR (101 MHz, D_2O , 4 °C, 17OR8-2019): δ/ppm = 181.8 (C1), 85.9 (C2), 75.2 (C3), 71.1 (C4), 63.3 (C5), 63.1 (C_q), 19.8 (CH₃), 29.1 (3 \times CH₃).

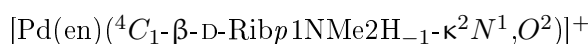
$[\{\text{Pd}(\text{en})\}_2(\text{D-Lyx}a1\text{NtBu}2,3,4\text{H}_{-3}\text{-}\kappa^2\text{N}^1, \text{O}^2:2\kappa^2\text{O}^{3,4})]^+$

^1H NMR (400 MHz, D_2O , 4 °C, 17OR10-2019): δ/ppm = 8.07 (s, H1, $J_{1,2}=1.5$ Hz), 4.37 $^3J_{2,3}=6.1$ Hz.

$^{13}\text{C}\{^1\text{H}\}$ NMR (101 MHz, D_2O , 4 °C, 17OR10-2019): δ/ppm = 183.0 (C1), 89.0 (C2), 87.4 (C3), 84.0 (C4), 64.5 (C5), 63.2 (C_q), 29.2 (3 \times CH₃).

5.6.3. Complexes featuring *N*-Alkyl-D-ribosylamines*N*-Methyl-D-ribosylamine and Pd-en

	D-Rib1NMe	Pd-en	HIO ₃	Pd-en chelate	%
1:1:1	110 mg 675 μmol	1.50 mL 675 μmol	119 mg 675 μmol	⁴ C ₁ -β-D-Ribp1NMe2H ₋₁ -κ ² N ¹ ,O ²	58
				⁴ C ₁ -α-D-Ribp1NMe2H ₋₁ -κ ² N ¹ ,O ²	25
				D-Riba1NMe2H ₋₁ -κ ² N ¹ ,O ²	13
				2 n. i. species	4
1:2:1	55.1 mg 338 μmol	1.50 mL 675 μmol	59.4 mg 338 μmol	⁴ C ₁ -β-D-Ribp1NMe2,3,4H ₋₃ -κ ² N ¹ ,O ² :κ ² O ^{3,4}	50
				α-D-Ribp1NMe2,3,4H ₋₃ -κ ² N ¹ ,O ² :κ ² O ^{3,4}	31
				D-Riba1NMe2,3,4H ₋₃ -κ ² N ¹ ,O ² :κ ² O ^{3,4}	8
				D-Riba1NMe2,4,5H ₋₃ -κ ² N ¹ ,O ² :κ ² O ^{4,5}	6
				1 n. i. species	5



¹H NMR (400 MHz, D₂O, 4 °C, 35OR7-2018): 4.04 (d, 1H, H1, ³J_{1,2}=9.1 Hz), 3.99 (t, 1H, H3, ³J_{2,3}=2.9 Hz, ³J_{3,4}=2.9 Hz), 3.94 (dd, 1H, H4), 3.77–3.72 (m, 1H, H5eq), 3.65–3.58 (m, 1H, H5ax), 3.26 (dd, 1H, H2), 2.45 (s, 3H, CH₃).

¹³C{¹H} NMR (101 MHz, D₂O, 4 °C, 35OR8-2018): δ/ppm = 90.8 (C1), 78.1 (C2), 72.1 (C3), 66.9 (C5), 64.8 (C4), 36.9 (CH₃).



¹H NMR (400 MHz, D₂O, 4 °C, 35OR8-2018): δ/ppm = 4.12 (d, H1, ³J_{1,2}=2.5 Hz).

¹³C{¹H} NMR (101 MHz, D₂O, 4 °C, 45OR5-2018): δ/ppm = 92.1 (C1), 73.3 (C2), 70.9 (C3), 66.6 (C4), 59.1 (C5), 36.8 (CH₃).

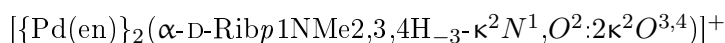


¹H NMR (400 MHz, D₂O, 4 °C, 35OR8-2018): δ/ppm = 7.99 (s, H1).

¹³C{¹H} NMR (101 MHz, D₂O, 4 °C, 35OR8-2018): δ/ppm = 186.4 (C1), 86.7 (C2), 74.4 (C3), 72.7 (C4), 63.4 (C5), 48.7 (CH₃).

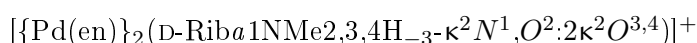


¹³C{¹H} NMR (101 MHz, D₂O, 4 °C, 36OR2-2018): δ/ppm = 91.2 (C1), 83.2 (C3), 77.9 (C2), 76.9 (C4), 67.6 (C5), 36.8 (CH₃).



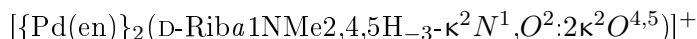
¹H NMR (400 MHz, D₂O, 4 °C, 36OR1-2018): δ/ppm = 8.11 (s, H1).

¹³C{¹H} NMR (101 MHz, D₂O, 4 °C, 36OR2-2018): δ/ppm = 91.2 (C1), 81.8 (C2), 75.8 (C3), 71.0 (C4), 60.4 (C5), 35.8 (CH₃).



¹H NMR (400 MHz, D₂O, 4 °C, 36OR1-2018): δ/ppm = 7.94 (s, H1).

¹³C{¹H} NMR (101 MHz, D₂O, 4 °C, 36OR2-2018): δ/ppm = 189.5 (C1), 87.7 (C2), 85.6 (C3), 82.6 (C4), 62.6 (C5), 48.8 (CH₃).



$^{13}\text{C}\{^1\text{H}\}$ NMR (101 MHz, D_2O , 4 °C, 36OR2-2018): δ/ppm = 185.8 (C1), 86.1 (C2), 82.1 (C4), 77.1 (C3), 73.5 (C5), 48.8 (CH_3).

N-Ethyl-D-ribosylamine and Pd-en

	D-Rib1NEt	Pd-en	HIO_3	Pd-en chelate	%
1:1:1	120 mg	1.50 mL	119 mg	$^4\text{C}_1\text{-}\beta\text{-D-Rib}p1\text{NEt}2\text{H}_{-1-\kappa^2}\text{N}^1,\text{O}^2$	88
	675 μmol	675 μmol	675 μmol	D-Rib a 1NEt2H $_{-1-\kappa^2}\text{N}^1,\text{O}^2$	12
1:2:1	59.8 mg	1.50 mL	59.4 mg	$^4\text{C}_1\text{-}\beta\text{-D-Rib}p1\text{NEt}2,3,4\text{H}_{-3-\kappa^2}\text{N}^1,\text{O}^2;\kappa^2\text{O}^{3,4}$	58
	338 μmol	675 μmol	338 μmol	D-Rib a 1NEt2,3,4H $_{-3-\kappa^2}\text{N}^1,\text{O}^2;\kappa^2\text{O}^{3,4}$	17
				D-Rib a 1NEt2,4,5H $_{-3-\kappa^2}\text{N}^1,\text{O}^2;\kappa^2\text{O}^{4,5}$	17
				$\alpha\text{-D-Rib}p1\text{NEt}2,3,4\text{H}_{-3-\kappa^2}\text{N}^1,\text{O}^2;\kappa^2\text{O}^{3,4}$	16



^1H NMR (400 MHz, D_2O , 4 °C, 28OR1-2018): δ/ppm = 4.14 (d, 1H, H1, $^3J_{1,2}=9.1$ Hz), 4.00 (t, 1H, H3, $^3J_{2,3}=2.8$ Hz, $^3J_{3,4}=2.8$ Hz), 3.76–3.71 (m, 1H, H5eq), 3.63 (dd, 1H, H5ax, $^3J_{4,5ax}=5.2$ Hz, $^2J_{5ax,5eq}=-11.5$ Hz), 3.52–3.46 (m, 1H, H4), 3.33–3.30 (sp, 1H, H2), 2.81 (dq, 1H, CH_2), 2.49 (dq, 1H, CH_2), 1.34 (t, 3H, CH_3).

$^{13}\text{C}\{^1\text{H}\}$ NMR (101 MHz, D_2O , 4 °C, 28OR2-2018): δ/ppm = 86.1 (C1), 78.0 (C2), 72.2 (C3), 66.9 (C5), 64.8 (C4), 42.4 (CH_2), 13.0 (CH_3).

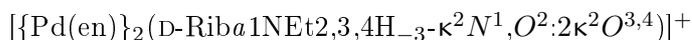


^1H NMR (400 MHz, D_2O , 4 °C, 28OR1-2018): δ/ppm = 7.99 (s, H1).

$^{13}\text{C}\{^1\text{H}\}$ NMR (101 MHz, D_2O , 4 °C, 28OR2-2018): δ/ppm = 184.9 (C1), 86.8 (C2), 74.2 (C3), 72.5 (C4), 63.4 (C5), 55.6 (CH_2), 15.0 (CH_3).

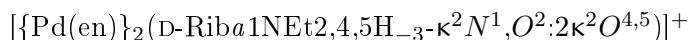


$^{13}\text{C}\{^1\text{H}\}$ NMR (101 MHz, D_2O , 4 °C, 28OR5-2018): δ/ppm = 86.2 (C1), 83.2 (C3), 77.7 (C2), 77.0 (C4), 67.7 (C5), 42.4 (CH_2), 13.0 (CH_3).



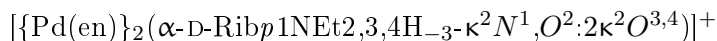
^1H NMR (400 MHz, D_2O , 4 °C, 28OR4-2018): δ/ppm = 8.12 (s, H1).

$^{13}\text{C}\{^1\text{H}\}$ NMR (101 MHz, D_2O , 4 °C, 28OR5-2018): δ/ppm = 187.8 (C1), 87.6 (C2), 85.7 (C3), 82.7 (C4), 62.6 (C5), 55.9 (CH_2), 15.3 (CH_3).



^1H NMR (400 MHz, D_2O , 4 °C, 28OR4-2018): δ/ppm = 7.95 (s, H1).

$^{13}\text{C}\{^1\text{H}\}$ NMR (101 MHz, D_2O , 4 °C, 28OR5-2018): δ/ppm = 184.3 (C1), 86.1 (C2), 82.2 (C4), 77.0 (C3), 73.5 (C5), 55.9 (CH_2), 12.4 (CH_3).



$^{13}\text{C}\{^1\text{H}\}$ NMR (101 MHz, D_2O , 4 °C, 28OR5-2018): $\delta/\text{ppm} = 86.0$ (C1), 81.6 (C2), 75.9 (C3), 70.9 (C4), 60.6 (C5), 40.7 (CH_2), 12.0 (CH_3).

N-Propyl-D-ribosylamine and Pd-en

	D-Rib1NPr	Pd-en	HIO_3	Pd-en chelate	%
1:1:1	129 mg	1.50 mL	119 mg	$^4\text{C}_1\text{-}\beta\text{-D-Ribp1NPr2H}_{-1}\text{-}\kappa^2\text{N}^1, \text{O}^2$	58
	675 μmol	675 μmol	675 μmol	D-Riba1NPr2H ₋₁ - $\kappa^2\text{N}^1, \text{O}^2$	26
				1 n. i. species	16
1:2:1	64.5 mg	1.50 mL	59.4 mg	$^4\text{C}_1\text{-}\beta\text{-D-Ribp1NPr2,3,4H}_{-3}\text{-}\kappa^2\text{N}^1, \text{O}^2; \kappa^2\text{O}^{3,4}$	25
	338 μmol	675 μmol	338 μmol	D-Riba1NPr2,3,4H ₋₃ - $\kappa^2\text{N}^1, \text{O}^2; \kappa^2\text{O}^{3,4}$	23
				D-Riba1NPr2,4,5H ₋₃ - $\kappa^2\text{N}^1, \text{O}^2; \kappa^2\text{O}^{4,5}$	22
				1 n. i. species	20
				$\alpha\text{-D-Ribp1NPr2,3,4H}_{-3}\text{-}\kappa^2\text{N}^1, \text{O}^2; \kappa^2\text{O}^{3,4}$	10

$[\text{Pd}(\text{en})(^4\text{C}_1\text{-}\alpha\text{-D-Ribp1NPr2H}_{-1}\text{-}\kappa^2\text{N}^1, \text{O}^2)]^+$

^1H NMR (400 MHz, D_2O , 4 °C, 38OR30-2018): $\delta/\text{ppm} = 4.12$ (d, 1H, H1, $^3J_{1,2}=9.4$ Hz), 4.01 (t, 1H, H3, $^3J_{2,3}=2.8$ Hz, $^3J_{3,4}=2.8$ Hz), 3.77–3.71 (m, 1H, H5eq), 3.65–3.60 (m, 1H, H5ax), 3.52–3.46 (m, 1H, H4), 3.33–3.30 (sp, 1H, H2), 2.76 (dt, 1H, NH– CH_2), 2.45 (dt, 1H, NH– CH_2), 1.84–1.78 (m, 1H, CH_2), 0.91 (t, 3H, CH_3).

$^{13}\text{C}\{^1\text{H}\}$ NMR (101 MHz, D_2O , 4 °C, 38OR31-2018): $\delta/\text{ppm} = 87.3$ (C1), 78.1 (C2), 72.2 (C3), 66.9 (C4), 64.8 (C5), 50.2 (NH– CH_2), 21.7 (CH_2), 11.4 (CH_3).

$[\text{Pd}(\text{en})(\text{D-Riba1NPr2H}_{-1}\text{-}\kappa^2\text{N}^1, \text{O}^2)]^+$

^1H NMR (400 MHz, D_2O , 4 °C, 38OR30-2018): $\delta/\text{ppm} = 7.98$ (s, H1).

$^{13}\text{C}\{^1\text{H}\}$ NMR (101 MHz, D_2O , 4 °C, 38OR31-2018): $\delta/\text{ppm} = 185.8$ (C1), 86.6 (C2), 74.4 (C3), 72.8 (C4), 63.4 (C5), 62.7 (NH– CH_2), 22.9 (CH_2), 10.8 (CH_3).

$[\{\text{Pd}(\text{en})\}_2(^4\text{C}_1\text{-}\beta\text{-D-Ribp1NPr2,3,4H}_{-3}\text{-}\kappa^2\text{N}^1, \text{O}^2; 2\kappa^2\text{O}^{3,4})]^+$

$^{13}\text{C}\{^1\text{H}\}$ NMR (101 MHz, D_2O , 4 °C, 28OR5-2018): $\delta/\text{ppm} = 91.2$ (C1), 83.2 (C3), 77.8 (C2), 76.9 (C4), 67.6 (C5), 50.2 (NH– CH_2), 21.7 (CH_2), 11.4 (CH_3).

$[\{\text{Pd}(\text{en})\}_2(\text{D-Riba1NPr2,3,4H}_{-3}\text{-}\kappa^2\text{N}^1, \text{O}^2; 2\kappa^2\text{O}^{3,4})]^+$

^1H NMR (400 MHz, D_2O , 4 °C, 28OR4-2018): $\delta/\text{ppm} = 8.09$ (s, H1).

$^{13}\text{C}\{^1\text{H}\}$ NMR (101 MHz, D_2O , 4 °C, 28OR5-2018): $\delta/\text{ppm} = 188.7$ (C1), 87.6 (C2), 85.6 (C3), 82.7 (C4), 62.8 (NH– CH_2), 62.5 (C5), 23.0 (CH_2), 10.8 (CH_3).

$[\{\text{Pd}(\text{en})\}_2(\text{D-Riba1NPr2,4,5H}_{-3}\text{-}\kappa^2\text{N}^1, \text{O}^2; 2\kappa^2\text{O}^{4,5})]^+$

^1H NMR (400 MHz, D_2O , 4 °C, 28OR4-2018): $\delta/\text{ppm} = 7.92$ (s, H1).

$^{13}\text{C}\{^1\text{H}\}$ NMR (101 MHz, D_2O , 4 °C, 28OR5-2018): $\delta/\text{ppm} = 185.2$ (C1), 86.0 (C2), 82.3 (C4), 77.0 (C3), 73.5 (C5), 62.9 (NH– CH_2), 23.0 (CH_2), 10.7 (CH_3).

$[\{\text{Pd}(\text{en})\}_2(\alpha\text{-D-Ribp1NPr2,3,4H}_{-3}\text{-}\kappa^2\text{N}^1, \text{O}^2; 2\kappa^2\text{O}^{3,4})]^+$

$^{13}\text{C}\{^1\text{H}\}$ NMR (101 MHz, D_2O , 4 °C, 28OR5-2018): $\delta/\text{ppm} = 87.3$ (C1), 81.6 (C2), 75.8 (C3),

70.8 (C4), 60.7 (C5), 48.4 (NH-CH₂), 20.8 (CH₂), 11.6 (CH₃).

N-(*iso*-Propyl)-*D*-ribosylamine and Pd-en

	D-Rib1 <i>Ni</i> Pr	Pd-en	HIO ₃	Pd-en chelate	%
1:1:1	129 mg	1.50 mL	119 mg	⁴ C ₁ -β- <i>D</i> -Rib <i>p</i> 1 <i>Ni</i> Pr2H ₋₁ -κ ² N ¹ ,O ²	71
	675 μmol	675 μmol	675 μmol	<i>D</i> -Rib <i>a</i> 1 <i>Ni</i> Pr2H ₋₁ -κ ² N ¹ ,O ²	29
1:2:1	64.5 mg	1.50 mL	59.4 mg	⁴ C ₁ -β- <i>D</i> -Rib <i>p</i> 1 <i>Ni</i> Pr2,3,4H ₋₃ -κ ² N ¹ ,O ² :κ ² O ^{3,4}	37
	338 μmol	675 μmol	338 μmol	<i>D</i> -Rib <i>a</i> 1 <i>Ni</i> Pr2,3,4H ₋₃ -κ ² N ¹ ,O ² :κ ² O ^{3,4}	27
				<i>D</i> -Rib <i>a</i> 1 <i>Ni</i> Pr2,4,5H ₋₃ -κ ² N ¹ ,O ² :κ ² O ^{4,5}	27
				α- <i>D</i> -Rib <i>p</i> 1 <i>Ni</i> Pr2,3,4H ₋₃ -κ ² N ¹ ,O ² :κ ² O ^{3,4}	5
				1 n. i. species	4



¹H NMR (400 MHz, D₂O, 4 °C, 28OR7-2018): δ/ppm = 4.13 (d, 1H, H1, ³J_{1,2}=9.4 Hz), 4.00 (d, 1H, H3, ³J_{3,4}=2.8 Hz), 3.86–3.81 (m, 1H, H5eq), 3.74 (dd, 1H, H5ax), 3.62 (dd, 1H, H4), 3.38 (dd, 1H, H2, ³J_{2,3}=2.8 Hz), 3.00 (m, 1H, CH), 1.30 (d, 3H, CH₃), 1.24 (d, 3H, CH₃).

¹³C{¹H} NMR (101 MHz, D₂O, 4 °C, 28OR8-2018): δ/ppm = 86.6 (C1), 78.3 (C2), 72.3 (C3), 66.8 (C4), 64.8 (C5), 50.9 (CH), 22.4 (CH₃), 21.1 (CH₃).

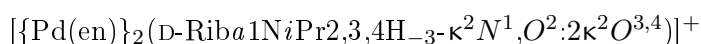


¹H NMR (400 MHz, D₂O, 4 °C, 28OR7-2018): δ/ppm = 7.98 (s, H1).

¹³C{¹H} NMR (101 MHz, D₂O, 4 °C, 28OR8-2018): δ/ppm = 182.0 (C1), 87.2 (C2), 74.1 (C3), 72.2 (C4), 63.4 (C5), 60.0 (CH), 22.2 (CH₃), 21.5 (CH₃).

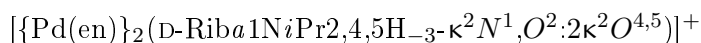


¹³C{¹H} NMR (101 MHz, D₂O, 4 °C, 28OR11-2018): δ/ppm = 86.9 (C1), 83.4 (C3), 78.0 (C2), 76.9 (C4), 67.7 (C5), 50.9 (CH), 22.5 (CH₃), 21.1 (CH₃).



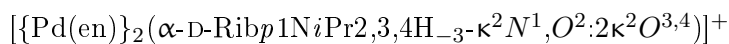
¹H NMR (400 MHz, D₂O, 4 °C, 28OR10-2018): δ/ppm = 8.14 (s, H1).

¹³C{¹H} NMR (101 MHz, D₂O, 4 °C, 28OR11-2018): δ/ppm = 184.4 (C1), 87.3 (C2), 86.1 (C3), 82.7 (C4), 62.6 (C5), 60.4 (CH), 22.3 (CH₃), 21.7 (CH₃).



¹H NMR (400 MHz, D₂O, 4 °C, 28OR10-2018): δ/ppm = 7.95 (s, H1).

¹³C{¹H} NMR (101 MHz, D₂O, 4 °C, 28OR11-2018): δ/ppm = 181.3 (C1), 86.2 (C2), 82.4 (C4), 77.0 (C3), 73.5 (C5), 60.5 (CH), 22.5 (CH₃), 21.9 (CH₃).



¹³C{¹H} NMR (101 MHz, D₂O, 4 °C, 28OR11-2018): δ/ppm = 86.7 (C1), 81.6 (C2), 75.9 (C3), 71.7 (C4), 60.4 (C5), 48.9 (CH), 21.6 (CH₃), 20.9 (CH₃).

***N*-(*tert*-Butyl)-*D*-ribosylamine and Pd-en**

	D-Rib1NtBu	Pd-en	HIO ₃	species	%
1:1:1	139 mg	1.50 mL	119 mg	D-Rib α 1NtBu2H ₋₁ - κ^2 N ¹ ,O ²	60
	675 μ mol	675 μ mol	675 μ mol	1 n. i. species	26
				⁴ C ₁ - β -D-Rib β 1NtBu2H ₋₁ - κ^2 N ¹ ,O ²	14
1:2:1	69.5 mg	1.50 mL	59.4 mg	D-Rib α 1NtBu2,3,4H ₋₁ - κ^2 N ¹ ,O ²	32
	338 μ mol	675 μ mol	338 μ mol	D-Rib α 1NtBu2,4,5H ₋₃ - κ^2 N ¹ ,O ² : κ^2 O ^{4,5}	24
				D-Rib α 1NtBu2,3,4H ₋₃ - κ^2 N ¹ ,O ² : κ^2 O ^{3,4}	22
				2 n. i. species	22

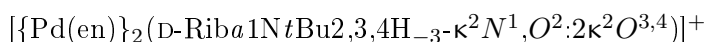


¹H NMR (400 MHz, D₂O, 4 °C, 38OR1-2018): δ /ppm = 7.90 (s, H1).

¹³C{¹H} NMR (101 MHz, D₂O, 4 °C, 38OR2-2018): δ /ppm = 180.3 (C1), 86.7 (C2), 74.1 (C3), 72.2 (C4), 63.5 (C5), 63.0 (C_q), 27.5 (3 \times CH₃).

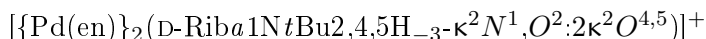


¹³C{¹H} NMR (101 MHz, D₂O, 4 °C, 38OR2-2018): δ /ppm = 94.4 (C1), 82.6 (C2), 71.6 (C3), 67.7 (C4), 63.6 (C5), 57.1 (C_q), 27.5 (3 \times CH₃).



¹H NMR (400 MHz, D₂O, 4 °C, 38OR4-2018): δ /ppm = 8.03 (s, H1).

¹³C{¹H} NMR (101 MHz, D₂O, 4 °C, 38OR5-2018): δ /ppm = 182.7 (C1), 87.6 (C2), 85.5 (C3), 82.7 (C4), 63.0 (C_q), 62.6 (C5), 29.3 (3 \times CH₃).



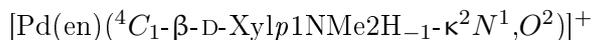
¹H NMR (400 MHz, D₂O, 4 °C, 38OR4-2018): δ /ppm = 7.79 (s, H1).

¹³C{¹H} NMR (101 MHz, D₂O, 4 °C, 38OR5-2018): δ /ppm = 179.5 (C1), 86.7 (C2), 82.5 (C4), 76.9 (C3), 73.5 (C5), 63.4 (C_q), 29.1 (3 \times CH₃).

5.6.4. Complexes featuring *N*-Alkyl-*D*-xylosylamines***N*-Methyl-*D*-xylosylamine and Pd-en**

	D-Xyl1NMe	Pd-en	HIO ₃	Pd-en chelate	%
1:1:1	110 mg	1.50 mL	119 mg	⁴ C ₁ - β -D-Xyl β 1NMe2H ₋₁ - κ^2 N ¹ ,O ²	85
	675 μ mol	675 μ mol	675 μ mol	D-Xyl α 1NMe2H ₋₁ - κ^2 N ¹ ,O ²	4
				α -D-Xyl β 1NMe2H ₋₁ - κ^2 N ¹ ,O ²	3
				1 n. i. species	8
1:1.5:1	73.4 mg	1.50 mL	79.2 mg	⁴ C ₁ - β -D-Xyl β 1NMe2,3,4H ₋₃ - κ^2 N ¹ ,O ² : κ^2 O ^{3,4}	47
	450 μ mol	675 μ mol	450 μ mol	⁴ C ₁ - β -D-Xyl β 1NMe2H ₋₁ - κ^2 N ¹ ,O ²	40
				D-Xyl α 1NMe2,3,4H ₋₃ - κ^2 N ¹ ,O ² : κ^2 O ^{3,4}	13
1:2:1	55.1 mg	1.50 mL	59.4 mg	⁴ C ₁ - β -D-Xyl β 1NMe2,3,4H ₋₃ - κ^2 N ¹ ,O ² : κ^2 O ^{3,4}	68
	338 μ mol	675 μ mol	338 μ mol	D-Xyl α 1NMe2,3,4H ₋₃ - κ^2 N ¹ ,O ² : κ^2 O ^{3,4}	24
				⁴ C ₁ - β -D-Xyl β 1NMe2H ₋₁ - κ^2 N ¹ ,O ²	8

After overlaying the aqueous reaction mixture containing all reactants in equimolar amounts with acetone and storing it at 4 °C for one week, colorless crystals of **8**IO₃-tetrahydrate were obtained that were suitable for structure analysis via single-crystal X-ray diffraction.



¹H NMR (400 MHz, D₂O, 4 °C, 33OR15-2017): $\delta/\text{ppm} = 3.90$ (dd, 1H, H5a, ³J_{4,5a}=5.4 Hz, ²J_{5a,5b}=-11.5 Hz), 3.81 (d, 1H, H1, ³J_{1,2}=8.9 Hz), 3.61 (dd, H4), 3.50 (sp, H3), 3.26 (t, 1H, H5b, ³J_{4,5b}=10.6 Hz), 3.16 (t, 1H, H2, ³J_{2,3}=9.1 Hz), 2.46 (s, 3H, CH₃).

¹³C{¹H} NMR (101 MHz, D₂O, 4 °C, 33OR16-2017): $\delta/\text{ppm} = 94.9$ (C1), 80.2 (C2), 78.0 (C3), 69.8 (C4), 68.6 (C5), 36.8 (CH₃).



¹H NMR (400 MHz, D₂O, 4 °C, 33OR15-2017): $\delta/\text{ppm} = 7.94$ (s, H1).

¹³C{¹H} NMR (101 MHz, D₂O, 4 °C, 33OR16-2017): $\delta/\text{ppm} = 187.4$ (C1), 87.3 (C2), 72.7 (C3), 71.1 (C4), 63.3 (C5), 48.6 (CH₃).

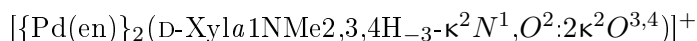


¹H NMR (400 MHz, D₂O, 4 °C, 33OR15-2017): 3.81 (d, 1H, H1, ³J_{1,2}=5.5 Hz).

¹³C{¹H} NMR (101 MHz, D₂O, 4 °C, 33OR16-2017): $\delta/\text{ppm} = 93.4$ (C1), 76.7 (C2), 73.4 (C3), 69.1 (C4), 63.5 (C5), 37.0 (CH₃).



¹³C{¹H} NMR (101 MHz, D₂O, 4 °C, 33OR18-2017): $\delta/\text{ppm} = 95.4$ (C1), 88.3 (C3), 82.1 (C2), 79.7 (C4), 68.2 (C5), 37.2 (CH₃).

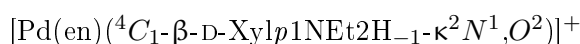


¹H NMR (400 MHz, D₂O, 4 °C, 33OR17-2017): $\delta/\text{ppm} = 8.91$ (s, H1).

¹³C{¹H} NMR (101 MHz, D₂O, 4 °C, 33OR18-2017): $\delta/\text{ppm} = 187.9$ (C1), 88.2 (C2), 85.2 (C3), 79.9 (C4), 65.6 (C5), 48.7 (CH₃).

N-Ethyl-D-xylosylamine and Pd-en

	D-Xyl11NEt	Pd-en	HIO ₃	Pd-en chelate	%
1:1:1	120 mg	1.50 mL	119 mg	⁴ C ₁ -β-D-Xylp1NEt2H ₋₁ -κ ² N ¹ ,O ²	98
	675 μmol	675 μmol	675 μmol	D-Xyla1NEt2H ₋₁ -κ ² N ¹ ,O ²	2
1:1.5:1	79.7 mg	1.50 mL	79.2 mg	⁴ C ₁ -β-D-Xylp1NEt2H ₋₁ -κ ² N ¹ ,O ²	58
	450 μmol	450 μmol	450 μmol	⁴ C ₁ -β-D-Xylp1NEt2,3,4H ₋₃ -κ ² N ¹ ,O ² :κ ² O ^{3,4}	27
				D-Xyla1NEt2,3,4H ₋₃ -κ ² N ¹ ,O ² :κ ² O ^{3,4}	9
				D-Xyla1NEt2H ₋₁ -κ ² N ¹ ,O ²	6
1:2:1	59.8 mg	1.50 mL	59.4 mg	⁴ C ₁ -β-D-Xylp1NEt2H ₋₁ -κ ² N ¹ ,O ²	48
	338 μmol	675 μmol	338 μmol	⁴ C ₁ -β-D-Xylp1NEt2,3,4H ₋₃ -κ ² N ¹ ,O ² :κ ² O ^{3,4}	31
				D-Xyla1NEt2,3,4H ₋₃ -κ ² N ¹ ,O ² :κ ² O ^{3,4}	12
				D-Xyla1NEt2H ₋₁ -κ ² N ¹ ,O ²	4
				1 n. i. species	5



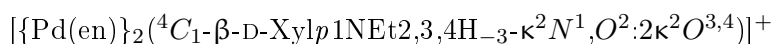
¹H NMR (400 MHz, D₂O, 4 °C, 33OR4-2017): 3.89–3.84 (sp, 1H, H5a) 3.85 (d, 1H, H1, ³J_{1,2}=7.8 Hz), 3.50 (td, 1H, H4), 3.29–3.22 (m, 3H, H3/H5b/H2), 2.83 (dd, 1H, CH₂) 2.49 (dd, 1H, CH₂), 1.35 (t, 3H, CH₃).

¹³C{¹H} NMR (101 MHz, D₂O, 4 °C, 33OR5-2017): δ/ppm = 90.2 (C1), 80.0 (C2), 78.0 (C3), 69.7 (C4), 68.6 (C5), 42.3 (CH₂), 12.9 (CH₃).

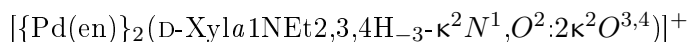


¹H NMR (400 MHz, D₂O, 4 °C, 33OR7-2017): δ/ppm = 7.96 (s, H1).

¹³C{¹H} NMR (101 MHz, D₂O, 4 °C, 33OR8-2017): δ/ppm = 185.9 (C1), 87.4 (C2), 72.8 (C3), 71.0 (C4), 63.3 (C5), 55.5 (CH₂), 14.8 (CH₃).



¹³C{¹H} NMR (101 MHz, D₂O, 4 °C, 33OR8-2017): δ/ppm = 90.6 (C1), 88.4 (C3), 81.9 (C2), 79.7 (C4), 68.2 (C5), 42.5 (CH₂), 12.8 (CH₃).

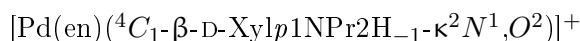


¹H NMR (400 MHz, D₂O, 4 °C, 33OR7-2017): δ/ppm = 8.91 (s, H1).

¹³C{¹H} NMR (101 MHz, D₂O, 4 °C, 33OR8-2017): δ/ppm = 186.1 (C1), 88.3 (C2), 85.2 (C3), 79.9 (C4), 65.6 (C5), 55.5 (CH₂), 14.9 (CH₃).

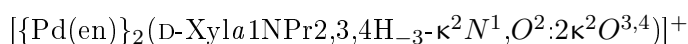
N-Propyl-D-xylosylamine and Pd-en

	D-Xyl1NPr	Pd-en	HIO ₃	Pd-en chelate	%
1:1:1	129 mg	1.50 mL	119 mg	⁴ C ₁ -β-D-Xylp1NPr2H ₋₁ -κ ² N ¹ ,O ²	76
	675 μmol	675 μmol	675 μmol	D-Xyla1NPr2H ₋₁ -κ ² N ¹ ,O ²	24
1:2:1	64.5 mg	1.50 mL	59.4 mg	D-Xyla1NPr2,3,4H ₋₃ -κ ² N ¹ ,O ² :κ ² O ^{3,4}	50
	338 μmol	675 μmol	338 μmol	⁴ C ₁ -β-D-Xylp1NPr2,3,4H ₋₃ -κ ² N ¹ ,O ² :κ ² O ^{3,4}	35
				n. i. species	15



¹H NMR (400 MHz, D₂O, 4 °C, 12OR1-2016): 3.85 (d, 1H, H1, ³J_{1,2}=8.2 Hz), 3.62 (dd, 1H, H5a, ³J_{4,5a}=5.5 Hz), 3.48 (dd, 1H, H4), 3.30–3.11 (m, 3H, H3/H5b/H2), 2.65–2.61 (sp, 2H, NH–CH₂) 1.82–1.73 (q, 2H, CH₂), 0.90 (t, 3H, CH₃).

¹³C{¹H} NMR (101 MHz, D₂O, 4 °C, 12OR2-2016): δ/ppm = 91.4 (C1), 80.1 (C2), 78.0 (C3), 69.7 (C4), 68.6 (C5), 50.0 (NH–CH₂), 21.6 (CH₂), 11.4 (CH₃).



¹H NMR (400 MHz, D₂O, 4 °C, 12OR1-2016): δ/ppm = 7.94 (s, H1).

¹³C{¹H} NMR (101 MHz, D₂O, 4 °C, 12OR2-2016): δ/ppm = 186.7 (C1), 87.3 (C2), 72.5 (C3), 71.4 (C4), 63.2 (C5), 62.6 (NH–CH₂), 22.8 (CH₂), 10.8 (CH₃).



¹H NMR (400 MHz, D₂O, 4 °C, 12OR4-2016): δ/ppm = 8.83 (s, H1).

¹³C{¹H} NMR (101 MHz, D₂O, 4 °C, 12OR5-2016): δ/ppm = 187.1 (C1), 88.2 (C2), 85.4 (C3), 80.1 (C4), 66.5 (C5), 62.8 (NH–CH₂), 23.1 (CH₂), 11.0 (CH₃).



¹³C{¹H} NMR (101 MHz, D₂O, 4 °C, 12OR5-2016): δ/ppm = 91.8 (C1), 88.4 (C3), 82.0 (C2), 79.7 (C4), 68.2 (C5), 50.2 (NH–CH₂), 21.5 (CH₂), 11.3 (CH₃).

N-(iso-Propyl)-D-xylosylamine and Pd-en

	D-Xyl1NiPr	Pd-en	HIO ₃	Pd-en chelate	%
1:1:1	129 mg	1.50 mL	119 mg	⁴ C ₁ -β-D-Xylp1NiPr2H ₋₁ -κ ² N ¹ ,O ²	78
	675 μmol	675 μmol	675 μmol	D-Xyla1NiPr2H ₋₁ -κ ² N ¹ ,O ²	14
				⁴ C ₁ -α-D-Xylp1NiPr2H ₋₁ -κ ² N ¹ ,O ²	8
1:2:1	64.5 mg	1.50 mL	59.4 mg	⁴ C ₁ -β-D-Xylp1NiPr2,3,4H ₋₃ -κ ² N ¹ ,O ² :κ ² O ^{3,4}	60
	338 μmol	675 μmol	338 μmol	D-Xyla1NiPr2,3,4H ₋₃ -κ ² N ¹ ,O ² :κ ² O ^{3,4}	29
				1 n. i. species	11



¹H NMR (400 MHz, D₂O, 4 °C, 32OR10-2017): 3.85 (d, H1, ³J_{1,2}=8.7 Hz), 3.84 (sp, H5a), 3.54–3.38 (m, H4), 3.30–3.16 (sp, H3/H5b), 3.09–2.97 (m, H2), 2.68–2.52 (m, CH), 1.30 (d, 2×CH₃).

$^{13}\text{C}\{^1\text{H}\}$ NMR (101 MHz, D_2O , 4 °C, 32OR11-2017): $\delta/\text{ppm} = 90.9$ (C1), 80.3 (C2), 78.1 (C3), 69.7 (C4), 68.5 (C5), 50.9 (CH), 22.4 (CH_3), 21.0 (CH_3).

$[\text{Pd}(\text{en})(\text{D-Xyl}a1\text{N}i\text{Pr}2\text{H}_{-1}-\kappa^2\text{N}^1,\text{O}^2)]^+$

^1H NMR (400 MHz, D_2O , 4 °C, 32OR10-2017): $\delta/\text{ppm} = 7.99$ (s, H1), 1.24 (d, $2\times\text{CH}_3$).

$^{13}\text{C}\{^1\text{H}\}$ NMR (101 MHz, D_2O , 4 °C, 32OR11-2017): $\delta/\text{ppm} = 183.2$ (C1), 87.7 (C2), 72.9 (C3), 70.9 (C4), 63.3 (C5), 59.7 (CH), 22.1 (CH_3), 21.4 (CH_3).

$[\text{Pd}(\text{en})(\alpha\text{-D-Xyl}p1\text{N}i\text{Pr}2\text{H}_{-1}-\kappa^2\text{N}^1,\text{O}^2)]^+$

^1H NMR (400 MHz, D_2O , 4 °C, 32OR10-2017): 4.66 (d, H1, $^3J_{1,2}=4.4$ Hz), 1.18 (d, $2\times\text{CH}_3$).

$^{13}\text{C}\{^1\text{H}\}$ NMR (101 MHz, D_2O , 4 °C, 32OR11-2017): $\delta/\text{ppm} = 88.9$ (C1), 78.2 (C2), 75.3 (C3), 69.1 (C4), 64.0 (C5), 52.3 (CH), 22.3 (CH_3), 21.1 (CH_3).

$[\{\text{Pd}(\text{en})\}_2(^4\text{C}_1\text{-}\beta\text{-D-Xyl}p1\text{N}i\text{Pr}2,3,4\text{H}_{-3}-\kappa^2\text{N}^1,\text{O}^2:2\kappa^2\text{O}^{3,4})]^+$

$^{13}\text{C}\{^1\text{H}\}$ NMR (101 MHz, D_2O , 4 °C, 32OR14-2017): $\delta/\text{ppm} = 91.6$ (C1), 88.4 (C3), 82.2 (C2), 79.7 (C4), 68.2 (C5), 50.9 (CH), 22.3 (CH_3), 20.8 (CH_3).

$[\{\text{Pd}(\text{en})\}_2(\text{D-Xyl}a1\text{N}i\text{Pr}2,3,4\text{H}_{-3}-\kappa^2\text{N}^1,\text{O}^2:2\kappa^2\text{O}^{3,4})]^+$

^1H NMR (400 MHz, D_2O , 4 °C, 32OR13-2017): $\delta/\text{ppm} = 8.94$ (s, H1), 1.16 (d, $2\times\text{CH}_3$).

$^{13}\text{C}\{^1\text{H}\}$ NMR (101 MHz, D_2O , 4 °C, 32OR14-2017): $\delta/\text{ppm} = 183.3$ (C1), 88.5 (C2), 85.4 (C3), 80.0 (C4), 65.6 (C5), 59.5 (CH), 22.8 (CH_3), 21.2 (CH_3).

***N*-(*tert*-Butyl)-D-xylosylamine and Pd-en**

	D-Xyl1N <i>t</i> Bu	Pd-en	HIO ₃	Pd-en chelate	%
1:1:1	139 mg	1.50 mL	119 mg	D-Xyl <i>a</i> 1N <i>t</i> Bu2H ₋₁ - $\kappa^2\text{N}^1,\text{O}^2$	49
	675 μmol	675 μmol	675 μmol	$^4\text{C}_1\text{-}\beta\text{-D-Xyl}p1\text{N}i\text{Pr}2,3,4\text{H}_{-3}-\kappa^2\text{N}^1,\text{O}^2:\kappa^2\text{O}^{3,4}$	20
				D-Xyl <i>a</i> 1N <i>t</i> Bu2,3,4H ₋₃ - $\kappa^2\text{N}^1,\text{O}^2:\kappa^2\text{O}^{3,4}$	18
				$^4\text{C}_1\text{-}\beta\text{-D-Xyl}p1\text{N}i\text{Pr}2\text{H}_{-1}-\kappa^2\text{N}^1,\text{O}^2$	11
1:2:1	69.5 mg	1.50 mL	59.4 mg	D-Xyl <i>a</i> 1N <i>t</i> Bu2,3,4H ₋₃ - $\kappa^2\text{N}^1,\text{O}^2:\kappa^2\text{O}^{3,4}$	75
	338 μmol	675 μmol	338 μmol	n. i. species	25

$[\text{Pd}(\text{en})(\text{D-Xyl}a1\text{N}i\text{Pr}2\text{H}_{-1}-\kappa^2\text{N}^1,\text{O}^2)]^+$

^1H NMR (400 MHz, D_2O , 4 °C, 32OR16-2017): $\delta/\text{ppm} = 7.90$ (s, H1).

$^{13}\text{C}\{^1\text{H}\}$ NMR (101 MHz, D_2O , 4 °C, 32OR17-2017): $\delta/\text{ppm} = 181.3$ (C1), 87.2 (C2), 72.8 (C3), 71.1 (C4), 63.2 (C5), 62.9 (C_q), 29.0 (CH_3).

$[\{\text{Pd}(\text{en})\}_2(^4\text{C}_1\text{-}\beta\text{-D-Xyl}p1\text{N}i\text{Pr}2,3,4\text{H}_{-3}-\kappa^2\text{N}^1,\text{O}^2:2\kappa^2\text{O}^{3,4})]^+$

$^{13}\text{C}\{^1\text{H}\}$ NMR (101 MHz, D_2O , 4 °C, 32OR17-2017): $\delta/\text{ppm} = 97.3$ (C1), 89.4 (C3), 82.8 (C2), 78.5 (C4), 68.4 (C5), 58.8 (C_q), 29.2 (CH_3).

$[\{\text{Pd}(\text{en})\}_2(\text{D-Xyl}a1\text{N}i\text{Pr}2,3,4\text{H}_{-3}-\kappa^2\text{N}^1,\text{O}^2:2\kappa^2\text{O}^{3,4})]^+$

^1H NMR (400 MHz, D_2O , 4 °C, 32OR16-2017): $\delta/\text{ppm} = 8.72$ (s, H1).

$^{13}\text{C}\{^1\text{H}\}$ NMR (101 MHz, D_2O , 4 °C, 32OR17-2017): $\delta/\text{ppm} = 181.9$ (C1), 88.0 (C2), 85.5 (C3), 80.3 (C4), 65.4 (C5), 61.1 (C_q), 28.6 (CH_3).

$[\text{Pd}(\text{en})(^4C_1\text{-}\beta\text{-D-Xylp1NtBu2H}_{-1}\text{-}\kappa^2N^1,O^2)]^+$

^1H NMR (400 MHz, D_2O , 4 °C, 32OR10-2017): 4.06 (d, H1, $^3J_{1,2}=12.9$ Hz).

$^{13}\text{C}\{^1\text{H}\}$ NMR (101 MHz, D_2O , 4 °C, 32OR17-2017): $\delta/\text{ppm} = 91.6$ (C1), 81.0 (C2), 78.2 (C3), 69.8 (C4), 68.6 (C5), 57.0 (C_q), 29.9 (CH_3).

5.6.5. Complexes featuring *N*-Alkyl-D-galactosylamines

N-Methyl-D-galactosylamine and Pd-en

	D-Gal1NMe	Pd-en	HIO_3	Pd-en chelate	%
1:1:1	110 mg	1.50 mL	119 mg	$\beta\text{-D-Galp1NMe2H}_{-1}\text{-}\kappa^2N^1,O^2$	98
	675 μmol	675 μmol	675 μmol	D-Gal α 1NMe2H $_{-1}\text{-}\kappa^2N^1,O^2$	2
1:2:1	55.1 mg	1.50 mL	59.4 mg	$\beta\text{-D-Galp1NMe2,3,4H}_{-3}\text{-}\kappa^2N^1,O^2:\kappa^2O^{3,4}$	92
	338 μmol	675 μmol	338 μmol	2 n. i. species	8

$[\text{Pd}(\text{en})(^4C_1\text{-}\beta\text{-D-Galp1NMe2H}_{-1}\text{-}\kappa^2N^1,O^2)]^+$

^1H NMR (400 MHz, D_2O , 4 °C, 11OR1-2016): $\delta/\text{ppm} = 3.72$ (m, 4H, H1/H4/H6/H6'), 3.63 (m, 1H, H5), 3.48 (dd, 1H, H3, $^3J_{2,3}=9.8$ Hz, $^3J_{3,4}=3.5$ Hz), 3.35 (dd, 1H, H2), 2.52 (s, 3H, CH_3).

$^{13}\text{C}\{^1\text{H}\}$ NMR (101 MHz, D_2O , 4 °C, 11OR2-2016): $\delta/\text{ppm} = 94.5$ (C1), 79.3 (C5), 77.3 (C2), 75.3 (C3), 69.3 (C4), 61.6 (C6), 36.9 (CH_3).

$[\text{Pd}(\text{en})(\text{D-Gal}\alpha\text{1NMe2H}_{-1}\text{-}\kappa^2N^1,O^2)]^+$

^1H NMR (400 MHz, D_2O , 4 °C, 11OR1-2016): 7.94 (d, H1).

$^{13}\text{C}\{^1\text{H}\}$ NMR (101 MHz, D_2O , 4 °C, 11OR2-2016): $\delta/\text{ppm} = 187.9$ (C1), 85.6 (C2), 70.8 (C3), 70.7 (C5), 70.2 (C4), 63.7 (C6), 48.6 (CH_3).

$[\{\text{Pd}(\text{en})\}_2(^4C_1\text{-}\beta\text{-D-Galp1NMe2,3,4H}_{-3}\text{-}\kappa^2N^1,O^2:2\kappa^2O^{3,4})]^+$

$^{13}\text{C}\{^1\text{H}\}$ NMR (101 MHz, D_2O , 4 °C, 11OR5-2016): $\delta/\text{ppm} = 94.6$ (C1), 85.3 (C3), 81.1 (C2), 79.8 (C4), 78.5 (C5), 62.5 (C6), 37.1 (CH_3).

N-Ethyl-D-galactosylamine and Pd-en

	D-Gal1NEt	Pd-en	HIO_3	Pd-en chelate	%
1:1:1	140 mg	1.50 mL	119 mg	$\beta\text{-D-Galp1NEt2H}_{-1}\text{-}\kappa^2N^1,O^2$	95
	675 μmol	675 μmol	675 μmol	D-Gal α 1NEt2H $_{-1}\text{-}\kappa^2N^1,O^2$	5
1:2:1	69.9 mg	1.50 mL	59.4 mg	$\beta\text{-D-Galp1NEt2,3,4H}_{-3}\text{-}\kappa^2N^1,O^2:\kappa^2O^{3,4}$	92
	338 μmol	675 μmol	338 μmol	2 n. i. species	8

$[\text{Pd}(\text{en})(^4C_1\text{-}\beta\text{-D-Galp1NEt2H}_{-1}\text{-}\kappa^2N^1,O^2)]^+$

^1H NMR (400 MHz, D_2O , 4 °C, 18OR7-2016): $\delta/\text{ppm} = 3.73$ (m, 4H, H1/H4/H6/H6'), 3.63 (m, 1H, H5), 3.47 (dd, 1H, H3, $^3J_{2,3}=9.7$ Hz, $^3J_{3,4}=3.4$ Hz), 3.35 (dd, 1H, H2), 2.96 (m, 1H, CH_2),

2.50 (m, 1H, CH₂), 1.37 (t, 3H, CH₃).

¹³C{¹H} NMR (101 MHz, D₂O, 4 °C, 18OR8-2016): δ/ppm = 89.6 (C1), 79.3 (C5), 77.2 (C2), 75.4 (C3), 69.3 (C4), 61.5 (C6), 42.2 (CH₂), 13.0 (CH₃).

[Pd(en)(D-Galα1NEt2H₋₁-κ²N¹,O²)]⁺

¹H NMR (400 MHz, D₂O, 4 °C, 21OR31-2016): δ/ppm = 7.96 (s, H1).

¹³C{¹H} NMR (101 MHz, D₂O, 4 °C, 18OR8-2016): δ/ppm = 186.3 (C1), 85.7 (C2), 70.8 (C3), 70.7 (C5), 70.2 (C4), 63.7 (C6), 55.6 (CH₂), 15.1 (CH₃).

[{Pd(en)}₂(⁴C₁-β-D-Galp1NEt2,3,4H₋₃-κ²N¹,O²:2κ²O^{3,4})]⁺

¹³C{¹H} NMR (101 MHz, D₂O, 4 °C, 18OR11-2016): δ/ppm = 89.5 (C1), 85.9 (C3), 80.9 (C2), 79.8 (C4), 78.5 (C5), 62.5 (C6), 42.2 (CH₂), 13.0 (CH₃).

N-Propyl-D-galactosylamine and Pd-en

	D-Gal1NPr	Pd-en	HIO ₃	Pd-en chelate	%
1:1:1	149 mg	1.50 mL	119 mg	β-D-Galp1NPr2H ₋₁ -κ ² N ¹ ,O ²	76
	675 μmol	675 μmol	675 μmol	1 n. i. species	9
				D-Galα1NPr2H ₋₁ -κ ² N ¹ ,O ²	8
				β-D-Galp1NPr2,3,4H ₋₃ -κ ² N ¹ ,O ² :κ ² O ^{3,4}	7
1:2:1	74.7 mg	1.50 mL	59.4 mg	β-D-Galp1NPr2,3,4H ₋₃ -κ ² N ¹ ,O ² :κ ² O ^{3,4}	94
	338 μmol	675 μmol	338 μmol	2 n. i. species	6

[Pd(en)(⁴C₁-β-D-Galp1NPr2H₋₁-κ²N¹,O²)]⁺

¹H NMR (400 MHz, D₂O, 4 °C, 23OR4-2016): δ/ppm = 3.72 (m, 4H, H1/H4/H6/H6'), 3.61 (m, 1H, H5), 3.46 (dd, 1H, H3, ³J_{2,3}=9.7 Hz, ³J_{3,4}=3.4 Hz), 3.38 (dd, 1H, H2), 2.82 (m, 1H, NH-CH₂), 2.45 (m, 1H, NH-CH₂), 1.82 (m, 2H, CH₂), 0.92 (t, 3H, CH₃).

¹³C{¹H} NMR (101 MHz, D₂O, 4 °C, 23OR5-2016): δ/ppm = 90.8 (C1), 79.2 (C5), 77.3 (C2), 75.4 (C3), 69.2 (C4), 61.4 (C6), 49.9 (NH-CH₂), 21.7 (CH₂), 11.4 (CH₃).

[Pd(en)(D-Galα1NPr2H₋₁-κ²N¹,O²)]⁺

¹H NMR (400 MHz, D₂O, 4 °C, 23OR4-2016): δ/ppm = 7.92 (s, H1).

¹³C{¹H} NMR (101 MHz, D₂O, 4 °C, 23OR5-2016): δ/ppm = 187.4 (C1), 85.8 (C2), 70.7 (C3), 70.6 (C5), 70.2 (C4), 63.7 (C6), 62.6 (NH-CH₂), 22.9 (CH₂), 11.5 (CH₃).

[{Pd(en)}₂(⁴C₁-β-D-Galp1NPr2,3,4H₋₃-κ²N¹,O²:2κ²O^{3,4})]⁺

¹³C{¹H} NMR (101 MHz, D₂O, 4 °C, 23OR8-2016): δ/ppm = 90.7 (C1), 85.9 (C3), 81.1 (C2), 79.7 (C4), 78.5 (C5), 62.4 (C6), 49.9 (NH-CH₂), 21.8 (CH₂), 11.5 (CH₃).

***N*-(*iso*-Propyl)-D-galactosylamine and Pd-en**

	D-Gal1N <i>i</i> Pr	Pd-en	HIO ₃	Pd-en chelate	%
1:1:1	149 mg	1.50 mL	119 mg	β -D-Galp1N <i>i</i> Pr2H ₋₁ - κ^2 N ¹ ,O ²	81
	675 μ mol	675 μ mol	675 μ mol	D-Gala1N <i>i</i> Pr2H ₋₁ - κ^2 N ¹ ,O ²	7
				D-Galactose	7
				1 n. i. species	5
1:2:1	74.7 mg	1.50 mL	59.4 mg	β -D-Galp1N <i>i</i> Pr2,3,4H ₋₃ - κ^2 N ¹ ,O ² : κ^2 O ^{3,4}	64
	338 μ mol	675 μ mol	338 μ mol	⁴ C ₁ - β -D-Galp1N <i>i</i> Pr2H ₋₁ - κ^2 N ¹ ,O ²	17
				D-Gala1N <i>i</i> Pr2H ₋₁ - κ^2 N ¹ ,O ²	11
				1 n. i. species	8



¹³C{¹H} NMR (101 MHz, D₂O, 4 °C, 38OR8-2016): δ /ppm = 90.4 (C1), 79.3 (C5), 77.5 (C2), 75.5 (C3), 69.1 (C4), 61.4 (C6), 50.8 (CH), 22.5 (CH₃), 21.0 (CH₃).



¹H NMR (400 MHz, D₂O, 4 °C, 38OR7-2016): δ /ppm = 7.99 (s, H1).

¹³C{¹H} NMR (101 MHz, D₂O, 4 °C, 38OR8-2016): δ /ppm = 183.5 (C1), 86.0 (C2), 70.9 (C3), 70.8 (C5), 70.2 (C4), 63.7 (C6), 60.0 (CH), 24.5 (CH₃), 21.2 (CH₃).



¹³C{¹H} NMR (101 MHz, D₂O, 4 °C, 38OR11-2016): δ /ppm = 90.6 (C1), 86.0 (C3), 81.2 (C2), 79.7 (C4), 78.6 (C5), 62.4 (C6), 50.6 (CH₂), 22.4 (CH₃), 21.2 (CH₃).

***N*-(*tert*-Butyl)-D-galactosylamine and Pd-en**

	D-Gal1N <i>t</i> Bu	Pd-en	HIO ₃	Pd-en chelate	%
1:1:1	159 mg	1.50 mL	119 mg	β -D-Galp1N <i>t</i> Bu2H ₋₁ - κ^2 N ¹ ,O ²	58
	675 μ mol	675 μ mol	675 μ mol	D-Gala1N <i>t</i> Bu2H ₋₁ - κ^2 N ¹ ,O ²	24
				3 n. i. species	18
1:2:1	79.4 mg	1.50 mL	59.4 mg	β -D-Galp1N <i>t</i> Bu2,3,4H ₋₃ - κ^2 N ¹ ,O ² : κ^2 O ^{3,4}	70
	338 μ mol	675 μ mol	338 μ mol	D-Gala1N <i>t</i> Bu2H ₋₁ - κ^2 N ¹ ,O ²	20
				β -D-Galp1N <i>t</i> Bu2H ₋₁ - κ^2 N ¹ ,O ²	10



¹³C{¹H} NMR (101 MHz, D₂O, 4 °C, 38OR25-2019): δ /ppm = 91.2 (C1), 79.4 (C5), 78.3 (C2), 75.5 (C3), 69.0 (C4), 61.4 (C6), 58.8 (C), 30.0 (3 \times CH₃).



¹H NMR (400 MHz, D₂O, 4 °C, 38OR24-2019): δ /ppm = 7.89 (s, H1).

¹³C{¹H} NMR (101 MHz, D₂O, 4 °C, 38OR25-2019): δ /ppm = 181.5 (C1), 85.6 (C2), 71.2 (C3), 70.8 (C5), 70.2 (C4), 63.7 (C6), 62.9 (C), 29.1 (3 \times CH₃).

$[\{\text{Pd}(\text{en})\}_2(^4\text{C}_1\text{-}\beta\text{-D-Galp1NtBu2,3,4H}_{-3}\text{-}\kappa^2\text{N}^1, \text{O}^2:2\kappa^2\text{O}^{3,4})]^+$
 $^{13}\text{C}\{^1\text{H}\}$ NMR (101 MHz, D_2O , 4 °C, 38OR28-2019): $\delta/\text{ppm} = 91.1$ (C1), 86.2 (C3), 82.0 (C2), 79.6 (C4), 78.6 (C5), 62.3 (C6), 58.7 (CH_2), 30.0 ($3 \times \text{CH}_3$).

5.6.6. Complexes featuring *N*-Alkyl-D-glucosylamines

N-Methyl-D-glucosylamine and Pd-en

	D-Glc1NMe	Pd-en	HIO ₃	Pd-en chelate	%
1:1:1	110 mg	1.50 mL	119 mg	$\beta\text{-D-Glcp1NMe2H}_{-1}\text{-}\kappa^2\text{N}^1, \text{O}^2$	84
	675 μmol	675 μmol	675 μmol	$\alpha\text{-D-Glcp1NMe2H}_{-1}\text{-}\kappa^2\text{N}^1, \text{O}^2$	12
				1 n. i. species	4
1:2:1	55.1 mg	1.50 mL	59.4 mg	$\beta\text{-D-Glcp1NMe2,3,4H}_{-3}\text{-}\kappa^2\text{N}^1, \text{O}^2:\kappa^2\text{O}^{3,4}$	72
	338 μmol	675 μmol	338 μmol	2 n. i. species	16
				$\beta\text{-D-Glcp1NMe2H}_{-1}\text{-}\kappa^2\text{N}^1, \text{O}^2$	12

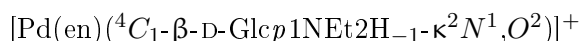
$[\text{Pd}(\text{en})(^4\text{C}_1\text{-}\beta\text{-D-Glcp1NMe2H}_{-1}\text{-}\kappa^2\text{N}^1, \text{O}^2)]^+$
 ^1H NMR (400 MHz, D_2O , 4 °C, 21OR25-2016): $\delta/\text{ppm} = 3.87$ (d, 1H, H1, $^3J_{1,2}=9.1$ Hz), 3.85–3.76 (m, 1H, H6a), 3.68 (dd, 1H, H6b, $^3J_{5,6b}=5.4$ Hz, $^2J_{6a,6b}=-12.2$ Hz), 3.39 (dd, 1H, H5), 3.34–3.27 (sp, H3/H4), 3.16 (t, 1H, H2, $^3J_{2,3}=9.1$ Hz), 2.49 (s, 3H, CH_3). $^{13}\text{C}\{^1\text{H}\}$ NMR (101 MHz, D_2O , 4 °C, 08OR5-2016): $\delta/\text{ppm} = 94.1$ (C1), 80.2 (C2), 79.0 (C3), 77.9 (C5), 69.8 (C4), 61.1 (C6), 36.8 (CH_3).

$[\text{Pd}(\text{en})(^4\text{C}_1\text{-}\alpha\text{-D-Glcp1NMe2H}_{-1}\text{-}\kappa^2\text{N}^1, \text{O}^2)]^+$
 ^1H NMR (400 MHz, D_2O , 4 °C, 21OR25-2017): 4.61 (d, H1, $^3J_{1,2}=5.8$ Hz), 2.40 (s, 3H, CH_3).
 $^{13}\text{C}\{^1\text{H}\}$ NMR (101 MHz, D_2O , 4 °C, 08OR5-2016): $\delta/\text{ppm} = 93.1$ (C1), 76.6 (C2), 74.0 (C3), 69.6 (C5), 69.3 (C4), 61.4 (C6), 36.6 (CH_3).

$[\{\text{Pd}(\text{en})\}_2(^4\text{C}_1\text{-}\beta\text{-D-Glcp1NMe2,3,4H}_{-3}\text{-}\kappa^2\text{N}^1, \text{O}^2:2\kappa^2\text{O}^{3,4})]^+$
 $^{13}\text{C}\{^1\text{H}\}$ NMR (101 MHz, D_2O , 4 °C, 21OR29-2016): $\delta/\text{ppm} = 95.0$ (C1), 88.3 (C3), 82.2 (C2), 80.1 (C4), 79.2 (C5), 61.6 (C6), 37.2 (CH_3).

N-Ethyl-D-glucosylamine and Pd-en

	D-Glc1NEt	Pd-en	HIO ₃	Pd-en chelate	%
1:1:1	140 mg	1.50 mL	119 mg	$\beta\text{-D-Glcp1NEt2H}_{-1}\text{-}\kappa^2\text{N}^1, \text{O}^2$	76
	675 μmol	675 μmol	675 μmol	D-Glc1NEt	10
				2 n. i. species	10
				$\text{D-Glca1NEt2H}_{-1}\text{-}\kappa^2\text{N}^1, \text{O}^2$	4
1:2:1	69.9 mg	1.50 mL	59.4 mg	$\beta\text{-D-Glcp1NEt2,3,4H}_{-3}\text{-}\kappa^2\text{N}^1, \text{O}^2:\kappa^2\text{O}^{3,4}$	54
	338 μmol	675 μmol	338 μmol	$\beta\text{-D-Glcp1NEt2H}_{-1}\text{-}\kappa^2\text{N}^1, \text{O}^2$	32
				1 n. i. species	8
			$\text{D-Glca1NEt2,3,4H}_{-3}\text{-}\kappa^2\text{N}^1, \text{O}^2:\kappa^2\text{O}^{3,4}$	6	



^1H NMR (400 MHz, D_2O , 4°C , 21OR31-2016): $\delta/\text{ppm} = 3.93$ (d, 1H, H1, $^3J_{1,2}=9.4$ Hz), 3.84 (dd, 1H, H6a, $^3J_{5,6a}=2.3$ Hz), 3.70 (dd, 1H, H6b, $^3J_{5,6b}=5.2$ Hz, $^2J_{6a,6b}=-12.4$ Hz), 3.42 (m, 1H, H3), 3.39–3.29 (sp, 2H, H4/H5), 3.24 (t, 1H, H2, $^3J_{2,3}=8.9$ Hz), 2.92 (dd, 1H, CH_2), 2.66 (dd, 1H, CH_2), 1.38 (t, 3H, CH_3).

$^{13}\text{C}\{^1\text{H}\}$ NMR (101 MHz, D_2O , 4°C , 21OR32-2016): $\delta/\text{ppm} = 89.5$ (C1), 80.2 (C2), 79.0 (C3), 77.9 (C5), 69.9 (C4), 61.1 (C6), 42.4 (CH_2), 13.0 (CH_3).

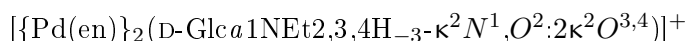


^1H NMR (400 MHz, D_2O , 4°C , 21OR31-2016): $\delta/\text{ppm} = 7.98$ (s, H1).

$^{13}\text{C}\{^1\text{H}\}$ NMR (101 MHz, D_2O , 4°C , 21OR32-2016): $\delta/\text{ppm} = 186.0$ (C1), 88.0 (C2), 71.9 (C3), 71.4 (C5), 69.3 (C4), 63.5 (C6), 55.3 (CH_2), 14.6 (CH_3).



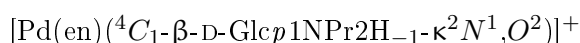
$^{13}\text{C}\{^1\text{H}\}$ NMR (101 MHz, D_2O , 4°C , 21OR35-2016): $\delta/\text{ppm} = 90.2$ (C1), 88.4 (C3), 82.0 (C2), 80.0 (C4), 79.3 (C5), 61.5 (C6), 42.5 (CH_2), 12.8 (CH_3).



^1H NMR (400 MHz, D_2O , 4°C , 21OR34-2016): $\delta/\text{ppm} = 9.18$ (s, H1). $^{13}\text{C}\{^1\text{H}\}$ NMR (101 MHz, D_2O , 4°C , 21OR35-2016): $\delta/\text{ppm} = 186.4$ (C1), 88.7 (C2), 85.4 (C3), 80.7 (C4), 73.5 (C5), 65.2 (C6), 55.3 (CH_2), 14.8 (CH_3).

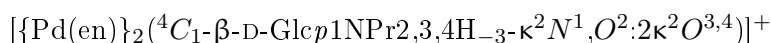
N-Propyl-D-glucosylamine and Pd-en

	D-Glc1NPr	Pd-en	HIO_3	Pd-en chelate	%
1:1:1	149 mg	1.50 mL	119 mg	$\beta\text{-D-Glcp1NPr2H}_{-1}\text{-}\kappa^2\text{N}^1, \text{O}^2$	94
	675 μmol	675 μmol	675 μmol	2 n. i. species	6
1:2:1	74.7 mg	1.50 mL	59.4 mg	$\beta\text{-D-Glcp1NPr2,3,4H}_{-3}\text{-}\kappa^2\text{N}^1, \text{O}^2:2\kappa^2\text{O}^{3,4}$	68
	338 μmol	675 μmol	338 μmol	$\beta\text{-D-Glcp1NPr2H}_{-1}\text{-}\kappa^2\text{N}^1, \text{O}^2$	14
				$\text{Glc1NPr2,3,4H}_{-3}\text{-}\kappa^2\text{N}^1, \text{O}^2:2\kappa^2\text{O}^{3,4}$	10
				1 n. i. species	10

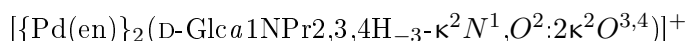


^1H NMR (400 MHz, D_2O , 4°C , 22OR63-2016): $\delta/\text{ppm} = 3.93$ (d, 1H, H1, $^3J_{1,2}=9.4$ Hz), 3.84 (dd, 1H, H6a, $^3J_{5,6a}=2.3$ Hz), 3.70 (dd, 1H, H6b, $^3J_{5,6b}=5.2$ Hz, $^2J_{6a,6b}=-12.4$ Hz), 3.42 (m, 1H, H3), 3.39–3.29 (sp, 2H, H4/H5), 3.24 (t, 1H, H2, $^3J_{2,3}=8.9$ Hz), 2.92 (dd, 1H, CH_2), 2.66 (dd, 1H, CH_2), 1.38 (t, 3H, CH_3).

$^{13}\text{C}\{^1\text{H}\}$ NMR (101 MHz, D_2O , 4°C , 22OR64-2016): $\delta/\text{ppm} = 90.7$ (C1), 80.1 (C2), 79.0 (C3), 77.9 (C5), 69.7 (C4), 61.0 (C6), 50.1 (CH_2), 21.7 (CH_2), 11.4 (CH_3).



$^{13}\text{C}\{^1\text{H}\}$ NMR (101 MHz, D_2O , 4°C , 22OR67-2016): $\delta/\text{ppm} = 91.3$ (C1), 88.3 (C3), 82.1 (C2), 79.9 (C4), 79.2 (C5), 61.5 (C6), 50.3 (CH_2), 21.5 (CH_2), 11.4 (CH_3).



^1H NMR (400 MHz, D_2O , 4 °C, 22OR66-2016): $\delta/\text{ppm} = 9.10$ (s, H1).

$^{13}\text{C}\{^1\text{H}\}$ NMR (101 MHz, D_2O , 4 °C, 22OR67-2016): $\delta/\text{ppm} = 187.4$ (C1), 88.2 (C2), 85.5 (C3), 80.8 (C4), 73.4 (C5), 65.2 (C6), 62.7 (NH-CH₂), 62.7 (NH-CH₂), 23.0 (CH₂), 11.1 (CH₃).

N-(*iso*-Propyl)-D-glucosylamine and Pd-en

	D-Glc1N <i>i</i> Pr	Pd-en	HIO ₃	Pd-en chelate	%
1:1:1	149 mg	1.50 mL	119 mg	$\beta\text{-D-Glc}p1\text{N}i\text{Pr}2\text{H}_{-1-\kappa^2}\text{N}^1, \text{O}^2$	78
	675 μmol	675 μmol	675 μmol	2 n. i. species	22
1:2:1	74.7 mg	1.50 mL	59.4 mg	$\beta\text{-D-Glc}p1\text{N}i\text{Pr}2,3,4\text{H}_{-3-\kappa^2}\text{N}^1, \text{O}^2:\kappa^2\text{O}^{3,4}$	48
	338 μmol	675 μmol	338 μmol	$\beta\text{-D-Glc}p1\text{N}i\text{Pr}2\text{H}_{-1-\kappa^2}\text{N}^1, \text{O}^2$	40
				D-Glc <i>a</i> 1N <i>i</i> Pr2,3,4H _{-3-κ^2} N ¹ ,O ² : κ^2 O ^{3,4}	12

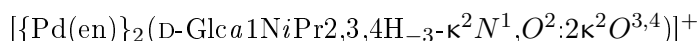


^1H NMR (400 MHz, D_2O , 4 °C, 27OR13-2018): $\delta/\text{ppm} = 3.92$ (d, 1H, H1, $^3J_{1,2}=7.9$ Hz), 3.81 (dd, 1H, H6a, $w^3J_{5,6a}=2.2$ Hz), 3.70 (dd, 1H, H6b, $^3J_{5,6b}=5.0$ Hz, $^2J_{6a,6b}=-12.4$ Hz), 3.39 (m, 1H, H3), 3.39-3.28 (sp, 3H, H4/H5/H2), 3.07 (s, 1H, CH), 1.27 (d, 6H, 2 \times CH₃).

$^{13}\text{C}\{^1\text{H}\}$ NMR (101 MHz, D_2O , 4 °C, 27OR14-2018): $\delta/\text{ppm} = 90.0$ (C1), 80.4 (C2), 79.1 (C3), 78.1 (C5), 69.7 (C4), 61.1 (C6), 50.9 (CH), 22.4 (CH₃), 21.0 (CH₃).



$^{13}\text{C}\{^1\text{H}\}$ NMR (101 MHz, D_2O , 4 °C, 27OR17-2018): $\delta/\text{ppm} = 91.0$ (C1), 88.4 (C3), 82.4 (C2), 79.9 (C4), 79.3 (C5), 61.5 (C6), 50.8 (CH), 22.3 (CH₃), 20.9 (CH₃).



^1H NMR (400 MHz, D_2O , 4 °C, 27OR16-2018): $\delta/\text{ppm} = 9.18$ (s, H1).

$^{13}\text{C}\{^1\text{H}\}$ NMR (101 MHz, D_2O , 4 °C, 27OR17-2018): $\delta/\text{ppm} = 183.5$ (C1), 88.5 (C2), 85.3 (C3), 80.7 (C4), 73.0 (C5), 65.3 (C6), 59.2 (CH), 23.2 (CH₃), 21.4 (CH₃).

N-(*tert*-Butyl)-D-glucosylamine and Pd-en

	D-Glc1N <i>t</i> Bu	Pd-en	HIO ₃	Pd-en chelate	%
1:1:1	159 mg	1.50 mL	119 mg	$\beta\text{-D-Glc}p1\text{N}t\text{Bu}2\text{H}_{-1-\kappa^2}\text{N}^1, \text{O}^2$	52
	675 μmol	675 μmol	675 μmol	D-glucose	31
				2 n. i. species	10
				D-Glc <i>a</i> 1N <i>t</i> Bu2H _{-1-κ^2} N ¹ ,O ²	7
1:2:1	79.4 mg	1.50 mL	59.4 mg	$\beta\text{-D-Glc}p1\text{N}t\text{Bu}2\text{H}_{-1-\kappa^2}\text{N}^1, \text{O}^2$	40
	338 μmol	675 μmol	338 μmol	D-Glc <i>a</i> 1N <i>t</i> Bu2,3,4H _{-3-κ^2} N ¹ ,O ² : κ^2 O ^{3,4}	20
				2 n. i. species	16
				$\beta\text{-D-Glc}p1\text{N}t\text{Bu}2,3,4\text{H}_{-3-\kappa^2}\text{N}^1, \text{O}^2:\kappa^2\text{O}^{3,4}$	14
				D-Glc <i>a</i> 1N <i>t</i> Bu2H _{-1-κ^2} N ¹ ,O ²	10



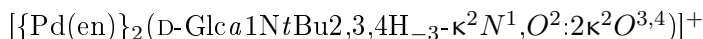
$^{13}\text{C}\{^1\text{H}\}$ NMR (101 MHz, D_2O , 4 °C, 27OR20-2018): $\delta/\text{ppm} = 90.7$ (C1), 81.0 (C2), 79.1 (C3),

78.2 (C5), 69.9 (C4), 61.3 (C6), 58.8 (C_q), 29.9 (CH₃).



¹H NMR (400 MHz, D₂O, 4 °C, 27OR19-2017): $\delta/\text{ppm} = 7.90$ (s, H1).

¹³C{¹H} NMR (101 MHz, D₂O, 4 °C, 27OR20-2018): $\delta/\text{ppm} = 181.5$ (C1), 87.9 (C2), 72.0 (C3), 71.4 (C4), 69.7 (C5), 63.6 (C6), 62.7 (C_q), 29.0 (CH₃).



¹H NMR (400 MHz, D₂O, 4 °C, 32OR25-2017): $\delta/\text{ppm} = 9.02$ (s, H1). ¹³C{¹H} NMR (101 MHz, D₂O, 4 °C, 27OR26-2018): $\delta/\text{ppm} = 182.2$ (C1), 88.1 (C2), 85.5 (C3), 80.9 (C4), 73.9 (C5), 65.1 (C6), 62.7 (C_q), 29.8 (CH₃).



¹³C{¹H} NMR (101 MHz, D₂O, 4 °C, 27OR26-2018): $\delta/\text{ppm} = 91.7$ (C1), 88.3 (C3), 83.4 (C2), 80.2 (C5), 79.0 (C4), 61.4 (C6), 58.8 (C_q), 29.6 (CH₃).

5.6.7. Complexes featuring *N*-Alkyl-L-gulosylamines

N-Methyl-L-gulosylamine and Pd-en

	L-Gul1NMe	Pd-en	HIO ₃	Pd-en chelate	%
1:1:1	110 mg	1.50 mL	119 mg	¹ C ₄ -β-L-Gulp1NMe2H ₋₁ -κ ² N ¹ , O ²	72
	675 μmol	675 μmol	675 μmol	¹ C ₄ -α-L-Gulp1NMe2H ₋₁ -κ ² N ¹ , O ²	16
				L-Gula1NMe2H ₋₁ -κ ² N ¹ , O ²	8
				1 n. i. species	4
1:2:1	55.1 mg	1.50 mL	59.4 mg	¹ C ₄ -β-L-Gulp1NMe2H ₋₁ -κ ² N ¹ , O ²	46
	338 μmol	675 μmol	338 μmol	L-Gula1NMe2,3,4H ₋₃ -κ ² N ¹ , O ² :κ ² O ^{3,4}	27
				1 n. i. species	19
			L-Gula1NMe2,3,4,5,6H ₋₅ -κ ² N ¹ , O ² :κ ² O ^{3,4} :κ ² O ^{5,6}	8	
1:3:1	36.7 mg	1.50 mL	39.7 mg	L-Gula1NMe2,3,4H ₋₃ -κ ² N ¹ , O ² :κ ² O ^{3,4}	37
	225 μmol	675 μmol	225 μmol	L-Gula1NMe2,4,5H ₋₃ -κ ² N ¹ , O ² :κ ² O ^{4,5}	21
				¹ C ₄ -β-L-Gulp1NMe2H ₋₁ -κ ² N ¹ , O ²	19
				L-Gula1NMe2,3,4,5,6H ₋₅ -κ ² N ¹ , O ² :κ ² O ^{3,4} :κ ² O ^{5,6}	17
				1 n. i. species	6



¹H NMR (400 MHz, D₂O, 4 °C, 24OR7-2016): $\delta/\text{ppm} = 4.01$ (d, 1H, H1, ³J_{1,2}=9.4 Hz), 3.94 (t, 1H, H3), 3.87 (m, 1H, H5), 3.72–3.70 (sp, H4), 3.64–3.58 (sp, 2H, H6/H6'), 3.43 (dd, 1H, H2, ³J_{2,3}=3.2 Hz), 2.51 (s, 3H, CH₃).

¹³C{¹H} NMR (101 MHz, D₂O, 4 °C, 24OR8-2016): $\delta/\text{ppm} = 91.2$ (C1), 76.5 (C5), 75.5 (C2), 72.5 (C3), 69.9 (C4), 61.6 (C6), 36.8 (CH₃).



¹H NMR (400 MHz, D₂O, 4 °C, 24OR7-2016): $\delta/\text{ppm} = 4.54$ (d, H1, ³J_{1,2}=5.9 Hz).

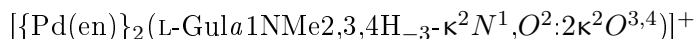
¹³C{¹H} NMR (101 MHz, D₂O, 4 °C, 24OR8-2016): $\delta/\text{ppm} = 92.2$ (C1), 70.4 (C2), 69.3 (C3),

69.3 (C4), 67.9 (C5), 61.9 (C6), 36.9 (CH₃).



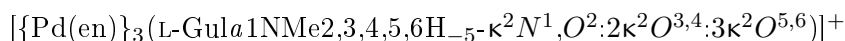
¹H NMR (400 MHz, D₂O, 4 °C, 25OR7-2016): 8.05 (s, H1).

¹³C{¹H} NMR (101 MHz, D₂O, 4 °C, 24OR8-2016): $\delta/\text{ppm} = 187.7$ (C1), 86.5 (C2), 75.2 (C3), 73.2 (C5), 70.8 (C4), 63.0 (C6), 48.8 (CH₃).



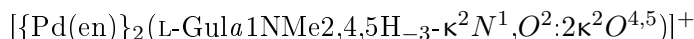
¹H NMR (400 MHz, D₂O, 4 °C, 14OR4-2017): 8.21 (s, H1).

¹³C{¹H} NMR (101 MHz, D₂O, 4 °C, 14OR5-2017): $\delta/\text{ppm} = 190.3$ (C1), 88.0 (C2), 85.8 (C3), 81.5 (C4), 73.9 (C5), 62.3 (C6), 48.8 (CH₃).



¹H NMR (400 MHz, D₂O, 4 °C, 14OR4-2017): 8.10 (s, H1).

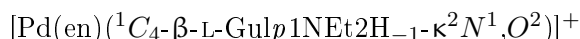
¹³C{¹H} NMR (101 MHz, D₂O, 4 °C, 14OR5-2017): $\delta/\text{ppm} = 190.9$ (C1), 88.8 (C2), 86.8 (C3), 85.3 (C4), 83.1 (C5), 72.4 (C6), 48.7 (CH₃).



¹³C{¹H} NMR (101 MHz, D₂O, 4 °C, 24OR35-2017): $\delta/\text{ppm} = 190.1$ (C1), 92.0 (C5), 88.8 (C2), 81.3 (C4), 79.5 (C3), 63.3 (C6), 48.7 (CH₃).

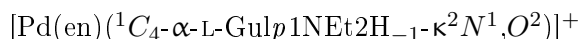
N-Ethyl-L-gulosylamine and Pd-en

	L-Gul1NEt	Pd-en	HIO ₃	Pd-en chelate	%
1:1:1	140 mg	1.50 mL	119 mg	¹ C ₄ -β-L-Gulp1NEt2H ₋₁ -κ ² N ¹ ,O ²	76
	675 μmol	675 μmol	675 μmol	¹ C ₄ -α-L-Gulp1NEt2H ₋₁ -κ ² N ¹ ,O ²	14
				L-Gula1NEt2H ₋₁ -κ ² N ¹ ,O ²	6
				1 n. i. species	4
1:2:1	69.9 mg	1.50 mL	59.4 mg	¹ C ₄ -β-L-Gulp1NEt2H ₋₁ -κ ² N ¹ ,O ²	48
	338 μmol	675 μmol	338 μmol	L-Gula1NEt2,3,4H ₋₃ -κ ² N ¹ ,O ² :κ ² O ^{3,4}	46
				¹ C ₄ -α-L-Gulp1NEt2H ₋₁ -κ ² N ¹ ,O ²	6



¹H NMR (400 MHz, D₂O, 4 °C, 24OR2-2016): $\delta/\text{ppm} = \delta/\text{ppm} = 4.09$ (d, 1H, H1, ³J_{1,2}=9.5 Hz), 3.96 (t, 1H, H3), 3.87 (m, 1H, H5), 3.72–3.70 (sp, H4), 3.64–3.58 (sp, 2H, H6/H6'), 3.49 (dd, 1H, H2, ³J_{2,3}=3.4 Hz), 2.72–2.51 (sp, CH₂), 1.37 (s, 3H, CH₃).

¹³C{¹H} NMR (101 MHz, D₂O, 4 °C, 14OR11-2017): $\delta/\text{ppm} = 86.3$ (C1), 76.5 (C5), 75.5 (C2), 72.5 (C3), 69.8 (C4), 61.5 (C6), 42.3 (CH₂), 13.2 (CH₃).



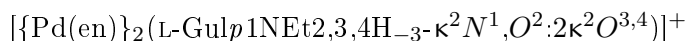
¹H NMR (400 MHz, D₂O, 4 °C, 24OR2-2016): $\delta/\text{ppm} = 4.65$ (d, H1, ³J_{1,2}=6.0 Hz).

¹³C{¹H} NMR (101 MHz, D₂O, 4 °C, 14OR11-2017): $\delta/\text{ppm} = 87.0$ (C1), 70.2 (C2), 69.3 (C3), 69.3 (C4), 68.0 (C5), 61.8 (C6), 41.7 (CH₂), 12.3 (CH₃).



^1H NMR (400 MHz, D_2O , 4 °C, 24OR2-2016): 8.07 (s, H1).

$^{13}\text{C}\{^1\text{H}\}$ NMR (101 MHz, D_2O , 4 °C, 14OR11-2017): $\delta/\text{ppm} = 186.2$ (C1), 86.5 (C2), 75.2 (C3), 73.3 (C5), 70.8 (C4), 63.0 (C6), 55.8 (CH_2), 15.0 (CH_3).

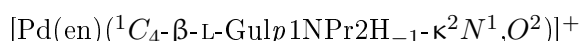


^1H NMR (400 MHz, D_2O , 4 °C, 24OR31-2016): 8.24 (s, H1).

$^{13}\text{C}\{^1\text{H}\}$ NMR (101 MHz, D_2O , 4 °C, 24OR32-2016): $\delta/\text{ppm} = 188.8$ (C1), 88.3 (C2), 85.7 (C3), 81.5 (C4), 74.0 (C5), 62.4 (C6), 55.8 (CH_2), 15.3 (CH_3).

***N*-Propyl-L-gulosylamine and Pd-en**

	L-Gul1NPr	Pd-en	HIO_3	Pd-en chelate	%
1:1:1	149 mg	1.50 mL	119 mg	$^1\text{C}_4\text{-}\beta\text{-L-Gulp1NPr2H}_{-1}\text{-}\kappa^2\text{N}^1,\text{O}^2$	52
	675 μmol	675 μmol	675 μmol	L-Gul1NPr	25
				L-Gul α 1NPr2H $_{-1}\text{-}\kappa^2\text{N}^1,\text{O}^2$	12
				L-gulose	6
				$^1\text{C}_4\text{-}\alpha\text{-L-Gulp1NPr2H}_{-1}\text{-}\kappa^2\text{N}^1,\text{O}^2$	5
1:2:1	74.7 mg	1.50 mL	59.4 mg	2 n. i. species	62
	338 μmol	675 μmol	338 μmol	$^1\text{C}_4\text{-}\beta\text{-L-Gulp1NPr2H}_{-1}\text{-}\kappa^2\text{N}^1,\text{O}^2$	38



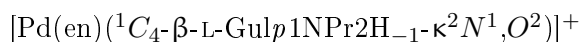
^1H NMR (400 MHz, D_2O , 4 °C, 36OR4-2019): $\delta/\text{ppm} = \delta/\text{ppm} = 4.07$ (d, 1H, H1, $^3J_{1,2}=9.2$ Hz), 3.94 (t, 1H, H3), 3.82 (m, 1H, H5), 3.72–3.66 (sp, H4), 3.64–3.58 (sp, 2H, H6/H6'), 3.46 (dd, 1H, H2, $^3J_{2,3}=3.4$ Hz), 2.67–2.60 (sp, NH– CH_2), 2.53 (t, NH– CH_2), 1.62 (m, CH_2), 0.89 (t, 3H, CH_3).

$^{13}\text{C}\{^1\text{H}\}$ NMR (101 MHz, D_2O , 4 °C, 36OR5-2019): $\delta/\text{ppm} = 87.5$ (C1), 76.5 (C5), 75.4 (C2), 72.5 (C3), 69.8 (C4), 61.4 (C6), 50.0 (NH– CH_2), 21.9 (CH_2), 11.5 (CH_3).



^1H NMR (400 MHz, D_2O , 4 °C, 36OR4-2019): 8.04 (s, H1).

$^{13}\text{C}\{^1\text{H}\}$ NMR (101 MHz, D_2O , 4 °C, 36OR5-2019): $\delta/\text{ppm} = 187.3$ (C1), 86.3 (C2), 75.3 (C3), 73.3 (C5), 70.8 (C4), 63.0 (C6), 62.8 (NH– CH_2), 22.9 (CH_2), 10.7 (CH_3).



^1H NMR (400 MHz, D_2O , 4 °C, 36OR4-2019): $\delta/\text{ppm} = 4.61$ (d, H1, $^3J_{1,2}=6.2$ Hz).

$^{13}\text{C}\{^1\text{H}\}$ NMR (101 MHz, D_2O , 4 °C, 36OR5-2019): $\delta/\text{ppm} = 88.2$ (C1), 70.1 (C2), 69.4 (C3), 69.3 (C3), 68.0 (C5), 61.6 (C6), 49.4 (CH_2), 20.9 (CH_2), 11.3 (CH_3).

***N*-(*iso*-Propyl)-L-gulosylamine and Pd-en**

	L-Gul1NiPr	Pd-en	HIO ₃	Pd-en chelate	%
1:1:1	149 mg	1.50 mL	119 mg	¹ C ₄ -β-L-Gulp1NiPr2H ₋₁ -κ ² N ¹ ,O ²	55
	675 μmol	675 μmol	675 μmol	L-Gula1NiPr2H ₋₁ -κ ² N ¹ ,O ²	23
				L-Gul1NiPr	10
				1 n. i. species	7
				¹ C ₄ -α-L-Gulp1NiPr2H ₋₁ -κ ² N ¹ ,O ²	5
1:2:1	74.7 mg	1.50 mL	59.4 mg	L-Gula1NiPr2,3,4H ₋₃ -κ ² N ¹ ,O ² :κ ² O ^{3,4}	46
	338 μmol	675 μmol	338 μmol	L-Gula1NiPr2,3,4H ₋₃ -κ ² N ¹ ,O ² :κ ² O ^{4,5}	35
				L-Gula1NiPr2,3,4,5,6H ₋₅ -κ ² N ¹ ,O ² :κ ² O ^{3,4} :κ ² O ^{5,6}	15
				¹ C ₄ -β-L-Gulp1NiPr2H ₋₁ -κ ² N ¹ ,O ²	4

[Pd(en)(¹C₄-β-L-Gulp1NiPr2H₋₁-κ²N¹,O²)]⁺

¹H NMR (400 MHz, D₂O, 4 °C, 36OR10-2019): δ/ppm = δ/ppm = 4.09 (d, 1H, H1, ³J_{1,2}=9.2 Hz), 3.94 (t, 1H, H3), 3.83 (m, 1H, H5), 3.72–3.66 (sp, H4), 3.64–3.58 (sp, 2H, H6/H6'), 3.46 (dd, 1H, H2, ³J_{2,3}=2.9 Hz), 3.09 (m, CH), 1.29 (sp, 6H, 2×CH₃).

¹³C{¹H} NMR (101 MHz, D₂O, 4 °C, 36OR11-2019): δ/ppm = 86.8 (C1), 76.7 (C5), 75.6 (C2), 72.7 (C3), 69.7 (C4), 61.4 (C6), 50.8 (NH–CH), 22.6 (CH₃), 21.2 (CH₃).

[Pd(en)(L-Gula1NiPr2H₋₁-κ²N¹,O²)]⁺

¹H NMR (400 MHz, D₂O, 4 °C, 36OR10-2019): 8.08 (s, H1).

¹³C{¹H} NMR (101 MHz, D₂O, 4 °C, 36OR11-2019): δ/ppm = 183.3 (C1), 86.7 (C2), 75.3 (C3), 73.3 (C5), 70.7 (C4), 63.0 (C6), 60.2 (CH), 22.2 (CH₃), 21.7 (CH₃).

[Pd(en)(¹C₄-α-L-Gulp1NiPr2H₋₁-κ²N¹,O²)]⁺

¹H NMR (400 MHz, D₂O, 4 °C, 36OR10-2019): δ/ppm = 4.58 (d, H1, ³J_{1,2}=6.0 Hz).

¹³C{¹H} NMR (101 MHz, D₂O, 4 °C, 36OR11-2019): δ/ppm = 88.2 (C1), 70.0 (C2), 69.4 (C3), 69.3 (C4), 67.8 (C5), 61.8 (C6), 51.3 (CH), 22.0 (CH₃), 20.7 (CH₃).

[{Pd(en)}₂(L-Gulp1NiPr2,3,4H₋₃-κ²N¹,O²:2κ²O^{3,4})]⁺

¹H NMR (400 MHz, D₂O, 4 °C, 36OR13-2019): 8.16 (s, H1).

¹³C{¹H} NMR (101 MHz, D₂O, 4 °C, 36OR14-2019): δ/ppm = 185.1 (C1), 88.3 (C2), 85.7 (C3), 81.5 (C4), 74.0 (C5), 62.4 (C6), 60.1 (CH), 22.3 (CH₃), 22.0 (CH₃).

[{Pd(en)}₂(L-Gulp1NiPr2,4,5H₋₃-κ²N¹,O²:2κ²O^{4,5})]⁺

¹H NMR (400 MHz, D₂O, 4 °C, 36OR13-2019): 8.26 (s, H1).

¹³C{¹H} NMR (101 MHz, D₂O, 4 °C, 36OR14-2019): δ/ppm = 185.5 (C1), 92.2 (C5), 88.8 (C2), 81.4 (C4), 79.5 (C3), 63.3 (C6), 60.3 (CH), 22.3 (CH₃), 22.2 (CH₃).

[{Pd(en)}₃(L-Gulp1NiPr2,3,4,5,6H₋₅-κ²N¹,O²:2κ²O^{3,4}:3κ²O^{5,6})]⁺

¹H NMR (400 MHz, D₂O, 4 °C, 36OR13-2019): 8.30 (s, H1).

¹³C{¹H} NMR (101 MHz, D₂O, 4 °C, 36OR14-2019): δ/ppm = 185.9 (C1), 89.0 (C5), 86.9 (C2), 85.6 (C3), 83.4 (C5), 72.4 (C6), 60.2 (CH), 22.4 (CH₃), 21.8 (CH₃).

***N*-(*tert*-Butyl)-*L*-gulosylamine and Pd-en**

	L-Gul1N <i>t</i> Bu	Pd-en	HIO ₃	Pd-en chelate	%
1:1:1	159 mg	1.50 mL	119 mg	L-Gul <i>a</i> 1N <i>t</i> Bu2H ₋₁ -κ ² N ¹ ,O ²	54
	675 μmol	675 μmol	675 μmol	¹ C ₄ -β-L-Gul <i>p</i> 1N <i>t</i> Bu2H ₋₁ -κ ² N ¹ ,O ²	27
				D-gulose	19
1:2:1	79.4 mg	1.50 mL	59.4 mg	L-Gul <i>a</i> 1N <i>t</i> Bu2,4,5H ₋₃ -κ ² N ¹ ,O ² :κ ² O ^{4,5}	61
	338 μmol	675 μmol	338 μmol	L-Gul <i>a</i> 1N <i>t</i> Bu2,3,4H ₋₃ -κ ² N ¹ ,O ² :κ ² O ^{3,4}	23
				L-Gul <i>a</i> 1N <i>t</i> Bu2,3,4,5,6H ₋₅ -κ ² N ¹ ,O ² :κ ² O ^{3,4} :κ ² O ^{5,6}	16

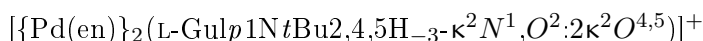


¹H NMR (400 MHz, D₂O, 4 °C, 37OR4-2019): 8.00 (s, H1).

¹³C{¹H} NMR (101 MHz, D₂O, 4 °C, 37OR5-2019): δ/ppm = 181.6 (C1), 86.1 (C2), 75.7 (C3), 73.3 (C5), 70.6 (C4), 63.1 (C), 62.9 (C6), 29.1 (3×CH₃).

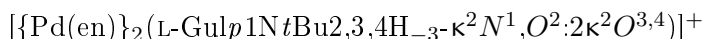


¹³C{¹H} NMR (101 MHz, D₂O, 4 °C, 37OR5-2019): δ/ppm = 87.3 (C1), 77.1 (C5), 76.3 (C2), 73.3 (C3), 69.7 (C4), 61.4 (C6), 58.8 (C), 27.4 (3×CH₃).



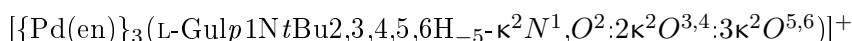
¹H NMR (400 MHz, D₂O, 4 °C, 37OR7-2019): 8.02 (s, H1).

¹³C{¹H} NMR (101 MHz, D₂O, 4 °C, 37OR8-2019): δ/ppm = 182.9 (C1), 92.6 (C5), 87.7 (C2), 82.0 (C4), 79.7 (C3), 63.3 (C6), 63.0 (C), 29.4 (3×CH₃).



¹H NMR (400 MHz, D₂O, 4 °C, 37OR7-2019): 8.18 (s, H1).

¹³C{¹H} NMR (101 MHz, D₂O, 4 °C, 37OR8-2019): δ/ppm = 183.6 (C1), 88.2 (C2), 86.2 (C3), 81.4 (C4), 74.0 (C3), 62.9 (C), 62.3 (C6), 29.3 (3×CH₃).

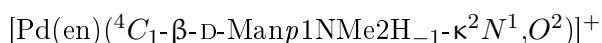


¹H NMR (400 MHz, D₂O, 4 °C, 37OR7-2019): 8.20 (s, H1).

¹³C{¹H} NMR (101 MHz, D₂O, 4 °C, 37OR8-2019): δ/ppm = 184.0 (C1), 88.8 (C5), 87.4 (C2), 85.7 (C3), 83.5 (C5), 72.5 (C6), 63.1 (CH), 29.5 (3×CH₃).

5.6.8. Complexes featuring *N*-Alkyl-D-mannosylamines***N*-Methyl-D-mannosylamine and Pd-en**

	D-Man1NMe	Pd-en	HIO ₃	Pd-en chelate	%
1:1:1	110 mg	1.50 mL	119 mg	β-D-Man <i>p</i> 1NMe2H ₋₁ -κ ² N ¹ ,O ²	40
	675 μmol	675 μmol	675 μmol	D-Man1NMe	22
				¹ C ₄ -α-D-Man <i>p</i> 1NMe2H ₋₁ -κ ² N ¹ ,O ²	20
				D-Man <i>a</i> 1NMe2H ₋₁ -κ ² N ¹ ,O ²	18



$^{13}\text{C}\{^1\text{H}\}$ NMR (101 MHz, D_2O , 4 °C, 10OR5-2016): $\delta/\text{ppm} = 94.2$ (C1), 78.7 (C5), 78.6 (C2), 72.6 (C3), 67.5 (C4), 61.8 (C6), 36.5 (CH_3).

$[\text{Pd}(\text{en})(^1\text{C}_4\text{-}\alpha\text{-D-Manp1NMe2H}_{-1}\text{-}\kappa^2\text{N}^1, \text{O}^2)]^+$

$^{13}\text{C}\{^1\text{H}\}$ NMR (101 MHz, D_2O , 4 °C, 10OR5-2016): $\delta/\text{ppm} = 97.0$ (C1), 79.1 (C2), 77.2 (C3), 72.8 (C5), 67.4 (C4), 61.8 (C6), 37.3 (CH_3).

$[\text{Pd}(\text{en})(\text{D-Man}\alpha\text{1NMe2H}_{-1}\text{-}\kappa^2\text{N}^1, \text{O}^2)]^+$

^1H NMR (400 MHz, D_2O , 4 °C, 10OR4-2016): 8.08 (s, H1).

$^{13}\text{C}\{^1\text{H}\}$ NMR (101 MHz, D_2O , 4 °C, 10OR5-2016): $\delta/\text{ppm} = 188.2$ (C1), 86.6 (C2), 73.8 (C3), 71.5 (C5), 70.2 (C4), 63.7 (C6), 48.8 (CH_3).

N-Ethyl-D-mannosylamine and Pd-en

	D-Man1NEt	Pd-en	HIO_3	Pd-en chelate	%
1:1:1	140 mg	1.50 mL	119 mg	$\beta\text{-D-Manp1NEt2H}_{-1}\text{-}\kappa^2\text{N}^1, \text{O}^2$	38
	675 μmol	675 μmol	675 μmol	$\text{D-Man}\alpha\text{1NEt2H}_{-1}\text{-}\kappa^2\text{N}^1, \text{O}^2$	36
				$^1\text{C}_4\text{-}\alpha\text{-D-Manp1NEt2H}_{-1}\text{-}\kappa^2\text{N}^1, \text{O}^2$	22
				1 n. i. species	4
1:1.5:1	93.3 mg	1.50 mL	79.3 mg	$\text{D-Man}\alpha\text{1NEt2,3,4H}_{-3}\text{-}\kappa^2\text{N}^1, \text{O}^2; \kappa^2\text{O}^{3,4}$	33
	450 μmol	675 μmol	450 μmol	$\beta\text{-D-Manp1NEt2H}_{-1}\text{-}\kappa^2\text{N}^1, \text{O}^2$	27
				$\text{D-Man}\alpha\text{1NEt2H}_{-1}\text{-}\kappa^2\text{N}^1, \text{O}^2$	24
				$^1\text{C}_4\text{-}\alpha\text{-D-Manp1NEt2H}_{-1}\text{-}\kappa^2\text{N}^1, \text{O}^2$	16
1:2:1	70.0 mg	1.50 mL	59.5 mg	$\text{D-Man}\alpha\text{1NEt2,3,4H}_{-3}\text{-}\kappa^2\text{N}^1, \text{O}^2; \kappa^2\text{O}^{3,4}$	95
	338 μmol	675 μmol	338 μmol	$\text{D-Man}\alpha\text{1NEt2H}_{-1}\text{-}\kappa^2\text{N}^1, \text{O}^2$	3
				$\beta\text{-D-Manp1NEt2H}_{-1}\text{-}\kappa^2\text{N}^1, \text{O}^2$	2

$[\text{Pd}(\text{en})(^4\text{C}_1\text{-}\beta\text{-D-Manp1NEt2H}_{-1}\text{-}\kappa^2\text{N}^1, \text{O}^2)]^+$

$^{13}\text{C}\{^1\text{H}\}$ NMR (101 MHz, D_2O , 4 °C, 45OR5-2015): $\delta/\text{ppm} = 89.9$ (C1), 79.2 (C2), 78.8 (C5), 72.7 (C3), 67.6 (C4), 61.7 (C6), 43.7 (CH_2), 11.6 (CH_3).

$[\text{Pd}(\text{en})(\text{D-Man}\alpha\text{1NEt2H}_{-1}\text{-}\kappa^2\text{N}^1, \text{O}^2)]^+$

^1H NMR (400 MHz, D_2O , 4 °C, 45OR4-2015): 8.09 (s, H1).

$^{13}\text{C}\{^1\text{H}\}$ NMR (101 MHz, D_2O , 4 °C, 45OR5-2015): $\delta/\text{ppm} = 186.6$ (C1), 86.5 (C2), 73.9 (C3), 71.2 (C5), 70.2 (C4), 63.7 (C6), 55.7 (CH_2), 15.1 (CH_3).

$[\text{Pd}(\text{en})(^1\text{C}_4\text{-}\alpha\text{-D-Manp1NEt2H}_{-1}\text{-}\kappa^2\text{N}^1, \text{O}^2)]^+$

$^{13}\text{C}\{^1\text{H}\}$ NMR (101 MHz, D_2O , 4 °C, 45OR5-2015): $\delta/\text{ppm} = 94.8$ (C1), 79.0 (C2), 77.9 (C3), 72.9 (C4), 67.3 (C5), 61.7 (C6), 45.3 (CH_2), 14.1 (CH_3).

$[\{\text{Pd}(\text{en})\}_2(\text{D-Manp1NEt2,3,4H}_{-3}\text{-}\kappa^2\text{N}^1, \text{O}^2; 2\kappa^2\text{O}^{3,4})]^+$

^1H NMR (400 MHz, D_2O , 4 °C, 46OR13-2015): 8.18 (s, H1).

$^{13}\text{C}\{^1\text{H}\}$ NMR (101 MHz, D_2O , 4 °C, 46OR14-2015): $\delta/\text{ppm} = 188.1$ (C1), 88.6 (C2), 87.8 (C3), 83.9 (C4), 73.3 (C5), 64.2 (C6), 55.9 (CH_2), 15.4 (CH_3).

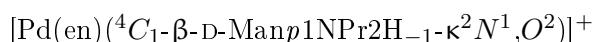
***N*-Propyl-D-mannosylamine and Pd-en**

	D-Man1NPr	Pd-en	HIO ₃	Pd-en chelate	%
1:1:1	149 mg	1.50 mL	119 mg	D-Man α 1NPr2H ₋₁ - κ^2 N ¹ ,O ²	40
	675 μ mol	675 μ mol	675 μ mol	β -D-Man p 1NPr2H ₋₁ - κ^2 N ¹ ,O ²	38
				D-Man f 1NPr2H ₋₁ - κ^2 N ¹ ,O ²	22
1:2:1	74.7 mg	1.50 mL	59.4 mg	D-Man α 1NPr2,3,4H ₋₃ - κ^2 N ¹ ,O ² : κ^2 O ^{3,4}	93
	338 μ mol	675 μ mol	338 μ mol	D-Man α 1NPr2H ₋₁ - κ^2 N ¹ ,O ²	5
				β -D-Man p 1NPr2H ₋₁ - κ^2 N ¹ ,O ²	2

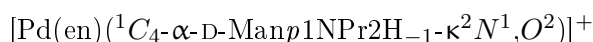


¹H NMR (400 MHz, D₂O, 4 °C, 47OR16-2015): δ /ppm = 8.07 (s, H1).

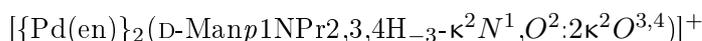
¹³C{¹H} NMR (101 MHz, D₂O, 4 °C, 47OR17-2015): δ /ppm = 187.7 (C1), 86.3 (C2), 74.0 (C3), 71.1 (C5), 70.2 (C4), 63.7 (C6), 62.8 (NH-CH₂), 22.9 (CH₂), 11.2 (CH₃).



¹³C{¹H} NMR (101 MHz, D₂O, 4 °C, 47OR17-2015): δ /ppm = 90.2 (C1), 79.2 (C2), 78.8 (C5), 72.8 (C3), 67.5 (C4), 61.7 (C6), 50.8 (NH-CH₂), 19.6 (CH₂), 10.8 (CH₃).



¹³C{¹H} NMR (101 MHz, D₂O, 4 °C, 47OR17-2015): δ /ppm = 94.9 (C1), 79.0 (C2), 77.8 (C3), 72.8 (C4), 67.2 (C5), 61.7 (C6), 52.1 (NH-CH₂), 22.5 (CH₂), 11.3 (CH₃).



¹H NMR (400 MHz, D₂O, 4 °C, 47OR19-2015): 8.15 (s, H1).

¹³C{¹H} NMR (101 MHz, D₂O, 4 °C, 47OR20-2015): δ /ppm = 189.2 (C1), 88.7 (C2), 87.6 (C3), 83.9 (C4), 73.3 (C5), 64.2 (C6), 62.9 (NH-CH₂), 23.2 (CH₂), 10.9 (CH₃).

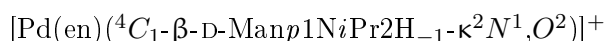
***N*-(*iso*-Propyl)-D-mannosylamine and Pd-en**

	D-Man1NiPr	Pd-en	HIO ₃	Pd-en chelate	%
1:1:1	149 mg	1.50 mL	119 mg	D-Man α 1NiPr2H ₋₁ - κ^2 N ¹ ,O ²	62
	675 μ mol	675 μ mol	675 μ mol	β -D-Man p 1NiPr2H ₋₁ - κ^2 N ¹ ,O ²	24
				3 n. i. species	14



¹H NMR (400 MHz, D₂O, 4 °C, 36OR13-2015): δ /ppm = 8.09 (s, H1).

¹³C{¹H} NMR (101 MHz, D₂O, 4 °C, 36OR14-2015): δ /ppm = 183.7 (C1), 86.6 (C2), 74.0 (C3), 71.1 (C5), 70.2 (C4), 63.7 (C6), 60.1 (CH), 22.3 (CH₃), 21.6 (CH₃).



¹³C{¹H} NMR (101 MHz, D₂O, 4 °C, 36OR14-2015): δ /ppm = 92.8 (C1), 79.2 (C2), 79.0 (C5), 73.0 (C3), 67.0 (C4), 61.6 (C6), 52.1 (CH), 23.0 (CH₃), 21.2 (CH₃).

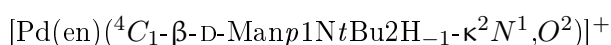
***N*-(*tert*-Butyl)-D-mannosylamine and Pd-en**

	D-Man1 <i>Nt</i> Bu	Pd-en	HIO ₃	Pd-en chelate	%
1:1:1	159 mg	1.50 mL	119 mg	D-Man α 1 <i>Nt</i> Bu2H ₋₁ - κ^2 N ¹ ,O ²	47
	675 μ mol	675 μ mol	675 μ mol	β -D-Man ρ 1 <i>Nt</i> Bu2H ₋₁ - κ^2 N ¹ ,O ²	29
				1 n. i. species	24
1:2:1	79.4 mg 338 μ mol	1.50 mL 675 μ mol	59.4 mg 338 μ mol	D-Man α 1 <i>Nt</i> Bu2,3,4H ₋₃ - κ^2 N ¹ ,O ² : κ^2 O ^{4,5}	100

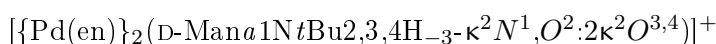


¹H NMR (400 MHz, D₂O, 4 °C, 47OR4-2015): δ /ppm = 8.02 (s, H1).

¹³C{¹H} NMR (101 MHz, D₂O, 4 °C, 47OR5-2015): δ /ppm = 182.1 (C1), 85.8 (C2), 74.7 (C3), 71.1 (C5), 70.1 (C4), 63.7 (C6), 63.1 (C), 29.1 (3 \times CH₃).



¹³C{¹H} NMR (101 MHz, D₂O, 4 °C, 47OR5-2015): δ /ppm = 93.5 (C1), 80.0 (C2), 78.8 (C5), 73.1 (C3), 66.8 (C4), 61.5 (C6), 57.7 (C), 29.9 (3 \times CH₃).

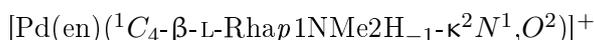


¹H NMR (400 MHz, D₂O, 4 °C, 47OR7-2015): δ /ppm = 8.12 (s, H1).

¹³C{¹H} NMR (101 MHz, D₂O, 4 °C, 47OR8-2015): δ /ppm = 183.1 (C1), 88.4 (C2), 87.9 (C3), 84.2 (C5), 73.3 (C4), 64.4 (C6), 63.1 (C), 29.3 (3 \times CH₃).

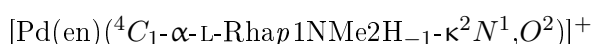
5.6.9. Complexes featuring *N*-Alkyl-L-rhamnosylamines***N*-Methyl-L-rhamnosylamine and Pd-en**

	L-Rha1 <i>N</i> Me	Pd-en	HIO ₃	Pd-en chelate	%
1:1:1	120 mg	1.50 mL	119 mg	¹ C ₄ - β -L-Rha ρ 1 <i>N</i> Me2H ₋₁ - κ^2 N ¹ ,O ²	58
	675 μ mol	675 μ mol	675 μ mol	⁴ C ₁ - α -L-Rha ρ 1 <i>N</i> Me2H ₋₁ - κ^2 N ¹ ,O ²	28
				L-Rha α 1 <i>N</i> Me2H ₋₁ - κ^2 N ¹ ,O ²	14



¹H NMR (400 MHz, D₂O, 4 °C, 17OR10-2017): δ /ppm = δ /ppm = 4.05 (d, 1H, H1, ³J_{1,2}=1.0 Hz), 3.81 (dd, 1H, H2, ³J_{2,3}=3.2 Hz), 3.57 (dd, 1H, H3, ³J_{3,4}=9.6 Hz), 3.49–3.45 (spj, H4/H5), 2.32 (s, 3H, CH₃), 1.38 (d, 3H, 3 \times H6).

¹³C{¹H} NMR (101 MHz, D₂O, 4 °C, 17OR11-2017): δ /ppm = 94.8 (C1), 78.9 (C2), 74.8 (C3), 72.8 (C5), 72.4 (C4), 36.4 (CH₃), 17.6 (C6).



¹H NMR (400 MHz, D₂O, 4 °C, 17OR10-2017): δ /ppm = 4.54 (d, H1, ³J_{1,2}=5.9 Hz), 1.34 (d, 3H, 3 \times H6).

¹³C{¹H} NMR (101 MHz, D₂O, 4 °C, 17OR11-2017): δ /ppm = 97.0 (C1), 77.2 (C2), 75.1 (C3),

72.5 (C4), 72.5 (C5), 37.3 (CH₃), 17.7 (C6).

$[\text{Pd}(\text{en})(\text{L-Rha}\alpha\text{1NMe2H}_{-1}\text{-}\kappa^2\text{N}^1,\text{O}^2)]^+$

¹H NMR (400 MHz, D₂O, 4 °C, 17OR10-2017): 8.08 (s, H1), 1.34 (d, 3H, 3×H6).

¹³C{¹H} NMR (101 MHz, D₂O, 4 °C, 17OR11-2017): $\delta/\text{ppm} = 187.9$ (C1), 86.8 (C2), 74.6 (C3), 73.8 (C4), 67.4 (C5), 48.8 (CH₃), 19.7 (C6).

***N*-Ethyl-L-rhamnosylamine and Pd-en**

	L-Rha1NEt	Pd-en	HIO ₃	Pd-en chelate	%
1:1:1	129 mg	1.50 mL	119 mg	¹ C ₄ -β-L-Rhap1NEt2H ₋₁ -κ ² N ¹ ,O ²	42
	675 μmol	675 μmol	675 μmol	⁴ C ₁ -α-L-Rhap1NEt2H ₋₁ -κ ² N ¹ ,O ²	26
				L-Rhaα1NEt2H ₋₁ -κ ² N ¹ ,O ²	20
				2 n. i. species	12

$[\text{Pd}(\text{en})(^1\text{C}_4\text{-}\beta\text{-L-Rhap1NEt2H}_{-1}\text{-}\kappa^2\text{N}^1,\text{O}^2)]^+$

¹H NMR (400 MHz, D₂O, 4 °C, 24OR43-2016): $\delta/\text{ppm} = 4.34$ (d, 1H, H1, ³J_{1,2}=1.2 Hz), 3.79 (dd, 1H, H2, ³J_{2,3}=3.4 Hz), 3.54 (dd, 1H, H3, ³J_{3,4}=8.8 Hz), 3.31–3.29 (dd, H4/H5), 3.16 (m, 1H, CH), 1.35 (d, 3H, 3×H6), 1.20 (d, 6H, 2×CH₃).

¹³C{¹H} NMR (101 MHz, D₂O, 4 °C, 24OR44-2016): $\delta/\text{ppm} = 94.8$ (C1), 78.9 (C2), 74.8 (C3), 72.8 (C5), 72.4 (C4), 36.4 (CH₃), 17.6 (C6).

$[\text{Pd}(\text{en})(^4\text{C}_1\text{-}\alpha\text{-L-Rhap1NEt2H}_{-1}\text{-}\kappa^2\text{N}^1,\text{O}^2)]^+$

¹H NMR (400 MHz, D₂O, 4 °C, 24OR43-2016): $\delta/\text{ppm} = 4.54$ (d, H1, ³J_{1,2}=6.2 Hz), 1.35 (d, 3×H6), 1.23 (d, 2×CH₃).

¹³C{¹H} NMR (101 MHz, D₂O, 4 °C, 24OR44-2016): $\delta/\text{ppm} = 97.0$ (C1), 77.2 (C2), 75.1 (C3), 72.5 (C4), 72.5 (C5), 37.3 (CH₃), 17.7 (C6).

$[\text{Pd}(\text{en})(\text{L-Rha}\alpha\text{1NEt2H}_{-1}\text{-}\kappa^2\text{N}^1,\text{O}^2)]^+$

¹H NMR (400 MHz, D₂O, 4 °C, 24OR43-2016): 8.07 (s, H1), 1.44 (d, 2×CH₃), 1.35 (d, 3×H6).

¹³C{¹H} NMR (101 MHz, D₂O, 4 °C, 24OR43-2016): $\delta/\text{ppm} = 186.4$ (C1), 86.8 (C2), 74.6 (C3), 73.9 (C4), 67.4 (C5), 55.7 (CH₂), 19.7 (C6), 15.1 (CH₃).

***N*-(*iso*-Propyl)-L-rhamnosylamine and Pd-en**

	L-Rha1NiPr	Pd-en	HIO ₃	Pd-en chelate	%
1:1:1	73.9 mg	800 μL	79.3 mg	L-Rhaα1NiPr2H ₋₁ -κ ² N ¹ ,O ²	46
	360 μmol	360 μmol	360 μmol	¹ C ₄ -β-L-Rhap1NiPr2H ₋₁ -κ ² N ¹ ,O ²	42
				¹ C ₄ -α-L-Rhap1NiPr2H ₋₁ -κ ² N ¹ ,O ²	12

$[\text{Pd}(\text{en})(^1\text{C}_4\text{-}\beta\text{-L-Rhap1NiPr2H}_{-1}\text{-}\kappa^2\text{N}^1,\text{O}^2)]^+$

¹H NMR (400 MHz, D₂O, 4 °C, 40OR1-2017): $\delta/\text{ppm} = \delta/\text{ppm} = 4.34$ (d, 1H, H1, ³J_{1,2}=1.2 Hz),

3.94 (t, 1H, H3), 3.87 (m, 1H, H5), 3.72–3.70 (sp, H4), 3.64–3.58 (sp, 2H, H6/H6'), 3.43 (dd, 1H, H2, $^3J_{2,3}=3.2$ Hz), 2.51 (s, 3H, CH₃).

$^{13}\text{C}\{^1\text{H}\}$ NMR (101 MHz, D₂O, 4 °C, 40OR2-2017): $\delta/\text{ppm} = 94.8$ (C1), 78.9 (C2), 74.8 (C3), 72.8 (C5), 72.4 (C4), 36.4 (CH₃), 17.6 (C6).

$[\text{Pd}(\text{en})(^4\text{C}_1\text{-}\alpha\text{-L-Rhap1NiPr2H}_{-1}\text{-}\kappa^2\text{N}^1, \text{O}^2)]^+$

^1H NMR (400 MHz, D₂O, 4 °C, 40OR1-2017): $\delta/\text{ppm} = 4.54$ (d, H1, $^3J_{1,2}=5.9$ Hz).

$^{13}\text{C}\{^1\text{H}\}$ NMR (101 MHz, D₂O, 4 °C, 40OR2-2017): $\delta/\text{ppm} = 97.0$ (C1), 77.2 (C2), 75.1 (C3), 72.5 (C4), 72.5 (C5), 37.3 (CH₃), 17.7 (C6).

$[\text{Pd}(\text{en})(\text{L-Rhaa1NiPr2H}_{-1}\text{-}\kappa^2\text{N}^1, \text{O}^2)]^+$

^1H NMR (400 MHz, D₂O, 4 °C, 40OR1-2017): 8.08 (s, H1).

$^{13}\text{C}\{^1\text{H}\}$ NMR (101 MHz, D₂O, 4 °C, 40OR2-2017): $\delta/\text{ppm} = 183.4$ (C1), 87.0 (C2), 74.6 (C3), 74.0 (C4), 67.4 (C5), 60.1 (CH), 22.3 (CH₃), 21.6 (CH₃), 19.7 (C6).

5.6.10. Complexes featuring *N*-Alkyl-2-deoxy-D-erythro-pentosylamines

N-Methyl-2-deoxy-D-erythro-pentosylamine and Pd-en

	D-ery-dPent1NMe	Pd-en	HIO ₃	Pd-en chelate	%
1:1:1	124 mg	1.87 mL	148 mg	D-ery-dPent	35
	843 μmol	843 μmol	843 μmol	D-ery-dPent a1NMe3H ₋₁ - $\kappa^2\text{N}^1, \text{O}^3$	29
				α -D-ery-dPent f1NMe3H ₋₁ - $\kappa^2\text{N}^1, \text{O}^3$	23
				1 n. i. species	13
1:2:1	73.9 mg	2.23 mL	88.3 mg	D-ery-dPent a1NMe3,4,5H ₋₃ - $\kappa^2\text{N}^1, \text{O}^3; \kappa^2\text{O}^{4,5}$	88
	502 μmol	1.00 mmol	502 μmol	complexed D-ery-dPent	12

$[\text{Pd}(\text{en})(\alpha\text{-D-ery-dPent f1NMe3H}_{-1}\text{-}\kappa^2\text{N}^1, \text{O}^3)]^+$

$^{13}\text{C}\{^1\text{H}\}$ NMR (101 MHz, D₂O, 4 °C, 46OR8-2015): $\delta/\text{ppm} = 92.4$ (C1), 90.7 (C4), 72.8 (C3), 62.8 (C5), 38.1 (C2), 36.8 (CH₃).

$[\text{Pd}(\text{en})(\text{D-ery-dPent a1NMe3H}_{-1}\text{-}\kappa^2\text{N}^1, \text{O}^3)]^+$

^1H NMR (400 MHz, D₂O, 4 °C, 46OR7-2015): $\delta/\text{ppm} = 7.75$ (s, H1).

$^{13}\text{C}\{^1\text{H}\}$ NMR (101 MHz, D₂O, 4 °C, 46OR8-2015): $\delta/\text{ppm} = 179.8$ (C1), 75.1 (C3), 68.4 (C4), 63.0 (C5), 51.1 (CH₃), 37.2 (C2).

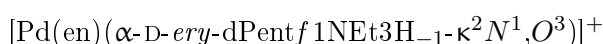
$[\{\text{Pd}(\text{en})\}_2(\text{D-ery-dPent a1NMe3,4,5H}_{-3}\text{-}\kappa^2\text{N}^1, \text{O}^3; 2\kappa^2\text{O}^{4,5})]^+$

^1H NMR (400 MHz, D₂O, 4 °C, 46OR10-2015): $\delta/\text{ppm} = 7.68$ (s, H1).

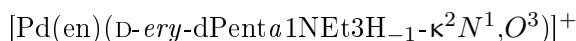
$^{13}\text{C}\{^1\text{H}\}$ NMR (101 MHz, D₂O, 4 °C, 46OR11-2015): $\delta/\text{ppm} = 174.0$ (C1), 84.8 (C3), 75.7 (C5), 69.3 (C4), 51.7 (CH₃), 39.3 (C2).

***N*-Ethyl-2-deoxy-D-erythro-pentosylamine and Pd-en**

	D-ery-dPent1NEt	Pd-en	HIO ₃	Pd-en chelate	%
1:1:1	197 mg	2.71 mL	215 mg	D-ery-dPent	34
	1.22 mmol	1.22 mmol	1.22 mmol	D-ery-dPent a1NEt3H ₋₁ -κ ² N ¹ ,O ³	31
				α-D-ery-dPentf1NEt3H ₋₁ -κ ² N ¹ ,O ³	20
				D-ery-dPent1NEt	12
				complexed D-ery-dPent	3
1:2:1	23.1 mg	636 μL	25.2 mg	β-D-ery-dPentf1NMe3,5,6H ₋₃ -κ ² N ¹ ,O ³ :κ ² O ^{5,6}	74
	143 μmol	286 μmol	143 μmol	complexed D-ery-dPent1NMe	26



¹³C{¹H} NMR (101 MHz, D₂O, 4 °C, 46OR2a-2015): δ/ppm = 92.3 (C1), 88.4 (C4), 73.0 (C3), 62.8 (C5), 40.3 (CH₂), 39.6 (C2), 14.0 (CH₃).



¹H NMR (400 MHz, D₂O, 4 °C, 46OR1a-2015): δ/ppm = 7.81 (s, H1).

¹³C{¹H} NMR (101 MHz, D₂O, 4 °C, 46OR2a-2015): δ/ppm = 173.3 (C1), 75.1 (C3), 68.1 (C4), 64.5 (C5), 57.9 (CH₂), 39.5 (C2), 16.4 (CH₃).

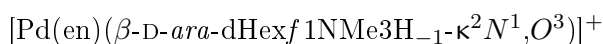


¹H NMR (400 MHz, D₂O, 4 °C, 46OR4-2015): δ/ppm = 7.75 (s, H1).

¹³C{¹H} NMR (101 MHz, D₂O, 4 °C, 46OR5-2015): δ/ppm = 173.3 (C1), 84.8 (C3), 75.6 (C5), 69.2 (C4), 58.1 (CH₂), 40.0 (C2), 16.4 (CH₃).

5.6.11. Complexes featuring *N*-Alkyl-2-deoxy-D-arabino-hexosylamines***N*-Methyl-2-deoxy-D-arabino-hexosylamine and Pd-en**

	D-ara-dHex1NMe	Pd-en	HIO ₃	Pd-en chelate	%
1:1:1	120 mg	1.50 mL	119 mg	β-D-ara-dHexf1NMe3H ₋₁ -κ ² N ¹ ,O ³	57
	675 μmol	675 μmol	675 μmol	1 n. i. species	26
				D-ara-dHexa1NMe3H ₋₁ -κ ² N ¹ ,O ³	17
1:2:1	59.8 mg	1.50 mL	59.4 mg	β-D-ara-dHexf1NMe3,5,6H ₋₃ -κ ² N ¹ ,O ³ :κ ² O ^{5,6}	41
	338 μmol	675 μmol	338 μmol	D-ara-dHexa1NMe3,5,6H ₋₃ -κ ² N ¹ ,O ³ :κ ² O ^{5,6}	39
				1 n. i. species	20



¹³C{¹H} NMR (101 MHz, D₂O, 4 °C, 44OR2-2016): δ/ppm = 89.6 (C1), 84.9 (C4), 70.3 (C5), 70.1 (C3), 64.6 (C6), 38.6 (C2), 37.0 (CH₃).



¹H NMR (400 MHz, D₂O, 4 °C, 42OR1-2016): δ/ppm = 7.80 (s, H1).

¹³C{¹H} NMR (101 MHz, D₂O, 4 °C, 44OR2-2016): δ/ppm = 175.3 (C1), 73.6 (C3), 73.4 (C5),

67.1 (C4), 63.3 (C6), 50.7 (CH₃), 41.1 (C2).



¹³C{¹H} NMR (101 MHz, D₂O, 4 °C, 44OR5-2016): $\delta/\text{ppm} = 89.5$ (C1), 87.5 (C4), 80.9 (C5), 78.3 (C3), 75.0 (C6), 38.4 (C2), 36.7 (CH₃).



¹H NMR (400 MHz, D₂O, 4 °C, 44OR4-2016): $\delta/\text{ppm} = 7.67$ (s, H1).

¹³C{¹H} NMR (101 MHz, D₂O, 4 °C, 44OR5-2016): $\delta/\text{ppm} = 178.8$ (C1), 86.7 (C5), 83.7 (C3), 76.0 (C6), 70.2 (C4), 50.9 (CH₃), 40.8 (C2).

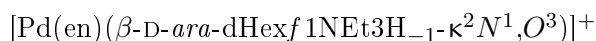
N-Ethyl-2-deoxy-D-*arabino*-hexosylamine and Pd-en

	D- <i>ara</i> -dHex1NEt	Pd-en	HIO ₃	Pd-en chelate	%
1:1:1	129 mg	1.50 mL	119 mg	D- <i>ara</i> -dHexa1NEt3H _{-1-κ²N¹, O³}	67
	675 μmol	675 μmol	675 μmol	β-D- <i>ara</i> -dHexf1NEt3H _{-1-κ²N¹, O³}	27
				1 n. i. species	6
1:2:1	64.5 mg	1.50 mL	59.4 mg	D- <i>ara</i> -dHexa1NEt3H _{-1-κ²N¹, O³}	60
	338 μmol	675 μmol	338 μmol	2 n. i. species	26
				β-D- <i>ara</i> -dHexf1NEt3H _{-1-κ²N¹, O³}	14



¹H NMR (400 MHz, D₂O, 4 °C, 42OR22-2015): $\delta/\text{ppm} = 7.87$ (s, H1).

¹³C{¹H} NMR (101 MHz, D₂O, 4 °C, 42OR23-2015): $\delta/\text{ppm} = 173.9$ (C1), 73.7 (C3), 73.2 (C5), 66.6 (C4), 63.4 (C6), 57.6 (CH₂), 41.1 (C2), 16.3 (CH₃).



¹³C{¹H} NMR (101 MHz, D₂O, 4 °C, 44OR2-2016): $\delta/\text{ppm} = 87.1$ (C1), 84.2 (C4), 70.4 (C5), 70.2 (C3), 64.7 (C6), 41.7 (CH₂), 38.9 (C2), 16.3 (CH₃).

N-(*iso*-Propyl)-2-deoxy-D-*arabino*-hexosylamine and Pd-en

	D- <i>ara</i> -dHex1NiPr	Pd-en	HIO ₃	Pd-en chelate	%
1:1:1	120 mg	1.30 mL	103 mg	D- <i>ara</i> -dHexa1NiPr3H _{-1-κ²N¹, O³}	75
	585 μmol	585 μmol	585 μmol	D- <i>ara</i> -dHex	15
				D- <i>ara</i> -dHex1NiPr	10
1:2:1	69.2 mg	1.50 mL	59.3 mg	D- <i>ara</i> -dHexa1NiPr3H _{-1-κ²N¹, O³}	64
	337 μmol	674 μmol	337 μmol	D- <i>ara</i> -dHex	24
				2 n. i. species	12

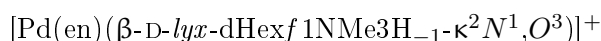


¹H NMR (400 MHz, D₂O, 4 °C, 15OR1-2016): $\delta/\text{ppm} = 7.87$ (s, H1).

¹³C{¹H} NMR (101 MHz, D₂O, 4 °C, 15OR2-2016): $\delta/\text{ppm} = 171.3$ (C1), 73.9 (C3), 73.3 (C5), 66.5 (C4), 63.5 (C6), 61.1 (CH), 42.4 (C2), 23.8 (CH₃), 21.5 (CH₃).

5.6.12. Complexes featuring *N*-Alkyl-2-deoxy-*D*-lyxo-hexosylamines*N*-Methyl-2-deoxy-*D*-lyxo-hexosylamine and Pd-en

	<i>D</i> -lyx-dHex1NMe	Pd-en	HIO ₃	Pd-en chelate	%
1:1:1	120 mg 675 μmol	1.50 mL 675 μmol	119 mg 675 μmol	β - <i>D</i> -lyx-dHexf1NMe3H ₋₁ -κ ² N ¹ ,O ³	63
				1 n. i. species	26
				<i>D</i> -lyx-dHexa1NMe3H ₋₁ -κ ² N ¹ ,O ³	11
1:2:1	59.8 mg 338 μmol	1.50 mL 675 μmol	59.4 mg 338 μmol	<i>D</i> -lyx-dHexa1NMe3,4,5H ₋₃ -κ ² N ¹ ,O ³ :κ ² O ^{4,5}	35
				β - <i>D</i> -lyx-dHexf1NMe3,5,6H ₋₃ -κ ² N ¹ ,O ³ :κ ² O ^{5,6}	32
				⁴ C ₁ - β - <i>D</i> -lyx-dHexp1NMe3H ₋₁ -κ ² N ¹ ,O ³	22
				1 n. i. species	11



¹³C{¹H} NMR (101 MHz, D₂O, 4 °C, 43OR17-2016): δ/ppm = 92.0 (C1), 90.9 (C4), 73.9 (C3), 72.2 (C5), 63.2 (C6), 38.0 (C2), 36.9 (CH₃).



¹H NMR (400 MHz, D₂O, 4 °C, 43OR16-2016): δ/ppm = 7.76 (s, H1).

¹³C{¹H} NMR (101 MHz, D₂O, 4 °C, 43OR17-2016): δ/ppm = 174.3 (C1), 73.8 (C5), 71.6 (C3), 67.2 (C4), 63.7 (C6), 51.4 (CH₃), 39.8 (C2).



¹H NMR (400 MHz, D₂O, 4 °C, 43OR19-2016): δ/ppm = 7.71 (s, H1).

¹³C{¹H} NMR (101 MHz, D₂O, 4 °C, 43OR20-2016): δ/ppm = 174.4 (C1), 87.2 (C5), 85.0 (C4), 68.9 (C3), 64.2 (C6), 51.6 (CH₃), 39.6 (C2).



¹³C{¹H} NMR (101 MHz, D₂O, 4 °C, 43OR19-2016): δ/ppm = 92.7 (C1), 90.3 (C4), 82.0 (C5), 74.0 (C6), 72.3 (C3), 37.5 (C2), 36.8 (CH₃).

N-Ethyl-2-deoxy-*D*-lyxo-hexosylamine and Pd-en

	<i>D</i> -lyx-dHex1NEt	Pd-en	HIO ₃	Pd-en chelate	%
1:1:1	129 mg 256 μmol	1.50 mL 512 μmol	119 mg 256 μmol	β - <i>D</i> -lyx-dHexf1NEt3H ₋₁ -κ ² N ¹ ,O ³	28
				<i>D</i> -lyx-dHex1N	28
				<i>D</i> -lyx-dHexa1NEt3H ₋₁ -κ ² N ¹ ,O ³	23
				<i>D</i> -lyx-dHex1NEt	11
				1 n. i. species	7
1:2:1	49.0 mg 338 μmol	1.14 mL 675 μmol	45.0 mg 338 μmol	<i>D</i> -lyx-dHexa1NEt3,4,5H ₋₃ -κ ² N ¹ ,O ³ :κ ² O ^{4,5}	92
				β - <i>D</i> -lyx-dHexf1NEt3,5,6H ₋₃ -κ ² N ¹ ,O ³ :κ ² O ^{5,6}	8



¹³C{¹H} NMR (101 MHz, D₂O, 4 °C, 43OR23-2016): δ/ppm = 91.9 (C1), 88.7 (C4), 74.1 (C3),

72.3 (C5), 63.3 (C6), 40.7 (CH₂), 38.1 (C2), 14.0 (CH₃).

[Pd(en)(D-lyx-dHexa1NEt3H₋₁-κ²N¹,O³)]⁺

¹H NMR (400 MHz, D₂O, 4 °C, 43OR22-2016): δ/ppm = 7.82 (s, H1).

¹³C{¹H} NMR (101 MHz, D₂O, 4 °C, 43OR23-2016): δ/ppm = 173.3 (C1), 73.8 (C5), 71.9 (C3), 67.2 (C4), 63.7 (C6), 57.9 (CH₂), 39.5 (C2), 16.4 (CH₃).

[{Pd(en)}₂(D-lyx-dHexa1NEt3,4,5H₋₃-κ²N¹,O³:2κ²O^{4,5})]⁺

¹H NMR (400 MHz, D₂O, 4 °C, 43OR27-2016): δ/ppm = 7.77 (s, H1).

¹³C{¹H} NMR (101 MHz, D₂O, 4 °C, 43OR26-2016): δ/ppm = 173.2 (C1), 87.3 (C5), 84.8 (C4), 68.6 (C3), 64.5 (C6), 58.1 (CH₂), 39.9 (C2), 16.3 (CH₃).

[{Pd(en)}₂(±D-lyx-dHexf1NEt3,5,6H₋₃-κ²N¹,O³:2κ²O^{5,6})]⁺

¹³C{¹H} NMR (101 MHz, D₂O, 4 °C, 43OR26-2016): δ/ppm = 92.6 (C1), 88.1 (C4), 82.1 (C5), 73.1 (C3), 73.0 (C6), 40.5 (CH₂), 37.5 (C2), 13.9 (CH₃).

5.6.13. Complexes featuring *N*-phenyl-D-glycosylamines

N-Phenyl-D-arabinosylamine and Pd-en

	D-Ara1NPh	Pd-tmeda	HIO ₃	Pd-en chelate	%
1:1:1	152 mg	1.50 mL	119 mg	D-Arabinose	55
	675 μmol	675 μmol	675 μmol	D-Ara1NPh	24
				¹ C ₄ -α-D-Arap1NPh2H ₋₁ -κ ² N ¹ ,O ²	21
1:2:1	76.0 mg	1.50 mL	59.4 mg	¹ C ₄ -α-D-Arap1NPh2,3,4H ₋₃ -κ ² N ¹ ,O ² :κ ² O ^{3,4}	60
	338 μmol	675 μmol	338 μmol	¹ C ₄ -α-D-Arap1NPh2H ₋₁ -κ ² N ¹ ,O ²	40

[Pd(tmeda)(¹C₄-α-D-Arap1NPh2H₋₁-κ²N¹,O²)]⁺

¹H NMR (400 MHz, D₂O, 4 °C, 41OR21-2018): δ/ppm = 4.47 (d, H1, ³J_{1,2}=7.8 Hz).

¹³C{¹H} NMR (101 MHz, D₂O, 4 °C, 41OR23-2018): δ/ppm = 143.0 (C_i), 130.8 (C_m), 128.8 (C_p), 124.1 (C_o), 98.0 (C1), 76.7 (C2), 75.3 (C3), 70.7 (C5), 68.5 (C4).

¹⁵N NMR (101 MHz, D₂O, 4 °C, 41OR22-2018): δ/ppm = -324.4.

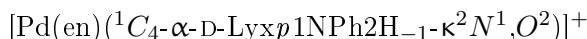
[{Pd(tmeda)}₂(⁴C₁-α-D-Arap1NPh2,3,4H₋₃-κ²N¹,O²:2κ²O^{3,4})]⁺

¹³C{¹H} NMR (101 MHz, D₂O, 4 °C, 41OR25-2018): δ/ppm = 143.0 (C_i), 130.8 (C_m), 128.8 (C_p), 124.1 (C_o), 98.0 (C1), 76.7 (C2), 75.3 (C3), 70.7 (C5), 68.5 (C4).

¹⁵N NMR (101 MHz, D₂O, 4 °C, 41OR26-2018): δ/ppm = -322.8.

N-Phenyl-D-lyxosylamine and Pd-en

	D-Lyx1NPh	Pd-en	HIO ₃	Pd-en chelate	%
1:1:1	152 mg	1.50 mL	119 mg	¹ C ₄ -α-D-Lyxp1NPh2H ₋₁ -κ ² N ¹ ,O ²	88
	675 μmol	675 μmol	675 μmol	D-Lyxa1NPh2H ₋₁ -κ ² N ¹ ,O ²	12



^1H NMR (400 MHz, D_2O , 4 °C, 04OR12-2018): $\delta/\text{ppm} = 4.60$ (d, H1, $^3J_{1,2}=9.3$ Hz).

$^{13}\text{C}\{^1\text{H}\}$ NMR (101 MHz, D_2O , 4 °C, 04OR14-2018): $\delta/\text{ppm} = 142.9$ (C_i), 130.8 (C_m), 128.2 (C_p), 122.3 (C_o), 90.9 (C1), 74.6 (C2), 72.5 (C3), 69.4 (C4), 68.2 (C5).

^{15}N NMR (101 MHz, D_2O , 4 °C, 04OR13-2018): $\delta/\text{ppm} = -328.0$.



^1H NMR (400 MHz, D_2O , 4 °C, 04OR12-2018): $\delta/\text{ppm} = 8.28$ (s, H1).

$^{13}\text{C}\{^1\text{H}\}$ NMR (101 MHz, D_2O , 4 °C, 04OR14-2018): $\delta/\text{ppm} = 190.0$ (C1), 148.5 (C_i), 130.5 (C_m), 129.4 (C_p), 123.4 (C_o), 87.3 (C2), 74.9 (C3), 71.2 (C4), 63.3 (C5).

^{15}N NMR (101 MHz, D_2O , 4 °C, 04OR13-2018): $\delta/\text{ppm} = -137.4$.

N-Phenyl-D-ribosylamine and Pd-en

	D-Rib1NPh	Pd-en	HIO ₃	Pd-en chelate	%
1:1:1	152 mg	1.50 mL	119 mg	$^4\text{C}_1\text{-}\beta\text{-D-Rib}p1\text{NPh}2\text{H}_{-1}\text{-}\kappa^2\text{N}^1, \text{O}^2$	69
	675 μmol	675 μmol	675 μmol	D-Rib a 1NPh2H ₋₁ - $\kappa^2\text{N}^1, \text{O}^2$ 1 n. i. species	17 14



^1H NMR (400 MHz, D_2O , 4 °C, 22OR9-2018): $\delta/\text{ppm} = 4.75$ (d, 1H, H1, $^3J_{1,2}=9.2$ Hz).

$^{13}\text{C}\{^1\text{H}\}$ NMR (101 MHz, D_2O , 4 °C, 22OR10-2018): $\delta/\text{ppm} = 142.8$ (C_i), 130.9 (C_m), 128.1 (C_p), 122.3 (C_o), 90.6 (C1), 77.5 (C2), 72.2 (C3), 66.6 (C4), 64.8 (C5).

^{15}N NMR (101 MHz, D_2O , 4 °C, 22OR12-2018): $\delta/\text{ppm} = -330.2$.



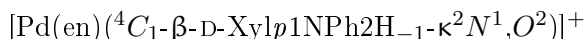
^1H NMR (400 MHz, D_2O , 4 °C, 22OR9-2018): $\delta/\text{ppm} = 8.15$ (s, H1).

$^{13}\text{C}\{^1\text{H}\}$ NMR (101 MHz, D_2O , 4 °C, 22OR10-2018): $\delta/\text{ppm} = 188.3$ (C1), 148.2 (C_i), 130.8 (C_m), 129.3 (C_p), 123.4 (C_o), 87.8 (C2), 74.1 (C3), 71.7 (C4), 63.5 (C5).

^{15}N NMR (101 MHz, D_2O , 4 °C, 22OR12-2018): $\delta/\text{ppm} = -142.4$.

N-Phenyl-D-xylosylamine and Pd-en

	D-Xyl1NPh	Pd-en	HIO ₃	Pd-en chelate	%
1:1:1	152 mg	1.50 mL	119 mg	$^4\text{C}_1\text{-}\beta\text{-D-Xyl}p1\text{NPh}2\text{H}_{-1}\text{-}\kappa^2\text{N}^1, \text{O}^2$	95
	675 μmol	675 μmol	675 μmol	D-Xyl a 1NPh2H ₋₁ - $\kappa^2\text{N}^1, \text{O}^2$	5
1:1.5:1	101 mg	1.50 mL	79.2 mg	$^4\text{C}_1\text{-}\beta\text{-D-Xyl}p1\text{NPh}2\text{H}_{-1}\text{-}\kappa^2\text{N}^1, \text{O}^2$	62
	450 μmol	675 μmol	450 μmol	$^4\text{C}_1\text{-}\beta\text{-D-Xyl}p1\text{NPh}2,3,4\text{H}_{-3}\text{-}\kappa^2\text{N}^1, \text{O}^2; \kappa^2\text{O}^{3,4}$ D-Xyl a 1NPh2,3,4H ₋₃ - $\kappa^2\text{N}^1, \text{O}^2; \kappa^2\text{O}^{3,4}$	31 7
1:2:1	76.0 mg	1.50 mL	59.4 mg	$^4\text{C}_1\text{-}\beta\text{-D-Xyl}p1\text{NPh}2,3,4\text{H}_{-3}\text{-}\kappa^2\text{N}^1, \text{O}^2; \kappa^2\text{O}^{3,4}$	75
	338 μmol	675 μmol	338 μmol	D-Xyl a 1NPh2,3,4H ₋₃ - $\kappa^2\text{N}^1, \text{O}^2; \kappa^2\text{O}^{3,4}$	15
				$^4\text{C}_1\text{-}\beta\text{-D-Xyl}p1\text{NPh}2\text{H}_{-1}\text{-}\kappa^2\text{N}^1, \text{O}^2$	10
1:2:2	76.0 mg	1.50 mL	119 mg	$^4\text{C}_1\text{-}\beta\text{-D-Xyl}p1\text{NPh}2\text{H}_{-1}\text{-}\kappa^2\text{N}^1, \text{O}^2$	85
	338 μmol	675 μmol	675 μmol	D-Xyl a 1NPh2H ₋₁ - $\kappa^2\text{N}^1, \text{O}^2$ 1 n. i. species	9 6



^1H NMR (400 MHz, D_2O , 4 °C, 37OR7-2017): δ/ppm = 7.54 (d, 2H, H_o), 7.45 (t, 2H, H_m), 7.31 (t, 1H, H_p), 4.49 (d, 1H, H1 , $^3J_{1,2}=8.4$ Hz), 3.73 (dd, 1H, H5a , $^3J_{4,5a}=5.5$ Hz, $^2J_{5a,5b}=-11.4$ Hz), 3.54 (dt, 1H, H4), 3.47–3.35 (m, 2H, H3/H5b), 3.15 (t, 1H, H2 , $^3J_{4,5b}=10.9$ Hz).

$^{13}\text{C}\{^1\text{H}\}$ NMR (101 MHz, D_2O , 4 °C, 37OR8-2017): δ/ppm = 142.5 (C_i), 130.9 (C_m), 128.2 (C_p), 122.3 (C_o), 94.4 (C1), 79.7 (C2), 78.0 (C3), 69.5 (C4), 68.5 (C5).

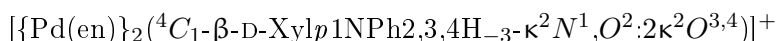
^{15}N NMR (101 MHz, D_2O , 4 °C, 51OR2-2017): δ/ppm = –329.0.



^1H NMR (400 MHz, D_2O , 4 °C, 37OR7-2017): δ/ppm = 8.16 (s, H1).

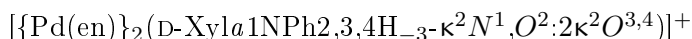
$^{13}\text{C}\{^1\text{H}\}$ NMR (101 MHz, D_2O , 4 °C, 37OR8-2017): δ/ppm = 189.8 (C1), 148.5 (C_i), 130.5 (C_m), 129.2 (C_p), 122.2 (C_o), 88.0 (C2), 73.6 (C3), 70.3 (C4), 63.4 (C5).

^{15}N NMR (101 MHz, D_2O , 4 °C, 51OR2-2017): δ/ppm = –145.2.



$^{13}\text{C}\{^1\text{H}\}$ NMR (101 MHz, D_2O , 4 °C, 37OR11-2017): δ/ppm = 142.8 (C_i), 130.5 (C_m), 128.1 (C_p), 122.0 (C_o), 94.7 (C1), 88.4 (C3), 81.4 (C2), 79.5 (C4), 68.3 (C5).

^{15}N NMR (101 MHz, D_2O , 4 °C, 51OR5-2017): δ/ppm = –329.5.



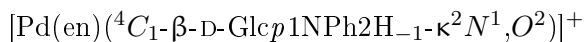
^1H NMR (400 MHz, D_2O , 4 °C, 37OR10-2017): δ/ppm = 9.22 (s, H1).

$^{13}\text{C}\{^1\text{H}\}$ NMR (101 MHz, D_2O , 4 °C, 33OR11-2017): δ/ppm = 190.2 (C1), 148.6 (C_i), 88.9 (C2), 85.7 (C3), 79.8 (C4), 65.9 (C5).

^{15}N NMR (101 MHz, D_2O , 4 °C, 51OR5-2017): δ/ppm = –148.6.

N-Phenyl-D-glucosylamine and Pd-en

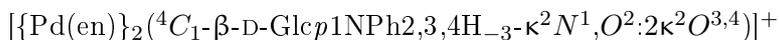
	D-Glc1NPh	Pd-en	HIO_3	Pd-en chelate	%
1:1:1	172 mg 675 μmol	1.50 mL 675 μmol	119 mg 675 μmol	$^4\text{C}_1\text{-}\beta\text{-D-Glcp1NPh2H}_{-1}\text{-}\kappa^2\text{N}^1, \text{O}^2$	100
1:2:1	76.0 mg 338 μmol	1.50 mL 675 μmol	59.4 mg 338 μmol	$^4\text{C}_1\text{-}\beta\text{-D-Glcp1NPh2H}_{-1}\text{-}\kappa^2\text{N}^1, \text{O}^2$ $^4\text{C}_1\text{-}\beta\text{-D-Glcp1NPh2,3,4\text{H}_{-3}\text{-}\kappa^2\text{N}^1, \text{O}^2:\kappa^2\text{O}^{3,4}$	51 49
1:2:2	76.0 mg 338 μmol	1.50 mL 675 μmol	119 mg 675 μmol	$^4\text{C}_1\text{-}\beta\text{-D-Glcp1NPh2H}_{-1}\text{-}\kappa^2\text{N}^1, \text{O}^2$ $^4\text{C}_1\text{-}\beta\text{-D-Glcp1NPh2,3,4\text{H}_{-3}\text{-}\kappa^2\text{N}^1, \text{O}^2:\kappa^2\text{O}^{3,4}$	81 19



^1H NMR (400 MHz, D_2O , 4 °C, 35OR31-2015): δ/ppm = 7.56 (d, 2H, H_o), 7.45 (t, 2H, H_m), 7.31 (t, 1H, H_p), 4.57 (d, 1H, H1 , $^3J_{1,2}=8.6$ Hz).

$^{13}\text{C}\{^1\text{H}\}$ NMR (101 MHz, D_2O , 4 °C, 35OR32-2015): δ/ppm = 142.8 (C_i), 130.8 (C_m), 128.1 (C_p), 122.3 (C_o), 93.6 (C1), 79.8 (C2), 79.2 (C3), 77.9 (C5), 69.3 (C4), 60.6 (C6).

$^{15}\text{N}\{^1\text{H}\}$ NMR (41 MHz, D_2O , 4 °C, 04OR2-2018): δ/ppm = –328.6.



^1H NMR (400 MHz, D_2O , 4 °C, 35OR31-2015): δ/ppm = 4.36 (d, 1H, H1 , $^3J_{1,2}=7.3$ Hz).

$^{13}\text{C}\{^1\text{H}\}$ NMR (101 MHz, D_2O , 4 °C, 04OR6-2018): $\delta/\text{ppm} = 143.1$ (C_i), 130.9 (C_m), 128.2 (C_p), 122.3 (C_o), 94.2 (C1), 88.3 (C3), 81.8 (C2), 79.8 (C4), 79.3 (C3), 61.4 (C6).

$^{15}\text{N}\{^1\text{H}\}$ NMR (41 MHz, D_2O , 4 °C, 04OR2-2018): $\delta/\text{ppm} = -329.0$.

N-Phenyl-L-gulosylamine and Pd-en

	L-Gul1NPh	Pd-en	HIO_3	Pd-en chelate	%
1:1:1	115 mg	1.00 mL	79.2 mg	L-Gulose	57
	450 μmol	450 μmol	450 μmol	$^1\text{C}_4\text{-}\beta\text{-L-Gulp1NPh2H}_{-1}\text{-}\kappa^2\text{N}^1, \text{O}^2$	37
				L-Gul1NPh	6

$[\text{Pd}(\text{en})(^1\text{C}_4\text{-}\beta\text{-L-Gulp1NPh2H}_{-1}\text{-}\kappa^2\text{N}^1, \text{O}^2)]^+$

^1H NMR (400 MHz, D_2O , 4 °C, 14OR1-2018): $\delta/\text{ppm} = 4.86$ (d, H1, $^3J_{1,2}=8.4$ Hz).

$^{13}\text{C}\{^1\text{H}\}$ NMR (101 MHz, D_2O , 4 °C, 14OR3-2018): $\delta/\text{ppm} = 143.0$ (C_i), 130.8 (C_m), 128.0 (C_p), 122.2 (C_o), 90.7 (C1), 76.7 (C5), 74.9 (C2), 72.6 (C5), 69.5 (C4), 61.0 (C6).

$^{15}\text{N}\{^1\text{H}\}$ NMR (41 MHz, D_2O , 4 °C, 14OR2-2018): $\delta/\text{ppm} = -329.0$.

N-Phenyl-D-mannosylamine and Pd-en

	D-Man1NPh	Pd-en	HIO_3	Pd-en chelate	%
1:1:1	115 mg	1.00 mL	79.2 mg	D-Man α 1NPh2H $_{-1}$ - $\kappa^2\text{N}^1, \text{O}^2$	74
	450 μmol	450 μmol	450 μmol	D-Man1NPh	26

$[\text{Pd}(\text{en})(\text{D-Man}\alpha\text{1NPh2H}_{-1}\text{-}\kappa^2\text{N}^1, \text{O}^2)]^+$

^1H NMR (400 MHz, D_2O , 4 °C, 02OR1-2018): $\delta/\text{ppm} = 8.31$ (d, H1).

$^{13}\text{C}\{^1\text{H}\}$ NMR (101 MHz, D_2O , 4 °C, 02OR2-2018): $\delta/\text{ppm} = 189.2$ (C1), 147.2 (C_i), 129.5 (C_m), 128.4 (C_p), 121.4 (C_o), 86.2 (C2), 73.3 (C3), 70.3 (C5), 69.3 (C5), 62.8 (C6).

$^{15}\text{N}\{^1\text{H}\}$ NMR (41 MHz, D_2O , 4 °C, 02OR3-2018): $\delta/\text{ppm} = -137.3$.

A. $^{13}\text{C}\{^1\text{H}\}$ NMR Spectra of coordinated Glycosylamines

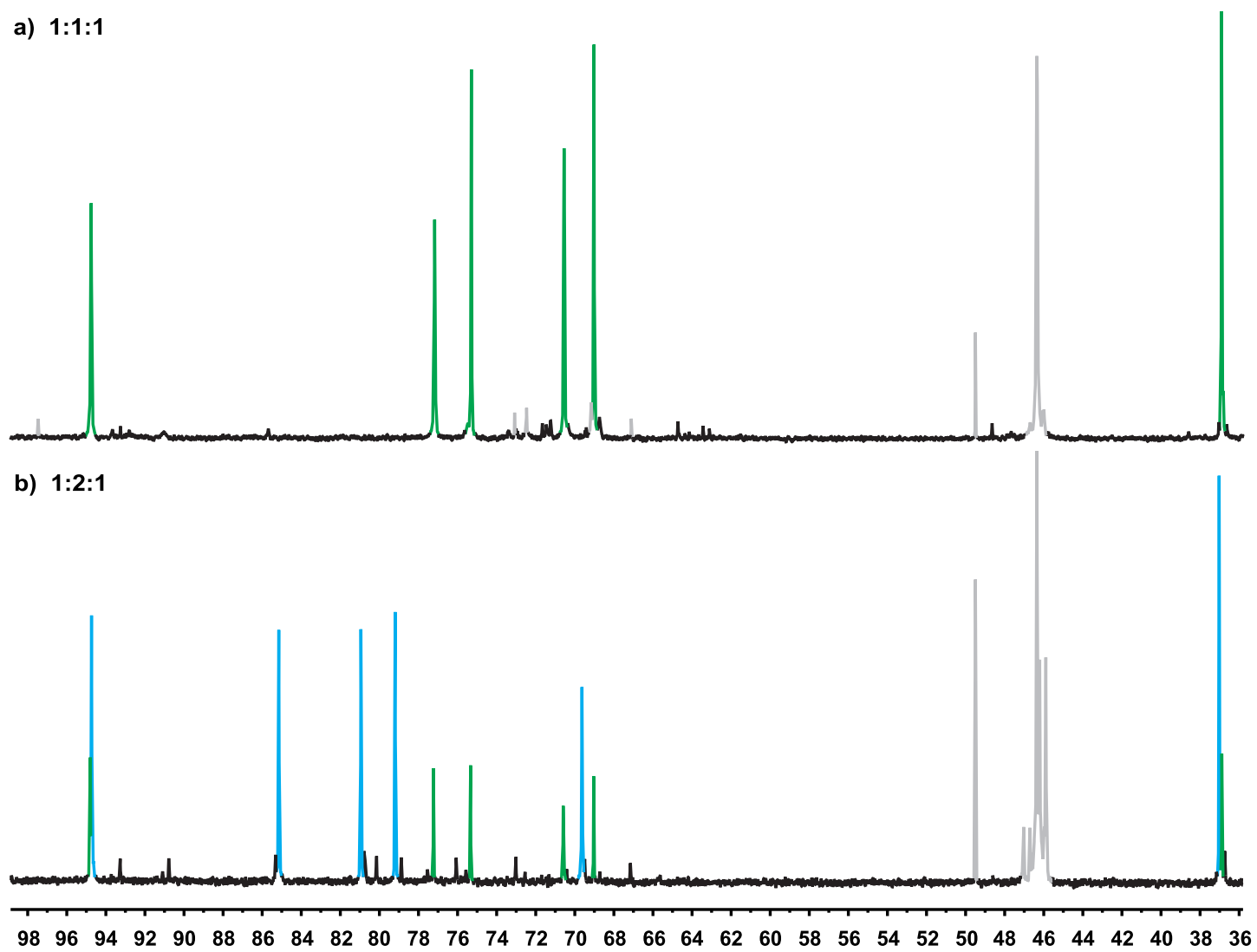
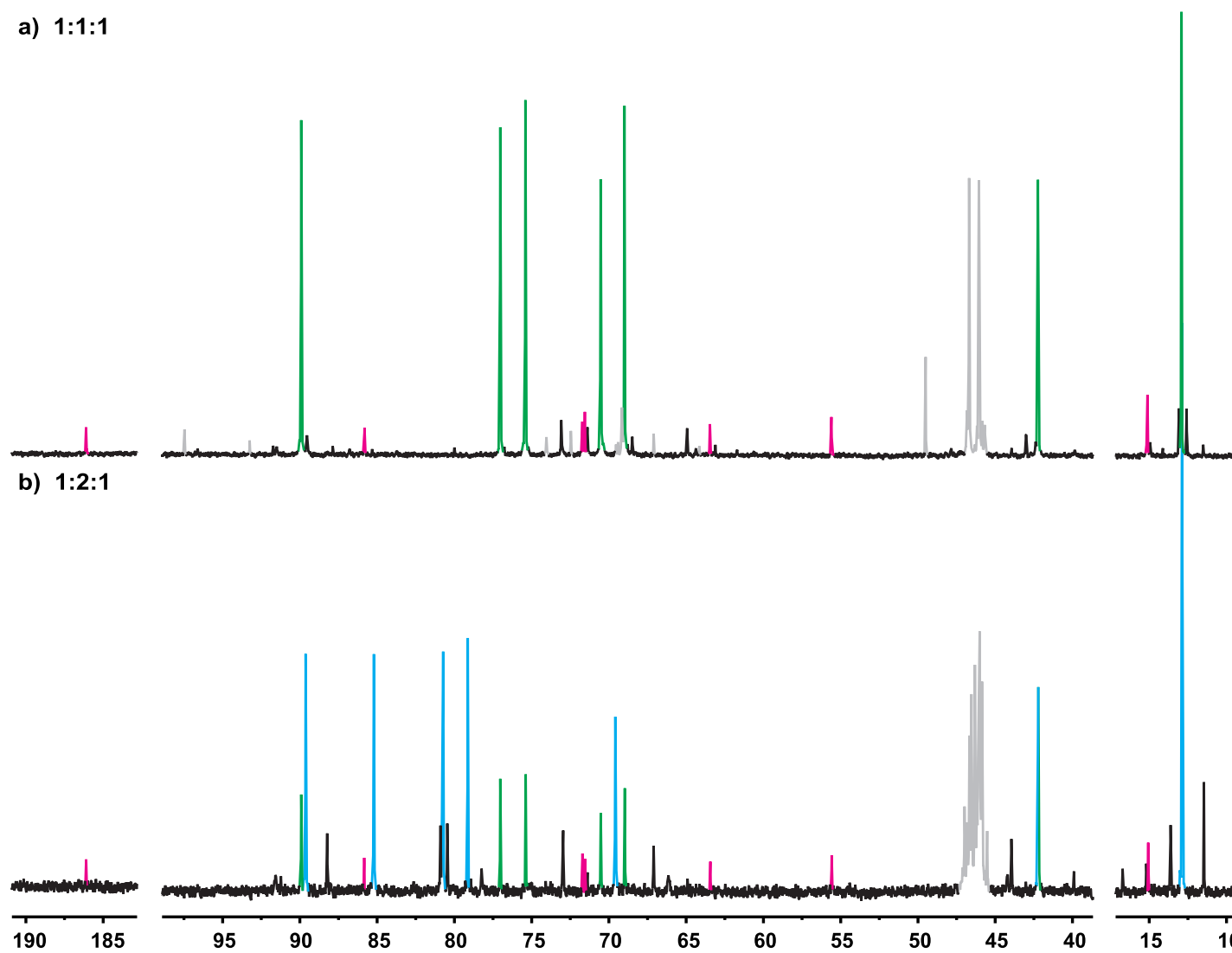


Figure A.1. Resulting $^{13}\text{C}\{^1\text{H}\}$ NMR spectra for the treatment of D-Ara1NMe with Pd-en and iodic acid in the molar ratios a) 1:1:1 and b) 1:2:1 after 3 h at 4°C in D_2O . Green: $^1\text{C}_4\text{-}\alpha\text{-D-Arap1NMe}_2\text{H}_{-1}$, cyan: $^4\text{C}_1\text{-}\alpha\text{-D-Arap1NMe}_{2,3,4}\text{H}_{-3}$, grey: D-Ara1NMe, Pd-en and MeOH.



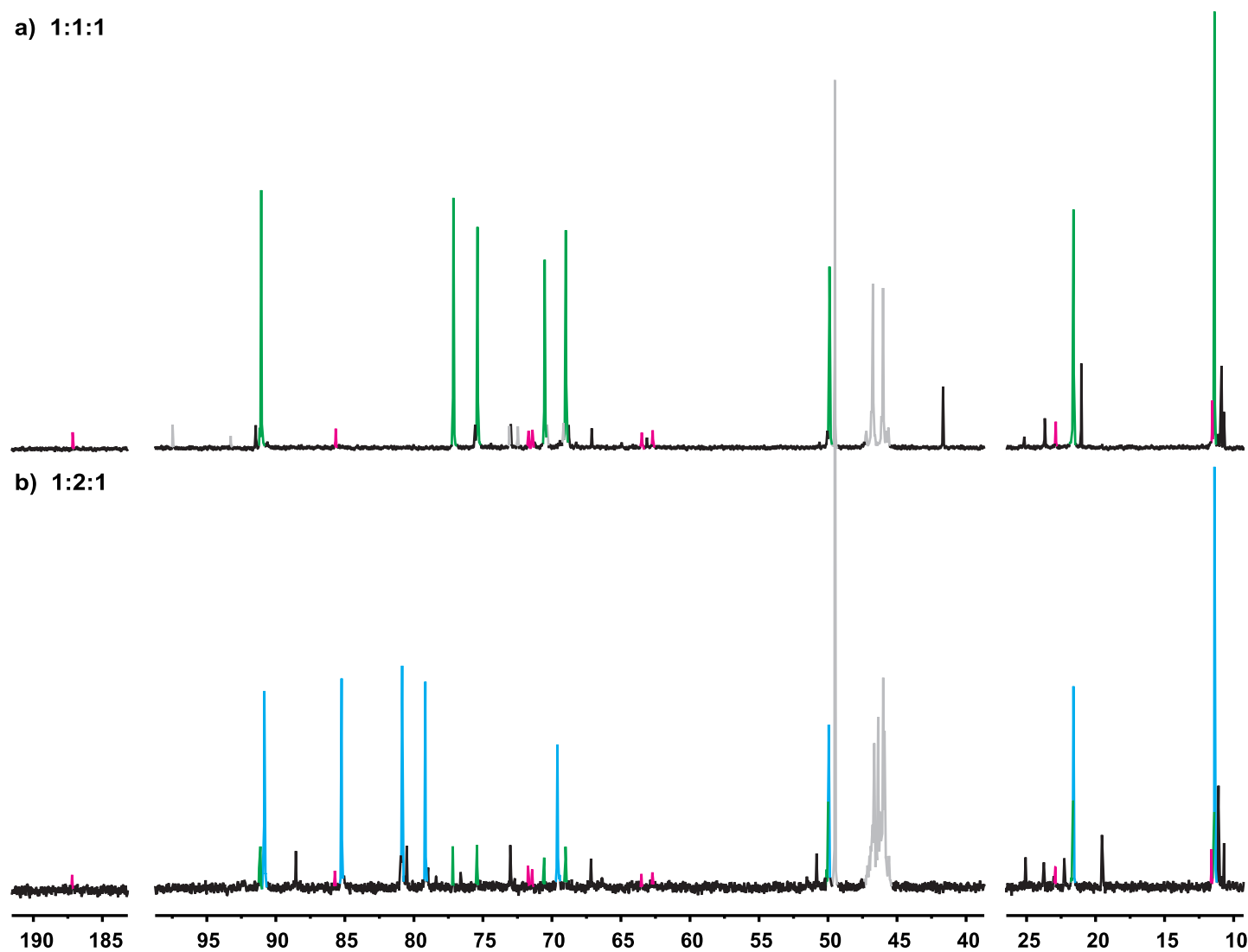


Figure A.3. Resulting $^{13}\text{C}\{^1\text{H}\}$ NMR spectra for the treatment of D-Ara1NPr with Pd-en and iodic acid in the molar ratios a) 1:1:1 and b) 1:2:1 after 3 h at 4 °C in D_2O . Green: $^1\text{C}_4\text{-}\alpha\text{-D-Arap1NPr2H}_{-1}$, magenta: D-Araa1NPr2H $_{-1}$, cyan: $^4\text{C}_1\text{-}\alpha\text{-D-Arap1NPr2,3,4H}_{-3}$, grey: Pd-en and MeOH.

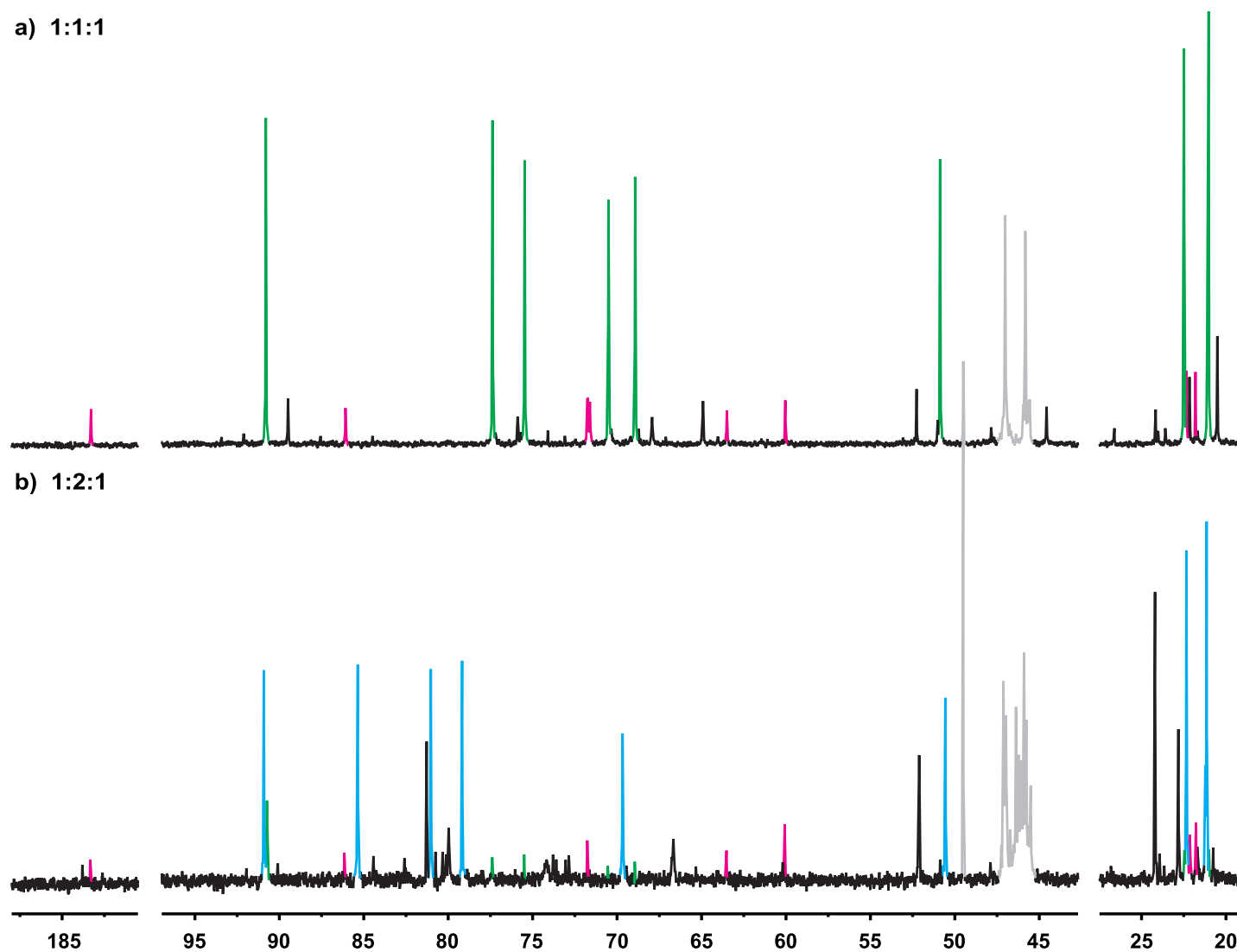


Figure A.4. Resulting $^{13}\text{C}\{^1\text{H}\}$ NMR spectra for the treatment of D-Ara1NiPr with Pd-en and iodic acid in the molar ratios a) 1:1:1 and b) 1:2:1 after 3 h at 4°C in D_2O . Green: $^1\text{C}_4\text{-}\alpha\text{-D-Arap1NiPr2H}_{-1}$, magenta: D-Araa1NiPr2H $_{-1}$, cyan: $^4\text{C}_1\text{-}\alpha\text{-D-Arap1NiPr2,3,4H}_{-3}$, purple: not identified species, grey: Pd-en and MeOH.

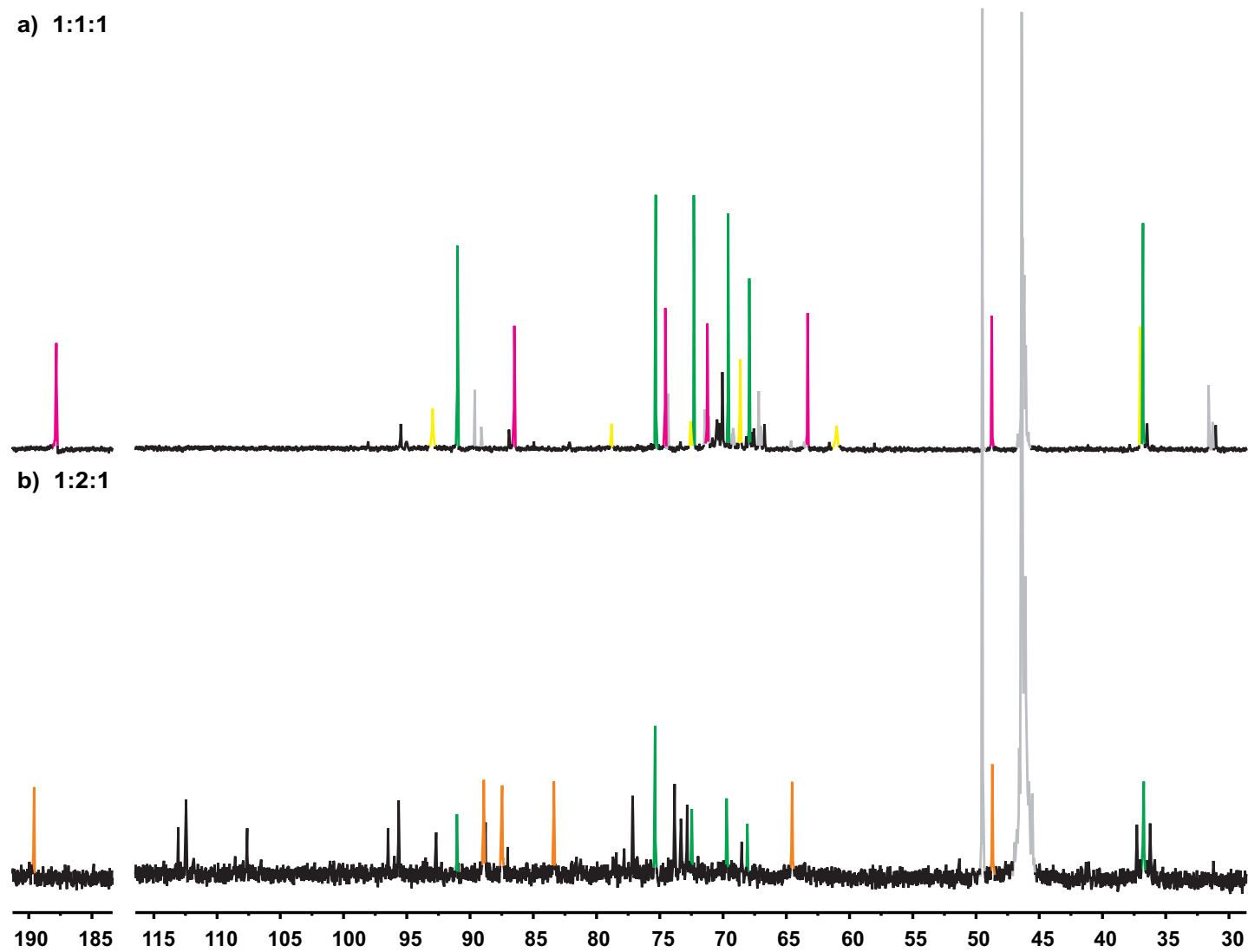


Figure A.5. Resulting $^{13}\text{C}\{^1\text{H}\}$ NMR spectra for the treatment of D-Lyx1NMe with Pd-en and iodic acid in the molar ratios a) 1:1:1 and b) 1:2:1 after 3 h at 4 °C in D₂O. Green: $^1\text{C}_4$ - α -D-Lyxp1NMe₂H₋₁, magenta: D-Lyxa1NMe₂H₋₁, yellow: $^1\text{C}_4$ - α -D-Lyxp1NMe₂H₋₁, orange: D-Lyxa1NMe_{2,3,4}H₋₃, grey: D-Lyx1NMe, Pd-en, MeNH₂ and MeOH.

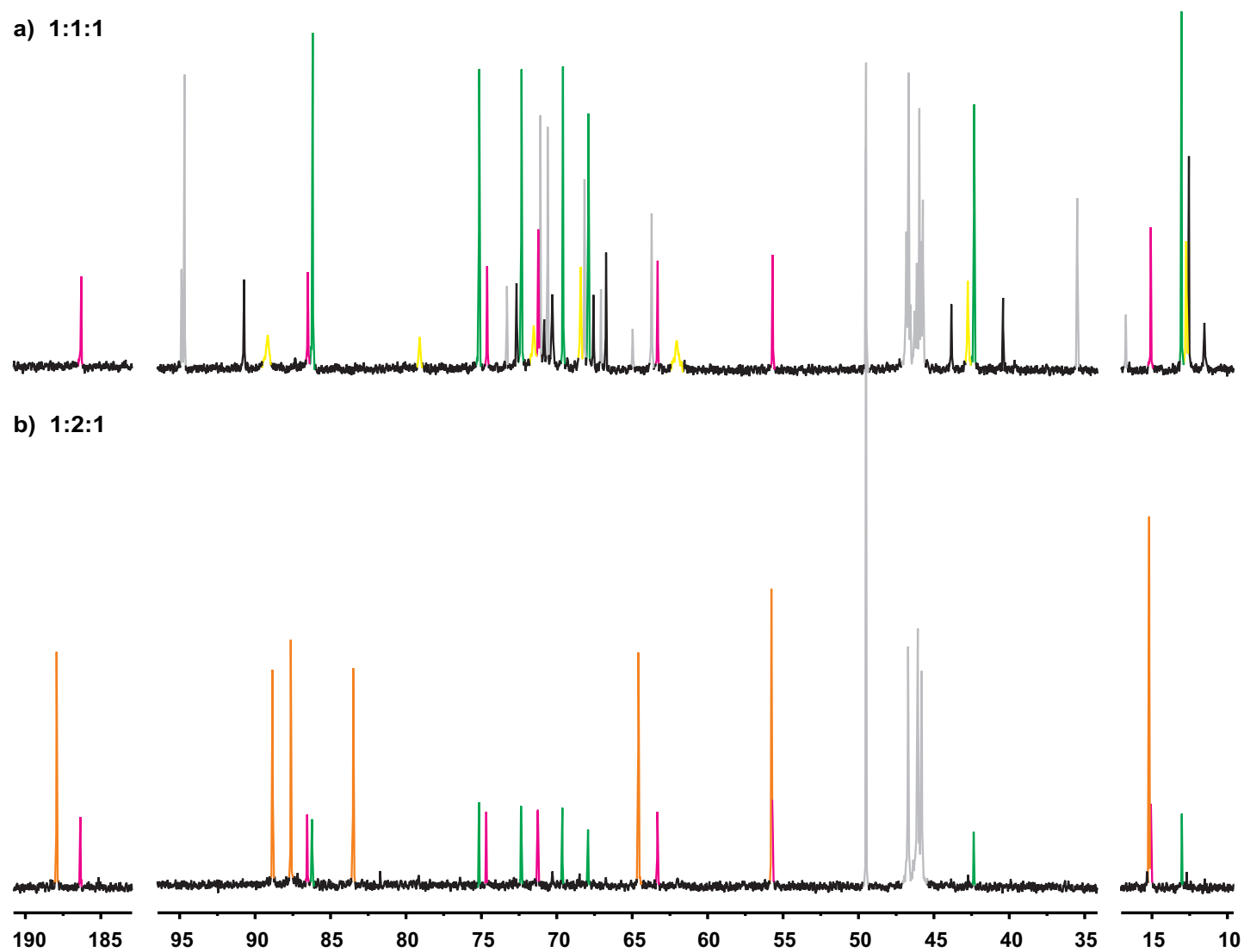


Figure A.6. Resulting $^{13}\text{C}\{^1\text{H}\}$ NMR spectra for the treatment of D-Lyx1NEt with Pd-en and iodic acid in the molar ratios a) 1:1:1 and b) 1:2:1 after 3 h at 4 °C in D_2O . Green: $^1\text{C}_4\text{-}\alpha\text{-D-Lyxp1NEt2H}_{-1}$, magenta: D-Lyxa1NEt2H $_{-1}$, yellow: $^1\text{C}_4\text{-}\alpha\text{-D-Lyxp1NEt2H}_{-1}$, orange: D-Lyxa1NEt2,3,4H $_{-3}$, grey: D-lyxose, Pd-en, EtNH $_2$ and MeOH.

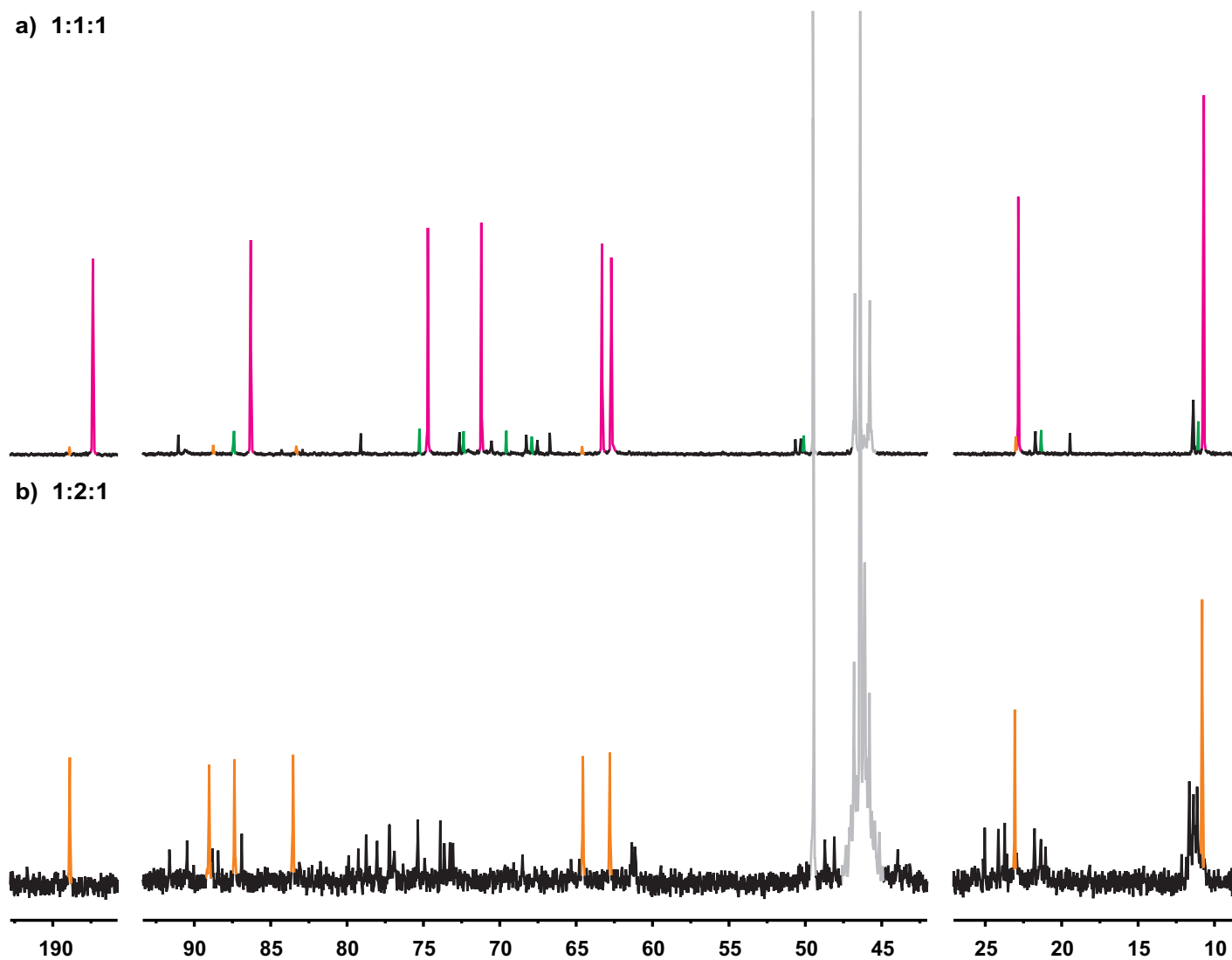


Figure A.7. Resulting $^{13}\text{C}\{^1\text{H}\}$ NMR spectra for the treatment of D-Lyx1NPr with Pd-en and iodic acid in the molar ratios a) 1:1:1 and b) 1:2:1 after 3 h at 4 °C in D_2O . Magenta: D-Lyxa1NPr2H₋₁, green: $^1\text{C}_4$ - α -D-Lyxp1NPr2H₋₁, yellow: $^1\text{C}_4$ - α -D-Lyxp1NPr2H₋₁, orange: D-Lyxa1NPr2,3,4H₋₃, grey: Pd-en and MeOH.

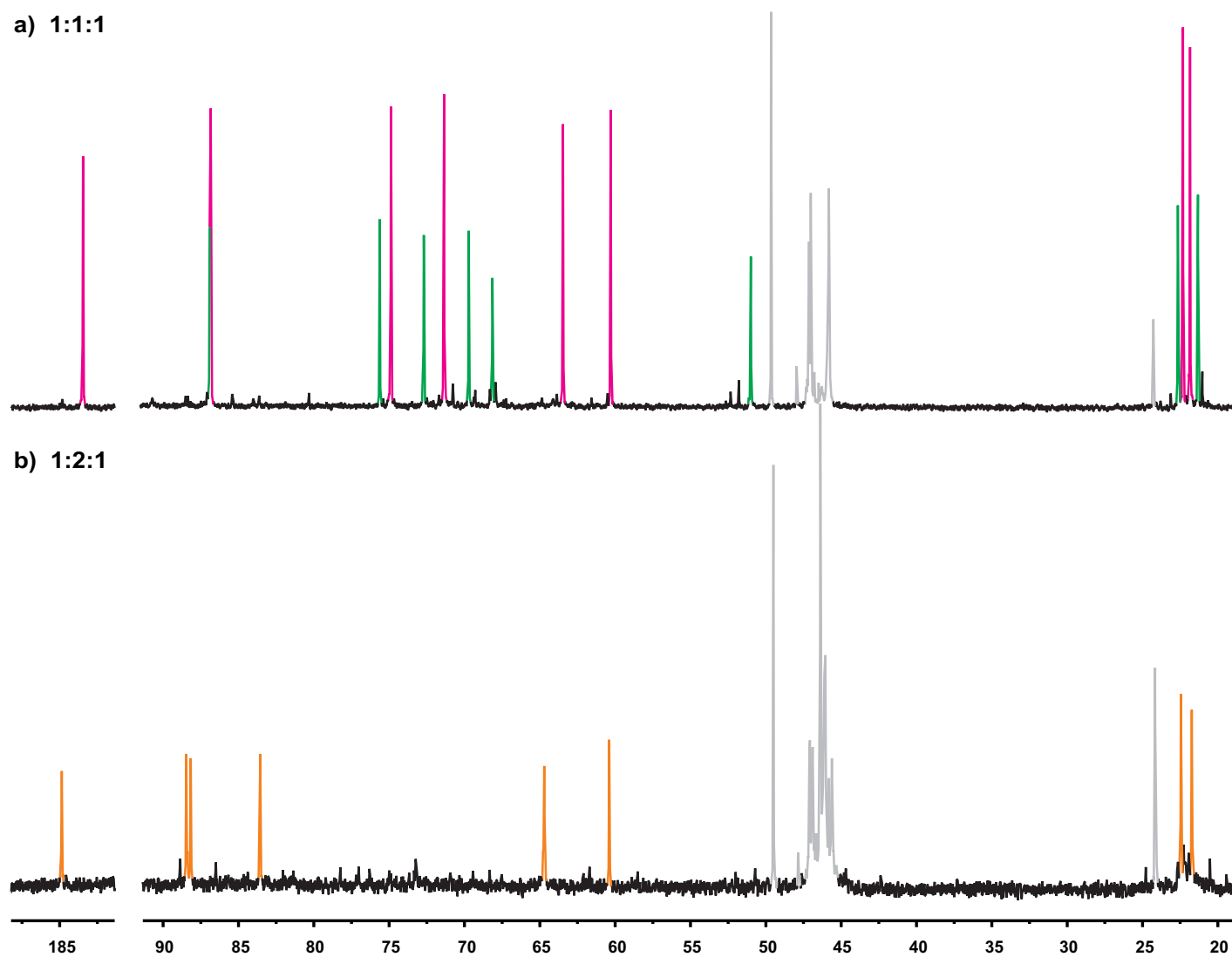


Figure A.8. Resulting $^{13}\text{C}\{^1\text{H}\}$ NMR spectra for the treatment of D-Lyx1*Ni*Pr with Pd-en and iodic acid in the molar ratios a) 1:1:1 and b) 1:2:1 after 3 h at 4 °C in D₂O. Magenta: D-Lyx*a*1*Ni*Pr2H₋₁, green: $^1\text{C}_4$ - α -D-Lyxp1*Ni*Pr2H₋₁, orange: D-Lyx*a*1*Ni*Pr2,3,4H₋₃, grey: Pd-en, *i*PrNH₂ and MeOH.

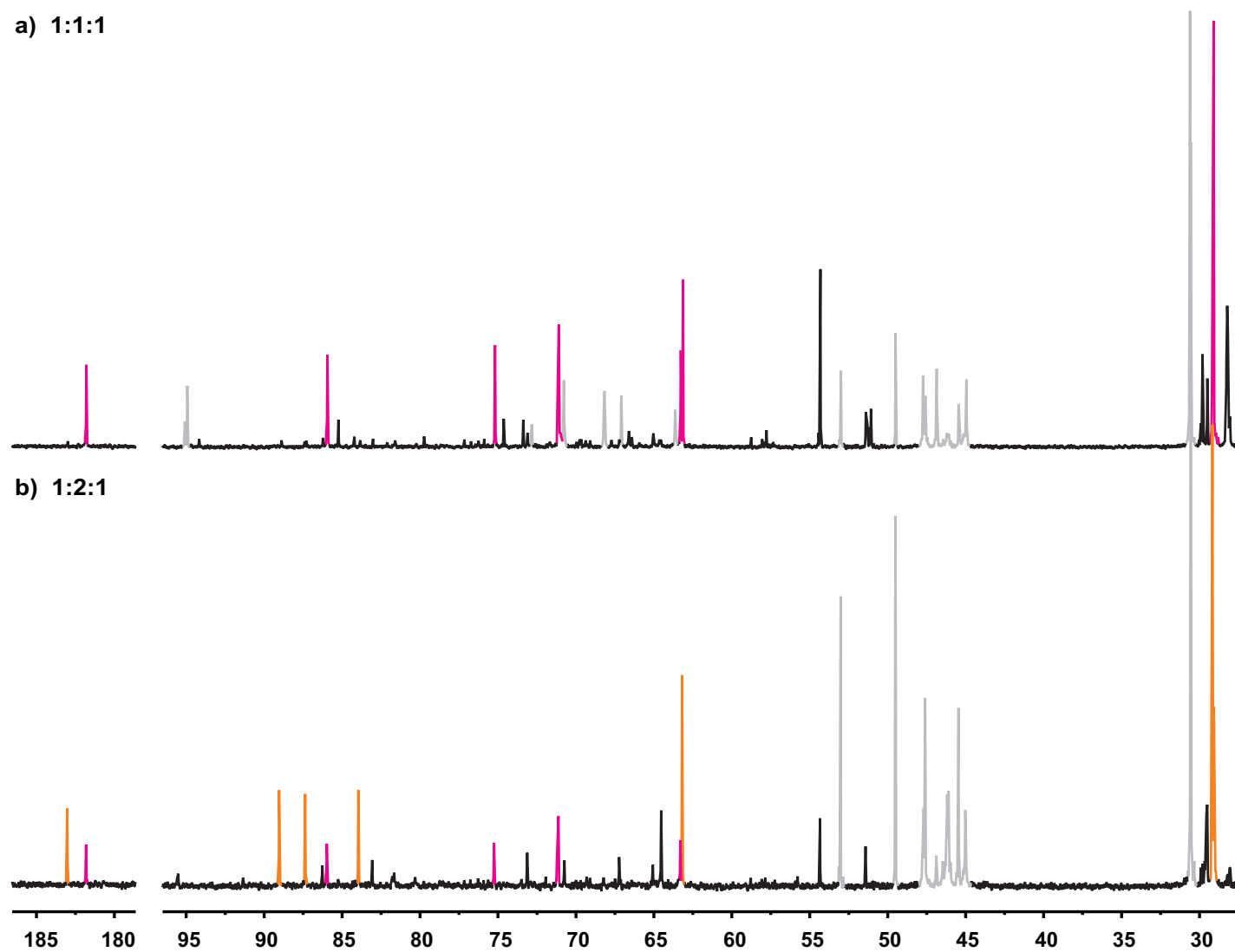


Figure A.9. Resulting $^{13}\text{C}\{^1\text{H}\}$ NMR spectra for the treatment of D-Lyx1NtBu with Pd-en and iodic acid in the molar ratios a) 1:1:1 and b) 1:2:1 after 3 h at 4°C in D_2O . Magenta: D-Lyxa1NtBu2H₋₁, orange: D-Lyxa1NtBu2,3,4H₋₃, grey: D-lyxose, Pd-en, *t*BuNH₂ and MeOH.

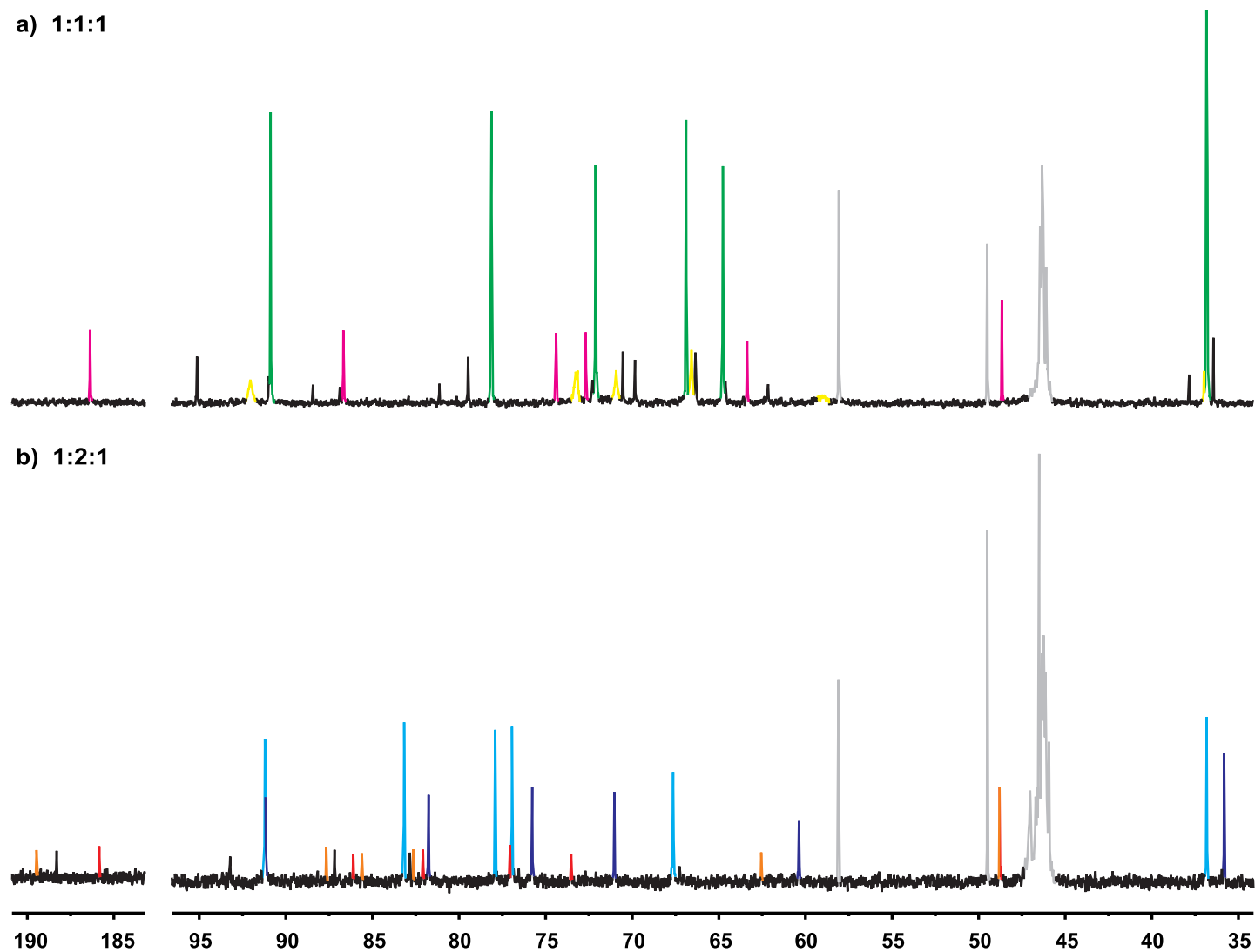


Figure A.10. Resulting $^{13}\text{C}\{^1\text{H}\}$ NMR spectra for the treatment of D-Rib1NMe with Pd-en and iodic acid in the molar ratios a) 1:1:1 and b) 1:2:1 after 3 h at 4 °C in D_2O . Green: $^4\text{C}_1$ - β -D-Ribp1NMe2H $_{-1}$, yellow: $^4\text{C}_1$ - α -D-Ribp1NMe2H $_{-1}$ - $\kappa^2\text{N}^1,\text{O}^2$, magenta: D-Riba1NMe2H $_{-1}$ - $\kappa^2\text{N}^1,\text{O}^2$, cyan: $^4\text{C}_1$ - β -D-Ribp1NMe2,3,4H $_{-3}$, purple: α -D-Ribp1NMe2,3,4H $_{-3}$, orange: D-Riba1NMe2,3,4H $_{-3}$, red: D-Riba1NMe2,4,5H $_{-3}$, grey: Pd-en, EtOH and MeOH.

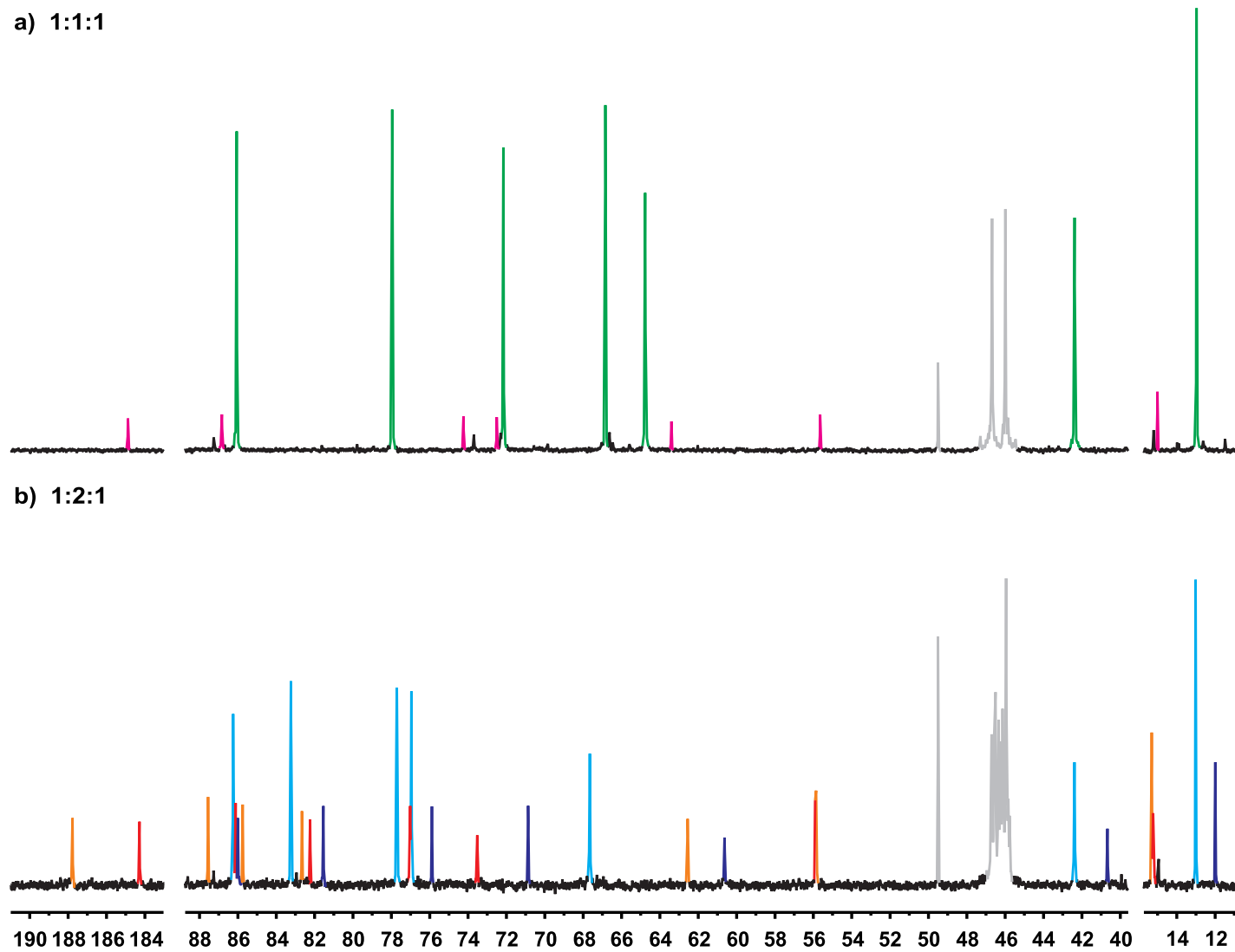


Figure A.11. Resulting $^{13}\text{C}\{^1\text{H}\}$ NMR spectra for the treatment of D-Rib1NEt with Pd-en and iodic acid in the molar ratios a) 1:1:1 and b) 1:2:1 after 3 h at 4°C in D_2O . Green: $^4\text{C}_1$ - β -D-Ribp1NEt2H $_{-1}$, magenta: D-Riba1NEt2H $_{-1}$ - $\kappa^2\text{N}^1, \text{O}^2$, cyan: $^4\text{C}_1$ - β -D-Ribp1NEt2,3,4H $_{-3}$, orange: D-Riba1NEt2,3,4H $_{-3}$, red: D-Riba1NEt2,4,5H $_{-3}$, purple: α -D-Ribp1NEt2,3,4H $_{-3}$, grey: Pd-en and MeOH.

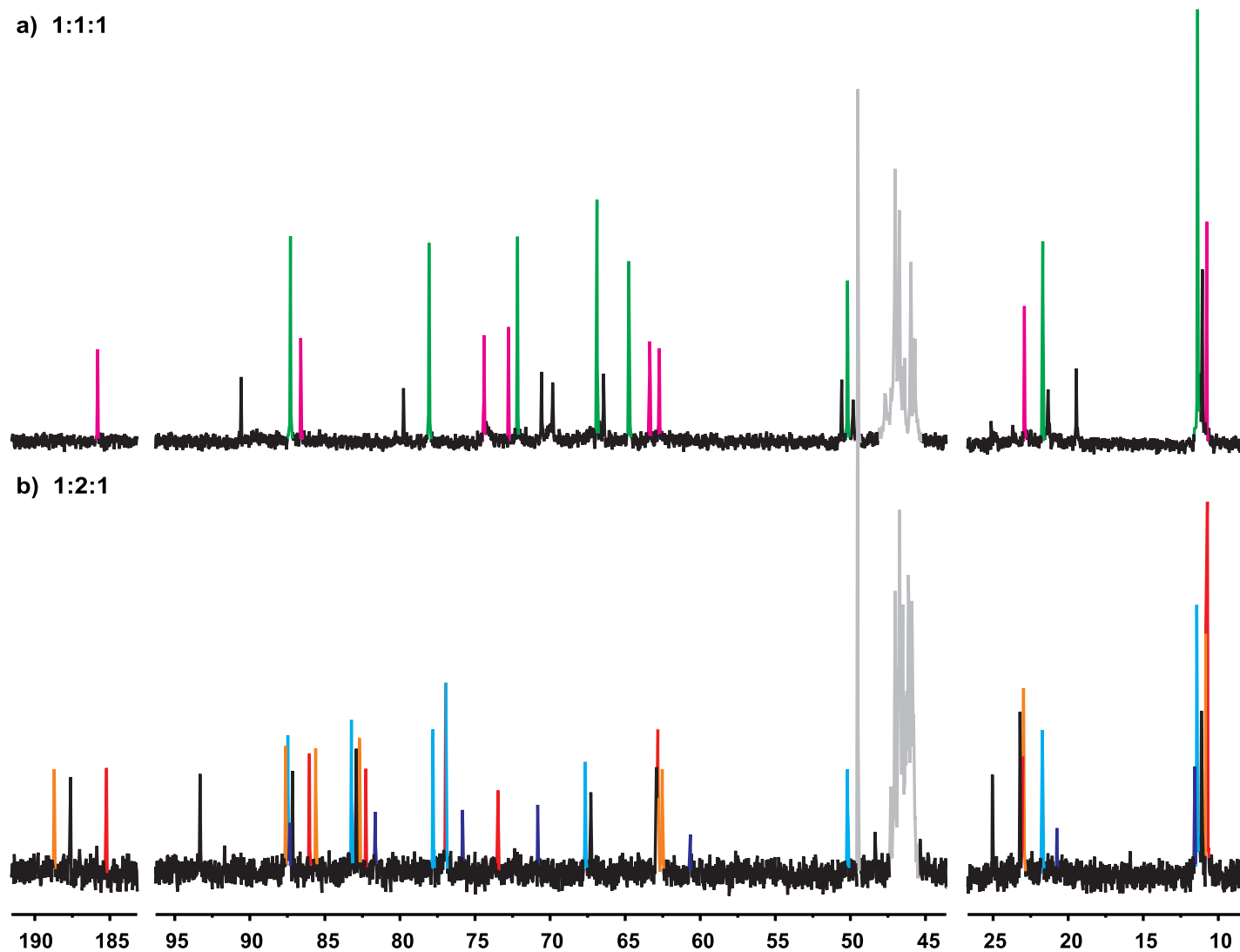


Figure A.12. Resulting $^{13}\text{C}\{^1\text{H}\}$ NMR spectra for the treatment of D-Rib1NPr with Pd-en and iodic acid in the molar ratios a) 1:1:1 and b) 1:2:1 after 3 h at 4°C in D_2O . Green: $^4\text{C}_1$ - β -D-Ribp1NPr2H $_{-1}$, magenta: D-Riba1NPr2H $_{-1}$ - $\kappa^2\text{N}^1, \text{O}^2$, cyan: $^4\text{C}_1$ - β -D-Ribp1NPr2,3,4H $_{-3}$, orange: D-Riba1NPr2,3,4H $_{-3}$, red: D-Riba1NPr2,4,5H $_{-3}$, purple: α -D-Ribp1NPr2,3,4H $_{-3}$, grey: Pd-en and MeOH.

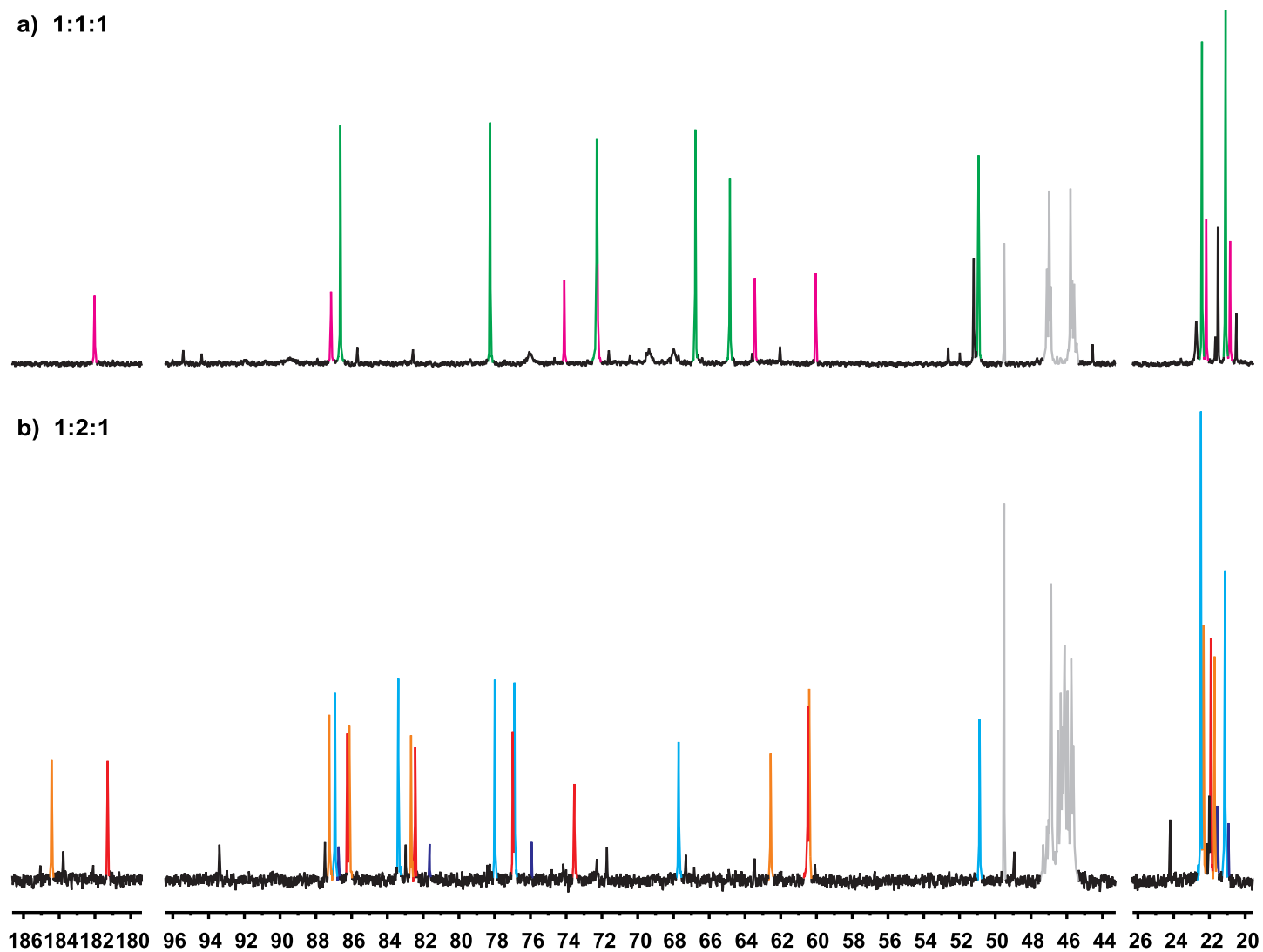


Figure A.13. Resulting $^{13}\text{C}\{^1\text{H}\}$ NMR spectra for the treatment of D-Rib1NiPr with Pd-en and iodic acid in the molar ratios a) 1:1:1 and b) 1:2:1 after 3h at 4°C in D_2O . Green: $^4\text{C}_1\text{-}\beta\text{-D-Ribp1NiPr2H}_{-1}$, magenta: D-Riba1NiPr2H₋₁- $\kappa^2\text{N}^1,\text{O}^2$, cyan: $^4\text{C}_1\text{-}\beta\text{-D-Ribp1NiPr2,3,4H}_{-3}$, orange: D-Riba1NiPr2,3,4H₋₃, red: D-Riba1NiPr2,4,5H₋₃, purple: $\alpha\text{-D-Ribp1NiPr2,3,4H}_{-3}$, grey: Pd-en and MeOH.

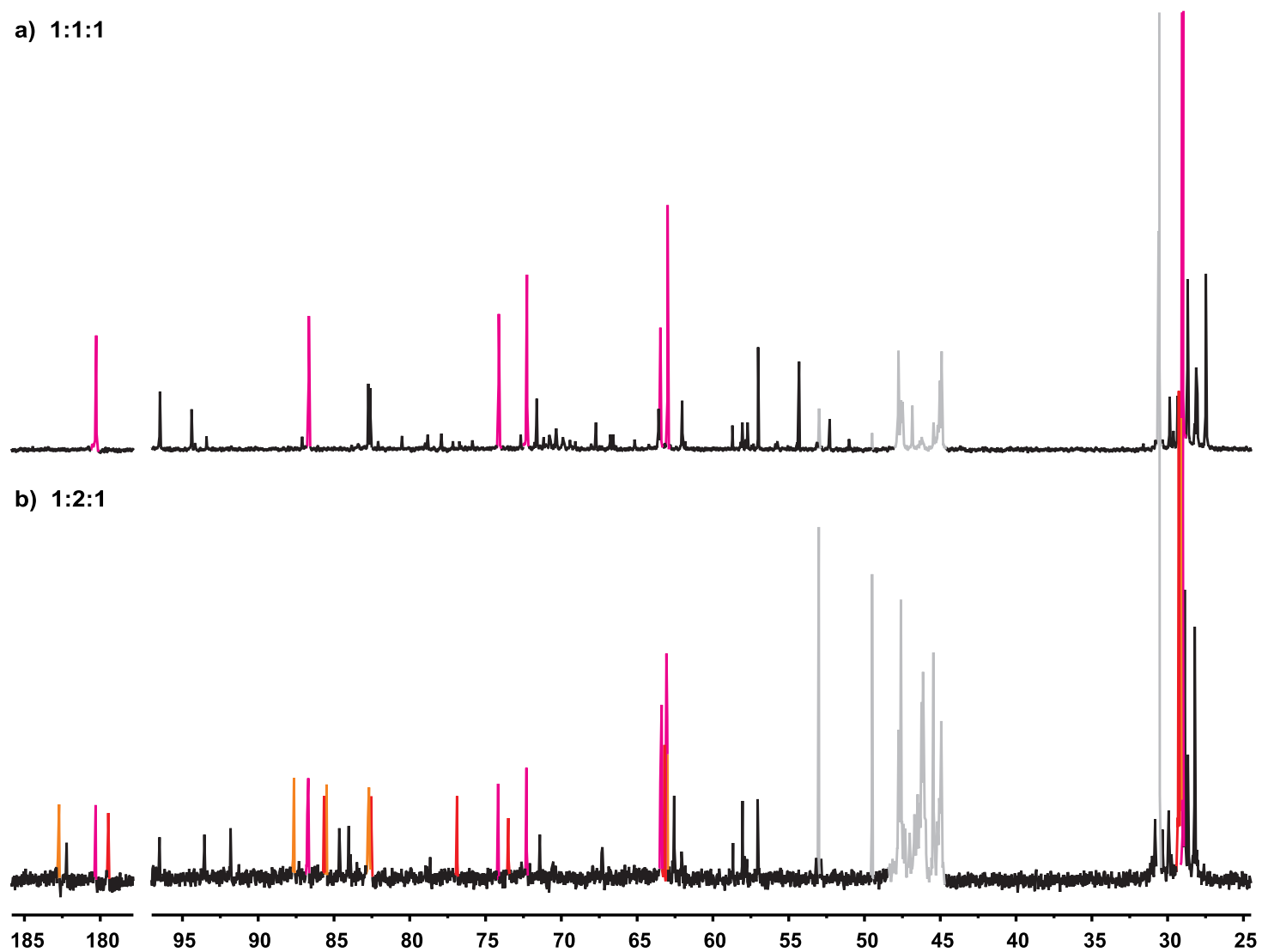


Figure A.14. Resulting $^{13}\text{C}\{^1\text{H}\}$ NMR spectra for the treatment of D-Rib1N*t*Bu with Pd-en and iodic acid in the molar ratios a) 1:1:1 and b) 1:2:1 after 3 h at 4 °C in D₂O. Magenta: D-Rib1N*t*Bu2H₋₁-κ²N¹,O², orange: D-Rib1N*t*Bu2,3,4H₋₃, red: D-Rib1N*t*Bu2,4,5H₋₃, grey: Pd-en, *t*BuNH₂ and MeOH.

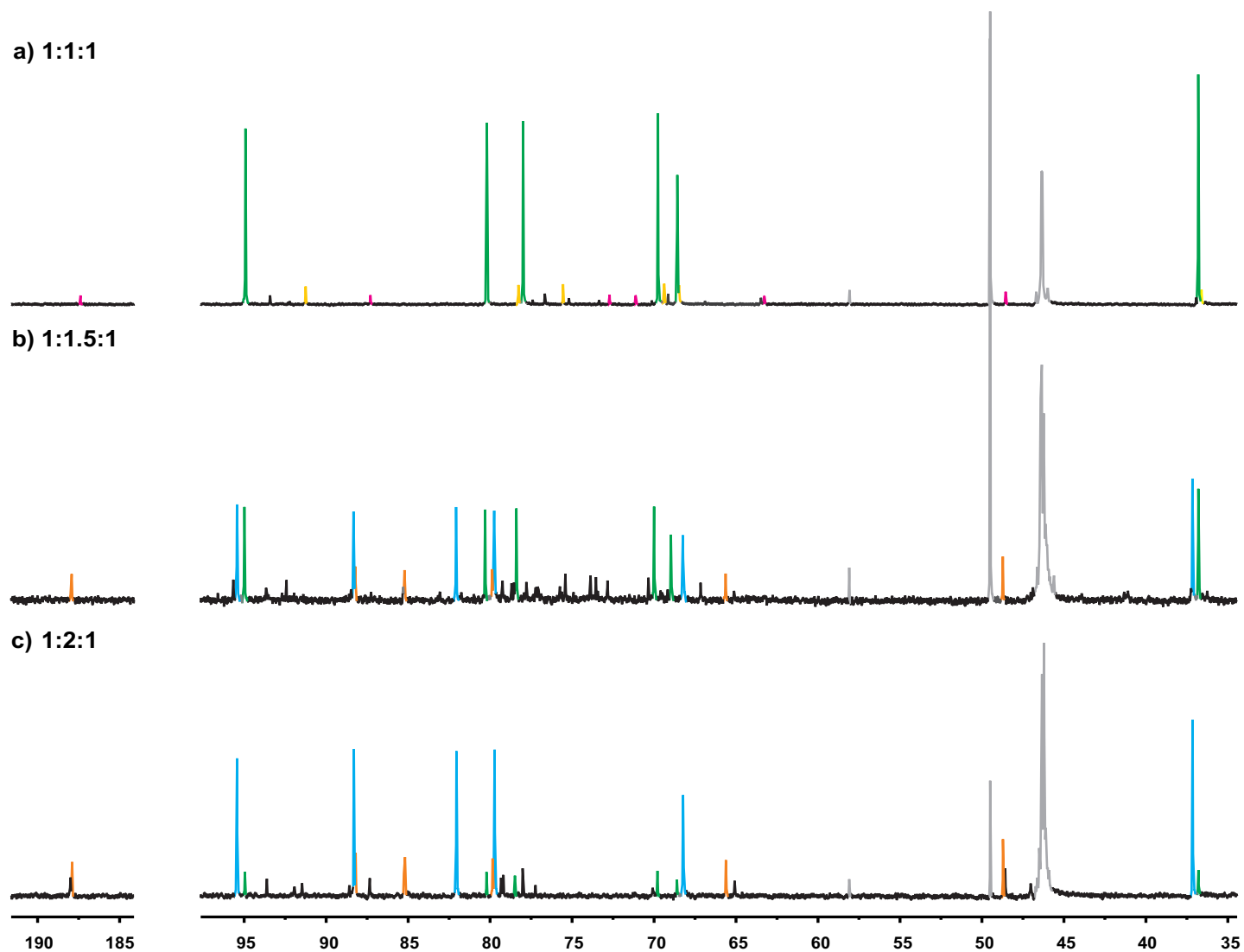


Figure A.15. Resulting $^{13}\text{C}\{^1\text{H}\}$ NMR spectra for the treatment of D-Xyl1NMe with Pd-en and iodic acid in the molar ratios a) 1:1:1, b) 1:1.5:1 and c) 1:2:1 after 3 h at 4°C in D_2O . Green: $^4\text{C}_1\text{-}\beta\text{-D-Xylp1NMe2H}_{-1}$, yellow: $\alpha\text{-D-Xylp1NMe2H}_{-1}$, magenta: D-Xyla1NMe2H_{-1} , cyan: $^4\text{C}_1\text{-}\beta\text{-D-Xylp1NMe2,3,4H}_{-3}$, orange: $\text{D-Xyla1NMe2,3,4H}_{-3}$, grey: Pd-en, EtOH and MeOH.

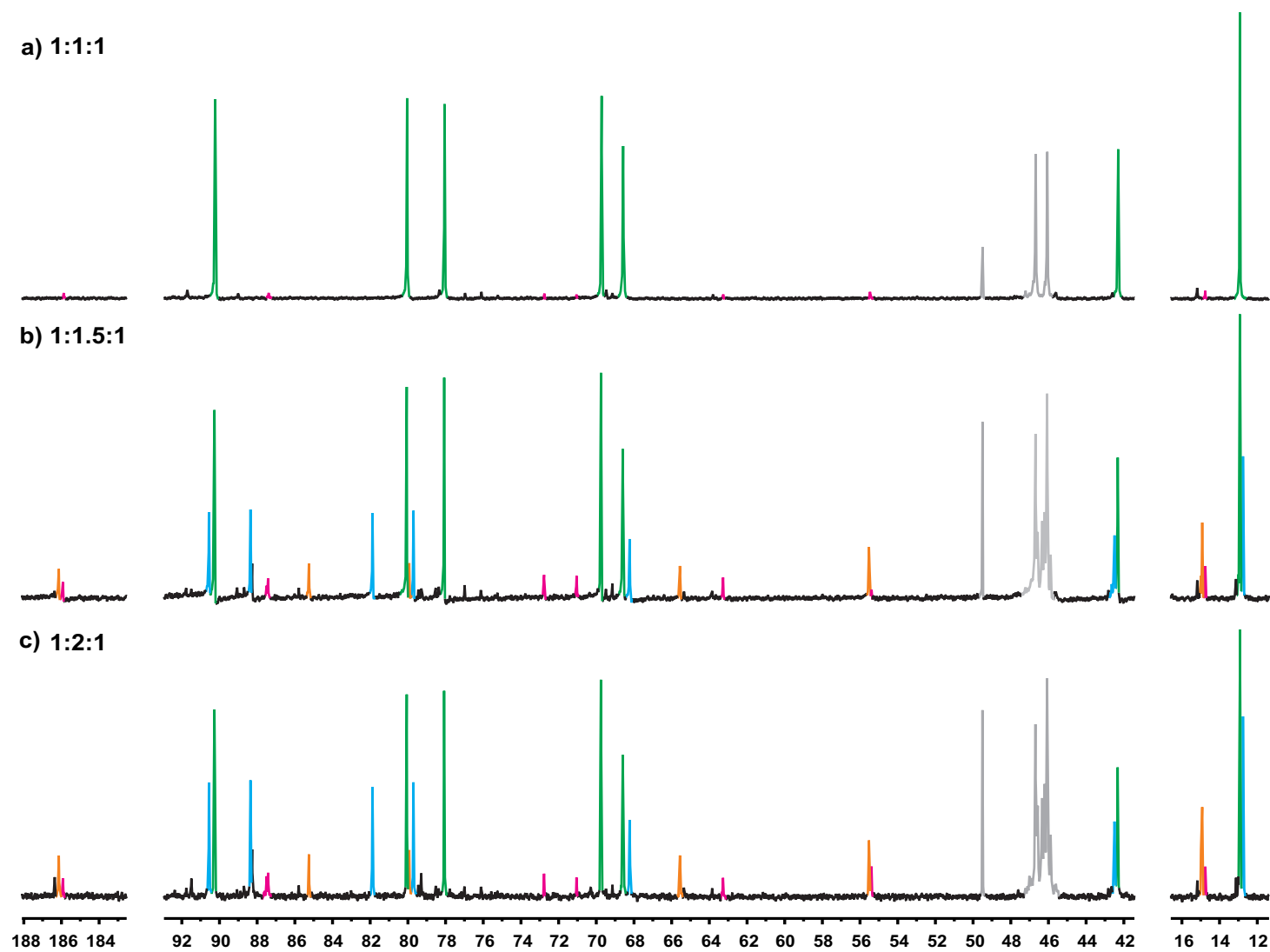


Figure A.16. Resulting $^{13}\text{C}\{^1\text{H}\}$ NMR spectra for the treatment of D-Xyl1NEt with Pd-en and iodic acid in the molar ratios a) 1:1:1, b) 1:1.5:1 and c) 1:2:1 after 3 h at 4 °C in D_2O . Green: $^4\text{C}_1$ - β -D-Xylp1NEt2H $_{-1}$, magenta: D-Xyla1NEt2H $_{-1}$, cyan: $^4\text{C}_1$ - β -D-Xylp1NEt2,3,4H $_{-3}$, orange: D-Xyla1NEt2,3,4H $_{-3}$, grey: Pd-en and MeOH.

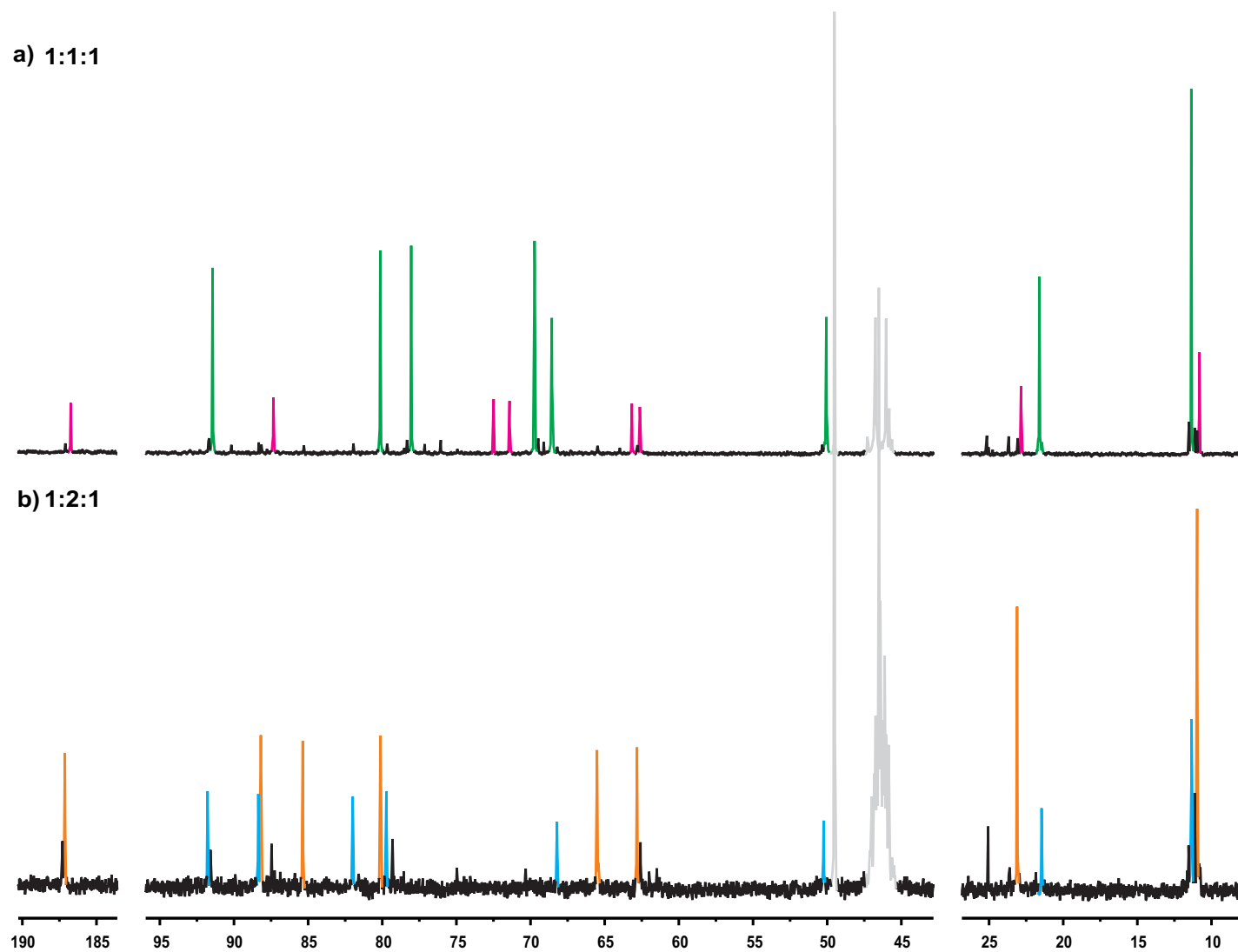


Figure A.17. Resulting $^{13}\text{C}\{^1\text{H}\}$ NMR spectra for the treatment of D-Xyl1NPr with Pd-en and iodic acid in the molar ratios a) 1:1:1 and b) 1:2:1 after 3 h at 4°C in D_2O . Green: $^4\text{C}_1$ - β -D-Xylp1NPr2H $_{-1}$, magenta: D-Xyla1NPr2H $_{-1}$, orange: D-Xyla1NPr2,3,4H $_{-3}$, cyan: $^4\text{C}_1$ - β -D-Xylp1NPr2,3,4H $_{-3}$, grey: Pd-en and MeOH.

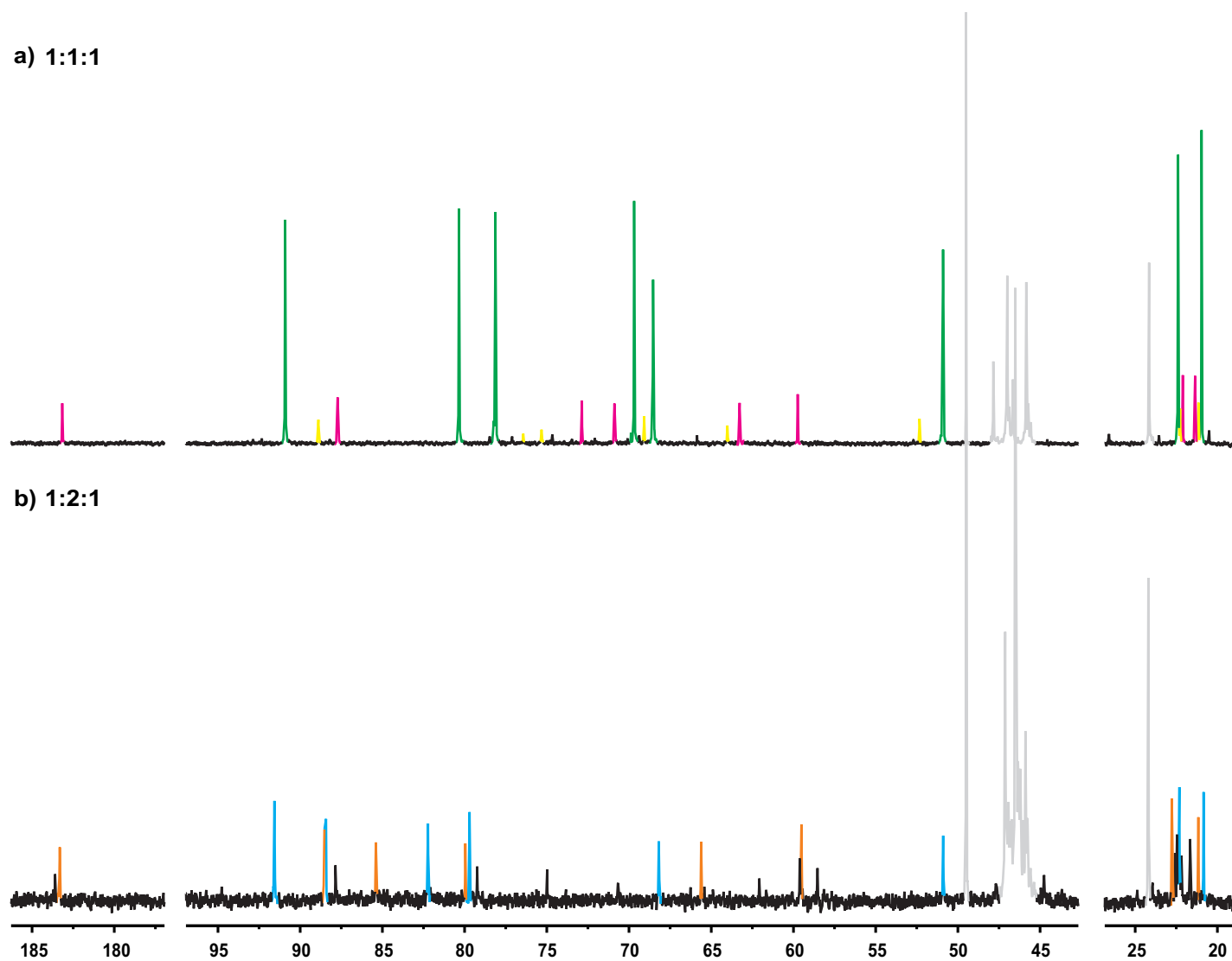


Figure A.18. Resulting $^{13}\text{C}\{^1\text{H}\}$ NMR spectra for the treatment of D-Xyl1NiPr with Pd-en and iodic acid in the molar ratios a) 1:1:1 and b) 1:2:1 after 3 h at 4 °C in D_2O . Green: $^4\text{C}_1\text{-}\beta\text{-D-Xylp1NiPr2H}_{-1}$, magenta: D-Xyla1NiPr2H₋₁, orange: D-Xyla1NiPr2,3,4H₋₃, cyan: $^4\text{C}_1\text{-}\beta\text{-D-Xylp1NiPr2,3,4H}_{-3}$, grey: Pd-en, *i*PrNH₂ and MeOH.

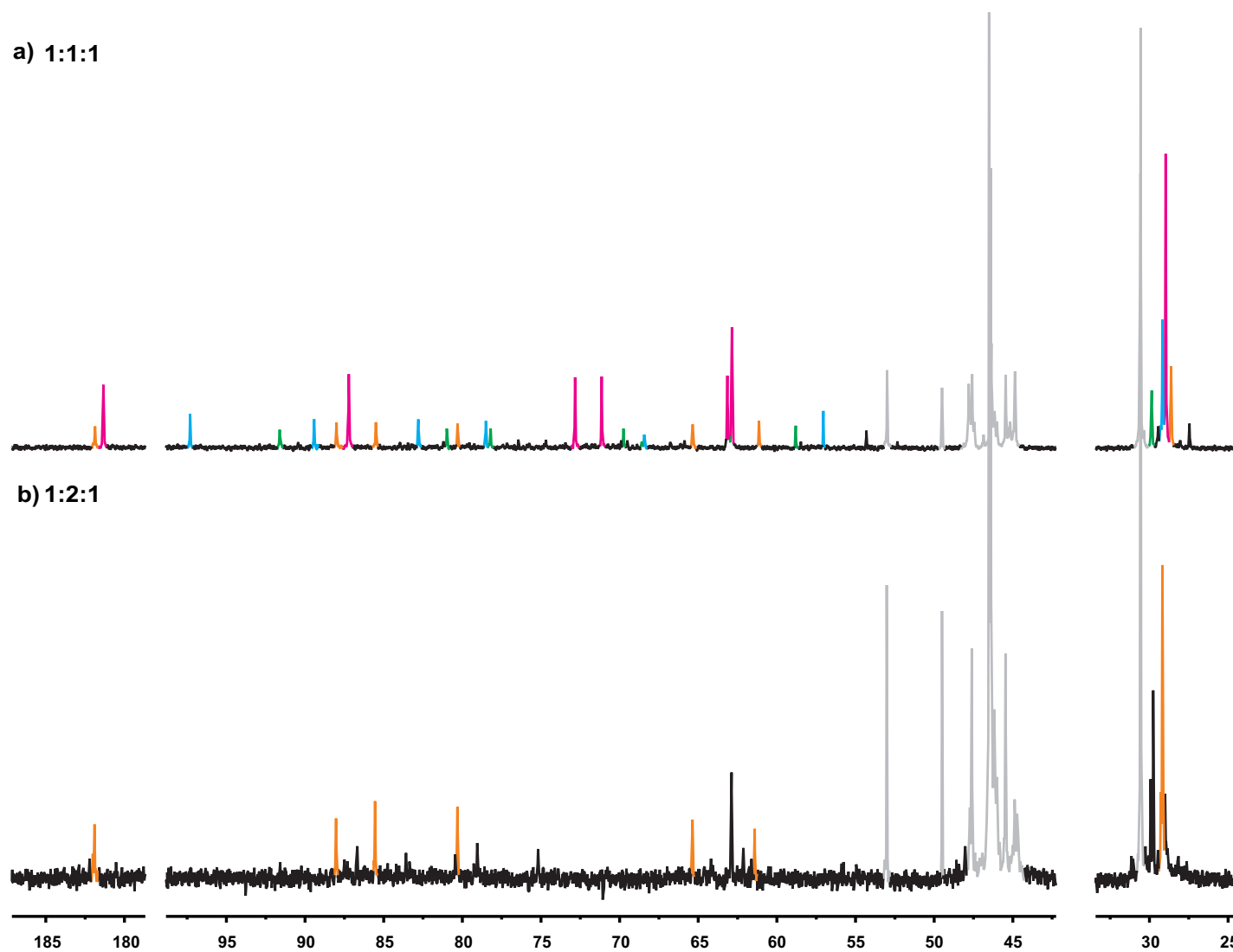


Figure A.19. Resulting $^{13}\text{C}\{^1\text{H}\}$ NMR spectra for the treatment of D-Xyl1N*t*Bu with Pd-en and iodic acid in the molar ratios a) 1:1:1 and b) 1:2:1 after 3 h at 4 °C in D₂O. Green: $^4\text{C}_1$ -β-D-Xylp1N*t*Bu2H₋₁, magenta: D-Xyla1N*t*Bu2H₋₁, orange: D-Xyla1N*t*Bu2,3,4H₋₃, cyan: $^4\text{C}_1$ -β-D-Xylp1N*t*Bu2,3,4H₋₃, grey: Pd-en, *t*BuNH₂ and MeOH.

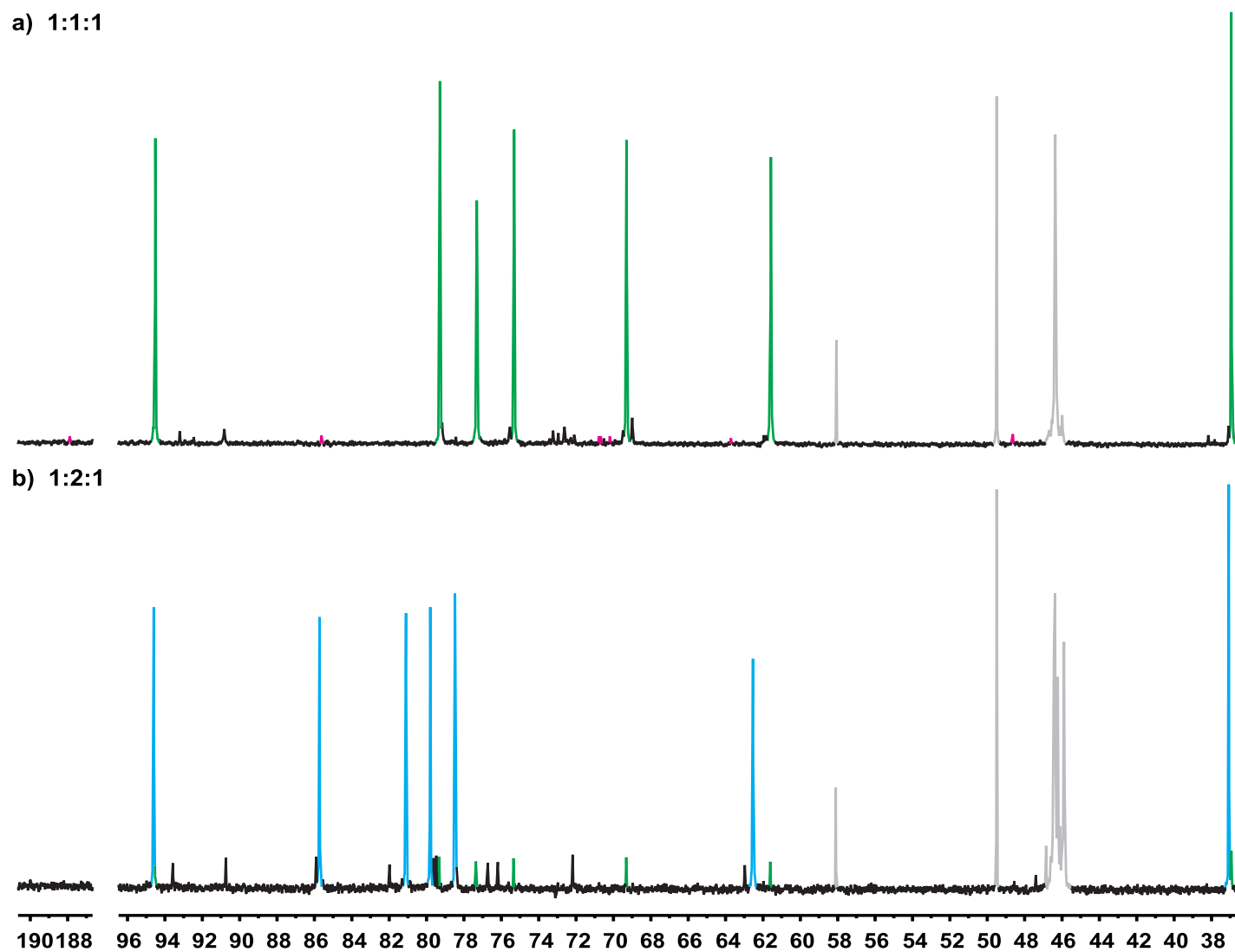


Figure A.20. Resulting $^{13}\text{C}\{^1\text{H}\}$ NMR spectra for the treatment of D-Gal1NMe with Pd-en and iodic acid in the molar ratios a) 1:1:1 and b) 1:2:1 after 3 h at 4 °C in D_2O . Green: β -D-Galp1NMe2H₋₁, magenta: D-Gala1NMe2H₋₁, cyan: β -D-Galp1NMe2,3,4H₋₃, grey: Pd-en, EtOH and MeOH.

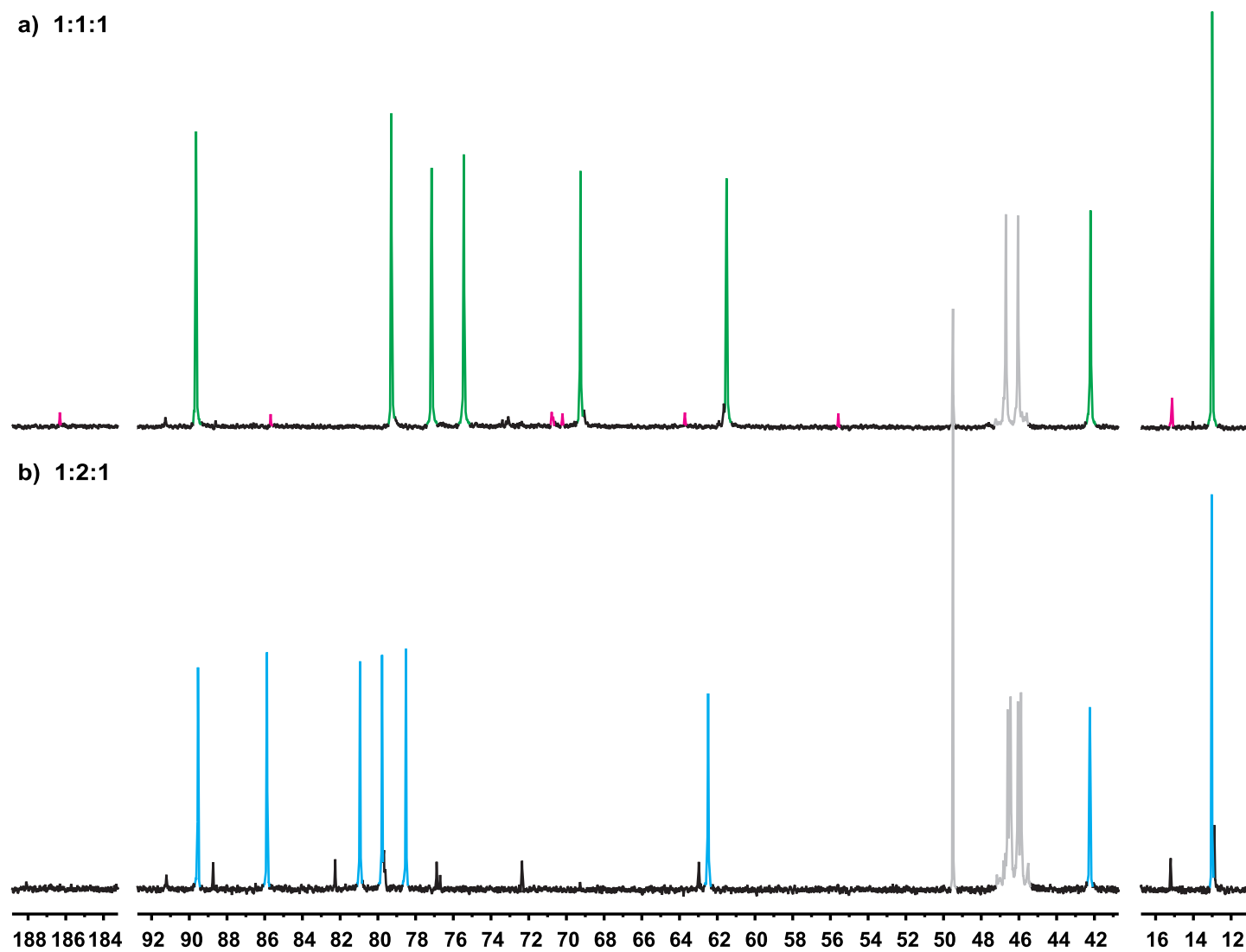


Figure A.21. Resulting $^{13}\text{C}\{^1\text{H}\}$ NMR spectra for the treatment of D-Gal1NEt with Pd-en and iodic acid in the molar ratios a) 1:1:1 and b) 1:2:1 after 3 h at 4 °C in D_2O . Green: $\beta\text{-D-Galp1NEt2H}_{-1}$, magenta: $\text{D-Gal}\alpha\text{1NEt2H}_{-1}$, cyan: $\beta\text{-D-Galp1NEt2,3,4H}_{-3}$, grey: Pd-en and MeOH.

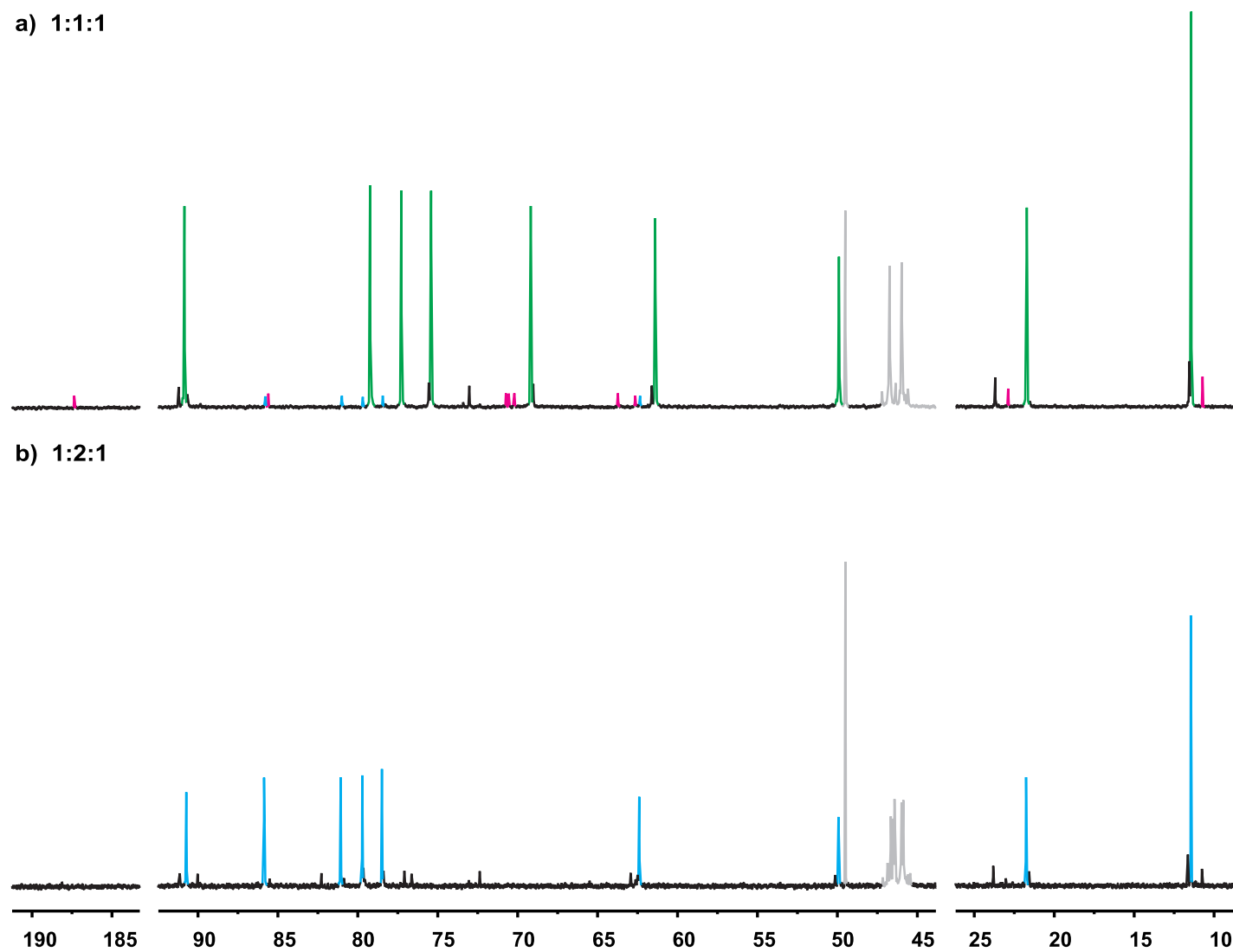


Figure A.22. Resulting $^{13}\text{C}\{^1\text{H}\}$ NMR spectra for the treatment of D-Gal1NPr with Pd-en and iodic acid in the molar ratios a) 1:1:1 and b) 1:2:1 after 3 h at 4 °C in D_2O . Green: $\beta\text{-D-Galp1NPr2H}_{-1}$, magenta: D-Gala1NPr2H_{-1} , cyan: $\beta\text{-D-Galp1NPr2,3,4H}_{-3}$, grey: Pd-en and MeOH.

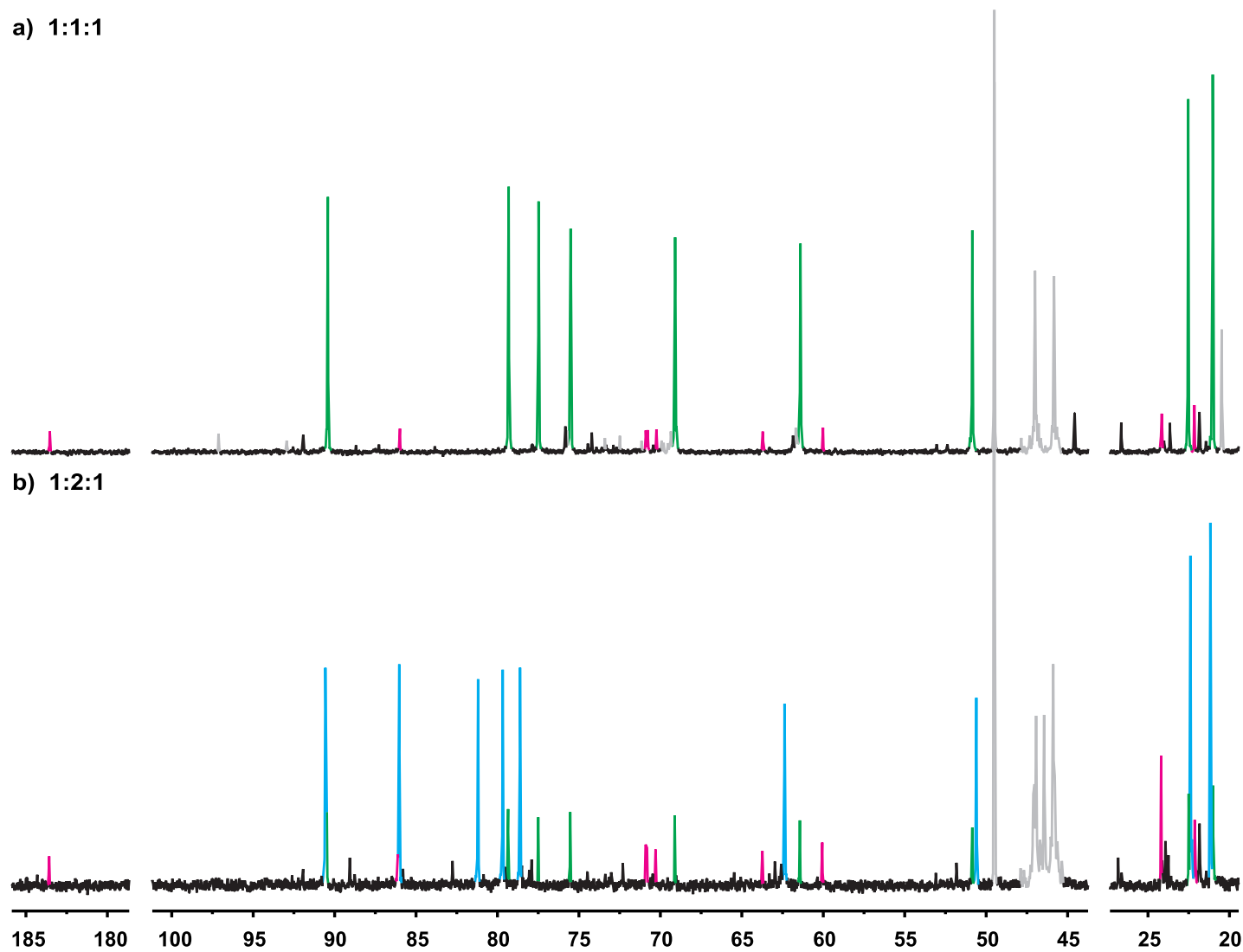


Figure A.23. Resulting $^{13}\text{C}\{^1\text{H}\}$ NMR spectra for the treatment of D-Galp1NiPr with Pd-en and iodic acid in the molar ratios a) 1:1:1 and b) 1:2:1 after 3 h at 4 °C in D_2O . Green: β -D-Galp1NiPr2H₋₁, magenta: D-Gal α 1NiPr2H₋₁, cyan: $^4\text{C}_1$ - β -D-Galp1NiPr2,3,4H₋₃, grey: Pd-en, *i*PrNH₂ and MeOH.

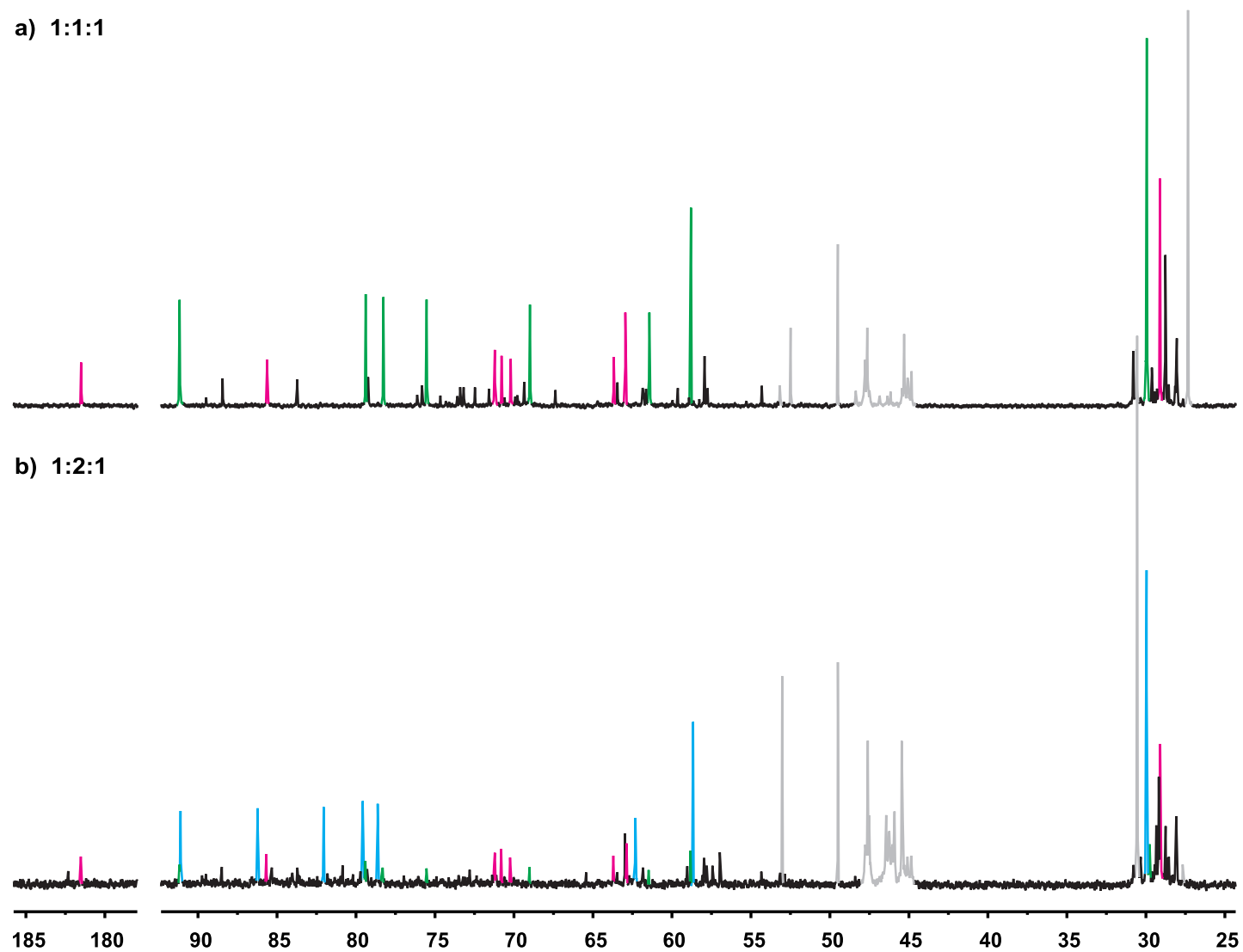


Figure A.24. Resulting $^{13}\text{C}\{^1\text{H}\}$ NMR spectra for the treatment of D-Galp1NtBu with Pd-en and iodic acid in the molar ratios a) 1:1:1 and b) 1:2:1 after 3 h at 4 °C in D_2O . Green: $\beta\text{-D-Galp1NtBu2H}_{-1}$, magenta: $\text{D-Gal}\alpha\text{1NtBu2H}_{-1}$, cyan: $^4\text{C}_1\text{-}\beta\text{-D-Galp1NtBu2,3,4H}_{-3}$, grey: Pd-en, $t\text{BuNH}_2$ and MeOH.

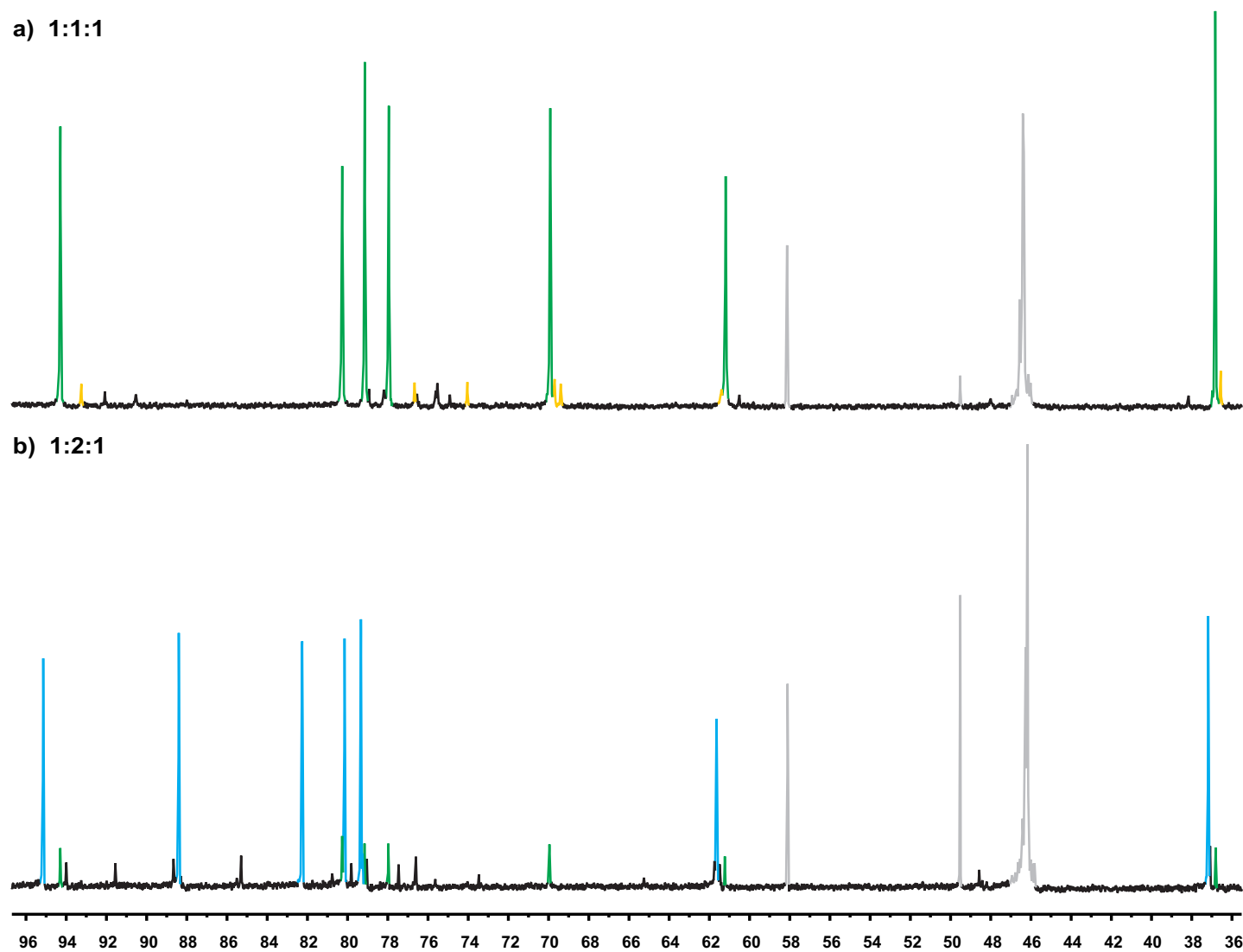


Figure A.25. Resulting $^{13}\text{C}\{^1\text{H}\}$ NMR spectra for the treatment of D-Glc1NMe with Pd-en and iodic acid in the molar ratios a) 1:1:1 and b) 1:2:1 after 3 h at 4 °C in D_2O . Green: β -D-Glc p1NMe₂H₋₁, yellow: α -D-Glc p1NMe₂H₋₁, cyan: β -D-Glc p1NMe_{2,3,4}H₋₃, grey: Pd-en, EtOH and MeOH.

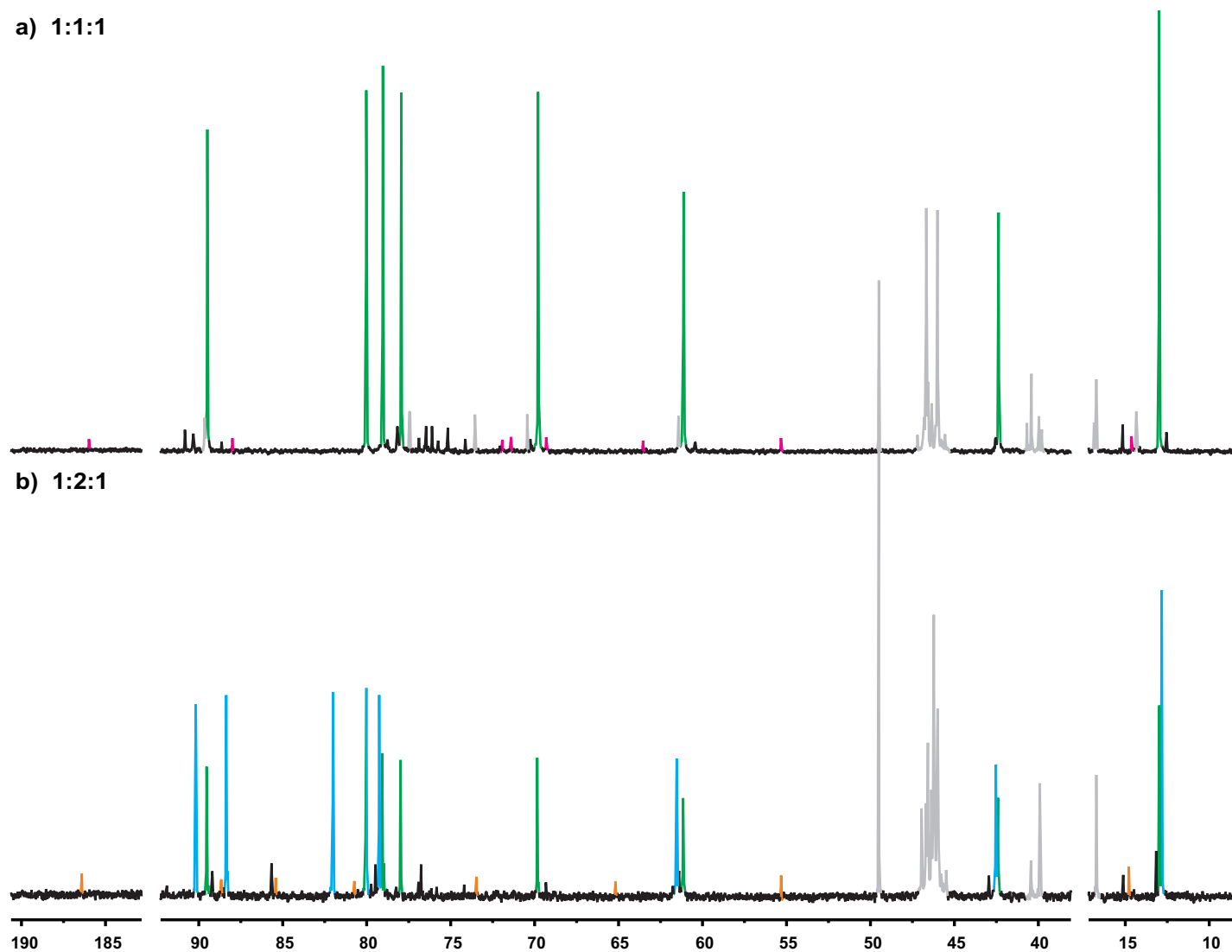


Figure A.26. Resulting $^{13}\text{C}\{^1\text{H}\}$ NMR spectra for the treatment of D-Glc1NEt with Pd-en and iodic acid in the molar ratios a) 1:1:1 and b) 1:2:1 after 3 h at 4 °C in D_2O . Green: $\beta\text{-D-Glcp1NEt2H}_{-1}$, magenta: D-Glca1NEt2H_{-1} , cyan: $\beta\text{-D-Glcp1NEt2,3,4H}_{-3}$, orange: $\text{D-Glca1NMe2,3,4H}_{-3}$, grey: D-Glc1NEt, Pd-en and MeOH.

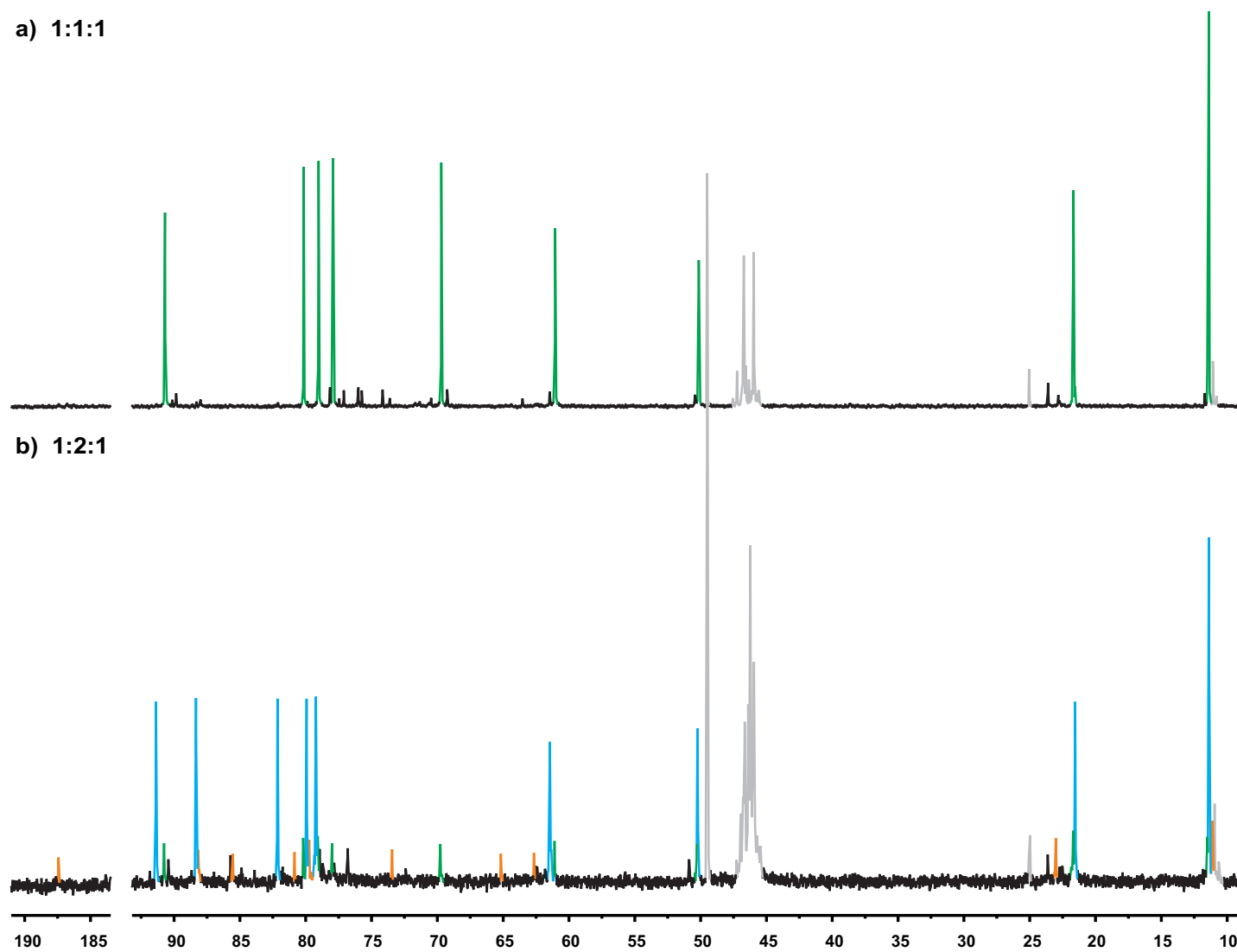


Figure A.27. Resulting $^{13}\text{C}\{^1\text{H}\}$ NMR spectra for the treatment of D-Glc1NPr with Pd-en and iodic acid in the molar ratios a) 1:1:1 and b) 1:2:1 after 3 h at 4 °C in D₂O. Green: $\beta\text{-D-Glcp1NPr2H}_{-1}$, cyan: $\beta\text{-D-Glcp1NPr2,3,4H}_{-3}$, orange: $\text{D-Glca1NEt2,3,4H}_{-3}$, grey: Pd-en, PrNH₂ and MeOH.

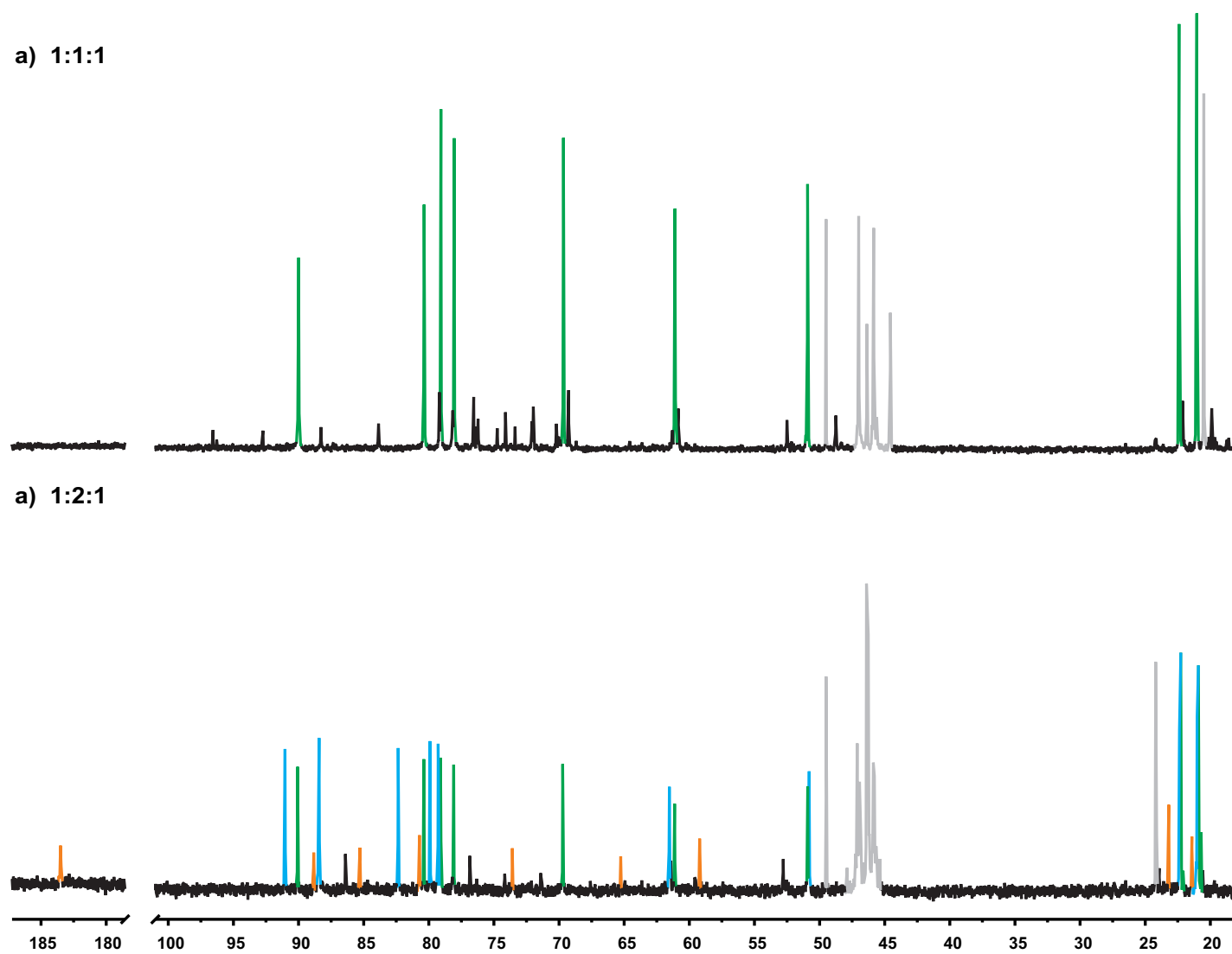


Figure A.28. Resulting $^{13}\text{C}\{^1\text{H}\}$ NMR spectra for the treatment of D-Glc1NiPr with Pd-en and iodic acid in the molar ratios a) 1:1:1 and b) 1:2:1 after 3 h at 4 °C in D_2O . Green: $\beta\text{-D-Glcp1NiPr2H}_{-1}$, cyan: $\beta\text{-D-Glcp1NiPr2,3,4H}_{-3}$, orange: $\text{D-Glca1NiPr2,3,4H}_{-3}$, grey: Pd-en, $i\text{PrNH}_2$ and MeOH.

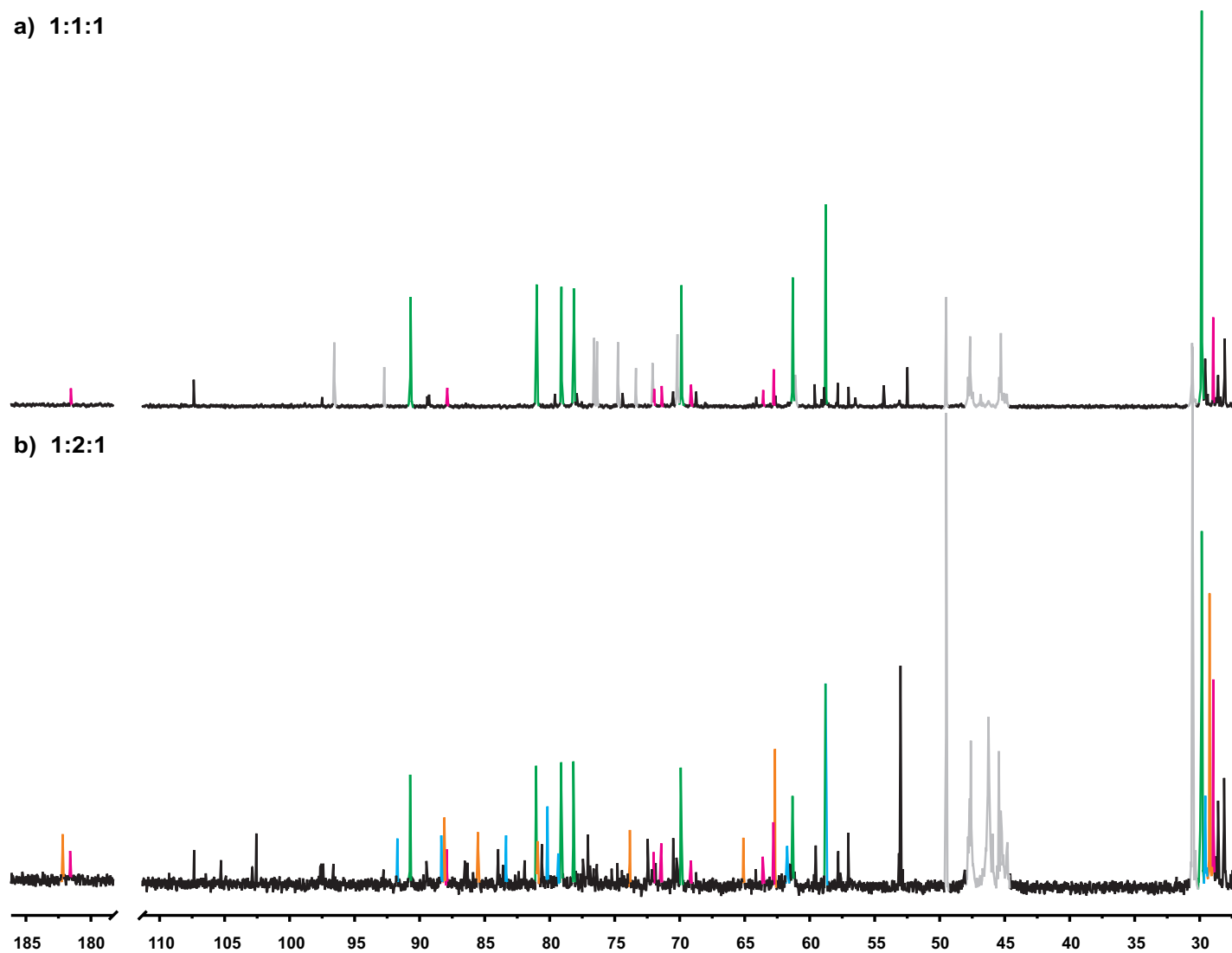


Figure A.29. Resulting $^{13}\text{C}\{^1\text{H}\}$ NMR spectra for the treatment of D-Glc1NtBu with Pd-en and iodic acid in the molar ratios a) 1:1:1 and b) 1:2:1 after 3 h at 4 °C in D_2O . Green: β -D-Glcp1NtBu2H₋₁, magenta: D-Glca1NtBu2H₋₁, orange: D-Glca1NtBu2,3,4H₋₃, cyan: β -D-Glcp1NtBu2,3,4H₋₃, grey: Pd-en, D-glucose, tBuNH₂ and MeOH.

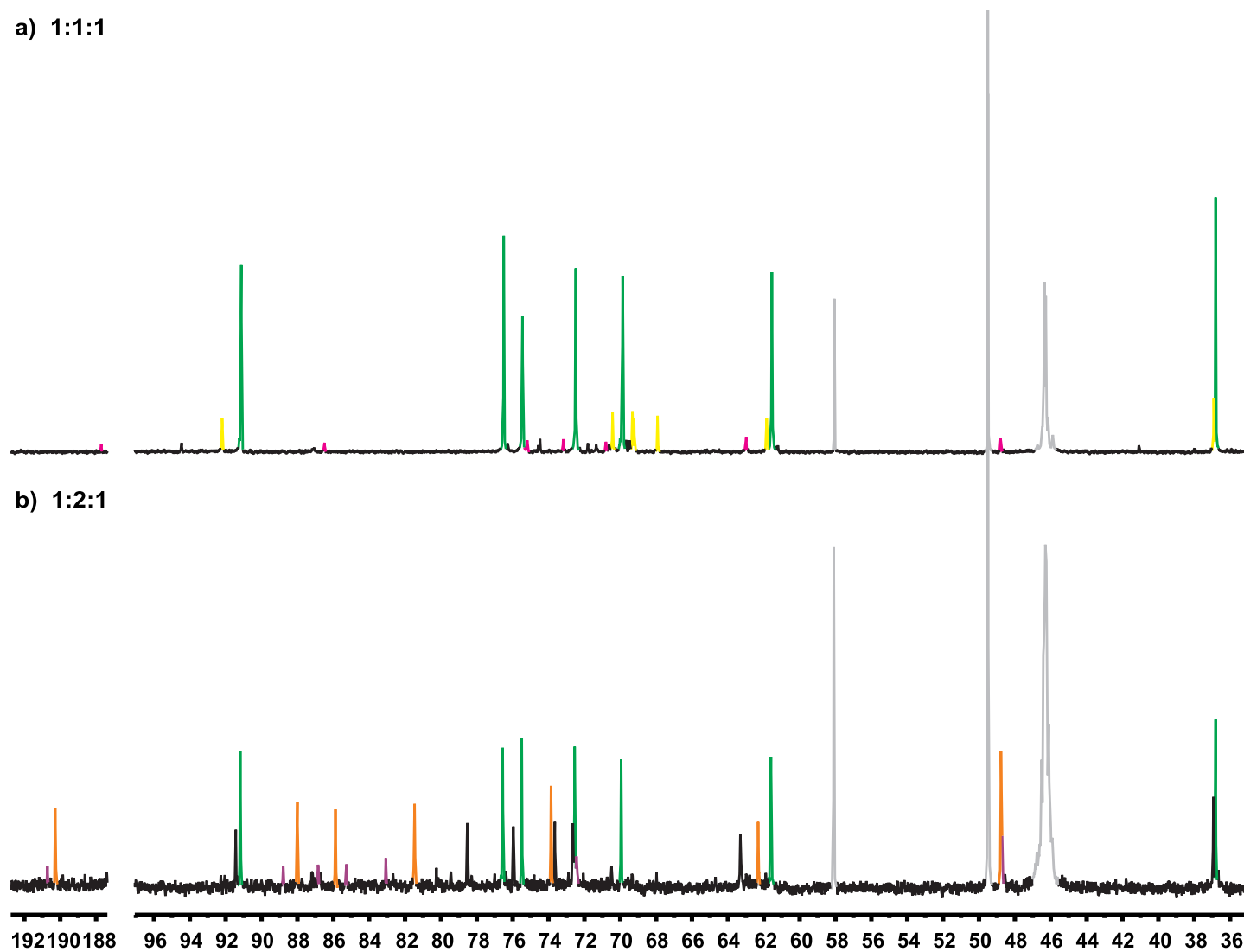


Figure A.30. Resulting $^{13}\text{C}\{^1\text{H}\}$ NMR spectra for the treatment of D-Gul1NMe with Pd-en and iodic acid in the molar ratios a) 1:1:1 and b) 1:2:1 after 3 h at 4 °C in D_2O . Green: $\beta\text{-D-Galp1NMe2H}_{-1}$, yellow: $^1\text{C}_4\text{-}\alpha\text{-D-Gulp1NMe2H}_{-1}$, magenta: D-Gula1NMe2H_{-1} , orange: $\text{L-Gula1NMe2,3,4H}_{-3}$, purple: $\text{L-Gula1NMe2,3,4,5,6H}_{-5}$, grey: Pd-en, EtOH and MeOH.

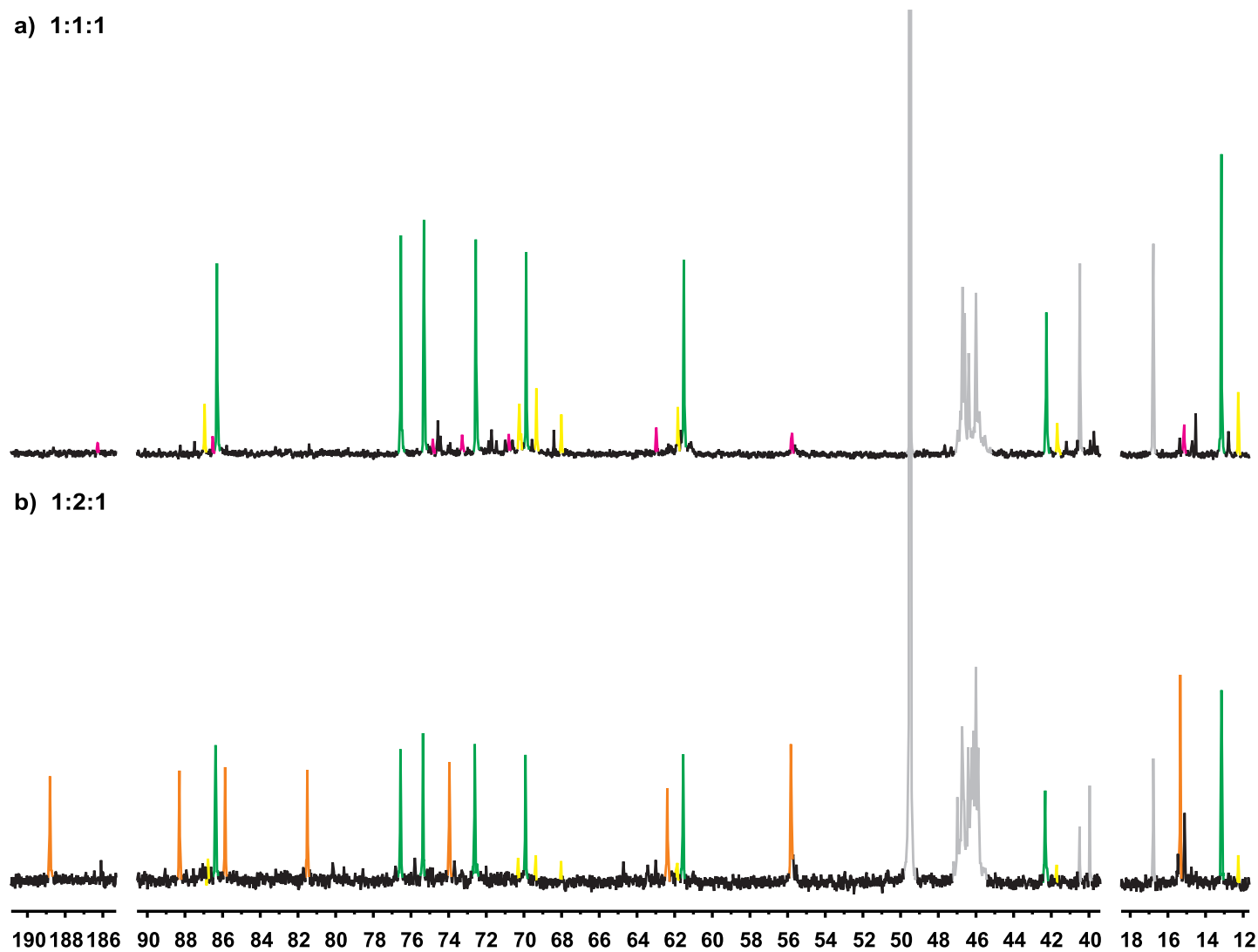


Figure A.31. Resulting $^{13}\text{C}\{^1\text{H}\}$ NMR spectra for the treatment of D-Gul1NEt with Pd-en and iodic acid in the molar ratios a) 1:1:1 and b) 1:2:1 after 3 h at 4 °C in D_2O . Green: $^1\text{C}_4$ - β -D-Gulp1NEt2H $_{-1}$, yellow: $^1\text{C}_4$ - α -D-Gulp1NEt2H $_{-1}$, magenta: D-Gula1NEt2H $_{-1}$, orange: L-Gula1NEt2,3,4H $_{-3}$, grey: Pd-en and MeOH.

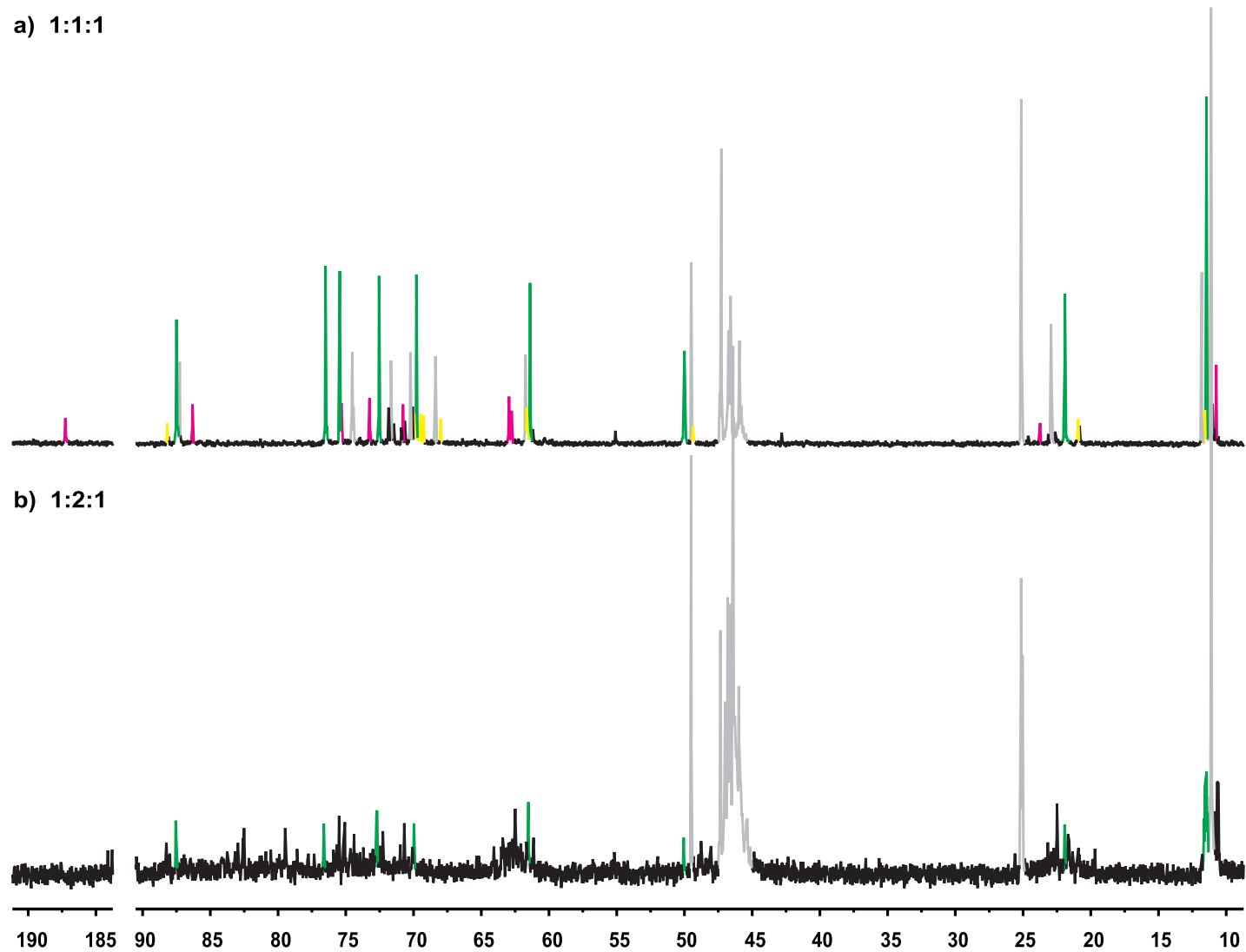


Figure A.32. Resulting $^{13}\text{C}\{^1\text{H}\}$ NMR spectra for the treatment of D-Gul1NPr with Pd-en and iodic acid in the molar ratios a) 1:1:1 and b) 1:2:1 after 3 h at 4°C in D_2O . Green: $^1\text{C}_4$ - β -D-Gulp1NPr2H $_{-1}$, yellow: $^1\text{C}_4$ - α -D-Gulp1NPr2H $_{-1}$, magenta: D-Gula1NPr2H $_{-1}$, yellow: $^1\text{C}_4$ - α -D-Gulp1NPr2H $_{-1}$, grey: D-Gul1NPr, Pd-en and MeOH.

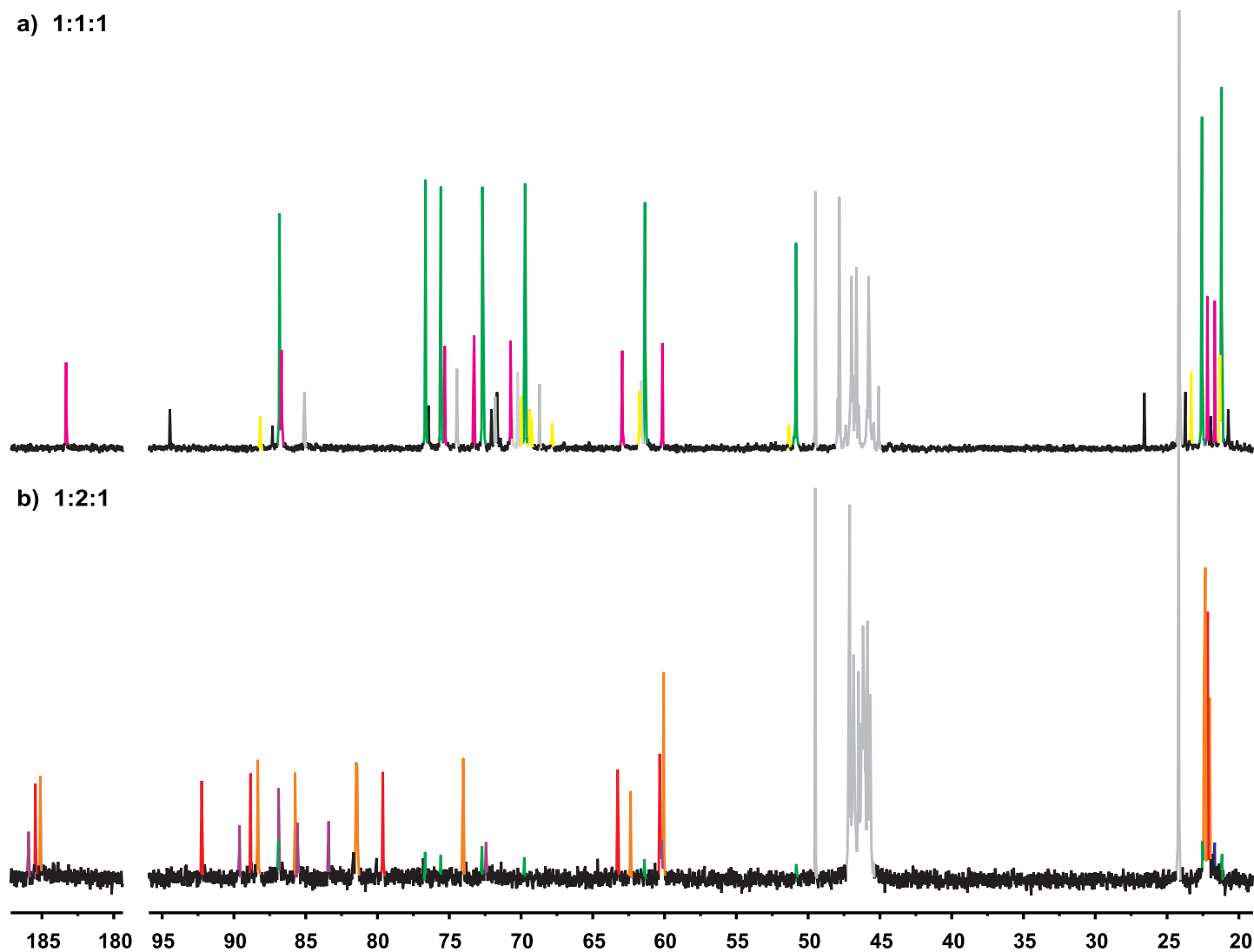


Figure A.33. Resulting $^{13}\text{C}\{^1\text{H}\}$ NMR spectra for the treatment of D-Gul1N*i*Pr with Pd-en and iodic acid in the molar ratios a) 1:1:1 and b) 1:2:1 after 3 h at 4 °C in D₂O. Green: $^1\text{C}_4$ -β-D-Gulp1N*i*Pr2H₋₁, magenta: D-Gula1NR2H₋₁, yellow: $^1\text{C}_4$ -α-D-Gulp1N*i*Pr2H₋₁, orange: L-Gula1N*i*Pr2,3,4H₋₃, red: L-Gula1N*i*Pr2,4,5H₋₃, purple: L-Gula1N*i*Pr2,3,4,5,6H₋₅, grey: D-Gul1N*i*Pr, Pd-en, *i*PrNH₂ and MeOH.

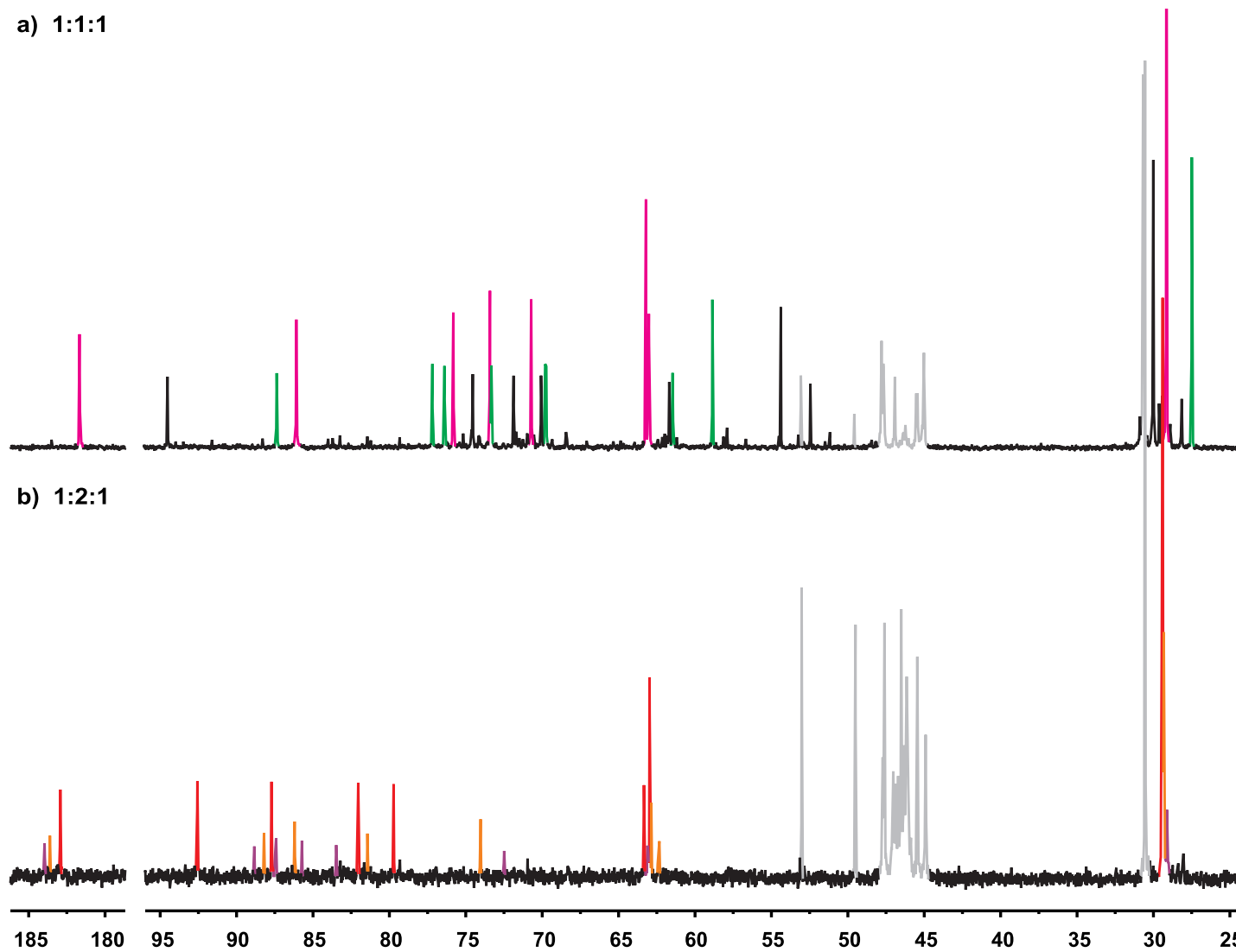


Figure A.34. Resulting $^{13}\text{C}\{^1\text{H}\}$ NMR spectra for the treatment of D-Gul1N*t*Bu with Pd-en and iodic acid in the molar ratios a) 1:1:1 and b) 1:2:1 after 3 h at 4 °C in D₂O. Magenta: D-Gul*a*1*t*Bu2H₋₁, green: $^1\text{C}_4$ -β-D-Gulp1N*t*Bu2H₋₁, red: L-Gul*a*1N*t*Bu2,4,5H₋₃, orange: L-Gul*a*1N*t*Bu2,3,4H₋₃, purple: L-Gul*a*1N*t*Bu2,3,4,5,6H₋₅, grey: Pd-en, *t*BuNH₂ and MeOH.

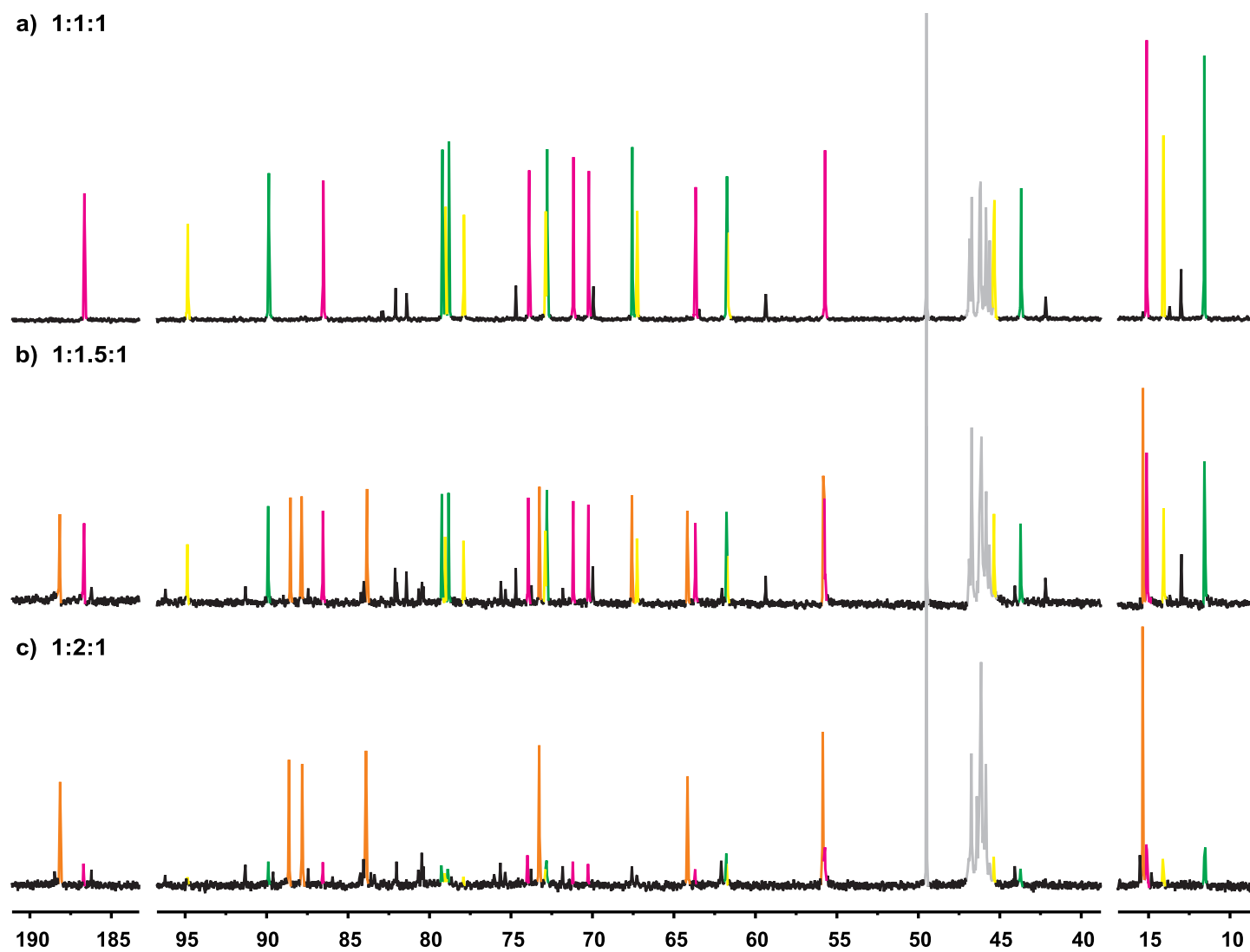


Figure A.35. Resulting $^{13}\text{C}\{^1\text{H}\}$ NMR spectra for the treatment of D-Man1NEt with Pd-en and iodic acid in the molar ratios a) 1:1:1, b) 1:1.5:1 and c) 1:2:1 after 3 h at 4 °C in D_2O . Green: $\beta\text{-D-Manp1NEt2H}_{-1}$, yellow: $^1\text{C}_4\text{-}\alpha\text{-D-Manp1NEt2H}_{-1}$; magenta: D-Mana1NEt2H₋₁, orange: D-Mana1NEt2,3,4H₋₃, grey: Pd-en and MeOH.

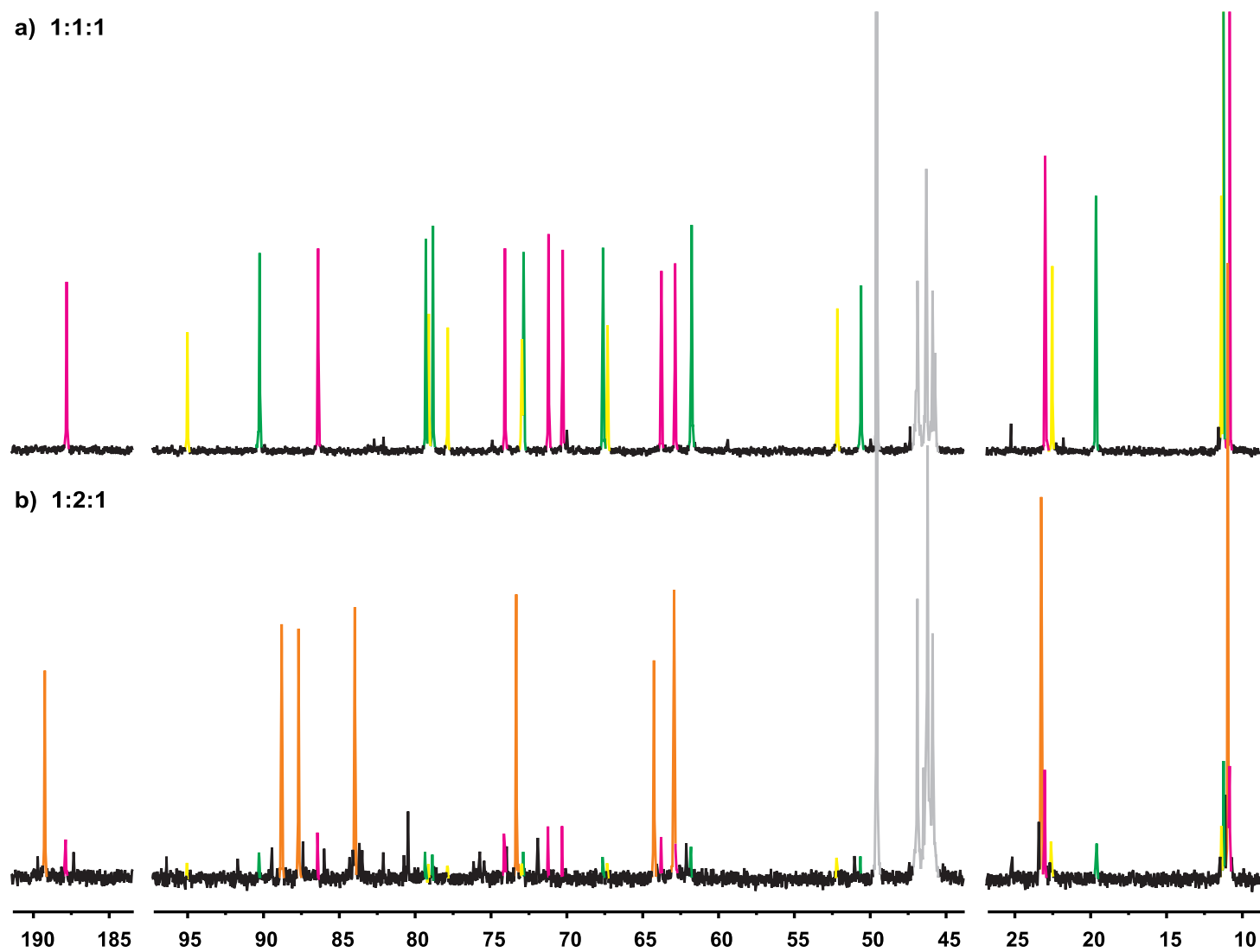


Figure A.36. Resulting $^{13}\text{C}\{^1\text{H}\}$ NMR spectra for the treatment of D-Man1NPr with Pd-en and iodic acid in the molar ratios a) 1:1:1 and b) 1:2:1 after 3 h at 4 °C in D_2O . Green: $\beta\text{-D-Man}p1\text{NPr}2\text{H}_{-1}$, yellow: $^1\text{C}_4\text{-}\alpha\text{-D-Man}p1\text{NPr}2\text{H}_{-1}$; magenta: $\text{D-Man}a1\text{NPr}2\text{H}_{-1}$, orange: $\text{D-Man}a1\text{NPr}2,3,4\text{H}_{-3}$, grey: Pd-en and MeOH

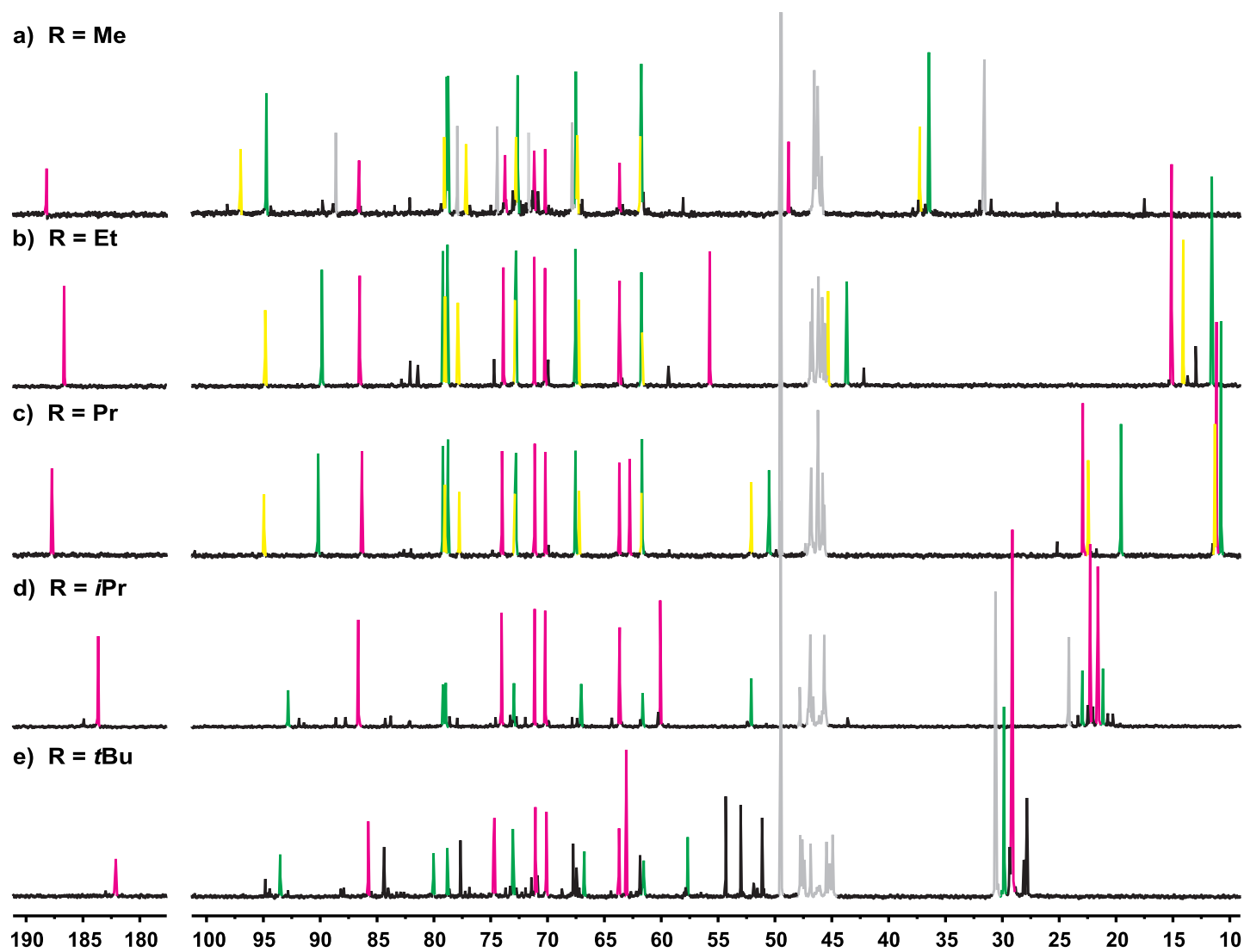


Figure A.37. Resulting $^{13}\text{C}\{^1\text{H}\}$ NMR spectra for the equimolar reactions of D-Man1NMe, D-Man1NEt, D-Man1NPr, D-Man1N*i*Pr and D-Man1N*t*Bu with Pd-en and iodic acid after 3 h at 4 °C in D₂O. Green: β -D-Manp1NR2H₋₁, yellow: $^1\text{C}_4$ - α -D-Manp1NR2H₋₁, magenta: D-Mana1NR2H₋₁, grey: Pd-en, EtOH and MeOH.

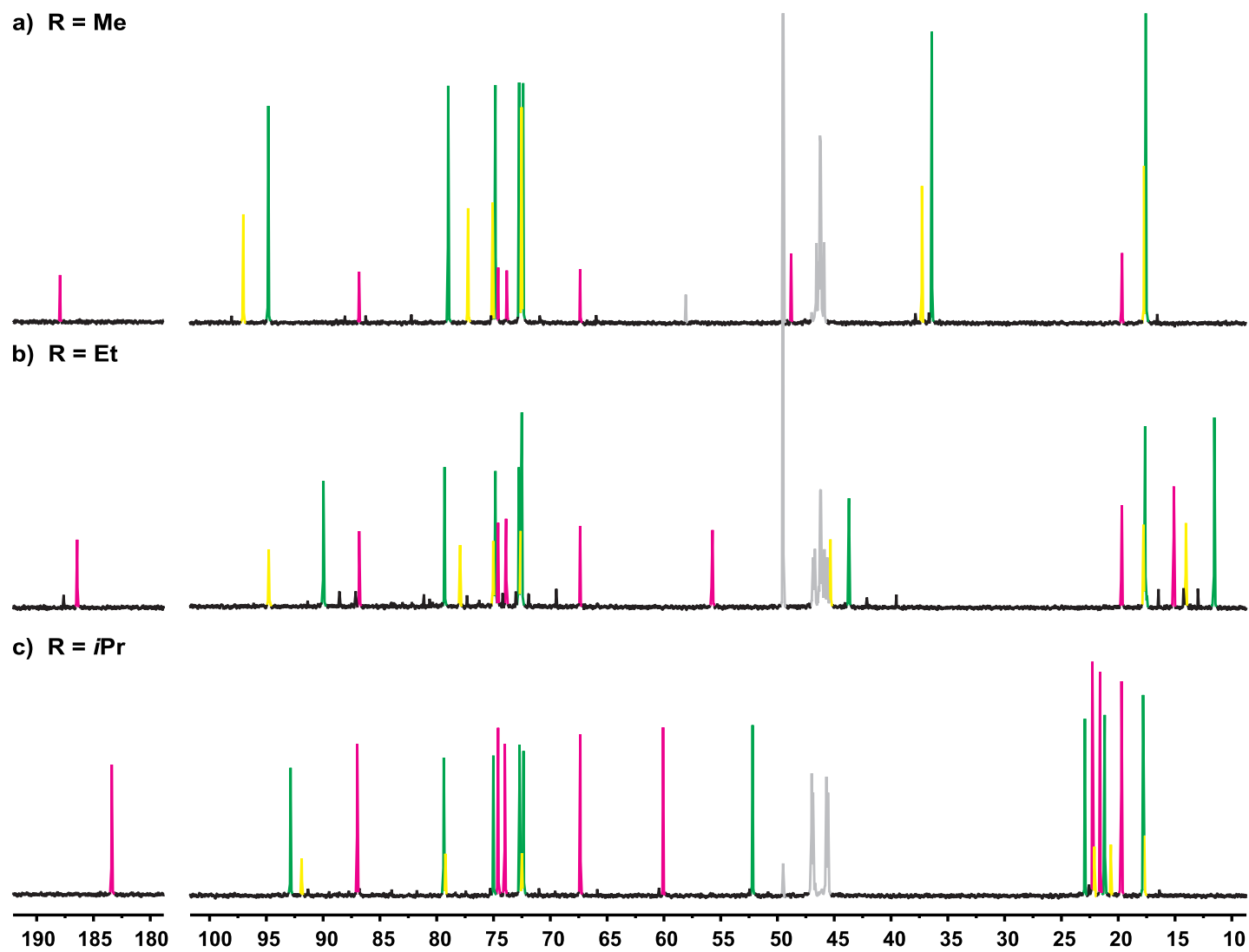


Figure A.38. Resulting $^{13}\text{C}\{^1\text{H}\}$ NMR spectra for the equimolar reactions of L-Rha1NMe, L-Rha1NEt and L-Rha1N*i*Pr with Pd-en and iodic acid after 3 h at 4 °C in D_2O . Green: β -D-Rhap1NR2H₋₁, yellow: $^1\text{C}_4$ - α -D-Rhap1NR2H₋₁, magenta: D-Rhaa1NR2H₋₁, grey: Pd-en, EtOH and MeOH.

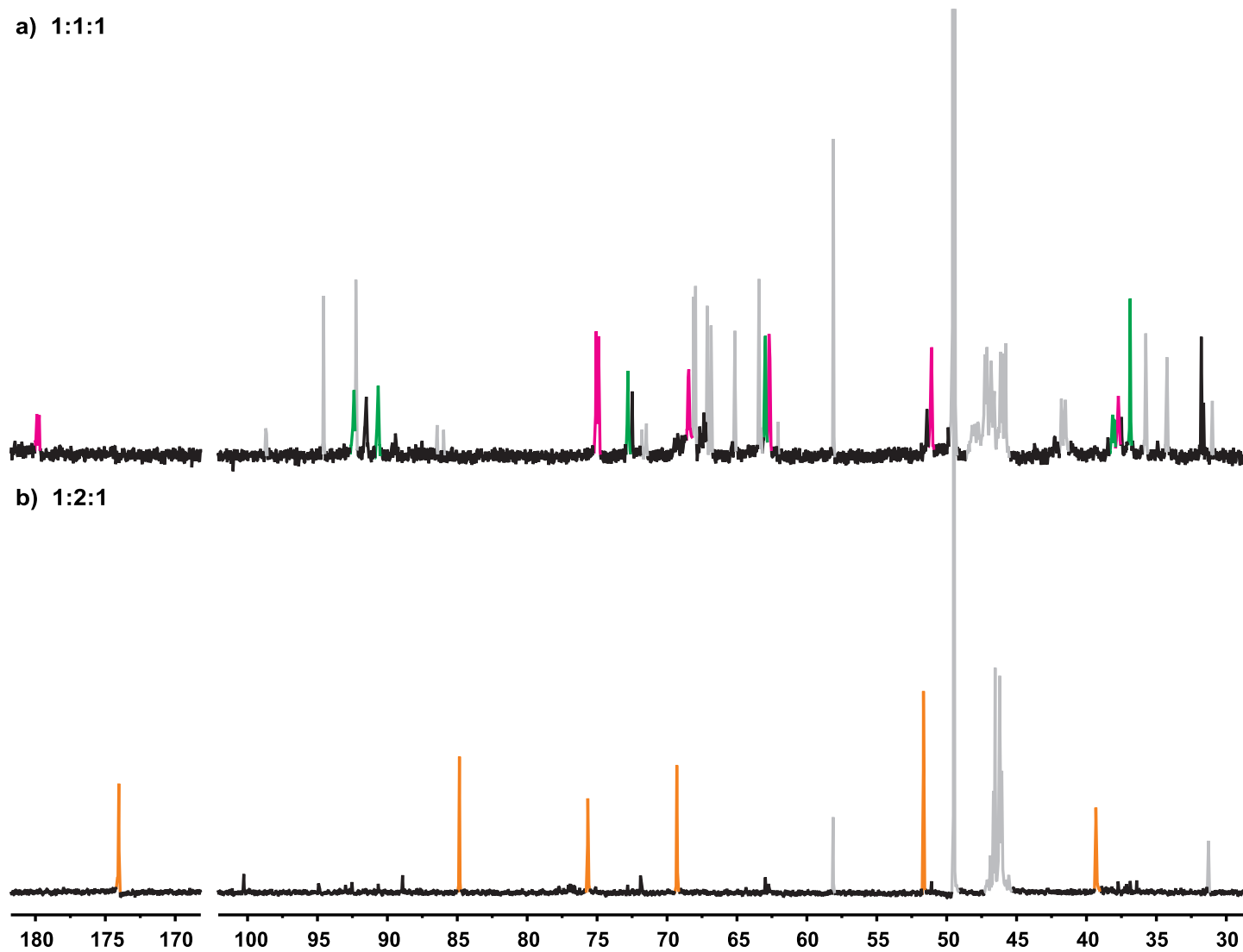


Figure A.39. Resulting $^{13}\text{C}\{^1\text{H}\}$ NMR spectra for the treatment of *D-ery*-dPent1NMe with Pd-en and iodic acid in the molar ratios a) 1:1:1 and b) 1:2:1 after 3 h at 4 °C in D_2O . Green: $^4\text{C}_1$ - α -*D-ery*-dPentf1NMe3H $_{-1}$, magenta: *D-ery*-dPenta1NMe3H $_{-1}$, orange: *D-ery*-dPenta1NMe3,4,5H $_{-3}$, grey: Pd-en, EtOH and MeOH.

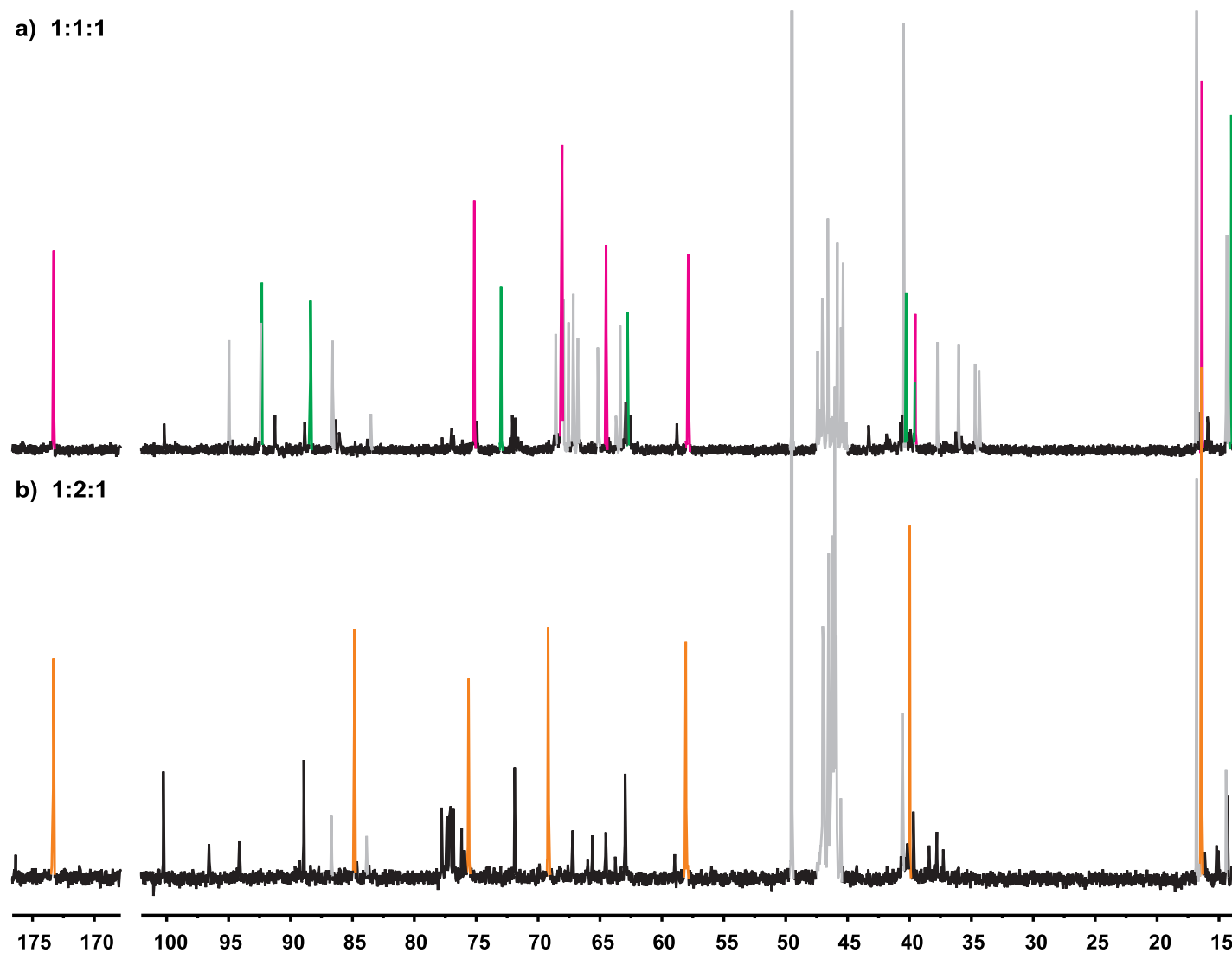


Figure A.40. Resulting $^{13}\text{C}\{^1\text{H}\}$ NMR spectra for the treatment of *D-ery*-dPenta1NEt with Pd-en and iodic acid in the molar ratios a) 1:1:1 and b) 1:2:1 after 3 h at 4 °C in D_2O . Green: $^4\text{C}_1$ - α -*D-ery*-dPentf1NEt3H $_{-1}$, magenta: *D-ery*-dPenta1NEt3H $_{-1}$ - $\kappa\text{N}^1, \kappa\text{O}^3$, orange: *D-ery*-dPenta1NEt3,4,5H $_{-3}$ - $\kappa\text{N}^1, \kappa\text{O}^3: \kappa\text{O}^{4,5}$, grey: Pd-en, EtOH.

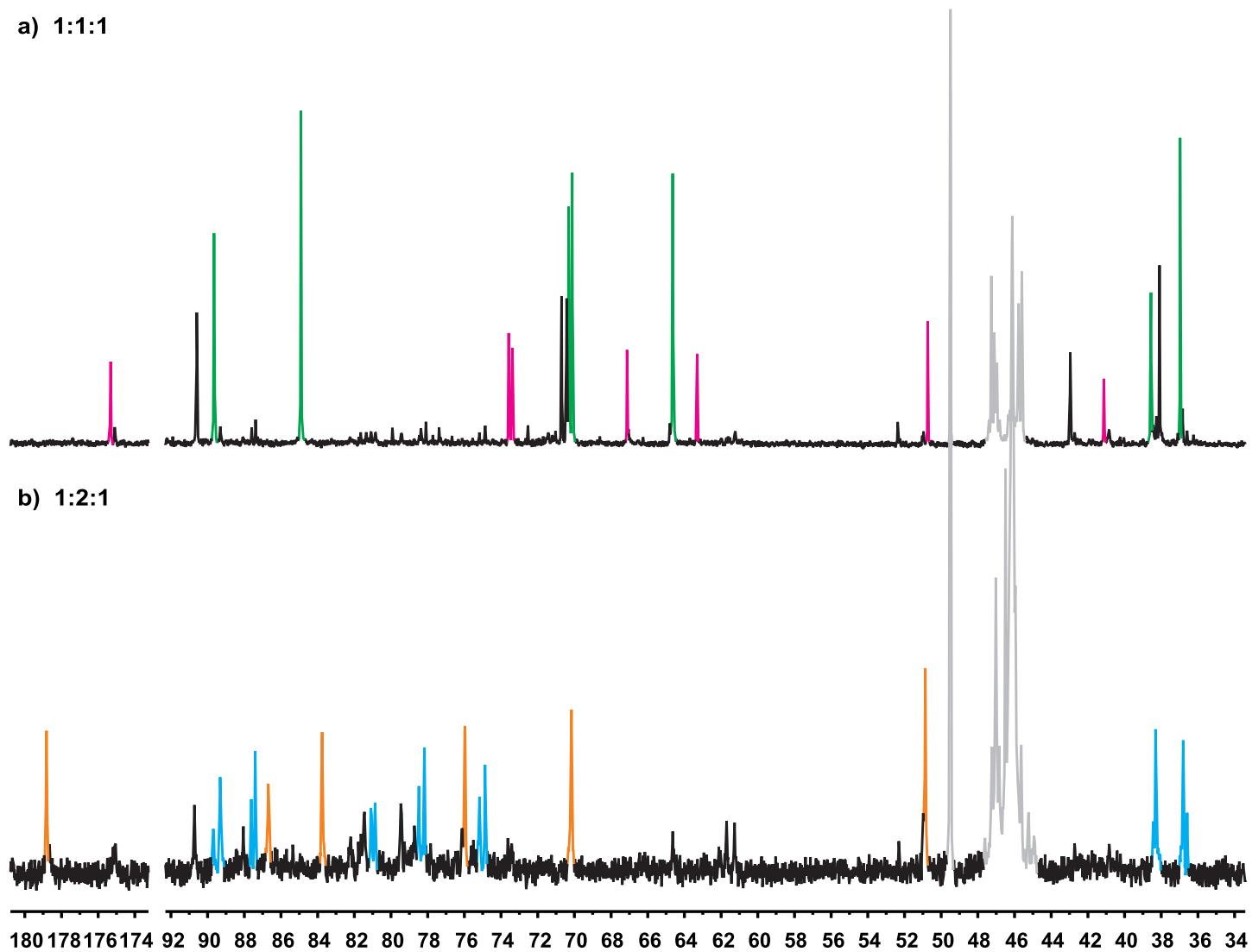


Figure A.41. Resulting $^{13}\text{C}\{^1\text{H}\}$ NMR spectra for the treatment of *D-ara*-dHex1NMe with Pd-en and iodic acid in the molar ratios a) 1:1:1 and b) 1:2:1 after 3 h at 4°C in D_2O . Green: β -*D-ara*-dHexf1NMe3H₋₁, magenta: *D-ara*-dHexa1NMe3H₋₁, cyan: β -*D-ara*-dHexf1NMe3,5,6H₋₃, orange: *D-ara*-dHexa1NMe3,4,5H₋₃, grey: Pd-en, EtOH and MeOH.

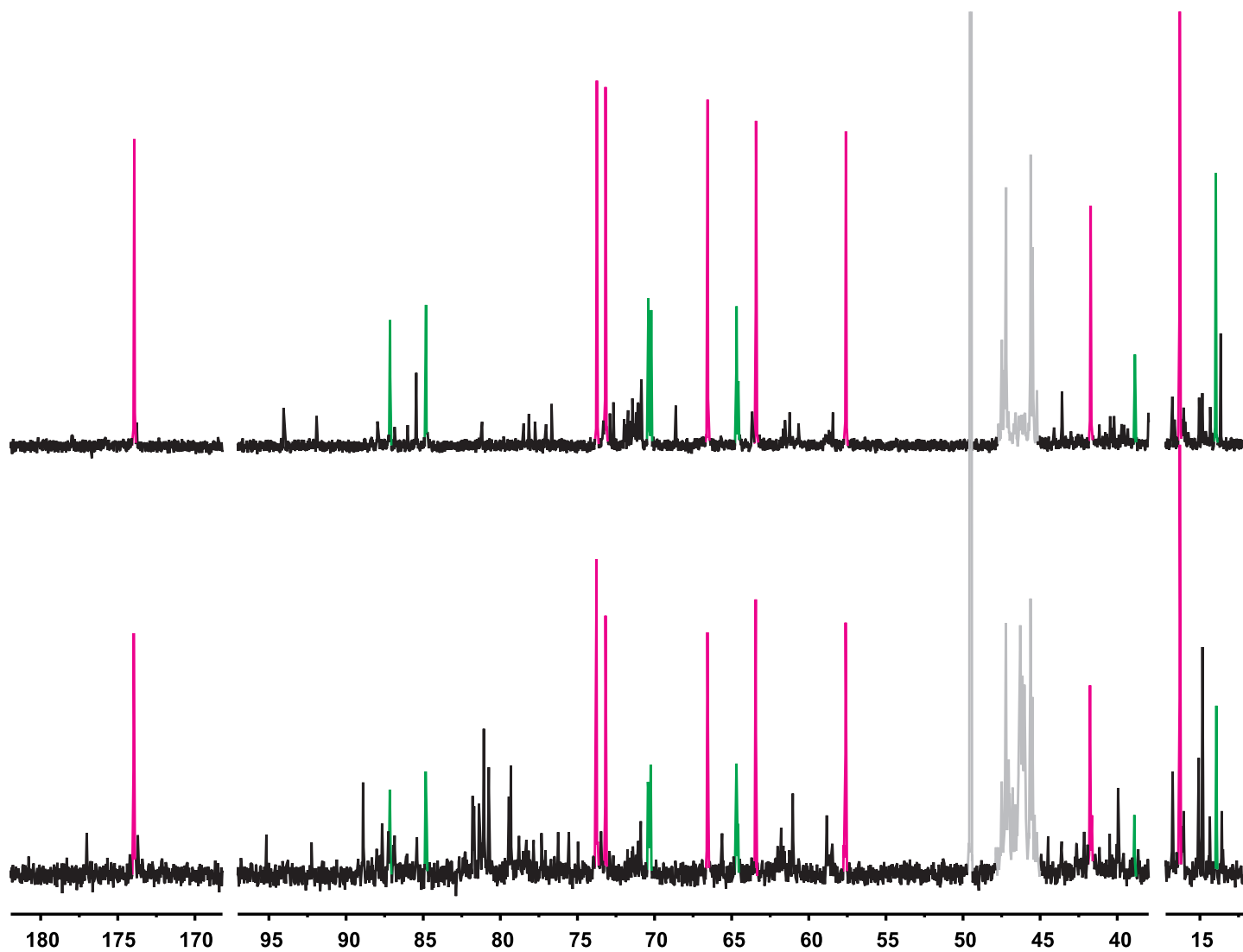


Figure A.42. Resulting $^{13}\text{C}\{^1\text{H}\}$ NMR spectra for the treatment of *D-ara*-dHex1NEt with Pd-en and iodic acid in the molar ratios a) 1:1:1 and b) 1:2:1 after 3 h at 4 °C in D_2O . Green: $^4\text{C}_1$ - β -*D-ara*-dHexf1NEt3H $_{-1}$, magenta: *D-ara*-dHexa1NEt3H $_{-1}$, grey: Pd-en and EtOH.

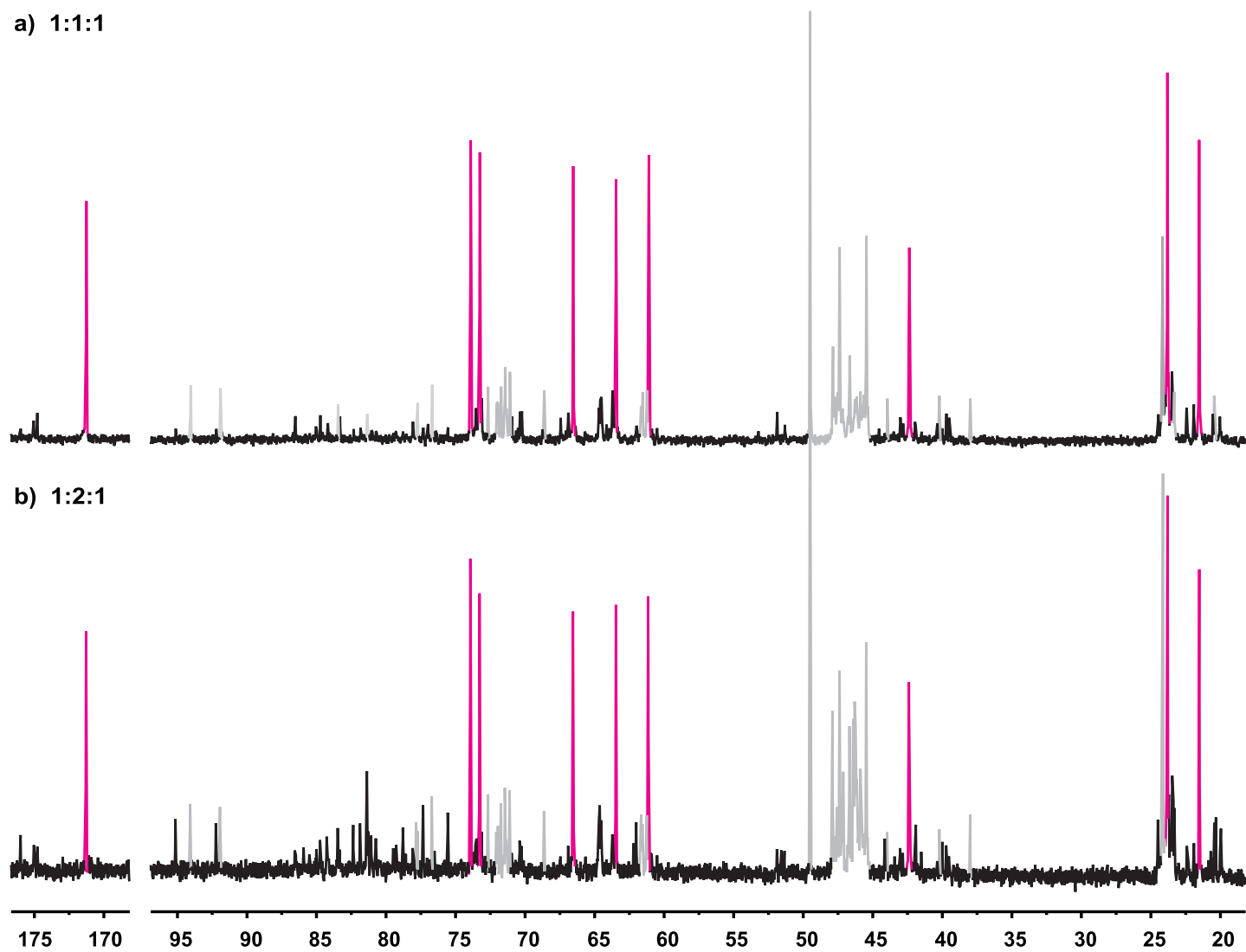


Figure A.43. Resulting $^{13}\text{C}\{^1\text{H}\}$ NMR spectra for the treatment of D-ara-dHex1NiPr with Pd-en and iodic acid in the molar ratios a) 1:1:1 and b) 1:2:1 after 3 h at 4°C in D_2O . Magenta: $\text{D-ara-dHexa1NiPr3H-1}$, grey: D-lyx-dHex , D-lyx-dHex1NiPr , Pd-en and EtOH.

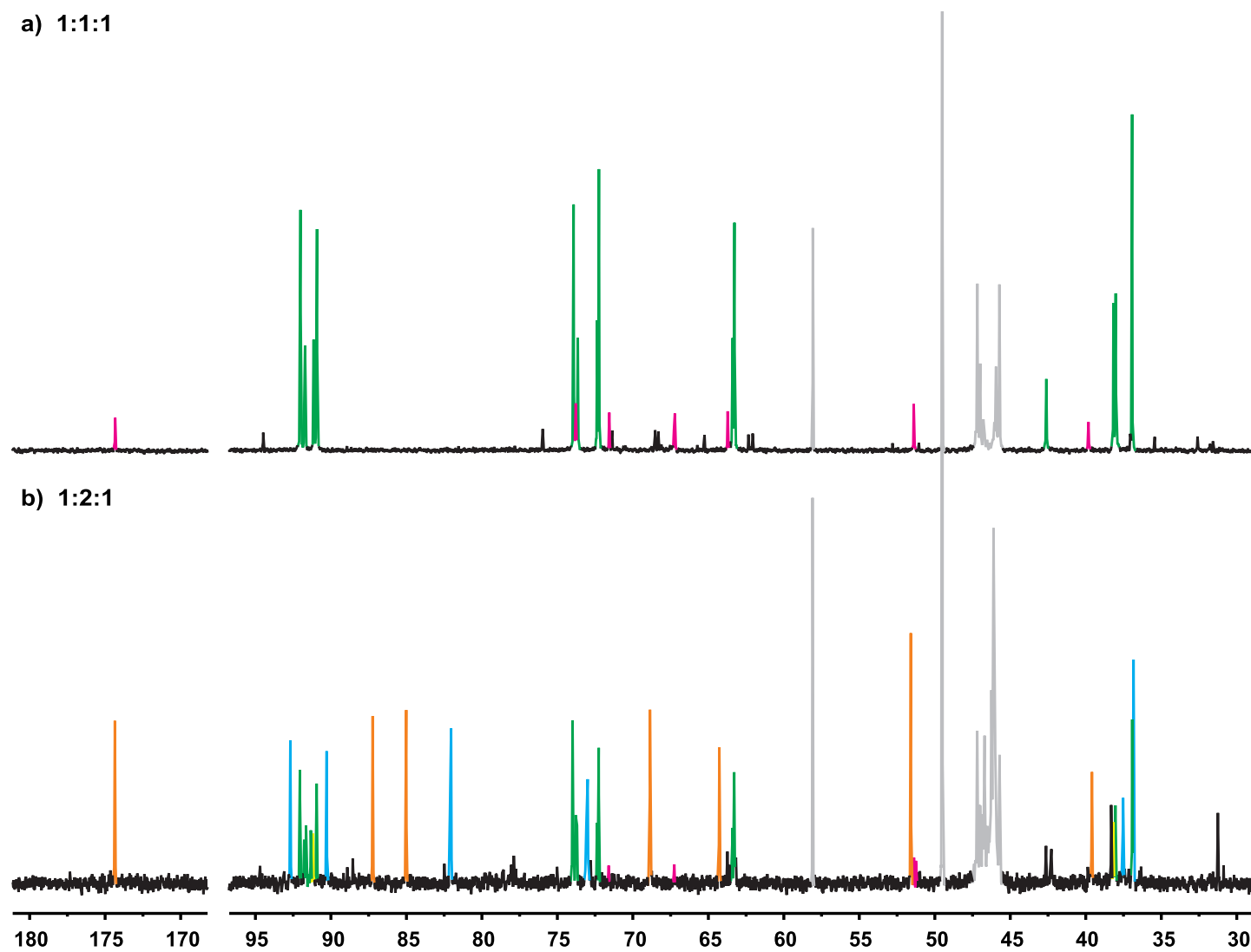


Figure A.44. Resulting $^{13}\text{C}\{^1\text{H}\}$ NMR spectra for the treatment of *D-lyx*-dHex1NMe with Pd-en and iodic acid in the molar ratios a) 1:1:1 and b) 1:2:1 after 3 h at 4 °C in D_2O . Green: $^4\text{C}_1$ - β -*D-lyx*-dHexf1NMe3H $_{-1}$, magenta: *D-lyx*-dHexa1NMe3H $_{-1}$, orange: *D-lyx*-dHexa1NMe3,4,5H $_{-3}$, cyan: β -*D-lyx*-dHexf1NMe3,5,6H $_{-3}$, grey: Pd-en, EtOH and MeOH.

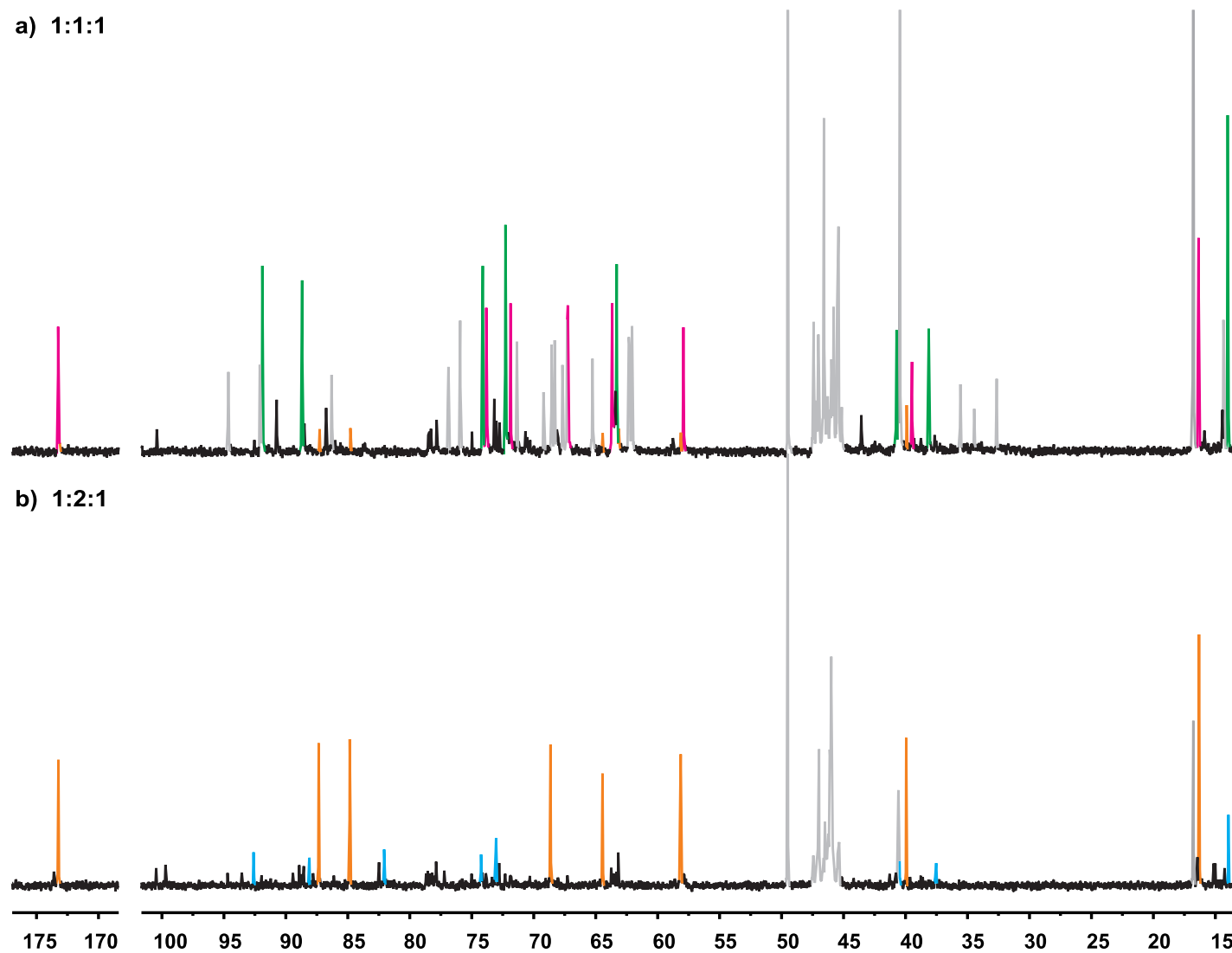


Figure A.45. Resulting $^{13}\text{C}\{^1\text{H}\}$ NMR spectra for the treatment of *D-lyx*-dHex1NEt with Pd-en and iodic acid in the molar ratios a) 1:1:1 and b) 1:2:1 after 3 h at 4 °C in D_2O . Green: $^4\text{C}_1$ - β -*D-lyx*-dHexf1NEt3H $_{-1}$, magenta: *D-lyx*-dHexa1NEt3H $_{-1}$, orange: *D-lyx*-dHexa1NEt3,4,5H $_{-3}$, cyan: β -*D-ara*-dHexf1NEt3,5,6H $_{-3}$, grey: *D-lyx*-dHex, *D-lyx*-dHex1NEt, Pd-en, EtOH.

B. Packing Diagrams of the Crystal Structures

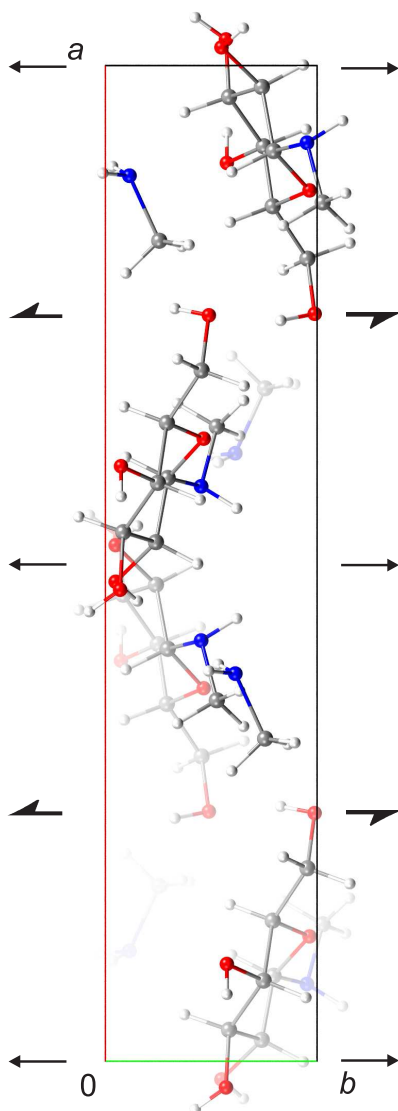


Figure B.1. Packing diagram of **1** in the monoclinic space group $C2$ with view along $[001]$. The symmetry elements of the space group $C2$ are overlaid. Atoms: carbon (grey), hydrogen (white), nitrogen (blue) and oxygen (red).

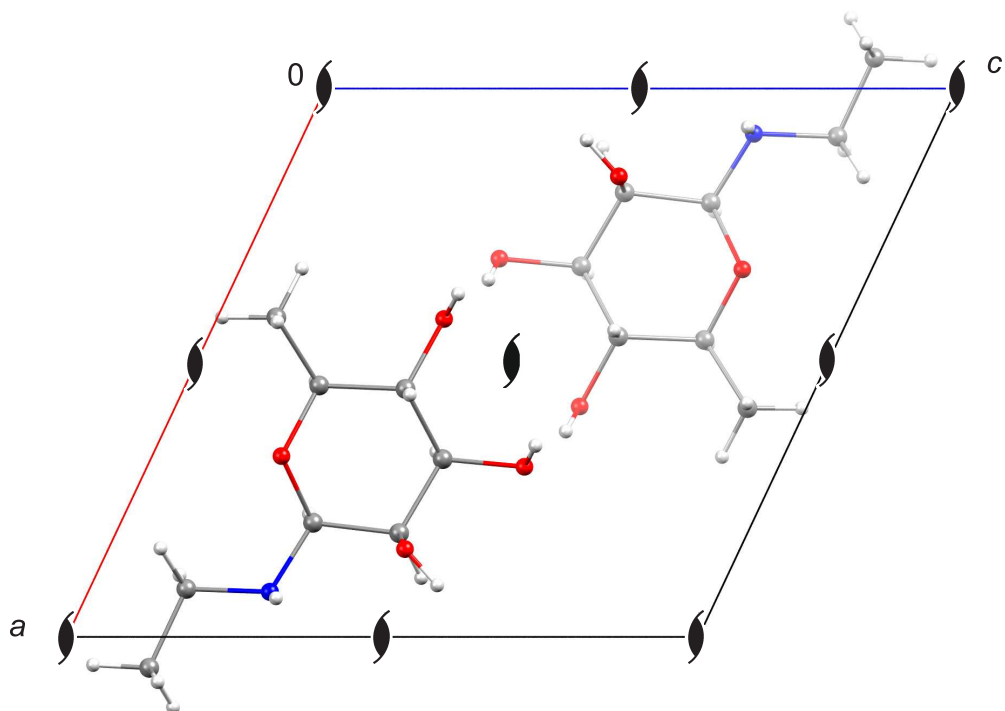


Figure B.2. Packing diagram of **2** in the monoclinic space group $P2_1$ with view along [010]. The symmetry elements of the space group $P2_1$ are overlaid. Atoms: carbon (grey), hydrogen (white), nitrogen (blue) and oxygen (red).

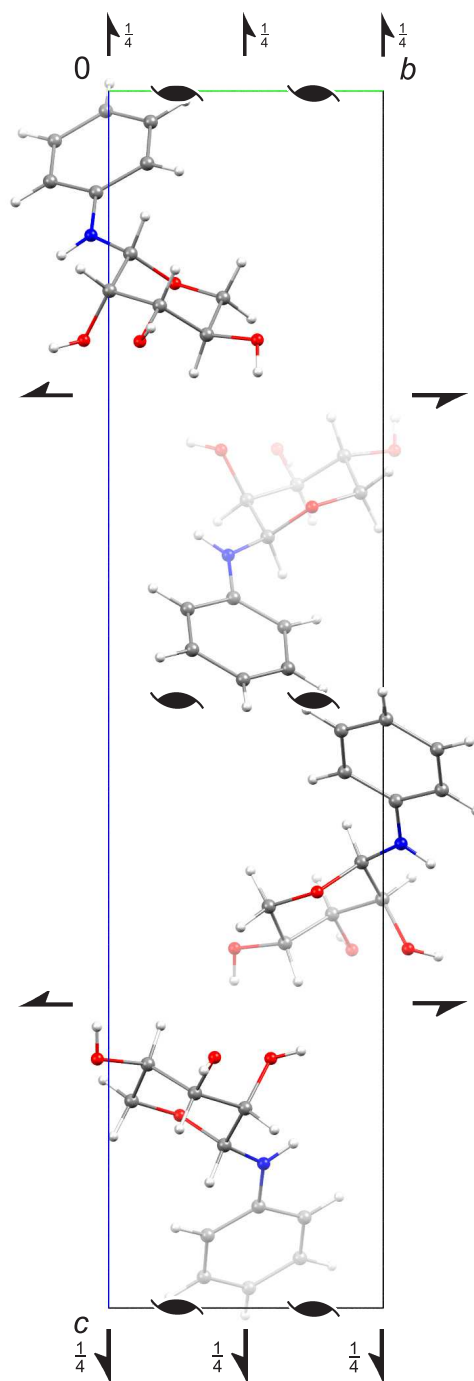


Figure B.3. Packing diagram of **3** in the orthorhombic space group $P2_12_12_1$ with view along $[100]$. The symmetry elements of the space group $P2_12_12_1$ are overlaid. Atoms: carbon (grey), hydrogen (white), nitrogen (blue) and oxygen (red).

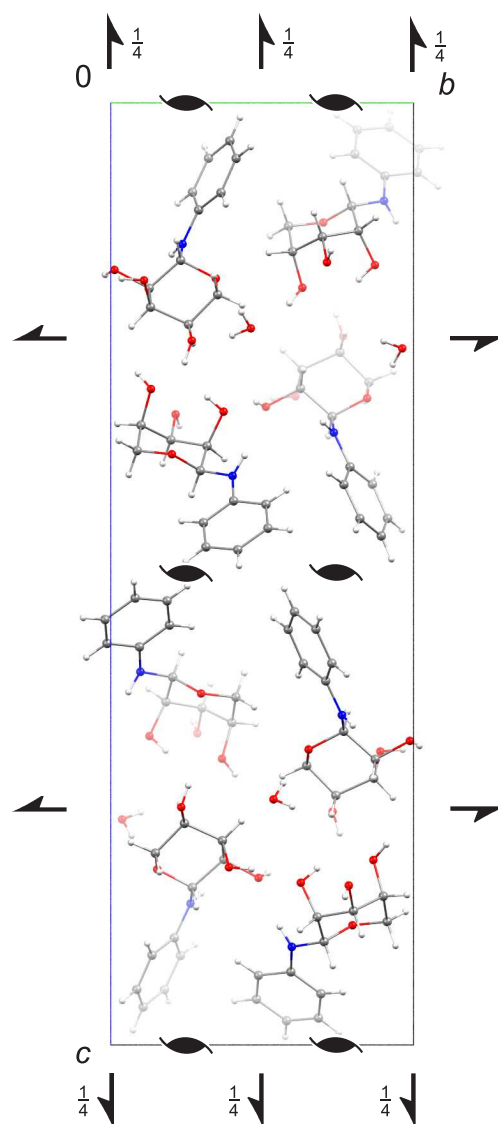


Figure B.4. Packing diagram of **4** in the orthorhombic space group $P2_12_12_1$ with view along $[100]$. The symmetry elements of the space group $P2_12_12_1$ are overlaid. Atoms: carbon (grey), hydrogen (white), nitrogen (blue) and oxygen (red).

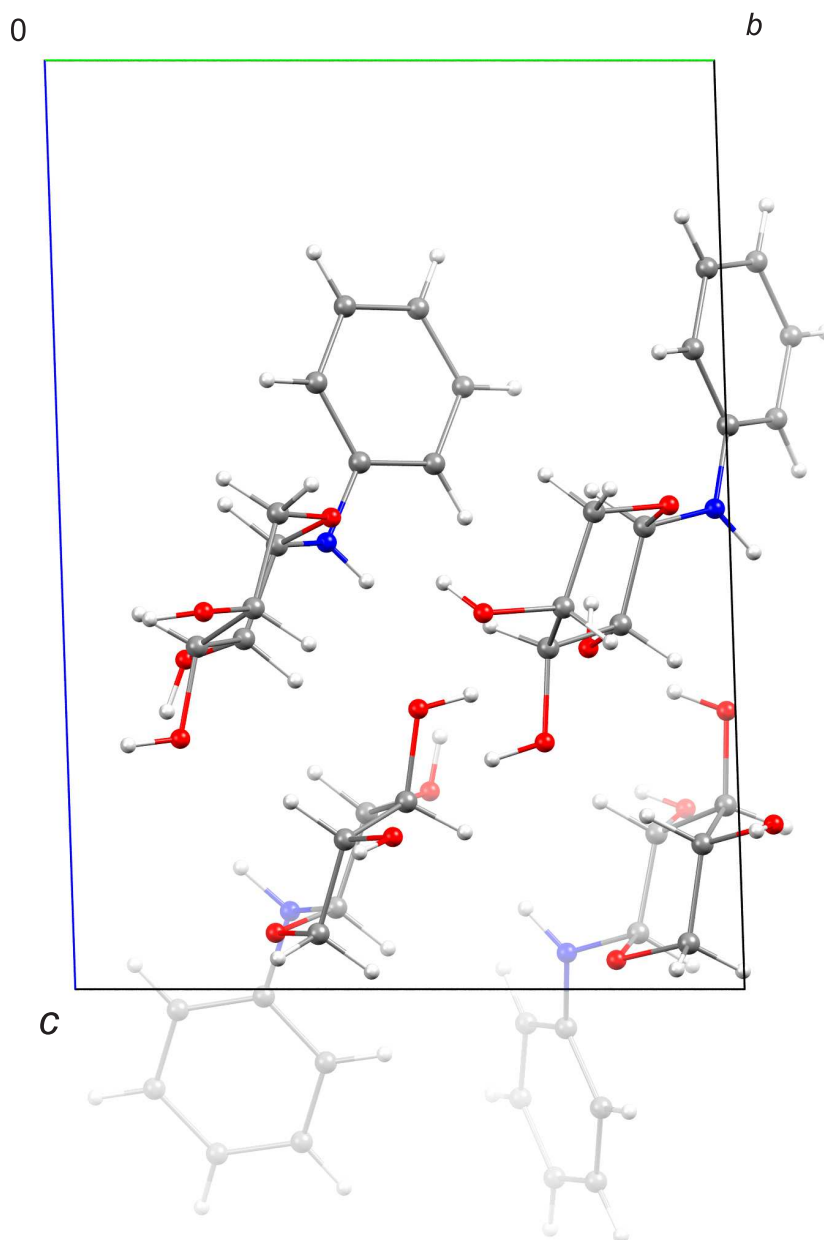


Figure B.5. Packing diagram of **5** in the triclinic space group $P1$ with view along $[100]$. Atoms: carbon (grey), hydrogen (white), nitrogen (blue) and oxygen (red).

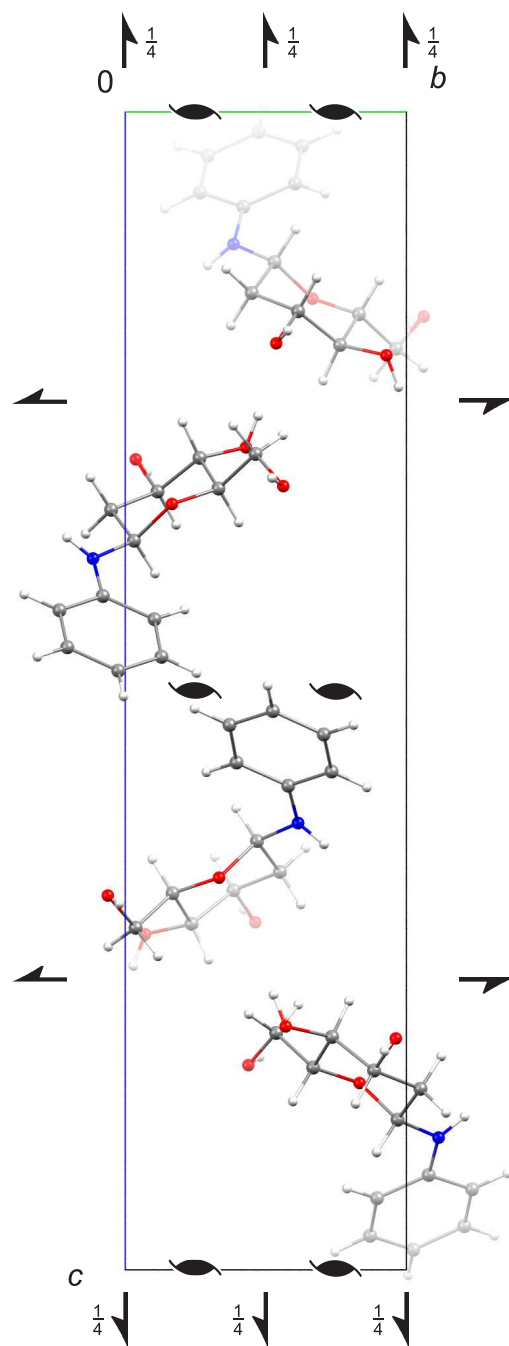


Figure B.6. Packing diagram of **6** in the orthorhombic space group $P2_12_12_1$ with view along $[100]$. The symmetry elements of the space group $P2_12_12_1$ are overlaid. Atoms: carbon (grey), hydrogen (white), nitrogen (blue) and oxygen (red).

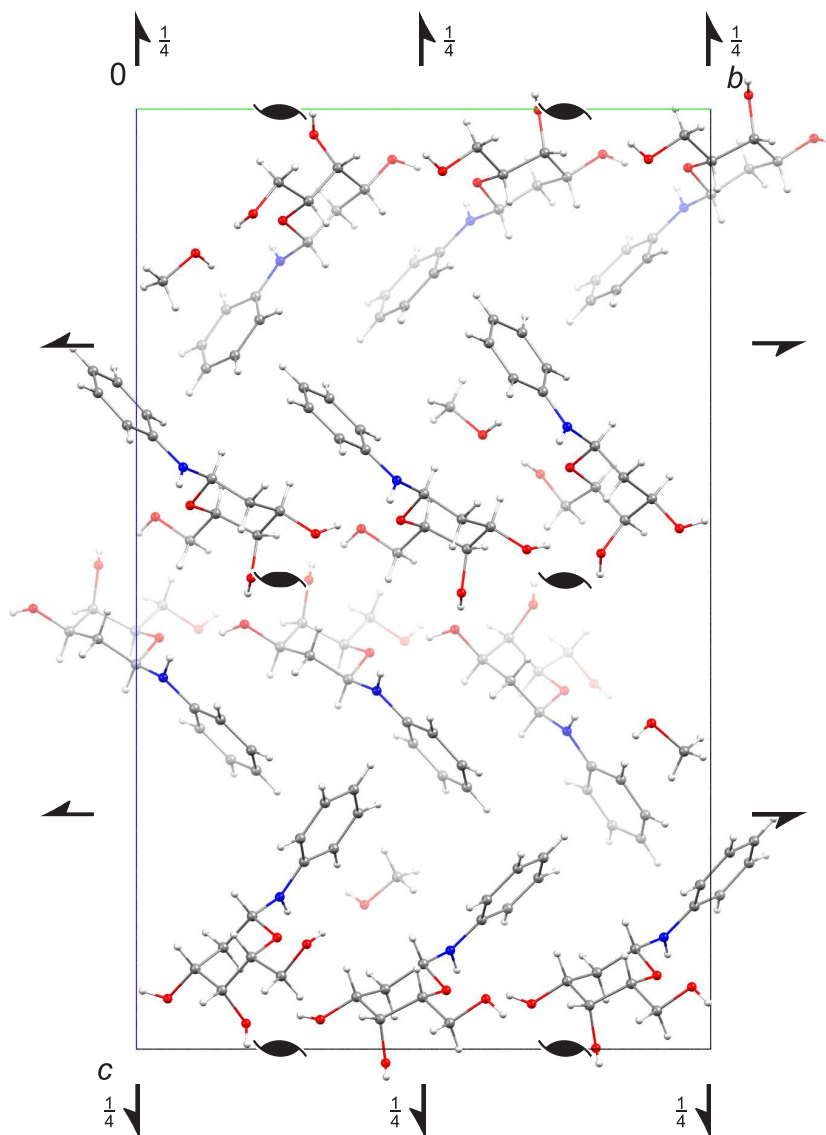


Figure B.7. Packing diagram of **7** in the orthorhombic space group $P2_12_12_1$ with view along $[100]$. The symmetry elements of the space group $P2_12_12_1$ are overlaid. Atoms: carbon (grey), hydrogen (white), nitrogen (blue) and oxygen (red).

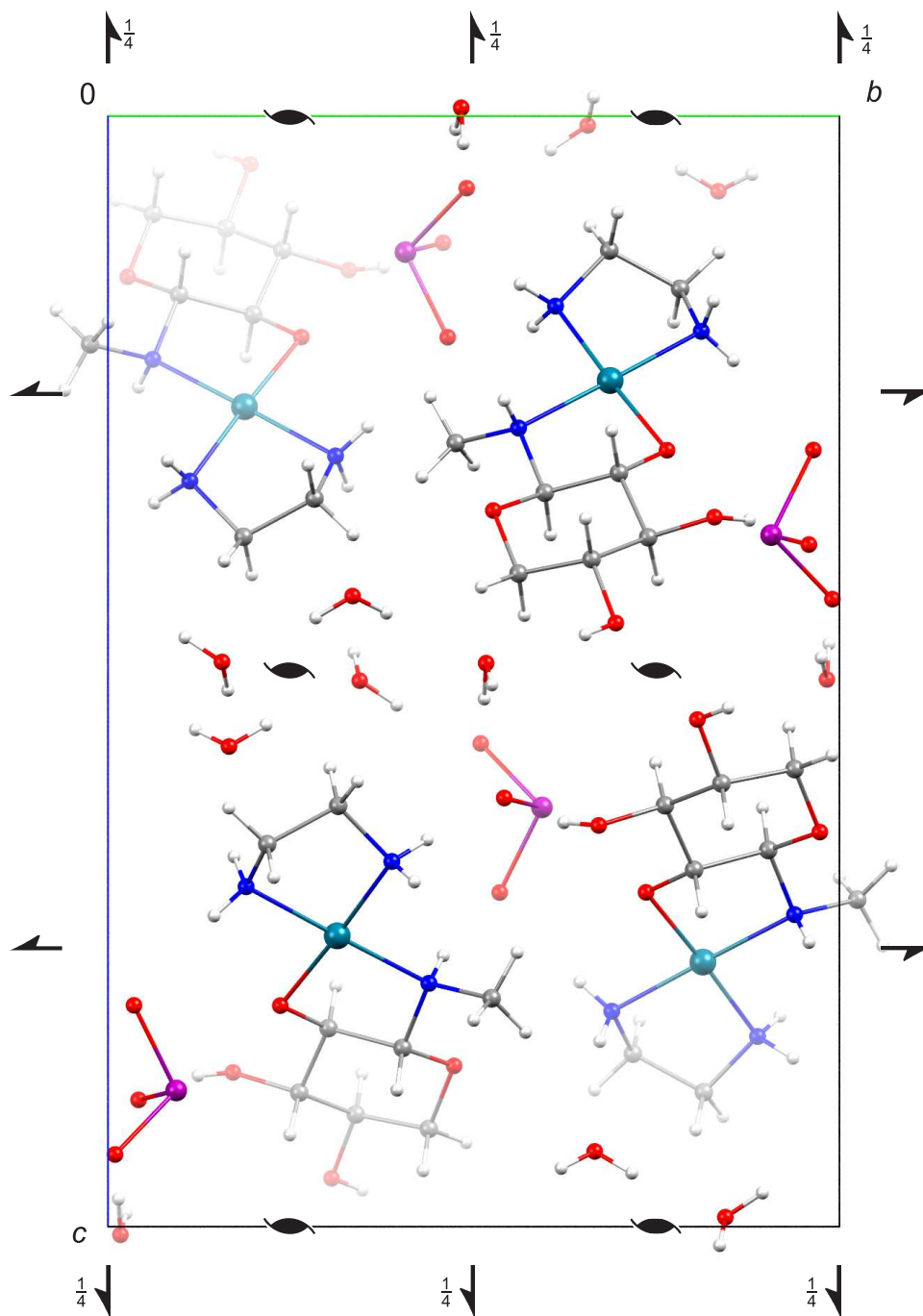


Figure B.8. Packing diagram of **8** in the orthorhombic space group $P2_12_12_1$ with view along $[100]$. The symmetry elements of the space group $P2_12_12_1$ are overlaid. Atoms: carbon (grey), hydrogen (white), iodine (purple), nitrogen (blue), oxygen (red) and palladium (turquoise).

C. Crystallographic Tables

Table C.1. Crystallographic data of 4C_1 - β -D-Glcp1NMe·MeNH₂ (**1**), 1C_4 - β -L-Rhap1NEt (**2**) and 4C_1 - β -D-Lyxp1NPh (**3**).

compound	1	2	3
empirical formula	C ₈ H ₂₀ N ₂ O ₅	C ₈ H ₁₇ NO ₄	C ₁₁ H ₁₅ NO ₄
M_r /g mol ⁻¹	224.26	191.22	225.24
crystal system	monoclinic	monoclinic	orthorhombic
space group	<i>C</i> 2	<i>P</i> 2 ₁	<i>P</i> 2 ₁ 2 ₁ 2 ₁
$a/\text{Å}$	23.5559(12)	10.4023(5)	6.0390(3)
$b/\text{Å}$	4.4523(3)	4.6613(2)	6.4195(3)
$c/\text{Å}$	12.3134(7)	10.8357(5)	28.4944(12)
$\alpha/^\circ$	90	90	90
$\beta/^\circ$	117.1375(18)	115.211(2)	90
$\gamma/^\circ$	90	90	90
$V/\text{Å}^3$	1149.24(12)	475.36(4)	1104.65(9)
Z	4	2	4
ρ /g cm ⁻³	1.296	1.336	1.354
μ /mm ⁻¹	0.107	0.106	0.103
crystal size/mm	0.40×0.10×0.03	0.10×0.10×0.03	0.12×0.09×0.04
temperature/K	100(2)	100(2)	100(2)
diffractometer	Bruker D8Venture	Bruker D8Venture	Bruker D8Venture
radiation	MoK α	MoK α	MoK α
anode	rotating anode	rotating anode	rotating anode
rate input/kW	2.5	2.5	2.5
θ range/°	3.245–26.37	3.583–29.61	3.253–27.12
reflexes for metric	3025	4183	5538
absorption correction	multi-scan	multi-scan	multi-scan
transmission factors	0.6980–0.7454	0.6482–0.7459	0.7015–0.7455
reflexes measured	11123	9138	10430
independent reflexes	2327	2631	2438
R_{int}	0.0466	0.0308	0.0223
mean $\sigma(I)/I$	0.0494	0.0465	0.0202
reflexes with $I \geq 2\sigma(I)$	2067	2292	2240
x, y (weighting scheme)	0.0429, 1.2670	0.0391, 0.0824	0.0317, 0.2016
hydrogen refinement	^a	^a	^a
Flack parameter	0.3(10)	1.6(7)	−0.4(3)
parameters	254	126	214
restraints	1	1	0
$R(F_{\text{obs}})$	0.0464	0.0400	0.0296
$R_w(F_2)$	0.1090	0.0934	0.0694
S	1.030	1.031	1.056
shift/error _{max}	0.001	0.001	0.001
max. electron density/e Å ³	0.515	0.370	0.206
min. electron density/e Å ³	−0.298	−0.188	−0.136

^a Coordinates of hydrogen were calculated in idealized positions, riding on their parent atoms.

Table C.2. Crystallographic data of 4C_1 - α -D-Ribp1NPh \cdot 0.5H $_2$ O (**4**), 4C_1 - β -D-Xylp1NPh (**5**) and 4C_1 - β -D-ara-dHexp1NPh (**6**).

compound	4	5	6
empirical formula	C ₂₂ H ₃₂ N ₂ O ₉	C ₁₁ H ₁₅ NO ₄	C ₁₂ H ₁₇ NO ₄
M_r /g mol ⁻¹	468.49	225.24	239.26
crystal system	orthorhombic	triclinic	orthorhombic
space group	$P2_12_12_1$	$P1$	$P2_12_12_1$
$a/\text{\AA}$	6.1211(2)	7.4696(5)	6.3074(5)
$b/\text{\AA}$	10.9298(4)	10.1415(7)	6.8393(6)
$c/\text{\AA}$	34.0162(12)	14.0776(9)	28.194(2)
$\alpha/^\circ$	90	87.934(2)	90
$\beta/^\circ$	90	87.0775(18)	90
$\gamma/^\circ$	90	86.3508(19)	90
$V/\text{\AA}^3$	2275.77(14)	1062.30(12)	1216.24(17)
Z	4	4	4
ρ /g cm ⁻³	1.367	1.408	1.307
μ /mm ⁻¹	0.106	0.107	0.098
crystal size/mm	0.10 \times 0.03 \times 0.10	0.25 \times 0.15 \times 0.10	0.05 \times 0.03 \times 0.02
temperature/K	298(2)	100(2)	100(2)
diffractometer	Bruker D8Venture	Bruker D8Venture	Bruker D8Venture
radiation	MoK $_{\alpha}$	MoK $_{\alpha}$	MoK $_{\alpha}$
anode	rotating anode	rotating anode	rotating anode
rate input/kW	2.5	2.5	2.5
θ range/ $^\circ$	3.035–25.73	2.442–27.14	3.065–23.28
reflexes for metric	9524	7322	3239
absorption correction	multi-scan	multi-scan	multi-scan
transmission factors	0.7102–0.7453	0.6434–0.7455	0.6027–0.7449
reflexes measured	47125	19581	8864
independent reflexes	4329	8370	1742
R_{int}	0.0584	0.0410	0.0616
mean $\sigma(I)/I$	0.0299	0.0560	0.0503
reflexes with $I \geq 2\sigma(I)$	3585	7356	1432
x, y (weighting scheme)	0.0338, 0.5078	0.0726, 1.0605	0.0338, 0.2823
hydrogen refinement	^a	^b	^b
Flack parameter	–0.2(4)	–0.1(5)	–1(2)
parameters	320	602	155
restraints	0	9	0
$R(F_{\text{obs}})$	0.0398	0.0551	0.0417
$R_w(F_2)$	0.0858	0.1488	0.0840
S	1.062	1.077	1.062
shift/error _{max}	0.001	0.005	0.001
max. electron density/e \AA^3	0.145	0.460	0.168
min. electron density/e \AA^3	–0.152	–0.341	–0.147

^a Coordinates of hydrogen atoms bonded to aqua ligands were refined freely, all other hydrogen atoms were calculated in idealized positions, riding on their parent atoms. ^b Coordinates of hydrogen were calculated in idealized positions, riding on their parent atoms.

Table C.3. Crystallographic data of ${}^4C_1\text{-}\beta\text{-D-lyx-dHexp1NPh}\cdot 0.33\text{H}_2\text{O}$ (**7**) and $[\text{Pd}(\text{en})({}^4C_1\text{-}\beta\text{-D-Xylp1NMe2H}_{-1}\text{-}\kappa N^1, \kappa O^2)]\text{IO}_3\cdot 4\text{H}_2\text{O}$ (**8**).

compound	7	8
empirical formula	$\text{C}_{37}\text{H}_{55}\text{N}_3\text{O}_{13}$	$\text{C}_8\text{H}_{26}\text{IN}_3\text{O}_{10}\text{Pd}$
$M_r/\text{g mol}^{-1}$	749.84	557.62
crystal system	orthorhombic	orthorhombic
space group	$P2_12_12_1$	$P2_12_12_1$
$a/\text{\AA}$	6.9077(2)	6.1659(2)
$b/\text{\AA}$	18.1692(6)	13.3545(5)
$c/\text{\AA}$	29.7678(9)	20.2868(9)
$\alpha/^\circ$	90	90
$\beta/^\circ$	90	90
$\gamma/^\circ$	90	90
$V/\text{\AA}^3$	3736.1(2)	1670.47(11)
Z	4	4
$\rho/\text{g cm}^{-3}$	1.333	2.217
μ/mm^{-1}	0.101	3.013
crystal size/mm	$0.10\times 0.08\times 0.03$	$0.09\times 0.07\times 0.03$
temperature/K	100(2)	100(2)
diffractometer	Bruker D8Venture	Bruker D8Venture
radiation	MoK_α	MoK_α
anode	rotating anode	rotating anode
rate input/kW	2.5	2.5
θ range/ $^\circ$	3.155–25.70	3.212–27.15
reflexes for metric	9847	7322
absorption correction	multi-scan	multi-scan
transmission factors	0.7006–0.7453	0.6897–0.7455
reflexes measured	100757	66324
independent reflexes	7146	3693
R_{int}	0.0592	0.0416
mean $\sigma(I)/I$	0.0317	0.0213
reflexes with $I \geq 2\sigma(I)$	6465	3602
x, y (weighting scheme)	0.0307, 1.4989	0.0114, 0.5094
hydrogen refinement	a	a
Flack parameter	0.8(3)	–0.004(8)
parameters	501	248
restraints	5	9
$R(F_{\text{obs}})$	0.0355	0.0138
$R_w(F_2)$	0.0802	0.0309
S	1.060	1.070
shift/error _{max}	0.001	0.002
max. electron density/ $e \text{\AA}^{-3}$	0.195	0.437
min. electron density/ $e \text{\AA}^{-3}$	–0.176	–0.367

^a Coordinates of hydrogen atoms bonded to aqua ligands were refined freely, all other hydrogen atoms were calculated in idealized positions, riding on their parent atoms.

Bibliography

- [1] P. M. DEWICK, *Medicinal Natural Products*; John Wiley and Sons Ltd, Chichester, 3rd edition **2009**.
- [2] T. W. RADEMACHER, R. B. PAREKH, R. A. DWEK, *Annu. Rev. Biochem.* **1988**, *57*, 785–838.
- [3] M. MILJKOVIĆ, in *Carbohydrates*, 221–244; Springer, New York, **2009**.
- [4] K. PAL, A. T. PAULSON, D. ROUSSEAU, in *Handbook of Biopolymers and Biodegradable Plastics*, 329–363; Elsevier, Amsterdam, **2013**.
- [5] G. LEDDERHOSE, *Ber. Dtsch. Chem. Ges.* **1876**, *9*, 1200–1201.
- [6] M.-P. MINGEOT-LECLERCQ, Y. GLUPCZYNSKI, P. M. TULKENS, *Antimicrob. Agents Chemother.* **1999**, *43*, 727–737.
- [7] J. E. HODGE, *J. Agric. Food. Chem.* **1953**, *1*, 928–943.
- [8] E. TAREKE, P. RYDBERG, P. KARLSSON, S. ERIKSSON, M. TÖRNQVIST, *J. Agric. Food. Chem.* **2002**, *50*, 4998–5006.
- [9] R. H. STADLER, I. BLANK, N. VARGA, F. ROBERT, J. HAU, P. A. GUY, M.-C. ROBERT, S. RIEDIKER, *Nature* **2002**, *419*, 449–450.
- [10] D. S. MOTTRAM, B. L. WEDZICHA, A. T. DODSON, *Nature* **2002**, *419*, 448–449.
- [11] D. V. ZYZAK, R. A. SANDERS, M. STOJANOVIC, D. H. TALLMADGE, B. L. EBERHART, D. K. EWALD, D. C. GRUBER, T. R. MORSCH, M. A. STROTHERS, G. P. RIZZI, M. D. VILLAGRAN, *J. Agric. Food. Chem.* **2003**, *51*, 4782–4787.
- [12] P. GREENBERG, A. H. MERRILL, D. C. LIOTTA, G. A. GRABOWSKI, *Biochim. Biophys. Acta Protein Struct. Molec. Enzym.* **1990**, *1039*, 12–20.
- [13] O. LOCKHOFF, P. STADLER, *Carbohydr. Res.* **1998**, *314*, 13–24.
- [14] V. NETO, A. VOISIN, V. HÉROGUEZ, S. GRELIER, V. COMA, *J. Agric. Food. Chem.* **2012**, *60*, 10516–10522.
- [15] S. J. ANGYAL, *Adv. Carbohydr. Chem. Biochem.* **1984**, *42*, 15–68.
- [16] Y. ZHU, J. ZAJICEK, A. S. SERIANNI, *J. Org. Chem.* **2001**, *66*, 6244–6251.
- [17] P. C. COLLINS, R. J. FERRIER, *Monosaccharides: Their Chemistry and Their Roles in Natural Products*; Wiley, Chichester, **1995**.

- [18] H. ISBELL, H. FRUSH, *J. Res. Nat. Bur. Stand.* **1951**, *46*, 132.
- [19] H. S. ISBELL, H. L. FRUSH, *J. Org. Chem.* **1958**, *23*, 1309–1319.
- [20] Y. ZHU, Q. PAN, C. THIBAudeau, S. ZHAO, I. CARMICHAEL, A. S. SERIANNI, *J. Org. Chem.* **2006**, *71*, 466–479.
- [21] T. SCHWARZ, *Synthese und Komplexchemie von Aminosuckern*, PhD thesis, Ludwig-Maximilians-Universität München, **2010**.
- [22] L. LINDNER, *Synthese und Komplexchemie von Glycosylaminen*, PhD thesis, Ludwig-Maximilians-Universität München, **2014**.
- [23] L. LINDNER, P. KLÜFERS, *Z. Anorg. Allg. Chem.* **2015**, *641*, 1869–1873.
- [24] H. PAULSEN, Z. GYÖRGYDEÁK, M. FRIEDMANN, *Chem. Ber.* **1974**, *107*, 1590–1613.
- [25] B. CAPON, W. G. OVEREND, in *Advances in Carbohydrate Chemistry*, 11–51; Elsevier, Amsterdam, **1961**.
- [26] H. A. TAHA, M. R. RICHARDS, T. L. LOWARY, *Chem. Rev.* **2012**, *113*, 1851–1876.
- [27] J. TSUJI, *Palladium Reagents and Catalysts*; John Wiley & Sons, Ltd, Chichester, **2004**.
- [28] B. ROSENBERG, L. VANCAMP, T. KRIGAS, *Nature* **1965**, *205*, 698–699.
- [29] B. ROSENBERG, L. VANCAMP, V. H. MANSOUR, *Nature* **1969**, *222*, 385–386.
- [30] B. WEBER, *Koordinationschemie*; Springer-Verlag GmbH, Berlin, **2014**.
- [31] M. FANELLI, M. FORMICA, V. FUSI, L. GIORGI, M. MICHELONI, P. PAOLI, *Coord. Chem. Rev.* **2016**, *310*, 41–79.
- [32] J. J. HLAVKA, R. G. CHILD, P. BITHA, Y. I. WANG, *Platinum complexes of polyhydroxylated alkylamines and 2-polyhydroxylated alkyl-1,2-diaminoethanes* **1986**, US4587331.
- [33] I. BERGER, A. NAZAROV, C. HARTINGER, M. GROESSL, S.-M. VALIAHDI, M. JAKUPEC, B. KEPPLER, *ChemMedChem* **2007**, *2*, 505–514.
- [34] Ž. D. BUGARČIĆ, J. BOGOJESKI, R. VAN ELDIK, *Coord. Chem. Rev.* **2015**, *292*, 91–106.
- [35] M. TANAKA, H. KATAOKA, S. YANO, H. OHI, K. KAWAMOTO, T. SHIBAHARA, T. MI-ZOSHITA, Y. MORI, S. TANIDA, T. KAMIYA, T. JOH, *BMC Cancer* **2013**, *13*, 237.
- [36] K. BOCK, C. PEDERSEN, in *Advances in Carbohydrate Chemistry and Biochemistry*, 27–66; Elsevier, Amsterdam, **1983**.
- [37] M. KARPLUS, *J. Am. Chem. Soc.* **1963**, *85*, 2870–2871.
- [38] T. ALLSCHER, Y. ARENDT, P. KLÜFERS, *Carbohydr. Res.* **2010**, *345*, 2381–2389.
- [39] B. N. STEPANENKO, R. D. GRESHNYKH, *Khim. Biokhim. Uglevodov, Mater. Vses. Konf., 4th* **1969**, 36–40.

- [40] D. CREMER, J. A. POPLE, *J. Am. Chem. Soc.* **1975**, *97*, 1354–1358.
- [41] F. CLORAN, Y. ZHU, J. OSBORN, I. CARMICHAEL, A. S. SERIANNI, *J. Am. Chem. Soc.* **2000**, *122*, 6435–6448.
- [42] F. BROTZEL, Y. C. CHU, H. MAYR, *J. Org. Chem.* **2007**, *72*, 3679–3688.
- [43] B. SOROKIN, *Ber. Dtsch. Chem. Ges.* **1886**, *19*, 513–513.
- [44] F. WEYGAND, *Ber. Dtsch. Chem. Ges.* **1939**, *72*, 1663–1667.
- [45] W. H. OJALA, J. M. OSTMAN, C. R. OJALA, *Carbohydr. Res.* **2000**, *326*, 104–112.
- [46] C. R. OJALA, J. M. OSTMAN, S. E. HANSON, W. H. OJALA, *Carbohydr. Res.* **2001**, *332*, 415–427.
- [47] R. AHLRICH, M. BALLAUFF, K. EICHKORN, O. HANEMANN, G. KETTENBACH, P. KLÜFERS, *Chem. Eur. J.* **1998**, *4*, 835–844.
- [48] Y. ARENDT, O. LABISCH, P. KLÜFERS, *Carbohydr. Res.* **2009**, *344*, 1213–1224.
- [49] T. ALLSCHER, *Carbohydrate-Metal Chemistry: Complexes of Palladium(II) and their Characterization via NMR Spectroscopy and X-Ray Crystallography*, PhD thesis, Ludwig-Maximilians-Universität München, **2011**.
- [50] C. ALTONA, M. SUNDARALINGAM, *J. Am. Chem. Soc.* **1972**, *94*, 8205–8212.
- [51] S. J. ANGYAL, *Angew. Chem. Int. Ed.* **1969**, *8*, 157–166.
- [52] G. F. BAUERFELDT, T. M. CARDOZO, M. S. PEREIRA, C. O. DA SILVA, *Org. Biomol. Chem.* **2013**, *11*, 299–308.
- [53] C. L. PERRIN, K. B. ARMSTRONG, *J. Am. Chem. Soc.* **1993**, *115*, 6825–6834.
- [54] M. MILJKOVIĆ, *Electrostatic and Stereoelectronic Effects in Carbohydrate Chemistry*; Springer US, New York, **2014**.
- [55] K. N. DREW, G. BONDO, B. BOSE, A. S. SERIANNI, *Carbohydr. Res.* **1998**, *307*, 199–209.
- [56] S. ANGYAL, V. PICKLES, *Aust. J. Chem.* **1972**, *25*, 1695.
- [57] T. SCHWARZ, D. HESS, P. KLÜFERS, *Dalton Trans.* **2010**, *39*, 5544.
- [58] H. E. GOTTLIEB, V. KOTLYAR, A. NUDELMAN, *J. Org. Chem.* **1997**, *62*, 7512–7515.
- [59] R. E. HOFFMAN, *Magn. Reson. Chem.* **2006**, *44*, 606–616.
- [60] J. L. MARKLEY, A. BAX, Y. ARATA, C. W. HILBERS, R. KAPTEIN, B. D. SYKES, P. E. WRIGHT, K. WÜTHRICH, *Pure Appl. Chem.* **1998**, *70*, 117–142.
- [61] R. K. HARRIS, E. D. BECKER, S. M. C. DE MENEZES, R. GOODFELLOW, P. GRANGER, *Pure Appl. Chem.* **2001**, *73*, 1795–1818.
- [62] A. GUTBIER, M. WOERNLE, *Ber. Dtsch. Chem. Ges.* **1906**, *39*, 2716–2720.

Danksagung

Ich bedanke mich herzlichst bei Prof. Dr. P. Klüfers für die interessante Themenstellung, den großen wissenschaftlichen Freiraum, die hervorragenden Arbeitsbedingungen, die vielen Ratschläge und Diskussionen als auch für die Geduld bei der Betreuung meiner Promotion.

Weiter bedanke ich mich bei Prof. Dr. H.-C. Böttcher für die wertvollen präparativen Anregungen, die angenehme Zusammenarbeit im Labor und die Übernahme der Zweitbegutachtung dieser Arbeit.

Mein ganz besonderer Dank gilt Christine Neumann für das Messen von über tausend NMR Spektren und die stete Hilfe in allen Belangen. Ohne diese Unterstützung wäre meine Forschung so nicht möglich gewesen.

Des Weiteren möchte ich Peter Mayer und Brigitte Breitenstein für die Messung der NMR-Spektren und Massenspektren sowie Susanne Ebert und Robert Eicher für die Durchführung der CHNS-Elementaranalysen danken.

Sandra Albrecht, Anja Belz, Leonie Lindner, Christine Sturm und Georg Monsch danke ich für das Messen meiner Kristalle. Ein besonderes Dankeschön geht zusätzlich an Markus Wolf, Jan Heinemann, Dr. Peter Mayer und vor allem Daniel Beck für ihre Unterstützung bei kristallographischen Probleme jeglicher Art.

Meinen Bachelor- und F-Praktikanten Maximilian Wurzenberger, Stefanie Heimsch, Laura Schwabauer, Marina Schmidt-Thomé, Lisa Gamperl, Yvonne Klingl, Jelena Reinhardt, Matthias Heiß, Katharina Hafner, Julian Brötzmann und Philip Watson danke ich für ihre fleißige und sorgfältige Mitarbeit.

Ich danke allen Mitgliedern des Arbeitskreises für ihre Unterstützung und die kollegiale Zusammenarbeit sowie die vielen unvergesslichen Abende innerhalb und außerhalb der Kaffeeküche. Hierbei möchte ich mich insbesondere bei Anja Belz bedanken, die mir nicht nur eine gute Freundin geworden ist, sondern die Jahre meiner Promotion besonders lustig und sportlich gemacht hat. Bei Jan Heinemann bedanke ich mich weiter für das sorgfältige und geduldige Korrekturlesen dieser Arbeit.

Ich danke von ganzen Herzen meinen Eltern und meinem Bruder, die mich seit jeher unterstützt und gefördert haben. Eine bessere Familie kann man sich nicht wünschen! Mein letzter Dank gilt Anna. Danke für deine Unterstützung, dein Verständnis und die Entbehrungen.